TN
1
A5
Vol.214
NIC

TRANSACTIONS

OF THE

AMERICAN INSTITUTE OF MINING, METALLURGICAL, AND PETROLEUM ENGINEERS

(INCORPORATED)

Volume 214

SOCIETY OF MINING ENGINEERS OF AIME

1959

Mining, Minerals Beneficiation, Coal,
Economics, Industrial Minerals,
Geology, Geophysics

THIS VOLUME IS MADE UP OF PAPERS AND DISCUSSIONS PRESENTED AT MEETINGS HELD AT NEW ORLEANS, FEB. 24-28, 1957; QUEBEC, OCT. 9-11, 1957; NEW YORK, FEB. 16-20, 1958; SPOKANE, APR. 17-19, 1958; LEXINGTON, KY., JUNE 13-14, 1958; SALT LAKE CITY, SEPT. 10-12, 1958; ST. LOUIS, OCT. 23-25, 1958; SAN FRANCISCO, FEB. 15-19, 1959; NEW YORK, FEB. 14-18, 1960.

PUBLISHED BY THE INSTITUTE
AT THE OFFICE OF THE SECRETARY
29 WEST 39TH STREET
NEW YORK 18, N. Y.

COPYRIGHT, 1960, BY THE
AMERICAN INSTITUTE OF MINING, METALLURGICAL, AND PETROLEUM ENGINEERS
(INCORPORATED)
PRINTED IN THE UNITED STATES OF AMERICA

CONTENTS

MINING ENGINEERING was paged consecutively throughout 1959. Thus, in this volume (214) of the Mining Transactions, there are interruptions in the pagination. The missing pages appeared in MINING ENGINEERING. This volume consists of all the Mining Transactions for 1959. Also listed are Extractive Metallurgy Division papers appearing in AIME Transactions Volume 215, 1959, published by The Metallurgical Society of AIME.

Mining

Basic Studies of Percussion Drilling. By H. L. HARTMAN 68
The 1959 Jackling Lecture—Economic History of the Lake Superior Iron District. By R. S. ARCHIBALD 513
Gyro-Compass Surveys Underground Workings and Boreholes. By E. P. PFLEIDER AND O. RELLENSMANN 521
Rock Breakage with Confined Concentrated Charges. By W. I. DUVALL AND T. C. ATCHISON 605
Case History in Pillar Recovery. By J. J. REED 701
Deflection of Mine Roof Supports. By L. ADLER 1027

Minerals Beneficiation

Polyacrylamides for the Mining Industry. By M. F. MCCARTY AND R. S. OLSON 61
Interaction of Minerals with Gases and Reagents in Flotation. I. PLASKIN 319
Experiments in Concentrating Iron Ore from the Pea Ridge Deposit, Missouri. By M. M. FINE AND D. W. FROMMER 325
Activation and Deactivation Studies with Copper on Sphalerite. By A. M. GAUDIN, D. W. FUERSTENAU, AND G. W. MAO 430
Recent Developments in Pebble Milling. By B. S. CROCKER 527
Application of Electron Diffraction and Electron Microscopy to Mineral Engineering. By J. E. LAWVER AND G. L. SAMSEL 535
Effect of Pulp Depth and Initial Pulp Density in Batch Thickening. By A. M. GAUDIN, M. C. FUERSTENAU, AND S. R. MITCHELL 613
Ferrograde Concentrates from Arkansas Manganiferous Limestone. By M. M. FINE 810
Economy Through Design. By R. J. LINNEY 909
Effects of Structure and Unsaturation of Collector on Soap Flotation of Iron Ores. By S. R. B. COOKE, I. IWASAKI, AND H. S. CHOI 920
Pebble Milling Practice at the South African Gold Mines of Union Corp. Ltd. By O. A. E. JACKSON 1133
Retention Time in Continuous Vibratory Ball Milling. By D. W. FUERSTENAU. (DISCUSSION, P. 1242) 1238
High-Intensity Magnetic Separation of Iron Ores. By O. E. PALASVIRTA 1244

Coal

Gravity Methods Clean Extreme Fine Sizes of Bituminous Coal. By H. B. CHARMBURY AND D. R. MITCHELL 211
Mineral Dressing Fundamentals Applied to the Fine Coal Problem. By M. C. CHANG AND J. DASHER 304
Permissible-Type Dust Counter for Coal Mines. By A. L. THOMAS, JR., AND S. OGLESBY, JR. 328
Laboratory Investigation—Flocculation to Improve Coal Slurry Filtration. By M. R. GEER, P. S. JACOBSEN, AND H. F. YANCEY. (DISCUSSION, P. 719) 715
Advancing Through Caved Ground with Yieldable Arches. By J. QUIGLEY 720
Face Ventilation for Continuous Miners. By J. D. KALASKY 928
Factors Affecting the Cleaning of Fine Coals by the Convertol Process. By S.-C. SUN AND W. L. MCMORRIS, III 1151

Economics

Trends in Real Prices of Representative Mineral Commodities, 1890-1957. By C. W. MERRILL 155

Industrial Minerals

Sand Deposits of Titanium Minerals. By J. L. GILLSON 421
Thorium and Uranium Resources in Monazite Placers of the Western Piedmont, North and South Carolina. By W. C. OVERSTREET, P. K. THEOBALD, JR., AND J. W. WHITLOW 709
Market Trends for Mineral Fillers in Western States. By W. F. DIETRICH 813
Relation of Land Subsidence to Ground-Water Withdrawals in the Upper Gulf Coast Region, Texas. By A. G. WINSLOW AND L. A. WOOD 1030

Geology

Tungsten in Searles Lake. By L. G. CARPENTER AND D. E. GARRETT 301
Midnite Mine—Geology and Development. By R. F. SHELDON 531
Drill Core Scanner Proved in Field. By W. W. VAUGHN, R. H. BARNETT, AND E. E. WILSON 617
The Gem Stocks and Adjacent Orebodies, Coeur d'Alene District, Idaho. By G. M. CROSBY 697
Bauxitization in the Pocos de Caldas District, Brazil. By B. N. WEBBER 805
Geology of the Ross-Adams Uranium-Thorium Deposit, Alaska, By E. M. MACKEVETT, JR., ... 915
Nuclear Detector for Beryllium Minerals. By T. CANTWELL, H. E. HAWKES, AND N. C. RASMUSSEN 938

The Electronic Computer and Statistics for Predicting Ore Recovery. By R. F. Shurtz 1035
Time Aspects of Geothermometry. By R. J. P. Lyon 1145
Quantitative Mineralogy as a Guide in Exploration. By R. J. P. Lyon and W. M. Tuddenham 1233

Geophysics

Geochemical Study of Soil Contamination in the Coeur d'Alene District, Shoshone County, Idaho. By F. C. Canney 205
Subsurface Investigations of a Plant Site. By L. Scharon, R. Uhley, and T. Meidav 215
A Decade of Development in Overvoltage Surveying. By R. W. Baldwin 307
Processing California Bastnasite Ore. By C. J. Baroch, M. Smutz, and E. H. Olson 315
Meteorological Influence on Radon Concentration in Drillholes. By A. B. Tanner 706
Airborne Gravity Meter—Description and Preliminary Results. By H. T. Lundberg and J. H. Ratcliffe 817
Scandinavian Electromagnetic Prospecting. By F. C. Frischknecht 932

Technical Notes

Beneficiation of Autunitic Ores. By W. C. Aitkenhead and J. A. Jaekel 66
Apparatus for Testing Coal Sedimentation. By S.-C. Sun 76
Sphalerite Flotation with Guanidine Compounds and Derivatives as Collectors. By P. R. Hines 219
Geochemical Study of Pb-Ag-Zn Ore from the Darwin Mine, Inyo County, California. By W. E. Hall 940
Fishing Tools for Retrieving Gamma-Ray Logging Components. By C. M. Bunker and J. M. Ohm 1045

Discussion of Papers Published Prior to 1957

Intergranular Comminution by Heating. By J. H. Brown, A. M. Gaudin, and C. M. Loeb, Jr. (1958), **211**, p. 490. 331
Grinding Ball Size Selection. By F. C. Bond (1958), **211**, p. 592 536
Lineament Tectonics and Some Ore Districts of the Southwest. By E. B. Mayo (1958), **211**, p. 1169 612
Scale-Up Relationships in Spodumene Flotation. By W. E. Horst (1958), **211**, p. 1182 616
Precision Survey for Tunnel Control. By D. D. Donald (1958), **211**, p. 977 723

Extractive Metallurgy

As many of members of the Society of Mining Engineers are interested in the papers of Extractive Metallurgy Division of The Metallurgical Society of AIME, the titles of the papers published for that Division in 1959 are listed below. These papers, and discussion, appear in AIME Transactions (1959), **215**, The Metallurgical Society.

Surface Tension and Contact Angles in Some Liquid Metal-Solid Ceramic Systems at Elevated Temperatures. By B. C. Allen and W. D. Kingery 30
Heat Flow and Temperature Distribution around a Copper Converter Tuyere. By W. A. Krivsky and R. Schuhmann, Jr. 82
Electrical Conductivity of Melts in the Systems NaCl-$ZrCl_4$ and NaCl-KCL (1:1 molar)-$ZrCl_4$. By L. J. Howell and H. H. Kellogg (Technical Note) 143
A Thermodynamic Study of The Titanium-Sulfur System in the Region $TiS_{1.93}$ to $TiS_{0.80}$. R. P. Abendroth and A. W. Schlechten 145
The Thermodynamics of the Liquidus-Solidus Gap in Binary Alloys: The Silver-Gold System. By J. L. White 178
Electrodeposition of Titanium from Fused Chloride Baths Using $TiCl_4$ as a Feed Material. By W. R. Opie and K. V. Svanstrom 253
Preparation of Two Lithium-Arsenic Compounds. By R. E. Tate and F. W. Schonfeld (Technical Note) 296
Preparation of Anhydrous Chlorides of Cerium and Thorium. By R. Didchenko (Technical Note) 401
The Preparation of High-Purity Uranium Metal by the Bomb Reduction of Uranium Tetrafluoride with Calcium. By R. W. Kewish, R. J. Bard, J. P. Bertino, O. E. Fry, S. W. Hayter, F. J. Hill, B. L. Kelchner, and A. W. Savage 425
The Separation of Rare Earths by Ion Exchange. By J. W. Powell and F. H. Spedding 457
High-Purity Tantalum. By R. F. Rolsten 472
A Redetermination of the Lead-Lead Sulfide Equilibrium Between 585° and 920°C. By J. R. Stubbles and C. E. Birchenall 535
The Present State of Titanium Extractive Metallurgy. By W. J. Kroll 546
Self and Interdiffusion in Liquid Zinc Amalgams. By H. W. Schadler and R. E. Grace 559
Equilibrium Electrode Potentials of Some Metal-Chlorine Galvanic Cells and Activities of Some Metal Chlorides in LiCl-KCL Eutectic Melt. By L. Yang and R. G. Hudson 589
Removal of Fission Products from Molten Thorium-Uranium Alloy. By A. G. Buyers, J. Chilton, and W. E. McKee 624
Separation of Yttrium and Rare-Earth Nitrates with the Solvent Extraction System-Tri-N-Butyl-amine-3 Methyl-2-Butanone. By W. G. Gruzensky and G. T. Engel 738
Oxidation of Sphalerite by Sulfur Trioxide. By A. W. Sommer and H. H. Kellogg 742
Stoichiometry of Lead Telluride. By E. Miller, K. Komarek, and I. Cadoff 882
Electrical Conductivity of Molten FeS. By D. Argyriades, G. Derge, and G. M. Pound 909

POLYACRYLAMIDES

FOR THE MINING INDUSTRY

A new type of flocculant is raising efficiency, lowering costs. Greater operating capacity made possible is changing plant set-ups, equipment design.

by MERRILL F. McCARTY and ROBERT S. OLSON

New organic flocculants of high-molecular weight are replacing lime, glue, and starch in liquid-solid separation. Of these synthetic materials, polyacrylamides are outstanding.

Polyacrylamides form a class of compounds varying widely in composition and activity. Separan 2610[R], one of the first of these flocculants[1] released to the mining industry in 1954, is described[2] as a high-molecular weight polymer of acrylamide with or without a copolymer material and with some replacement of amide by carboxylic groups.

MECHANISM OF FLOCCULATION

In practice, flocculation makes solids settle faster and filter better. But two opposing factors control it. The random motion that causes particles to collide favors Van der Waals' forces, which hold the particles together. The effect of zeta potential opposes this contact, and particles are mutually repelled. Flocculation can be achieved by reducing the magnitude of the zeta potential; this is the mechanism of flocculation by lime addition.

The way in which polyacrylamides accomplish flocculation is not fully understood, but the action is undoubtedly complex and probably varies considerably depending on the system. To begin with, the active groups of these compounds have an extremely high affinity for solid surfaces, probably by hydrogen bonding.[3] Initially some active groups of the molecule attach themselves to the solids with a large portion of the molecule extending into the solution. Two particles can become tied together by long flocculant molecules in the following ways—by bonding between the active groups of two flocculant molecules on different particles, or by an extended molecule from one particle attaching itself directly to the surface of the other particles.[4,5] These flocculant bridges prevent the particles from moving apart through random motion, but when such motion moves them together other active groups on the flocculant bridge bond to the solids, holding them in the closer position. This process is repeated until the particles are close together.

F. F. McCARTY, Member AIME, is a Metallurgist with Dow Chemical Co., Midland, Mich. R. S. Olson, Member AIME, is Project Leader, Dow Chemical Co., Pittsburgh, Calif. TP 4775B. Manuscript, May 6, 1958. New Orleans Meeting, February 1957. AIME Trans., Vol. 214, 1959.

Although bridging is probably a major flocculation mechanism, it is not the only phenomenon involved. Relatively neutral acrylamide flocculants reduce the magnitude of the zeta potential by increasing the viscosity of solution in the immediate vicinity of the solid surface which contains the mobile counter ions of the double layer. In other words, it moves the shear surface which bounds the zeta potential out into the solution containing counter ions which tend to neutralize the zeta potential. This effect is probably more pronounced during the initial adsorption period, before the flocculant molecules are pulled close to the solid.

In some cases the slight charge of the polyacrylamide molecule tends to neutralize a zeta potential. However, this is not a primary flocculation mechanism, as evidenced by the fact that the polyacrylamides will flocculate solids with either positive or negative zeta potential.

Adsorption of polyacrylamide flocculants by a solid is substantially an irreversible reaction. Since the flocculant molecule is attached to the particle surface by many active groups of high bonding strength, desorption would require the simultaneous breaking of many bonds—an unlikely occurrence.

UNIQUE PROPERTIES

The irreversible adsorption of certain polyacrylamides, the flocculant's high affinity for solid surfaces and its rapid adsorption make it effective, but these unique properties require special techniques to achieve maximum flocculation.

If flocculants of this type are added to a pulp as a relatively concentrated solution, the solids in the

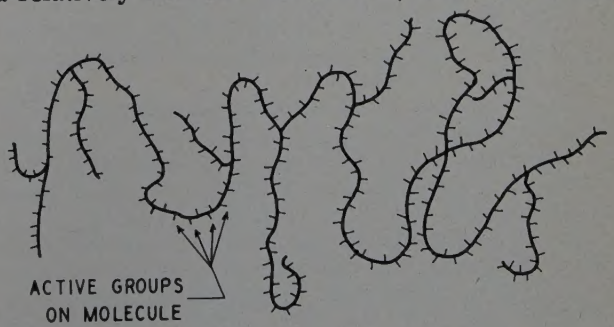

Fig. 1—Representation of a flocculant molecule.

Fig. 2—Mechanics of flocculation by Separan 2610.

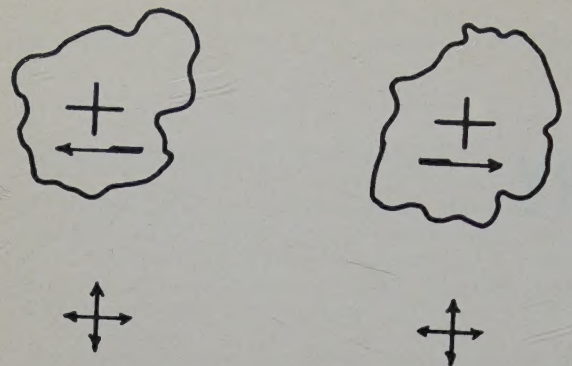

A—Two particles in suspension.

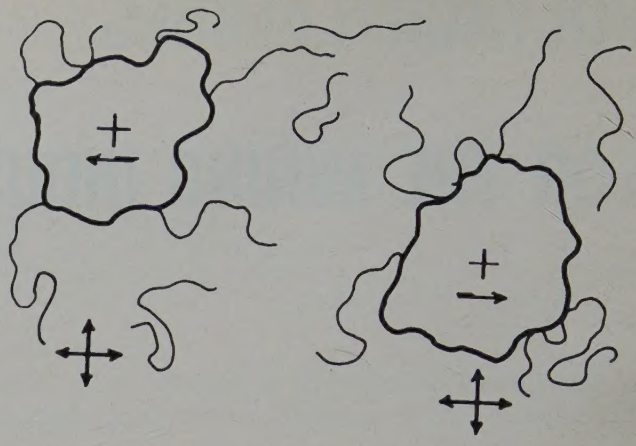

B—Flocculant sorbing.

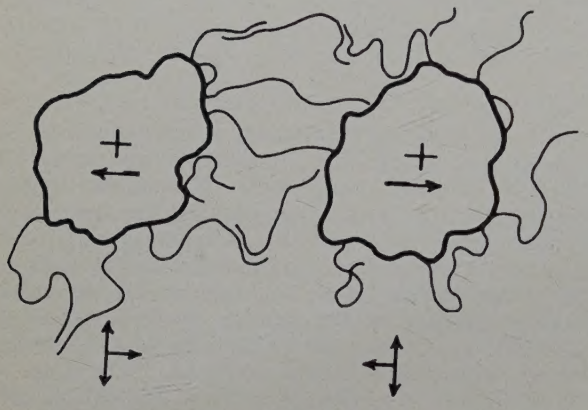

C—Flocculant bridging.

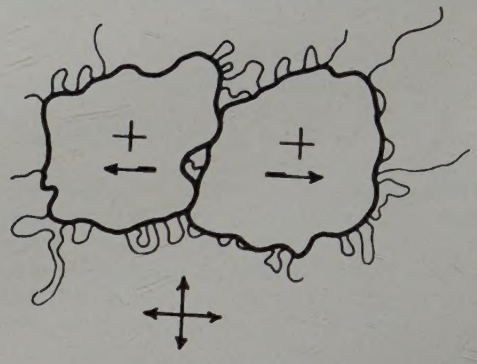

D—Particles flocculated.

vicinity of the addition point adsorb all of the flocculant rapidly and completely. The bulk of the pulp thus remains unflocculated—an undesirable condition. To insure optimum flocculation the reagent must be distributed uniformly throughout the pulp.

Better distribution can be obtained by slowly adding the reagent solution to the system while gently agitating the pulp, so that all the pulp is exposed to the flocculant addition point. This method is not very practical in flowing systems, but it can be approximated by multiple point addition of solution to the system. If dilute solutions are used distribution is further improved, since the large solution volume mixes more uniformly with the pulp in a short period of time. These effects are illustrated in Fig 3, which shows the free settling rate (initial rate) of an acid leach uranium ore pulp flocculated with 0.23 lb of Separan 2610 per ton. The 30 pct solids pulp was flocculated with different concentrations of solution added in either one or three increments. The pulp was diluted to 16 pct solids after flocculation to insure identical conditions during determination of settling rates.

The advantages of dilute multiple point addition are quite pronounced, as these data show. However, the magnitude of this effect varies considerably from system to system. In one unusual case solid flocculant is added to a pulp[6] with good results.

Ease of reagent distribution varies markedly with the concentration and characteristics of the individual pulp to be flocculated. In general the more concentrated the pulp the more difficult distribution becomes. This fact is shown in Fig. 4, which summarizes tests in which various dilutions of the pulp used in previous tests were treated with 0.23 lb of Separan 2610 per ton, added as a 0.2-gpl solution in three increments. Initial settling rate was determined after dilution to 16 pct solids.

With most pulps, the effect of increasing the reagent dosage is to increase degree of flocculation. Fig. 5 illustrates the plateau reached with the addition of 0.2 lb Separan 2610 per ton. The same pulp was flocculated at 30 pct solids with varying amounts of flocculant diluted with a constant volume of liquor, so that the solids content of the pulp after flocculation was 16 pct in all cases.

At moderate levels polyacrylamide is almost quantitatively adsorbed by the solids. Non-adsorbed molecules do not remain in the liquid until amounts far beyond those required for effective flocculation are applied. This quantitative adsorption is, in part, responsible for the sensitivity of the flocs to more than mild agitation. When the flocs are degraded by mechanical agitation no unadsorbed flocculant is available and reflocculation does not usually occur, except to a small degree, until more is added to the system.

Sensitivity to agitation varies considerably from pulp to pulp. Fig. 6 shows the effect of agitation on one pulp, as well as the effect of additional reagent after extreme floc break-up. In these tests the 30 pct solids pulp was flocculated with 0.23 lb per ton Separan 2610 added as a 0.028-gpl solution in three increments. The pulp after flocculation contained 16 pct solids. One-liter portions of flocculated pulp were agitated with a 1½-in. four-bladed turbine

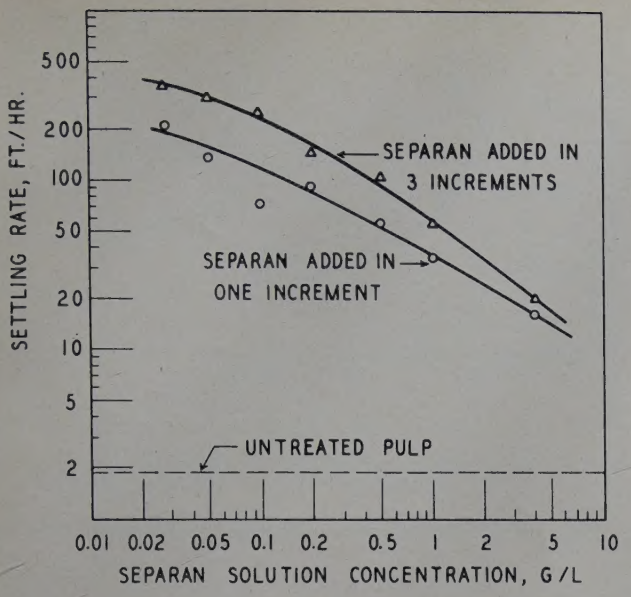

Fig. 3—Effect of Separan dilution on settling rate.

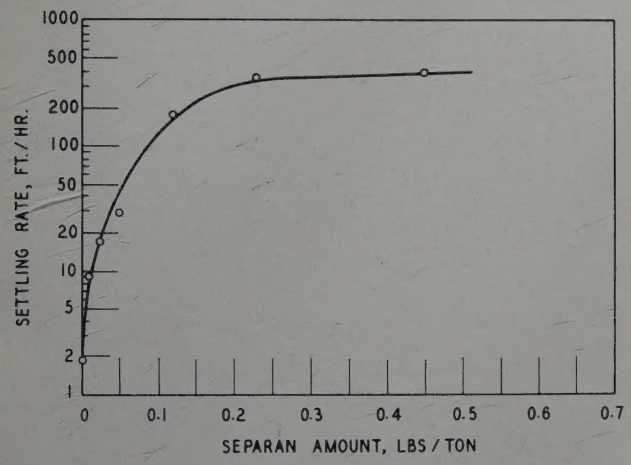

Fig. 5—Settling rate varies with amount of Separan.

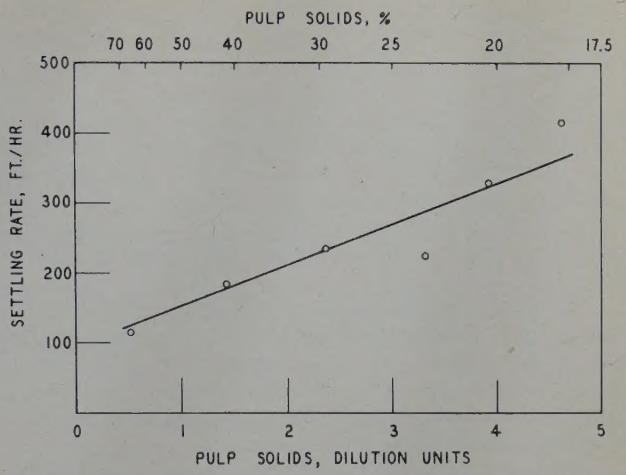

Fig. 4—Effect of initial pulp density on flocculation.

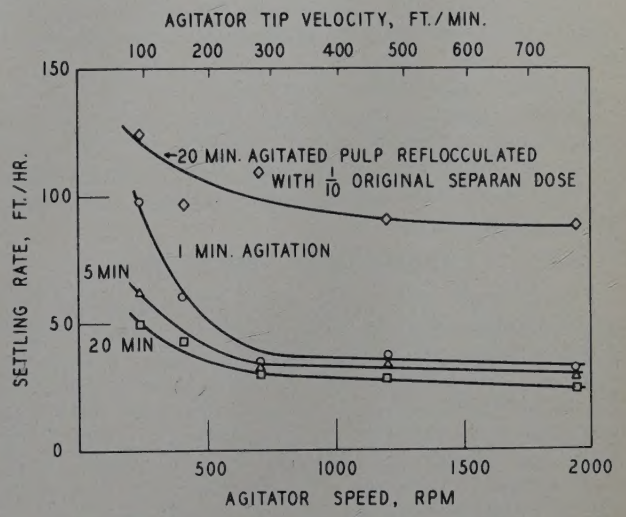

Fig. 6—Agitation of a flocculated pulp. (Unagitated rate: 460 ft per hr.)

type (Rushton) impeller in a 4-in. diam vessel 5 in. high, equipped with four baffles 0.4 in. wide. Settling rate of the pulp after agitation at various speeds and times was determined. The settling rate of the flocculated pulp agitated for 20 min and reflocculated with 0.023 lb per ton Separan 2610 added under the above conditions was also determined. In general, an agitation-degraded floc can be restored to its original flocculated condition by a small fraction of the original amount of reagent.

APPLICATION METHODS

In plant application the unique properties of polyacrylamide flocculants must be considered. It is generally impractical, because of the volume required, to prepare a solution at optimum application strength in a mixing tank, so a relatively concentrated (about 1 pct) stock solution is prepared and diluted continuously to the strength required. Laboratory tests should be made to determine the optimum concentration—usually less than 0.05 pct (0.5 gpl) is desirable.

It is often undesirable to add to the plant circuit the relatively large volume of water arising from the dilute reagent stream. Where this is true the stock solution is diluted to application strength with recycle plant solution, filtrate in a filtration operation, or thickener overflow in thickening or clarification. By this means solution at any concentration can be added without diluting soluble values. The stock solution should be prepared with water to eliminate the possibility of high viscosity, resulting from reaction of the flocculant with soluble iron or other ions.

At first glance, dilution of pulps with flocculant solutions might seem detrimental to liquid-solid separations but in clarification operations (very low pulp density) dilution is so small that this effect is not observed. In thickening operations, requirements are governed, not by the feed dilution, but by a more concentrated pulp zone in the thickener so that here, too, dilution has little adverse effect. In filtration a definite optimum reagent concentration will be found at which the increasing filtration rate result-

ing from an increased volume of the reagent solution is overcome by the decreasing filtration rate caused by pulp dilution. This effect is illustrated by Fig. 7, which shows the filtration of another 66 pct solids acid leached uranium ore pulp as a function of reagent dilution at two treatment levels. The pulp was flocculated by three increment additons, and filtration was determined on a 0.1-sq ft test leaf, with 35 sec submergence, 10 sec dry, 25 sec wash, 20 sec dry, and a 10-sec discharge cycle at 17-in. vacuum.

Optimum concentration is a function of the treatment level. Mechanical details of plant set-ups for using flocculants generally depend on problems of individual plants, and any discussion of application systems includes stock solution preparation, feed control and dilution, and application.

Importance of Thorough Dispersion: Fig. 8 illustrates two ways to obtain the even dispersion essential in preparing stock solutions of polyacrylamides. The first method uses high-power agitation (1.5 hp per 100 gal). The second adds dry flocculant to the tank through the Dow-developed Separan disperser, a water jet device. The dispersed solids are then dissolved by mild air or mechanical agitation for 1 to 2 hr.

Stock solutions are usually prepared in 50-lb increments (shipping bag size). Daily preparation is convenient, although polycrylamide solutions are stable for much longer intervals. Batch sizes as large as 1000 lb (12,000 gal of 1 pct solution) have been prepared in 2 hr.

LABORATORY METHODS

Preliminary laboratory tests are essential. Test work should simulate plant practice, using multiple point addition of a dilute solution. With thick pulps, such as those for filtration, this can be accomplished by dividing the dilute flocculant solution into three portions and simultaneously pouring together the pulp and successive portions of the solution with mild agitation between additions. In preparing more dilute pulps for thickening tests it is convenient to add reagent increments to the pulp in a graduate, gently rocking the graduate several times after each addition.

Laboratory filtration tests are usually carried out with standard test leaves. The filtration rate from a single test can be taken as the average of the rate calculated from the cake weight and that calculated from the filtrate volume. Alternatively, the filtration can be repeated on a batch of flocculated pulp until consistent cake weights and filtrate volumes are obtained.

As pointed out by Talmage and Fitch,[7] the classic Coe and Clevenger[8] thickening test method is not reliable when applied to flocculated pulps. This method necessitates determining settling rates of the pulp over a range of densities, but the problem of insuring the same degree of flocculation at the different densities is almost insurmountable. It might be attempted in two ways, flocculating the pulp at various dilutions or decanting varying amounts of liquid from a settled flocculated pulp and resuspending before it settles again. The data previously given prove the first method invalid, and the second is questionable because the flocs may have been compressed in settling or the agitation to resuspend the pulp may break up the floc. It should be noted that the Coe and Clevenger method generally gives settling areas greater than the true areas.

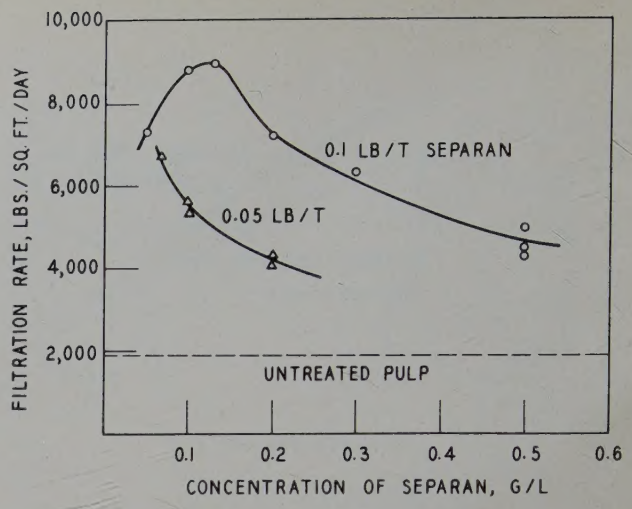

Fig. 7—Effect of Separan dilution on filtration rate.

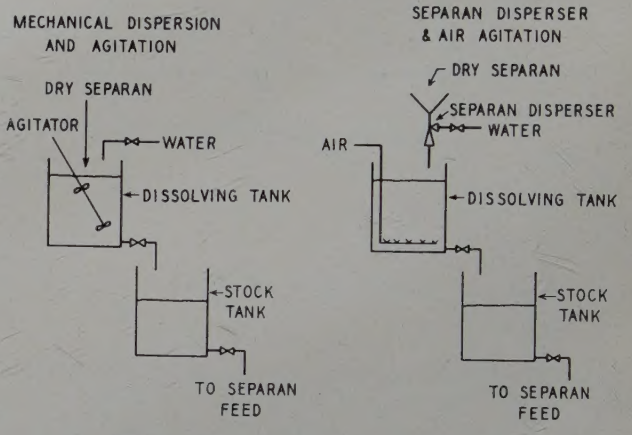

Fig. 8—Stock solution preparation.

At present there is no *completely* satisfactory thickening test for flocculated pulps, but the single-settling test developed by Talmage and Fitch, in conjunction with the compression point determination proposed by Roberts,[9] has been found useful and is probably as good as any method now available.

TYPICAL USES OF POLYACRYLAMIDES

The high-molecular weight polymers are remarkably versatile, flocculating a wide range of suspended solids, from coal and sewage to minerals and chemical precipitates. They are effective even when the suspending solution is strongly acid or basic or a strong salt solution. Particles ranging in size from colloidal clays to sands are flocculated by materials of this type.

Uranium Leaching: Leaching operations create some of the most difficult liquid-solid separations in the mining industry. Separan 2610 is used in uranium mills to thicken the ore pulp before leaching, to flocculate both acid and carbonate-leached pulp, and to flocculate high grade precipitates.[6, 10, 12] Hannay, for example, reports the use of 0.05 lb per ton of solids in ground ore thickening and 0.2 lb per ton to flocculate carbonate leach pulp before filtration.

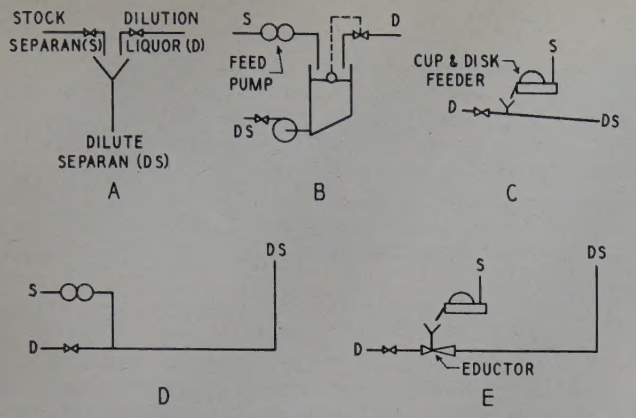

Fig. 9—Feed control and dilution.

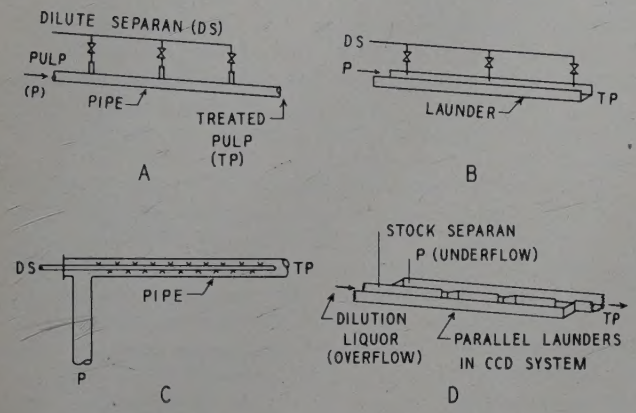

Fig. 10—Application to pulp.

Cyanidation, Zinc Leaching: Polyacrylamides are used extensively in gold cyanidation, which presents many problems similar to those of uranium leaching. They are effective on leached zinc calcines prior to electrolytic refining and recovery of the zinc and are also utilized in the neutral or primary leach thickeners, as well as in a number of thickening applications during purification of the zinc electrolyte. At Cerro de Pasco, Separan 2610 has been found to decrease zinc leach residue filtration time.[13]

Nickel Recovery: The study of flocculants made by Evans, Kunda, and Chiang[14] for Sherritt-Gordon's complex nickel recovery showed that 0.03 lb of Separan per ton of concentrate decreased the required thickener diameter from 103 to 73 ft on an ammonia leach slurry. In plant practice further capital expenditure for thickeners and filters was eliminated by using Separan 2610 at 0.03 lb per ton in the leach thickener, 0.06 lb per ton in the final thickener, and 0.12 per ton before final filtration.

Increased Tonnage without Expansion: Recognizing that dispersed pulp is desirable in flotation, operators naturally hesitated to use flocculants to thicken flotation feed. But laboratory results have indicated that where most of the mineral to be recovered occurs in the slimes, flocculants are not harmful and actually offer an advantage. Difficulties arise chiefly when slimes are mostly gangue minerals. When this occurs, flocculants may increase slime coatings on the minerals to be recovered and reduce concentrate grade or recovery.

By thickening flotation concentrates with flocculants, many plants have increased concentrate tonnage without expanding thickener capacity. Flocculant requirements for this purpose average 0.01 to 0.02 lb per ton.

To recover water and prevent stream pollution, it is increasingly important to thicken concentrator tailings. Polyacrylamide flocculants in tailings have improved operations without expenditure for additional thickeners. In several cases, flocculant is added directly to the tailing launder to facilitate dam building and obtain maximum clarity of tailing dam overflow.

Unique Application: Polyacrylamide flocculants have been used as electrolyte additives in refining and plating metals. One large copper refinery reports a 3 to 5 pct increase in current efficiency, as well as a smoother and higher-density copper deposit on the cathode. The additive's function in this application is apparently twofold. First, it effectively flocculates the slimes and causes them to settle to the bottom of the cell, eliminating the nuclei causing rough spots on the cathode. Second, the adsorption of the large molecule is concentrated at those points on the cathode which protrude toward the anode. This reduces current density at these points, rounding off the rough spots. A similar procedure is being investigated in zinc electrolysis.

Further Uses: Polyacrylamides are also effective in recovery of flue gas solids in scrubbing plants and removal of solids from the mine water before it is pumped. In areas where streams are unusually turbid, they are used to clarify the raw river water.

These applications by no means conclude the list. In almost every type of mining operation, polyacrylamide flocculants have improved thickening, filtration, and clarification. The increased capacity of liquid-solids separation equipment so obtained is having a pronounced effect on equipment and mill design.

The authors are indebted to E. C. Tveter and A. W. Hart for suggestions and editorial assistance in preparing this article.

REFERENCES

[1] Anon.: Dow Product Announcement, September 1954.
[2] Anon.: Information Release. Dow Chemical Co., Midland, Mich., Feb. 13, 1956.
[3] R. O. French, et al.: The Quantitative Application of Infrared Spectroscopy to Studies in Surface Chemistry. *Journal of Physical Chemistry*, 1954, vol. 58, pp. 805-811.
[4] R. A. Ruerhwein and D. W. Ward: *Soil Science*, June 1952, vol. 73, p. 485.
[5] A. S. Michaels and O. Morelos: Polyelectrolyte Adsorption by Kaolinite. *Industrial Engineering Chemistry*, 1955, vol. 47, pp. 1801-1808.
[6] R. L. Hannay: Milling at Beaverlodge. *Canadian Mining Journal*, 1956, vol. 77, no. 6, pp. 136-140.
[7] W. P. Talmage and E. G. Fitch: Determining Thickener Unit Areas. *Industrial Engineering Chemistry*, 1955, vol. 47, pp. 38-41.
[8] H. S. Coe and G. H. Clevenger: Methods for Determining the Capacities of Slime-settling Tanks. *AIME Trans.*, 1916-17, vol. 55, pp. 356-384.
[9] E. J. Roberts: Thickening—Art or Science? *Mining Engineering*, 1949, vol. 1, pp. 61-64.
[10] J. B. Huttl: Vitro's Keys to Successful Uranium Leaching, *Engineering and Mining Journal*, vol. 156, no. 9, pp. 100-4.
[11] F. A. Brinker: Concentration of Vanadium and Uranium Ore at Monument No. 2 Mine of Vanadium Corporation of America. Presented at Colorado Mining Ass'n, Denver, February 1956.
[12] J. B. Rosenbaum and J. B. Clemmer: Accelerated Thickening and Filtering of Uranium Leach Pulps. International Conference on the Peaceful Uses of Atomic Industry A/Conf. 8/P/528, July 6, 1955.
[13] I. L. Barker: Complex Metallurgy by Cerro de Pasco. Presented at the AIME Annual Meeting, New York, February 1956.
[14] O. J. I. Evans, W. Kunda, and P. Chiang: Laboratory Studies on Flocculants for Settling, Thickening, and Filtration in the Sherritt Gordon Process. Presented at Third Western Regional Conference of Chemical Institute of Canada, Edmonton, September 1956.

Discussion of this article sent (2 copies) to AIME before Feb. 28, 1959, will be published in MINING ENGINEERING.

Technical Note

BENEFICIATION OF AUTUNITIC ORES

Experiments have developed a highly successful collector for this mineral component of a low grade uranium ore.

By WILLIAM C. AITKENHEAD and JOHN A. JAEKEL

Uranium deposits in the Spokane Indian Reservation, as well as those around Mt. Spokane, are essentially low grade, much of the ore containing less than 0.2 pct U_3O_8. The Mining Experiment Station of the Division of Industrial Research, State College of Washington, has been engaged in intensive research on the amenability of these low grade ores to froth flotation. The results: successful flotation of autinite, chief mineral constituent.

At the outset of this work the goal was a concentrate of 1 pct U_3O_8 with a 90 pct recovery from ores containing less than 0.2 pct U_3O_8. Most of the work has been done on argillite ore from the Midnight mine on the Spokane Indian Reservation. The goal has not been attained using this ore, but samples of the granite ore from Mt. Spokane yielded successful results. For example, a concentrate containing 11.2 pct U_3O_8 was produced from a Mt. Spokane high grade ore containing 1.27 pct U_3O_8, with a recovery of 97.8 pct. Another Mt. Spokane ore yielded a concentrate of 5.0 pct U_3O_8 from an ore containing 0.13 pct U_3O_8, with a recovery of 85 pct. This same ore gave a recovery of 93.5 pct when the grade of concentrate was reduced to 2.0 pct.

It has been concluded that a successful method for floating autunite has been developed and that the mediocre results from the Midnight argillite ore are probably caused by the presence of some other uranium mineral or minerals less amenable to these reagents.

The experimenters tested a third type of Washington ore, found on the Northwest Uranium Mines Inc. property on the Spokane Indian Reservation. This is a conglomerate of pebbles and small boulders of partially decomposed granite and is shot through with autunite. Its characteristics lie between those of the Midnight ore and the granite ore from the Spokane district. It responds better than the ore from Midnight but not as well as that from Mt. Spokane.

As the fatty acids are the only type of collectors showing promise, investigation has been concerned with these acids and the optimum conditions for their use. The first method for treating the argillite ore from the Spokane Indian Reservation made use of Cyanamid's R-708 as a collector, a tall oil product described as a substitute for oleic acid. Although the investigators proved that R-708 is a collector for autunite when mixtures of autunite and silica sand are used, results on the ore were mediocre. Tests of other fatty acids revealed that the solid fatty acids of the saturated series are collectors for autunite and that their collecting power increases with the length of the carbon chain. The even carbon members of the whole series were tested from the 10 carbon acid (capric) to the 22 carbon acid (behenic). The least expensive collector, stearic acid (18 carbon), proved to be a good one, so this was used in most of the tests.

In first attempts with stearic acid, the collector was dissolved in various hydrocarbons and the solutions were added to the flotation cell. Cyclohexane, gasoline, fuel oil, kerosene, and other solvents were tried. Small amounts of high grade concentrates could be brought up, but recoveries were low. Finally emulsions of stearic acid were tried. It was discovered that stearic acid alone has little collecting power except when conditioning is carried out at high temperature. When hydrocarbon solvents were also present, it proved to be an excellent collector. An example of one emulsion that proved satisfactory for some ores is given as follows: 1 part stearic acid by weight, 1 part sodium oleate by weight, 1.2 parts kerosene by weight, 100 parts water. In some successful tests part of the stearic acid was replaced by oleic acid.

The emulsions were made by agitating the stearic acid and sodium oleate together with hot water, then adding the kerosene and agitating while cooling.

In the five tests reported in Table I, 650 g of ore were ground with 650 cc water in a laboratory rod mill. The pulp was filtered to eliminate excess water and the ground ore transferred to a stainless steel beaker for conditioning at high pulp density. In most of the tests sodium hydroxide was added to the conditioner during agitation, then the collector emulsion, and finally the sodium silicate. The amount of alkali was adjusted to give a pH of 8.5 to 9.0 in the flotation cell. After conditioning the pulp was transferred to a laboratory flotation cell and the test completed in a normal manner.

It is interesting to note that a deposit of high grade concentrate forms on the conditioning agitator and in the conditioning vessel, and at times on the agitator of the flotation cell itself. A few grams of concentrate running as high as 4 pct U_3O_8 were recovered from the conditioner when Midnight ore containing less than 0.2 pct U_3O_8 was treated. In the examples given in Table I this conditioner concentrate is calculated as part of the total concentrate. The authors have not yet fully explored the possi-

W. C. AITKENHEAD and J. A. JAEKEL, Members AIME, are, respectively, Director and Metallurgist, Mining Experiment Station, State College of Washington, Division of Industrial Research, Pullman, Wash. TN 463B. Manuscript, May 26, 1958. AIME Trans., Vol. 214, 1959.

bility of making use of this tendency for the concentrate to stick to metallic surfaces.

Table I reports details of tests on five ores. Test AU 185 shows results on a sample of low grade Midnight argillite ore, the most difficult of all ores tested. Concentrates from this ore always contained large amounts of ferruginous slime and decomposed biotite mica, so the concentrate grade was invariably low. Low recoveries may have been due to nondescript uranium minerals in the extremely fine sizes.

Test 140 records data on a conglomerate ore, which gave results better than those obtained on the Midnight sample, but inferior to the good recoveries with high grade concentrates that result from the Mt. Spokane granite ores.

Tests 108 and 114 show results on undecomposed granite ore from Mt. Spokane. Test 116 treated a decomposed granite ore in which the feldspar was largely kaolinized. The clay in this ore does not interfere with production of high grade concentrates with good uranuim recovery.

Table II shows results of tests for maximum recovery compared with tests for maximum grade of concentrate.

Use of the stearic acid-kerosene emulsion has not been investigated as a collector for other uranium minerals more common than autunite. So far there have been no studies of concentrate cleaning and recirculation of the cleaner tailings, which should give a higher grade concentrate with little or no sacrifice of recovery.

Table I. Test Results for Five Uranium Ores

Test Factors	Test AU 185 Dawn Mining Co. (Midnight Ore) 0.12 Pct U_3O_8 −35 Mesh	Test No. 140 N.W. Uranium Inc. 0.148 Pct U_3O_8 −48 Mesh	Test No. 108 Mt. Spokane (Granite) 0.215 Pct U_3O_8 −35 Mesh	Test No. 114 Mt. Spokane (Granite) 0.390 Pct U_3O_8 −35 Mesh	Test No. 116 Mt. Spokane (Decomposed Granite) 0.131 Pct U_3O_8 −48 Mesh
Conditioning Reagents, Lb Per Ton					
NaOH	1.2	—	0.3	0.15	0.15
Collector emulsion					
Stearic acid	1.5	1.5	2.25	1.0	1.5
Oleic acid	1.5	—	—	—	—
Sodium oleate	3.0	1.5	2.25	1.0	1.5
Kerosene	2.4	1.2	4.8	1.1	1.7
Sodium silicate	—	0.3	0.3	0.3	0.3
Sodium metasilicate	1.2	—	—	—	—
Pulp density, pct	59	59	61	61	60
Temperature, °C	24	28	29	29.5	26.3
Time, min					
NaOH	26	25	21	21	21
Collector emulsion	20	20	20	20	20
Sodium silicate	—	2	2	2	2
Sodium metasilicate	26	—	—	—	—
Flotation Reagents, Lb Per Ton					
B-23	—	—	0.2	0.3	0.35
Pine oil	—	0.18	—	—	—
Collector emulsion*					
Stearic acid	—	1.5	—	—	—
Sodium oleate	—	1.5	—	—	—
Kerosene	—	1.2	—	—	—
Temperature, °C	24	27	26	26	26
pH	8.3	8.15	9.0	9.0	8.7
Pulp density, pct	19.0	25	25	25	25
Recovery, pct	75.7	89.6	95.0	89.3	93.5
Concentrate, pct U_3O_8	0.434	0.44	3.06	12.04	2.0
Ratio of concentration	4.8	3.3	14.9	34.6	16.5
Tailings, pct U_3O_8	0.037	0.022	0.011	0.043	0.009
Total reagent cost per ton, $	1.13	1.09	0.84	0.40	0.56

* Four-stage additions.

Table II. Recovery vs Grade

Ore from Daybreak Mines Inc. (Mt. Spokane)		U_3O_8, Pct				
Objective	Test No.	Heads	Recovery	Concentrate	Tails	Ratio Conc.
Maximum recovery	AU 230	0.125	96.6	0.87	0.006	7.1
Maximum recovery	116	0.131	93.5	2.00	0.009	16.5
Maximum grade	116-b	0.131	85.0	5.00	0.020	45.1
Ore from Mt. Spokane (Granite)		U_3O_8, Pct				
Objective	Test No.	Heads	Recovery	Concentrate	Tails	Ratio Conc.
Maximum recovery	108	0.215	95.8	2.29	0.010	11.2
Maximum recovery	109	0.226	94.3	2.70	0.014	12.7
Maximum grade	111	0.348	83.3	19.4	0.059	67.0
Maximum grade	114	0.390	89.3	12.0	0.043	34.6
Recovery and grade	113-b	0.385	93.1	6.0	0.028	16.8
Ore from Mt. Spokane (Decomposed Granite)		U_3O_8, Pct				
Objective	Test No.	Heads	Recovery	Concentrate	Tails	Ratio Conc.
Maximum recovery	93	1.49	98.6	7.0	0.026	4.8
Maximum grade	92	1.27	97.8	11.2	0.032	9.0
Ore from Northwest Uranium Mines Inc. (Conglomerate)		U_3O_8, Pct				
Objective	Test No.	Heads	Recovery	Concentrate	Tails	Ratio Conc.
Maximum recovery	140	0.148	89.6	0.44	0.022	3.3
Maximum grade	140-b	0.148	80.1	1.14	0.033	9.6

BASIC STUDIES OF PERCUSSION DRILLING

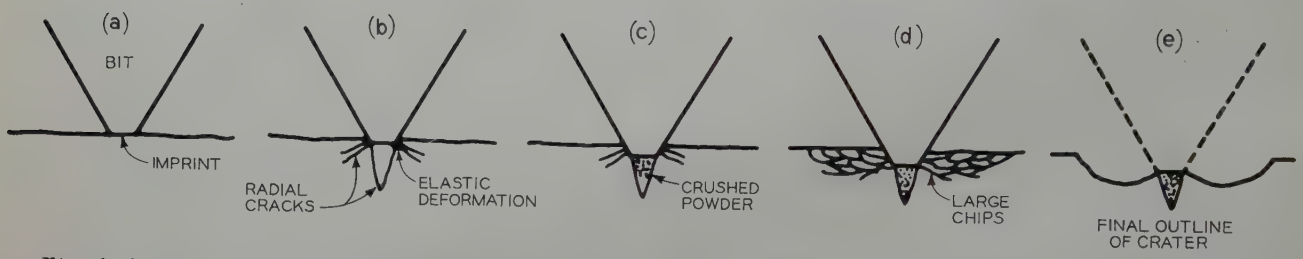

Fig. 1—Sequence of rock failure and crater formation when a blunt, wedge-shaped bit strikes an impact blow.

The author contends that for more than 70 years there has been no major improvement in percussion drills, that rock drilling remains an art when it should become a science, and that faster rates of penetration depend on advances in basic research.

BY HOWARD L. HARTMAN

The past 15 years have seen rapid advances in the metallurgy of materials for drill machinery and bits, but rock drilling itself continues to be largely an art. Jet piercing, roller bit rotary drilling, and rotary percussion are all promising new techniques, but the percussion rock drill, still used for 90 pct of the blastholes in U. S. hard-rock mining, has undergone no major modification since pneumatic machines were first used successfully in the 1860's.

This singular lack of progress stems directly from ignorance of the nature of impact failure of rock and the fundamentals of rock penetration in general. For nearly three-quarters of a century, mining engineers did not know what went on at the bottom of a drillhole.

More and more, in recent years, investigators in the field have come to realize that to understand percussion drilling they must study the basic action of percussion bits penetrating rock—not the performances of commercial rock drills, with their many attendant variables that cannot be isolated or controlled.

Using a vertical drop tester, the writer investigated the sequence of rock failure under the impact of a simple, chisel-shaped bit when changes were made, singly, in significant variables. Results of this and other research are reported here.

BASIC CONCEPTS

The formation of a crater in rock under the impact blow of a bit can be observed experimentally. Directly beneath the edge of the bit the rock is crushed into fine powder; toward the sides of the crater it chips out into relatively large fragments.

An explanation of these phenomena has been offered by Drilling Research Inc. on the basis of work sponsored by this organization at Battelle Memorial Institute (Ref. 1, 1954, Summary, pp. 9-18). High-speed photography and force waveforms obtained from strain gages mounted on the bit near the cutting edges recorded the sequence of events in crater formation with a die-shaped or blunt, wedge-

H. L. HARTMAN, Member AIME, is Professor and Head, Department of Mining, The Pennsylvania State University, University Park, Pa. TP 4785A. Manuscript, Aug. 11, 1958. New York Meeting, February 1958. AIME Trans., Vol. 214, 1959.

shaped bit. The events may be summarized briefly as follows, with reference to Fig. 1:

1) Crushing of surface irregularities as bit first makes contact with rock.

2) Elastic deformation of rock from continued application of load by bit. Subsurface cracks radiate out from lines of stress concentration at boundaries of cutting edge; two major cracks propagating downward converge and outline V-shaped wedge.

3) Crushing of central wedge of rock into fine fragments.

4) Chipping out of large fragments along curved trajectory to surface adjacent to crushed zone.

5) Crumbling away of crushed zone and displacement by bit as it continues to penetrate. Entire sequence may be repeated if blow energy is sufficient.

With a sharp, wedge-shaped chisel bit the same phenomena of rock failure are evident as with the die-shaped bit, but essentially they occur simultaneously instead of successively. The crushing and chipping processes follow many times in succession, almost continuously, until the blow energy is dissipated. The outward appearance of the crater is the same, but somewhat less subsurface damage (fracturing, cracking, and crushing) occurs.

Crushing vs Chipping: In the DRI discussion of crater formation, it was pointed out that some of the rock was displaced by crushing and some by chipping. It has long been maintained that in percussion drilling the fastest penetration is attained when the greatest proportion of chipping to crushing takes place. Basic energy relations can be used to demonstrate that the most efficient drilling is accompanied by the fewest and coarsest cuttings per unit volume.[2]

Consider a wedge-shaped bit. The predominance of crushing or chipping depends chiefly on the included angle of the wedge—more crushing and less chipping occurs as the cutting angle of bit increases. More of the compressional loading applied to the rock by the bit with an obtuse-angled wedge is directed downward, so that higher forces are needed for fracturing chips to surface. The area of contact between bit and rock is larger for a given depth of penetration, also necessitating higher forces to deliver the same stress to the rock. In practice, bits with included angles over 90° produce relatively little rock damage by chipping. For that reason, acute-angled bits are definitely preferable from the standpoint of drilling speed, although they wear more rapidly.

Two investigators (Ref. 1, 1953, 2nd Qtr., pp. 11-14; Ref. 3) have reported that at constant blow energy, depth of penetration of the bit varies inversely as the square root of the tangent of half the wedge angle, and the area or volume of the crater formed is a function of the reciprocal of the tangent of half the wedge angle.

Mechanism of Rock Failure: Rock failure under an impact blow appears to be related to the number and magnitude of local flaws or cracks in the rock structure and to their distribution geometrically about the line of load. As the bit penetrates the crushed zone, stresses build up in the adjacent *solid* rock until a crack propagates from one of the points of stress concentration and a chip is formed.

Griffith[4] states that failure of brittle material, such as rock, under a compressive load actually occurs in tension, along cracks or planes of weakness oriented at 45° to the axis of load. Stress tends to concentrate at the tip of a crack, causing it to propagate and the material to rupture at loads only a fraction of the cohesive (compressive) strength. Griffith's mathematical deductions, based on the theory of elasticity, may be applicable to rock penetration under impact, although his work is theoretically correct only for static loading conditions.

Mathematical Analysis of Effect of Bit Shape on Penetration: It is highly desirable to obtain a mathematical relation between energy of blow and depth of penetration, cross-sectional area, or volume of

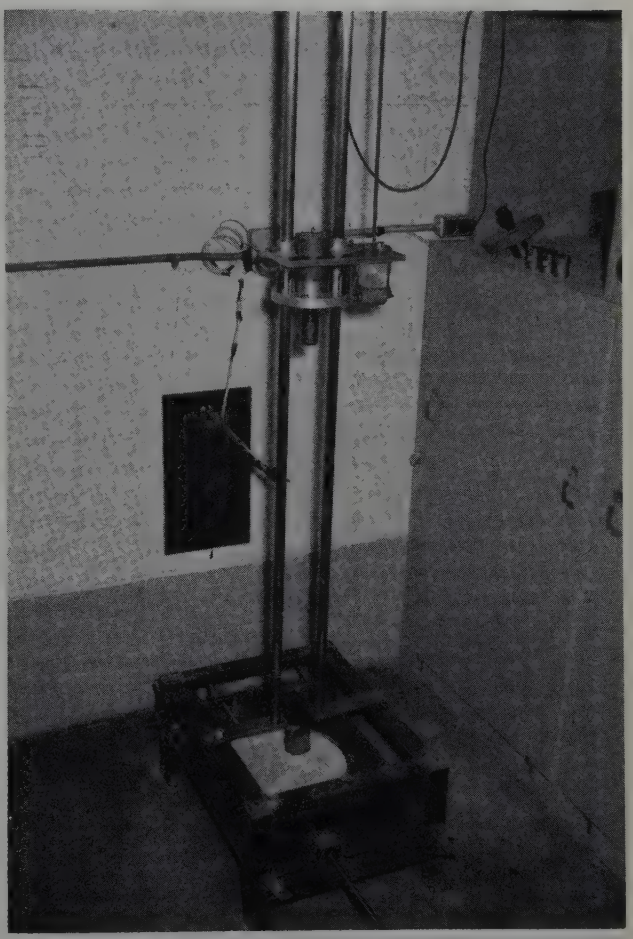

Fig. 2—The laboratory drop tester. The plate with the attached bit and the weights is held by the triggering device, ready for a drop onto the test rock below.

Fig. 3—Various bit shapes used in the experimental work. Left, die; center, wedge; right, hemisphere.

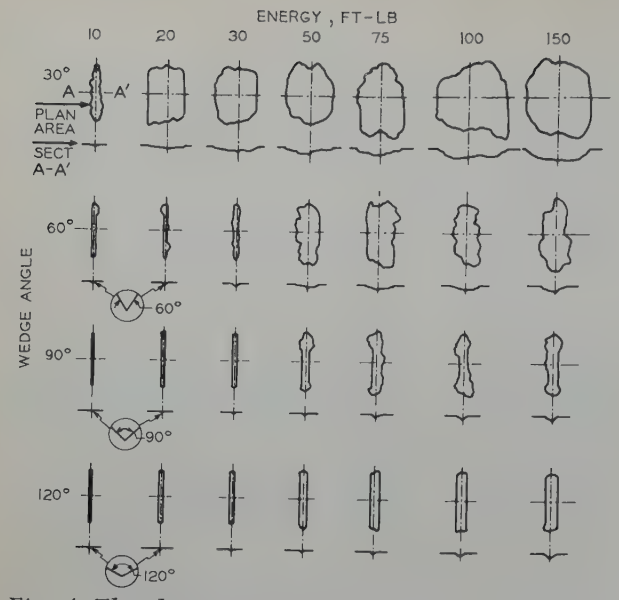

Fig. 4—The shapes of typical craters that are formed by sharp, wedge-shaped bits with varying blow energy.

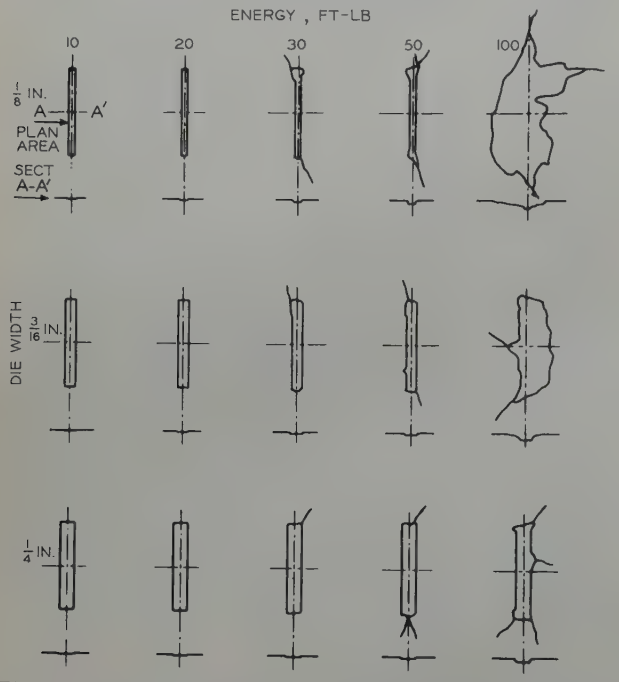

Fig. 6—The shapes of typical craters that are formed by die-shaped bits striking with varying blow energy.

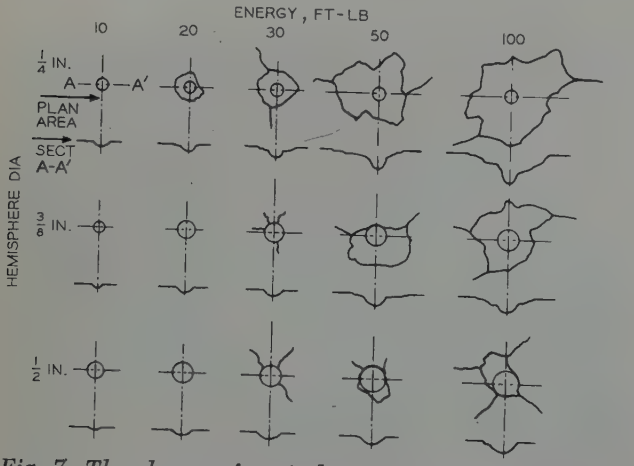

Fig. 7—The shapes of typical craters formed by hemispherical-shaped bits striking with varying blow energy.

crater for any shape of bit. This relationship is needed to determine an expression for the rate of penetration of a drill bit, since the amount of rock broken out per blow per unit of time is a measure of drilling speed.

The approach adopted here was suggested by Drilling Research Inc. (Ref. 1, 1953, 2nd Qtr., pp. 14-18) for die and wedge-shaped bits. Although over-simplified, it is believed to indicate the basic relationship between blow energy and crater dimensions. The author independently arrived at the same relation for the wedge-shaped bit, which led him to extend the derivation to other bit shapes.

Consider a chisel bit of any shape. The resistive force the rock offers to bit penetration is assumed to act over the horizontal projection of the area of contact of bit and rock, the area being a function of depth of penetration for that particular shape of bit. Let the unit resistance of the rock to penetration be f and the horizontal projection of the area be a. Then the work, w, in penetrating the rock is a function of the force developed, F $(=fa)$ and the depth of penetration of the bit, h, or

$$w = \int_0^h F\,dh \qquad [1]$$

At the maximum depth penetrated, the work done is equal to the energy of the blow, E. After substituting fa for F (with a a function of h) and setting the equation equal to E when integrating, the expression can then be solved for h in terms of E.

The procedure is demonstrated below for the wedge, a typical bit shape:

Let l = length of cutting edge and
θ = included angle of wedge;
then $a = 2\,lh \tan \theta/2$ and
$F = fa = 2flh \tan \theta/2$;
therefore, $w = \int_0^h 2flh \tan \theta/2\,dh$.
Integrating, $E = flh^2 \tan \theta/2$
and

$$h = \sqrt{\frac{E}{fl \tan \theta/2}} \qquad [2]$$

This relation demonstrates theoretically that the depth of penetration is inversely proportional to the square root of the tangent of half the wedge angle, *but more important, it shows that the depth varies directly as the square root of the blow energy,* or $h \propto E^{1/2}$. Further, it can be shown that since l is independent of h and since the cross-sectional area of the crater varies as the square of h, *the volume of the crater V is directly proportional to the blow energy:* $V \propto E$. This demonstrates the dependence of crater formation on blow energy.

This expression is of tremendous importance in determining and explaining percussion drilling performance. It can be shown mathematically that *the above relation between V and E should be valid for any shape of bit*: wedge, die, blunt wedge, cylindrical, conical, prismatic, or hemispherical.

One reason this relationship is over-simplified is that a threshold energy E_o exists below which only elastic deformation occurs and no damage is done to the rock. A more correct version of the above expression is then:

$$V \propto (E - E_o).$$

E_o is almost negligible for sharp wedges or soft rocks but may be rather large for blunt bits or hard rock.

Within limits, the experimental work will be shown to substantiate this theory.

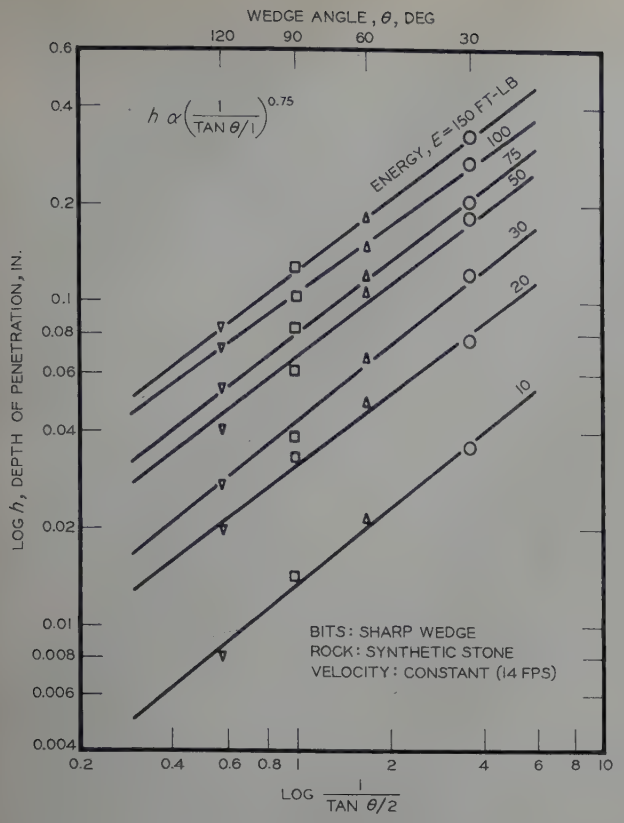

Fig. 5—Effect of included angle of cutting edge (wedge angle) on penetration depth of sharp, wedge-shaped bits.

Blow Dynamics: Those factors in drilling which can be grouped under blow dynamics include: 1) energy, 2) velocity, 3) mode of transfer, 4) force, 5) contact time, 6) momentum, 7) impulse, and 8) acceleration. All these factors may influence rock failure and crater formation and hence rate of penetration in drilling. The first three are reported experimentally in this article.

The most significant dynamic factor is blow energy; the importance of blow velocity is debatable. Battelle (Ref. 1, 1953, 3rd Qtr., p. 7) and Shepherd[5] have reported a negligible effect of this variable on crater formation, while Freudenthal (Ref. 1, Oct. 15, 1952, pp. 20-37) claims an inverse relationship. Shepherd's work, however, was apparently complicated by down-hole conditions, and the velocity and energy ranges of the two DRI studies were too limited.

The different principles involved in transferring the impact of a percussion blow are demonstrated by the old piston machine and the present hammer drill. Coupling of the piston and steel is an important consideration with the hammer principle, and elastic waves set up in the steel may aid or hinder penetration. On the other hand, the piston drill must overcome higher inertias as the steel length or size increases. Mode of blow transfer has never received adequate study.

Multiple Blows: The relationship of adjacent blows to crater formation and rate of penetration is complex. A study of single unrelated blows logically progresses to consideration of multiple blows struck a given, indexed distance apart. In a conventional rock drill using a radial-wing bit, indexing is achieved by rotating the steel and bit through a prescribed arc.

Rock breakage is substantially increased by the existence of an additional free-face to break to when adjacent craters are close enough together to cause crater 2 to break into crater 1. Theoretically, the maximum effect is realized when the indexing distance is at an optimum. When the indexing is less than optimum, energy is wasted and the average crater volume diminishes; when the indexing is greater than optimum, the craters will not break into one another and the average volume is the same as for an individual blow.

Drilling Research Inc. devoted considerable study to this factor (Ref. 1, Summary, pp. 25-33; Ref. 6). DRI's so-called *universal indexing curve*, based on drop tester studies, indicates that the average volume of rock per blow is independent of the indexing distance, provided that distance exceeds a minimum value. In an actual drilling process with a radial-wing bit, indexing has much less influence, because multiple wings form W craters per blow, and there are then W craters to break to after only $1/W$ rev of the bit (where W is number of bit wings). Almost infinite statistical variations in the indexing distance are encountered after $1/W$ rev, which complicates theoretical analysis. Experimental work on this factor will be reported later.

Rate of Penetration: The ultimate goal of fundamental studies of rock drilling is to achieve faster rates of penetration by increasing knowledge of the basic mechanism of rock penetration. Another objective is to predict or calculate rates of penetration from basic parameters of the process.

To date there have been two formulas developed to express the linear rate of penetration, S, of a multi-wing chisel bit. One, reported by Simpson and Parry,[7] is in terms of the average distance of advance, d, of the bit per blow:

$$S = \frac{WdB}{B/R} = WdR \qquad [3]$$

where R is frequency of rotation and B is frequency of reciprocation. A second, proposed by Battelle (Ref. 1, 1954, Summary, pp. 3-5), involves the average cross-sectional area of crater A broken per wing at the periphery of the bit:

$$S = \frac{WAB}{\pi D} = \frac{WAB}{C} \qquad [4]$$

where D is gage (diameter) and C is circumference of bit. Actually, both expressions are equivalent, because $d = (A/C)\ (B/R)$.

Still a third and more useful expression may be obtained from Eq. 3 or 4 relating S and the volume of crater V broken per wing by any chisel-shaped bit:

$$S = \frac{W\frac{4V}{D}B}{\pi D} = \frac{VBW}{A_b} \qquad [5]$$

where $A = 4V/D$ and $A_b = 1/4\pi D^2$ is plan area of the bit (or hole, more correctly). Recalling that $V \propto E$ for any shape of bit (actually, WV and E, considering the bit as an entity), then

$$S \propto \frac{BE}{A_b}.$$

Thus, *energy of blow, frequency of blows, and plan area of bit are the principal variables on which rate of penetration depends.*

It is definitely an advantage that with all three formulas the crater dimension (h, A *or* V) can be determined experimentally, probably by drop tester.

Simon[6] has also obtained an experimental relation between rate of penetration and power, P, of a drilling process:

$$S = 2.4 \frac{P - P_0}{D^2 c} \qquad [6]$$

where P_0 is threshold power and c is drilling strength of the rock. Note the similarity between the last two formulas. Since $P = BE$ for a percussion drill, it can be shown by either relation that

$$S \propto P$$

or, *the rate of penetration is directly proportional to the power of the process.* This is a basic premise of percussion drilling.

Experimental evidence from actual drilling has been offered by several investigators[2,8,9] to confirm this relation. As mentioned before, evidence from drop tests will be offered to verify the relation $V \propto E$, which then may be considered substantiation of the $S \propto P$ expression.

EXPERIMENTS WITH DROP TESTER

The principal laboratory equipment used in carrying out the present investigations was an impact drop tester (Fig. 2), calibrated to obtain a wide range of blow energy, velocity, and load. Bits of the desired shape (Fig. 3) were attached to a weighted plate and permitted to strike blows on rock specimens. Synthetic stone was used for the entire series of tests, prepared from high, early-strength cement and FF-grade pumice in a 4:1 weight ratio that averaged 5000 psi compressive strength. The use of synthetic stone reduced the effects of heterogeneity and variability between specimens and still faithfully demonstrated the mechanism of failure in rock types such as shale, siltstone, and the younger sediments whose behavior is termed both brittle and ductile.

Before each test, the rock specimen was clamped in the position desired for receiving the blow. The height of fall to produce the required velocity and energy of blow had been previously calculated and the plate was raised to that height. A cardboard cylinder was placed on the rock at the location of the intended blow to prevent scattering of cuttings. Then with the desired bit attached to the plate, the blow was struck.

All dimensions of the resulting crater were determined, either by direct measurement or by calculation, as follows:

1) Weight of cuttings, by direct weighing.
2) Volume of crater, by weight of dental wax required to fill the impression, converted to volume.
3) Depth of crater, by micrometer depth gage.
4) Length of crater, by scale.
5) Plan area of crater, by planimetering the outline traced on paper.
6) Width of crater, by calculation (the plan area divided by the length).
7) Cross-sectional area of crater, by calculation (the volume divided by the length).

In addition to dimensions, observations on crater formation were recorded with each series of drops. The cross section of each crater was sketched, and notes were made on chipping, crushing, and cracking.

At least ten tests were carried out at each level of variable studied. Results of the acceptable tests were averaged together, while those affected by cracks from other craters, the edges of the rock, or imperfections in the rock were discarded. (About one in ten was not acceptable.) Even with all precautions, variations up to 50 pct were noted in data from ten tests, ample evidence that: 1) even synthetic rock is lacking in homogeneity, and 2) brittle failure is complex and non-uniform.

Tests on the following variables in rock penetration were conducted in the manner indicated:

1) Blow energy varied from 10 to 150 ft-lb for wedge-shaped bits of included angle 30° to 120°, and from 10 to 100 ft-lb for die-shaped bits ⅛ to ¼ in. wide and hemispherical bits ¼ to ½ in. diam; blow velocity was 14 fps.
2) Blow velocity varied from 8.6 to 20.4 fps for 30° wedge-shaped bits and blow energy was 22.2 ft-lb.
3) Mode of blow transfer varied with bit in motion or bit at rest; wedge angle was 30° and blow energy 30 ft-lb.
4) Indexing studies were conducted with blows struck on previously cratered surface, wedge angle 30°, blow energy 30 ft-lb, and indexing 1 in.

DISCUSSION OF TEST RESULTS

Bit Shape, Wedges: The importance of the included angle of sharp, wedge-shaped bits on crater formation was confirmed. As the blow energy was varied with bits of different angles, two separate and distinct phases in the cutting action were observed, namely, the crushing and chipping phases. This behavior can be seen in the sketches of typical craters, appearing in Fig. 4, which may be summarized as follows:

1) Both crushing and chipping were not obtained with all wedges—the 30° wedge always penetrated by chipping, whereas the 90° and 120° wedges never left the crushing phase, even at high blow energies.
2) Craters were formed principally by crushing *or* chipping; some chipping occurred when crushing was predominant (particularly at the ends of the pit) and crushing continued even after chipping began, but there was a fairly sharp demarcation in cutting.
3) Chipping did not predominate until a certain energy level was attained; this was low with the 30° bit and apparently infinite with bit angles greater than 90°.
4) There was similitude in the crushing or chipping phase for a given bit, although at the highest blow energies (150 ft-lb) the craters appeared to deepen with little or no increase in volume.

The relationship between depth of penetration and wedge angle was determined by plotting a family of curves at constant energy (Fig. 5). The slope of the straight lines obtained indicated that

$$h \propto \left(\frac{l}{\tan 0/2} \right)^{0.75}$$

This deviates somewhat from the square-root relation expected, indicating that the earlier explanation is over-simplified. Likewise, the relation between the volume of crater and the function $\frac{l}{\tan 0/2}$ was exponential to the power 1.5 instead of 1.

Dies and Hemispheres: The other two shapes of bits behaved in a manner similar to that of the wedge. The appearance of the craters (Figs. 6 and 7) revealed a predominance of either crushing or chipping at various energy levels, although the transition between the two phases was less sharply de-

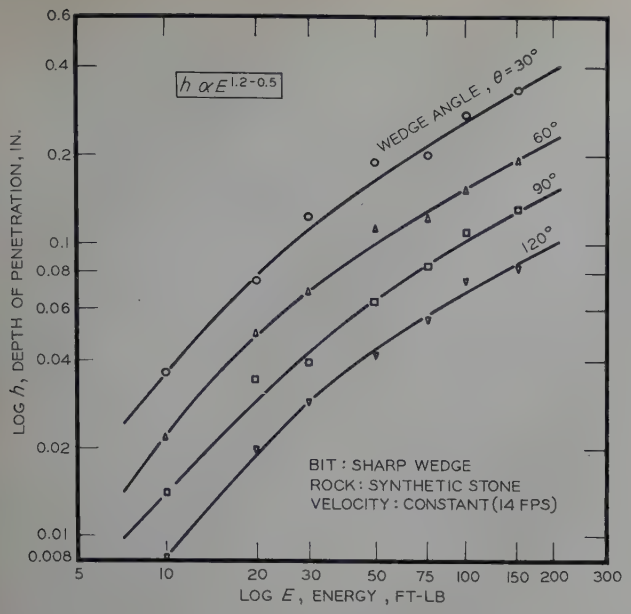

Fig. 8—Plotted results show effect of energy of blow on depth of penetration of sharp, wedge-shaped bits.

fined. More radial cracking was observed with these bit shapes than with the wedges, indicating a proportionately higher expenditure of energy for cracking than for crater formation. There was a strong tendency with both dies and hemispheres for adjacent craters to index across at higher blow energies. Rebound was not significant (less than 1 pct) with any bit shape.

Blow Energy, Wedges: The depth of penetration of sharp, wedge-shaped bits was plotted against energy of blow (Fig. 8). Again, some departure from theory was evident, because this relation varied from $h \propto E^{1.2}$ at low energies to $h \propto E^{0.5}$ at high energies. The varying geometry of the falling mass as well as end effect (due to inconstant crater length) probably were responsible for some of the variation in slope of this family of curves.

For the 90° and 120° bits, the length of crater 1 varied with energy to the 0.03 and 0.05 power, respectively: $l \propto E^{0.03 \text{ or } 0.05}$. The exponent varied from 0.05 to 0.15 for the 60° bit and 0.05 to 0.25 for the 30°. At low energies, length is nearly constant, but at high energies it increases significantly for acute-angled bits.

Volume of crater plotted against energy of blow (Fig. 9) indicated that $V \propto E$, approximately, in either the crushing or chipping phase. This is an important confirmation of theory. Two phases, crushing and chipping, were evident, which partly explains why these data fluctuate more than the values for depth of penetration. With all the bits tested, there was some indication that when blow energy is increased beyond a certain point the benefit decreases, i.e., the crater volume appears to taper off at 150 ft-lb. More longitudinal cracks and subsurface damage appeared to accompany high-energy blows, however, and there was more tendency for craters to index across, which may compensate for the crater volume.

Divergence in crater similitude for a given wedge angle can be ascertained by comparing the effect of blow energy on other crater dimensions. Cross-sectional area, like volume, varied directly as blow energy $A \propto E$, approximately, with sharp breaks between the crushing and cutting phases. However, the

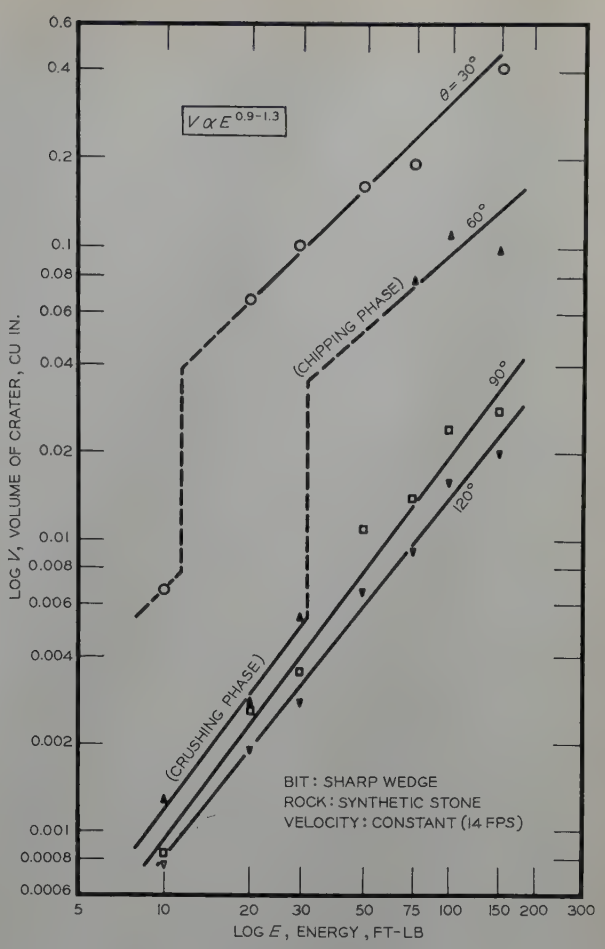

Fig. 9—Effect of energy of blow on volume of the crater that is formed by sharp, wedge-shaped bits.

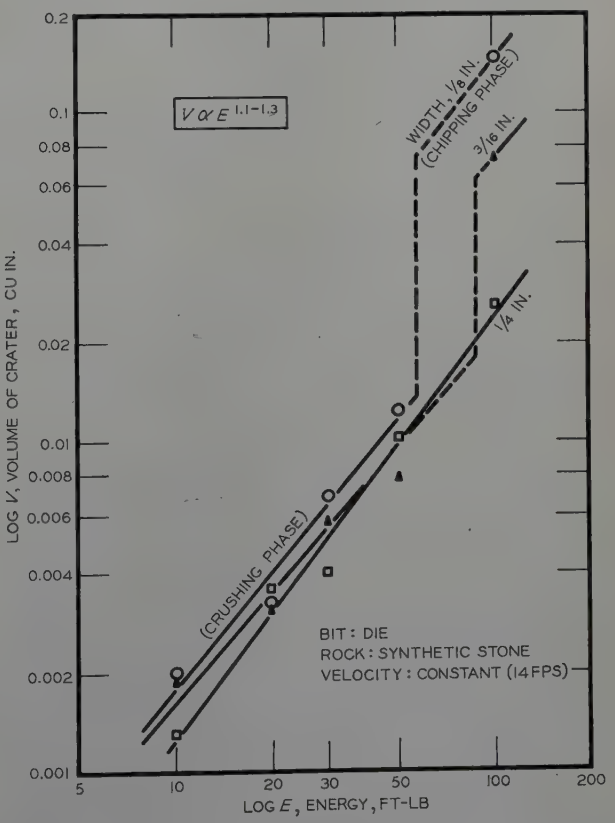

Fig. 10—The effect of energy of blow on volume of the crater that is formed by die-shaped bits.

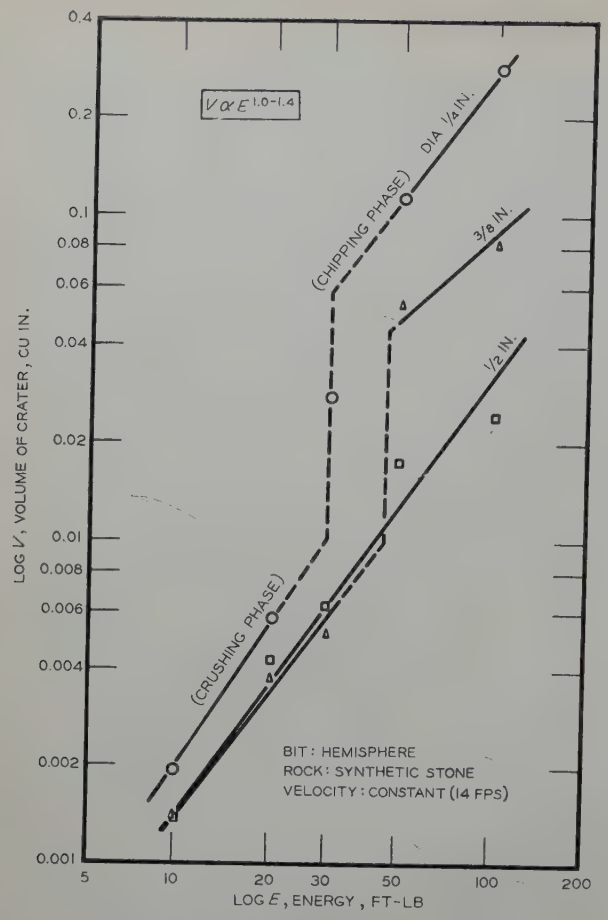

Fig. 11—The effect of energy of blow on volume of the crater that is formed by hemispherical-shaped bits.

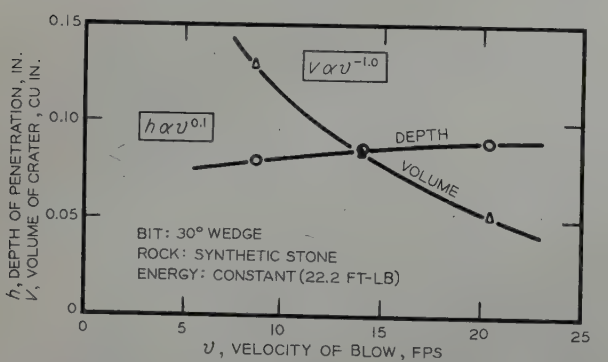

Fig. 12—Effect of velocity of blow on penetration depth and volume of crater formed by 30° wedge-shaped bit.

plan area of the crater A_p (as well as the width b) varied with energy approximately to the 0.6 power, or

$$A_p \propto b \propto E^{0.6}.$$

Again, the different cutting actions were plainly visible. These relations confirm the earlier observation that as energy rises the crater increases less rapidly in plan dimensions than in depth. With all crater dimensions except depth, there was a marked tendency to level off or even decrease at high blow energies.

Dies: The effect of blow energy on the depth of penetration of die-shaped bits only approximated the linear relation anticipated: $h \propto E^{1.3}$. The variation of volume of crater with energy (Fig. 10) agreed somewhat better with theory, because $V \propto E^{1.2}$, approximately.

Hemispheres: The hemispherical bits also departed from theory in the behavior of depth of penetration with varying energy. The data demonstrated that $h \propto E^{0.9}$, rather than the cube-root relation that would be expected. Again, the crater volume showed closer conformity because, as illustrated in Fig. 11, $V \propto E^{1.2}$.

It is very significant that for all three bit shapes tested—the wedge, die, and hemisphere—an essentially linear relationship between volume of crater and energy of blow was obtained for the crushing and chipping phases, in spite of variance in h vs E. *This is an important verification of the theory advanced earlier.*

Blow Velocity: Studies of blow velocity carried out with the 30° wedge at constant blow energy indicated diverging trends of h and V (Fig. 12). Depth of penetration remained practically constant over a wide range of velocity, v: $h \propto v^{0.1}$, while volume of crater varied inversely with velocity: $V \propto \frac{l}{v}$. Furthermore, while the length of crater remained constant, the plan area also fell off as velocity increased:

$$A_p \propto \frac{l}{v^{0.6}}.$$

These three relations indicate that a very definite change was taking place in the cross section of the crater as the velocity was varied over the range (8.6 to 20.4 fps) studied. While the depth was practically unchanged, the craters appeared to narrow and developed less of a U-shape and more of a V-shape. At least for this bit shape, blow energy, and rock type, an increase in blow velocity proved detrimental to crater formation. The effect of this variable is complicated by the interaction of contact time and the geometry of striking mass, however.

Blow Transfer: As the following data show, crater formation was considerably improved when velocity of the falling mass was imparted to the bit:

	Blow Velocity, Fps	Depth, In.	Plan Area, Sq In.	Volume, Cu In.
Bit at rest	0	0.108	1.143	0.084
Bit dropped	14	0.124	1.546	0.101

(30° wedge, kinetic energy 30 ft-lb, synthetic stone)

When the bit rested on the rock and the falling weight transferred the energy of the blow to the bit, the volume of crater produced was only 84 pct as large as that formed when the bit was attached to the falling weight and struck the rock at high velocity. The craters were similar in appearance but narrower when the bit was at rest.

Although care was taken to insure good coupling between the falling weight and the bit at rest, it is possible that loss of energy when the blow was transferred accounted for the reduced crater volume. However, since more than ten tests were conducted for each condition to eliminate such variability, it appears more likely that the decreased volume reflected the effect of the different manner of blow transfer and, to some extent, the difference in geometry of the striking mass. The coupling in the tests was probably superior to that attained in actual drilling.

Indexed Blows: Investigation of this factor was not exhaustive but aimed mainly at a study of in-

dexed blows struck on a previously cratered surface, the situation in an actual drilling process. Although several tests were run, results described here represent one typical test rather than the average of several tests, because too many different craters were involved in each test for averaging to be significant.

A succession of blows struck adjacent to one another on a fresh surface produced indexed craters four times, i.e., each crater broke into the preceding one. But on the fifth blow, breakage into the adjacent crater did not occur. Indexing was beneficial to craters 2 to 4, the volume broken being three times that of the first or last blows. Crater depths were constant.

A second row of blows, struck on the previously cratered surface, behaved unexpectedly. Each was struck midway between the axes of adjacent craters of the first row. The craters formed were similar in appearance, depth, and volume; however, they did not index together but seemed to break independently, none cratering beyond the axes of the original row. Average volume of the indexed craters was only 20 pct greater than that of crater 1 and less than half the volume of indexed craters 2 to 4.

The lack of benefit from indexed blows on a previously cratered face was apparently due to the crushed zone and subsurface fracturing produced along the axes of impact of the first row of blows. Stresses set up by a blow struck on this surface were unable to progress beyond the ruptured zone, and thus craters could not index across.

The phenomenon of indexing is also a function of bit shape, blow energy, index distance, and rock type, factors not studied here.

CONCLUSIONS

The present fundamental studies of rock penetration under impact suggest certain conclusions generally applicable to percussion drilling of soft brittle to ductile rocks.

Bit Shape: The most desirable bit shape is the wedge, because it promotes chipping in crater formation, but a wedge with an included angle greater than 90° has little merit in this regard. Particularly in soft rock, the included angle should be as small as commensurate with bit strength and resistance to wear.

Blow Energy: A high blow energy is desirable to penetrate the rock and break a large crater, since the volume of crater is approximately proportional to the energy, regardless of bit shape. But just as a threshold energy to achieve any failure exists at the low end of the scale, so an optimum energy appears to govern in the upper range of blow energies. Both undoubtedly vary with rock properties. An optimum energy exists partly because the bit length ceases to be a constant, but also because the energy is not effectively used for crater formation.

Blow Velocity: To break the maximum volume per crater, a low-velocity blow is preferable to a high one. There is probably an optimum velocity for any combination of bit shape, blow energy, and rock type.

Blow Transfer: Crater formation is aided by imparting the blow velocity to the bit, rather than by striking the blow on a bit at rest. This is a function of the geometry of the striking mass, but in general the old piston-drill principle appears to have merit, particularly when applied in a down-hole design to reduce inertia of the reciprocating mass.

Indexed Blows: Indexing is cyclical, and the critical index distance to insure 100 pct indexing with sharp wedges is almost prohibitively small. Blow energy, bit shape, and rock type all influence the critical index distance. It is even harder to insure indexing in actual drilling, since blows are struck on a previously cratered surface.

Power of Drilling Process: The linear relationship between energy of blow and volume of crater has been established. Actual drilling is concerned with advance, or volume per unit of time, and this in turn is proportional to the power, or energy multiplied by blow frequency. Thus power is even more critical than energy in a percussion drilling process. If an optimum level of blow energy does exist for penetrating a given type of rock, then faster drilling speeds can be attained only by increasing the blow frequency. This factor should be a most rewarding subject for future study.

Mechanism of Brittle Failure and Rock Penetration: In relating penetration to energy, power, and drilling speed, the most useful property is crater volume, but this is subject to the greatest deviation between runs under identical conditions. The most consistent and reproducible dimension is depth, but with all the bits studied, its behavior deviated from theory as energy was varied. Although in general the crater volume behaved as expected, it is evident that the basic assumptions for the mathematical derivation of the V-E relation are oversimplified and not entirely correct. There is still greater need for a comprehensive theory that satisfactorily explains all the puzzling aspects of percussion drilling in terms of a workable concept of dynamic brittle fracture. Improved penetration techniques depend on a solution to this problem.

The writer's experimental studies of percussion drilling fundamentals, beginning in 1954, originated with the establishment of a rock penetration laboratory at the Colorado School of Mines and are continuing at The Pennsylvania State University.

This research was made possible by a faculty grant from the Foundation of the Colorado School of Mines. The author extends his appreciation to the Foundation and to Dean Truman H. Kuhn of the school for his encouragement in the project. The Gardner-Denver Co. and the Timken Roller Bearing Co. supplied special test bits, and these and many other companies shared technical knowledge. Special commendation is due Drilling Research Inc. for having released copies of its Collected Reports to universities, making available a mass of fundamental data as guideposts to investigators in the field.

REFERENCES

[1] Drilling Research Inc.: *Collected Reports*, vols. 1-6, 1949-1954.
[2] H. L. Hartman and E. P. Pfleider: *Exhaust Dust Control in Dry Percussion Drilling. AIME Trans.*, 1955, TP 4005 A, 36 pp.
[3] S. Tandanand: *Effect of Bit Shape on Cutting Action of Percussion-Type Bits.* Colorado School of Mines Master's thesis, 1956, T837, pp. 25-26.
[4] A. A. Griffith: The Theory of Rupture. *Proc.*, First International Congress of Applied Mechanics, Delft, 1924, pp. 53-63.
[5] B. F. Shepherd: The Connecting Link in Percussion Drilling: the Problem—What—Why—How? *Mining Congress Journal*, 1954, vol. 40, no. 11, pp. 28-31.
[6] R. Simon: Theory of Rock Drilling. *Proc.*, Sixth Annual Drilling Symposium, University of Minnesota, 1956, pp. 1-14.
[7] D. N. Simpson and V. S. Parry: Percussion Drilling in Hard Rock, Parts I-IV. *Iron and Coal Trade Review*, 1951, vol. 163, no. 4346, pp. 173-178; no. 4347, pp. 239-243; no. 4348, pp. 301-304; no. 4349, pp. 347-354.
[8] E. J. Wells: Penetration Speed References for the Drillability of Rocks. *Proc.*, Australian Institute of Mining and Metallurgy, 1950, no. 158-159, N. S. pp. 453-464.
[9] E. Ryd and J. Holdo: Percussion Rock Drills—Their Construction and Method of Operation. *Manual of Rock Blasting*, Stockholm, 1956, sec 12:01, pp. 12-14.

Discussion of this article sent (2 copies) to AIME before Feb. 28, 1959, will be published in MINING ENGINEERING.

by SHIOU-CHUAN SUN

APPARATUS FOR TESTING COAL SEDIMENTATION

Most previous work on sedimentation of coal[1] and mineral[2,3] suspensions has been conducted in graduated 1-liter glass cylinders of 6-cm diam. With this type of large container it is often difficult to see through the suspension and tedious to perform a large number of tests. Furthermore, the heavy glass walls and the graduation lines of glass cylinders cause internal and stray reflections, respectively. To obviate these difficulties, an Atlab Emulsion Viewer from Arthur H. Thomas Co. was adopted as an alternative apparatus.

Equipment: The viewer,[4] shown in Fig. 1, consists of: 1) a stainless steel frame rack holding 21 flat-bottom Nessler tubes or an ungraduated replica 1.64 cm ID and 1.80 cm OD, 2) a movable masked 150-w lumaline lamp behind the tubes, and 3) a scaled glass panel with 100 vertical divisions in front of the tubes. The tubes are snugly held by springs in slots formed by spacer bars, which also serve as shields to eliminate stray light. The lumaline lamp is mounted behind a slit in a movable housing so that it can be positioned behind the suspension to be examined. The lowest or 100-division line on the front glass plate is leveled with the upper side of the bottom of all tubes. The scaled portion of each tube, roughly 19 cm high and 40 ml in volume, is used to study coal and mineral suspensions.

Procedure: The following procedure was used in many tests. A 1.6-gm sample of dry coal was mixed with 16 ml of distilled water in an ordinary test tube and allowed to stand for three days, with occasional shaking to insure thorough wetting of all particles. The slurry was transferred to a Nessler tube and diluted to 32 ml. The pH regulator and flocculating reagent were added, and the slurry was diluted to reach the uppermost or zero-division line. The tube was immediately stoppered and inverted downward and up again ten times during a period of 35 to 40 sec. The lumaline lamp was turned on during the inversion period. After inversion the tube was quickly returned to the viewer rack. The time elapsed for each 10-division drop of the demarcation line between solid and liquid was recorded by stopwatch until the 80-division line was reached in the zone of compression. Additional readings were taken at 15, 30, and 60 min after settling began.

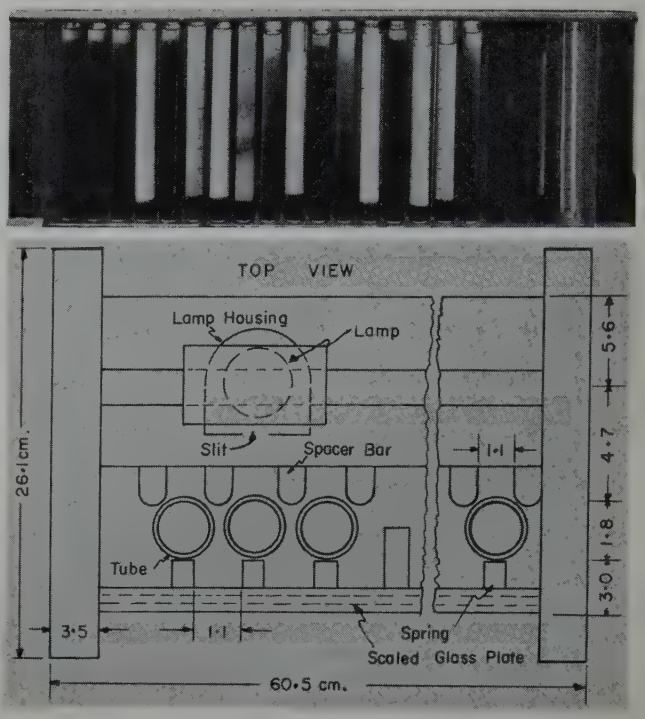

Fig. 1—The Atlab Emulsion Viewer.

The clarity of the supernatent liquid was observed also. As the settling rate became considerably slower at the 75-division line, it was convenient at this time to start the next test in a separate Nessler tube. This was continued until the suspensions in any number of the 21 tubes were tested.

An attempt was made to correlate the experimental results between the Nessler tube and a 1-liter glass cylinder. Table I shows that coal particles settle much faster in the cylinder than in the tube, which has a large wall effect.[5] The correction factor for the tube impedance is 1.662 ± 0.145 at the 40-division line in the hindered settling zone, and 1.614 ± 0.139 at the 75-division line in the compression zone. This rough correlation was established by dividing the pulp height of each container into 100 divisions and comparing the settling rates of the two containers at the same divisions. Tests were also performed to determine the accuracy of the viewer. The results, not presented, showed that error was within 10 pct.

Table 1. Effects of Containers on Settling Rate of 200/270 Mesh R & P Coal in a 4 Pct Slurry, Using 30 Mg Per Liter of Glue 2611 As Flocculant at pH 6.4

1000-Ml Glass Cylinder* (Fisher No. 8-564)			40-Ml Nessler Tube** of Atlab Viewer			
Settling Distance		Cumulative Settling Rate, Cm per Hr (Average of Two Tests)	Settling Distance		Cumulative Settling Rate, Cm per Hr (Average of Three Tests)	Settling Rate, Ratio of Cylinder to Viewer
Division	Centimeters		Division	Centimeters		
0 to 10	3.6	418±12	0 to 10	1.9	196±24	2.135±0.267
0 to 20	7.2	481±18	0 to 20	3.8	259±19	1.860±0.152
0 to 30	10.8	507±27	0 to 30	5.7	295±19	1.719±0.143
0 to 40	14.4	515±30	0 to 40	7.6	308±20	1.662±0.145
0 to 50	18.0	483±20	0 to 50	9.5	291±16	1.661±0.114
0 to 60	21.6	367±17	0 to 60	11.4	228±6	1.660±0.088
0 to 70	25.2	194±3	0 to 70	13.3	119±8	1.672±0.121
0 to 75	27.0	113±1	0 to 75	14.25	70±6	1.614±0.139

* 36-cm graduated height, 5.94-cm diam.
** 19-cm scaled height, 1.64-cm diam.

S. C. SUN, Member AIME, is Professor, Department of Mineral Preparation, The Pennsylvania State University, University Park, Pa. TN 461 H. Manuscript, June 16, 1958. College of Mineral Industries Contribution No. 58-38. AIME Trans., Vol. 214, 1959.

REFERENCES

[1] D. R. Mitchell: *Coal Preparation*, pp. 609-647. AIME, New York, 1950.
[2] S. R. B. Cooke, N. F. Schulz, and E. W. Lindroos: The Effect of Certain Starches on Quartz and Hematite Suspensions. *AIME Trans.*, 1952, vol. 193, pp. 697-793.
[3] M. E. Wadsworth and I. B. Cutler: Flocculation of Mineral Suspensions with Coprecipitated Polyelectrolytes. *AIME Trans.*, 1956, vol. 205, pp. 830-833.
[4] W. C. Griffen and R. W. Behrans: Apparatus for Observing Emulsions. *Analytical Chemistry*, June 1952, vol. 24, p. 1076.
[5] A. M. Gaudin: *Principles of Mineral Dressing*, pp. 183-186. McGraw-Hill Book Co. Inc., New York, 1939.

TRENDS IN REAL PRICES OF REPRESENTATIVE MINERAL COMMODITIES, 1890-1957

by CHARLES W. MERRILL

The price records of seven representative mineral commodities for the 68-year period 1890 through 1957 have been compiled and analyzed for significant trends. When these records are reduced to *real* prices in terms of dollars of constant purchasing power or to the purchasing power of industrial wages at average rates, a substantial overall fall in prices is revealed. This downtrend contradicts the widely held concept that heavy drafts on a mineral resource must lead to scarcity, reflected in rising prices.

Three metals (aluminum, copper, and pig iron), two fuels (bituminous coal and petroleum), and two nonmetals (sulfur and cement) have been chosen because of their pre-eminence in their respective categories, their significance in an industrial economy, and the ready availability of their price records. It might be added that these seven commodities were selected before any price figures were compiled; none was selected or rejected to substantiate any preconceived notions as to price trends. The overall importance of the seven is demonstrated by the fact that, taken together, they composed over three-fourths of the value of all minerals produced in the U. S. in 1957.

The first step in the analysis was to reduce the price records to a basis for significant comparisons. Two such comparisons have been made: 1) The quantities of each of the commodities that could have been purchased for an average hour's wage in each year, and 2) the unit price of each commodity through the years in terms of deflated dollars. These data are set forth in the accompanying table and two charts.

The quantities of the mineral commodity purchasable with the average wage for one hour's work in all manufacturing industries through 1926 were based on annual average prices and on average annual wage rates determined by Paul H. Douglas and published in his "Real Wages in the United States, 1890-1926." The series was extended through 1957 by the Bureau of Labor Statistics, U. S. Department of Labor.

Calculations based on these data show that the average worker could have purchased 1.28 lb of copper with his hourly wage in 1890, whereas his hourly wage would have purchased 8.11 lb in 1957, an increase of 633 pct in the 68-year period. An average hour's wage would have bought 10.85 gal of petroleum in 1890, compared with 33.04 gal in 1957. Even more spectacular is the increase in sulfur, of which 25.25 lb could have been purchased with the 1904 average hourly wage; 223.08 lb were purchasable with the wage in 1957—an increase of 883 pct. Comparable price data for sulfur are not available for years earlier than 1904. For every commodity, the calculations show an improvement in the wage earner's purchasing power in 1957 compared with the early years.

Measuring purchasing power in terms of wages does not give an entirely fair picture of the availability of a commodity in an economy. When the efficiency of an economy changes and the balance shifts among such elements as raw-material production, manufacturing, and service trade, the economic significance of an hour's work changes. Partly to meet such criticism, but mostly to present another interesting measure of the response of minerals to changing market conditions, a second set of calculations has been made to deflate unit prices for the seven commodities into terms of 1954 dollars. To accomplish this adjustment to a common 1954 parity, the Gross National Product Price Deflator, developed by the Office of Business Economics, U. S. Department of Commerce, was used. Although the results of these calculations are not as striking as those based on labor's increasing purchasing power, nevertheless the declines outweigh the rises in the prices of the mineral commodities. In terms of these deflated prices, aluminum and sulfur are much cheaper today than in the early years; copper was substantially cheaper in 1957 than in 1890; pig iron and petroleum are little changed; and only bituminous coal and cement have increased substantially. Strangely, the two mineral commodities with the strongest reserve positions are the two to exhibit rising real prices.

Now this apparent overall downtrend in prices has taken place during a period of almost fantastic increase in the demand for mineral products. The value of minerals consumed in the world during the period greatly exceeds all mineral consumption up to 1890. A stage has been reached in the U.S. in which 95 pct of the energy used is of mineral origin and in which machines, structures, roadways, communication facilities, and most other elements in the industrial economy are primarily of mineral origin. Even agricultural fertility is maintained, in large measure, by mineral fertilizers. A series published in Minerals Yearbook shows that the value of U. S. mineral products has risen from $615 million in 1890 to $18,000 million in 1957, a 29-fold increase. Even in deflated dollars, the increase has been eightfold, while population has expanded less than threefold.

Not only are demands of the industrial nations—the U. S., countries of Western Europe, and Japan—increasing at rapid rates, but those countries with agrarian economies are calling themselves underdeveloped and clamoring to industrialize. The ever-expanding mineral requirements in the U. S. and throughout the world show no abatement.

Mineral reserves frequently have been described as wasting assets. Much concern has been shown for future users, who have been pictured as finding themselves on a plundered planet. Conservationists have viewed the future with alarm and have demanded legislation and regulations to reduce the drain on mineral reserves.

C. W. MERRILL, Member AIME, is Chief, Division of Minerals, U. S. Bureau of Mines, Washington, D. C. TP 4792K. Manuscript, Nov. 12, 1958. San Francisco Meeting, February 1959. AIME Trans., Vol. 214, 1959.

It seems strange, then, that rapidly rising demand met from irreplaceable reserves should be accompanied by a downtrend in prices when measured in terms of average wages or even in deflated dollars. What factors have made this anomaly possible? There are many, but advancing technology and discovery are by far the most important.

It is interesting to note that industrialization, which has been made possible by minerals for machines, structures, and energy, has made a tremendous return to mineral exploitation through mechanization of mining, beneficiation, smelting, refining, and processing. In the early years of the period under discussion, hand drilling was common, and virtually all ore not drawn from chutes was hand-loaded. Hand tramming was as widespread as hand loading. Crushing and grinding were mechanized early, but the increase in efficiency since 1890 has been very great. Almost every phase of the processing of minerals has increased in efficiency through technologic advance. In fact, when a deposit or an ore was not amenable to major technologic advance, exploitation declined and in some instances stopped. For example, narrow veins containing free gold that would have been worked with profit in 1890 lie idle today, and the very large slate industry of 50 years ago survives only because artistic considerations cause a few architects to specify slate roofs on special jobs.

Technology's contributions to the mineral industry are not confined to mechanization, however. Many ores yielded only part of their content in the form of salable products when treated by the older metallurgical processes. Before selective flotation was developed, lead-zinc ores yielded only the lead and were penalized at the smelter for their zinc, whereas selective flotation yielded two or more marketable products. The percentage of valuable products recovered from other ores rose substantially. The higher recoveries and new coproducts and byproducts made it possible to work lower grade and less accessible orebodies. Frequently lowering the cutoff grade for ore added enormously to reserves.

Technology, science, and engineering also contributed to discovery through geology, geophysics, exploratory drilling, more reliable sampling, and many other ways. Discovery is of particular importance in petroleum and natural gas where new and improved exploration techniques have been major factors in maintaining reserves despite ever-increasing drains on known oil pools.

In addition to advancing technologies in discovery, extraction, and processing, technology in utilization also moves forward. Thus the growing demand for energy, which in 1890 was met largely by coal, has shifted progressively to petroleum and later to natural gas. Moreover, the efficiency of thermoelectric plants has risen, as evidenced by the fact that 7.05 lb of coal were burned to generate 1 kw-hr in 1890 compared with only 0.93 lb in 1957. Aluminum has assumed a larger role in transmitting electricity, relieving copper of some of the sharply rising demand. Looking to the future, there is strong evidence that the fissionable elements soon will carry part of the ever-rising burden that otherwise would have to be assumed by the fossil fuels.

This long record of downtrends in the prices of basic mineral raw materials is most encouraging to those looking into the future. Here is positive evidence to refute the alarmists who propose hoarding mineral resources in the name of conservation. Although wastefulness is not to be condoned, there is little to sustain the argument that use of minerals leads to an impoverished future. Those countries that have put their minerals to work have the high standards of living today and the bright futures.

The fact that the rapidly rising drafts on virtually all minerals in the 68-year period under review have been accompanied by falling prices, in terms of wages, has been a principal factor in the rising standard of living in countries industrialized during this period. With no sign that industrialization will slow, there is good reason to look toward a continuing rise in living standards.

Although there have been some painful consequences of a local nature, the general trends usually have been upward. Progress and change leave ghost towns and obsolete plants behind, but the replacements almost always are better and more efficient.

Exploration and technological research to maintain reserves and rising output cannot be taken for granted. A substantial part of the income from current production must be available to assure the future. Taxation must recognize the wasting nature of particular orebodies, and management must provide for future mineral supplies through exploration and technological research. Moreover, it is essential that such research take the bold approach that any rock formation may be transformed into ore through science, engineering, and new needs. The transformation of taconite from country rock to ore is an example of what certainly will be repeated many times in the future.

This presentation has been general. More detailed analysis of the data will show minor trends which have been obscured when averaged into the long-term trends. The effects of such factors as tariffs, quotas, subsidies, wartime regulations, discriminatory taxation and freight rates, and many other factors have been passed by. Some may think that they detect evidence that the downtrends in prices have been faltering in the last decade and will conclude that industrialization is about to outrun the mineral-supply base. However, it seems much too soon to reach any such conclusion. Major scientific and technologic discoveries have met many situations where stringencies were developing. The impending entry of nuclear energy into the power field could affect profoundly the trend lines for the fossil fuels.

It should be recognized that data like these permit many interpretations. Industrialists will justify accelerated industrialization; labor leaders will demand new pay increases; investors will insist on their share of the rising productivity. Moreover, by selecting segments of the series, special trends, each with its own interpretation, can be developed. The data are left with the reader.

In closing, the writer is convinced that the 68-year record of downtrends on the whole of the real prices of seven major mineral products gives a basis for forecasting a continued downtrend. Increasing attention is indicated to exploration for workable orebodies and to research in mineral processing and utilization. Today's submarginal deposits will provide the ore of tomorrow. Extraction efficiency will improve. The products of abundant resources will replace the products from reserves that are growing scarce. At the very least, we can look forward with confidence that the mineral industries with their allied engineers, technologists, and scientists will be able to provide the principal material basis for an expanding industrial economy at reasonable and probably lower real prices.

Table I. Market prices, quantities purchasable in terms of average hourly wages, and deflated prices for representative mineral commodities in the United States, 1890-1957

Year	Hourly Wage, $[1]	Gross National Product Deflator Reciprocal[2]	Prices: Metals: Aluminum, $ per Lb[3]	Metals: Copper, $ per Lb[4]	Metals: Pig Iron, $ per Long Ton[3]	Fuels: Bituminous Coal, $ per Ton[4]	Fuels: Petroleum, $ per 42-Gal Bbl[4]	Nonmetals: Sulfur, $ per Long Ton[4]	Nonmetals: Cement, $ per 376 Lb Bbl[4]	Quantity of Commodity Purchasable for Wage of One Hour of Labor: Aluminum, Lb	Copper, Lb	Pig Iron, Lb	Bituminous Coal, Lb	Petroleum, Gal	Sulfur, Lb	Cement, Lb	Adjusted Price (In 1954 Dollars): Aluminum, $ per Lb	Copper, $ per Lb	Pig Iron, $ per Lb	Bituminous Coal, $ per Lb	Petroleum, $ per 42-Gal Bbl	Sulfur, $ per Long Ton	Cement, $ per 376-Lb Bbl
1890	0.199	3.416	[5]	0.1560	17.00	0.99	0.77	[5]	0.58	[5]	1.28	26.22	402	10.85	[5]	129	[5]	0.533	58.07	3.38	2.63	[5]	1.98
1891	0.202	3.465	[5]	0.1280	14.82	0.99	0.56	[5]	0.56	[5]	1.58	30.53	408	15.15	[5]	136	[5]	0.444	51.35	3.43	1.94	[5]	1.94
1892	0.203	3.601	[5]	0.1160	13.48	0.99	0.51	[5]	0.59	[5]	1.75	33.73	410	16.72	[5]	129	[5]	0.418	48.54	3.56	1.84	[5]	2.12
1893	0.205	3.526	[5]	0.1080	12.20	0.96	0.60	[5]	0.55	[5]	1.90	37.64	427	14.35	[5]	140	[5]	0.381	43.02	3.38	2.12	[5]	1.94
1894	0.200	3.770	[5]	0.0950	10.39	0.91	0.72	[5]	0.60	[5]	2.11	43.12	440	11.67	[5]	125	[5]	0.358	39.17	3.43	2.71	[5]	2.26
1895	0.200	3.818	[5]	0.1070	11.71	0.86	1.09	[5]	0.63	[5]	1.87	38.26	465	7.71	[5]	119	[5]	0.409	44.71	3.28	4.16	[5]	2.41
1896	0.205	3.918	[5]	0.1080	11.14	0.83	0.96	[5]	0.68	[5]	1.90	41.22	494	8.97	[5]	113	[5]	0.423	43.65	3.25	3.76	[5]	2.66
1897	0.203	3.906	[5]	0.1200	9.98	0.81	0.68	[5]	0.75	[5]	1.69	45.56	501	12.54	[5]	102	[5]	0.469	38.98	3.16	2.66	[5]	2.93
1898	0.204	3.794	[5]	0.1240	10.41	0.80	0.80	[5]	0.81	[5]	1.65	43.90	510	10.71	[5]	95	[5]	0.470	39.50	3.04	3.04	[5]	3.07
1899	0.209	3.667	[5]	0.1710	17.34	0.87	1.13	[5]	0.83	[5]	1.22	27.00	480	7.77	[5]	95	[5]	0.627	63.59	3.19	4.14	[5]	3.04
1900	0.216	3.506	0.330	0.1655	17.82	1.04	1.19	[5]	0.77	0.65	1.31	27.15	415	7.62	[5]	105	1.157	0.580	62.48	3.65	4.17	[5]	2.70
1901	0.219	3.526	0.330	0.1640	14.35	1.05	0.96	[5]	0.79	0.66	1.34	34.19	417	9.58	[5]	104	1.164	0.578	50.60	3.70	3.38	[5]	2.79
1902	0.227	3.416	0.330	0.1197	19.89	1.12	0.80	[5]	0.98	0.69	1.90	25.56	405	11.92	[5]	87	1.127	0.409	67.94	3.83	2.73	[5]	3.35
1903	0.236	3.377	0.330	0.1362	17.75	1.24	0.94	[5]	1.07	0.72	1.73	29.78	381	10.54	[5]	83	1.114	0.460	59.94	4.19	3.17	[5]	3.61
1904	0.236	3.340	0.330	0.1311	13.34	1.10	0.86	20.93	0.82	0.72	1.80	39.63	429	11.53	25.25	108	1.102	0.438	44.56	3.67	2.87	69.91	2.74
1905	0.239	3.258	0.332	0.1598	15.96	1.06	0.62	20.40	0.90	0.72	1.50	33.54	451	16.19	26.24	100	1.082	0.520	52.00	3.45	2.02	66.46	2.93
1906	0.248	3.180	0.394	0.1977	18.84	1.11	0.73	17.33	1.08	0.63	1.25	29.49	447	14.27	32.06	86	1.253	0.629	59.91	3.53	2.32	55.11	3.43
1907	0.257	3.059	0.379	0.2086	22.49	1.14	0.72	17.55	1.07	0.68	1.23	25.60	451	14.99	32.80	90	1.159	0.638	68.80	3.49	2.20	53.68	3.27
1908	0.250	3.082	0.293	0.1339	16.02	1.12	0.72	18.05	0.84	0.85	1.87	35.00	446	14.58	31.02	112	0.903	0.413	49.37	3.45	2.22	55.63	2.59
1909	0.252	2.982	0.240	0.1311	16.23	1.07	0.70	18.52	0.80	1.05	1.92	34.78	471	15.12	30.48	118	0.716	0.391	48.40	3.19	2.09	55.23	2.39
1910	0.260	2.896	0.220	0.1288	15.55	1.12	0.61	18.02	0.88	1.18	2.02	37.45	464	17.90	32.32	111	0.637	0.373	45.03	3.24	1.77	52.19	2.55
1911	0.263	2.910	0.204	0.1255	14.00	1.11	0.61	18.02	0.84	1.29	2.10	42.08	474	18.11	32.69	118	0.594	0.365	40.74	3.23	1.78	52.44	2.44
1912	0.274	2.801	0.205	0.1648	14.82	1.15	0.74	17.32	0.81	1.34	1.66	41.41	477	15.55	35.44	127	0.574	0.462	41.51	3.22	2.07	48.51	2.27
1913	0.285	2.788	0.214	0.1552	15.42	1.18	0.95	17.59	1.00	1.33	1.84	41.40	483	12.60	36.29	107	0.597	0.433	42.99	3.29	2.65	49.04	2.79
1914	0.287	2.756	0.194	0.1331	13.52	1.17	0.81	18.17	0.92	1.48	2.16	47.55	491	14.88	35.38	117	0.535	0.367	37.26	3.22	2.23	50.08	2.54
1915	0.287	2.670	0.246	0.1747	14.15	1.13	0.64	16.87	0.86	1.17	1.64	45.43	508	18.83	38.11	125	0.657	0.466	37.78	3.02	1.71	45.04	2.30
1916	0.320	2.370	0.355	0.2846	20.31	1.32	1.10	15.97	1.10	0.90	1.12	35.29	485	12.22	44.88	109	0.841	0.675	48.13	3.13	2.61	37.85	2.61
1917	0.364	1.921	0.378	0.2919	39.99	2.26	1.56	21.41	1.35	0.96	1.25	20.39	322	9.80	38.08	101	0.726	0.561	76.82	4.34	3.00	41.13	2.59
1918	0.448	1.649	0.329	0.2468	34.38	2.58	1.98	22.00	1.59	1.36	1.82	29.19	347	9.50	45.61	106	0.543	0.407	56.69	4.25	3.27	36.28	2.62
1919	0.529	1.609	0.330	0.1890	29.91	2.49	2.10	15.12	1.71	1.60	2.80	39.62	425	10.58	78.37	116	0.531	0.304	48.13	4.01	3.38	24.33	2.75
1920	0.663	1.414	0.333	0.1750	43.80	3.75	3.08	19.77	2.01	1.99	3.79	33.91	354	9.04	75.12	124	0.471	0.247	61.93	5.30	4.36	27.95	2.84
1921	0.607	1.658	0.263	0.1265	24.05	2.89	1.73	17.81	1.89	2.31	4.80	56.54	420	14.74	76.34	121	0.436	0.210	39.87	4.79	2.87	29.53	3.13
1922	0.574	1.755	0.209	0.1356	25.00	3.02	1.61	16.37	1.76	2.74	4.23	51.43	380	14.97	78.54	123	0.367	0.240	43.88	5.30	2.83	28.73	3.09
1923	0.620	1.708	0.260	0.1461	27.15	2.68	1.34	16.06	1.89	2.38	4.24	51.15	463	19.43	86.48	123	0.444	0.250	46.37	4.58	2.29	27.43	3.23
1924	0.636	1.728	0.278	0.1316	21.87	2.20	1.43	16.26	1.80	2.29	4.83	65.14	578	18.68	87.62	133	0.480	0.227	37.79	3.80	2.47	28.10	3.11
1925	0.645	1.698	0.282	0.1416	21.32	2.04	1.68	15.61	1.77	2.29	4.56	67.77	632	16.13	92.55	137	0.479	0.240	36.20	3.46	2.85	26.51	3.01
1926	0.647	1.691	0.275	0.1393	21.06	2.06	1.88	18.00	1.71	2.35	4.64	68.81	628	14.45	80.52	142	0.465	0.236	35.61	3.48	3.18	30.44	2.89
1927	0.647	1.733	0.258	0.1305	19.35	1.99	1.30	18.00	1.62	2.51	4.96	74.90	650	20.90	80.52	150	0.447	0.226	33.53	3.45	2.25	31.19	2.81
1928	0.662	1.720	0.243	0.1468	18.32	1.86	1.17	18.00	1.57	2.72	4.51	80.94	712	23.76	82.38	159	0.418	0.252	31.51	3.20	2.01	30.96	2.70
1929	0.662	1.713	0.243	0.1823	19.15	1.78	1.27	18.00	1.48	2.72	3.63	77.43	744	21.89	82.38	168	0.416	0.312	32.80	3.05	2.18	30.83	2.54
1930	0.647	1.779	0.238	0.1311	18.18	1.70	1.19	18.00	1.44	2.72	4.94	79.72	761	22.84	80.52	169	0.423	0.233	32.34	3.02	2.12	32.02	2.56
1931	0.602	1.988	0.233	0.0824	16.45	1.54	0.65	18.00	1.11	2.58	7.31	81.97	782	38.90	74.92	204	0.463	0.164	32.70	3.06	1.29	35.78	2.21
1932	0.528	2.208	0.233	0.0567	14.99	1.31	0.87	18.00	1.02	2.26	9.31	78.90	806	25.50	65.71	195	0.514	0.125	33.10	2.89	1.92	39.74	2.23
1933	0.521	2.220	0.233	0.0715	16.30	1.34	0.67	18.00	1.33	2.24	7.29	71.60	778	32.66	64.84	147	0.517	0.159	36.19	2.97	1.49	39.96	2.95
1934	0.625	2.092	0.222	0.0853	18.64	1.75	1.00	18.00	1.54	2.82	7.33	75.11	714	26.25	77.78	153	0.464	0.178	38.99	3.66	2.09	37.66	3.22
1935	0.647	2.115	0.195	0.0876	19.12	1.77	0.97	18.00	1.51	3.32	7.39	75.80	731	28.01	80.52	161	0.412	0.185	40.44	3.74	2.05	38.07	3.19
1936	0.654	2.064	0.190	0.0958	20.00	1.76	1.09	18.00	1.51	3.44	6.83	73.25	743	25.20	81.39	163	0.392	0.198	41.28	3.63	2.25	37.15	3.12
1937	0.736	2.025	0.198	0.1327	23.60	1.94	1.18	18.00	1.48	3.72	5.55	69.86	759	26.20	91.59	187	0.401	0.269	47.79	3.93	2.39	36.45	3.00
1938	0.736	2.053	0.200	0.1010	22.35	1.95	1.13	17.00	1.45	3.68	7.29	73.76	755	27.36	96.98	191	0.411	0.207	45.88	4.00	2.32	34.90	2.98
1939	0.743	2.071	0.200	0.1107	21.75	1.84	1.02	16.00	1.47	3.72	6.71	76.52	808	30.59	104.02	190	0.414	0.229	45.04	3.81	2.11	33.14	3.04
1940	0.773	2.046	0.188	0.1140	23.15	1.91	1.02	16.00	1.46	4.11	6.78	74.80	809	31.83	108.22	199	0.385	0.233	47.36	3.91	2.09	32.74	2.99
1941	0.855	1.881	0.165	0.1187	24.10	2.19	1.14	16.00	1.47	5.18	7.20	79.47	781	31.50	119.70	219	0.310	0.223	45.33	4.12	2.14	30.10	2.77
1942	1.004	1.684	0.150	0.1187	24.19	2.36	1.19	16.00	1.53	6.69	8.46	92.97	851	35.44	140.56	247	0.253	0.200	40.74	3.97	2.00	26.94	2.58
1943	1.130	1.551	0.150	0.1187	24.19	2.69	1.20	16.00	1.56	7.53	9.52	104.64	840	39.55	158.20	272	0.233	0.184	37.52	4.17	1.86	24.82	2.44
1944	1.197	1.522	0.150	0.1187	24.17	2.92	1.21	16.00	1.59	7.98	10.08	110.93	820	41.55	167.58	283	0.228	0.181	36.79	4.44	1.84	24.35	2.42
1945	1.204	1.477	0.150	0.1187	25.19	3.06	1.22	16.00	1.63	8.03	10.14	107.06	787	41.45	168.56	278	0.222	0.175	37.21	4.52	1.80	23.63	2.41
1946	1.278	1.340	0.150	0.1392	27.84	3.44	1.41	16.00	1.72	8.52	9.18	102.83	743	38.07	178.92	279	0.201	0.187	37.31	4.61	1.89	21.44	2.30
1947	1.449	1.119	0.150	0.2115	34.86	4.16	1.93	17.00	1.90	9.66	6.85	93.11	697	31.53	190.93	287	0.168	0.237	39.01	4.66	2.16	19.02	2.13
1948	1.583	1.136	0.155	0.2220	43.38	4.99	2.60	18.00	2.18	10.21	7.13	81.74	634	25.57	196.99	273	0.176	0.252	49.28	5.67	2.95	20.45	2.48
1949	1.642	1.125	0.170	0.1936	46.98	4.88	2.54	18.00	2.30	9.66	8.48	78.29	673	27.15	204.34	268	0.191	0.218	52.85	5.49	2.86	20.25	2.59
1950	1.716	1.113	0.176	0.2146	48.24	4.84	2.51	18.00	2.35	9.75	8.00	79.68	709	28.71	213.55	275	0.196	0.239	53.69	5.39	2.79	20.03	2.62
1951	1.865	1.034	0.190	0.2437	53.62	4.92	2.53	22.00	2.55	9.82	7.65	77.91	758	30.96	189.89	275	0.196	0.252	55.44	5.09	2.62	22.75	2.63
1952	1.962	1.025	0.194	0.2437	54.84	4.90	2.53	22.50	2.54	10.11	8.05	80.14	801	32.57	195.33	290	0.199	0.250	56.21	5.02	2.59	23.06	2.60
1953	2.081	1.008	0.209	0.2892	57.00	4.92	2.68	22.50	2.68	9.96	7.20	81.78	846	32.61	207.18	292	0.211	0.292	57.46	4.96	2.70	22.68	2.70
1954	2.126	1.000	0.218	0.2982	57.61	4.51	2.78	26.50	2.78	9.75	7.13	82.66	943	32.12	179.71	288	0.218	0.298	57.61	4.51	2.78	26.50	2.78
1955	2.208	0.989	0.237	0.3739	58.77	4.50	2.77	26.50	2.89	9.32	5.91	84.16	982	33.48	186.64	287	0.234	0.370	58.12	4.45	2.74	26.21	2.86
1956	2.327	0.960	0.260	0.4188	62.22	4.82	2.79	26.50	3.08	8.95	5.56	83.78	966	35.03	196.70	284	0.250	0.402	59.73	4.63	2.68	25.44	2.96
1957	2.431	0.945	0.275	0.2999	65.40	5.08	3.09	24.41	3.21	8.84	8.11	83.26	957	33.04	223.08	285	0.260	0.283	61.80	4.80	2.32	25.07	3.08

[1] The average hourly earnings series is that developed for all manufacturing industries by Paul H. Douglas and published in his *Real Wages in the United States, 1890-1926*, Houghton Mifflin Co., New York, 1930, and extended 1927-57 by the U.S. Bureau of Labor Statistics, Department of Labor. [2] The Gross National Product Implicit Price Deflator Reciprocals are based on the series developed by the Office of Business Economics, U.S. Dept. of Commerce and published in *National Income—1954 Edition*, pp. 216-17 for 1929-1953 reciprocals, in *Survey of Current Business*, February 1957, p. 7 for 1954-56 reciprocals, and *Economic Report of the President, January 1958*, p. 122 for 1957 reciprocal; the 1890-1928 reciprocals are based on unpublished work sheets of John Kendrick. [3] *Metal Statistics* series, *American Metal Market*. [4] *Minerals Yearbook* series, U.S. Bureau of Mines. [5] Data not available.

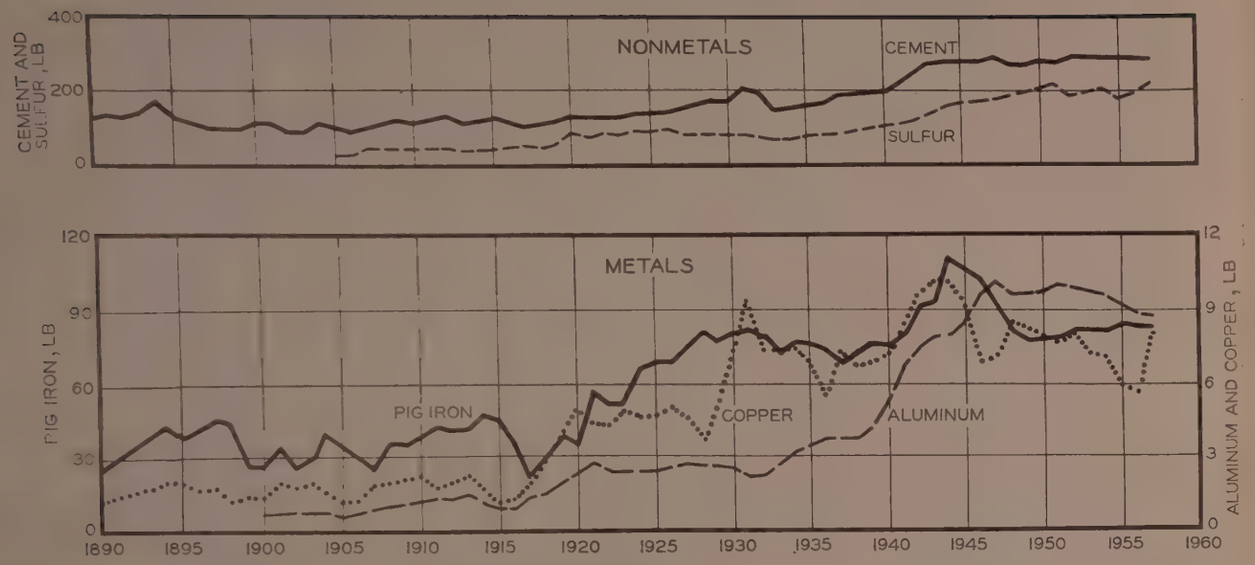

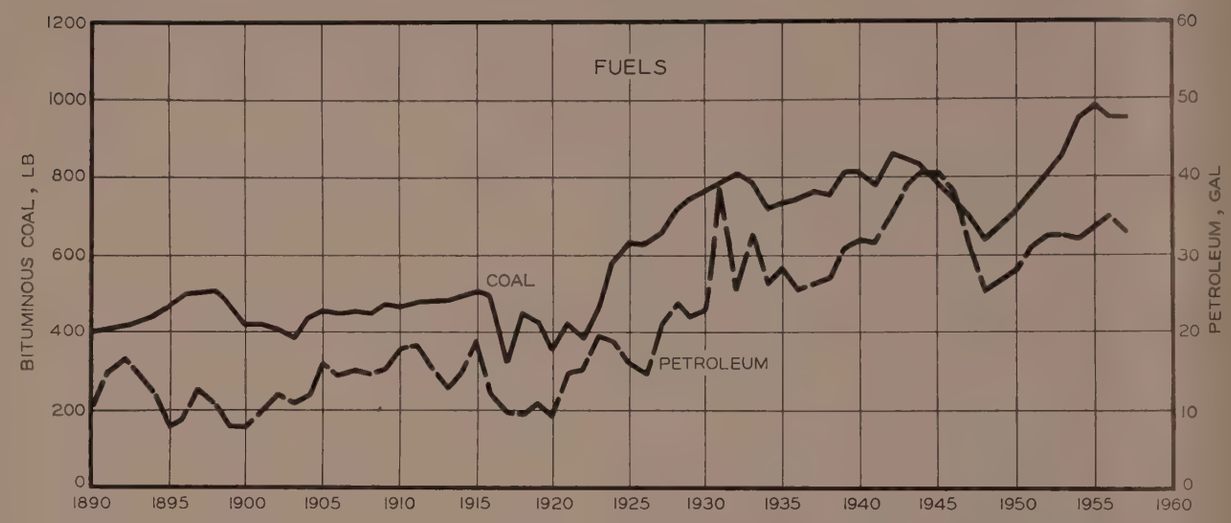

Figs. 1 and 2—Quantities of selected mineral commodities purchasable for wage of one hour's labor. Average hourly earnings series used is the one developed for all manufacturing industries by Paul H. Douglas for 1890-1926 and extended 1927-1957 by the U. S. Department of Labor.

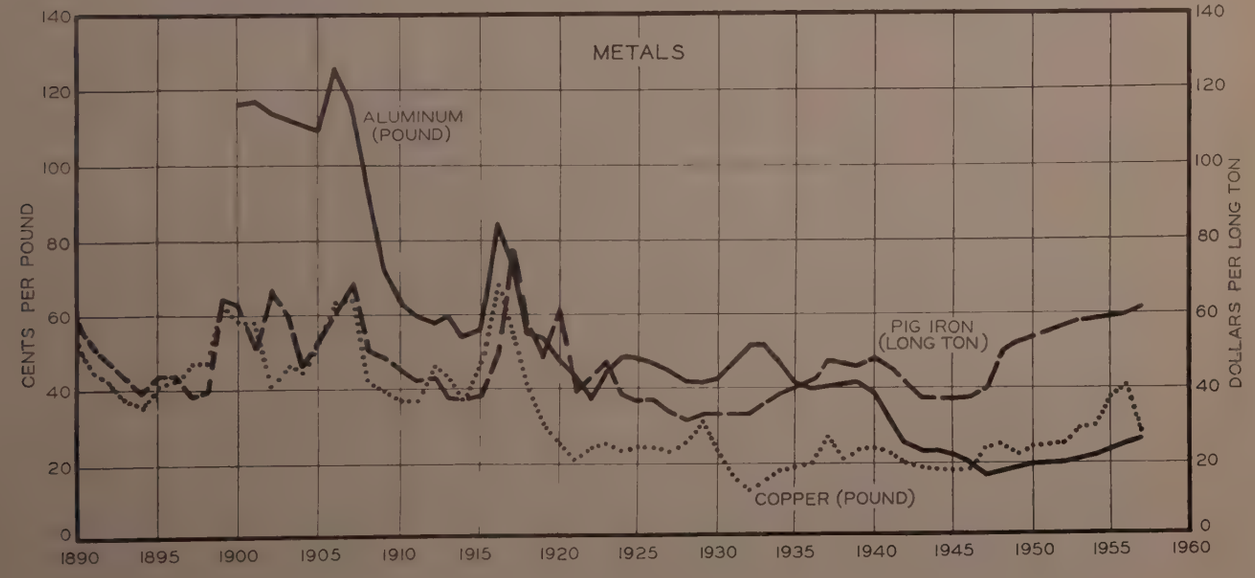

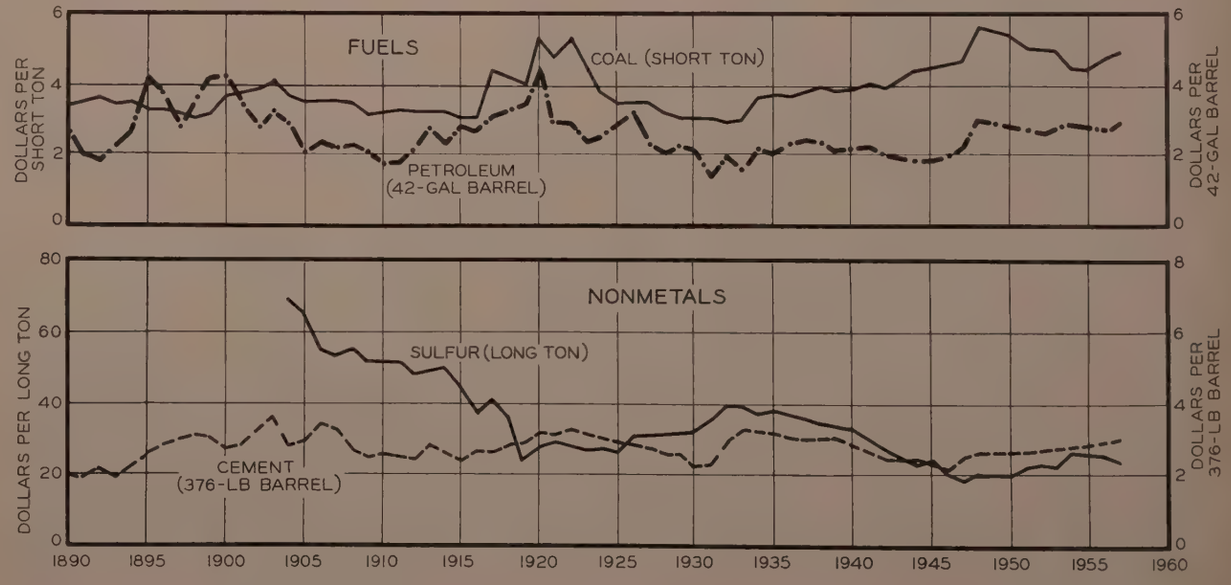

Figs. 3 and 4—Deflated prices (in 1954 dollars) of selected mineral commodities, 1890-1957. The Gross National Product Implicit Price Deflators used are based on the series developed by the Department of Commerce, 1929-1957, and on unpublished work sheets of John Kendrick for 1890-1928.

GEOCHEMICAL STUDY OF SOIL CONTAMINATION IN THE COEUR D'ALENE DISTRICT, SHOSHONE COUNTY, IDAHO

by F. C. CANNEY

Geochemical prospecting seeks hidden mineral deposits by sampling for variations in the chemical composition of naturally occurring materials. Usually the samples are of soils and other products of weathering and erosion—surface materials extremely susceptible to contamination by human activities. Except when a survey is conducted well away from populated areas, contamination is an ever-present hazard.

The program's success is particularly endangered when the contaminants are the elements sought; if these occur erratically throughout an area, spurious anomalies completely unrelated to mineralized areas can be formed. Evenly distributed contamination can be dangerous too, if it raises the background to such a level that true anomalies can no longer be easily detected. Suppose, for example, that in an area where the lead background is 20 parts per million the soil over a lead vein contains 1000 ppm of lead. Here the contrast would be 50 to 1, which is very satisfactory for geochemical surveying. Now if 1000 ppm of lead from some source were added evenly to the soil in this area, the contrast would be reduced to about 2 to 1, and the anomaly would no longer be readily detectable because a threshold of significance twice the value of the background is the minimum generally used for interpreting geochemical data.

Of the many possible sources of contamination, probably most important are smelter fumes, which may distribute large quantities of metal contaminants over many square miles of ground.

For several reasons, the investigation reported here was begun in the Coeur d'Alene district in northern Idaho: 1) a lead smelter has been operated in this district since 1917 and an electrolytic zinc plant since 1928, and presumably the contamination patterns are strongly developed; 2) to evaluate the usefulness of certain geochemical techniques, V. C. Kennedy and S. W. Hobbs of the USGS had already studied the distribution of copper, lead, and zinc in the soils (both in background areas and other veins) and in the water and plants, providing a criterion for measuring the magnitude and effect of soil contamination; 3) one of the economically important parts of the district lies south of the South Fork of Coeur d'Alene River and within a radius of five miles of the reduction plants near Smelterville (Fig. 1). In this area, and in the entire district, conventional methods of prospecting are hindered by heavy vegetation and thick soil cover, and the possibility of contamination by smelter fumes has discouraged geochemical prospecting. Should data reveal that geochemical prospecting could be done successfully in such an area, a particularly useful tool would be available to mining companies and prospectors searching for concealed orebodies in this economically important part of the district.

The field work on which this report is based was done from July 28 to 31, 1955. It should be emphasized that this was reconnaissance study only, and therefore far from exhaustive.

Previous Investigations in U. S. : The first geochemical survey known to have been affected by contamination was conducted in 1940—a geobotanical reconnaissance made in the Michigan copper district by a private company. Geologists found striking variations in the copper content of oak and maple leaves, but unfortunately the high copper isograds of the study seemed to be related more to the Calumet and Hecla copper smelter fall-out than to mineralized ground.[1] The leaves of one oak tree near the smelter contained 0.4 pct Cu.

Similar contamination was reported by Clarke (Ref. 2, p. 41), who conducted experimental geochemical soil and botanical surveys at Ray, Ariz. He found that the leaves of oak trees growing in unmineralized ground near Superior, Ariz., contained more copper than the leaves of oak trees growing on the capping of the Ray orebody and attributed this fact to contamination from the fumes of the Magma smelter at Superior. According to H. E. Hawkes,[3] soils and stream sediments in the Superior area are also severely contaminated. Hawkes' work there has shown a copper content averaging 0.5 pct in the surface horizons of soils within one mile of the smelter stack. Samples taken only a few inches below the anomalous surface samples showed only background copper values.

In 1950 L. C. Huff[4] of the USGS made a geochemical survey in an area near Jerome, Ariz., and found considerable zinc and copper in the soils over unmineralized basalt close to Clarkedale, Ariz., and over limestone close to Jerome. As the amounts were notably greater than could reasonably be expected to be derived from the underlying rocks, Huff suspected airborne contamination from the smelter at Clarkedale.

Description of Area: The area sampled in detail (Fig. 1) for the study presented here is one of strong relief. The dominant watercourse is the westward-flowing South Fork of the Coeur d'Alene River. East of Kellogg the South Fork flows in a rather narrow canyon, but its valley floor widens considerably to the west where much of the flood plain is covered by an extensive veneer of mining, milling, and smelting debris. South of the South Fork and between Big Creek and Pine Creek is a mountainous area where

F. C. CANNEY is a Geologist with the Mineral Deposits Branch, U. S. Geological Survey, Denver, Colo. TP 4784L. Manuscript, May 8, 1958. New York Meeting, February 1958. AIME Trans., Vol. 214, 1959.

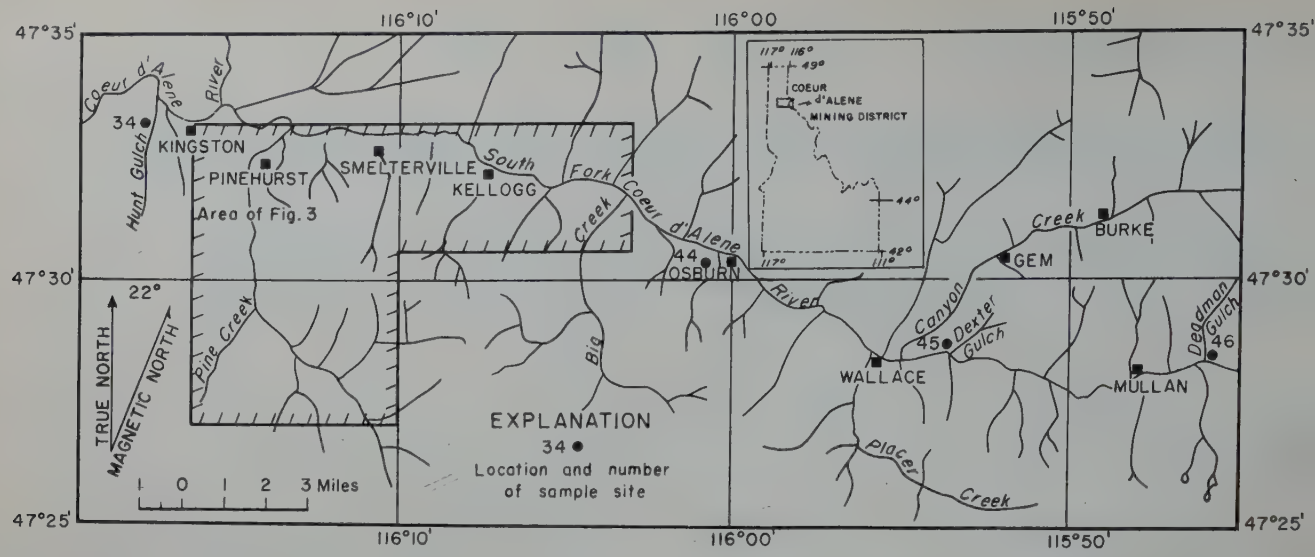

Fig. 1—Map of part of Coeur d'Alene district, Idaho, shows outlying sample sites and area sampled in detail.

many of the ridge crests and peaks rise 1500 to 3000 ft above the valley floors. The tributary gulches that enter the South Fork from the south are mostly short and steep-sided.

For some distance around the smelter most of the vegetation has been killed by the fumes. Surrounding the almost completely denuded region is a barren bordering zone covered with grass, stunted shrubs, and small trees. Where the vegetative cover has been destroyed, the soil is extremely susceptible to erosion.

Sample Collection and Analysis: To guide the location and spacing of the sample sites, two assumptions were made: first, that the heaviest contamination would be found along the sides and floor of the valley of the South Fork of Coeur d'Alene River, and second, that the profile of particle fall-out from the smelter fumes would resemble an asymmetrical curve skewed to the east, downwind of prevailing winds.

Accordingly a basic traverse (labeled AA′ in Fig. 2) was located roughly parallel to the South Fork in a general easterly direction. The smelter area near Smelterville was, of course, the focal point of the sample pattern. Since time was short, the sample sites had to be reasonably accessible by car; this, and the somewhat limited distribution of terrace gravels (the material sampled wherever possible) account for the lack of a definite factor controlling the interval between samples.

Of the 46 sites visited in this investigation, 42 (those in the area sampled in detail) are shown in Fig. 2, and the rest (four outlying sites) in Fig. 1. It will be observed that in addition to the sites along AA′ there are many others in several of the major gulches, especially to the east of the smelter area. Sites were also located in the Pine Creek drainage to furnish data that would show the extent of soil contamination from fumes that cross the intervening mountainous area.

For the ideal sampling medium the author wanted a soil that had developed from parent material relatively uniform in its lead-zinc content and probably without abnormal amounts of these metals.

Extensive patches of terrace gravels mantle many of the slopes in a strip about one mile wide bordering the South Fork on its southern side. Although they are called gravels, the materials in the surface layer of these deposits—at least at most of the samples sites visited in this investigation—are mainly in the clay, silt, and sand-size fractions, with only very scattered well-rounded pebbles and cobbles. Deposited by river action, this material is a naturally composited sample of all the rock types in the river's drainage basin. It is therefore believed that the soils developed on these terrace gravels were originally of fairly uniform, low heavy-metal content similar to the metal content of residual soils developed on the sedimentary rocks—although perhaps somewhat lower, since there was probably more quartzose material in the gravels. All sample sites on traverse AA′, therefore, were located in areas of the terrace gravels. However, of the sites off traverse AA′ only two—9 and 34—are in areas of terrace gravels; the rest are located where soils have developed directly from weathering of the slightly metamorphosed sedimentary rocks of the Belt series of Pre-Cambrian age. In these areas, sites were selected where no mineralization was evident in a cursory examination of the immediate vicinity.

To determine the depth of contamination, profile samples were collected at each site. The desirability of sampling individual horizons in the soil profile was considered, but much of the soil had been washed away, especially in the barren zone surrounding the smelter area, and it was decided to sample at fixed vertical intervals. At 22 sites vertical channel samples were collected through each of the following intervals: 0 to 2 in., 2 to 6 in., and 6 to 12 in. The top of the A_1 soil horizon was used as a reference plane for depth measurements where it was present; in truncated profiles, the top of any available surface mineral horizon was used. At the remaining 24 sites only two samples were taken, one from the 0 to 2-in. interval and the other from an interval of about 1 in. centered at a depth of 6 in. At certain sites, samples of the surface material also were collected, either humus from the A_0 horizon, or the top half-inch of the surface mineral horizon.

About 25 g of material were collected for each sample. R. R. Beins and W. J. Breed of the USGS laboratories analyzed the samples for lead and zinc by rapid colorimetric field methods, which are usually precise to within ± 30 pct. The size fraction

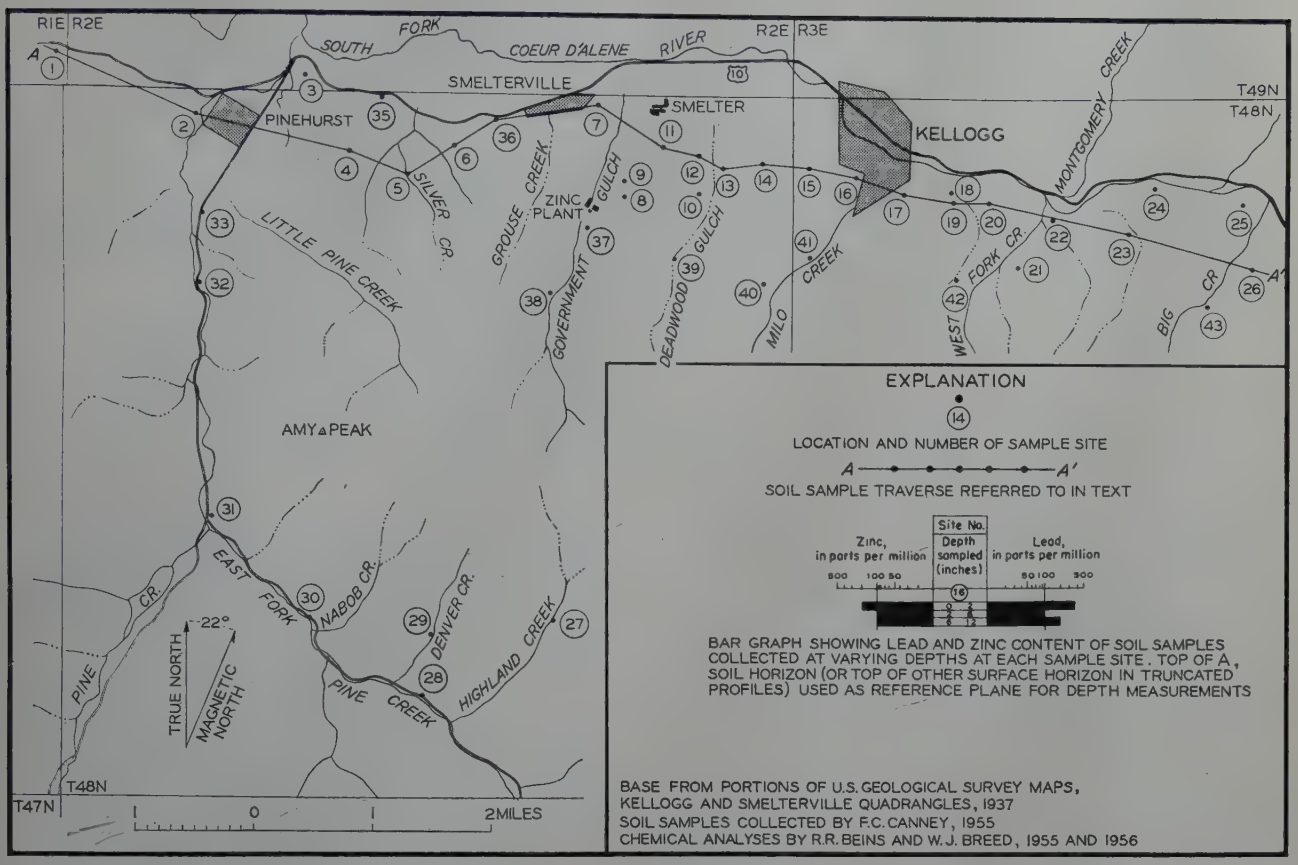

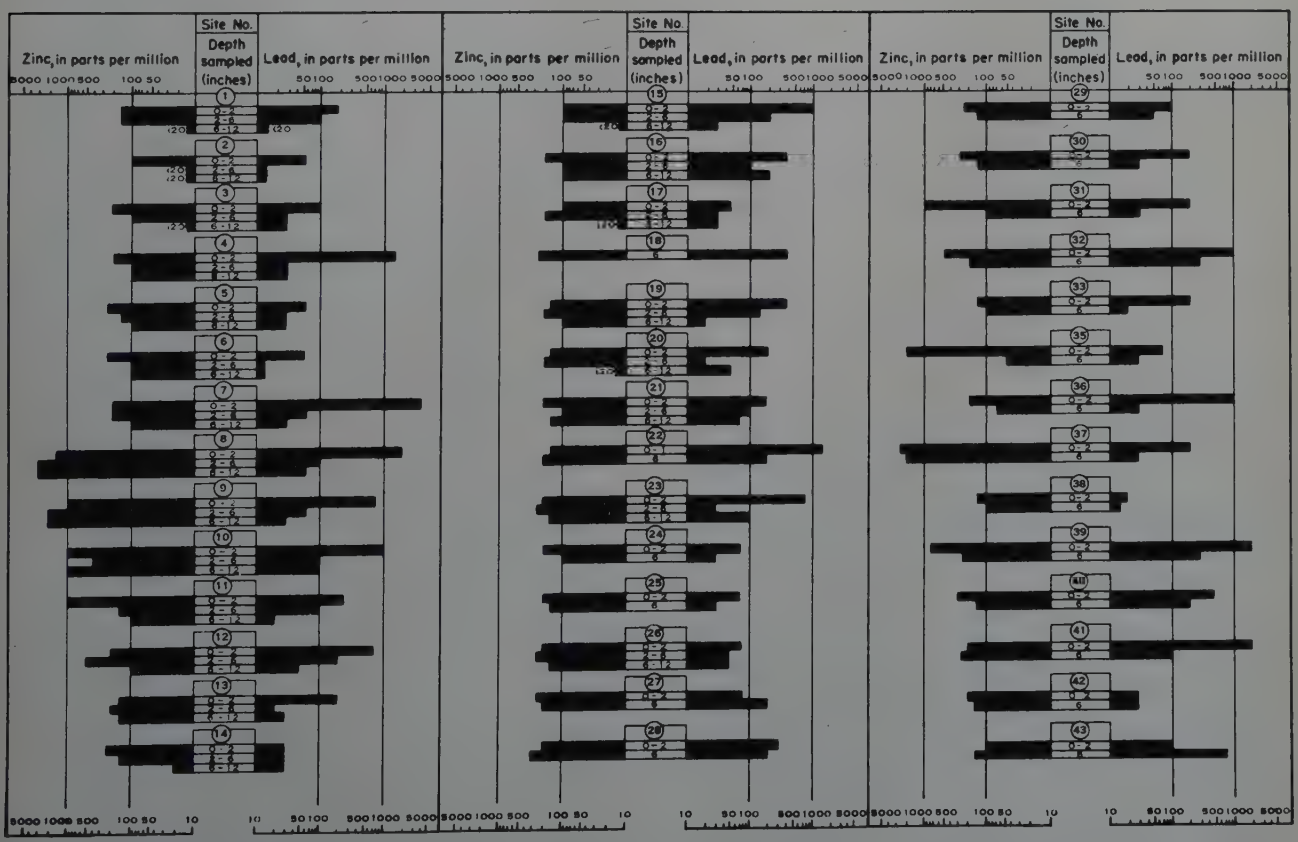

Fig. 2A (top)—Map showing sample sites. Fig. 2B (bottom)—Histogram showing lead and zinc contents of samples.

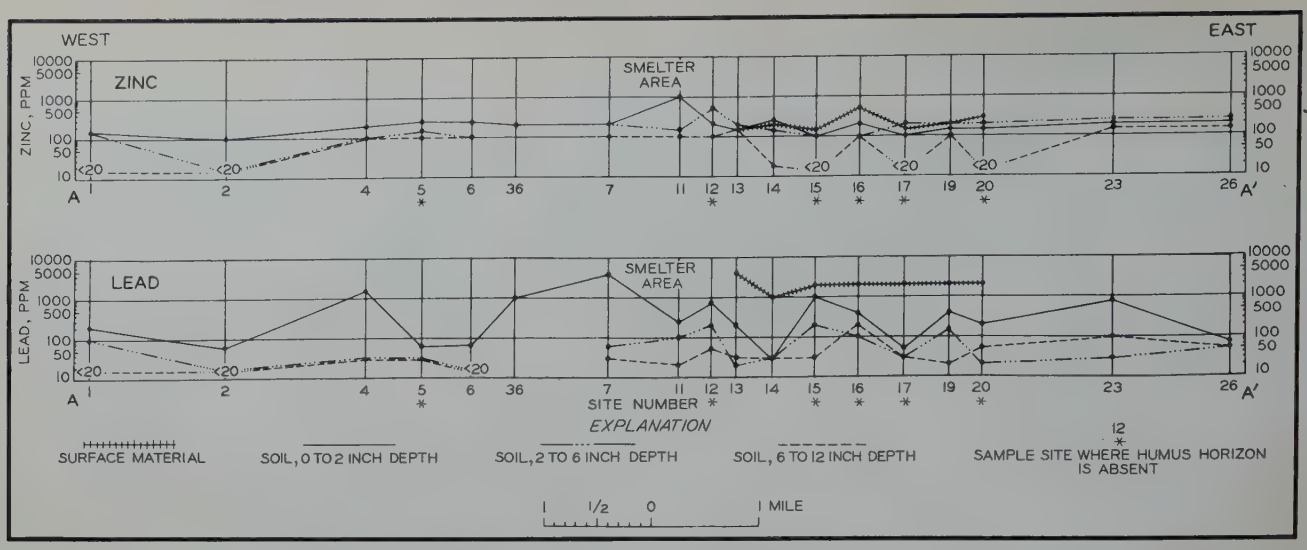

Fig. 3—Vertical distribution of metal along traverse AA'.

that passed through an 80 mesh sieve was used for all analyses.

RESULTS OF INVESTIGATIONS

The lead and zinc content of each soil sample is shown in Figs. 2 and 3 and in Table I. Fig. 2 presents the analytical data in a series of bar graphs to facilitate comparing the lead and zinc contents of the various sets of profile samples. Fig. 3 shows the vertical distribution of metal along traverse AA'.

Because these determinations were semi-quantitative, and the field work only reconnaissance, too much significance should not be given to small differences in metal content of the samples. Much more sampling and analysis would be needed, moreover, to account for both the horizontal and vertical distribution of metal contaminants as revealed by the data.

Lead and Zinc Contamination Patterns: Kennedy and Hobbs,[5] conducting the earlier program, collected soil samples in the vicinity of the sub-outcrops of many known veins, as well as beyond the periphery of the district known to be mineralized. On the basis of resulting data, they concluded that background values for copper, lead, and zinc in the Coeur d'Alene area are about 25, 20, and 100 ppm, respectively. It may be seen that by comparison many samples of the present writer's study contain highly anomalous quantities of both lead and zinc, but the distribution is somewhat erratic, both horizontally and vertically.

Actual distribution of metal along traverse AA' bears only slight resemblance to an asymmetrical curve skewed to the east. In some locations there are wide differences in metal content of the samples, even between those from closely adjacent sites. There are several possible explanations for this discrepancy.

First, although it might be expected that the metal contaminants would be evenly spread over large tracts of ground, this may not be so. Owing to the funneling action of the topography in this area, there may be significant long-term variations in the intensity of fall-out at different localities.

Second, it is very probable that many of the irregularities are caused by differential erosion of the metal-rich surface layer, and by variations in the amount of metal filtering down into the soil owing to differences in soil porosity and permeability. In many portions of the barren zone around the smelter, as well as in outlying areas where most of the vegetative cover is gone, much of the soil is being actively eroded by sheet wash and deflation. In such areas any layer of metal contaminants probably would not be preserved to any extent. It is conceivable that at the bases and at topographic benches on these barren slopes, deposits of metal-rich colluvium have attained considerable thickness, perhaps accounting for the appreciable metal content, especially lead, of both the 0 to 2-in. and the 6-in. samples at sites 39, 40, and 41.

The contrast between lead profiles at sites 14 and 15 is a striking example of discrepancy possibly produced by differences in soil porosity and permeability. At site 14, in spite of a surface humus layer containing 0.1 pct Pb, there has been no contamination of the lower horizons, which contain only 30 ppm lead. At site 15, on the other hand, an appreciable amount of lead has been dispersed through the first 6 in. of the soil from a similar lead-rich surface layer. Both these sites, less than half a mile apart, are on slopes of about the same degree of steepness and have the same amount of vegetative cover. If only these two sites were considered, it could be postulated that at site 14, which has a humus horizon, the lead has been immobilized by formation of complex metallo-organic compounds, whereas at site 15 the lack of a humus horizon has prevented any complexing action. But this hypothesis is probably incorrect, as shown by the lead profiles at sites 17 and 19, where exactly the opposite situation prevails.

Another fact requiring explanation, if these differences are caused by variations in permeability, is the absence of any similarity between zinc and lead profiles at these sites. For example, at site 14 there has been appreciable downward migration of zinc, but almost no migration of lead. Looking at all the profiles in Fig. 3, the author believes that many of these apparent discrepancies are due to different dispersal mechanisms for lead and zinc in the soil profile. As a working hypothesis, he suggests that much of the zinc is dissolved out of the surface layer and migrates downward in solution, whereas most of the lead is carried down mechanically in suspension. This theory helps explain many of the distributional patterns, and it seems reasonable because the degree of mechanical

infiltration of lead particles should be much more dependent on soil porosity than is the diffusion of material carried in true solution. Of course, at those sites where the soil is very porous, much of the zinc, as well as the lead, may be moved mechanically in a suspension.

The rather low and uniform zinc content of the soil at most of the sites is worth noting. Most values are between 100 and 300 ppm. Only at sites 8, 9, 10, and 37, all in the immediate smelter area, do most of the samples contain highly anomalous amounts of zinc. At six of the sites along traverse AA', the low zinc values of the samples taken from 6 to 12 in. seem to show that the average zinc content of the terrace gravels is considerably under the 100 ppm that Kennedy and Hobbs consider normal for soils. But no correspondingly lower value is evident for lead. It may be that the 100-ppm zinc values for the 6 to 12-in. samples at such sites as 4, 5, and 6 merely indicate areas where there is somewhat more zinc than is average for soils developed on the terrace gravels, or, of course, these values may represent sites where zinc-bearing solutions had penetrated to greater than average depth in the profile. The similarity in zinc content of the surface samples, the 0 to 2-in. samples, and the 2 to 6-in. samples is probably due to the greater mobility of zinc; this is in striking contrast to the lead pattern, in which concentration usually falls off rapidly with depth. As shown by the profiles in Fig. 3, in nearly all instances the lead content of the surface material is considerably higher than that of the immediately underlying material, but there is little difference in the amount of zinc. At some sites, in fact, the top layer may have a slightly lower zinc content than the material immediately underlying, as is true along the eastern third of traverse AA'.

At two sites, 27 and 43, the fact that the lead content of the 6-in. samples exceeds that of the 0 to 2-in. samples suggests that mineralization near these sites may be contributing some metal to these samples.

It was surprising to find above-normal amounts of lead in the 6-in. samples taken at the outlying sites (Fig. 1, Table I). Only at site 45, at the mouth of Dexter Gulch, does the lead content of the 6-in. sample exceed the critical value for lead discussed later. The reason for these above-normal values is not known. It is worth pointing out, however, that site 46 is not far from an area that was sampled in detail by Kennedy and Hobbs and found to have only background quantities of lead in the soil over much of the locality.

The generally lower zinc values give the impression that fall-out intensity of zinc contaminants is considerably less than that of lead. The different mobilities of lead and zinc are undoubtedly responsible for this impression; as most of the zinc contamination is distributed through at least 6 in. of soil, there is no extremely high zinc value in any one section, whereas most of the lead is concentrated in the top 2 in. of the profile. To illustrate: suppose that 1500 ppm of lead and zinc are added to the top half-inch of a soil layer 6 in. thick with a normal lead and zinc content of 20 ppm and 100 ppm, respectively. Should the excess zinc in the surface layer be distributed evenly throughout the 6-in. layer, the zinc content would be increased from 100 ppm to only 200 ppm, whereas distribution of the excess lead through the upper 2 in. of this layer would increase the lead concentration from 20 ppm to about 300 ppm.

Discussion of Data: In evaluating the data contained in this report, it must be realized that the Coeur d'Alene district has been extensively mined and prospected since the early eighties, and the amount of metallic contamination at each site undoubtedly represents an integrated total of contaminants from more than one source. The geochemical data of Kennedy and Hobbs warrants a tentative conclusion that smelter fumes contributed most of the metal contaminants to the majority of samples collected for this study. Much of their geochemical work was done near Burke and Mullen, more than 15 miles from the smelter. Nearly all the samples they collected over unmineralized bedrock contained only background quantities of lead and zinc. As most of their samples were composites of the first 4 in. of soil directly underlying the humus horizon, any contamination would be reflected in the metal content of these samples. Presumably, since Kennedy and Hobbs sampled chiefly in active or previously active mining areas, their sites were as subject to contamination by windblown tailings and dump material as the sample sites selected by the writer. Therefore it is reasonable to assume that most of the contamination found in the present writer's investigation is due to smelter fumes.

Table I. Metal Content of Samples Collected from Outlying Sites Shown in Fig. 1

Depth, In.	Number of Samples	Percent of Samples in which Metal Content Exceeds: 100 Ppm Lead	200 Ppm Zinc
34	0 to 2	400	200
	6	70	50
44	0 to 2	400	250
	6	100	150
45	0 to 2	250	200
	6	150	150
46	0 to 2	250	100
	6	100	100

Table II. Summary of Data Presented in Table I and Fig. 2

Site Number	Sample Depth, In.	Parts Per Million Lead	Zinc
0 to 2	45	67	38
2 to 6, 6	46	24	24
6 to 12	22	5	14

Effect of Contamination on Geochemical Soil Surveys: Before the effect of contamination on any geochemical soil survey can be appraised, it is necessary to determine what contamination level is critical. Widespread, fairly even contamination of an area will raise the local background; the difficulty of prospecting will increase as contamination increases, with no real critical points. Very spotty contamination, on the other hand, does have a critical value; it is that amount of metal which, added to a background sample, will raise the concentration above the threshold value. The threshold value, as defined by Hawkes (Ref. 6, p. 338) is the limiting anomalous value below which variations represent only normal background effects, and above which they are significant in terms of possible mineral deposits.

The data of this survey show that in the Coeur d'Alene district the contaminants are distributed somewhat erratically; therefore it would seem that in this area the greatest danger from contamination to geochemical soil surveys is the presence of spurious anomalies. For an estimate of how much lead and zinc would have to be added to soil of background composition to create such a spurious anomaly, the threshold values for these metals must be known. The data of Kennedy and Hobbs on soils collected in mineralized areas show that near 11 of the 13 veins they studied, lead is concentrated above background to a much greater extent than zinc. The ratio of highest lead concentration to background ranged from 20 to as much as 1500. The zinc content was much less satisfactory—at only two veins did the zinc content exceed six times the background value. As the lead anomalies generally show a substantially higher contrast to the background, Kennedy and Hobbs concluded that lead is the best element to use when prospecting for orebodies expected to contain much lead and zinc, and that analyses for zinc would be useful primarily in searching for ore where the zinc-lead ratio would probably be high. They believe that soil samples should be considered probably anomalous if the metal concentration is two to four times the normal concentration, and almost certainly anomalous if the concentration is more than four times background.

Considering lead first, it seemed that 100 ppm would be a conservative threshold value. Although 100 ppm is five times the background value (20 ppm) and therefore falls just past the limit of the "probably anomalous" range of Kennedy and Hobbs, in view of the large contrast for lead over most ore zones, lead values of 100 ppm or under would probably not be taken very seriously. Even if the lead background were raised to 100 ppm, the 11 lead anomalies of Kennedy and Hobbs would still be very striking in their contrast to this higher background.

The effect of zinc contamination on geochemical prospecting in this district is not so critical where lead has been found the more valuable indicator in locating ore. The lowest threshold of practical application in geochemical prospecting is about twice the background value. For zinc, therefore, the threshold value was set at 200 ppm, twice the average background value. This figure, which gives a lower ratio than was used for lead, was selected because near most of the veins studied by Kennedy and Hobbs zinc is not concentrated in amounts above background to the extent that lead is, and also because it would take only a slight increase in the zinc background to submerge many of the very weak zinc anomalies completely. Soil analyses over two veins that did contain appreciable amounts of zinc yielded satisfactory contrasts—at one site the ratio of the highest zinc concentration to background was 15; at the other, 36. It should be emphasized again, however, that as most of the veins contain a high lead-to-zinc ratio—at least near the surface—it is unlikely that analysis would be made only for zinc.

It is suggested, then, that at the depth sampled, contamination by more than 80 ppm lead and 100 ppm zinc would raise the lead and zinc content above the threshold values and might make it difficult to interpret soil survey data. Evaluation can best be accomplished by referring to Table II, which summarizes the data of Fig. 2 and Table I. It must be admitted that a somewhat lower threshold value for zinc should be probably used for those sites located on the terrace gravels, since the zinc background of soils developed on this material is probably lower; even had this been done, however, the figures in Table II would not have been changed appreciably.

The data in Table II indicate that within the area studied the upper 6 in. of soil should not be sampled in any geochemical soil survey, as there are probably excessive amounts of lead and zinc contaminants that would raise the metal content of the samples above the limiting threshold values, thereby creating spurious anomalies. The data strongly suggest that below 6 in. serious contamination is so rare that the metal content of the soil samples taken below this depth could be used with confidence in prospecting for concealed mineral deposits. It should be emphasized, however, that these findings are specific for this district and it would be hazardous to attempt to extrapolate them to other districts.

CONCLUSIONS AND RECOMMENDATIONS

Results of this survey indicate that the degree of contamination below about 6 in. is not enough to interfere seriously with geochemical prospecting techniques in this area. Some samples taken below this depth (especially in the immediate vicinity of the smelters and in very loose-textured soils) may be contaminated to some extent, particularly with zinc, because of its greater mobility. But it seems unlikely that an occasional contaminated sample would seriously interfere with interpretation of data, since a geochemical anomaly is rarely indicated by a single high sample.

To be on the safe side, however, it would be wise to collect all samples in this area from a depth of at least 10 in., although this may be difficult in the rocky soil of certain sections. It is important to prevent any soil above this depth from mixing with the sample, particularly surface material, which is extensively contaminated, especially with lead. Because there are not enough data from this survey to delimit completely the area of badly contaminated ground, no distance can be given beyond which contamination would not have to be considered; however, the 10-in. depth is highly recommended within at least a five-mile radius of the smelter area. Beyond this distance, suitable orientation sampling should be done if there is any question at all about the presence of contamination.

Results of the Kennedy and Hobbs study to date were generously made available to the author, who has indicated at appropriate places in the text where this information was utilized.

Publication of this article has been authorized by the Director, U. S. Geological Survey.

REFERENCES

[1] H. L. Cannon: Written communication.
[2] O. M. Clarke: Geochemical Prospecting for Copper at Ray, Ariz. *Economic Geology*, 1953, vol. 48, pp. 39-45.
[3] H. E. Hawkes: Written communication, 1957.
[4] L. C. Huff: Written communication, 1950.
[5] V. C. Kennedy and S. W. Hobbs: Written communication.
[6] H. E. Hawkes: Principles of Geochemical Prospecting. *USGS Bull. 1000F*, 1957.

Discussion of this article sent (2 copies) to AIME before Mar. 31, 1959, will be published in MINING ENGINEERING.

GRAVITY METHODS CLEAN EXTREME FINE SIZES OF BITUMINOUS COAL

Low-cost recovery and simple operation, with reduced ash and sulfur content in the yield of clean coal.

by H. B. CHARMBURY and D. R. MITCHELL

Recovery of fine coal from solids reporting to wash water has become increasingly important. These solids range from about 28 mesh to 0 and constitute 3 to 7 pct by weight of the feed tonnage to a coal preparation plant. In the past they were usually wasted to streams, but present clean stream legislation makes it necessary to remove them from the wash water and, if economically possible, recover the associated coal as a saleable product.

Where these solids are not wasted to streams or to slime ponds they are recovered by thickeners and filters. Since filter cake is often high in ash or sulfur, or both, it is not readily marketed or used. Common practice is to mix it with other plant products, generally slack or cleaned run-of-mine. Uniform blending is difficult, not only because the impurity is usually high, but also because during certain operating periods it is possible to get a concentration of this filter cake in a railroad or barge.

At some plants filter cake has been derived from the froth flotation clean-up of Dorr thickener underflow. The operating circuits required for a froth flotation plant make this a comparatively high-cost treatment, and in the last few years experiments have been carried out with bulk oil methods. These also are quite expensive and lend themselves only to special situations.

Table I gives some characteristics of thickener underflows for plants in the Pittsburgh area treating Pittsburgh seam coal. It will be noted that there is a concentration of impurities in the -200 mesh sizes.

H. B. CHARMBURY and D. R. MITCHELL, Members AIME, are respectively, Professor and Head, Department of Mineral Preparation, and Professor and Chairman, Division of Mineral Engineering, College of Mineral Industries, The Pennsylvania State University, University Park, Pa. TP 4787F. Manuscript, October 31, 1957. Joint Solid Fuels Conference AIME-ASME, Quebec, Canada, October 1957. AIME Trans., Vol. 214, 1959.

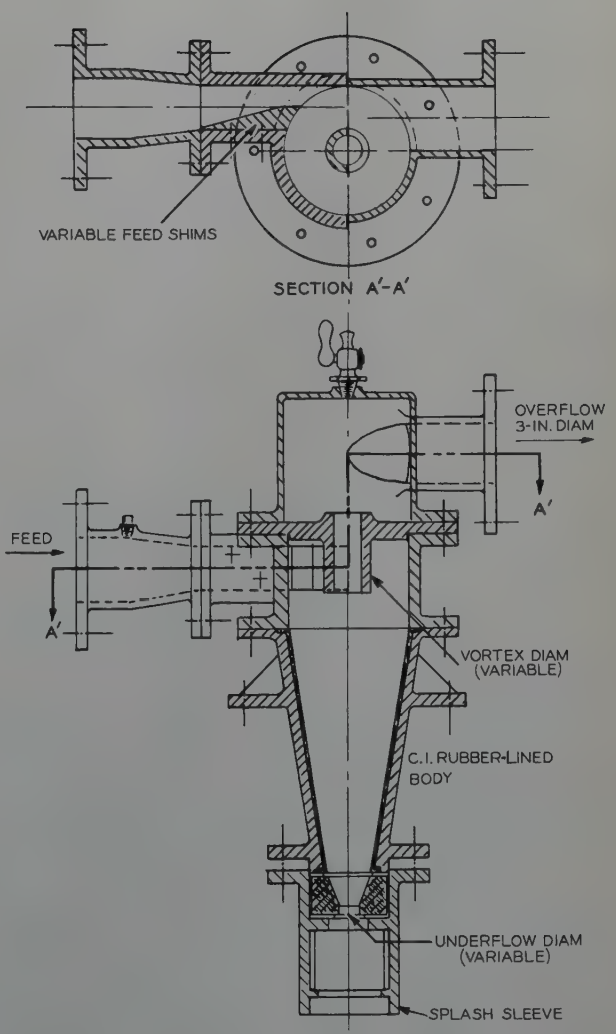

Fig. 1—The 6-in. Dorrclone for A and B samples.

Table I. Size, Ash, and Sulfur Analysis for Thickener Underflows

Mesh		Direct			Cumulative Retained		
Passing	Retained	Wt, Pct	Ash, Pct	S, Pct	Wt, Pct	Ash, Pct	S, Pct
			Plant A				
	48	13.2	7.8	1.46	13.2	7.8	1.46
48	100	45.4	6.0	1.52	58.6	6.4	1.51
100	200	23.5	18.3	2.76	82.1	9.8	1.87
200	325	14.3	34.2	5.37	96.4	13.4	2.39
325		3.6	40.1	6.44	100.0	14.4	2.53
			Plant B				
	48	20.0	6.1	1.40	20.0	6.1	1.40
48	100	22.7	6.6	1.46	42.7	6.4	1.43
100	200	24.5	14.8	2.36	67.2	9.4	1.77
200		32.8	41.8	2.52	100.0	20.1	2.02
			Plant C				
	48	17.7	8.0	1.65	17.7	8.0	1.65
48	100	24.5	10.5	1.87	42.2	9.5	1.78
100	200	20.7	19.1	2.63	62.9	12.7	2.06
200	325	17.3	27.2	2.30	80.2	15.8	2.11
325		19.8	43.7	2.27	100.0	21.3	2.14

Table II. Washability Data for +200 Mesh Fraction Thickener Underflow, Plant C

−200 mesh — 62.9 Pct—11.1 Pct Ash—2.02 Pct S
+200 mesh — 37.1 Pct—39.0 Pct Ash—2.21 Pct S
Head Analysis—100.0 Pct—21.3 Pct Ash—2.14 Pct S

Specific Gravity		Direct			Cumulative Float		
Sink	Float	Wt, Pct	Ash, Pct	S, Pct	Wt, Pct	Ash, Pct	S, Pct
	1.30	84.4	4.2	1.23	84.4	4.2	1.23
1.30	1.40	2.5	16.0	2.40	86.9	4.5	1.27
1.40	1.50	1.7	22.7	3.06	88.6	4.8	1.30
1.50	1.60	2.3	24.4	3.52	90.9	5.3	1.36
1.60	1.70	1.3	35.5	4.54	92.2	6.8	1.40
1.70		7.8	75.0	9.34	100.0	11.1	2.02

Table III. Results of Cleaning Thickener Underflow Material from Plant *A* in a 6-In. Cyclone

Conditions	Feed Inlet to Cyclone	Clean Coal Overflow Product	Refuse Underflow Product
Pulp, gpm	69.4	54.1	15.3
Solids, tph	10.8	5.9	4.9
Solids in pulp, pct	32.2	30.5	56.2
Total solids, pct	100.0	54.7	45.3
Ash in solids, pct	13.6	10.8	16.9
Sulfur in solids, pct	2.24	1.66	2.93

Table V. Results of Cleaning Thickener Underflow Material from Plant *B* in a 6-In. Cyclone

Conditions	Feed Inlet to Cyclone	Clean Coal Overflow Product	Refuse Underflow Product
Pulp, gpm	73.1	59.3	14.8
Solids, tph	8.45	5.89	2.56
Solids in pulp, pct	40.4	35.6	56.3
Total solids, pct	100.0	70.0	30.0
Ash in solids, pct	19.3	17.5	23.4
Sulfur in solids, pct	2.02	1.66	2.83

Table VII. Results of Gravity Belt Test with Thickener Underflow Material from Preparation Plant C

Product	Wt, Pct	Ash, Pct	Ash Distribution, Pct	S, Pct	Sulfur Distribution, Pct
Clean coal	88.2	19.2	77.5	1.65	70.5
Refuse	11.8	42.3	22.5	5.18	29.5
Calc. head	100.0	21.9	100.0	2.07	100.0

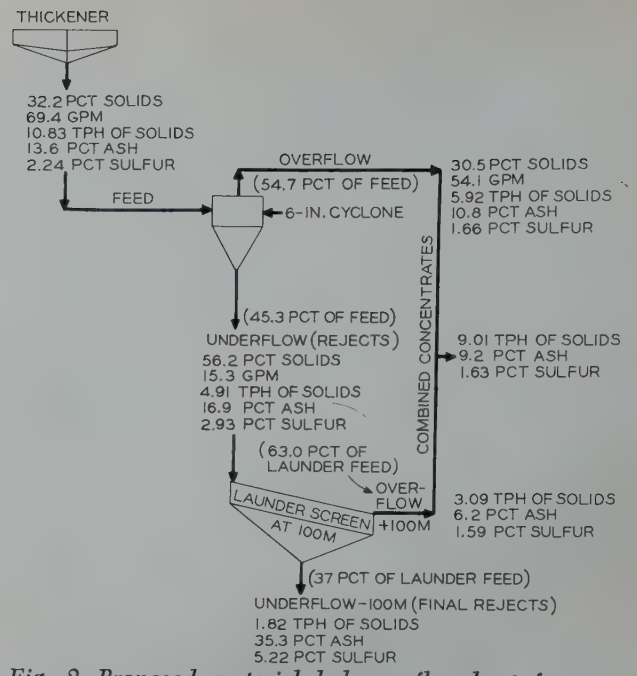

Fig. 2—Proposed material balance flowsheet for preparing clean coal from Plant A thickner underflow.

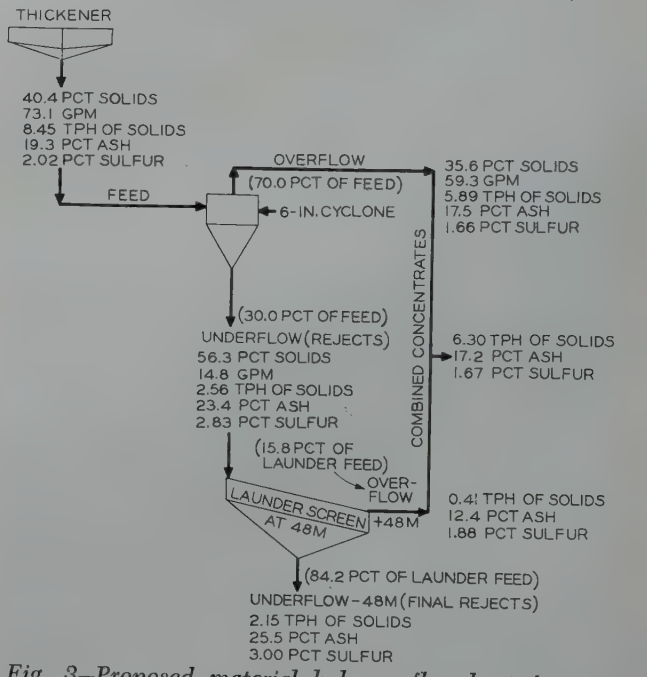

Fig. 3—Proposed material balance flowsheet for preparing clean coal from Plant B thickener underflow.

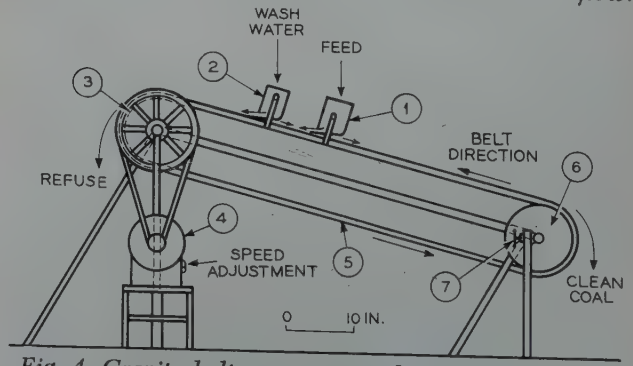

Fig. 4—Gravity belt separator used for plant C product. Legend: 1) feed box; 2) wash water box; 3) drive or head end; 4) variable speed motor; 5) waffle-grid, belt, ⅛-in. pockets; 6) tail end; and 7) separator slope adjustment.

Development of the launder screen, particularly in the anthracite region, has made it economically possible to do a partial cleaning job on fines of this character by sizing on the screen. With this type of screen, size separation is held to a lower limit of about 100 mesh, with coal loss, of course, in the undersize.

In recent years slimes have been effectively removed by low-pressure cyclones, which are economically sound for those plants where an underflow product of marketable grade can be obtained. The possibility of using high-pressure cyclones as concentrators for cleaning Dorr thickener underflow has been under investigation in the mineral dressing laboratories of The Pennsylvania State University for some time. Results have been encouraging, and at least one plant installation has been made for this purpose and is now operating. The laboratory has also developed a gravity method of separation that utilizes stream flow action on a specially designed traveling belt machine. These two units, cyclones and gravity belt separators, have proved effective in removing sulfur from Dorr thickener underflows, so that it is possible to obtain a low sulfur product suitable for blending with other products of the preparation plant. This is particularly important to plants preparing coal for metallurgical purposes.

Coals Investigated: The coals used in these tests were obtained from slurry samples taken as thickener underflows from three preparation plants in the Pittsburgh area of Pennsylvania. These coals, which vary from 2.02 to 2.53 pct sulfur and 14.4 to 21.3 pct ash, represented an enormous quantity of marketable material if the ash content could be reduced and, more particularly, if the sulfur content could be lowered below 1.70 pct.

Table I shows the size, ash, and sulfur analyses of the coals from the three different preparation plants, *A*, *B*, and *C*. Calculations of the cumulative oversize indicate that specification grades of less than 1.70 pct sulfur may be attained by sizing. If samples *A* and *B* were separated at some size in the range of 100 to 200 mesh, specification grade clean coal with less than 1.70 pct sulfur could be obtained. The ash content of the coal from plant *A* would be lowered from 20.1 to less than 9.0 pct. Recoveries, in these cases, would range from 60 to 70 pct.

The sample from plant *C*, however, would have to be sized at about 48 mesh to meet specification grade. In this instance the ash would be lowered from 21.3 to 8.0 pct, but clean coal recovery would amount to only 17.7 pct of the total coal.

Table II lists washability data on the +200 mesh fraction of thickener underflow material from plant *C*. Calculations using these data indicate that cleaning only the +200 mesh material at a gravity of 1.70 will increase recovery from the 17.7 pct shown above to 58.0 pct (62.9 x 0.922). In this case sulfur would be lowered from 2.14 to 1.40 pct and ash from 21.3 to 6.8 pct. Also, should the −200 mesh fraction representing 37.1 pct of the coal and having 39.0 pct ash and 2.2 pct sulfur be blended into the clean portion of the +200 mesh obtained at a gravity of 1.50, a clean coal with less than 1.65 pct sulfur and 18.5 pct ash could be produced and recovery could be raised to 92.8 pct. Thus the combination of sizing and gravity concentration with reasonable recovery to meet specification grade appears theoretically possible and attractive.

Cyclone Tests with Samples A and B: Details of the 6-in. diam cyclone used in this work are presented in Fig. 1. The feed inlet opening to the

Table IV. Size, Ash, and Sulfur Analyses of Cyclone Products from Plant *A* Slurry

Mesh		Direct			Cumulative Retained			Cumulative Passing		
Passing	Retained	Wt, Pct	Ash, Pct	S, Pct	Wt, Pct	Ash, Pct	S, Pct	Wt, Pct	Ash, Pct	S, Pct
				Clean Coal Overflow Product 54.7 Pct of Feed						
	48	9.6	10.0	1.27	9.6	10.0	1.27	100.0	10.8	1.66
48	65	18.6	4.8	1.38	28.2	6.6	1.34	90.4	10.9	1.70
65	100	26.8	6.4	1.45	55.0	6.5	1.40	71.8	12.5	1.79
100	200	24.8	9.3	1.66	79.8	7.4	1.48	45.0	16.1	1.99
200	325	16.6	23.2	2.36	96.4	10.1	1.63	20.2	24.5	2.39
325		3.6	30.2	2.54	100.0	10.8	1.66	3.6	30.2	2.54
				Refuse Underflow Product 45.3 Pct of Feed						
	48	17.2	6.1	1.44	17.2	6.1	1.44	100.0	16.9	2.93
48	65	20.5	5.2	1.50	37.7	5.6	1.47	82.8	19.2	3.24
65	100	25.3	7.0	1.76	63.0	6.2	1.59	62.3	23.8	3.82
100	200	22.2	28.2	2.86	85.2	11.9	1.92	37.0	35.3	5.22
200	325	11.9	44.9	8.39	97.1	15.9	2.71	14.8	45.9	8.77
325		2.9	50.0	10.34	100.0	16.9	2.93	2.9	50.0	10.34

Table VI. Size, Ash, and Sulfur Analyses of Cyclone Products from Plant *B* Slurry

Mesh		Direct			Cumulative Retained			Cumulative Passing		
Passing	Retained	Wt, Pct	Ash, Pct	S, Pct	Wt, Pct	Ash, Pct	S, Pct	Wt, Pct	Ash, Pct	S, Pct
				Clean Coal Overflow Product 70.0 Pct of Feed						
	48	10.1	4.5	1.28	10.1	4.5	1.28	100.0	17.5	1.66
48	100	25.0	5.6	1.31	35.1	5.3	1.30	89.9	19.0	1.70
100	200	22.8	8.6	1.58	57.9	6.6	1.41	64.9	24.2	1.85
200		42.1	32.6	2.00	100.0	17.5	1.66	42.1	32.6	2.00
				Refuse Underflow Product 30.0 Pct of Feed						
	48	15.8	12.4	1.88	15.8	12.4	1.88	100.0	23.4	2.83
48	100	24.9	15.2	2.14	40.7	14.1	2.04	84.2	25.5	3.00
100	200	24.2	17.5	3.16	64.9	15.4	2.46	59.3	29.8	3.37
200		35.1	38.3	3.51	100.0	23.4	2.83	35.1	38.3	3.51

cylindrical part of the cyclone was 1½ in. square. Vortex diameter was 2½ in. and overflow outlet diameter 3 in. Underflow was discharged through a ⅝-in. diam orifice.

Plant *A* thickener underflow containing 32.2 pct solids was pumped into the cyclone at 69.4 gpm at 40-psi inlet pressure. Details of the sample to the cyclone and the clean coal and refuse products from the cyclone are presented in Table III. From these results it may be seen that the clean coal met specification grade with 1.66 pct sulfur and that ash was reduced from 13.6 to 10.8 pct. Recovery of clean coal was 54.7 pct.

The size, ash, and sulfur analyses of the overflow and underflow products are presented in Table IV. From these results it appears that, under the conditions tested, the cyclone acted as a concentrating unit rather than as a classifier. It may also be seen that if the underflow were sized at 100 mesh, more specification grade material could be recovered and overall recovery of the clean coal with less than 1.65 pct sulfur could be raised to 83.2 pct. Fig. 2, based on the above results, is the proposed flowsheet for recovering specification grade clean coal from thickener underflow fines from preparation plant *A*.

Similar results of a cyclone test with the thickener underflow material from preparation plant *B* are presented in Tables V and VI and Fig. 3. From these results it may be seen that a clean coal with 1.66 pct sulfur and 17.5 pct ash was obtained from a feed to the cyclone with 2.02 pct sulfur and 19.3 pct ash. Clean coal recovery in this test was about 70 pct. Sizing the underflow material from the cyclone at 48 mesh raised recovery to 74.6 pct.

In the above cases the cyclone acted as a concentrator rather than as a sizing classifier because inlet pressures and specific gravities of the inlet suspension were relatively high. The high inlet pressures resulted in greater centrifugal force to throw the particles to the periphery of the cylindrical section, and the high percentage of solids created a barrier on the periphery, forcing the lighter coal particles into the center and the heavier refuse particles to the outside.

Other factors of importance in this type of cyclone operation were the vortex and underflow diameters. These were adjusted so that some 80 pct of the pulp reported in the overflow and about 20 pct in the underflow.

It is to be noted that the high-pressure cyclone is particularly effective in concentrating sulfur in the underflow. This is undoubtedly due to the higher specific gravity of pyrite compared to slate and coal and is especially important at metallurgical coal plants. Usually a relatively high ash filter cake product can be mixed in with the overall plant product, but not a high sulfur filter cake. Also, since the cyclone can be operated on straight thickener underflows without added water, processing by the cyclone method is much simpler than by other methods requiring large quantities of water.

The attrition effect in pumps and in the cyclone tends to free coal particles from impurities and gives recoveries higher than indicated by sizing and sink-float tests of the feed. Tests are projected to determine the effect of closer sizing or classification on results that might be obtained on processing thickener underflows in high-pressure cyclones.

Gravity Belt Test with Sample C: Since the thickener underflow product from preparation plant *C* had a size consist and analysis entirely different from the products of plants *A* and *B*, a different method of concentration was investigated. Washability data on the plant *C* product indicated that gravity concentration was feasible.

The apparatus used for concentration was the gravity belt separator illustrated in Fig. 4. This is a continuous belt separator set at a slope, with the belt traveling uphill. This rectangular belt is 5 in. wide and 1 in. deep and has a waffle-type surface with ⅛-in. cubes. Other waffle-type surfaces are available.

Feed suspension flows by gravity through a ¾-in. hose into a feed box over the belt center, giving an even distribution of pulp across the width of the belt, which travels counter to the flow. Heavy refuse particles are trapped in the waffles, carried over the top of the belt, and washed with spray water into a launder; the lighter clean coal particles flow over the belt and are discharged at the lower end. Upstream from the feed, provisions are made to dilute the original pulp with water from a box similar to the feed box.

Operation variables are slope, belt speed, feed flow rate, density, and amount of wash water. An increase in slope increases the yield of clean coal but also raises the percent sulfur. Greater belt speed decreases the yield with very little change in percent sulfur. Faster flow rate rapidly increases recovery of clean coal but usually sacrifices cleanliness of products. The percent sulfur in the clean coal rises with increased flow rate, particularly at the higher rates. Changes in feed pulp density have very little effect on the recovery or grade of clean coal. Increases in pulp density do slightly increase the percent sulfur in the refuse. The use of wash water increases recovery of clean coal but also the percent sulfur in the clean coal. It also increases sulfur in the refuse.

As a result of these findings, tests were conducted with thickener underflow material from plant *C*, using a slope of 9°, belt speed of 6.5 fpm, and a pulp rate of about 1 gpm with 17 pct solids. No wash water was used during the test. Results under these conditions (Table IV) show a clean coal recovery of 88.2 pct with specification grade sulfur. Sizing and washability data indicated a theoretical recovery of 92.8 pct with 1.65 pct sulfur. Theoretical data also indicated 18.5 pct ash with this sulfur value. The belt test showed an ash reduction from 21.9 pct in the feed to 19.2 pct in the clean coal. This indicates that the belt was removing mainly the heavy particles, such as pyrite, in the refuse.

Further reductions in sulfur content of the clean coal were made by passing the clean coal product from the first test over the belt a second time, which produced a recleaned coal and middling product in addition to the refuse. Conditions were the same for test No. 2, except that pulp density was reduced to 15 pct solids. The second test showed reduction of sulfur to 1.54 pct, with a clean recovery reduction to 79.4 pct. The middling product amounted to 8.8 pct of the total feed and contained 34.1 pct ash and 2.51 pct sulfur.

A number of tests were made on this traveling belt separator. At optimum conditions it proved an effective machine for removing fine pyritic sulfur from thickener underflows. The machine is easy to construct, and in normal plant operation maintenance cost would be low.

Discussion of this article sent (2 copies) to AIME before March 31, 1959, will be published in MINING ENGINEERING.

SUBSURFACE INVESTIGATIONS OF A PLANT SITE

by LeROY SCHARON, ROBERT UHLEY, and TSVI MEIDAV

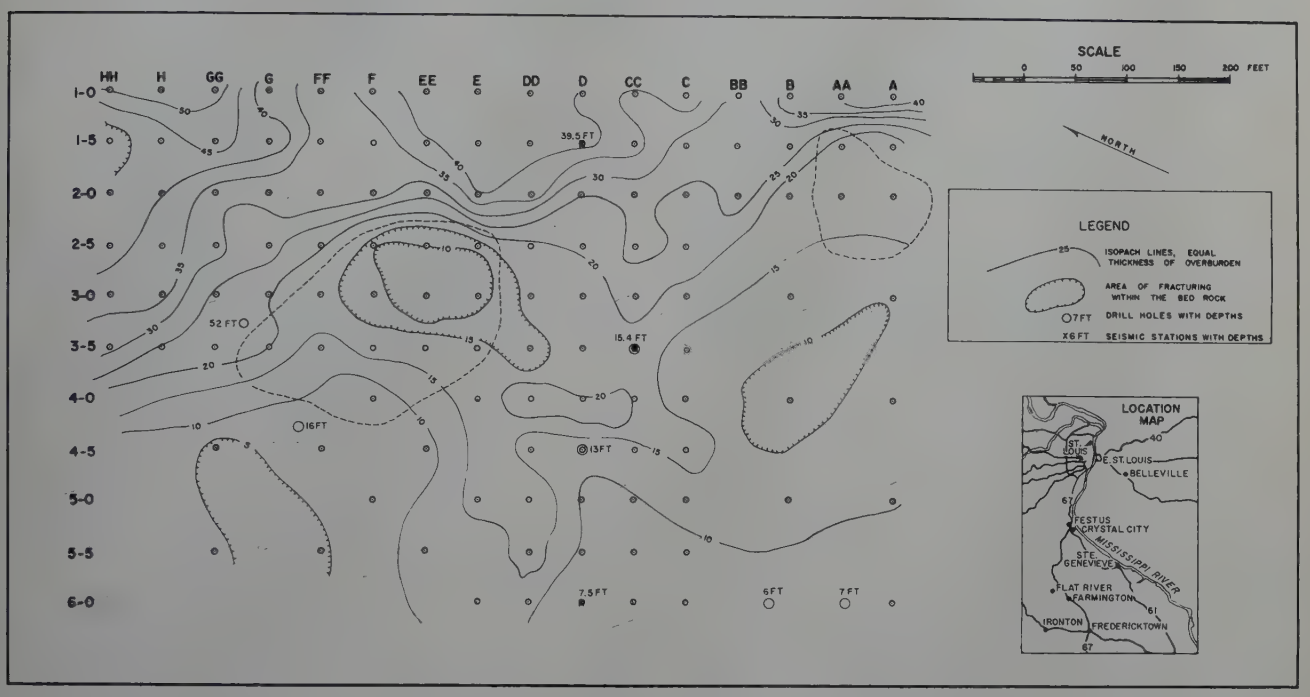

Fig. 1—Isopach map of overburden showing areas of deeply fractured bedrock.

Before National Lead built an industrial plant on its Fredricktown property, some 100 miles south of St. Louis, a 750x500-ft area on the proposed site was investigated by electrical resistivity, seismic refraction, and churn drilling. Data were accumulated to prepare an isopach map of the overburden and to determine soundness of the dolomite bedrock and the depth to bedrock at fixed points.

The site was on a gently sloping hillside. Elevations above sea level ranged from 760 ft in the northwest corner to 820 ft along the eastern edge, giving a total relief of 60 ft. There were no major drainage features, but in the northern part of the plant site there was an indicated depression area which later was interpreted as reflecting subsurface conditions in the bedrock. No rock was exposed in the entire plant site area; the surface was characterized by soil and overburden.

GEOLOGY

Prevailing geology in the area of investigation was relatively simple—Bonneterre dolomite overlain by residuum. The red overburden was that derived from the weathered Bonneterre. Some chert was present, interpreted in the general area as a weathering of both the Bonneterre dolomite and younger sedimentary rocks such as the Potosi dolomite. During the period of actual measurements the residuum varied from moist near surface on the western edge of the proposed site to dry near surface on the eastern edge, and for this reason overburden resistivities ranged from low on the west to high on the east. Seismic velocities were low, since the material was not well packed.

The bedrock encountered was dolomite, specifically the Bonneterre of Upper Cambrian age which, according to McQueen,[1] consists of an upper dark gray member and a lower light gray member. These have been further divided into four zones, in ascending sequence a dark gray, sandy argillaceous dolomite; a dark brown or black, fine-grained dolomite; a light gray, finely crystalline, compact dolomite; and, at the top, a dark brown, finely crystalline, compact dolomite. In the area of investigation the upper two zones were encountered in the drilling tests as constituting the bedrock. The dolomite varies widely in porosity, which is low in the dense, fine-grained layers. In this area, therefore, both electrical resistivities and seismic velocities were high.

Fracture zones in the Bonneterre are nearly vertical and may extend to some depth, causing considerable deep weathering. It was realized that over deep fracturing the apparent resistivities

L. Scharon, Member AIME, is Professor of Geophysics, Washington University, St. Louis, Mo.; R. Uhley is Chief Geologist, St. Louis Smelting & Refining Div., National Lead Co., Fredericktown, Mo.; and T. Meidav is Washington University Fellow in Geology, Washington University, St. Louis, Mo. TP 4789L. Manuscript, April 11, 1958. New Orleans Meeting, February 1957. AIME Trans., Vol. 214, 1959.

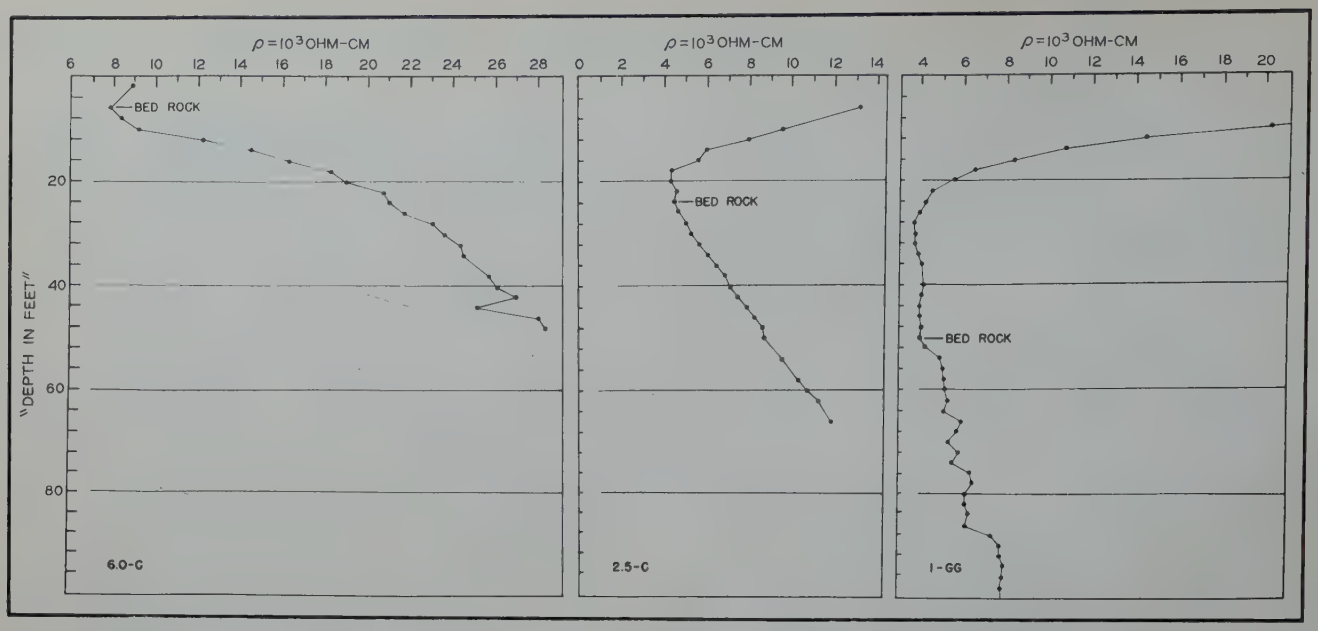

Fig. 2—Correlation chart showing increase in depth to bedrock from west to east in the area.

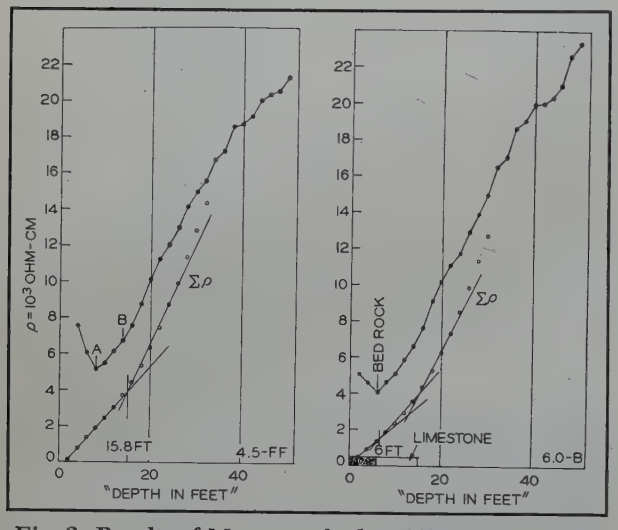

Fig. 3—Results of Moore method at 4.5-FF and 6.0-B.

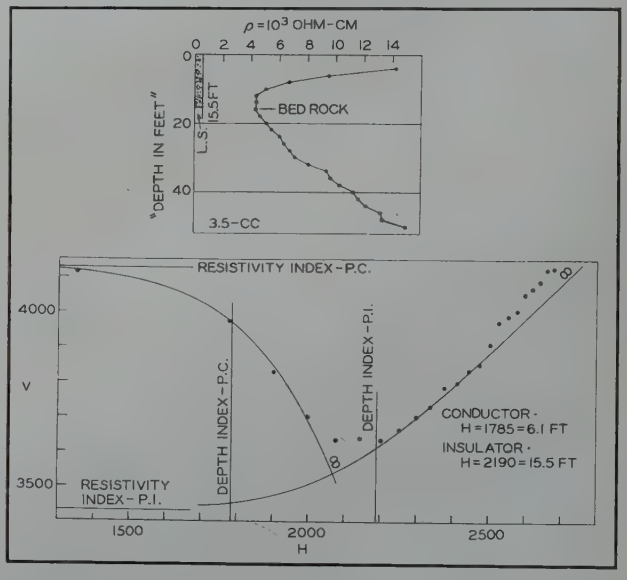

Fig. 4—Roman superposition results for station 3.5-CC.

would be extremely low, owing to the presence of mineralized waters and clays, and it was believed important to the investigation to recognize and outline such conditions.

Two holes were drilled in the plant site area, one at 4.5-D and the other at 3.5-CC. Data were available from four previous holes, but locations and information were considered doubtful. Reportedly they were 15 ft west of 6.0-B, 45 ft west of 6.0-A, 25 ft northwest of 4.5-FF, and near stations 3.0-GG and 3.5-G. All four yielded data indicating bedrock to be the Bonneterre dolomite with a clay and chert residuum.

GEOPHYSICS

Electrical resistivity was measured with equipment of the Gish-Rooney type[2] according to the Wenner[3] electrode configuration. At 124 stations, located on 50 and 100-ft centers (Fig. 1), profiles were measured by an interval of $a = 2$ ft to depths of 50 to 100 ft. Ten working days were required to make those measurements and determine the elevations at each station.

Following preliminary interpretation of the electrical data, shallow seismic refraction measurements were made at three points: 1) shallow depth to bedrock at 6.0-D, 2) medium depth to bedrock at 3.5-CC, and deep bedrock at 1.5-D. The seismic work was completed in less than a day.

Results: The aims of the subsurface investigation were readily met by combining results of the two types of geophysics and the check drilling. Compiled as an isopach map of the overburden, these results are given in Fig. 1, which shows the seismic stations and drillholes and their indicated depth to bedrock. Two areas of highly fractured zones in the bedrock are presented, one centered at coordinate 2.0-AA and the other at 3.5-F.

Interpretation of Electrical Data: When all the electrical resistivity depth profiles for the survey were assembled, one fact about depth to bedrock was revealed—it increased from the west to the east side of the area. The correlation of three profiles (6.0-C, 2.5-C, and 1.0-GG) in Fig. 2 shows that as depth to bedrock increases there is a marked change in apparent resistivities of the dolomite.

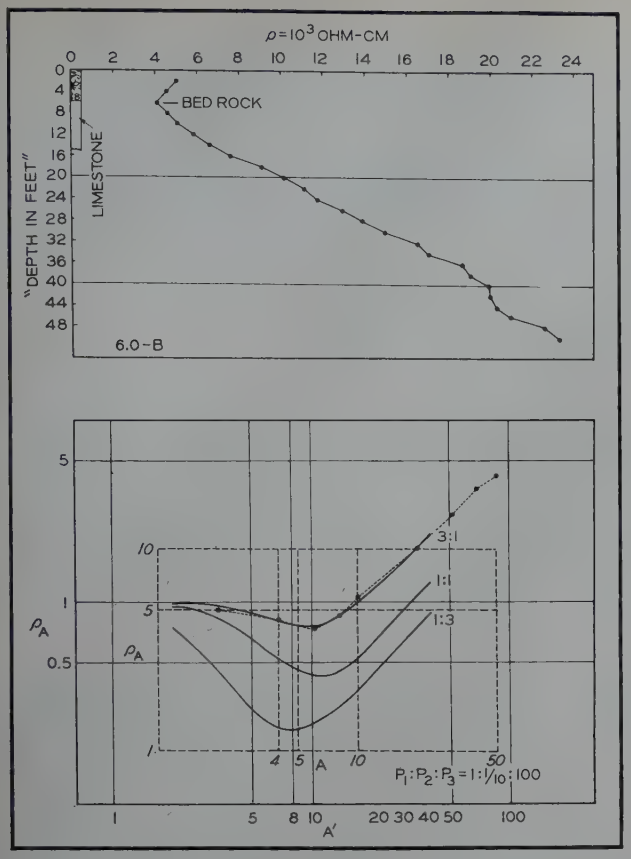

Fig. 5—Wetzel-McMurry interpretation for station 6.0-B.

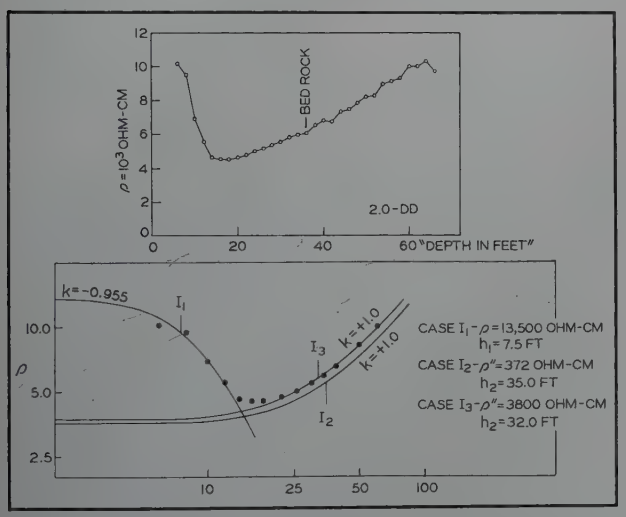

Fig. 6—Successive interpretation for station 2.00-DD.

Overburden resistivities, also given on this map, are directly associated with surface moisture content at the various elevations. At lowest elevation the resistivities are low; at maximum elevation they are very high.

Cumulative Resistivities: For most of the profiles the unknown depths to bedrock could be calculated from those already known, and early interpretations of electrical data seemed fairly straightforward because of the extreme contrast in resistivities between dolomite bedrock and residuum. But when the seismic refraction and drilling results became available, they pointed up the need for more precise interpretations. Depth to bedrock at station 4.5-FF was originally interpreted as 8 ft (break A, Fig. 3), while a drillhole 25 ft northwest of this station indicated dolomite at 16 ft. Because of the resistivity contrast, it was believed that point A was the depth to dolomite. A cumulative resistivity profile after Moore's method,[4] however, showed the break at point B, or a depth of 15.8 ft. To test the validity of this method still further, cumulative resistivity data were made for station 6.0-B (Fig. 4), where a drill check gave bedrock at a depth of 6 ft. A good resistivity break occurs on both the apparent and summation apparent resistivity curves at 6 ft. After all profiles of the general character of 4.5-FF and 6.0-B had been analyzed by the Moore method, it was concluded that this method can be applied only to profiles having a definite character. Mooney[5] has described the limitations of Moore's approach.

Roman Superposition Method: When the Moore analysis proved unsuitable for these data, they were interpreted by theoretical procedures. The following application of Roman's superposition method[6] is summarized in Fig. 4:

At station 3.5-CC both seismic and drilling checks were made, giving a calculated depth of 15.5 ft and 15.33 ft, respectively. Depth to the perfect insulator was calculated to be 15.5 ft—a very close agreement with seismic and drilling results. Since it was possible to correlate a portion of the resistivity curve with the "Reference Chart for Buried Conductors," depth to the perfect conductor was found to be 6.1 ft, which may be a reflection of the top of the water table.

Wetzel-McMurry Standard Curves: The Wetzel-McMurry set of standard apparent resistivity curves[7] for the three-layer case, using the Wenner electrode configuration, were matched with the field curves obtained. Typical results are given in Fig. 5, in which the original curve for station 6.0-B is superposed on a set of standard curves. The standards have the ratios for the three layers $\rho_1:\rho_2:\rho_3 = 1:1/10:100$, with h_2 (thickness of overburden) equal to 8 units on the standards. It will be seen that the number 8 on the standard curves corresponds to a, equal to 4.7 ft. This is the interpreted depth to bedrock. At this station, as indicated in Fig. 6, a drillhole available for checking purposes gave bedrock at 6 ft. Apparently depth to bedrock is more precise on the original field curve.

Successive Approximation Method: Hummel[8] has shown that a three-layer case may be solved by combining the thickness and resistivities of the upper two layers, using Kirchoff's Law:

$$\frac{d_1 + d_2}{\rho''} = \frac{d_1}{\rho_1} + \frac{d_2}{\rho_2}$$

where ρ_1 and ρ_2 are resistivities; d_1 and d_2 are thicknesses of the first and second layers, respectively; and ρ'' is the composite resistivity of the two layers. The solution for the third layer is found by using Roman's two-layer case. Watson and Johnson[9] and Spicer[10] have demonstrated that under favorable conditions this technique can be applied to the multi-layer case.

Analysis of the apparent resistivity profile at station 2.0-DD (Fig. 6) gives the application of this technique. First a Roman two-layer curve (I_1) was matched with the shallow part of the field profile, giving a value of $k = -0.96$, depth of h_1 as 7.5 ft, and ρ_1 equal to 13,500 ohm cms. When the resistivity ρ_2 was computed in the following equation, it was found to equal 311 ohm cms:

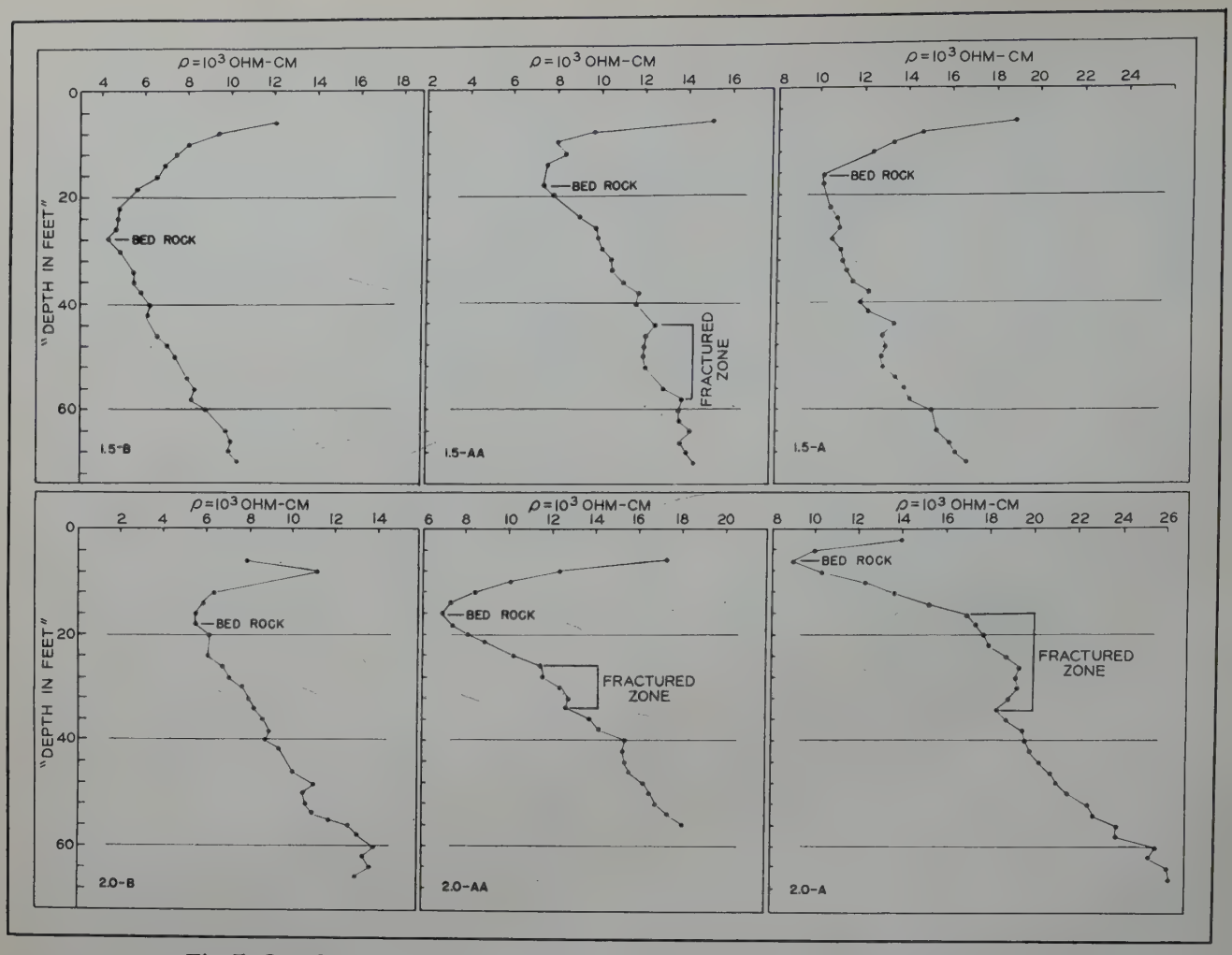

Fig. 7—Correlation chart showing method of delineating fractured zones in bedrock.

$$\rho_2 = \rho_1\left(\frac{1+k_1}{1-k_1}\right) =$$

$$13{,}500\left(\frac{1-0.955}{1+0.955}\right) = 311 \text{ ohm cms}$$

To determine the composite resistivity (ρ'') of the first two layers it is necessary to know the thickness of the second layer, d_2. This is approximated by applying Roman's two-layer curves to the deeper part of the field profile. In this operation h_2, the total depth to the bottom of the second layer, was found to be 35 ft; d_2 was then equal to 27.5 ft. Using Kirchoff's Law, the composite resistivity is computed as 372 ohm cms. The master curve is then superposed on the field curve with depth and resistivity indices corresponding to 35 ft and 372 ohm cms respectively, as shown by curve I_2. It is obvious that this fit is incorrect. A much better match can be obtained, however, by shifting the curve horizontally to the left. Correspondingly, the depth index shifts to 32 ft, and recomputing with the new d_2 gives ρ'' a value of 3800 ohm cms. When the new depth and resistivity indices are matched a better fit is obtained, as shown by curve I_3. The interpreted depth to bedrock in this example is then 32 ft, not 35 ft as obtained by the first approximation or 36 ft as empirically interpreted on the original field profile.

Fractured Zones: As indicated in Fig. 1, two areas of fractured zones have been outlined. To determine the presence of such zones the original field profiles were used in the manner shown in Fig. 7. These data illustrate the interpretation of the fractured zone centered at coordinate 2.0-AA. As demonstrated throughout the survey, when the dolomite bedrock was encountered the apparent resistivities increased rapidly. As long as these resistivities continued to increase to the depth measured, it could be assumed that the rock was sound and free from fractures or cavernous conditions. Wherever such conditions do prevail in the dolomite a reversal or decrease in apparent resistivity would be expected, especially during the time of the survey when the water table was high. Of the six curves shown in Fig. 7, three exhibit reversals in resistivity trends and have been noted as the "fractured zone." The fractured zone centered at coordinate 3.5-F affected many more stations than the one illustrated. In this latter case it is quite possible that fracturing extended up to the overburden. This is probably reflected in the slight drainage pattern in the original topography.

Conclusions: From a practical point of view the survey was successful, for it indicated that bedrock would not be encountered in any excavation required for the proposed buildings. The interpretation of results, however, points up the need for both empirical and theoretical analysis even on what appear to be the most obvious in field results, and experience in this particular survey shows the advisability of several methods of interpretation.

REFERENCES

[1] H. S. McQueen: Occurrence of Dolomite in the Frederick Area, Madison County, Missouri. Missouri Geological Survey and Water Resources, *62nd Biennial Report*, State Geologist, 1941-42.
[2] O. H. Gish: Improved Equipment for Measuring Earth-Current Potentials and Earth Resistivity. National Research Council *Bull.*, November 1926, vol. 2, part 2.
[3] F. Wenner: A Method of Measuring Earth Resistivity. National Bureau of Standards *Bull.*, 1916, vol. 12, no. 3.
[4] R. W. Moore: An Empirical Method of Interpretation of Earth Resistivity Measurements. AIME, *TP 1743*, 1944.
[5] H. M. Mooney: Depth Determinations by Electrical Resistivity. *AIME Trans.*, 1954, vol. 199, pp. 915-918.
[6] I. Roman: Superposition in the Interpretation of Two-Layer Earth Resistivity Curves. *USGS Bull. 927-A*, 1941.
[7] W. W. Wetzel and H. V. McMurry: A Set of Curves to Assist in the Interpretation of the Three-Layer Resistivity Problem. *Geophysics*, 1937, vol. 2.
[8] J. N. Hummel: A Theoretical Study of Apparent Resistivity in Surface Potential Methods. AIME, Geophysical Papers, 1932.
[9] R. J. Watson and J. F. Johnson: On the Extension of Two-Layer Methods of Interpretation of Earth Resistivity Data to Three or More Layers. *Geophysics*, vol. 3, 1938.
[10] H. C. Spicer: Handbook for Resistivity Exploration Using Gish-Rooney Equipment. *USGS Bull.* In preparation.

Discussion of this article sent (2 copies) to AIME before Mar. 31, 1959, will be published in MINING ENGINEERING.

Technical Note

SPHALERITE FLOTATION WITH GUANIDINE COMPOUNDS AND DERIVATIVES AS COLLECTORS

by PIERRE R. HINES

Diphenyl guanidine is used as an accelerator in vulcanizing rubber. Other rubber accelerators are also flotation collectors, e.g., dithiocarbamate, thiazole, and the xanthates.

Urea and its derivatives are good flotation collectors,[1] and guanidine is the nitrogen analog of urea. These two characteristics suggested testing diphenyl guanidine as a flotation collector. Diphenyl guanidine has been tried in flotation work previously, but references give no details.[2-4]

Bunker Hill Co. of Kellogg, Idaho, supplied the ore sample used in these tests. The sample was typical of the ore milled in 1949 and contained 4.52 pct Pb and 1.08 pct Zn. A flotation test made by the author with potassium ethyl xanthate as a collector, the same flotation reagents, and the same grind employed in regular Bunker Hill mill practice was the standard for comparing results with the compounds and derivatives of guanidine.

The compounds and derivatives of guanidine are only fair collectors of galena. However, if potassium ethyl xanthate were used in the galena float, its presence later in the sphalerite float would make it impossible to introduce another type of collector and be certain which collector contributed the result, so the compound or derivative of guanidine under test was used in both the galena and sphalerite floats in Table I. On both the galena and the sphalerite in the Bunker Hill ore, the depressing action of sodium cyanide and zinc sulfate is much greater with collectors of the guanidine type than with the xanthates. If the depressing agents are left out when a guanidine type of collector is used, but a pH of 8.6 is maintained with either lime or sodium carbonate, the depressing action is approximately the same as in the standard xanthate test. Consequently the depressing agents, sodium cyanide and zinc, were not used in the galena floats of tests 1226, 1228, and 1286, Table I, so the galena floats would be on a comparable basis with the standard xanthate test.

As shown by the tests in Table I, the loss in the tail when diphenyl guanidine is used is 8.3 to 9.3 pct, as compared to 17.6 pct with potassium ethyl xanthate, or a recovery of 2.3 to 2.0 lb more zinc. Concentrate grade is 13.7 pct with potassium ethyl xanthate and increases to 22.9 and 31.8 pct with diphenyl guanidine, showing a much higher selectivity. Unless the Barrett's No. 4 coal tar creosote is considered to be a collector, no collector other than diphenyl guanidine is present in the tests, Nos. 1226, 1228, and 1286.

Tests 1218, 1253, and 1263 in Table II were run to check the effect of the depressing agents used in flotation of the galena (sodium cyanide and zinc sulfate) upon subsequent flotation of sphalerite by diphenyl guanidine. Urea was substituted for potassium ethyl xanthate in tests 1253 and 1263 because it is a good collector for galena and a poor one for sphalerite, and the effect of the depressing agents is more marked with urea than with potassium ethyl xanthate. Test 1205 checks the effect of urea alone without any depressing agents when used for the flotation of galena.

Table II shows that diphenyl guanidine as a collector for sphalerite is compatible with other flotation reagents used in floating galena. When the depressing agents sodium cyanide and zinc sulfate are used in the galena flotation step, the amount of lime in the sphalerite flotation must be increased (compare 1253 and 1263).

Table III gives some of the compounds of guanidine which were tested and compared. Some of the compounds and derivatives of guanidine* are soluble in water and others are not. Those tested were fed dry.

* Diphenyl guanidine is in commercial production and is available on the market.

When an organic collector is promising, its compounds and derivatives should be tested and their comparative collecting power recorded. Eventually, in this way, it may be possible to discover some of the essential chemical characteristics of a good collector. For example, it is interesting to compare the diphenyl and dibutyl derivatives in Table IV with those of urea in Table III, Example 3, U. S. Patent 2,664,198. All are good collectors.

Table I shows some of the effects of lime on recovery of sphalerite by diphenyl guanidine. Table V

P. R. HINES, Member AIME, is a Mining Engineer in Portland, Ore. TN 462B. Manuscript, Sept. 29, 1958.

Table I. Compounds and Derivatives of Guanidine in Floats

	Tail Assay and Zinc, Pct	Total Zinc Lost in Tail, Pct	Concentrate Grade, Zn, Pct	Collector
Standard Z-3	0.22	17.6	13.7	Z-3
1226	0.11	8.3	24.0	DPG
1228	0.09	8.5	22.9	DPG
1286	0.12	9.3	31.8	DPG

Reagents, Lb per Ton, Standard Test

Galena Float	Sphalerite Float
0.06 Z-3, 1.1 Na_2CO_3	0.33 $CuSO_4$, 0.1 CaO, 0.066 Z-3
0.15 NaCN, 0.40 $ZnSO_4$	Pine oil as needed
Bunker Hill frother as required	

Reagents, Lb per Ton, Tests 1226, 1228, and 1286 with Diphenyl Guanidine

1226 0.1 DPG, 1.0 CaO	0.33 $CuSO_4$, 0.1 DPG
1228 0.1 DPG, 1.0 CaO	0.33 $CuSO_4$, 0.1 DPG, 2.0 CaO
1286 0.1 DPG, 2.0 Na_2CO_3	0.33 $CuSO_4$, 0.1 DPG, 3.0 CaO
Bunker Hill frother as required	Pine oil as needed

Bunker Hill Frother	Pct
Amyl alcohol	5
Pine oil	10
Barrett's No. 4 coal tar creosote	85

Table II. Amounts of Galena and Sphalerite Float Reagents

Galena Float Reagents, Lb per Ton				
1218	0.06 Z-3	1.1 Na_2CO_3	0.15 NaCN	0.4 $ZnSO_4$
1253	0.1 Urea	4.0 Na_2CO_3	0.15 NaCN	0.4 $ZnSO_4$
1263	0.1 Urea	4.0 Na_2CO_3	0.15 NaCN	0.4 $ZnSO_4$
1205	0.3 Urea	2.0 Na_2CO_3	— —	— —

Sphalerite Float Reagents, Lb per Ton				Tail Assay, Zn, Pct	Total Zinc Lost in Tail, Pct	Concentrate Grade, Zn, Pct
1218	0.1 DPG	0.33 $CuSO_4$	1.5 CaO	0.12	10.9	18.4
1253	0.1 DPG	0.33 $CuSO_4$	1.0 CaO	0.22	18.2	30.8
1263	0.1 DPG	0.33 $CuSO_4$	3.0 CaO	0.13	11.9	24.6
1205	0.1 DPG	0.33 $CuSO_4$	1.5 CaO	0.09	7.8	17.9

Table III. Test Results for Guanidine Compounds

Compound	Tail Assay, Zn, Pct	Total Zinc Lost in Tail, Pct	Grade of Concentrate, Zn, Pct
Guanidine nitrate	0.15	13.5	26.3
Guanidine hydrochloride	0.17	17.1	23.4
Guanidine acetate	0.18	17.6	21.1
Amino-guanidine bicarbonate	0.30	32.4	13.2
Cyano guanidine	0.41	38.1	15.0
Guanidine carbonate	0.46	40.4	15.7
Guanidine sulfate	0.49	40.8	14.5

Table IV. Some Derivatives of Guanidine Tested and Compared

Derivative	Tail Assay, Zn, Pct	Total Zinc Lost in Tail, Pct	Grade of Concentrate, Zn, Pct
1-3 Di-o-tolyl-guanidine	0.12	9.8	24.1
Dibutyl guanidine picrate	0.12	10.9	12.1
N N′ di-n-butyl guanidine nitrate	0.12	12.2	11.7
Diphenyl guanidine	0.12	9.3	31.8
Methyl guanidine sulfate	0.13	13.8	11.7
Triphenyl guanidine	0.19	16.4	21.6
Dimethyl guanyl guanidine	0.27	25.3	22.6
Potassium ethyl xanthate	0.22	17.6	13.3

Table V. Effects of Lime on Recovery of Sphalerite by Diphenyl Guanidine

Lime, Lb per Ton	pH	Assay Zinc in Tail, Pct	Loss Total Zinc in Tail, Pct	Concentrate Grade Assay, Zn, Pct
		Diphenyl Guanidine		
1.0	8.6	0.13	11.4	20.3
2.0	9.2	0.13	11.5	28.6
3.0	9.8	0.13	11.2	30.2
		Guanidine Nitrate		
1.0	8.6	0.16	14.7	21.4
2.0	9.2	0.16	14.6	25.6
3.0	9.8	0.15	13.5	27.6

shows it even more clearly, for both diphenyl guanidine and guanidine nitrate.

Zinc loss in the tail goes down slightly as pH is raised with lime, but concentrate grade rises rapidly, contrary to the action of most collectors.

The concentrates produced from the Bunker Hill ore by the guanidine-type collectors all have a salt-and-pepper appearance, unlike the uniform ochre color of concentrates produced by xanthates. This pepper-and-salt appearance is due to a greater proportion of a black resinous sphalerite, not to the cleaner grade of concentrate. Edwards[5] gives the percentages of iron in sphalerite with the corresponding shades of color, from 1 pct Fe (colorless to pale brown) up to 10 pct Fe or more (practically black). The Bunker Hill ore is reported to have zinc as "marmatite plus some sphalerite."[6] It is reasonable to assume that the increased recovery by the guanidine type of collectors is due to better recovery of marmatite or *black jack*.

Marmatite is frequently blamed for poor metallurgical results in flotation of zinc ores.[7] Very little is known about the flotation of marmatite apart from sphalerite.[8,9] An example from practice was a rich zinc ore in which the sphalerite occurred in all shades from pale yellow to brown and black. The light-colored sphalerite floated rapidly with very little xanthate, the dark shades only when the amount of xanthate was greatly increased. It would be valuable to know more about the flotation of marmatite, separate from that of sphalerite. There is no proof that marmatite is accountable for the high zinc losses in some mill tails, and no information as to the nature of these losses. The most frequent excuse for such poor results is that a high grade concentrate is more profitable than a high recovery.

CONCLUSION

Diphenyl guanidine gives a better recovery of the sphalerite and marmatite in the Bunker Hill ore, and with a higher grade concentrate than potassium ethyl xanthate. Further test work on other zinc ores is needed to determine fully what the characteristics of the guanidine-type collectors are and whether or not these collectors can be generally applied.

The diphenyl and dibutyl derivatives of both urea and guanidine are excellent flotation collectors. The relationship of diphenyl and dibutyl structures to their collecting properties has not been determined.

REFERENCES

[1] P. R. Hines: Differential Froth Flotation Process. U.S. Patent 2,664,198. Dec. 29, 1953.
[2] A. R. Taggart, T. C. Taylor, and C. R. Ince: Experiments with Flotation Reagents. *Milling Methods*, p. 285. AIME, New York, 1930.
[3] E. M. C. Barthe'lemy: Differential Flotation of Sulphureted Copper and Zinc Ores. U.S. Patent 1,950,537. Aug. 11, 1932.
[4] A. O. Jaeger and R. Herrlinger: Guanidine Xanthate. U. S. Patent 2,198,774. April 30, 1940.
[5] A. B. Edwards: *Textures of the Ore Minerals*, p. 84.
[6] A. F. Taggart: *Handbook of Mineral Dressing*, Sect. 2, p. 167.
[7] A. M. Gaudin: *Flotation*, pp. 214, 215, 258, and 266.
[8] I. W. Wark: *Principles of Flotation*, pp. 166, 253, 260.
[9] I. W. Wark: *AIME Trans.*, 1934, vol. 112, pp. 245, 253, 265.

TUNGSTEN IN SEARLES LAKE

An unexploited reserve promises more tungsten than the total contained in all other known U. S. sources. The problem now: commercial recovery.

by L. GRAYDON CARPENTER and DONALD E. GARRETT

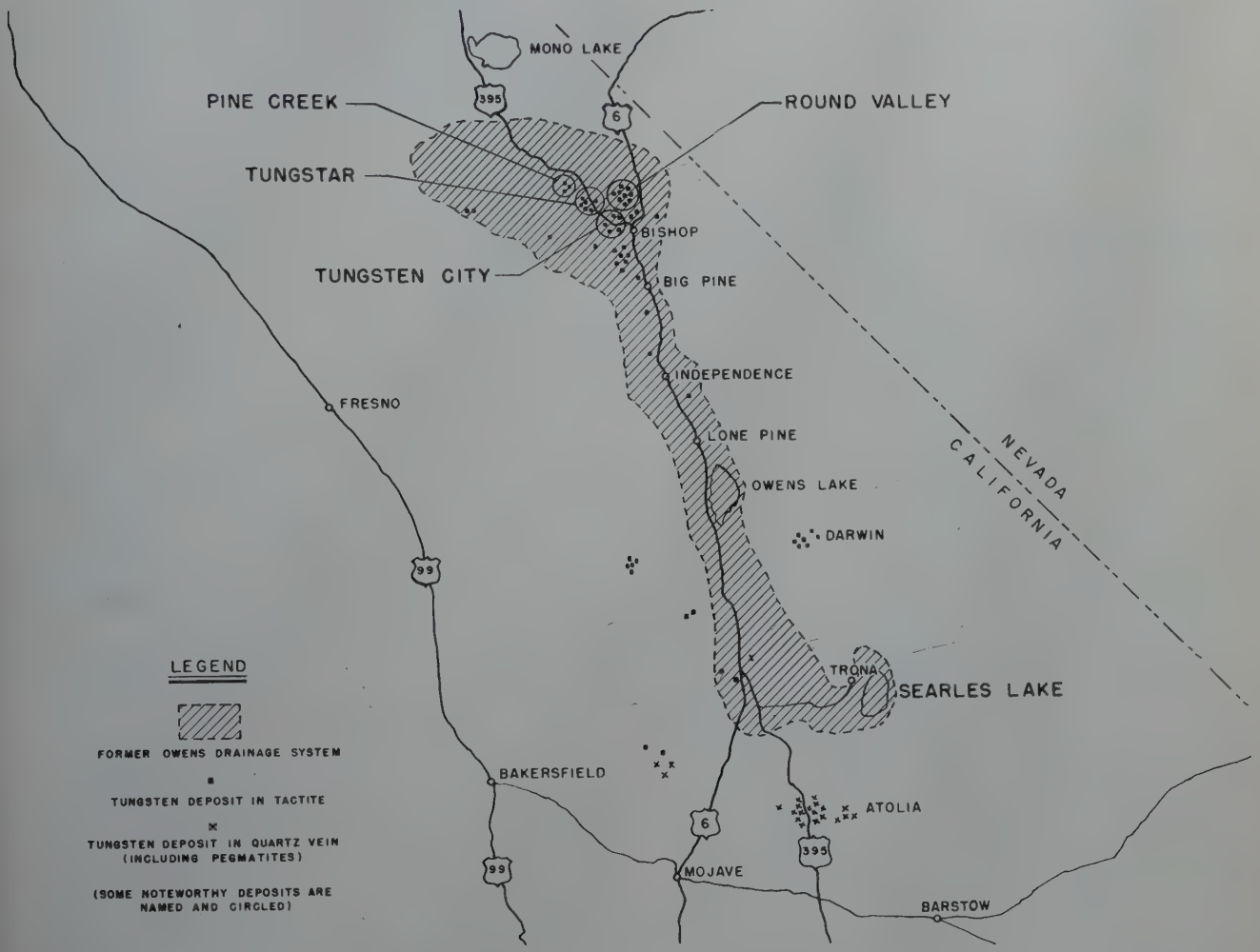

Fig. 1—Relation of tungsten deposits to former Owens drainage system.

Probably the largest single tungsten deposit in the U. S. is one that has yet to produce any tungsten; it is not even listed in tables showing U. S. reserves. This deposit is at Searles Lake, Calif., where the brine contains about 70 ppm WO_3. Small though the concentration is, the amount of brine in the lake is so great that it is estimated at 170 million lb of WO_3 (8.5 million units), equaling the total of all other known reserves in the U. S.

This dry lake is located in the basin formed by the Argus and Slate ranges in the northeastern corner of the Mojave Desert (Fig. 1). It consists of a massive salt body some 35 sq miles in extent, varying in thickness from 0 to 120 ft and containing more than 3 billion tons of salt. A central section of about 8 sq miles is exposed salt; the remaining area is overlain by mud. Except for the exposed sodium chloride (10 to 15 ft thick) the body consists of a very complex and heterogenous mixture of soluble crystals, containing at least eight major phases. It is only about 53 pct solid, the voids being occupied by a dense brine which is the raw material for two chemical companies operating in the valley.

The deposit is believed to be made up of salts present in the runoff waters from the last two ice stages. Searles Lakes was the third in a chain of five lakes that received waters from the Owens Valley drainage of the Sierra Nevada Mts. After leaving Owens Lake the waters could flood in succession into the Indian Wells, Searles, Panamint, and Death valleys (Fig. 2). During the first two ice stages of the Pleistocene Epoch most of the waters eventually arrived at Death Valley; consequently the lower 3300 ft of Searles Valley contain only mud

L. G. CARPENTER and D. E. GARRETT are with the Research Dept., American Potash & Chemical Corp., Trona, Calif. TP 4788I. Manuscript, Nov. 4, 1958. AIME Trans., Vol. 214, 1959.

This page of Mining Transactions AIME follows p. 220. The intervening non-Transactions pages appeared in MINING ENGINEERING.

Table I. Typical Upper Structure Brine Analysis from Searles Lake

Constituent	Upper Structure Brine, Wt Pct
NaCl	16.10
Na_2SO_4	6.75
KCl	4.90
Na_2CO_3	4.75
$Na_2B_4O_7$	1.58
$NaHCO_3$	0.15
Na_3PO_4	0.14
Na_2S	0.12
Na_3AsO_4	0.05
Br^-	0.085
Li_2O	0.018
WO_3	0.007
I^-	0.003
F^-	0.002
H_2O (by diff)	65.34

and insoluble salts with thin and scattered seams of sodium chloride, trona, and nahcolite. Following the second ice stage, however, there was volcanic activity in the Mono area and in the White Mts. (both extending into the Owens drainage area). Considerable volcanic ash and debris resulted, and numerous hot springs were formed. This greatly enriched the mineral content of the runoff waters.

In the succeeding glacial periods, the Tahoe and the Tioga, there appears to have been little, if any, overflow of waters from Searles Lake, so that it became the repository for most of the salts. During the Tahoe period about 40 ft of mixed salts were deposited, with six mud seams from 2 in. to 2 ft banded through the deposit. Later, in the Tioga period, about 14 ft of mud were deposited and then about 80 ft of salts. The top of the 14-ft mud seam is approximately 10,000 years old and the bottom 24,000 years, as indicated by carbon 14 dating.

The complexity of the brine mixture within the salt beds is shown by the list of major constituents in Table I. The tungsten in the brine probably exists as a large heteropoly ion, $(M_xW_yO_z)^{n-}$, where M may be boron, arsenic, or phosphorus and $y{:}x$ may be numbers between 6 and 12. Such ions are very soluble in water but will form insoluble precipitates with complex organic compounds, such as proteins and various alkaloids.[1] The concentration in the brine is only 0.005 to 0.008 pct WO_3, and 0.2 to 0.25 pct in some of the plant liquors—well under the saturation concentrations that would allow a solid phase of tungsten to crystallize out.

The tungsten in the Searles Lake deposit probably resulted from a combination of the leaching of minerals and from the tungsten content of waters from hot springs. Many known tungsten deposits are within the drainage basins (Fig. 1) of the Owens, Indian Wells, and Searles valleys. The largest is in the Bishop district, principally the Pine Creek mine of U. S. Vanadium Corp. There are known reserves of more than one million units of tungsten in the ore, which generally contains 0.3 to 1 pct WO_3, averaging 0.45 pct. In a portion of the ore zone molybdenum disulfide is about 1 pct and copper 0.2 pct. Silver is also present. Other mines in the area, such as the Black Rock mines, contain ore averaging 0.6 pct WO_3.

One of the country's largest producers has been the Atolia district somewhat to the south, although its reserves are now small. This deposit differs from most of the others associated with the Sierra Nevada batholith in that the scheelite is associated with quartz and quartz monzonite. Some of the deposits were of high grade, averaging 4 pct WO_3. About 10 pct of production was from placer deposits, where concentration was much lower.

Most of these California deposits are scheelite, generally in tactite, a rock formed by the alteration of limestone or marble by intrusive granitic magma. It is thought[3] that the tungsten deposits were formed following the intrusion of quartz monzonite and granite into overlying sedimentary deposits. Mineralizing solutions were rich in silicon, aluminum, and ferric iron but poor in sulfur. They carried tungsten, which was precipitated by the limestone at the contact zone as calcium tungstate (scheelite). The solutions may well have been at high temperatures, perhaps even in the gaseous state. The deposits were thus of the contact-metamorphic type, and as would be expected from this mode of deposition, the tungsten content of the ore is generally low.

The present-day Keough hot spring possibly resembles the original tungsten-depositing waters, for it analyzes 0.3 ppm WO_3.[4] It is very likely that this hot spring was formed during the last period of volcanic activity in the area and can be assumed to have played a major part in supplying tungsten to Searles Lake. Assuming a dilution factor of 300 for the Keough to total Owens River waters, the total tungsten concentration (from that source) would be about one part per billion. When the Searles Lake ratio of total sodium chloride to total tungsten was compared with the assumed average sodium chloride content of the Owens River waters (the 1908 to 1958 average was used), the total tungsten content of the ice age Owens River waters was calculated to be 4 parts per billion. Considering that the saturation value of scheelite in water is about 0.2 g per 100 g of water, and taking into account the large amount of exposed tungsten in the drainage basins, the additional 3 parts per billion in excess of that from the one hot spring is reasonable. The comparatively high solubility of scheelite and the complex tungstates would indicate that no tungsten precipitated or crystallized during evaporation of the ancient lakes and that essentially all the tungsten originally present is now in the brines of Searles Lake.

Tungsten was first recognized in Searles Lake brines in 1937 when the scale clogging a condenser line was analyzed. Since then considerable study has been directed toward developing an economic process to recover tungsten from the plant liquors. It is estimated that processing the higher strength plant liquor would recover approximately 1000 lb of tungsten per day. Processing the brine directly from the lake, of course, would produce a larger amount, but recovery would be much more costly, since concentration would be thirtyfold less.

Solvent extraction or ion exchange methods would appear attractive, in view of the uranium industry's success with low concentrations of metal ion in concentrated salt or acid solutions. Unfortunately such processes have not been effective with Trona liquors. A large number of ion exchange resins have been tested, including chelating resins specific for tungsten, without any removal of tungsten from the brine. Similar tests with a wide variety of potential solvents or complexing agent-solvent mixtures have been made with the same negative results. This would appear to indicate that the tungsten complex exists as a low-valenced ion and that it is relatively stable and not easily dissociated.

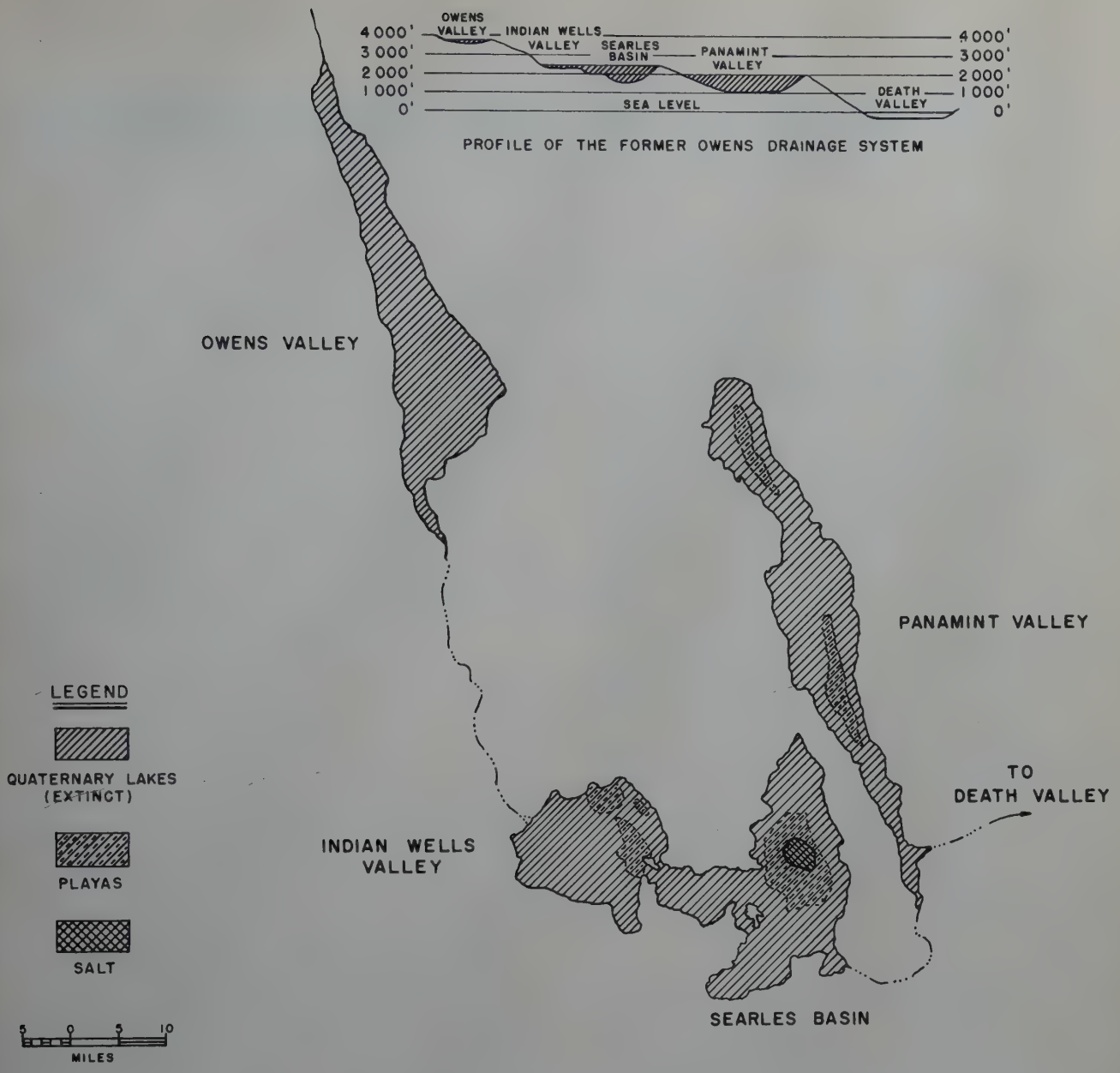

Fig. 2—The former Owens drainage system.

Tungstic acid is quite insoluble, so by suitable acidification of the liquors, tungsten can be precipitated. It is possible to acidify the liquor directly or to use an indirect method, such as electrolysis to generate chlorine, thus acidifying the solution and simultaneously oxidizing the tungsten. The tungsten recovered by acidification is very impure, even after the soluble salts have been removed, containing large quantities of arsenic, phosphorus, and molybdenum. An extensive purification step is required, further adding to the expense and impractibility of such a method.

If a precipitant such as iron or blood meal is used, less acidification is needed and the process is cheaper. However, considerable acid is still necessary, and the product is again very impure. Although they are an improvement on direct acidification, these precipitants do not provide an economical process.

A much more promising approach has recently been studied involving precipitation of tungsten with an organic complexing agent. An essentially complete precipitation of tungsten may be made from liquor at a pH that can be reached by the comparatively easy device of carbonating the liquor with flue gas. The precipitate is considerably less contaminated than by previous methods, but purification is still required if the tungsten is to be of filament grade. The economics of this process are not yet defined, and it is not known whether a commercial process will result, but the studies have added to the knowledge of tungsten as it occurs at Searles Lake. It is believed that eventually this tungsten reserve, the country's largest, will be at least partially recovered.

References

[1] H. F. Walton: *Principles and Methods of Chemical Analysis.* Prentice-Hall Inc., New York, 1952.
[2] Materials Survey—Tungsten. U. S. Department of Commerce, December 1956.
[3] A. Knopf: Tungsten Deposits in Northwestern Inyo County, California. *USGS Bull. 640*, p. 229, 1917.
[4] L. L. Louden (Los Angeles Department of Water and Power): Private communication.

by M. C. CHANG and JOHN DASHER

MINERAL DRESSING FUNDAMENTALS

The Crucible mine in Pennsylvania, operating on Pittsburgh seam coal, is rated at 5000 tpd. The washing plant, built in 1943, is rated at about 400 tph, using hydroseparator boxes to wash the coarse coal (4 x 5/16 in.) and hydrotator units for the fine coal (5/16 x 0).

It is generally acknowledged that gravity concentration equipment cannot be used efficiently to beneficiate coal finer than about 65 mesh. Before the present flotation circuit was installed, Crucible recovered its fine coal slurry, predominantly —24 mesh material, by passing it through a battery of five 14-in. and one hundred and ten 3-in. Heyl & Patterson cyclones in parallel with a 75-ft Dorr thickener. About two thirds went to the cyclones and one third to the thickener. Underflows from cyclones and thickener were filtered, respectively, in one 12-disk Eimco and two 4-disk Oliver filters fitted with stainless steel cloth. The resulting cakes were added to the coarse metallurgical coal. The filtrates, overflow from the 3-in. cyclones, and thickener overflow were recycled to the coarse coal plant.

The three major problems encountered in this system became acute when the mine switched from track-mounted machinery to the more economical off-track equipment. The quality and uniformity of product declined, too much slime accumulated in the circuit, and waste pond disposal became highly impracticable.

Lowering of Quality and Uniformity: Since the filter cake was not beneficiated in any way, addition of this material, which contained about 18 pct ash, would certainly lower the quality of metallurgical coal. Difficulties of handling the high-ash, high-moisture cake were compounded by the lack of adequate blending facilities at the mine, making it impossible to maintain uniform feed for the coke ovens. For a two-month test period, to verify the source of trouble, all filter cake was excluded from the metallurgical coal. The excluded filter cake was stocked in the yard.

Slime Buildup: The moisture retained in the coarse coal products and the filter cake provided daily the only means of slime bleed from the circuit. As this bleed was not enough to offset the incoming fines in the raw coal feed, there was excessive buildup of slimes. To operate at all, it was necessary to purge the system each weekend by pumping all the solids from the thickener to a waste pond. The slimes built up during the week progressively increased the apparent viscosity and density of the circulating plant water, so that hydroseparators and hydrotator units had to be constantly adjusted. Uniformity, yield, and quality of the metallurgical coal suffered in consequence, and the filter cake ash and moisture contents increased from Monday to Friday.

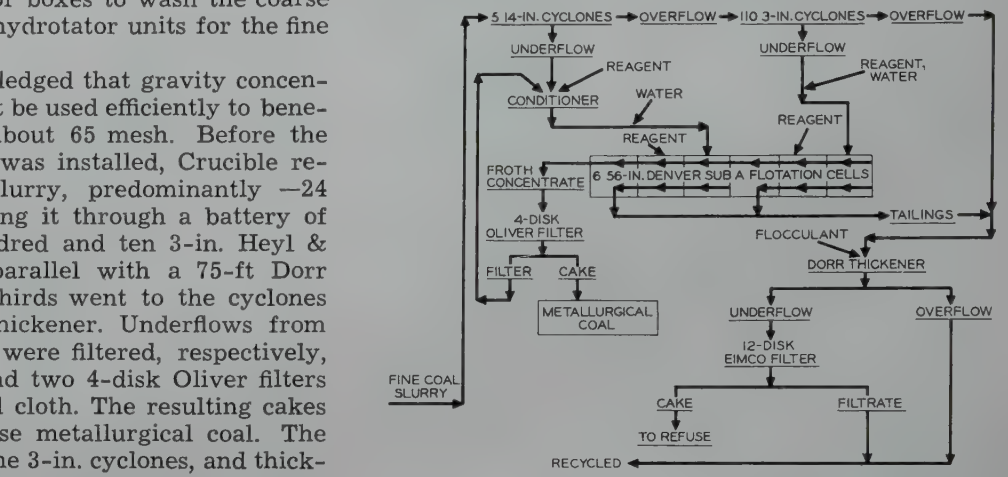

Fig. 1—The flowsheet for Crucible's fine coal plant.

Limited Waste Disposal: Location of the plant does not permit unlimited waste pond area. Maintenance of a waste pond for the purpose of emptying the thickener during weekends became a costly burden that could not be tolerated.

HOW THE PROBLEMS WERE SOLVED

The flowsheet (Fig. 1) chosen to overcome these difficulties is considered the one most economical to install and operate. In a preliminary change made before the flotation circuit was installed, the cyclones and thickener were first operated in series, the overflow from the 3-in. cyclones, after flocculation, being discharged into the thickener and the thick-

Table I. Average Analysis of Filter Cakes

Date	Ash, Pct	Sulfur, Pct	Remarks
January 1956	18.41	—	Old practice
September 1956	15.80	2.29	Cyclone and thickener in series, before flotation
August 1957	8.17	2.02	After flotation

Table II. Estimated Cost of Beneficiating Filter Cake by Flotation

Fixed Charges, Based on New Equipment		Clean Filter Cake, Cost Per Ton, $
Taxes, etc., at 2 pct of $50,000		0.013
Depreciation at 10 pct of $50,000		0.063
	Total	0.076
Operating Costs:		
Power at $0.01 per kw-hr		0.030
Reagent at $0.17 per lb and 0.1 lb per ton		0.017
Maintenance at 2 pct of $50,000		0.013
	Total	0.060

M. C. CHANG, Member AIME, is Research Mineral Engineer and J. DASHER, Member AIME, is Research Supervisor, Central Research Laboratory, Crucible Steel Co. of America, Pittsburgh. TP 4795F. Manuscript, March 31, 1958. New York Meeting, February 1958. AIME Trans., Vol. 214, 1959.

APPLIED TO THE FINE COAL PROBLEM

ener underflow being pumped to a temporary waste pond.

Series Operation of Cyclones and Thickener with Flocculation of Thickener Feed: The flowsheet was first arranged so that all fine coal slurry was classified in the cyclones, only the final overflow discharging into the thickener. In this operation the cyclones removed the relatively coarser material and rejected the high-ash fines. Cyclone performance is shown by the size and weight distribution of feed and products given in Fig. 2. About 25 pct of the solids fed into the cyclones was rejected in the final overflow. Subsieve sizing of solids in the final overflow showed that 92 pct was finer than 600 mesh. In the 3-in. cyclone underflow 88 pct of the material was coarser than 600 mesh.

To provide a clear overflow for recycle, the thickener feed was flocculated with causticized potato starch. This change of circuit, made before flotation, somewhat improved the quality of product in the cyclone underflows.

Preparing the Feed: Rarely used in soft coal beneficiation, flotation in this field has generally been considered unfeasible and uneconomical, an opinion based on results from plants where the process has been misapplied. When minerals are coated, for example, by excessive slimes, surface properties of the various phases are equalized, making it impossible to separate by flotation. The high specific surface of slimes demands excessive reagent and causes considerable difficulty in handling the froth product, and the fine coal slurry contains much fine clay. Success in flotation of coal depends on proper desliming of feed.

It also depends on uniformity of feed. The flotation rate of a mineral finer than 100 mesh usually decreases with decreasing size. When a feed consists of discrete particles of different minerals with wide differences in floatability, particles in a wider range of sizes can be separated with reasonable efficiency. Fine coal particles, however, are middling, that is, each contains some coal and some ash. To separate those which are mostly ash from those which are mostly coal, it is necessary not only to minimize the proportion of slimes, but also to have a feed of reasonably uniform size. Only under these conditions will it be possible to achieve good separation, reagent and power economy, and efficient use of equipment.

The existing 14-in. and 3-in. cyclones at the Crucible plant could be used to deslime and classify the flotation feed. The underflows, which consisted of different size ranges, were floated separately.

Operation: Each of the cyclone underflows was floated in three No. 30 Denver Sub A cells. The bank of six cells can handle 20 tons of clean coal per hr.

Feed is maintained at about 20 pct solids. The reagent in the 14-in. cyclone underflow is Aerofroth No. 73 and in the 3-in. cyclone underflow methyl isobutyl carbinol. Average reagent consumption is about 0.1 lb per ton of clean filter cake.

The froth product filters readily and is being handled in a 4-disk Oliver filter. The same material, unbeneficiated, required about three times as much filter area. The tailing is discharged into the thickener for dewatering and disposal.

Performance: The improvement in quality of the filter cake by flotation can best be described by comparing the average analysis of the various filter cakes given in Table I. Flotation reduced the ash and sulfur in the cake; rejection of ash, however, is more effective than that of sulfur. Weight recoveries are 8 to 90 pct for the 14-in. cyclone underflow and 80 to 85 pct for the 3-in. underflow.

Cost: The estimated cost of beneficiating the filter cake by flotation is given in Table II. Total cost is about 14¢ per ton of clean filter cake. Since this product is about 8 pct of the total tonnage produced, the additional cost for cleaning the filter cake is a little more than 1¢ per ton of total product. Labor cost is not included in the estimate, since no extra labor was required to operate the flotation units.

Efficiency of separation by size and ash distribution on samples of the flotation feeds, concentrates, and tailings is shown in Figs. 3 and 4 for the 14-in.

Table III. Comparison of Product Quality

Date	Mine Coal Analysis		Remarks
	Ash, Pct	Sulfur, Pct	
January 1956	8.74	1.60	Previous practice, filter cake to barges
April 1956	8.07	1.61	Previous practice, filter cake excluded
September 1956	8.65	1.49	New practice, before flotation
August 1957	7.44	1.35	New practice, after flotation

Table IV. Comparison of Product Uniformity

Date	Coke Plant Coal Analysis			Remarks
	Ash, Pct	Variant	Mean Deviation	
January 1956	9.11	0.79	0.66	Previous practice, filter cake to barges
April 1956	7.82	0.30	0.42	Previous practice, filter cake excluded
September 1956	8.62	0.56	0.60	New practice, before flotation
August 1957	7.30	0.25	0.42	New practice, after flotation

Table V. Results of Geisler Plastometer Test

Sample	Start, °C	Final, °C	Range, °C	Max, °C	Fluidity, DDPM
Clean production filter cake	386	473	87	432	55,550
Unclean stock filter cake	385	469	84	439	37,500
Clean stock filter cake	368	466	98	429	41,700
Run-of-mine washed coal	381	478	97	438	33,400

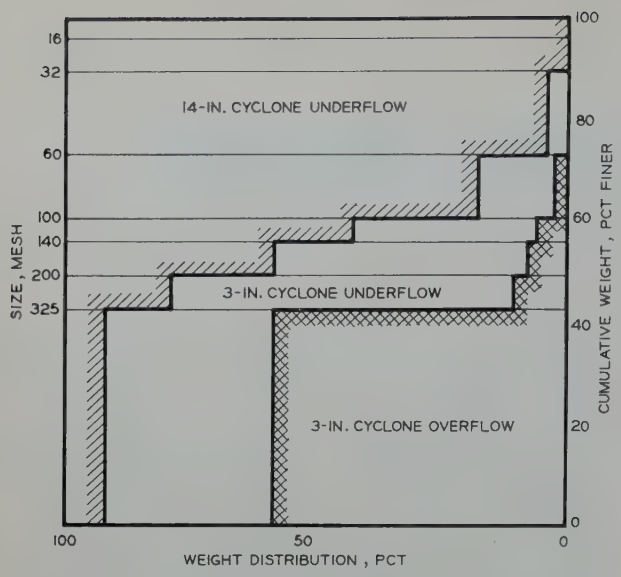

Fig. 2—The size and weight distribution of cyclone feed and products. Approximately 25 pct of the solids fed into the cyclones was rejected in the final overflow.

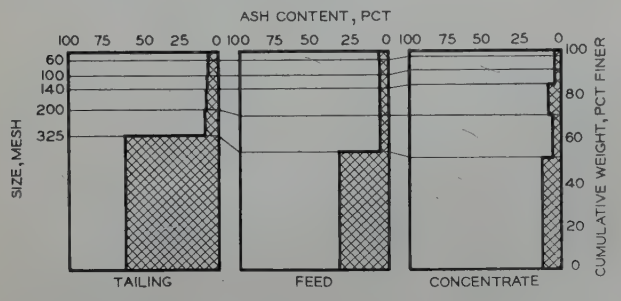

Fig. 4—Size and ash distribution, 3-in. cyclone underflow.

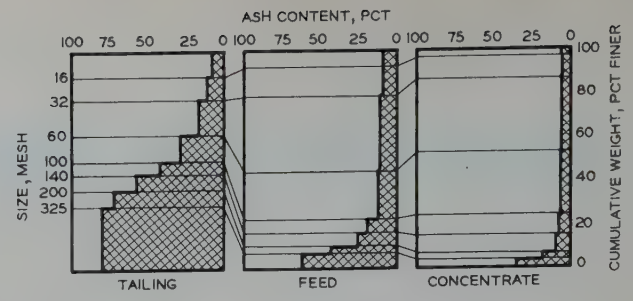

Fig. 3—Size and ash distribution, 14-in. cyclone underflow.

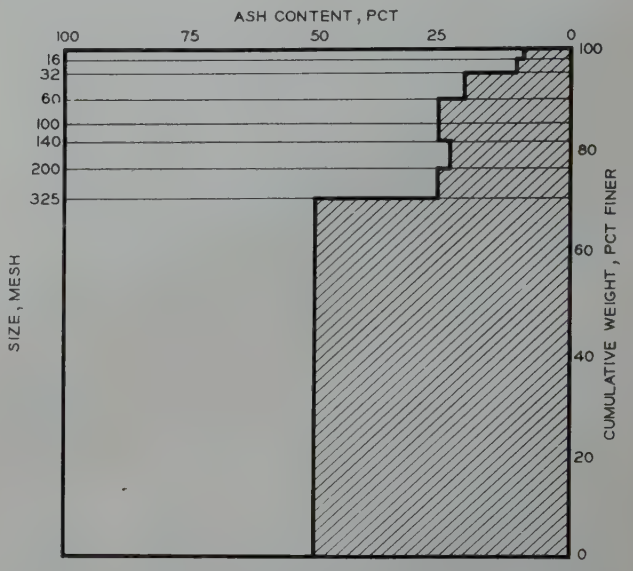

Fig. 5—Size and ash distribution of the fine refuse.

and 3-in. cyclone underflows, respectively. It may be noted that a good separation (concentrate containing less than about 10 pct ash) is obtained in the 14-in. cyclone underflow circuit only above 200 mesh; in the 3-in. cyclone underflow circuit, a good separation is obtained on the —325 mesh (but deslimed) fraction. This verifies the necessity of classifying feed.

Filtration of Thickener Underflow: Thickener feed now consists of the 3-in. cyclone overflow and the flotation tailings. For flocculation the starch consumption is approximately 0.6 lb per ton of solids. Thickener underflow is filtered in the 12-disk Eimco filter fitted with polyethylene bags. The cake, containing 40 to 50 pct ash and 30 to 35 pct moisture, is combined with the plant refuse for disposal via aerial tram buckets to the gob pile located across the river. This closed circuit operation of the plant eliminates the need for a waste pond, except for emergencies, and helps remedy the problem of stream pollution.

Size and ash distribution of solids in the filter cake refuse is shown in Fig. 5.

RESULTS EVALUATED

Product Quality: The improved quality of products resulting from these changes is shown by the average analysis of the various products given in Table III. Quality of the metallurgical coal has been significantly improved, as shown by the lower ash and sulfur contents.

Product Uniformity: At Midland a barge is unloaded by a clamshell, which dumps the coal in a hopper for discharge onto a conveyor belt to the coke plant. Any variation in uniformity of product would be reflected in the daily Midland analysis of the coal. The increased uniformity of product quality is evident from Table IV, which gives the average calculated variant and mean deviation under the various washer operations.

Geisler Plastometer Tests: Results of the Geisler plastometer test on the clean production filter cake; the stock filter cakes, clean and unclean; and the run-of-mine washed coal are given in Table V. It is interesting to note that all of the filter cakes tested give higher fluidity reading than the run-of-mine washed coal.

Data presented in this article were based largely on samples taken by the staff of Heyl & Patterson. The authors express their appreciation to Crucible Steel Co. of America for permission to publish this information.

Discussion of this article sent (2 copies) to AIME before April 30, 1959, will be published in MINING ENGINEERING.

A DECADE OF DEVELOPMENT IN OVERVOLTAGE SURVEYING

by ROBERT W. BALDWIN

As used in geophysical exploration, the term *overvoltage* applies to secondary voltages set up by a current into the earth which decay when the current is interrupted. These secondary effects may be measured by pick-up electrodes. The term *induced polarization* has often been employed to describe this same phenomenon. In its own operations Newmont Exploration Ltd. commonly uses the word *pulse*.

The basis of this method in prospecting is that metallic particles, sulfides in particular, give a high response, whereas barren rock, with certain exceptions, gives a low response. Overvoltage has been tried in searching for many types of mineral occurrence but has been most successful in outlining the widespread disseminated mineralization associated with porphyry coppers.

History:[1] Newmont Mining Corp. has been interested in overvoltage since 1946, when Radio Frequency Laboratories of Boonton, N. J., drew the company's attention to phenomena observed in the laboratory. At the instigation of A. A. Brant further model studies were undertaken, and the first tests were performed in 1947. Tests at San Manuel, Ariz., in 1948 were very encouraging, clearly demonstrating that the method could be used to distinguish scattered sulfides at depth. H. O. Seigel followed up the San Manuel work with a study to determine the phenomena involved.[2]

R. W. BALDWIN, Member AIME, is with the Geophysical Department, Newmont Exploration Ltd., Danbury, Conn. TP 4793L. Manuscript, June 25, 1958. New York Meeting, February 1958. AIME Trans., Vol. 214, 1959.

Fig. 1—Current and voltage sequences, typical measurement. Overvoltage response to be plotted equals integrated secondary voltage divided by primary voltage.

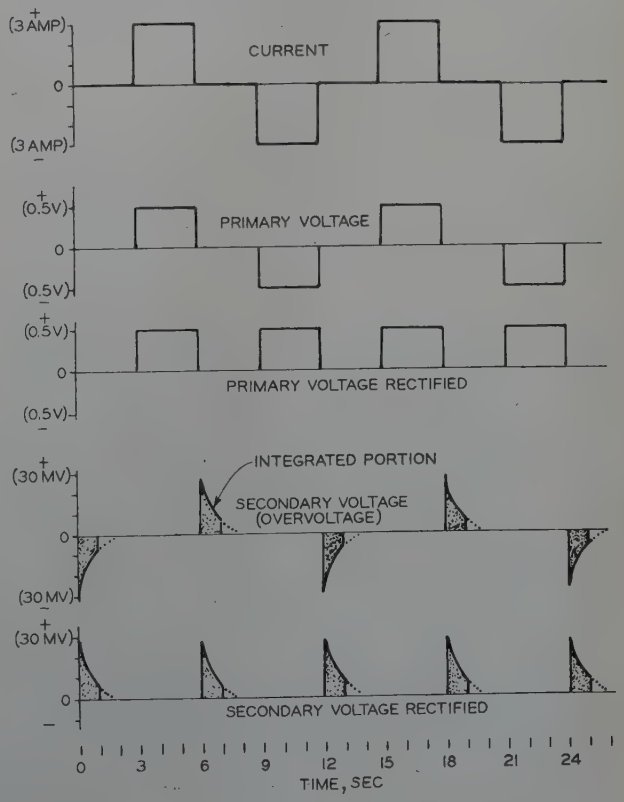

Further field experiments took place at Jerome, Ariz., in 1949-1950. Since 1950 this method has been a standard prospecting tool of Newmont Exploration Ltd. Overvoltage surveys have been carried out in the U. S., Canada, Latin America, and Africa. Field equipment has been constantly improved.

Concurrent with field exploration, theoretical and experimental investigations were pursued at Jerome. H. O. Seigel, J. R. Wait, V. Mayper, E. H. Bratnober, and L. S. Collett were notable contributors. Work at the Jerome laboratories included:

1) Study of the phenomena involved, with extensive investigation into the causes of background nonsulfide effects.

2) Study of the possibilities of taking induced polarization measurements with low-frequency alternating current instead of pulsed direct current.

3) Mathematical development of type curves showing the anomalies to be expected from mineralized bodies of various shapes and sizes under varying depths and conditions of cover.

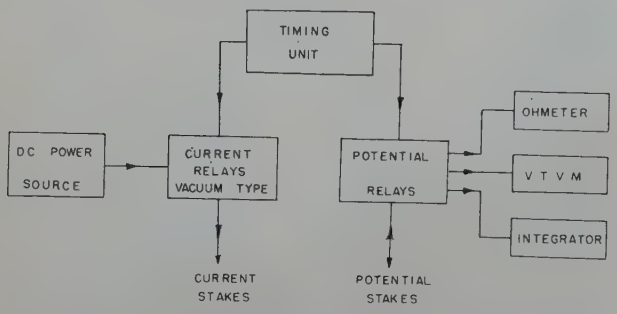

Fig. 2–Block diagram of typical field equipment.

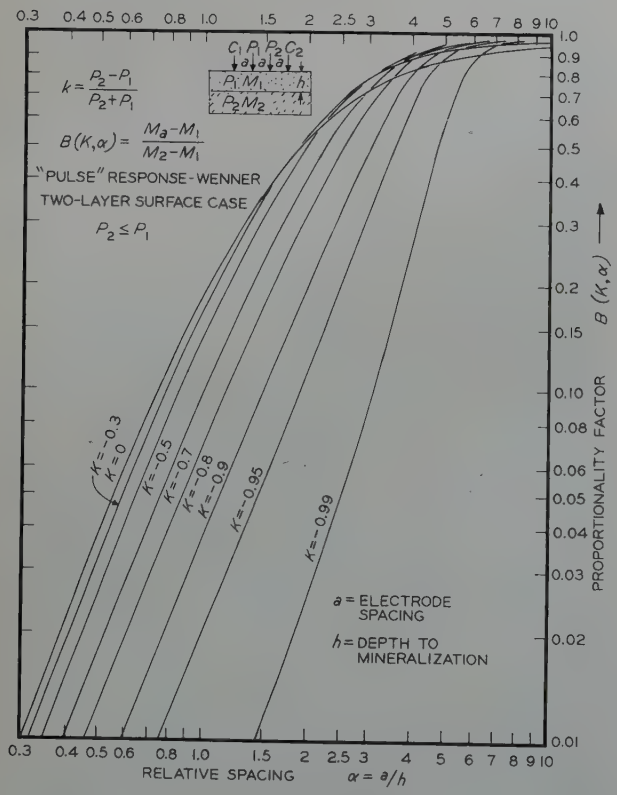

Fig. 3–Typical theoretical overvoltage response curves.

4) Laboratory testing of rock samples, study of the form of overvoltage decay and the a-c response for various types and sizes of mineral particles, and model orebody studies.

Operational Methods: The overvoltage method requires direct connection to the ground, by means of two current electrodes and two potential electrodes. Field methods are thus similar to those of resistivity surveys. Various electrode arrays have been used; electrode spacings are chosen according to the type of target and expected depth. Spacings as wide as 1500 ft have been regularly employed. In laboratory work also, four direct connections must be made to the specimen or model.

Fig. 1 illustrates, in idealized form, the sequences encountered in a typical d-c overvoltage measurement.* While the current is on there is a primary

* The voltage and current values quoted are samples to indicate an order of magnitude.

voltage across the potential electrodes which may be measured with a vacuum tube voltmeter—a simple resistivity measurement. On cessation of current (allowing 10 to 15 milliseconds for inductive and capacitive coupling effects to disappear) the decaying secondary voltage or overvoltage appears at the potential electrodes. This decay curve may be presented on an oscilloscope and photographed—the procedure in many laboratory experiments. Field practice is to integrate the decay voltage over an interval following current cessation. Common operating times are 3 sec of current pulse and 1 sec of integrating time. To obtain a reading the integrated secondary voltage is divided by the primary voltage. The units are then millivolt-seconds per volt.

In practice, of course, not just one pulse of current is applied but a succession of pulses as shown, every second pulse being of reversed polarity. Rectifying relays are provided so that the primary and secondary voltages always read positively.

Field Equipment:[3] Fig. 2 is a block diagram of typical field equipment. The heart of the equipment is the timing unit, which controls both current switching and the connections of potential electrodes to the vacuum tube voltmeter for primary voltage and to the integrator for secondary voltage measurement. Two types of timing units have been employed: the first electronic, using multivibrators, and the second mechanical, using a constant-speed motor and cam-operated switches. The integrating device is a General Electric fluxmeter, model 32C248. The d-c power supply has usually consisted of a gasoline-motor a-c generator followed by a high-voltage d-c rectifier unit. The smaller units (order of 1000 to 1500 w) are relatively mobile and have been transported by burros; the larger units (up to 25,000 w) are mounted in heavy-duty trucks.

Most field equipment was designed and constructed in the Jerome laboratories by A.W. Love, K. E. Ruddock, and W. E. Bell.

Type Curves:[4] H. O. Seigel has developed mathematical expressions for the overvoltage response to be expected from mineralized bodies of various geometric forms. The analysis is equally applicable if the source of overvoltage effects is not mineralization. Seigel uses an electrodynamic model of overvoltage which considers the effect of resistivity contrasts within the region of measurement on both primary and secondary fields. His basic postulate is that the action of the primary field sets up a volume distribution of current dipoles—all antiparallel to the primary field—whose moment equals the product

of the primary current density and a mineralization*

* The term *mineralization* is understood to include other sources of overvoltage effects.

factor which is a property of the medium. He then develops a procedure for calculating overvoltage responses from associated resistivity curves by weighting the overvoltage contribution of any medium according to the logarithmic derivative of apparent resistivity with respect to the resistivity of that medium.

Mathematically,

$$M_a = \sum_i M_i \frac{\partial \log \rho_a}{\partial \log \rho_i}$$

where M_i and ρ_i are the *mineralization* factor and apparent resistivity of the ith medium, M_a and ρ_a are the overvoltage response and apparent resistivity at the point of measurement and $\sum_i$ represents a summing of the terms for all media.

Where there are only two media concerned the above formula reduces to

$$\frac{M_a - M_1}{M_2 - M_1} = \frac{\delta \log \rho_a}{\delta \log \rho_a}$$

where the subscripts 1 and 2 refer to media 1 and 2.

An important approximation of overvoltage surveys is the two-layer case. This assumes a horizontal layer of barren material overlying an infinite layer of mineralized material. The overvoltage responses have been derived directly from the well known resistivity two-layer formula. Fig. 3 gives the type curves when the lower layer has the lower resistivity. The abcissa is relative electrode spacing (i.e., in terms of thickness of top layer) and the ordinate, in effect, indicates what proportion of the lower layer mineralization factor should appear in the observed reading. The different curves are for different resistivity contrast conditions. Note that the plotting is logarithmic. Examples of the use of these curves are given in the field results to follow.

Phenomenological Theory:[5] To account for overvoltage effects, J. R. Wait has proposed the following theoretical model:

Each conducting particle is considered to be coated with a thin dielectric film that poses a block action to current flow into the particle. Thus the action at the interface of each particle is somewhat comparable to that of a lossy condensor, and any ground exhibiting an overvoltage response may be considered to contain in effect a large number of tiny condensers. It should be noted, however, that the dielectric constant of these condensers may vary with frequency.

Wait applied his model theory to predict the form of the decay curve and its variation with particle size. His predictions have been borne out by laboratory experiments. Some typical results are shown in Fig. 4. The tests were performed on a compact mixture of 98 pct andesite and 2 pct pyrite particles, plus a weak electrolyte. Different samples contained different sizes of pyrite particles, ranging from 0.25 to 12-mm diam. Duration of current pulse was 1 sec. Primary voltage was the same in all cases. Note that the time scale is logarithmic. It will be observed that decay is more rapid with the smaller sulfide particles. It can also be noted that at any time following the cessation of current there is an optimum particle size for which the decay voltage is maximum.

A-C Overvoltage Methods:[6] As is perhaps suggested by the condenser analogy mentioned above,

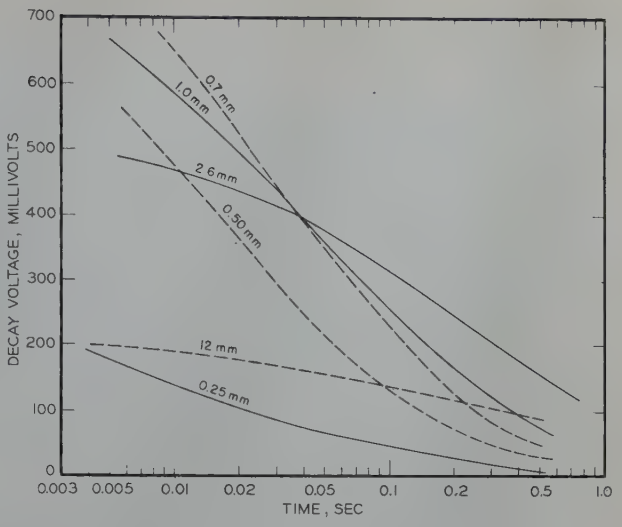

Fig. 4—Observed decay voltage $e(t)$ as a function of time. For $V = 15$ volts, $v = 0.02$ and $\sigma = 5x10^{-3}$ mhos/m. This graph and Fig. 5 are examples of extensive overvoltage experiments at Newmont's laboratories in Jerome, Ariz. Fig. 4 illustrates work in transient domain, Fig. 5 work in frequency domian.

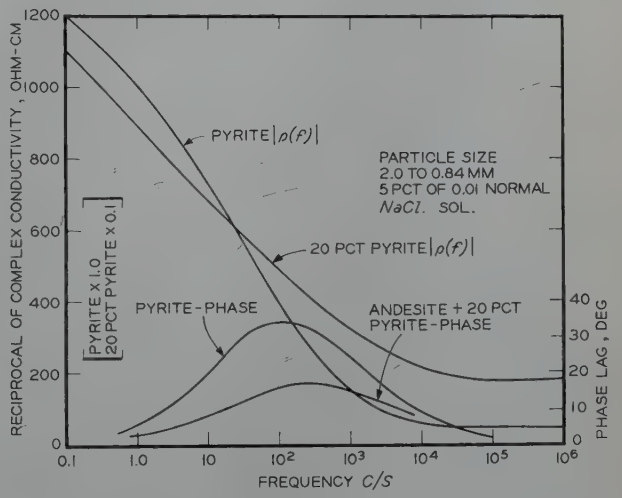

Fig. 5—Variation of complex conductivity with frequency. From experiments at Newmont laboratories.

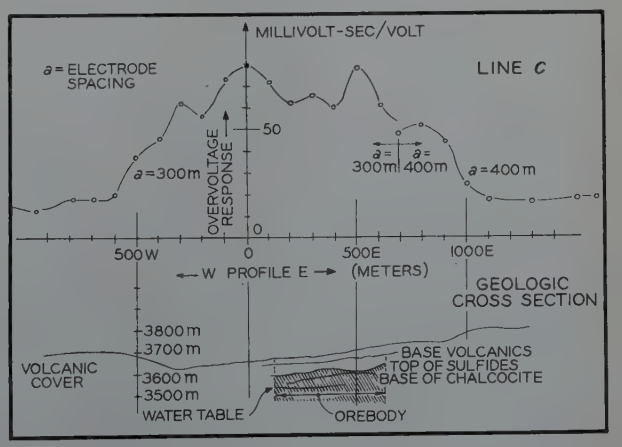

Fig. 6—Overvoltage profile, north end, Quellavaco.

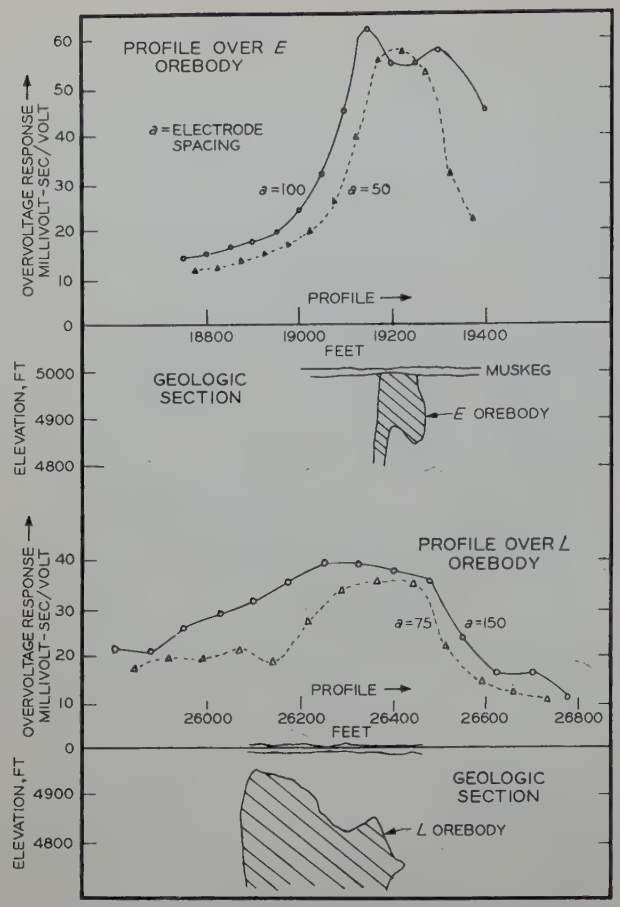

Fig. 7—Overvoltage profiles at Lynn Lake, Manitoba.

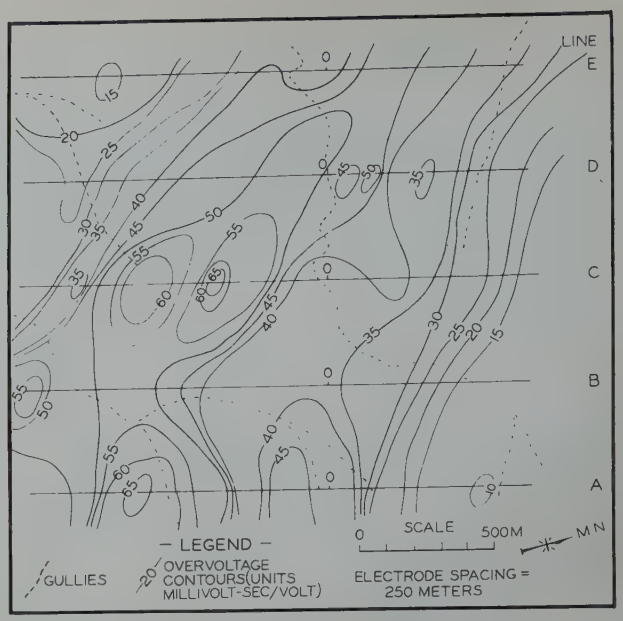

Fig. 8—Copper prospect, Peru. Overvoltage contours here directly outline distribution of sulfides.

the overvoltage phenomena may be measured in the frequency domain instead of in the transient domain, that is, by applying alternating current instead of pulsed direct current. The earth in general has a complex impedance in which the d-c resistivity is a pure resistive component and the overvoltage contributes a somewhat complicated combination of capacitance and resistance. The complex impedance and the phase angle vary with frequency. This variation is especially pronounced in the case of sulfides.

Results of some complex impedance measurements in the laboratory are shown in Fig. 5. Complex impedance and phase angle for pyrite and for pyrite in andesite particles are plotted against log frequency. The maximum slope of the impedance curve occurs at that frequency at which phase angle is a maximum. In comparison, impedance vs frequency curves for barren rock material (over the frequency range up to the order of several hundred cycles) are almost flat and the phase angle remains low.

It should be noted that a-c overvoltage measurements should be made in the low frequency range where electromagnetic propagation effects are negligible. Caution should also be taken to avoid excessive line coupling between the current and potential circuits. Probably several tens of cycles is about the upper frequency limit for operations in the field.

Wait has demonstrated the relation between the response in the frequency domain and that in the transient domain. From experimentally observed frequency response data he derived the overvoltage decay curve to be expected following a pulse of direct current. The agreement with the experimentally observed decay curve was excellent.

Field Results:[7] To date pulsed d-c methods have been used in field exploration. The technique of measurement is described above under Operational Methods and Field Equipment.

To repeat, the basis of the overvoltage method as a prospecting device is that metallic particles, especially sulfides, give a high response, whereas barren rock, with certain exceptions, gives a low response.

In the earlier days it was not realized that barren rock could display a considerable range of response, and minor anomalies of less than 50 pct of background were deemed evidence of sulfides. At Jerome, Ariz., anomalies of this order were found to be caused by certain portions of the Pre-Cambrian basement beneath the Palaeozoic cover. At the present time overvoltage readings of two to three times background are usually necessary to excite interest. Even then it must be recognized that some anomalies may have causes other than sulfides.

In overvoltage surveys results fall into four classes:

1) No significant anomalies.
2) Anomalies due to economic sulfides.
3) Anomalies due to noneconomic sulfides.
4) Anomalies due to nonsulfides.

Groups 2 and 3 above may both be considered geophysical successes if not exploration successes. The ratio of noneconomic to economic mineralization disclosed is certainly no worse than for other geophysical methods. The chief villain has been disseminated pyrite. Many porphyry copper deposits have a surrounding halo of disseminated pyrite, and the zone of maximum sulfides is not necessarily the zone of maximum copper.

While there have been a few striking examples of nonsulfide anomalies, most major anomalies have been explained by sulfides. For example, in almost four years of work in Peru, only one recommended

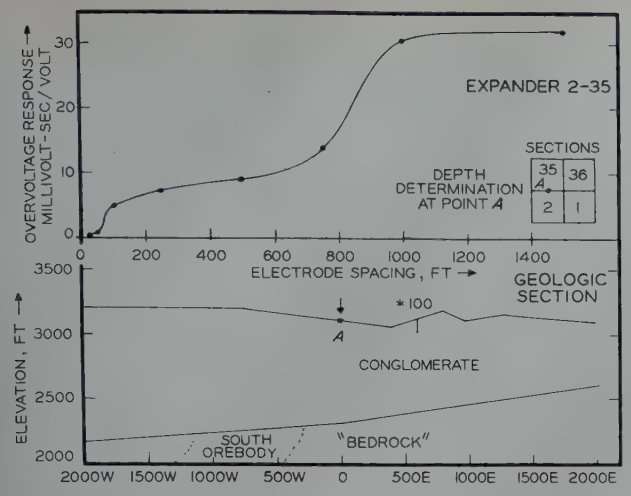

Fig. 9—Detection of deep mineralization is possible at San Manuel by use of large electrode spacings.

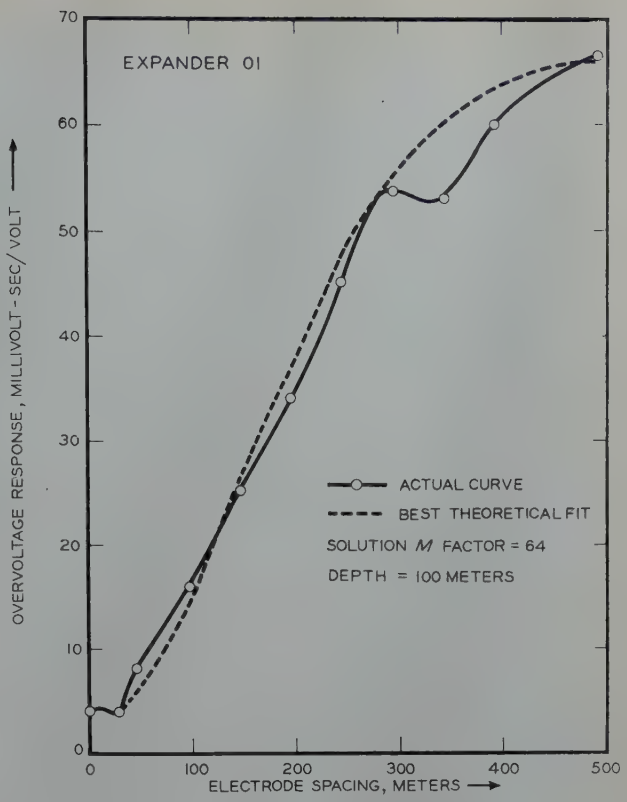

Fig. 10—Mineralization and depth, Cuajone.

drillhole completely failed to find a reasonable quantity of sulfides.

Over a disseminated sulfide deposit the anomalous overvoltage response (i.e., in addition to the rock background) will depend on:

1) The percentage by volume of sulfides.
2) The geometry of the deposit with respect to surface and the electrode array in use. Geometry thus includes size and depth below surface.
3) The resistivity contrast conditions between the sulfide zone and the cover and surroundings.

In any one area the overvoltage response of a mineralized zone has been found to vary more or less directly with the percent of volume of sulfides for moderate percentages of sulfides. It is not safe, however, to project from one area and type of mineral occurrence to another.

A fair number of the examples to follow were obtained over known or later proven orebodies. In attacking any new area, it has been the general policy to test over known mineralization first, where possible, and work out from there, so that the type of anomaly to be sought is known.

Fig. 6 shows an overvoltage profile over the north end of the orebody at Quellaveco, Peru. The ore zone is covered by about 40 meters of postmineral volcanics, and depth to sulfides is from 60 to 100 meters. The orebody is well detected; however, it is to be noted that the anomaly is some 800 meters wider than the orebody, presumably because of a surrounding zone of disseminated pyrite.

Fig. 7 shows the response over an entirely different type of orebody, the *E* and *EL* orebodies at Lynn Lake, Manitoba. The scale of operations is reduced here: to discriminate those relatively narrow bodies, an electrode spacing of about 100 ft was used as opposed to 300 meters at Quellaveco, and readings were taken every 50 ft instead of every 100 meters. The smaller *E* body gives a better response than the *EL*. Some reasons for this are: 1) the *EL* body has massive sulfides, whereas the *E* is more disseminated,*

* The overvoltage method works best with disseminated sulfides.

and 2) the overburden is deeper over the *EL*. While both these bodies are adequately detected from their immediate surroundings, varying rock backgrounds reduce the certainty of the method in this area. For instance, not far to the west of the *EL* a quartzite formation gave response in the 50's, higher than that obtained over the *EL* itself. Disseminated pyrite possibly contributed to the high quartzite response.

A contour map of anomalous overvoltage response provides a good picture of the distribution of sulfide mineralization; in regions where the depth to top of sulfides is less than about a third the electrode spacing and resistivity contrasts are not extreme. An example is given in Fig. 8, which is from a prospect in Peru; the contours here include a background response of about 5. Drilling in the highs provided approximate confirmation of the distribution in a limited portion.

A reading on one electrode spacing only gives no indication of depth of cover. This information can be obtained from expanders. An expander is a series of readings at different electrode spacings taken at one station. The results are then compared with type curves. In a great many cases the simple two-layer approximation is adequate. The derivation of two-layer type curves has been discussed under Type Curves. The investigator solves for depth and for anomalous response or mineralization factor of the underlying zone. The examples below are plotted linearly for greater clarity, but the method of solution requires the field results to be plotted on two-cycle logarithmic paper of the same size as the type curve paper. An expander is entirely analogous to the vertical profile of resistivity surveys.

Fig. 9 shows an expander taken at San Manuel, Ariz., plus a geological section in the region. The surrounding pyrite mineralization presumably renders the two-layer case applicable. This example is particularly interesting in illustrating how such deep mineralization as San Manuel's is detectable.

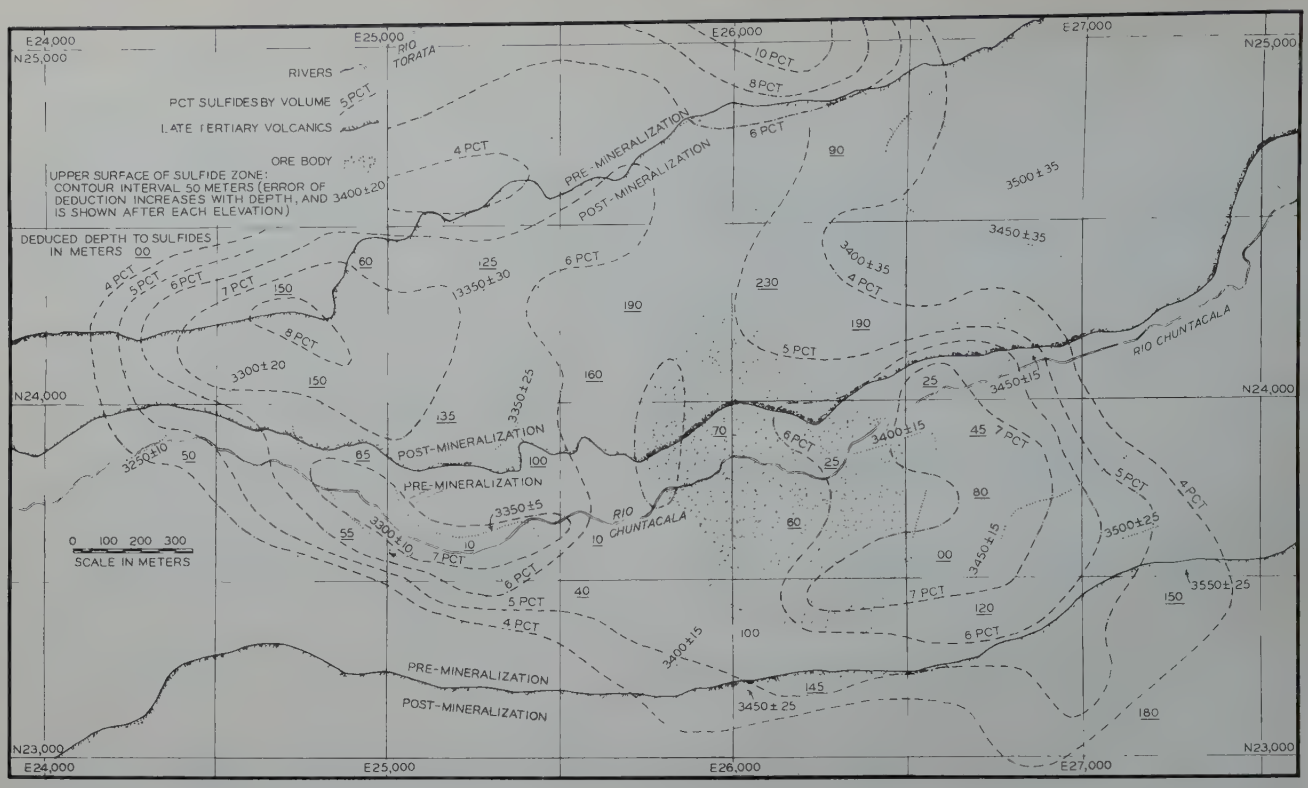

Fig. 11—The sulfide distribution at Cuajone, Peru, as deduced from the overvoltage data. Note the great variation in depth to the top of the sulfides. The mineralization that is outside the orebody consists mostly of pyrite.

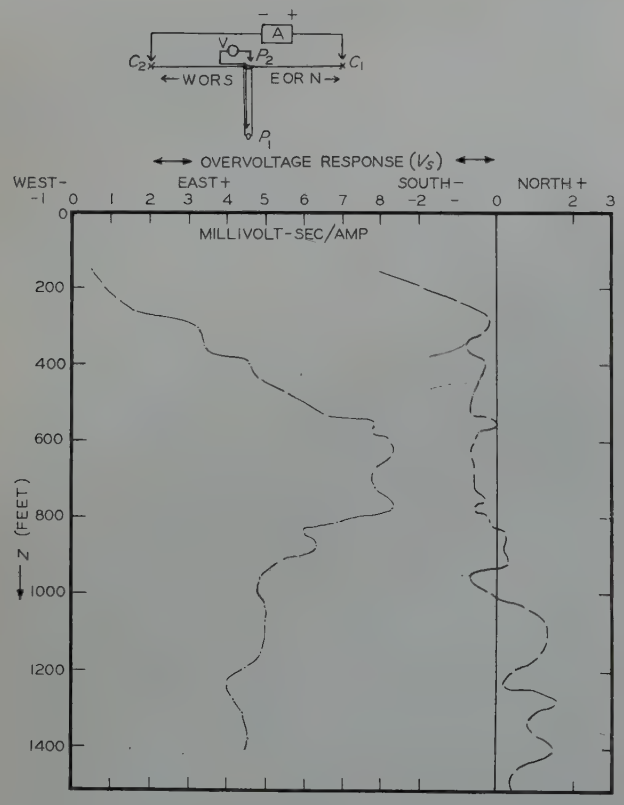

Fig. 12—Nababeep West, South Africa, borehole WP 12. The direction of mineralization from a drillhole is indicated here by the overvoltage azimuth survey.

An expander across the south end of the orebody at Cuajone, Peru (Fig. 10) gives depth to sulfides as 100 meters. Depth actually is about 90 meters.

With the aid of readings on more than one electrode spacing over a large area, it is possible to obtain mineralization factors and depths at a great number of points and then to contour this deduced data. At Cuajone two electrode spacings, one twice the other, were used on every line throughout the anomalous area, and additional control was provided by short spacing readings on several lines and by a few formal expanders. Fig. 11 shows a portion of the deduced mineralization and top of sulfide contour map; Fig. 11a, an aerial photograph of the region, illustrates to some extent the type of topography. For mineralization, it was assumed that a mineralization factor of 10 represented 1 pct sulfides by volume.* Depth to sulfides varies from less than 10 meters in the Chuntacala Valley to more than 160 meters where the late Tertiary volcanics cap the pampa or mesa to the north. The Cuajone orebody has now been extensively drilled and a rough outline is shown on the map. The deduced mineralization extends more than a kilometer to the west and more than half a kilometer to the east of the orebody, also (not shown here) far to the northwest. The deduced mineralization is at some points actually higher on the rim than directly over the orebody. The mineralization rim is disseminated pyrite. The drilling has in general verified the deduced mineralization pattern, but only relatively. A recent study of the assays from 35 drillholes has revealed that predicted sulfide content was on the average 1.95 times actual

* This factor was based on tests made in Arizona.

Fig. 11a--Air photo of Cuajone site shows steep hillsides, especially bordering the Rio Torata.

sulfide content. If this correction had been known in advance, the probable error of mineralization prediction at any point would have been about 30 pct of the predicted sulfide content, or less than 1 pct sulfides by volume. The probable error of depth prediction at Cuajone was 10 meters.

The overvoltage method has been tried in drillholes. This application, though it has given useful indications, has not had the widespread success that was first expected. One major problem has been correcting for the masking effect of low resistivity fluid in the drillhole, especially when working in very high resistivity Pre-Cambrian formations.

One important sideline to drillhole work is azimuth determinations. Once a significant anomaly is obtained in a drillhole using normal electrode arrays, direction is determined by placing the two current electrodes on surface an equal distance on each side of the collar, lowering one potential electrode down the hole, and measuring the overvoltage response with respect to a reference electrode. A positive response indicates that the source of the anomaly lies in the direction of the negative current electrode and vice versa. Two azimuth runs (north-south and east-west) are necessary to fully establish direction. Results in Nababeep West, South Africa, drillhole No. 12 (Fig. 12), suggest that in the upper part of the hole mineralization lies chiefly west, whereas in the lower part it lies chiefly to the south. These deductions were confirmed in the course of drilling the orebody.

There remain to be mentioned those unfortunate cases where overvoltage anomalies are not caused by sulfides.

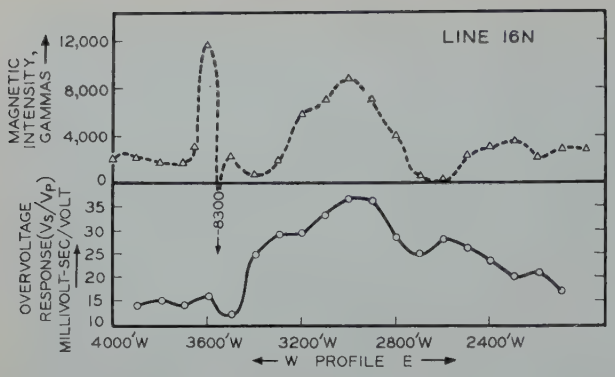

Fig. 13—Magnetic and overvoltage profiles at Engels, Calif. Overvoltage anomaly is attributed to magnetite.

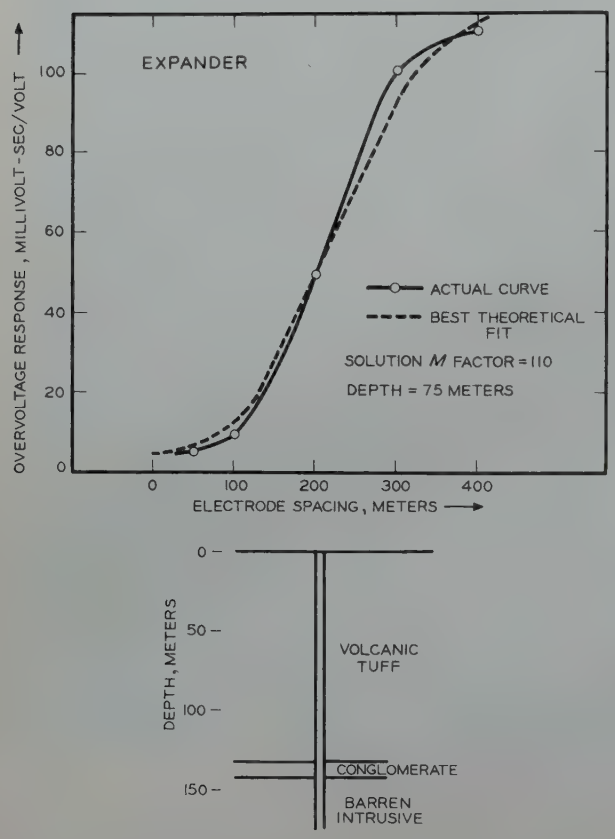

Fig. 14—Unexplained anomaly, Wildcat prospect, Peru.

Magnetite, being a metallic substance, gives an overvoltage response. An example of an anomaly presumably caused by disseminated magnetite comes from Engels, Calif. (Fig. 13). There is good correlation between the overvoltage and magnetic profiles. Of course the presence of an associated magnetic anomaly is not necessarily unfavorable. The two Lynn Lake examples both had excellent magnetic anomalies also.

Response from graphite has been observed in the laboratory, and in Southern Rhodesia a field anomaly was attributed to this mineral. However, graphite has not proved generally troublesome, for the simple reason that most surveys have not been in graphitic areas.

A wildcat anomaly obtained in Peru is still not satisfactorily explained. This occurred in a trough of post-mineral volcanic tuff. The expander taken at the center of the anomaly is shown in Fig. 14. Mineralization was predicted at less than 100 meters, the best solution being about 75 meters. In fact, drilling disclosed no lithological change for nearly twice this depth and the basement was only negligibly mineralized.

Victor Mayper[8] has shown that clay minerals with high ion exchange capacity can give a considerable overvoltage response. Notable extraneous anomalies were obtained in low resistivity phyllites in South West Africa and in certain schists in British Columbia.

The process of taking an overvoltage reading provides a resistivity reading automatically. The resistivity data are of direct use to the overvoltage survey in providing information necessary in depth calculations. A resistivity survey also has many well known applications—such as determining depth of overburden—and in itself is often a guide to mineralization. Porphyry coppers, for example, offer a fairly limited range of resistivity values. Most of the examples given in this article have accompanying resistivity anomalies. It is standard practice always to consider overvoltage results in conjunction with resistivity data.

Despite some unforeseen complications, e.g., the high response from certain nonsulfide material, the overvoltage method has proved its usefulness in detecting and outlining disseminated sulfide mineralization, even at depths as great as 200 meters.

The following firms have kindly granted permission to publish various items of information: Newmont Mining Corp., American Smelting & Refining Co., Cerro de Pasco Corp., San Manuel Copper Corp., Sherritt Gordon Mines Ltd., and O'okiep Copper Co. Ltd.

REFERENCES

[1] A. A. Brant: *Overvoltage Developments and Geophysical Application by Newmont Exploration Limited 1946-1955.**

[2] H. O. Seigel: *Theoretical and Experimental Investigations into the Application of the Phenomenon of Overvoltage to Geophysical Prospecting.* University of Toronto doctoral thesis, May 1949.

[3] K. A. Ruddock: *Field Equipment for Prospecting by the Overvoltage Method.**

[4] H. O. Seigel: *A Theory of Induced Polarization Effects for Step-Function Excitation.**

[5] J. R. Wait: *A Phenomenological Theory of Induced Electrical Polarization.**

[6] J. R. Wait: *The Variable-Frequency Overvoltage Method in Electrical Prospecting.**

[7] R. W. Baldwin: *Overvoltage—Field Results.**

[8] V. Mayper, Jr.: *The Normal Effect.**

[9] A. A. Brant: U.S. Patent 2,611,004, Sept. 16, 1952. Geophysical Exploration.

[10] S. Glasstone: *Textbook of Physical Chemistry*, p. 1017.

[11] J. A. V. Butler: *Electrical Phenomena at Interfaces*, especially Chapter VII, by J. O'M. Bockris.

[12] V. Vacquier, C. R. Holmes, P. P. Kintzinger, and M. Lavergne: Prospecting for Ground Water by Induced Electrical Polarization. *Geophysics*, July 1957, vol. 22, no. 3, p. 660.

[13] R. Frische and H. von Buttlar: A Theoretical Study of Induced Electrical Polarization. *Geophysics*, July 1957, vol. 22, no. 3, p. 688.

[14] D. F. Bleil: Induced Polarization: A Method of Geophysical Prospecting. *Geophysics*, July 1953, vol. 22, no. 3, p. 636.

[15] J. H. Henkel and R. G. Van Nostrand: Experiments in Induced Polarization. *AIME Trans.*, March 1957, vol. 208, p. 355.

[16] L. S. Collett: *Laboratory Investigation of Overvoltage.**

* These items are private company papers, but it is hoped that they will soon be presented in a monograph to be published by the Pergamon Press.

Discussion of this article sent (2 copies) to AIME before April 30, 1959, will be published in MINING ENGINEERING.

PROCESSING CALIFORNIA BASTNASITE ORE

by CHARLES J. BAROCH, MORTON SMUTZ, and EDWIN H. OLSON

IN 1949 an orebody containing some 10 billion lb of recoverable rare earth metals was discovered in the Mountain Pass district of San Bernardino County, California.[1] The following year Molybdenum Corp. of America purchased a number of claims at the deposit and a mill on the property which had been constructed to process the district's gold ores.

Average composition of ore from the San Bernardino deposit is less than 0.1 pct ThO_2, 25 to 35 pct calcite, 10 pct rare earth oxides, 15 to 20 pct silica, and 30 to 40 pct barite.[2] Rare earth content of the ore analyzes 50.7 pct CeO_2, 4.2 pct Pr_6O_{11}, 11.7 pct Nd_2O_3, 1.3 pct Sm_2O_3, and 34.3 pct La_2O_3 and others.[2]

By floating the barite and depressing the bastnasite, Molybdenum Corp. of America produced a concentrate that contained 60 to 70 pct rare earth oxides. More than 25 pct of the rare earths, however, was lost in flotation. It seemed likely that a more economical method could be found.

At the present time most of the rare earths in the concentrates are converted to rare earth chlorides, which are either fed to ion exchange columns for separation of the individual rare earths or reduced to misch metal. Current investigation shows that solvent extraction may achieve this separation more economically than ion exchange. The study reported here was undertaken to develop an economical method of preparing a pure rare earth nitrate mixture from California bastnasite ore. Results indicated that more than 98 pct of the rare earths could be recovered.

Several possibilities were considered for processing bastnasite ore, but only the method outlined in Fig. 1 was investigated. This involved leaching the calcined ore with nitric acid. The nitric acid process is discussed under the following headings: 1) calcination of the ore, 2) leaching of calcine, 3) filtration studies, 4) solvent extraction, and 5) nitric acid recovery.

C. J. BAROCH, Junior Member AIME, formerly at the Ames Laboratory of the U. S. Atomic Energy Commission, Ames, Iowa, is now in the Army. M. SMUTZ is Assistant to the Director and E. H. OLSON is an Associate Engineer at the Ames Laboratory.
TP 4794L. Manuscript, May 21, 1958. AIME Trans., Vol. 214, 1959.

Calcination: Since California bastnasite ore contains 25 to 35 pct calcite and about 10 pct bastnasite, calcination was needed to reduce the violence of reaction with nitric acid. Weight losses of 26 to 30 pct were obtained by calcining the ore at 900°C for 1 hr or at 800°C for 4 hr. Longer periods resulted in no further weight loss.

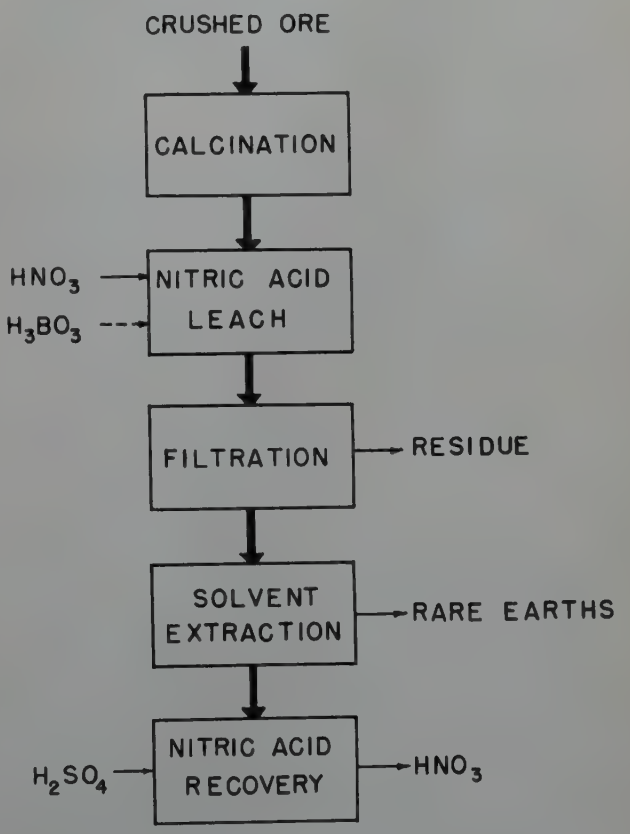

Fig. 1—Proposed method of processing bastnasite ore.

Leaching the Calcine: When the bastnasite calcine was leached with 30 pct nitric acid for 8 to 10 days, rare earth recoveries of only 45 to 50 pct were

obtained. Because of the low rare earth recoveries, another method of opening the ore was sought.

C. J. Rodden[3] had stated that the rare earth fluorides were soluble in a mixture of concentrated nitric acid and boric acid. Leaching the calcine with this mixture for 8 to 10 days indicated rare earth recoveries of more than 90 pct. Further tests showed that boric acid was not required. The major disadvantage was the high cost of the concentrated nitric acid, but the commercial preparation of about 57 pct, costing only 2.2¢ per lb, proved equally effective.

Additional tests showed that leaching the calcine for only 1 hr liberated over 93 pct of the rare earths. The percentage recovered was not appreciably affected by increasing the leach time to 2 hr or more. These experiments also revealed that size of calcine particles had very little effect on the percentage of rare earths recovered. For economic reasons, —10 mesh particles were considered satisfactory.

A 1-hr leach and a nitric acid/calcine weight ratio of 2.2 were required to liberate 93 pct of the rare earths. Larger-scale leachings using the same acid/calcine ratio resulted in the liberation of over 99 pct of the rare earths from the calcine. This minimum nitric acid/calcine weight ratio was not the optimum required for the overall process. It will be shown that efficiency of filtration and of solvent extraction depends on the ratio of acid to calcine weight.

Filtration Studies: It is difficult to predict accurately, from small-scale laboratory tests, the filter area needed in commercial plants. Several standard tests have been devised, however, from which it is possible to predict semi-quantitatively the requirements for a large plant.

In the filtration experiments Eimco media No. Dy-452 was used on a standard leaf test. This cloth resisted the attack of hot concentrated nitric acid and was capable of retaining particles as fine as 200 mesh. A vacuum of 10 in. of mercury was used, and a plot was made of time vs volume of filtrate.

A standard lot of calcined ore was prepared for the tests. Owing to the small size of the leaching vessel, two equal batches of slurry were prepared and mixed, and when the temperature of the combined slurries dropped to 45°C, the filtration tests were started. Results showed that filtration was best with an acid/calcine weight ratio of 2.96. To simplify calculations, a ratio of 3.00 was used.

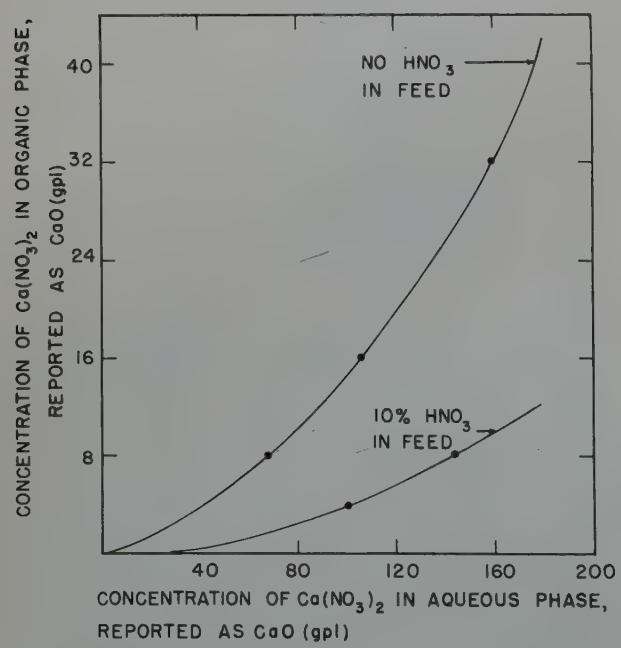

Fig. 2—The calcium nitrate distribution curves used in determining amount of calcium transferred to TBP.

Table I. Results of Typical Solvent Extraction Operation

Stage	Volume, Cm^3 In	Volume, Cm^3 Out	Analysis of Exit Streams RE_2O_3, Gpl	Analysis of Exit Streams CaO, Gpl
Extract 1				
Aqueous	716*	690	25.74	91.10
Organic	358	400	32.26	1.23
Extract 2				
Aqueous	690	675	12.34	91.86
Organic	345	360	26.51	3.71
Extract 3				
Aqueous	675	658	2.58	87.58
Organic	338	340	19.31	9.00
Extract 4				
Aqueous	658	655	0.00	79.56
Organic	329	330	4.85	16.07
Scrub 1				
Aqueous	96	93	20.16	76.46
Scrub 2				
Aqueous	96	96	40.12	28.58
Organic	1430	1430	17.38	0.00

* The feed to Extract 1 of the extraction section consisted of scrub 1 and 2, 25 cm^3 of 57 pct HNO_3, and 500 cm^3 of fresh feed (see Fig. 4). The fresh feed contained 53.95 gpl RE_2O_3 and 107.40 gpl CaO and had an acid normality of 2.46.

Table II. Composition of Various Streams of a Bench-Scale Test

Material	Quantity	RE_2O_3, G	CaO, G	SiO_2, G	$BaSO_4$, G	HNO_3, G
Raw ore	7044.2 g	734.4	1554.3	118.3	1767.4	—
Calcine	5000.0 g	733.1	1538.1	91.5	1690.0	—
Leached ore	1876.0 g	—	—	92.3	1667.0	—
HNO_3 feed	11.0 L	—	—	—	—	8299.7
Leach liquor	14.0 L	755.5	1503.6	—	—	2173.2
Additional HNO_3 to feed	0.7 L	—	—	—	—	528.8
Raffinate	18.1 L	—	1440.0	—	—	120.9
TBP product	40.0 L	699.9	—	—	—	2424.0
$CaSO_4$ precipitate	3190.0 g	—	1488.0*	—	—	—
HNO_3 recovered	6.3 L	—	—	—	—	4752.0

* Estimated from weight of the $CaSO_4$ precipitate.

Filterability was influenced by many properties of the slurries, such as viscosity of the clear leach liquor and size of the reacted calcine particles. When the calcine was leached with a nitric acid/calcine weight ratio of 3.00 or less, a nearly saturated solution of calcium nitrate was obtained. When the solution cooled to room temperature, some calcium nitrate and some of the rare earths were crystallized. Crystallization of the calcium nitrate greatly reduced filterability of the slurries.

Crystallization of the calcium nitrates and rare earth nitrates can be prevented by diluting the leach liquor with water or by heating the liquor to 40°C or higher. It would be much more costly to maintain the leach liquor at 40°C or higher than it would be to dilute it. Most of the calcium nitrate was kept in solution, therefore, by adding water equal to 35 to 40 pct of the volume of the leach liquor.

Still another variable influenced filtration characteristics of the slurries—the greater the tetravalent cerium concentration, the poorer the filterability. Addition of hydrogen peroxide, powdered iron, or magnesium to the slurry reduced the tetravalent

cerium concentration, but the cost of these reagents would not be offset by the reduction in filtration costs.

No effort was made to determine the minimum amount of water required to wash the filter cake, but over 99 pct of the soluble rare earths was recovered when the cake was washed with water equivalent to about 25 pct of the volume of the leach liquor. It can be assumed, therefore, that the amount of water necessary to keep all of the calcium nitrate in solution would be a good measure of the amount required to wash the filter cake satisfactorily.

Solvent Extraction: Solvent extraction should be one of the cheapest and simplest methods of removing the combined rare earth nitrates from the leach liquor. According to Knapp,[4] the distribution coefficient of the combined rare earths was greatly increased by the presence of salting agents such as calcium and ferric nitrates. Since California bastnasite ore contains about twice as much soluble calcium as rare earths, the distribution coefficient of the combined rare earth nitrates should be very favorable. The distribution curves for the combined rare earth nitrates were obtained by three to six successive contacts of the leach liquor with tributyl phosphate (TBP) which contained no diluent. The TBP used in these tests was pre-equilibrated with nitric acid of varying strengths so that a series of distribution curves could be obtained. The equilibrium curves indicated that in most cases the distribution coefficient of the combined rare earths varied inversely as the nitric acid concentration in the TBP. In determining the rare earth distribution curves, it was noticed that some calcium was transferred to the TBP. However, when the nitric acid concentration in the fresh TBP was greater than 1.26 *N*, no calcium was detected in the TBP product.

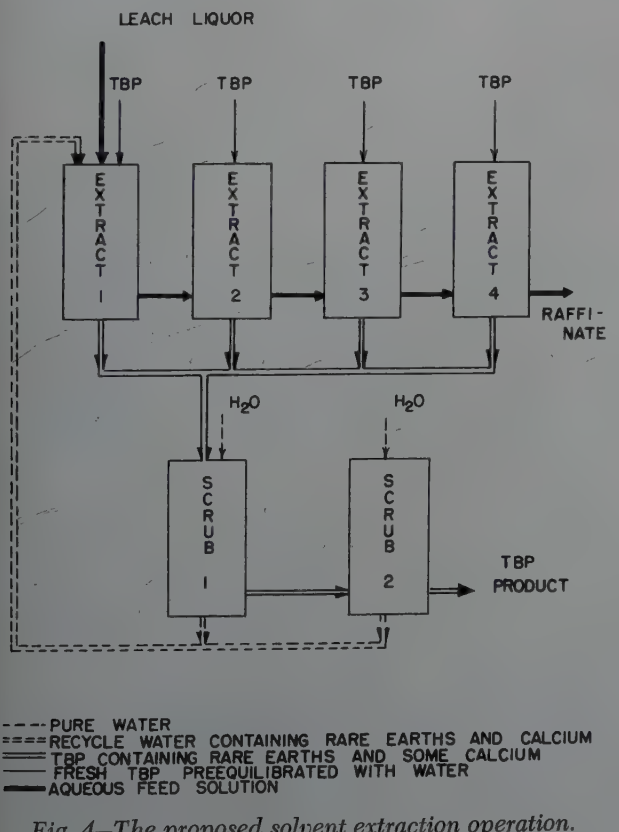

Fig. 4—The proposed solvent extraction operation.

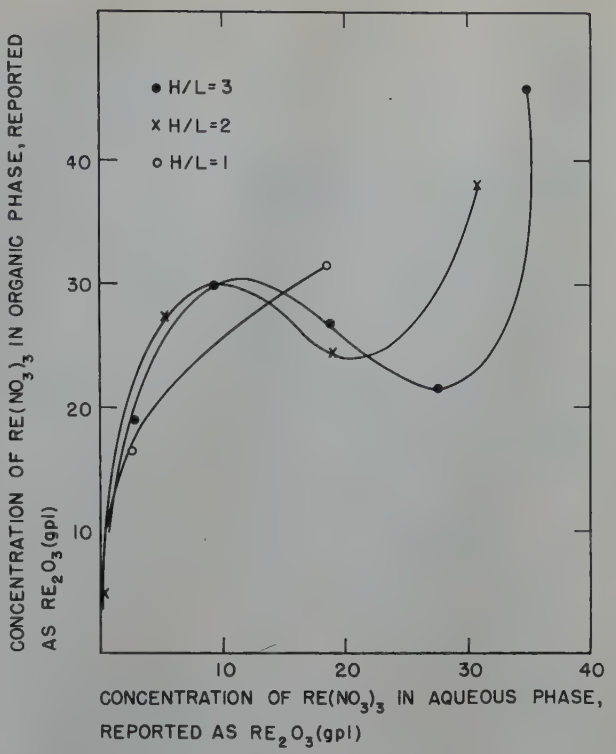

Fig. 3—Effect of H/L volume ratio on total rare earth nitrate distribution curve. Best cocurrent extraction is obtained with H/L ratio of 2, using four extract stages, but for cocurrent extraction to apply in this process, the calcium must be separated from the rare earths.

To determine the amount of calcium transferred to the TBP, the distribution curve for a calcium nitrate solution was determined. The calcium nitrate distribution curves in Fig. 2 indicate that the distribution coefficient of the calcium nitrate varies inversely as the nitric acid concentration.

Effectiveness of the solvent extraction operation was determined by making a simulated countercurrent solvent extraction run. The rare earth distribution curve for this run did not duplicate the curves obtained using cocurrent extractions. In fact, in some of the extract stages the rare earth concentration in the aqueous phase increased about 50 pct. Also the extraction was less than 35 pct effective in removing rare earths from the aqueous feed.

Several attempts were made to improve the efficiency of countercurrent extractions. However, varying the number of extract stages, the aqueous to organic (*H/L*) volume ratio, the nitric acid concentration in the TBP, and the amount of scrub solution had very little effect. Varying the operating conditions seemed only to influence the distribution curve, and in no instance was the rare earth recovery greater than 50 pct.

Cocurrent extraction did overcome the difficulties found in the countercurrent operation, but the application of cocurrent extraction might be limited by the amount of calcium transferred to the TBP, as well as by the quantity of TBP required to recover 98 pct of the rare earths in the aqueous feed solution.

Effectiveness of the cocurrent extractions was determined by making several runs using *H/L* ratios of 1, 2, and 3. In all instances the TBP contained no diluent or nitric acid. The rare earth distribution curves obtained in the cocurrent runs

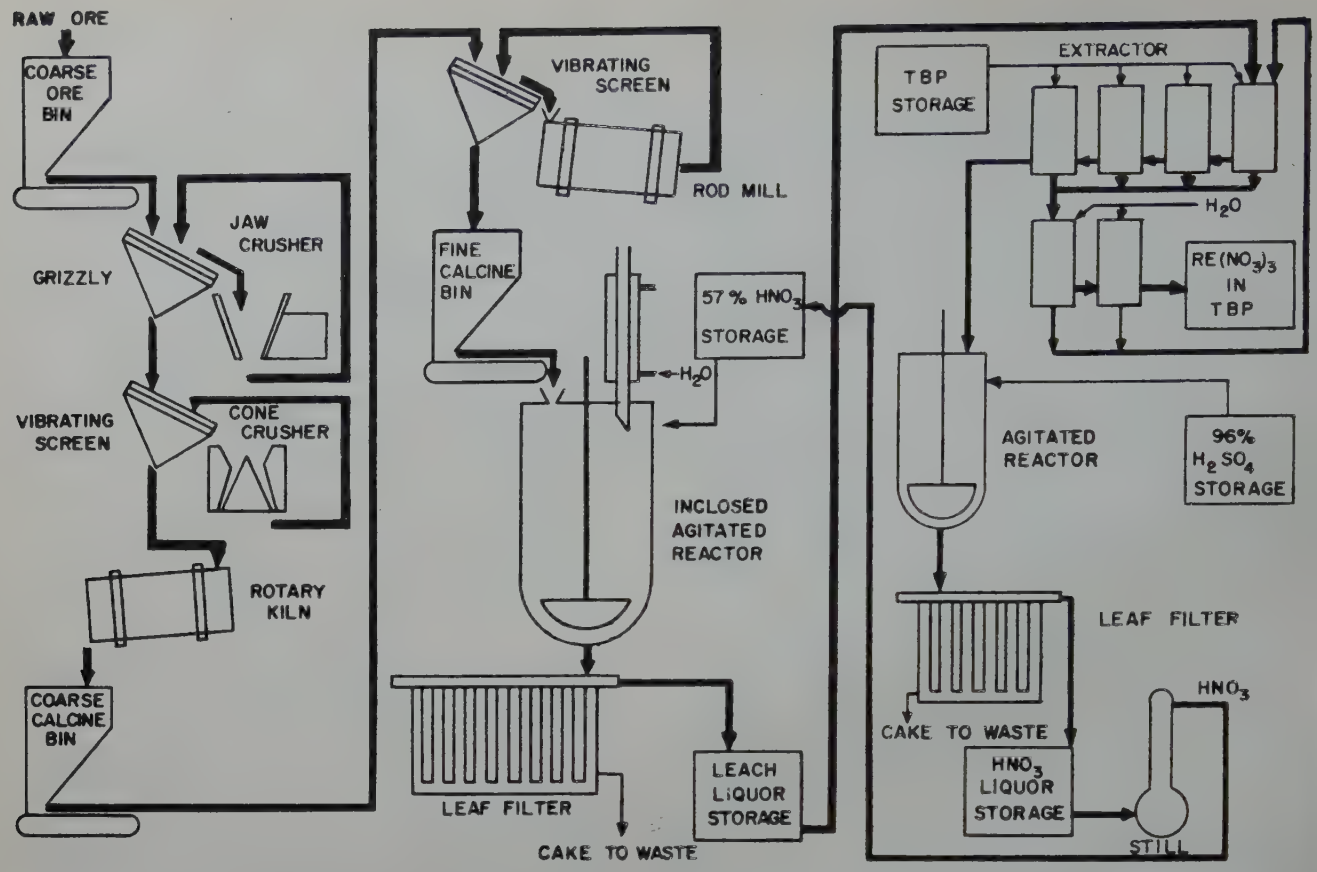

Fig. 5—Process or preparing rare earth nitrate mixture from California bastnasite ore gives over 98 pct recovery.

are shown in Fig. 3. Variability in the curves can probably be attributed to the difference in extractability of the tetravalent cerium, nitric acid, and the remainder of the rare earths.

Calculations using the curves in Fig. 3 indicated that best cocurrent extraction can be obtained with an *H/L* ratio of 2, using four extract stages. However, in order for the cocurrent extraction to be applicable to this process, the calcium must be separated from the rare earths. The low distribution coefficient of the calcium nitrate suggested that if the TBP containing both calcium and rare earth nitrates were scrubbed with water, the calcium nitrate might be preferentially extracted. The scrubbing operation proved to be effective—in fact, practically all of the calcium was scrubbed from the TBP by two cocurrent contacts of the combined TBP products with water, using an *H/L* ratio of 0.067 in each contact. Since some of the rare earths were also removed, the scrub solutions must be processed to recover them.

A method for recovering the rare earths in the scrub solution is outlined in Fig. 4. Several simulated runs with this method indicated that recycling the scrub solution had very little effect on the rare earth distribution curve and that a TBP product could be obtained which was virtually free of calcium.

Nitric Acid Recovery: In the leaching operation over 60 pct of the nitric acid is consumed by the calcite and other impurities. Therefore the nitric acid would have to be recovered from the calcium nitrate and other nitrate compounds. The nitric acid recovery operation would involve a chemical reaction between calcium nitrate and sulfuric acid which would produce calcium sulfate and nitric acid. The resulting slurry would be filtered and the filtrate processed by extractive distillation.

Details of the extractive distillation operation were not investigated in this project. A 96 pct sulfuric acid to raffinate volume ratio of 0.15 would be required to liberate most of the nitric acid. Because of the variable composition of the raffinate, however, an acid to raffinate volume ratio of 0.18 might prove more satisfactory.

BENCH-SCALE INVESTIGATIONS

Several bench tests of the process outlined in Fig. 5 provided information for a more reliable material balance and also indicated where difficulties might arise in scaling up the process. By increasing the size of the operation, it was possible to study the processing steps more easily.

About 7200 g of raw ore were thoroughly mixed, sampled, and calcined. After the calcine had cooled, it was crushed to pass a 10-mesh screen, remixed, and sampled. Five kilograms of the calcine were slowly fed to 11,000 ml of about 57 pct nitric acid. The slurry was thoroughly agitated throughout the leaching operation. Originally it was planned to feed the calcine at a rate of 5000 g per hr, but its reaction with nitric acid was so violent that excessive amounts of steam and nitric acid were produced. To minimize the loss of nitric acid, the calcine feed rate was reduced to about 4000 g per hr. The reaction slurry was then agitated for one additional hour after all the calcine had been fed.

The nitric acid vapors evolved by the hot slurry made the filtration immediately after leaching very difficult; for this reason the slurry was allowed to cool for about 2 hr before it was filtered. The filter cake was then washed with about 2500 ml of water.

Any calcium nitrate that crystallized upon cooling was dissolved by diluting the leach liquor with water. A small portion of the leach liquor was then used in the solvent extraction operation.

In the first experiment with cocurrent solvent extraction, the feed solution had an acid normality of about 2.5, and the run yielded a TBP product that contained about 1.3 gpl of calcium oxide. Therefore, a second solvent extraction run was performed in which the nitric acid concentration of the fresh feed was increased to about 3.0*N*. The use of this additional nitric acid yielded a TBP product that was free of calcium. Results of this solvent extraction run are presented in Table I.

A fraction of the raffinate from the solvent extraction operation was processed to recover the nitric acid that had combined with the calcium and other impurities. Over 92 pct of the nitric acid in the raffinate was recovered in this operation. Undoubtedly greater nitric acid recoveries can be obtained; however, the optimum conditions could be more easily determined in a pilot plant operation.

The various streams, raw materials, and products of the bench-scale tests were analyzed for rare earths, calcium, barium, silica, and nitric acid content. Table II presents the analysis of the various streams of a typical bench-scale operation.

Summary: The process developed during this investigation consisted of the following steps:

1) Calcination of ore for 1 hr at 900°C or 4 hr at 800°C.

2) Digestion of the calcine in 57 pct nitric acid for 1 hr. Almost all of the rare earths and calcium were readily dissolved from −10 mesh calcine particles. An acid to calcine weight ratio of 3.00 was required.

3) Filtration of reaction slurry and washing of filter cake. At least a 35 pct dilution of the leach liquor was required to keep all of the calcium nitrate in solution.

4) Recovery of the combined rare earth nitrates from the leach liquor in a solvent extraction operation using TBP as the solvent. The operation was performed in four cocurrent extract stages using an *H/L* volume ratio of 2.00 in each stage. To remove the calcium nitrate, the TBP products were combined and scrubbed twice with water, using an *H/L* ratio of 0.067. The scrub solutions were recycled to the first extract stage. An overall *H/L* ratio of 0.38 was required in the solvent extraction operation.

5) Recovery of the nitric acid combined with the calcium and other impurities. A sulfuric acid to raffinate volume ratio of 0.18 was required to liberate most of the nitric acid. Nitric acid in the reaction slurry was recovered by filtration and then concentrated by extractive distillation.

Results obtained in this study showed that over 98 pct of the rare earths could be recovered. About 18 pct of the nitric acid fed to the leaching operation was combined with the rare earths or was lost in the nitric acid recovery operation.

This article is a condensation of a dissertation presented by C. J. Baroch in partial fulfillment of the requirements of a Doctor of Philosophy degree at Iowa State College, Ames, Iowa. Work was performed in the Ames Laboratory of the U. S. Atomic Energy Commission.

REFERENCES

[1] J. Olson, D. R. Shawe, L. C. Pray, and W. N. Sharp: Rare-Earth Mineral Deposits of the Mountain Pass District, San Bernardino County, Calif. *USGS Prof. Paper 261*, 1954.

[2] R. J. Lund and R. E. Holmes: Survey Report on Potential Supplies of Thorium from the Rare Earth Industry of the United States. *AEC Report BMI-257*, September 1951.

[3] C. J. Rodden (Ed.): *Analytical Chemistry of the Manhattan Project.* McGraw-Hill Book Co. Inc., New York, 1950.

[4] L. L. Knapp: *Solvent Extraction Equilibria for Rare Earth Nitrate-Tributyl Phosphate System.* Graduate thesis, Iowa State College, August 1956.

Discussion of this article sent (2 copies) to AIME before April 30, 1959, will be published in MINING ENGINEERING.

INTERACTION OF MINERALS WITH GASES AND REAGENTS IN FLOTATION

by IGOR PLAKSIN

Interaction of sulfide minerals and native metals with reagents in flotation is largely determined by particle-surface changes resulting from action of the medium and dissolved gases.

A number of early studies were devoted to the selective action of various gases on minerals.[1] McLachlan[2] paid attention to oxygen as the most active gas affecting flotation properties of sulfide minerals.

I. N. PLASKIN is Professor, Moscow Mining Institute, Academy of Sciences of USSR, and Chief, Department of Mineral Dressing, and Corresponding Member, Academy of Sciences of USSR, Moscow.
TP 4790B. AIME Trans., Vol. 214, 1959.

Opposing views were expressed concerning the influence of sulfide oxidation on xanthate flotation: Taggart[3] recognized the positive influence of oxygen, and I. W. Wark[4] rejected it. Shvedov[5] offered the hypothesis of partial oxidation. As to the influence of such gases as hydrogen[6] and carbon dioxide on mineral floatability, opinions also differed.

Effect of Oxygen on Sulfide Mineral Flotation: Research on the influence of oxygen and other gases on the floatability of sulfide minerals and native metals has been carried out at the Institute of Mining of the USSR Academy of Sciences in

Behavior of both sulfide and nonsulfide minerals depends on the concentration of oxygen in solution. The response of these minerals to variations in oxygen level is affected significantly by their crystal structure.

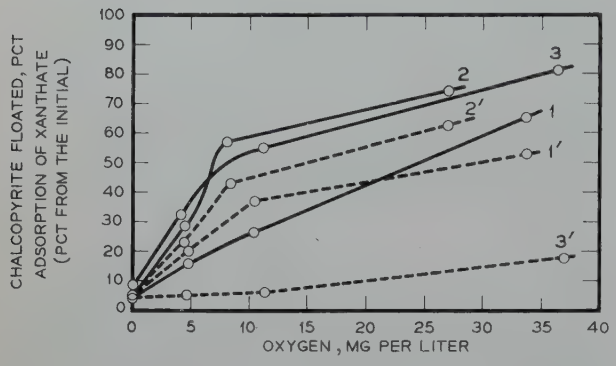

Fig. 1—Influence of oxygen on chalcopyrite flotation (from mixture with quartz) in an argon atmosphere, following additions of S-35 marked potassium ethyl xanthate. Solid lines represent mineral recovery and dotted lines the xanthate adsorption. Curves 1 and 1', xanthate addition at 10 g per ton; curves 2 and 2', xanthate addition at 100 g per ton; curves 3 and 3', xanthate addition at 1000 g per ton; and terpineol, 50 g per ton.

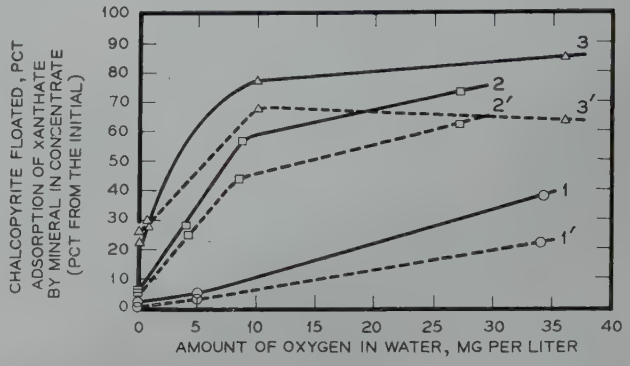
CHALCOPYRITE FLOATED, PCT
ADSORPTION OF XANTHATE
BY MINERAL IN CONCENTRATE
(PCT FROM THE INITIAL)
AMOUNT OF OXYGEN IN WATER, MG PER LITER

Fig. 2—Influence of minor quantities of oxygen on chalcopyrite flotation (from mixture with quartz) in atmospheres of hydrogen, argon, and carbon dioxide, using potassium ethyl xanthate (100 g per ton) and terpineol (50 g per ton) as reagents. The solid lines represent mineral recovery and the dotted lines xanthate adsorption. Curves 1 and 1', with hydrogen as the principal gas; curves 2 and 2', with argon as the principal gas; curves 3 and 3', with carbon dioxide as the principal gas.

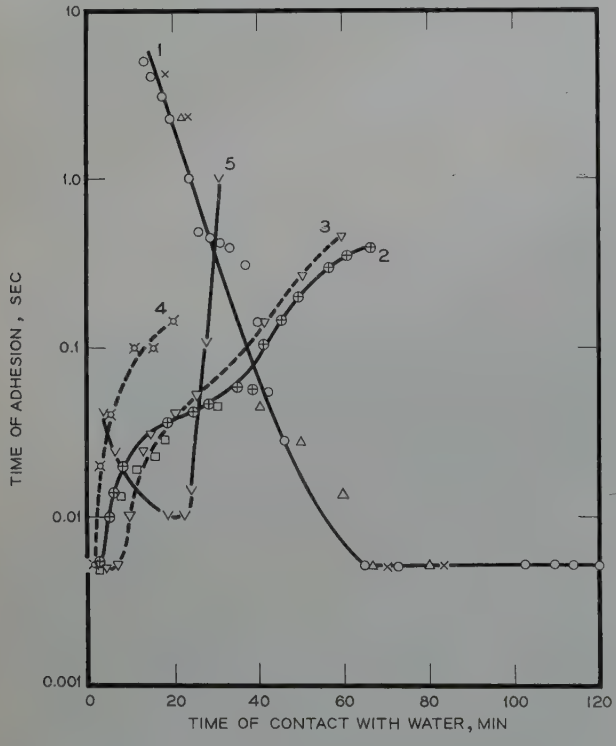

Fig. 3—Glembotsky times of bubble adhesion as a function of duration of mineral-water contact for pyrite, galena, and chalcopyrite. Curve 1, chalcopyrite (various experiments); curve 2, galena ground in water; curve 3, galena ground in air; curve 4, oxidized galena that is preliminarily sulfidized; curve 5, pyrite.

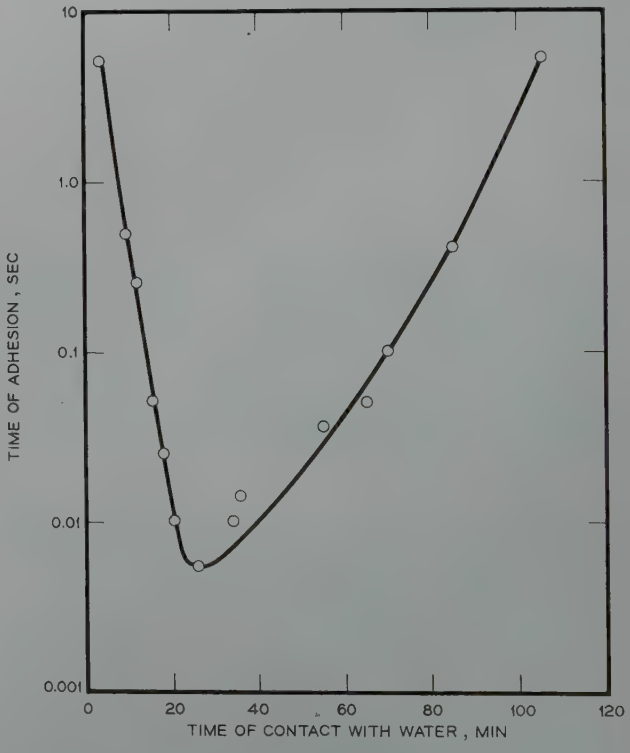

Fig. 4—Glembotsky times of bubble adhesion to the galena as a function of the mineral-water contact, the water being at first deoxygenated and then oxygenated.

Moscow.[7-15] The basic method was flotation of ground minerals in water containing strictly measured amounts of oxygen in an inert gas atmosphere. A standard mineral surface was achieved by grinding and classifying pure sulfide mineral in an oxygen-free atmosphere (nitrogen or argon). Thus treated, the mineral was floated in deoxygenated water by an inert gas, or in water with a definite oxygen content (from traces to 20 to 30 mg per liter).

The apparatus was considerably more elaborate than usual in flotation testing. It included a device for purifying the gas used and for distilling water under a controlled gas atmosphere. Special grinding mills, screens, and flotation cells were designed to permit carrying out these operations under closely controlled gas composition.

Floatability increases with increased oxygen content, in different ratios for various minerals. The most complete flotation of galena is obtained with water having an oxygen content of 1 to 1.5 mg per liter, whereas complete flotation of chalcopyrite requires tens of milligrams of oxygen per liter. Different quantities of oxygen in solution are necessary for the flotation of various sulfides, and rate of floatability increases for various sulfides depending on their activity with relation to oxygen. This has been established by the flotation of monomineral powders as well as by flotation of mineral mixtures. The following mineral sequence has been found with regard to increasing oxygen content of the atmosphere in order to attain complete flotation with a collector: galena, pyrite, sphalerite, chalcopyrite, pyrrhotite, arsenopyrite.

The nonfloatability of chalcopyrite in the absence of oxygen was proved by experiments in the above-mentioned apparatus, using xanthates up to 1 kg per ton.[11] Fig. 1 shows the recovery of chalcopyrite obtained with various quantities of collector added at various oxygen levels; this recovery increases with oxygen level and is very low when the level is under 1 mg per liter. Fig. 1 also shows the xanthate consumed by the mineral (dotted lines) as determined by assays based on S-35.

Carbon dioxide favorably influences floatability of chalcopyrite. In this case, in the absence of oxygen, a noticeable recovery is obtained (Fig. 2). This action may be explained by the decrease of pH from about 7 to 6 in the presence of carbon dioxide; if pH is increased to 6 to 8 by addition of NaOH, this flotation effect practically disappears. Hydrogen does not increase the flotation of chalcopyrite;[13] in fact, it lowers it somewhat in comparison with argon or nitrogen, whose bubbles serve only as *carriers* for the mineral particles (Fig. 2).

It is interesting that conditions of gas composition producing good mineral recovery also produce substantial collector adsorption; conversely, lack of recovery corresponds to lack of adsorption. This is shown by the accord between solid and dotted lines in Figs. 1 and 2.

During flotation tests without collector or frother, floatability was noticed in the presence of oxygen. This natural floatability, or ability of minerals to float in the water without reagents, agrees with the oxygen sulfide activity sequence. In the absence of oxygen and reagents, however, none of the sulfides float. Experiments have proved that on the fresh surface of a sulfide mineral the oxygen is adsorbed first, and then the xanthate is fixed.

Action of oxygen and other gases upon sulfide minerals and native metals has been studied by several methods other than direct flotation: measurement of the contact angle, measurement of adhesion time of particles to bubbles in an electronic contact device,[16] determination of oxygen abstraction from a sulfide mineral pulp,[17] study of the ionic composition of the liquid phase of sulfide suspensions, measurements* of irreversible sulfide-mineral potentials;[14,15] and others.[34,35] The data obtained make it possible to offer a consistent explanation of the phenomena observed. The study of the adhesion time of the mineral particles to air bubbles in the Glembotsky contact device[16] is particularly revealing. The Glembotsky apparatus is an electronic mechanism that evaluates the time required for adhesion to occur between a bubble and a mineral surface. In many measurements this time ranges from 10 to 10^{-3} sec.* Of course, the more hydrophobic the mineral, the shorter this induction time, and a completely hydrophilic surface should require an infinite induction time. Practically, if the induction time exceeds 5 m-sec the mineral is unfloatable. Measurements by the Glembotsky device using pure water on minerals prepared in various ways are summarized in Fig. 3, which illustrates not only the reproducibility of the data, but also substantial differences in behavior between the various sulfides. Also, galena (curves 2 and 3) behaves in much the same way whether prepared by grinding in water or in air, whereas oxidized galena preliminarily sulfidized behaves differently (curve 4).

The author's interpretation of these facts is that the change of surface properties of galena and pyrite proceeds rapidly, whereas for chalcopyrite it occurs slowly. Oxygen adsorption on galena is so rapid that in water with ordinary oxygen content (7 to 8 mg per liter), initial surface wettability is not detected. Galena wettability is found if the ad-

* We study the electrochemical unevenness of a surface of sulfide minerals,[34, 35] and also the electrochemical properties of mineral surface in general.[14, 15] We use a method of anode and cathode polarization of sulfide. We have studied by this method anode and cathode parts on the surface of a sulfide mineral. Uneven surface chemical compounds of sulfide minerals have been proved by these tests. Such unevenness of electrochemical potential on the sulfide mineral surface influences the distribution of reagents on mineral particles of flotation pulp.[36]

* Sven Nilson and then M. A. Eigeless were the first to register the time of contact between mineral particle and air bubble. Glembotsky's device is unique in that it is an electronic mechanism with a moving holder of the bubble.

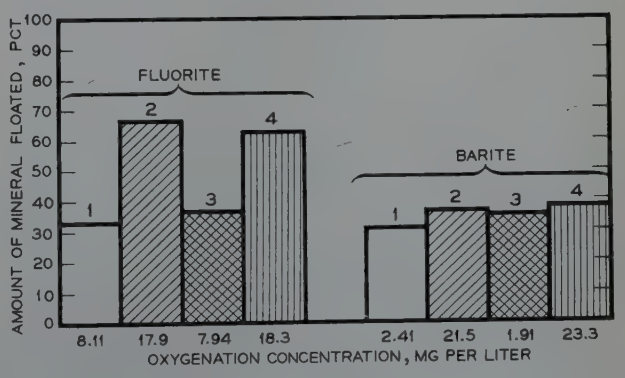

Fig. 5—Effect of aerating gas on recovery of fluorite (left) and barite (right). The numbers 1, 2, 3, and 4 refer to flotation condition as follows: 1, without deliberately added gases; 2, following oxygenation; 3, following nitrogen addition after oxygenation; 4, after second oxygenation. Numbers at base of blocks represent oxygen concentration in milligrams per liter.

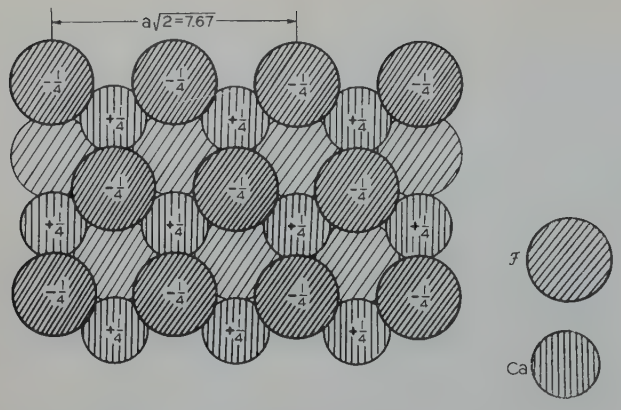

Fig. 6—Diagram illustrating the projection of the fluorite structure upon the cleavage plane (111).

hesion time measurements are conducted first in deoxidized water and then while oxygen is dissolved in the water (Fig. 4, left branch of the curve). These tests prove that sulfide mineral particles can adhere to a bubble in the presence of oxygen.[18] It should be noted that in this study the relations obtained between galena adsorption of oxygen dissolved in water and galena adsorption of oxygen from the air are very close to the results published in Hagihara's work on electron diffraction of galena oxidation.[19]

Thus it has been established that in the absence of oxygen the fresh surface of a sulfide mineral or of a metal is wettable to some extent. The oxygen dissolved in water is adsorbed on the surface of minerals before the other gases (nitrogen, carbon dioxide, etc.) are adsorbed. Plaksin and Bessonov[8] distinguish successive stages of the action of oxygen with a transition from a labile form of fixing through a stable one to forming of chemical compounds, which can be shown, for instance, by the following sequence: 1) adsorption, 2) activated adsorption with fixing of oxygen, 3) oxidation of the surface with oxygen diffusion in the surface layer. For various sulfides and metals these stages occur at different rates, depending on the chemical activity of the sulfide (or metal) for oxygen. Flotation properties of mineral surfaces under the influence of oxygen and collector change accordingly. In the initial period of its action, oxygen promotes dehydration of the mineral surface, facilitating penetration of xanthate groups and their consequent fixation. In case of long exposure to oxygen the flotation properties of a surface become worse.

These observations and results have made it possible to classify gold ores and the sulfides of nonferrous metals as to their oxygen demand during flotation. Proceeding from the experience of one USSR dressing plant, a direct selective method of flotation for copper-lead-zinc ores with oxygen control has been introduced.

Experiments have been made with controlled oxygen content in flotation of sulfide minerals with xanthate in respect to modifiers, activators, and depressants, in particular on the action of sodium sulfide.[20] The experiments show that a certain average concentration of sodium sulfide exists when adsorption of the collector by galena reaches a peak. The peak is explained by an initial oxidation of the galena and agrees well with the depression of galena due to excess sodium sulfide.[21]

Effect of Oxygen on Flotation of Nonsulfide Minerals: The influence of oxygen and other gases on the floatability of nonsulfide minerals (fluorite, barite, calcite, quartz) has also been studied, with unexpected results. Phosphorite was studied first. It was found that flotation properties of the ore changed in relation to the gas blown into the pulp. The phosphorite ore was ground to 0.15 to 0.05 mm and after preliminary desliming was placed in a laboratory flotation machine of 350-cc capacity. The machine had a gas-tight cover and at the side there was a device for supplying gas to the flotation chamber. Reagents used were carboxylic acid (or tall oil soap), caustic soda, and sodium silicate. The other experiments were carried out first without addition of gases. When gases were used they were allowed to remain in contact with the pulps for 3 to 75 min. After gasification, the flotation reagents were introduced and the pulp and reagents thoroughly mixed, after which flotation was carried out. Temperature of the pulps was maintained at 18° to 20°C for 5 to 60 min. In the experiments with oxygen and air, flotation was carried out with tap water and distilled water, but for experiments with nitrogen fresh doubly-distilled water was used. It was found that introduction of air and/or oxygen in the pulps increased the recoveries, whereas nitrogen decreased them.[22–25]

Particles of fluorite and quartz (0.15 to 0.06 mm) were floated with sodium oleate (100 to 500 g per ton) by passing oxygen or nitrogen through the pulp for varying lengths of time. On addition of 100 g of sodium oleate per ton of fluorite the collector abstraction corresponded initially to 94 pct of a monomolecular layer and increased to 137 pct after 60 min. The thickness of the layer was approximately twice as great at 200 g per ton. Further increases in reagent addition are generally without effect. The change in thickness of the adsorbed layer brought about by continued oxygen treatment has no significant effect on recovery of fluorite or of quartz in the concentrate.[26]

The experiments, conducted under the usual precise conditions of flotation, showed that recovery of nonsulfide minerals in the froth product was greatly increased if oxygen had previously been admitted to the mineral surface.

Motion pictures made it possible to observe the progress of mineralization of the air bubble with mineral grains under dynamic conditions. The experiments were carried out in a cuvette with plane parallel walls, filled with water or with aqueous solution of the collector, in which the motion of the air bubbles and mineral particles was effected. Pictures were taken at 400, 900, and 1500 frames per sec with bubbles 2 mm in diam ascending at 18 to 27 cm per sec.

By speed filming, then, it was possible to determine that additional adsorption of oxygen on the surface of fluorite produces:

1) Higher mineralization of the bubble with the particles of fluorite.

2) Five to ten times longer contact between mineral grain and air bubbles.

3) Air flocculant attachment of fluorite grains to the air bubble.

Relation Between Crystal Structure and Influence of Gases: Study of the combined action of gases and

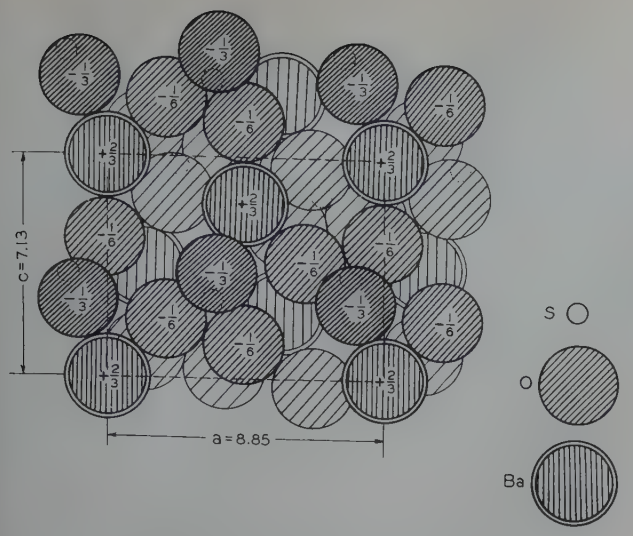

Fig. 7—Projection of barite structure upon cleavage plane (110). Here and in Fig. 6 the varying intensities of shading indicate distances of the ions from a geometrical plane that is tangent to the outermost atoms.

reagents on flotation of nonsulfide minerals brings out peculiarities that can be rationalized in terms of crystal structure. The complex effects for fluorite and barite are shown in Fig. 5. Blocks 1 and 2, left, show that oxygen markedly favors recovery of fluorite, while the corresponding blocks in the right half of the illustration show that there is no such effect with barite. Blowing nitrogen after oxygen (block 3) shows reversion to unoxygenated recoveries, while secondary oxygen blowing (block 4) restores the oxygen effect. Thus changes in the floatability of certain nonsulfide minerals by dissolved gases is not a general phenomenon.

To explain the flotation behavior of fluorite and barite, peculiarities of their crystal structure may be used, considering that the breaking of minerals occurs mainly along the cleavage faces and that the molecular-physical properties of the surfaces are determined by their crystal chemistry.

Study of the projection of fluorite and barite structures on the cleavage plane (Figs. 6 and 7) shows that the fluorite surface is distinguished by a low relief, and its surface molecular field is characterized by evenness and a small value for the intensity (the value of separate noncompensated electrostatic charges is not above ¼). On the contrary, the surface of barite is distinguished by substantial differences in the values of noncompensated charges and a radically expressed unevenness of their distribution. This, together with a certain softness in the structural setting of ions and the presence of great unevenness, predetermines the heterogeneity of the surface molecular field and its greater intensity in the places of localization —in the active centers, that is—having charges of ½ to 2/3.

Thus the wettability of a fluorite surface, which is low compared with that of a barite surface, is predetermined first by a lower value of the noncompensated charges, second by a poorer distribution of spaces for the adsorbed molecules of water. A part of the water molecules cannot approach the attracting ion up to immediate contact. The relative evenness of the surface, together with the absence of strong charges, promotes the instability and lability of the hydrate layer.

In a similar way, the peculiarities of the surface molecular field determine the behavior of gases dissolved in the pulp. As the result of screening by the adsorbed molecules of the surface force field, the total surface wetting is changed. In turn the diffusion of gases to the surface, which precedes the adsorption, depends on correct orientation of the dipoles of the hydrate layer. There is an apparent and direct relation between the degrees of surface wetting and the surface adsorption of gases.

The degree of hydrophobicity, which is increased as a result of the physical adsorption of gases from the solution, may on the whole be associated with the intensity value of the surface field. The dependence is reversed: the smaller the intensity of the field, the greater the screening effect by the adsorbed molecules.[27]

Similar considerations apply in the case of some other nonsulfide minerals.[32,33] Pyrite and arsenopyrite have also been the object of considerable study at the Institute of Mining in Moscow, and three methods[28,29] have been proposed for their separation. In the last analysis these methods rest on the crystal-chemical differences in the structure of the minerals.

Influence of Oxygen and Oxydizers on Selective Flotation of Pyrite and Arsenopyrite as a Function of Their Crystal Structure: In certain cases oxygen and the oxydizing chemicals can facilitate the selective separation of minerals with different crystal structure but similar flotation properties.

In modern practice selective flotation of such sulfide minerals as pyrite and arsenopyrite has not found complete practical solution. Both for industry and flotation theory, therefore, the selection of pyrite and arsenopyrite is of great importance, because with very similar flotation properties these minerals differ substantially in structure.

In the crystal structure of pyrite the ions of iron seem to be separated by ions of sulfur. The sulfur ions, being situated in pairs close to every ion of iron, are mainly concentrated at the surface and at the intersections of the crystal lattice of the minerals.

As to the morphologic peculiarities of crystals, arsenopyrite is classed with the markezite row. However, x-ray study shows certain deviations from this structure. The ideal structure of this mineral is monolithic; it becomes rhombic only when it is doubled. In the crystal structure of arsenopyrite-markesite the situation and the bonds of atoms are much more complex for arsenopyrite than for pyrite. In the former, every atom of iron has six neighbors in the corners of a somewhat displaced octahedron; one face of the octahedron is a triangle composed of three atoms of sulfur, whereas the opposite face is composed of three atoms of arsenic. An atom of sulfur is surrounded by three atoms of iron and one of arsenic, which are situated in the corners of a somewhat elongated tetrahedron. Accordingly, an atom of arsenic is surrounded by three atoms of iron and one of sulfur. The peculiarities of the crystal structure of pyrite and arsenopyrite reveal the different influence of oxidation upon them. The position of atoms of sulfur in pyrite on the faces and on the ribs of cells makes them more accessible for the joining of oxygen. In the first phase of oxidation it probably occurs without the destruction of the crystal lattice of the mineral.

Alteration of the ionic content of the aqueous part of the pyrite pulp which follows is associated with the dissolving of the oxidation products which takes place owing to weakening of the bond between the same adjacent atoms of sulfur and iron. However, the break-off of separate atoms apparently does not completely destroy the general structure of the mineral's crystal cell, and its newly revealed surface remains capable of interaction with flotation reagents. This is why even a protracted influence of oxidation does not depress floatability of the pyrite. As for the arsenopyrite, which has a more complicated structure both as regards its content and composition, the sulfur atoms are within the crystal cell in complex interrelation with the atoms of iron and arsenic and, consequently, are not accessible to oxygen influence in the first stage of oxidation. Hence, oxidation of arsenopyrite proceeds more slowly than that of pyrite. The processes of deep oxidation caused by prolonged oxidation in its more active form change the mineral structure by breaking the sulfurous and arsenic bonds. The arsenic ion is oxidized predominantly with the formation of arsenic oxide groups which remain on arsenopyrite surface. The study of flotation properties of pyrite and arsenopyrite has helped to establish the difference in their behavior under definite conditions of selective flotation, outlining three methods of separating pyrite and arsenopyrite: 1) use of oxidizers as reagents which differentiate the floatability of these minerals, 2) selective flotation in lime media with preliminary activation by $CuSO_4$, and 3) selective flotation with ammonium compounds and lime.

The third of these methods depends on the use of a relatively high concentration of ammonium chloride to favor flotation of pyrite and discourage flotation of arsenopyrite. This experimental result is corroborated by measurements of xanthate adsorption on both minerals made through xanthate tagged with S-35.

SUMMARY

In this necessarily very brief review of a very large research program, the writer has touched only the highlights. These include the following ideas:

1) Gases play an important chemical role in flotation. The behavior of minerals in particular depends on the concentration of oxygen in solution.

2) The effect of oxygen is not limited to sulfide minerals but, surprisingly, enters also into the behavior of nonsulfides.

3) The crystal structure of minerals, sulfides and nonsulfides alike, is a major factor in their response to variations in oxygen level.

REFERENCES

[1] A. S. Adams: Gas Sorption in Flotation. *AIME Trans.*, 1928, vol. 79 *(Flotation Practice)*, pp. 216-225.

[2] C. G. MacLachlan: Synthetic Testing for Flotation. Canadian Institute of Mining and Metallurgy *Bulletin*, vol. 173, September 1926.

[3] A. F. Taggart, T. C. Taylor, and A. G. Knoll: Chemical Reactions in Flotation. *AIME Trans.*, 1930, vol. 87 *(Milling Methods)*, pp. 217-260.

[4] I. W. Wark: *Principles of Flotation.* Melbourne, 1938.

[5] D. A. Shvedov: Hypothesis on the Good Floatability of Sulphide Minerals and Poor Floatability of Oxidized Ones. *Magazine of Ore Dressing*, 1936, no. 6, pp. 24-27.

[6] A. K. Podnek and Z. I. Emmanuilova: On the Mechanism of Interaction of Xanthates with Sulphides in Flotation. Collection of questions on flotation theory. *Metallurgisdat*, 1941, pp. 69-75.

[7] I. N. Plaksin, A. J. Sinelnikova, and G. N. Hazinskaya: Influence of Oxidation upon Floatability and Separation of Sulphide Minerals. *Trans.*, USSR Academy of Sciences, Technical Science Department, 1947, pp. 425-437.

[8] I. N. Plaksin and S. B. Bessonov: On the Part of Oxygen and Other Gases in Flotation. *Trans.*, USSR Academy of Sciences, Technical Science Department, 1948, no. 11, pp. 1773-1788.

[9] I. N. Plaksin: Role of Gases and Their Chemical Interaction with Reagents in Flotation Processes. Collection: *Role of Gases and Reagents in Flotation Processes.* USSR Academy of Sciences, 1950, pp. 32-62.

[10] S. V. Bessonov and I. N. Plaksin: Influence of Oxygen on Floatability of Galena and Chalcopyrite. *Trans.*, USSR Academy of Sciences, Technical Science Department, 1954, no. 1, pp. 114-127 et seq.

[11] I. N. Plaksin, S. V. Bessonov, and V. I. Turnikova: On Mechanism of Xanthates Interaction with Sulphide Mineral Surface. *Reports*, USSR Academy of Sciences, 1955, vol. 102, no. 2, pp. 331-333.

[12] I. N. Plaksin and S. P. Zaitseva: Influence of Oxygen, Nitrogen and Hydrogen upon the Ethyl Xanthate Adsorption by Gold, Silver, Copper and Their Alloys. *Reports*, USSR Academy of Sciences, 1955, vol. 101, no. 4, pp. 727-730.

[13] S. V. Bessonov, I. N. Plaksin, and V. I. Turnikova: Influence of Various Gases upon Chalcopyrite Floatability. *Trans.*, USSR Academy of Science, Technical Science Department, 1955, no. 10, pp. 125-130.

[14] I. N. Plaksin, S. V. Bessonov, and L. R. Solovjeva: On the Study of Changes in Flotation Properties of the Surface of Sulphides under the Action of Gases and Reagents. *Proceedings*, Institute of Mining, Academy of Sciences, USSR, 1955, vol. 2, pp. 193-206.

[15] I. N. Plaksin, S. V. Bessonov, and L. R. Solowjowa: Anderungen der Flotationseigenschaften von Sulfidoberfiachen unter dem Einfluss von Gasen und Reagenzien. Freiberger Forschungshefte, 1955, H. A. 33, s. 60.

[16] V. A. Glembotsky: Rate of Adhesion to Air Bubbles to Mineral Particles during Flotation and Methods for Its Measurement. *Trans.*, USSR Academy of Sciences, Technical Science Department, 1953, no. 11, pp. 1524-31.

[17] I. N. Plaksin and S. B. Bessonov: Oxygen Adsorption in Sulphide Suspension. *Reports*, USSR Academy of Sciences, 1954, vol. 98, no. 2.

[18] I. N. Plaksin and S. V. Bessonov: On Sulphide Mineral Adhesion to Air Bubbles in the Absence of Reagents. *Reports*, USSR Academy of Sciences, 1954, vol. 97, no. 3, pp. 495-498.

[19] H. Hagihara: Surface Oxidation of Galena in Relation to Its Flotation as Revealed by Electron Diffraction. *Journal of Physical Chemistry*, May 1952, vol. 56, p. 610.

[20] S. I. Mitrofanov, V. G. Kushnikova, I. A. Strigin, and G. S. Rozhavsky: The Study of Sulfidization Reactions of Oxidized Minerals. Collection of papers: Nonferrous Metals Metallurgy and Methods of Analysis. Gonty Literature of Ferrous and Nonferrous Metals, 1955, no. 10, pp. 7-29.

[21] D. Ny-lian, I. N. Plaksin, and V. I. Turnikova: Influence of the Oxygen on the Interaction of Sulfide Minerals with Xanthate in the Presence of Sodium Sulfide. *Trans.*, USSR Academy of Sciences, Technical Science Department, no, 12, 1957.

[22] I. N. Plaksin and E. M. Doubrovsky: The Influence of Gases upon the Flotation of Phosphorite Ores. *Reports*, USSR Academy of Sciences, 1949, vol. 68, no. 2, pp. 361-363.

[23] I. N. Plaksin and E. M. Doubrovsky: The Influence of Adsorption Interaction of Gases upon the Floatability of Phosphatites. *Trans.*, USSR Academy of Sciences, Technical Science Department, 1949, no. 7, pp. 1030-1037.

[24] I. N. Plaksin and E. M. Chaplygina: The Influence of Gases upon Flotation of Nonsulfide Minerals. *Reports*, USSR Academy of Sciences, 1952, vol. 82, no. 3, pp. 451-453.

[25] I. N. Plaksin and E. M. Chaplygina: The Influence of Gases upon Flotation of Nonsulfide Minerals, USSR Academy of Sciences, Technical Science Department, 1952, vol. 82, no. 9, pp. 1353-1359.

[26] I. N. Plaksin and E. M. Chaplygina: On the Question of the Influence of Gases upon the Density of the Adsorption Layer of Sodium Oleate in Flotation of Some Nonsulfide Minerals. *Reports*, USSR Academy of Sciences, 1953, vol. 91, no. 2, pp. 301-303.

[27] V. V. Bakakin, I. N. Plaksin, and E. M. Chaplygina: The Influence of Gases upon Flotation of Fluorite and Barite. *Trans.*, USSR Academy of Sciences, Technical Sciences Department, 1957, no. 9, pp. 96-100.

[28] I. N. Plaksin and N. S. Vlassova: Concerning Oxygen Influence upon Separation of Pyrite and Arsenopyrite by Selective Flotation. *Reports*, USSR Academy of Sciences, 1946, vol. 52, no. 1, pp. 55-56.

[29] I. N. Plaksin, G. A. Myasnikova, and A. M. Okolovitch: *Flotation of Arsenic-Pyrite Ores.* Akademizdat, Moscow, 1955.

[30] I. N. Plaksin: The Problems of Finding Flotation Reagents and the Study of Their Interaction with Minerals. *Proceedings*, USSR Academy of Sciences, 1952, no. 8, pp. 57-65.

[31] I. N. Plaksin: Results and Prospects of Research into the Interaction of Reagents with Minerals during Flotation. *Trans.*, USSR Academy of Sciences, Technical Science Department, 1955, no. 1, pp. 109-134.

[32] I. N. Plaksin and E. M. Chaplygina: The Influence of Oxygen and Nitrogen upon Selective Flotation of the Titanium and Zirconium Minerals. *Reports*, USSR Academy of Sciences, 1958, vol. 119, no. 4.

[33] V. V. Bakakian, I. N. Plaksin, and E. M. Chaplygina: The Influence of Oxygen and Nitrogen upon Selective Flotation of the Titanium and Zirconium Minerals and Their Crystal Structure. *Trans.*, USSR Academy of Sciences, Technical Science Department, 1958, no. 6, pp. 84-90.

[34] I. N. Plaksin and R. Sh. Shafeev: Influence of the Electric Potential on the Xanthate Distribution on the Sulfide Minerals Surface. *Reports*, USSR Academy of Sciences, 1958, vol. 118, no. 3.

[35] I. N. Plaksin and R. Sh. Shafeev: Influence of the Electrochemical Unevenness of Sulfide Minerals Surfaces on the Xanthate Distribution in the Flotation Condition. *Reports*, USSR Academy of Sciences, 1958, vol. 121, no. 1.

[36] I. N. Plaksin, et al.: Microradiographic Study of the Action of Flotation Reagents. *Transactions*, Institution of Mining and Metallurgy, vol. 67, 1957-1958, part I, no. 1, pp. 1-7; discussion, no. 4, pp. 251-257, and no. 5, pp. 370-371. Vol. 68, 1958-1959, no. 2, author's reply to discussion.

Discussion of this article sent (2 copies) to AIME before April 30, 1959, will be published in MINING ENGINEERING.

EXPERIMENTS IN CONCENTRATING IRON ORE FROM THE PEA RIDGE DEPOSIT, MISSOURI

by M. M. FINE and D. W. FROMMER

Mineral dressing research showed that iron concentrates of commercial quality could be produced from the Pea Ridge deposit near Sullivan, Mo. Magnetic separation and flotation, on a laboratory scale, yielded concentrates ranging from 60.0 to 71.4 pct Fe at recoveries of 89.9 to 97.6 pct.

Early in 1957 St. Joseph Lead Co. announced discovery of three new centers of iron ore deposition in east central Missouri.[1] The discovery resulted from exploratory drilling in the vicinity of a magnetic anomaly or *high*. A deep hole, drilled into the Pre-Cambrian porphyry to determine the cause of anomaly, penetrated a magnetite-rich deposit.[2]

The magnetic surveys that revealed the anomalies were begun by the Missouri Geological Survey in 1929 and were continued into the 1930's.[3] At that time an area in Crawford County known as the Bourbon magnetic high was located. A second anomaly, similar in size and intensity, was discovered about six miles to the northeast in Franklin County in the vicinity of Sullivan. This area was not studied in detail until the early 1940's.

To determine the cause of the anomalies, the USBM drilled four holes at the Bourbon site in 1943-1944.[4] The most productive hole penetrated four mineralized zones having a total thickness of 127.5 ft. These zones contained magnetite in rhyolite porphyry at depths between 1600 and 2000 ft. Additional iron ore below 2000 ft was considered a possibility at the time.

Some years later, the USGS, Missouri Geological Survey, St. Joseph Lead Co., and others cooperated in sponsoring an aeromagnetic survey of the Bourbon-Sullivan area which resulted in discovery of a third high, about eight miles distant at Pea Ridge. This deposit, with an estimated reserve of 50 to 100 million tons of iron ore, is considered the main find, although other orebodies in the same general area are of definite interest.[4]

When this discovery was announced, St. Joseph Lead also revealed plans to exploit the deposit jointly with Bethlehem Steel Co. A new corporation, Meramec Mining Co., was established, and 1962 was set as the target date for completing physical plant.[2] Annual production goals of 2 million tons of beneficiated and pelletized iron ore were proposed. Preparation of the site for shaft sinking was begun in June 1957.

Orebody and Character of Samples: Drilling to date has established the Pea Ridge orebody as a crescent-shaped pipe about 300 ft wide. Some drillholes were bottomed at 2800 ft in very good iron ore.[6] The orebody is predominantly magnetite, although hematite and a mixture of hematite and magnetite occur in the upper areas and peripheral walls.

Table I. Partial Chemical Analyses of Composite Samples

Number	Character	Analysis, Pct Fe	P	SiO_2	S	Cu
1	Medium grade mixed hematite and magnetite	40.3	0.87	27.2	0.35	0.04
2	High grade mixed hematite and magnetite	59.6	1.14	5.3	0.52	0.02
3	High grade magnetite	64.1	0.75	4.1	0.37	0.03

Drillhole cores representing ore from different areas and depths of mineralization were grouped into composites for testing. These composites consisted of: 1) medium grade mixed hematite and magnetite, 2) high grade mixed hematite and magnetite, and 3) high grade magnetite. The medium grade ore came from three holes with depths of 1350 to 1900 ft. The high grade mixed hematite and magnetite cores came from the 1790 to 2812-ft interval of one hole.

Partial chemical analyses of the three samples, given in Table I, reveal that all are excessively high in phosphorus and sulfur, and sample 1 is

M. M. FINE, Member AIME, is Chief Mineral Dressing Section, Division of Mineral Technology, Region IV, U. S. Bureau of Mines, Rolla, Mo. D. W. FROMMER is a Metallurgist, Region V, U. S. Bureau of Mines, Minneapolis, Minn. TP 4791B. Manuscript, Sept. 8, 1958. Mid-America Minerals Conference, St. Louis, Mo., October 1958. AIME Trans., vol. 214, 1959.

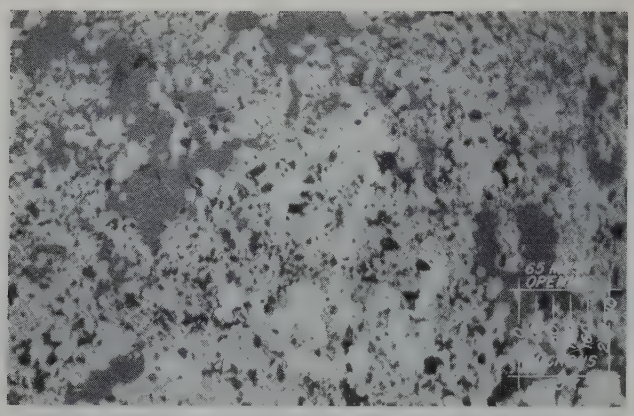

Fig. 1— Pyrite and gangue in magnetite. 75X, ¼ reduction.

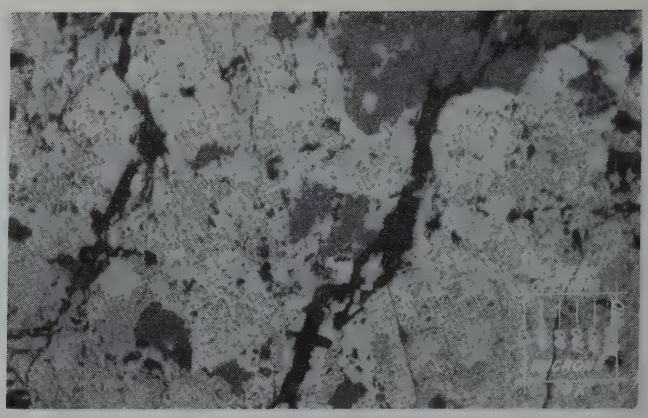

Fig. 2—Magnetite, hematite, gangue. 75X, ¼ reduction.

over the silica specification as well. It is notable, too, that samples 2 and 3 would be direct-shipping ore were it not for the phosphorous and sulfur contamination.

A petrographic examination of sample 1 revealed hematite and magnetite in a gangue comprised primarily of orthoclase, quartz, and chlorite. Smaller amounts of apatite, pyrite, chalcopyrite, and traces of tremolite and calcite were noted. Hematite and magnetite were in sample 2, of course, and the gangue minerals included quartz, feldspar, apatite, pyrite, and chalcopyrite. Finally, magnetite was the essential constituent of sample 3, accompanied by small quantities of the same gangue minerals noted for sample 1.

Figs. 1 through 3 are micrographs of polished sections made from random fragments at a magnification of 75X. In Fig. 1 the light-colored material is pyrite, the gray is magnetite, the dark gray is gangue (in this case, primarily apatite), and the black areas are depressions in the section. The grain size may be gaged by comparison with the photographic insert of a 65-mesh opening. Fig. 2 shows hematite (light gray) as an alteration product of magnetite (medium gray), and the gangue is represented by the dark gray areas. The light-colored area in the center of Fig. 3 is a grain of chalcopyrite; the light gray and the medium gray areas are hematite and magnetite, respectively; and the dark gray area is apatite. The micrographs, particularly Figs. 1 and 2, are eloquent evidence of the intimate association of iron oxides and gangue in the samples.

BENEFICIATION RESEARCH

Magnetic Separation: Since most of the Pea Ridge samples were comprised of magnetite, the initial experiment was recovery of iron by magnetic methods. From the intergrowth of minerals revealed in polished sections, it was anticipated that fine grinding would be required for adequate liberation. Accordingly a portion of sample 3 was ground to —48 mesh and sized by screening, and the individual fractions were separated in a Davis magnetic tube. These results, presented in Table II, showed a gradual reduction in phosphorous analysis of the magnetic concentrates down to 325 mesh and then a sharp drop to a value about half that of the coarser fractions. This suggested that the phosphorous content of magnetic concentrates produced from sample 3 would be a function of the quantity of —325 mesh material in the feed. In Table II it is evident that sulfur was also efficiently eliminated by fine grinding and magnetic separation.

Subsequent wet separations on a laboratory drum-type machine showed that grinding to at least —100 mesh was required to yield magnetic concentrates with a satisfactory iron-to-phosphorus ratio. A nominal 100 mesh grind created about 50 pct —325 material. The ground samples were given a two-stage magnetic treatment at a current of 0.5 amp; tailings from the first stage were thickened and passed through the unit a second time to recover additional magnetic values.

Table II. Sample 3, Separation in Davis Tube

Product	Mesh	Weight, Pct	Analysis, Pct				Pct of Total	
			Fe	P	SiO_2	S	Fe	P
Magnetic	−48 +100	22.6	69.0	0.35	2.7	0.17	24.2	10.1
Nonmagnetic	−48 +100	1.6	10.0	6.44	—	—	0.2	13.2
Magnetic	−100 +150	12.2	68.7	0.35	2.0	0.11	13.0	5.4
Nonmagnetic	−100 +150	1.1	8.8	7.08	—	—	0.2	10.0
Magnetic	−150 +200	12.0	69.7	0.31	1.8	0.07	13.0	4.7
Nonmagnetic	−150 +200	1.0	8.6	7.08	—	—	0.2	9.1
Magnetic	−200 +325	11.7	70.7	0.27	1.3	0.06	12.9	4.1
Nonmagnetic	−200 +325	1.2	12.5	6.77	—	—	0.2	10.4
Magnetic	−325	32.1	71.2	0.15	0.80	0.03	35.5	6.1
Nonmagnetic	−325	4.5	7.9	4.64	—	—	0.6	26.9
Composite		100.0	64.3	0.78	—	—	100.0	100.0

Table III. Sample 3, Magnetic Separation in Drum-Type Separator

Product	Weight, Pct	Analysis, Pct				Pct of Total	
		Fe	P	SiO_2	S	Fe	P
1st magnetic	85.9	71.5	0.21	1.1	0.047	94.0	21.3
2nd magnetic	3.0	68.0	0.45	2.8	0.14	3.1	1.5
Nonmagnetic tailings	11.1	17.0	5.87	—	—	2.9	77.2
Composite	100.0	63.3	0.84	—	—	100.0	100.0
Total magnetic concentrate	88.9	71.4	0.22	1.2	0.05	97.1	22.8

The results of separating sample 3 magnetically at —100 mesh are given in Table III. Recovery of 97.1 pct Fe was effected in a product grading 71.4 pct Fe, 1.2 pct SiO_2, 0.22 pct P, and 0.05 pct S. The second magnetic product (Table III) was made part of the total concentrate without appreciable detriment to the overall analysis, although it contained many locked magnetite-gangue grains. Their pres-

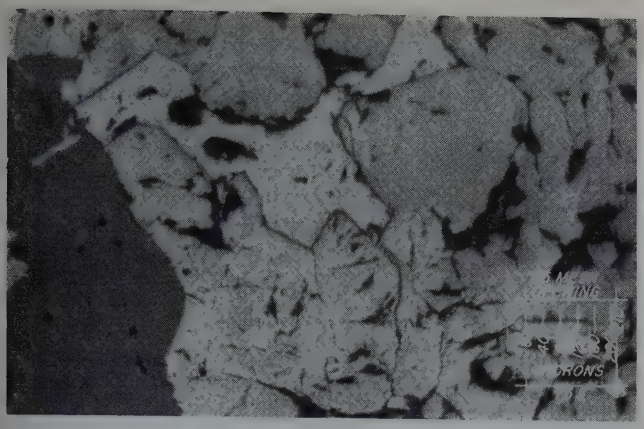

Fig. 3—Magnetite, hematite, chalcopyrite, and apatite. Micrograph reduced about one-fourth for reproduction.

ence, however, emphasized the importance of sufficient grinding to prevent too many of these highly magnetic middling particles from reporting with the concentrate.

Flotation: Samples 1 and 2, with hematite contents of about 55 and 40 pct respectively were, in the natural state, only partially responsive to low-intensity magnetic separation. Accordingly, research was undertaken to develop flotation procedures for concentrating these materials. With regard to major impurities, there was no difficulty in removing sulfur by conventional sulfide flotation or some variation of this method. Silica was a problem only on sample 1, and there the difference in floatability of iron oxides and the quartz-silicate gangue was so great that the gangue was readily rejected. Phosphorus was much more of a problem, since both the crystalline apatite and iron oxides were receptive to anionic collectors.

Research on flotation of iron ores has been under way in industrial and government laboratories for many years, and technical literature contains a profusion of related experimental data. Most of the research has been devoted to separation of siliceous ores, for which at least three solutions have been proposed and one (fatty acid flotation) applied commercially.[7] One reference[8] to flotation of iron ore containing apatite suggests that in an acid pulp fluorides or fluosilicates should help depress the phosphate mineral during anionic flotation of iron oxides. A similar combination of reagents has been notably successful, on an industrial scale, in floating ilmenite in the presence of apatite.[9]

Much the same approach was made with the samples of Pea Ridge ore, but it was soon evident that although the reagent combination of sodium fluoride and sulfuric acid was an excellent depressant for quartz and silicate minerals, it did little to discourage flotation of apatite. The iron oxides, on the other hand, could be depressed by alkaline silicates while floating apatite with moderate quantities of fatty acid or tall oil soaps. Iron minerals were easily reactivated with larger quantities of anionic collector. On this basis samples 1 and 2 were successfully concentrated.

The medium grade ore, sample 1, was wet-ground to −65 mesh and conditioned with soda ash and sodium silicate. Apatite and the sulfides were then promoted in succession with a tall oil soap and xanthate, respectively. The pulp was settled and thickened by decantation. A small amount of slime,

Table IV. Sample 1, Flotation

Product	Weight, Pct	Analysis, Pct Fe	P	SiO_2	S	Pct of Total Fe	P
Apatite concentrate	6.6	8.6	11.5	—	—	1.4	83.0
Apatite middling	3.0	33.0	0.47	—	—	2.5	1.5
Sulfide concentrate	0.9	37.3	0.44	—	—	0.9	0.5
Sulfide middling	1.2	26.3	0.31	—	—	0.8	0.5
Iron concentrate	58.9	60.0	0.19	9.8	0.075	89.9	12.1
Iron middling	6.6	10.0	0.06	—	—	1.7	0.3
Tailing	20.2	4.0	0.04	—	—	2.0	0.9
Slime	2.6	11.8	0.42	—	—	0.8	1.2
Composite	100.0	39.3	0.91	—	—	100.0	100.0

Metallurgical Results

Operating Data. Apatite and Sulfide Flotation

Reagents	Pounds Per Ton of Crude Ore: Apatite Flotation, Conditioners 1	Conditioners 2	Rougher	Cleaner	Sulfide Flotation, Conditioner	Rougher	Cleaner
Sodium carbonate	2.0						
Sodium silicate	2.0						
AC 710*		0.5					
Secondary butyl xanthate					0.10		
Aerofroth 65*					0.02		
pH	10.2						
Time, min	5	5	5	5	5	5	3

Operating Data. Iron Flotation

Reagents	Pounds Per Ton of Crude Ore: Conditioners 1	Conditioners 2	Rougher	Cleaners 1	Cleaners 2
Sulfuric acid	0.67			0.20	0.20
Sodium fluoride	0.25			0.08	0.08
Pamak No. 1**		0.90			
pH	7.5				
Time, min	5	10	5	5	5

* American Cyanamid Co.
** Hercules Powder Co.

Table V. Sample 2, Flotation

Product	Weight, Pct	Analysis, Pct Fe	P	SiO_2	S	Pct of Total Fe	P
Apatite concentrate	9.5	11.8	11.25	—	—	1.9	85.4
Apatite middling	1.9	50.8	0.79	—	—	1.6	1.2
Sulfide concentrate	0.9	39.0	0.58	—	—	0.6	0.4
Sulfide middling	1.1	49.0	0.54	—	—	0.9	0.5
Iron product	86.6	65.5	0.18	6.4	0.067	95.0	12.5
Composite	100.0	59.7	1.25	—	—	100.0	100.0

Metallurgical Results

Operating Data

Reagents	Pounds Per Ton of Crude Ore: Apatite Flotation, Conditioners 1	Conditioners 2	Rougher	Cleaner	Sulfide Flotation, Conditioner	Cleaner	Rougher
Sodium carbonate	2.0						
Sodium silicate	2.0						
Sodium oleate		0.5					
Secondary butyl xanthate					0.12		
Aerofroth 65					0.02		
pH	10.2						
Time, min	5	5	5	5	5	5	5

containing less than 1 pct of the total iron, was decanted in the process. The thickened slurry, at about 40 pct solids, was conditioned with sulfuric acid and sodium fluoride to establish a near-neutral pH. A rougher concentrate was floated with a refined tall oil fatty acid and cleaned twice to produce a finished concentrate.

Details and results are presented in Table IV. Recovery of 89.9 pct was attained from sample 1 at a grade of 60.0 pct Fe, 0.19 pct P, 9.8 pct SiO_2, and 0.075 pct S.

The high grade mixed ore, sample 2, was treated similarly, but since this material contained little silica it was necessary only to float the apatite and sulfides to yield a nonfloat product of acceptable quality. Table V gives the results and operating data in flotation of sample 2, from which 95.0 pct recovery was effected at a grade of 65.5 pct Fe, 0.18 pct P, 6.4 pct SiO_2, and 0.067 pct S.

As a sidelight of the flotation research it was discovered that in upgrading the iron, the apatite could be recovered as a byproduct of possible commercial value. In some tests, recoveries of 75 to 80 pct of the phosphorus were effected at grades of 66 to 71 pct tricalcium phosphate (BPL). The Pea Ridge iron ore deposit, it has been announced, will be brought into production within the next five years at an annual output of 2 million tons of concentrate. At that rate, Pea Ridge could also be a source of some 100,000 tons of apatite concentrate per year. Apatite does not compete with phosphate rock for production of wet-process superphosphate because it is less reactive with sulfuric acid, but it should be a satisfactory raw material for electric-furnace phosphorus.

If a market is developed for the apatite, the logical flowsheet for all three types of Pea Ridge ore would consist of magnetic separation followed by flotation, which would insure maximum recovery of apatite and both iron oxides. Research to confirm this premise was conducted on samples 1 and 2 under this agreement and products of satisfactory quality were recovered. Recoveries were somewhat lower than those presented here, but only because time limitations prevented achieving optimum results.

The work on which this report is based was done under a cooperative agreement between the U. S. Bureau of Mines and St. Joseph Lead Co.

The authors wish to acknowledge the complete cooperation of St. Joseph Lead Co., which supplied not only the samples with which the research was conducted, but also funds for the experimental and analytical work.

REFERENCES

[1] *Mining World*, May 1957, p. 35.
[2] L. Kohlmeier: Mountain is Being Moved to Get at Missouri's Iron Ore. *St. Louis-Globe-Democrat*, Nov. 17, 1957.
[3] J. G. Grohskopf and C. O. Reinoehl: Magnetic Surveys, Missouri Bureau of Geology and Mines, *57th Biennial Report*, Appendix IV, 1933, pp. 5-20.
[4] W. D. McMillan: Exploration of the Bourbon Magnetic Anomaly, Crawford County, Mo. *USBM R. I. 3961*, 1946, 9 pp.
[5] *Engineering and Mining Journal*, April 1957, p. 72.
[6] *Engineering and Mining Journal*, April 1958, p. 179.
[7] L. A. Roe: *Iron Ore Beneficiation*, pp. 115-132. Minerals Publishing Co. Inc., Lake Bluff, Ill., 1957.
[8] A. M. Gaudin: *Flotation*, p. 476. McGraw-Hill Publishing Co., New York, 1957.
[9] F. R. Milliken: Metallurgy at National Lead Co., MacIntyre Development. *AIME Trans.*, 1949, vol. 183, p. 108.

Discussion of this article sent (2 copies) to AIME before April 30, 1959, will be published in MINING ENGINEERING.

PERMISSIBLE-TYPE DUST COUNTER FOR COAL MINES

by ALBERT L. THOMAS, JR., and SABERT OGLESBY, JR.

Until recently, probably the best means of sampling airborne dusts has been the impinger method. Dust-laden air is drawn into a sampling tube, and the particulate matters separated from the air and collected in the liquid in the impinger. A sample of the suspension is prepared on a slide and counted through a projection microscope.

This method is simple and reliable, but it does suffer drawbacks. Since the collected particles must be counted visually, results of the dust count are not immediately available at the time the sample is taken. This seriously impedes studying the effectiveness of dust inhibitors, such as water sprays, or making adjustments in equipment. Greatest disadvantage of all, however, is the tedious task of counting particles in the sample. With the growing desirability of taking more samples, the effort involved in making these counts is a real factor in the cost of dust control. Finally, it is generally recognized that impinger dust counts can be related to health hazard only for specific kinds of dust and under similar conditions. This is because the rather complex mechanism of dust damage depends so much on size distribution of the dust. Counts determined by impinger samples cover a limited size range that does not necessarily corre-

A. L. THOMAS, JR., is Head of the Instrument Development Section and S. OGLESBY, JR., is Head of the Engineering Division, Southern Research Institute, Birmingham, Ala. TP 4797F. Manuscript, March 28, 1958. New York Meeting, February 1958. AIME Trans., Vol. 214, 1959.

late with retention by the lungs and upper respiratory tract.

Several other methods for making dust counts in the mine offer advantages over impinger sampling, especially in giving instantaneous readings of the dust concentration or dust level. These methods will not be evaluated here, but it is generally recognized that each has its own particular shortcoming.

In considering development of a counter for use in coal mines, the writers set forth the following desirable properties:

1) It should read number of particles rather than mass concentration. This is important, since it is recognized that it is primarily the number of irritation centers that create respiratory damage, rather than the total quantity inhaled.

2) It should read dust concentration directly. This is a requisite for any improved dust sampling method because of the labor associated with visual counts.

3) It should be capable of reading particles down to the smallest retained in the lungs, although it will not be used at that sensitivity for comparison with counts made by the impinger method.

4) It should be possible to correlate data obtained with results of impinger sampling methods. This is important because of the great amount of work already done in attempting to get agreement between potential hazard and dust levels as measured by impingers.

5) It must be a type permissible in gassy mines.

The type of counter the present investigators are working on is a particle photometer operating on the forward scattering of light from an aerosol or dust particle. The optical layout of the counter, shown in Fig. 2, is composed of a light source, a system of lenses and stops, a photoelectric tube, and the associated electronic circuitry. The light source in this counter is a No. 13 flashlight bulb.

The lens system gives a condensed image of the light filament just over the end of the tube shown in the lower part of Fig. 2; the beam is then stopped in the lower light trap. The photoelectric tube *looks* across the nozzle and the light path into a dark, velvet-lined chamber. The area above the nozzle that is illuminated by the lamp and the area seen by the phototube form the sensitive volume. Now if this volume contains no particles, the phototube will see nothing but the dark chamber. However, if there is a particle in the view volume, light will be scattered from the particle onto the sensitive cathode of the phototube. If the particle is moving there will be a pulse from the phototube, the amplitude of the pulse being generally proportional to the size of the particle, for constant illumination and phototube characteristics.

Fig. 1, showing the view volume for a particle counter, was made with a dense smoke passing through the nozzle and with considerable background light. The camera in this instance replaces the phototube and the smoke is considerably denser than in normal counting, but if sensitive enough film were available, it would be possible to record the trail of a particle across the illuminated area.

The phototube is sensitive enough to record the light from the small particles, so that in practice the electrical pulse from the phototube, rather than the film, is used to record or count the particles.

This particular optical arrangement may be used not only for counting particles but, with suitable

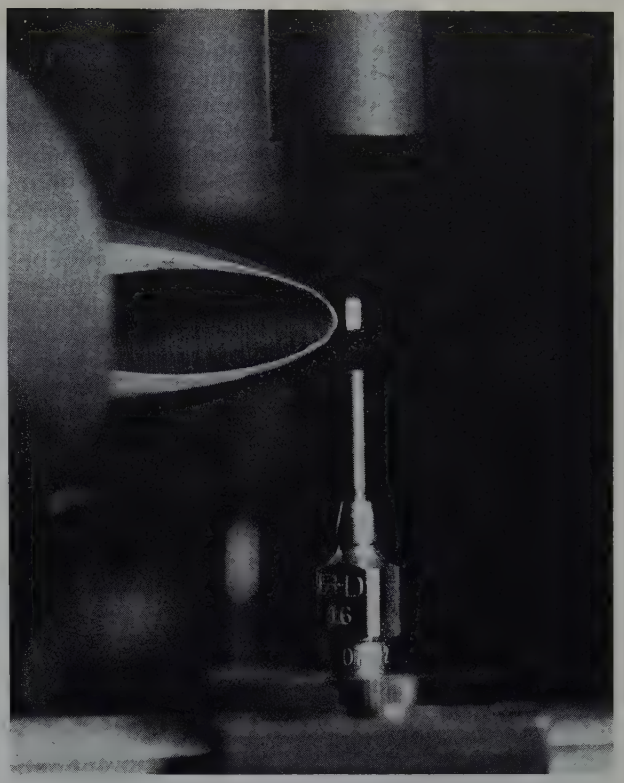

Fig. 1—Smoke through nozzle.

circuitry, can be made to give the particle size as well. If the particles are homogeneous, and if the light intensity and phototube characteristics do not change, the size or height of the electrical signal from the phototube will be proportional to particle

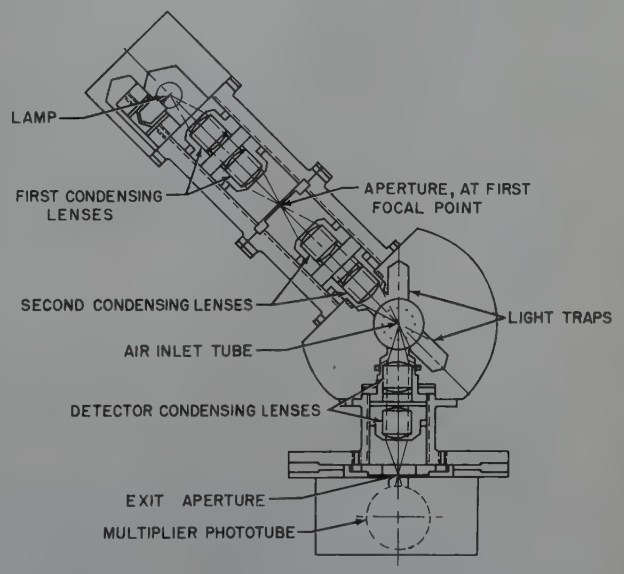

Fig. 2—Optical layout of particle counter.

size. It is relatively easy then to show not only the particle count, but also to draw a histogram of particle size distribution. This is not a feature of the present model counter, but it does have a number of applications.

The relationship between the height of the electrical pulse and the particle size is important in

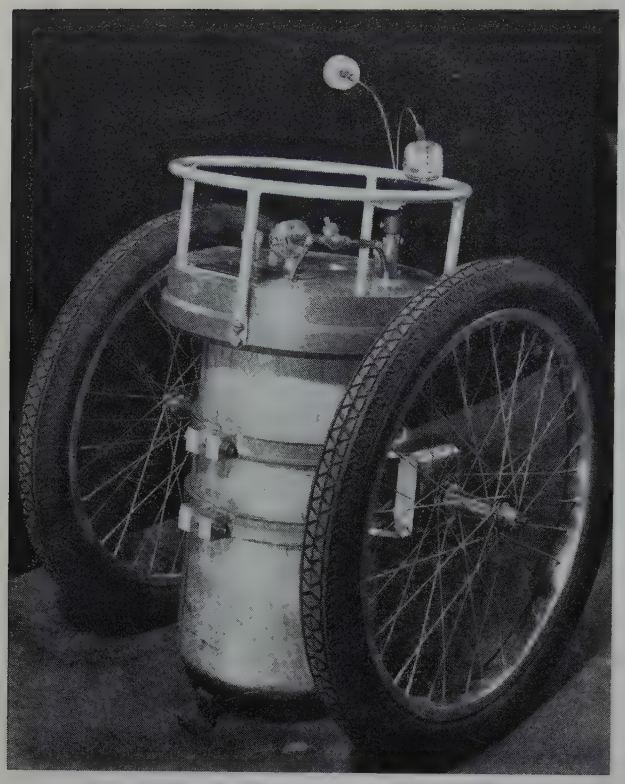

Fig. 3–View of instrument in case.

other regards, because it establishes the minimum particle size that can be counted. This minimum size depends on a number of factors in design and layout of the counter's optical system, on the optical properties of the particles being counted, and on characteristics of the phototube and electronic circuitry. To be counted, the pulse amplitude must be great enough so that the electronic circuitry can distinguish it from the random current in the phototube. This will be discussed later in more detail.

The electrical circuit of the counter is shown in Fig. 4 in block diagram form. Chief purpose of the electronic circuitry is to convert the pulses from the phototube into a voltage proportional to the number of pulses per second. The voltage is displayed on a meter that is calibrated in particles per second.

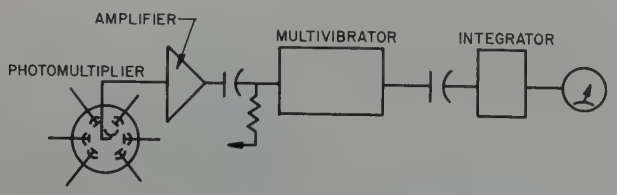

Fig. 4–Block diagram of electrical circuit.

The first block in the diagram is an amplifier, which increases the height of the pulses so that they can be handled by the remaining circuits. The output of the amplifier is fed to a multivibrator circuit. Each pulse from the amplifier above a given minimum voltage triggers the multivibrator, giving an output pulse of constant height regardless of the height of the input pulse.

Finally, the output of the multivibrator is fed to an integrating circuit whch gives an output voltage proportional to the number of pulses per unit of

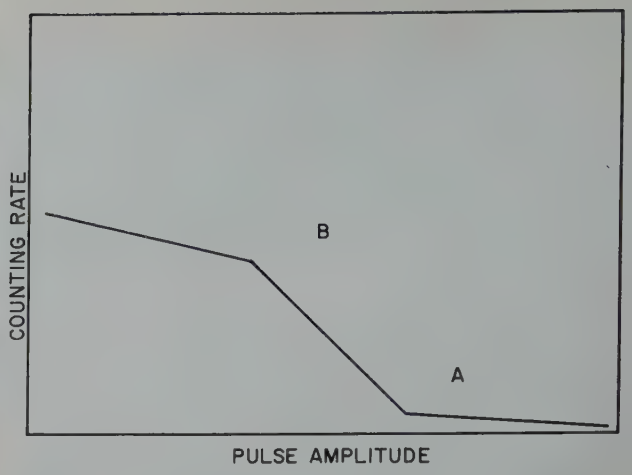

Fig. 5–Counting rate vs discriminator setting.

time. This voltage is indicated by the panel meter inside the top of the counter case.

It is apparent from the operation of the counter that not more than one particle should be in the view volume at one time. Otherwise the output would be a single pulse of larger size than is indicated by a single particle, resulting in erroneously low dust counts. Consequently, in order to count the heavy concentrations found in the mines, input must be greatly diluted.

Dilution of aerosols or dusts is, of course, a very tricky problem. If it is not performed accurately the apparent counts will be in error. Also, the dilution system should not alter the resistance to flow; otherwise the flow rate would change with dilution, Finally, any dilution method should not alter the particle size distribution. It all sums up that the diluted sample should be representative.

In the Southern Research Institute counter dilution is accomplished by a special value that mixes filtered air with the unfiltered air, then samples the mixture and discards the excess isokinetically. This is done in a novel device for which a patent has been applied. Accurate dilutions up to 10/1 are possible with this valve.

The basic counter is capable of counting a particle density of 10 million per cu ft of air with no dilution. Consequently, a maximum density of 100 million per cu ft can be counted with a 10/1 dilution; greater dilutions approaching infinity are possible, though less accurate.

As mentioned previously, one of the requirements was that the counter be approved for use in gassy mines. The case for housing the counter, therefore, had to meet USBM requirements of containing an explosion set off within the case. To meet these requirements, the case was made of a heavy aluminum pipe. A brass, screw-type lock ring fastens the instrument to the case.

The most difficult problems in development of the dust counter were in adapting it as a field instrument. Basic techniques for the counter as a laboratory device had previously been worked out. As the instrument was developed, it was decided to have it completely self-contained with all batteries inside the case. It is also important that these batteries have a long life to reduce maintenance problems. This means low current drain. On the other hand, it is important that light intensity be high in the view volume. An ideal light source would be a ribbon filament lamp with filament

dimensions about ⅛ in. square. This filament could be focused by the lens system on the view area and would give the best illumination pattern. This would give the best signal-to-noise ratio and would permit counting the smallest particle size. Unfortunately such a lamp is not available, and if it were, the voltage-current characteristics would probably not be suitable. The No. 13 flashlight lamp used as a compromise gives low current drain and enough illumination to count particles down to about 0.3μ, although the illumination is not as uniform as from a ribbon lamp.

Calibration of the dust counter is done by sampling an aerosol of known particle size. Polystyrene latex is available from Dow Chemical Co. in various measured sizes from 0.1 to 2.0 μ, and the range of particle size in each sample is extremely narrow. The procedure for setting the sensitivity of the counter is to generate an aerosol of the desired minimum size to be counted and to vary the discriminator setting. Counting rate will change with discriminator setting, as shown in Fig. 5. The plateau on the curve indicates the setting at which all of the particles in this size range are being counted.

Two points on the curve, *A* and *B*, are used to indicate sensitivity of the counter. Point *A* is the discriminator setting at which the counter just begins to count the particles and point *B* the setting at which all the particles are being counted. Once these points are established for a given aerosol, the counter can be set to, and returned to, any desired sensitivity.

One difficulty in using polystyrene latex for calibration is that the reflectance for polystyrene is considerably different from that of coal dust. The minimum size coal dust that can be counted therefore is smaller than that of the polystyrene particle, for which the minimum size has not yet been determined. However, it has been established that the counter can be set to be sensitive to particles smaller than are countable with the usual projection microscope technique.

Fig. 6 compares readings of the particle counter with impinger counts to show agreement between the two methods. Data for this curve were taken by simultaneously sampling coal dust from a chamber with the particle counter and with an impinger. Agreement is well within the variability of counts by impinger methods.

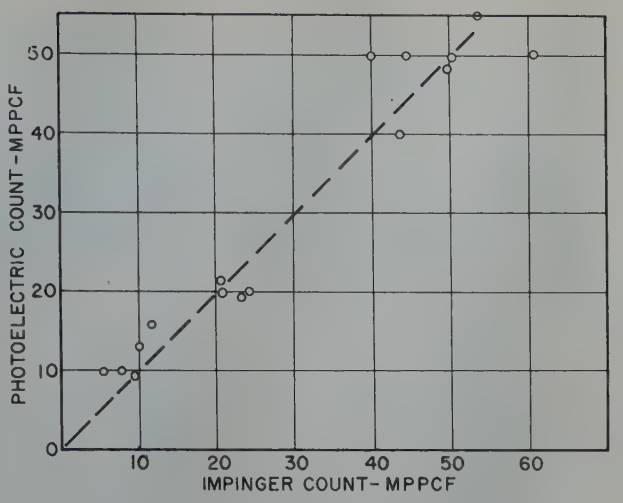

Fig. 6—Correlation of impinger and photoelectric data.

Before it can be declared operational, the counter must be tested extensively in the mine. To be successful, it must give long trouble-free service and survive rough handling. There must be a rapid and convenient way to check calibration in order to develop confidence in the counter's reliability.

Work has now reached the field trial stage. The counter is being used by the industrial engineering department at Alabama Power Co.'s Gorgas mine, where the mechanics are being checked as well as the optical and electrical features. Several factors have already been found to influence operation of the instrument, which is being modified accordingly. There is every hope that it will prove successful in coal mine dust sampling and that it will significantly reduce the cost of mine dust control.

Discussion of this article sent (2 copies) to AIME before April 30, 1959, will be published in MINING ENGINEERING.

Discussion

INTERGRANULAR COMMINUTION BY HEATING

by J. H. BROWN, A. M. GAUDIN, and C. M. LOEB, JR.

(MINING ENGINEERING, page 490, April 1958, AIME Trans., Vol. 211)

R. E. Carter *(General Research Laboratory, Schenectady, N. Y.)*—Brown, Gaudin, and Loeb in their study of intergranular comminution by heating attempt to find one explanation for all types of rock in terms of the properties of the phases present. The *only* necessary condition for intergranular cracking by heating is the setting up of high stresses at the grain boundaries.

Such stresses may be set up in multiphase isotropic mixtures if the thermal expansions of the phases are different, in non-cubic single phases because of the anisotropy of thermal expansion in the various crystallographic directions, and in materials containing quartz because of the α-β transformation at 575°C. In addition, for intergranular comminution by heating, the cooling and not the heating is most important.

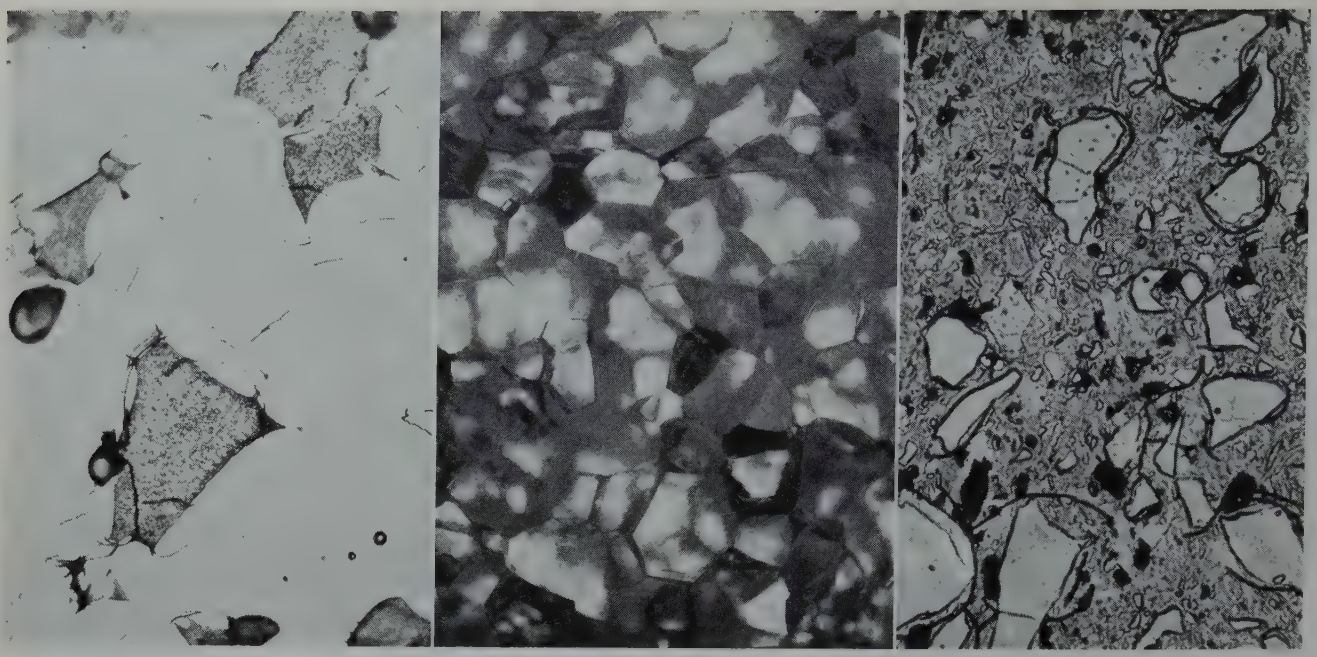

Fig. 9—Microcracks formed during cooling. (Photographs reduced approximately 15 pct for reproduction.) Section A (left)—Magnesium ferrite plus a Wüstite-like precipitate SnCl,HCl etch. Reflected light. X500. Section B (center)—Single-phase alumina. Unetched. Transmitted light. X30. The intergranular cracks reflect light and make the grains visible. Section C (right)—Porcelain containing undissolved quartz. Phosphoric acid etch. Reflected light. X500.

Almost all the cracking must occur on cooling, since on heating part or all of the stress may be relieved by plastic flow, but on cooling plastic flow will be almost absent. An extension of this argument suggests that the faster the cooling the less the plastic flow and the greater the stress; hence the greater the possibility of intergranular cracking.

In Fig. 9 there are three sintered materials, all of which show intergranular or near intergranular cracking as a result of cooling from the sintering temperatures. Section A shows a cubic magnesium ferrite containing a cubic Wüstite-like precipitate. The precipitate has a higher coefficient of thermal expansion than does the ferrite phase and on cooling from 1400°C a tensile radial stress of 40,000 psi is set up at the interface if no relaxation occurs during cooling.[14] Section B shows a specimen of single phase alumina which R. L. Coble of the G. E. laboratory reports was sintered at 1800°C and then air-quenched. During cooling, stresses are set up at the grain boundaries because of the anisotropy of the thermal expansion of this rhombohedral material. The formation of the cracks may be observed with a binocular microscope using transmitted light. In many cases the cracking was accompanied by an audible ring.[15] Section C shows a porcelain containing large pieces of undissolved quartz. These cracks could not have formed during heating, since the material placed in the furnace was a mechanical mixture of quartz, feldspar, and clay which then reacted at the sintering temperature. The cracks must therefore have resulted from the high radial tensile stresses set up in the porcelain on cooling because of the volume contraction of the quartz particles during β to α transformation.

J. H. Brown, A. M. Gaudin, and C. M. Loeb, Jr. *(authors' reply)*—We wish to thank R. E. Carter for his contribution. His observation that the only condition necessary for intergranular cracking by heating is the setting up of high grain boundary stresses seems accurate to us, and we agree with his listing of several methods by which this could occur.

On the other hand, we cannot agree with his statement that for intergranular comminution by heating the cooling and not the heating is most important. It may be true that plastic flow will be more likely on heating than on cooling, but we are not aware of any indication that plastic flow rates for these materials are so highly temperature-dependent in this temperature range that it is particularly significant that a rock is either heating or cooling. Certainly the figures presented to support the hypothesis of cracking during cooling do not clarify the point, since in these specimens no structure was available to fracture during heating. We feel that Carter has specified still another method by which heat treatment prior to crushing may affect the rock. There is merit in the suggestion that fracture may occur when the cooling rate is high enough to cause large temperature differentials in the cooling specimen.

In support of our hypothesis that intergranular fracture occurs during heating to a significant extent, we refer again to the data presented in Figs. 2 and 5. If the cooling rate is important, it is difficult to explain why at least as great an effect, if not a greater one, was observed when the specimen was not allowed to cool at all before crushing.

A final test of the cracking-during-heating proposal was made in our laboratory recently. A specimen of granite about ½x½x3 in. was held by one end on a block to leave about 2½ in. of unsupported specimen. This cantilever was then loaded with a weight which we estimated as being 10 to 15 pct of the load required to fracture the piece in the unheated state. The entire system was then set into a furnace and a signal system by which the moment of fracture could be detected was attached to the specimen. The furnace was then closed and heated gradually. At a temperature of about 500°C *during heating* the specimen broke.

We do not deny the possibility that fracture may occur during cooling. We merely state that the fracture that occurs during heating was highly significant and we hope that a report on further work in this area which is now in preparation will contribute to this question.

REFERENCES

[14] R. E. Carter: Effect of Oxygen Pressure on the Microstructure and Coercive Force of Magnesium Ferrite. Submitted to the *Journal of the American Ceramic Society.*

[15] R. L. Coble: In *Effect of Microstructure on Mechanical Properties* (edited by W. D. Kingery), p. 213. John Wiley & Sons Inc., New York, 1958.

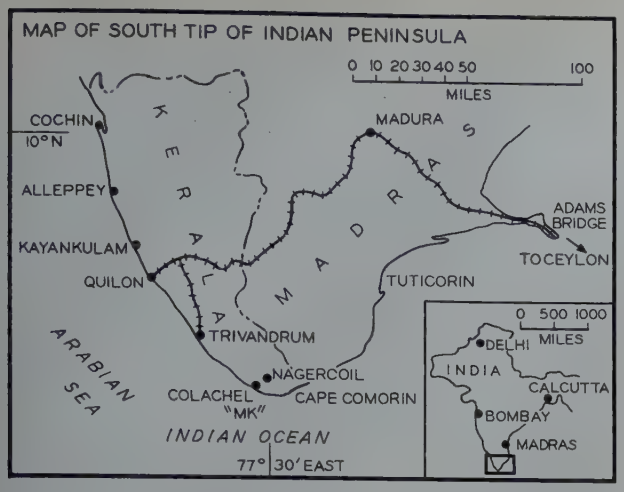

SAND DEPOSITS OF TITANIUM MINERALS

by J. L. GILLSON

A world survey of processes as illustrated by Indian deposits.

Historically, rock deposits and sand deposits of titanium minerals came into production about the same time, although there may be some argument as to what is meant by production. Beach deposits of heavy minerals in India (Figs. 1-4) and Brazil (Figs. 5) were worked for monazite about the turn of century, but as there was then no market for titanium minerals, these were thrown away. The rock rutile deposits at Roseland, Va., Fig. 6, were worked to supply rutile for titanium chemicals and for coloring ceramics long before there was a titanium pigment business. The pigment industry started about the middle twenties, both in Europe and the U. S., and almost simultaneously the rock deposits at Ponte Vedra Beach near Jacksonville, Fla., were worked for titanium content.

Since those days, production from both types of deposits has continued to grow at a rapid rate; many deposits of both types have been found, and reserves have grown to very large figures. In total tonnage of reserves, there is no doubt that the rock deposits are far ahead of the sand deposits; nevertheless there is a very large tonnage of commercial sands available. It is the quality of titanium mineral in the sand and the relatively lower costs of operating sand deposits that have kept them abreast, at least in annual tonnage produced, with the rock deposits.

The principal titanium mineral used is ilmenite, but as soon as that mineral began to be sought as a titanium ore, it was obvious that there are ilmenites and ilmenites. Textbook ilmenite should have the composition $FeOTiO_2$ and should analyze 52.6 pct TiO_2 and 36.8 pct iron as Fe. The Indian ilmenite, for almost a generation the standard ore for manufacturing pigment in the U. S., was found to analyze about 60 pct TiO_2 and only 24 pct Fe, and most of the iron is in the ferric condition. The whole process of pigment manufacture in the U. S. was built up on the use of a raw material of that grade, and the American chemical engineers who operate the pigment plants shuddered at the thought of using a rock ilmenite with 45 pct or so of TiO_2 and nearly 40 pct Fe.

J. L. GILLSON, Member AIME, is Chief Geologist, E. I. du Pont de Nemours & Co., Wilmington, Del. Manuscript, May 1, 1958. New York Meeting, February 1958. TP 4799H. AIME Trans., Vol. 214, 1959.

Intensive search was made around the world to find other deposits of rich black sand, like the Indian beaches, but although a few were found, there was some objectionable feature about each. A deposit in Senegal, south of Dakar (Fig. 7), was worked for a while, but an organic coating on the grains made attack by acid difficult. Modern practice would have included a scrubbing operation, in a caustic soda bath, to eliminate the organic coating. Brazilian deposits were numerous, but individually small, and shipping from them difficult. Deposits on the east coast of Ceylon had many attractive features, but the ilmenite analyzed only 54 pct TiO_2 and could have been used only with a penalty. Sand deposits with 2 pct ilmenite, like those now worked in Florida, would not have been considered commercial ore, even if they had been known at that time.

Most rock ilmenites are associated or mixed with hematite or magnetite, which accounts for the lower titanium and higher iron values than in the sand ilmenites. The Norwegians, English, and Germans, with cheap Norwegian rock ore at hand, learned to install in their pigment plants adequate capacity on *the black side*, as it is called, and counterbalanced the extra cost of plant, and larger amount of acid used, by the lower cost of ore.

When World War II arrived, two of the largest pigment manufacturers in the U. S. had to learn how to use the Adirondack ilmenite, but one of them very gladly went back to sand ores when the Florida deposits came into large-scale production after the war. The other continues to use Adirondack ilmenite and finds it commercially attractive to do so.

Rutile is not a raw material for titanium pigment manufacture by the sulfate process, since it is insoluble in sulfuric acid. In addition to its small consumption in chemicals and ceramics it began to be used in quantity in welding rod coatings. With the outbreak of World War II, and the tremendous need for welding rods in shipbuilding and other structural steel construction, rutile suddenly became in heavy demand. The sand deposits on the eastern shore of Australia (Fig. 8A) which had been worked in a small way since 1934 were brought into production, and some stream placers in Brazil were worked and rutile concentrates shipped to American

This page of Mining Transactions AIME follows p. 332. The intervening non-Transactions pages appeared in MINING ENGINEERING.

consumers. But Australia was a long way off, and the need for a domestic deposit was urgent.

An elongated ridge between Jacksonville and Jacksonville Beach, Fla., recognized later as an elevated sand bar, had been found before the war, but no one had considered the possibility of working it for its rutile content, which was very low.

About 1942 the Titanium Alloy Mfg. Co., a producer of titanium products from rutile, acquired the Jacksonville deposit and tried to concentrate the minerals in the low grade sand by froth flotation and magnetic separation. At the same time electrostatic equipment was installed at Titanium Alloy's research facility at Niagara Falls, N. Y. J. Hall Carpenter, a young man trained in ceramic engineering, was employed at that laboratory and worked on the electrostatic equipment. He was transferred to the Jacksonville plant to assist in the technical phases of the operation, including integration of electrostatic methods of concentration with the other equipment.

Out in Oregon the War Production Board had arranged with Humphreys Gold Corp. to dredge some beach placers of chromite ore, and to concentrate the sands in a gravity device just developed by I. D. Humphreys, one of the partners in the company. This was a spiral consisting of three to five turns, down which a slurry was caused to flow. Under the centrifugal action the light gravity minerals were thrown out toward the outside lip of the spiral, whereas the heavy minerals dragged bottom and remained in a path near the inside edge, from which they were drawn out through conveniently spaced ports. The gangue minerals whirled around the lip until they reached the bottom end. Thus a separation occurred between minerals of high and low specific gravity.

Soon the shortage of chromium concentrates was alleviated by other producers, and the Oregon operation was not needed. A staff member of the War Production Board, Dean Frasche, now with Union Carbide Corp., was familiar with the spiral operation in Oregon and also with the difficulties being encountered in concentrating a similar sand near Jacksonville for its rutile values. At the suggestion of the WPB, Humphreys Gold Corp. was moved to Florida, and concentration of titanium minerals with the Humphreys spiral began. Today it is the key unit in most of the sand operations in the U. S. and Australia that are producing titanium minerals.

J. H. Carpenter stayed on with the Humphreys Gold Corp., which has continued to operate the Jacksonville plant under contract for Titanium Alloy Mfg. Co.* He has since founded Carpco Mfg. Co. and has contributed more improvements to the science, art, and engineering of electrostatic separation of titanium minerals and other oxide ores than any other man of his time.

* Now a part of the National Lead Co.

The Jacksonville operation demonstrated that low grade sand containing only 2 to 3 pct titanium minerals could be concentrated successfully and economically with the Humphreys spiral and that the oxides could be separated from the heavy silicates by electrostatic methods. This experiment encouraged extensive search for similar deposits.

Search for additional deposits of such sand ores in Florida and other states was begun by both Federal and private groups. The U. S. Bureau of Mines deserves the credit for discovery of Trail Ridge, which is probably the largest deposit of high grade titanium-bearing sands yet found. Active search has now revealed many others, not only in North America but in other parts of the world. For a long time the search was confined almost entirely to marine sands of Pleistocene age, although a fossil placer in the Tokio sandstone of Cretaceous age near Nashville, Ark., has been known for a long time. That deposit was small and irregular, so that little attention was paid to coastal plain sediments until recently.

In 1956 and early 1957 Cretaceous sands of Tennessee and Miocene and Pliocene sands of New Jersey were found to contain important quantities of titanium minerals. The first deposits are marine, the second are probably terrestrial. About the same time the wide-ranging uranium prospectors with their airborne scintillation counters picked up sand deposits carrying monazite, and some ilmenite in Cretaceous sands in a number of places in the Rocky Mountain states. Those found to date are relatively small and difficult to reach by transportation.

Rutile as an important titanium ore became in great demand with development of the process for making titanium metal by reducing the chloride $TiCl_4$. Titanium tetrachloride could be made from ilmenite, but the consumption of chloride by the iron made it a very unattractive raw material. However, rutile, with almost no iron, chlorinated readily, and after much effort and expense in developing processes and, especially, equipment to handle the reactive chlorine, manufacture of titanium tetrachloride became big business. Many companies went into it, stimulated principally by government prodding and purchases of titanium metal.

It was found also that another titanium mineral of uncertain composition and heritage, leucoxene, was desirable feed for chlorination. This was important, since many of the sand deposits contain substantial quantities of leucoxene, which is of no value to the pigment manufacturers using the sulfate process, because it is insoluble in sulfuric acid. Leucoxene never was acceptable to the welding rod manufacturers.

Mineralogy of the Titanium Sand Deposits: Black sands in streams and on the beaches of volcanic regions are widespread and well known. Some beaches in these regions are very black indeed, but the principal black minerals are magnetite, titaniferous magnetite, and black silicates, chiefly augite and hornblende. From such sands, it was never possible to produce an ilmenite concentrate of a grade acceptable to pigment manufacturers. The best known deposit of this kind is on the southwest shore of the North Island of New Zealand (Fig. 8B) where there is a tremendous reserve on the beaches and in the dunes along the Taranaki coast. Undoubtedly the minerals were ejected as ash from Mount Egmont nearby. The heavy mineral concentrate analyzes about 9 pct TiO_2 and most of it is in ilmenite interground with magnetite, or magnetite partly altered to hematite.

Black sand concentrations, rich in magnetite, occur on many shores in northern latitudes. One such deposit is at Natashquan, on the north shore of the St. Lawrence in Canada. Natashquan is the next major river east of the Romaine, which discharges at Havre St. Pierre, where the Allard Lake ilmenite ores are shipped. The Natashquan deposit probably contains several million tons of magnetite, with just enough titanium to be a nuisance rather than an asset.

It is not these black sands rich in magnetite that are titaniferous ores, but rather the sands containing no magnetite at all, or very little. Why none is present is one of the major geological factors needing emphasis.

These titaniferous black sands with little or no magnetite are found on the shores, or in the streams of continental masses, and only in temperate and tropical zones. The minerals were concentrated out of granitic and gneissic rocks, following a period of peneplaination. Few if any of the rocks from which the minerals came were particularly rich in either ilmenite or rutile.

The mineral composition of most of the deposits around the world is remakably similar, differing only in percentages of each mineral present. All of the minerals are characteristic of gneisses, granites, and pegmatites. They are physically hard and chemically resistant to attack by earth acids and weathering. The minerals are ilmenite, leucoxene, rutile, monazite, zircon, sillimanite, cyanite, andalusite, garnet, spinel (usually more than one variety), corundum, staurolite, tourmaline, and epidote. Patient search through scores of mounts may find a stray grain of xenotime, vesuvianite, or some unknown that is lost before it can be identified and is never seen again. In fine-grained deposits like those in Tennessee, which were obviously deposited in quiet water, there is some mica. Various authors have reported anatase present instead of rutile. This the writer has never seen, except in very small quantities, and obviously as a secondary recrystallization.

Epidote and garnet are abundant in some assemblies, absent in many. The grain size of the mineral is usually in inverse proportion to their specific gravity. Staurolite, tourmaline, garnet, and sillimanite are coarser than the ilmenite, zircon is fine, and monazite is very fine, in the heavy mineral concentrates. An exception is rutile, and in the sands of most deposits in eastern U.S. the grains of rutile are finer than those of the ilmenite. Presumably the rutile grains were finer than the ilmenite grains in the original rocks.

Average grain size varies with the deposit and is an indication of the conditions of deposition. Most stream deposits are composed of coarser grains than marine deposits, and these vary through a wide range. The coarsest sands in a deposit considered to be of commercial size and grade are those in Horse Creek, near Aiken, S. C., which are in a delta deposit. The heavy minerals at Trial Ridge, Fla., which are Middle Pleistocene, are much coarser than those in the Jacksonville deposit, which are probably of Wisconsin age. The latter may have been deposited after a longer journey from their source, the coarser grains having been deposited along the way. A deposit on a marine terrace, east of Trail Ridge, at Folkston, Ga., seems to be made up of the fines washed out of Trail Ridge. What happened to the coarse fraction is not known.

The grains in the Tennessee sands, although very fine, show little wear, and crystal faces on many of the minerals are seen frequently. Zircon, usually the only mineral showing crystal faces, was probably more likely to have been formed originally in euhedral crystals than other minerals, and being hard, it has resisted wear. Monazite is found in most mounts in rounded grains, its hardness being only 5 to 5.5.

Grains in eluvial deposits are the coarsest of all.

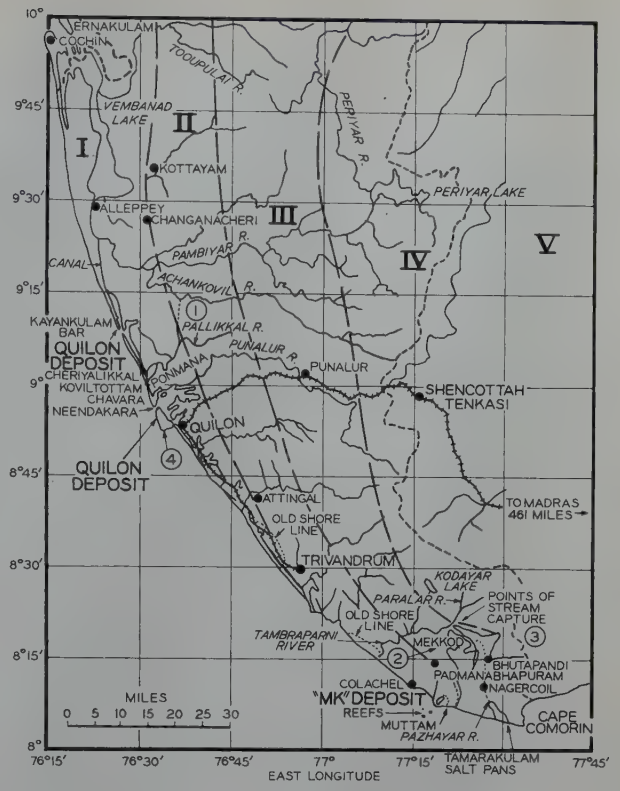

Fig. 2—Ilmenite deposits of Travancore, India, are related here to geology and physiography. Physiographic areas are indicated by roman numerals: I. Lowland, recent emergence. II. Laterite plain. III. Recently uplifted intermediate plateau. IV. High plateau. V. Interior plain, old age; eastern mountain face is an eroded fault scarp, probably thrust from the west. For the circled arabic numbers, read as follows: 1. Achankovil River formerly discharged through the Pallikal. 2. Ruttenar channel passes through the wind gap at Mekkod. 3. Anandunar channel uses the wind gap at Sungananda. 4. Laterite bluffs at Tangacheri show the old headland. In the mountains deeply entrenched meanders and numerous high hanging valleys indicate recent uplift. Water falls indicate repetition of uplifts.

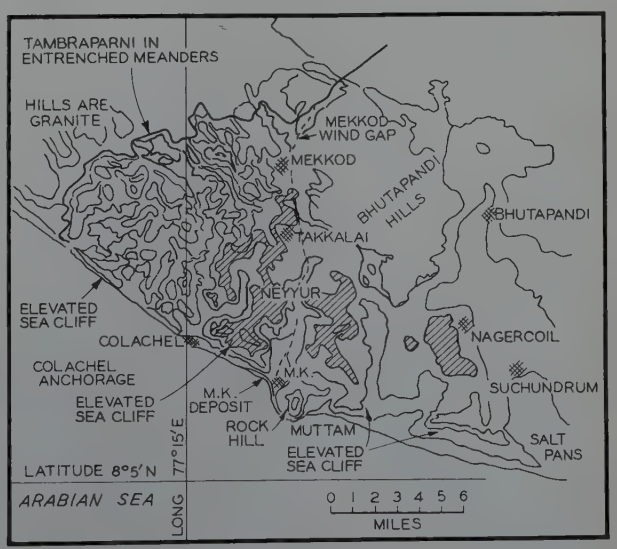

Fig. 3—Map showing the M. K. ilmenite deposits.

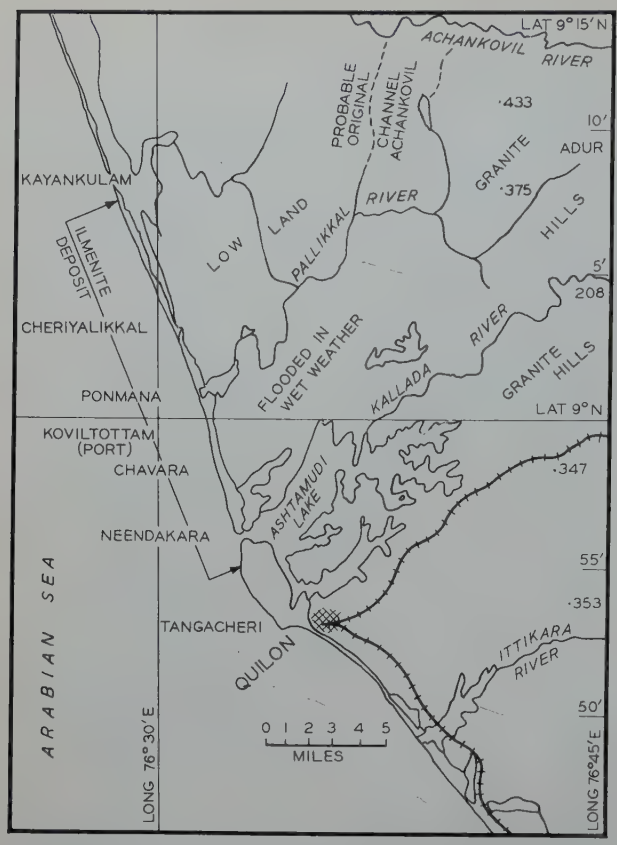

Fig. 4—Map locating the Quilon deposit, Travancore.

Grains of nut or pea size are common in the soil in Hanover and Gooch counties, Virginia; Murphy, N. C.; Young Harris, Ga.; and Ceara, Brazil. Many eluvial and stream placers have been worked for rutile and for monazite, which has had a high unit value, permitting small deposits to be worked. The fossil stream placer in New Jersey and the delta deposit at Aiken, S. C., are the first river deposits of titanium minerals now known to be large enough to permit economic mining for ilmenite. Old gold placers in the Boise Basin in Idaho were worked several years ago for monazite, and the byproduct ilmenite was sold for pigment manufacture.

Zircon is the one mineral of the assemblage that has been and is coming almost exclusively from these placer deposits. In fact, the large-scale production of titanium minerals has made zircon abundantly available and encouraged its use in relatively low-valued outlets, such as foundry sands. No shortage of zircon can be anticipated, unless unforeseen uses are developed which will require very large quantities.

Monazite has come exclusively from these sand deposits, except for one rock deposit in South Africa. Currently monazite is a doubtful asset in these sands because it commands only a small market, which may decrease rather than grow as thorium becomes available from such uranium deposits as Blind River, Ont., and from various carbonatites which may be worked for pyrochlore, but which contain thorium, perhaps as monazite. The presence of monazite in sands in India and Brazil has brought about government restrictions on prospecting and developing that may actually have reduced or prevented development.

Although sillimanite, cyanite, and corundum are abundant in most of these sands, there has been little or no production of these minerals as byproducts, although the techniques are known and have been used. The markets are not large, and many users want a coarser grain than is found in the sands.

Weathering of the Titanium Minerals: The leaching of the iron during weathering, with consequent enrichment of the mineral in titanium oxide, was established by Lynd and his associates.[17] The importance of this step in increasing the value of using ilmenite from beach sands cannot be over-emphasized. Nearly all the titaniferous beach sands around the world show some enrichment of the ilmenite, but in only a few deposits had the process been carried far enough to raise the analysis of the ilmenite to 60 pct TiO_2. In the Indian sands a substantial part of the ilmenite concentrate has a brownish cast, but the grains are still strongly magnetic. There is little or no leucoxene, which is recognized as a gray or white mineral that is weakly magnetic or nonmagnetic. In the Brazilian sand there is a substantial fraction of rusty-brown grains, but these seem to be limonite after magnetite and degrade rather than upgrade the concentrate. Treatment in hot HCl dissolves them. The Florida, Tennessee, and New Jersey ilmenites contain a substantial amount of the chalky grains. What is called *ilmenite concentrate* is determined by the amount of current put into the electromagnets, but from those sands an "ilmenite" is made analyzing 60 to 63 pct TiO_2 and a "nonmagnetic" (of course, *nonmagnetic* is a relative term) fraction that analyzes from 75 to 90 pct TiO_2, depending upon how much partially altered ilmenite was left in the product, and the proportion of rutile present.

The weathering process included some activities that were not so beneficial to mining of the deposit. The sands now making up Trail Ridge must have been underlying swamps for a long time, and pods or lenses of the sand are cemented with an organic coating. Such hard pan must be blasted ahead of dredging and the chunks disintegrated by crushing. Grains must then be scrubbed and leached to permit electrostatic separation and subsequent sulfuric acid decomposition in the pigment plant.

The McNary sand in Tennessee is for the most part uncemented, but there are layers locally called *iron stone* in which the sand is cemented by iron oxide, and some layers are almost as firmly cemented as quartzite. In most places the cemented layers are only an inch or so thick, but their presence demands a type of drilling equipment entirely different from that used in Florida.

The Cretaceous sands in the Rocky Mountain states are typical sandstones. Had the deposits been of commercial size they would have required typical hard rock mining methods.

Classification of Deposits: The descriptions above have indicated that the commercial titanium sand deposits vary in age from Cretaceous to recent (even forming at the present time) and they are eluvial, fluvial, and marine in origin. There is no reason why commercial deposits in geological ages earlier than the Cretaceous should not exist. Certainly black sand concentrations are known in earlier rocks, and some large enough and sufficiently accessible to be considered commercial may some day be found. One feature common to all of the deposits is that they occur on continental land masses; are derived directly, or indirectly, from granitic rocks and gneisses; and were formed following a long enough

period of peneplaination for a deep soil zone to have accumulated in which all of the magnetite, feldspar, and more easily weathered minerals had been decomposed.

A classification, with some examples of each type, is as follows:

Residual: With little or no transportation. Shooting Creek, N. C.; Young Harris, Ga.; Hanover, Va.

Eluvial: Residual with some transportation by water. Rutile deposits in Ceara and in Goiaz, Brazil, and the Cameroons of West Africa.

Fluvial: Black sand zones in the Cretaceous of many Mountain states; the sands of Ocean County, New Jersey. Miocene and Pliocene. Delta deposits in Horse Creek, near its mouth and junction with the Savannah River. Pleistocene. Rutile and monazite deposits of the Carolinas, black sands in sand bars of major rivers such as the Arkansas. Recent.

Marine: In most cases reconcentrated from previously formed sediments, rather than directly from the granitic soil. There are two principal types—offshore bars and spits and shore line deposits. Erosion, old or recent, has modified the deposits in many places.

Most of the major deposits of the world were formed as sand bars or spits that have been uplifted during later times. Trail Ridge was once a spit in the Sunderland Sea. Most of the deposits along the Atlantic Seaboard were formed when the sea stood 15 to 75 ft higher than it does today. A number of shoreline deposits, both fossil and modern, are known in Brazil. A shore line deposit lies at the base of a marine cliff of sediments containing heavy minerals. The waves undercut the cliff, digesting the fallen material; the heavies remain on the beach and the light minerals are washed out to sea. If the beach is wide, and only the highest waves of severe storms reach the marine cliff, the enriched zone lies just at the base of the cliff, or dunes, and is called a storm line deposit. Elevation of these has left long and narrow but rich layers parallel to the shore. Many, if not most, of the deposits along the east coast of Australia are of this type. If the waves of the present shore line reach into these elevated storm line deposits, a very black modern beach will result, particularly during a storm. Such is the Manavalakurichi deposit of South Travancore.

Aeolian: Dunes and wind-blown sand. Wherever there is some black sand accumulated on barren beaches exposed to the wind, the dunes will carry heavy minerals, but in most such dunes the medium *heavies* dominate over the heavier grains, i.e., staurolite, tourmaline, sillimanite, etc. are more abundant than in the marine sands, and the ilmenite and zircon are less abundant. Sometimes these dunes are very large, so that the aggregate tonnage is very considerable. The dunes at Nags Head, N. C., offer an outstanding example. It was from such dunes that the Wright brothers flew the first plane at Kitty Hawk. The dunes behind the beach at Panama City, Fla., carry up to 5 pct heavy mineral, but the titanium mineral forms only about 25 to 30 pct of the heavies. Very large dunes are found on Stradbroke Island, off Brisbane, Queensland, although the major deposits there are marine, under the dunes. A large part of the readily mineable material on the Travancore beaches is in the dunes, since the richer layers are below water table and are not readily mineable.

Examples of Ilmenite Sand Deposition: Formation of sand deposits is related to the physiographic history of the region in which they occur. The science called *geomorphology* and the science called *economic geology* have some overlapping areas, as for example, in the development of the processes of secondary enrichment in some ore veins. However, most economic geologists, including the writer, never had had formal training in the science of geomorphology. Except for an elementary course in his early college days, and the opportunity of listening on a few occasions to some stimulating lectures from that great teacher who was one of the founders of the science, William Morris Davis, the writer had little guidance in his early years of field work. However, when the study of and search for concentrations of heavy minerals became an important part of his duties, he found himself much involved in problems of peneplaination, stream piracy, drowning of river valleys, and emergence of old shore lines and offshore sand bars.

The search for black sand deposits along the U.S. Atlantic Seabord involves a study of the Pleistocene stages of glaciation, particularly in the interglacial epochs; it was during those times that the ocean levels were high because all or much of the ice was melted, and the water once locked up in continental ice sheets was returned to the ocean in liquid form. Sand bars and old shore lines then formed are now found above the sea level, since much water is still tied up in Arctic and Antarctic ice. It is a very provocative thought that interglacial periods of the middle Pleistocene were longer in duration than the period since the last withdrawal of the Wisconsin ice sheet, and the climate was warmer than it is today. There is still a very large amount of ice at both polar caps, and on the Greenland plateau. It can very seriously be wondered whether the present epoch is not just another interglacial one. No one now living, nor those engaged in long-range planning, must lie awake nights worrying about the matter, since these climatic changes occur very slowly, and the processes are measured in thousands, rather than in tens or hundreds of years.

Russell[20] has summarized the evidence of many glacialogists who agree that changes in ocean level

Fig. 5—Sand deposits of titanium minerals in Brazil.

resulting from maximum advance of the glaciers—when about 30 pct of the land surface was covered with ice—to complete melting varied from 300 to 600 ft. Flint[9] gives 400 ft as the maximum lowering of ocean level. There have been other changes in at least post-Cretaceous times that are too great to be explained by climatic changes that have stored more or less water in continental glaciers. There are the flat-topped submarine mountains called *guyots* found by Hess[14] and described in a memoir by Hamilton.[13] The eroded tops of these guyots are as much as 4000 ft below the present ocean level. There are continental shelves around most of the continents, and across them are the seaward continuation of major valleys, like the Hudson, Delaware, and Susquehanna. The edge of the shelf off the eastern U.S. lies at 100 fathoms. There are many submarine valleys, like those off the California coast, off Japan, Ceylon, and in the Mediterranean. These are over 1000 ft down, some much deeper. There are the steep canyons along the front of the continental shelf of the U.S., which Kuenen[15] calls the "New England type." They continue down to 1500 fathoms.

It is not the purpose here to try to explain these profound changes in level. In fact, no one has yet had much success in explaining them.

Shepard[22], in his closing paragraph of a book of 338 pages on submarine geology wrote, in 1948:

> The fact that the evidence is world-wide and comes from stable and unstable areas alike, naturally leads one to suspect changes of sea level as the cause. On the other hand the magnitude of displacement which seems to be required causes much hesitation in the acceptance of such a conclusion. Still greater difficulty appears to lie in the path of any conclusion that the continental margins and ocean basins have been undergoing tremendous oscillations in comparatively recent geologic times, and especially, that they have all now been submerged. This is a serious predicament and requires much thought and still more investigations in the field. Whatever we find, the indications are that something has been radically missing from our knowledge of past geologic conditions.

Landis,[16] in his retiring address as vice-president of Section E of the AAAS, suggested in all seriousness in 1951 that these great changes in ocean level were caused by profound changes in the level of the bottom of the oceans, particularly the Pacific. He postulated some sort of a tremendous graben into which tens of thousands of cubic miles of ocean water conveniently entered, like pulling the plug in a bath tub. This lowered the ocean and caused erosion of the guyots. Later this graben was filled or re-elevated, and the ocean level came back up where it had been. No one seems to have paid much attention to this idea, but at least it fits many of the facts much more closely than some other ideas that have been offered to explain these profound changes in level.

This world-wide submergence and drowning of old river valleys comes into the discussion of the origin of many of the ilmenite deposits, particularly those in India, as will be explained on a later page. Almost certainly out on the continental shelves are submerged sand bars as large and as rich in heavy minerals as those known on shore today, but we would not know how to work them, even if we could find them.

Although not pertinent to the problem under consideration, the thought that the whole maritime existence of the peoples of this earth would have been vastly different if this drowning had not occurred is also very provocative. Certainly, if the last major movement had been emergence, rather than submergence, we would have no capacious harbors and estuaries to provide havens for our shipping. There would be no great harbor at New York, Norfolk, San Francisco, Rio de Janeiro, or Sydney, no deep estuaries like the St. Lawrence, Delaware, Thames or La Plata where cities could develop far inland as major ports for world-wide shipping. All would have been like Los Angeles, Lima, or Valparaiso, where such harbors as exist are man-made extensions of the protection of a headland, or entirely man-made as at Chicago, Toronto, Cleveland, or Atlantic City.

The series of Pleistocene terraces and shore lines are identified along the Atlantic Coast of the U.S. by names of localities where they are well marked, as cited by Cooke.[5] They range in height from 275 ft down to 25 ft. The implication that the water levels were lowered in step-like progression was not the case, for there were five major advances of the ice, with long interglacial epochs. In fact, the interglacial epochs were much longer than the glacial. Some features formed in an early interglacial level, when much or all of the ice was melted and the water was back in the seas, may have been destroyed in the next interglacial epoch.

The world-wide level of about 25 ft found by Daly[7] is probably a level established in a mid-Wisconsin interglacial period called Pamlico. The most important ilmenite sand deposits connected with that stage are probably those in Brazil, Australia, West Africa, South Africa, and the lower ones in Florida and Georgia. However, the low-lying flat surface or marine terrace is a most important feature that has provided suitable sites for many of our major cities. At no place is this more striking than at Rio de Janeiro where that great city sprawls around the base of mountains rising sheer above that terrace. Had there been no marine terrace above the water, there would have been no room for the city. Except for Beacon Hill, Boston is another good example, as is Philadelphia.

If and when all of the ice now in Polar regions melts, the sea level will rise about 100 ft (Flint[9] says 165 ft), which will be a little hard on those who are then inhabitants of those cities. Of course, it will take place gradually. The severe destruction caused by high tides along the Dutch and English coasts a short time ago resulted perhaps from the general glacial retreat which has taken place in the last 50 years and which has raised the ocean level perhaps one foot.

The relation of sand deposits to these physiographic changes has been described earlier by the writer[10, 1] for deposits in Brazil and in Florida. The important deposits of Travancore in relation to changes in sea level were described briefly by the writer[11] in the second edition of the volume *Industrial Minerals and Rocks*. Opportunity is taken here to expand the previous brief description and to illustrate the changes with maps. Tilting seems to have been effective in Travancore, but not in these other localities.

The Indian Ilmenite Deposits: The former native states of Travancore and Cochin, once ruled as

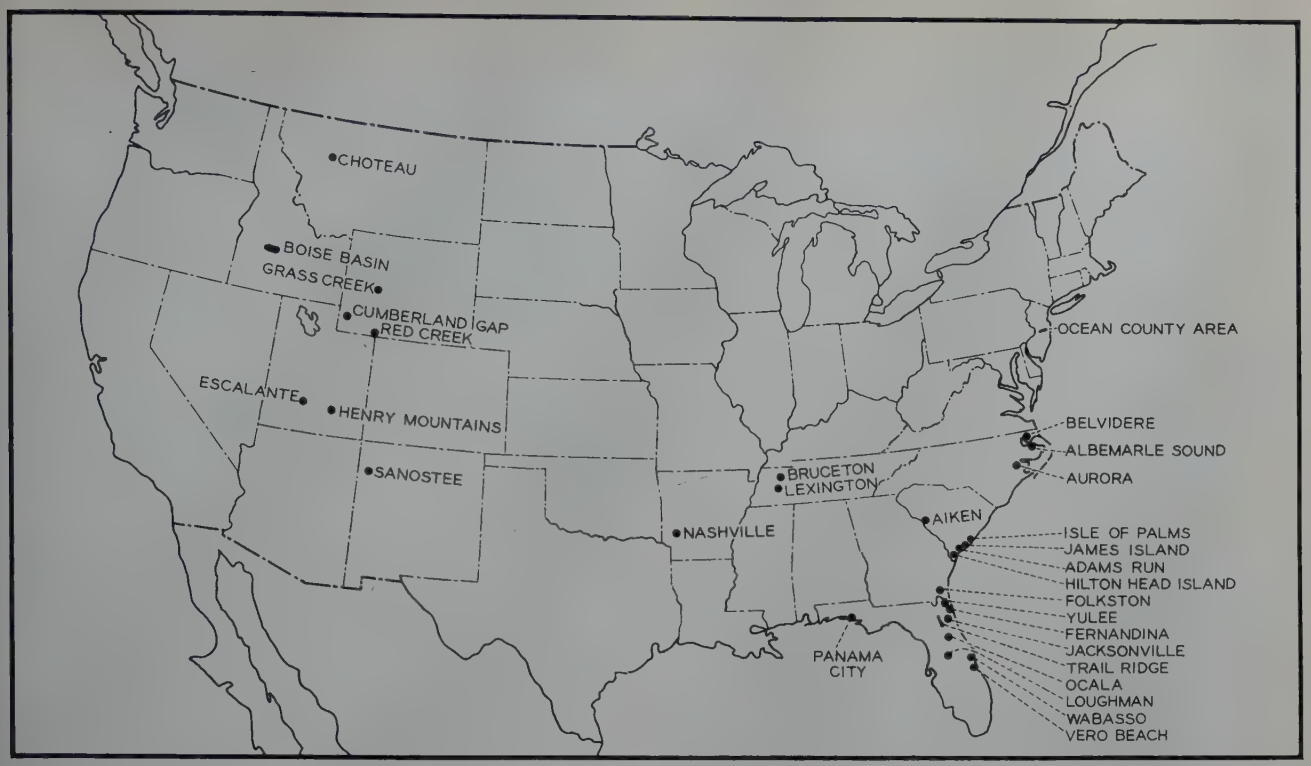

Fig. 6—Sand deposits of titanium minerals in the U. S.

princely states by Maharajas, have now been combined into the Indian state of Kerala. This state forms the southwest tip of the Indian Peninsula (Fig. 1) and is joined on the east and north by the state of Madras. The southernmost tip of India, Cape Comorin, lies close to the eastern boundary of the state at its south end. The state faces the Arabian Sea, and the coast had been known long to Venetian trader and Portuguese explorer as the Malabar Coast. Then the Dutch came and stayed for a hundred years, but then traded their holdings in India to the British for the Spice Islands and Java, Borneo, and Sumatra. The era of the British in India, like the Dutch in the East Indies, has just closed, but this is not a political dissertation in the relative importance of Travancore as a source of titanium minerals.

A visit to that section of India shows that is consists of several physiographic provinces (see Fig. 2). There is a coastal strip of recent emergence, marked by an inland waterway. Like its counterpart along our eastern coast, this waterway is made up of dug canals connecting estuaries and the lagoons and channels between the barrier beaches and the mainland. Inland from the coastal strip, with its coconut palms, is a laterite plain of poor soil, planted mostly to mandioca. Wherever water runs in ditches on that plain, the black minerals settle out in heavy deposits. The erosion of that laterite is the source of the black minerals on the beach and the sand bars.

Inland from the laterite plain is a deeply dissected plateau with an erosion surface shown as remnants on the ridges at around 1000 ft. This is the rubber-growing country.

Further inland is the mountain ridge called the Western Ghats, a high and old erosion surface, the drainage of which is entirely unrelated to the modern streams working headwards from the coast. This plateau in Travancore stands at elevations of 5000 to 6000 ft; further north it is higher. Where the streams from the coast have worked back to intersect the old mature drainage of the high plateau there are most spectacular waterfalls with drops of hundreds of feet. Since this high plateau receives a high precipitation, of hundreds of inches per year, these falls present great potential of water power. Some initial development of the falls has already taken place at the Periyar Lake, shown on Sheet 58 G/2 of the Indian Survey. This high plateau is the tea-growing country.

The east face of the high plateau is even more abrupt than the west. The writer believes it is an eroded fault scrap, probably an overthrust, pushed from the west. To the east stretches the wide Madras plain—a surface of old age.

The rocks of the plateau country are basic gneisses, given Scandinavian names, but American petrologists would call them simple gabbro or diorite gneisses. Intrusive (?) into these are garnetiferous granites or granite gneisses. There is no question that the ilmenite (and the other heavy minerals of the beach sands) came originally from these rocks, but were concentrated first in the red soil of the laterite plain. During the long period of tropical weathering that formed the laterite, any magnetite present was converted to limonite and the minerals of poor chemical stability, such as the feldspars and pyroxene, apatite and amphiboles, disappeared.

It has been stated above that these deposits supplied the bulk of the titanium ore used by American pigment plants prior to World War II. Even now more than 200,000 tons of ilmenite are shipped annually to the U.S. and additional substantial tonnages to France, Italy, and Japan.

The black sand deposits occur at two places. The southernmost deposit (Fig. 3), one no longer worked, is near the southern end of the coast, close to a village called Manavalakurichi, a name abbreviated to M.K. for rather obvious reasons. The northern deposit, which has been worked since about 1933, extends along the coast for 15 miles from the Neendakara Estuary to Kayankulam Bar.

The two deposits have more differences than similarities. The ilmenite in the M.K. deposit analyzed only 54 pct TiO_2, and the sand was rich in garnet and monazite. The ilmenite in the Quilon deposit analyzes about 60 pct TiO_2. The sand carries almost no garnet, and the monazite content is high in only two sections of the beach later described.

The M.K. deposit consisted of buried seams of rich black sand at or just above the present ocean level, and the beach sands that were rich only when the monsoon storms sorted out the light minerals from the heavy ones. The deposit lies in a cove between the headland at Muttam and a smaller one cut in the laterite at Kolachel, as shown on Indian Survey Sheets 58 H-4 and 58 H-8, surveyed in 1918-1919.

The localization of the deposit at that particular place, and its character, can be explained after a careful study of the geological and geomorphological history. The deposit is on the sea side of an embayment between the granite hills that reach elevations up to 500 ft north and northeast of Kolachel, and the outlying mountain mass, east of Padmanabhapuram, called the Bhutapandi Hills, that rise abruptly to over 3000 ft. This embayment is a rather deeply eroded laterite terrace, the remnants of which lie just about at the 200-ft contour. Since this laterite carries abundant ilmenite and the other minerals of the coastal sands, there is no doubt that the intermediate source of these minerals is this laterite, just as the Brazilian and Florida deposits came out of Tertiary sediments. The dissection of this laterite terrace could not have resulted from the streams flowing in it today. The Valliyar, which discharges at the east end of the deposit, is a puny sluggish stream and does not even reach back into the head of the very valley in which it flows. The next valley to the east, at the mouth of which are the Rajakkamangalam salt flats, has no permanent stream at all. A study of the larger streams up country shows

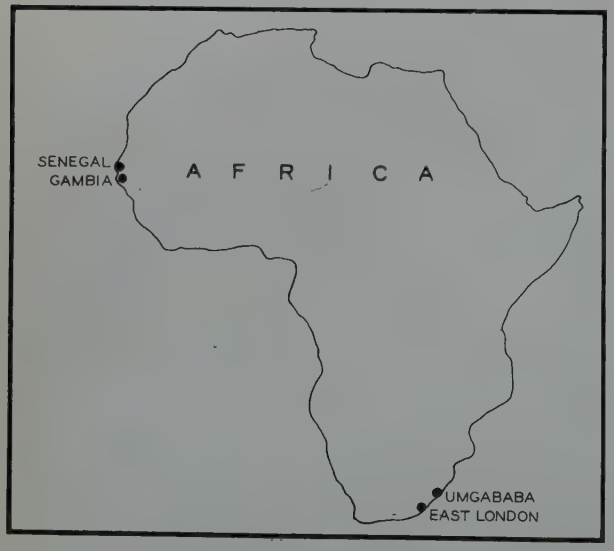

Fig. 7—Sand deposits of titanium minerals in Africa.

that a beautiful case of stream piracy is recorded. The Tambraparni, which is the downstream name for the very large Kodayar, captured the Paralar, leaving a wind gap at Mekkod, probably in Tertiary time. More recently, with uplift, but before the Paralar was captured and its seaward end diverted north, dissection of the laterite plain occurred, and the products of erosion were carried to the sea. Some of the heavy minerals may have remained about where they fell, but the quartz sand was carried away by alongshore currents (probably to the northwest). As emergence continued, waves attacked the laterite and made *storm line deposits* at the top of the beach, generally called the berm, by washing away the light gravity minerals and leaving the heavy where they fell. With further emergence, these storm line deposits were buried by wind-blown sand. These are the "buried" seams worked actively by the Hopkin-Williams Travancore Ltd. from about 1902 to 1935. The overburden was stripped off by hand, but as the sand of the overburden carried considerable ilmenite and monazite, all of it was put through the plant, which was called a *factory*.

The monsoon storms drove the beach back and produced very rich beach deposits, by the destruction of the buried seams that became exposed under the fury of the waves. After nearly 30 years of operation, the buried seams were about exhausted and there was nothing more for the waves to concentrate.

Before leaving the description of the M.K. deposits, it is interesting to recall how an old theory of the early operators—that the ilmenite washed in from the sea—was quickly disposed of by determining that the ocean bottom only a few hundred feet offshore is composed only of coral rock. The writer engaged a pearl diver, who dived from a dugout canoe at numerous places along the shore line, trying without success to scrap bottom sand into an empty can, but finding only rock. As the water was shallow for a long way from shore, the lowest depth reached was 30 ft and the longest dive 55 sec.

The northern beach (Fig. 4), called the Quilon deposit, is not only very much larger and with an ilmenite of better quality, but is also of a different genesis from the one at M.K. Obviously the emergence there has not been so great, suggesting that the south Indian coast has been tilted, with greater movement to the south. Back from the M.K. beach are elevated beach cliffs above the 50-ft contour. At Quilon, the river mouths are still deep estuaries, and for miles inland from the barrier beach that is the ilmenite deposit, the land is so low that it is flooded widely during the rainy season.

A barrier beach is like the ones at Miami, Atlantic City, Coney Island, or along the Texas Coast. It is an elevated offshore bar, and what was formerly deep water between bar and original mainland is now a lagoon, used as an inland waterway, as along the Atlantic and Gulf Coasts of the U.S.

The low-lying flat, now densely covered with coconut palms, was a laterite plain formed on detritus brought down by the major streams, the Punalur and the Pallikal. The drowning of the valleys during submergence terminated the discharge directly into the sea, so that the sands now making the barrier beach were brought down before the submergence. That the sands did not move very far is shown by the mineral composition and grain

Fig. 8a—Sand deposits of titanium minerals, Australia.

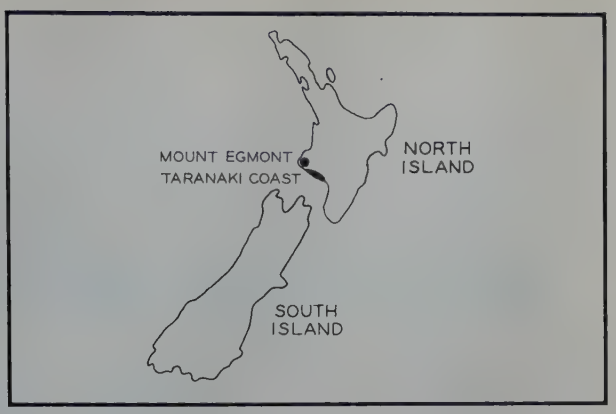

Fig. 8b—The sand deposits in New Zealand.

size of the sands at Neendakara estuary and at Ponmana, which is obviously the original point of discharge of the Pallikal River, until it was captured by the Achankovil and diverted north. The coarser grains, and the concentration of the heavier minerals like monazite and zircon, are more abundant near the point of discharge of these major rivers.

The enrichment of heavy minerals in the offshore bars was done by ocean currents moving north parallel to the coast, as the writer has described[10,1] for the Brazilian and Floridian deposits. Heavy minerals moved shorter distances, and the lighter minerals were carried on, probably most of them for miles beyond the enriched zones. As emergence occurred, the heavy surf broke on the bars, and the waves picked up the minerals of lighter gravity and carried them across the bar and into the deeper water on the land side. Hence the bar acted like the riffles on a Wilfley table. Further elevation made a beach out of the bar, and storm line deposits were developed on the berm by the highest waves. With further emergence these storm line deposits were covered by dune sand. So much black mineral was available that the dunes carry as much as 50 pct heavies. Destruction of the dunes by advancing waves formed rich concentrations on the beach. For years one company, Travancore Minerals Co. Ltd. (now Travancore Minerals Private Ltd.) worked the beach concentrations, while three others have worked the dunes and buried seams.

That emergence is continuing is suggested by the writings of Marco Polo, who waited out a monsoon in Quilon in the late 1200's until he could embark on a Chinese junk for Cathay. He reported that a ship carrying 700 people was in the harbor. Today only a dugout canoe can get into Neendakara estuary, if the boatman is careful to ride in with a big roller.

The ilmenite mining and concentration has been described recently by P. Viswanathan,[24, 25] who is the plant manager for the Travancore Minerals Private Ltd.

The concentrating plants are located at Chavara. The products are shipped from Koviltottam, first in canoes launched through the surf, each canoe carrying 20 bags of concentrate. The bags are transferred to sailing lighters called *dhonies,* which sail out to the steamers, anchored four miles off shore.

The sand is mined by hand tools, transported in baskets carried on the heads of boys to the inland water way, and moved down in bulk to the concentrating plants in canoes called *wallums.*

Densely populated villages like Cheriyalikkal,* shown in Fig. 4, restrict the section of beach and dune land available for mining.

* Estimated population 30,000.

Unless and until dredges are used for mining, reserves below sea level are unavailable. The titanium minerals lying above water table, and in open land between villages, are measured in only a few millions of tons.

REFERENCES

[1] J. H. Carpenter, J. C. Detweiler, J. L. Gillson, and E. C. Weichel, Jr.: Mining and Concentration of Ilmenite and Associated Minerals at Trail Ridge, Fla. *AIME Trans.*, 1953, vol. 196, pp. 789-795.

[2] C. W. Cooke: Geology of the Coastal Plain of South Carolina. *USGS Bull. 867*, 1936 (especially p. 130).

[3] C. W. Cooke: Geology of the Coastal Plain of Georgia. *USGS Bull. 941*, 1943 (especially p. 103).

[4] C. W. Cooke: The Scenery of Florida. Fla. Geol. Survey, *Geol. Bull. 17*, 1939, p. 32.

[5] C. W. Cooke: Correlation of Coastal Terraces. *Journal of Geology*, 1930, vol. 38, pp. 577-589.

[6] J. C. Crowell: Submarine Canyons Bordering Central and Southern California. *Journal of Geology*, 1952, vol. 60, pp. 58-83.

[7] R. A. Daly: *The Changing World of the Ice Age.* Yale University Press, 1934, p. 271.

[8] K. O. Emery, W. S. Butcher, H. R. Gould, and F. C. Shepard: Submarine Geology off San Diego, Calif. *Journal of Geology*, 1952, vol. 60, pp. 511-548.

[9] R. F. Flint: *Glacial Geology of the Pleistocene Epoch*, 589 pp. John Wiley, New York, 1947, (see especially p. 427).

[10] J. L. Gillson: Deposits of Heavy Minerals on the Brazilian Coast. *AIME Trans.*, vol. 187, pp. 685-693, 1950.

[11] J. L. Gillson: *Industrial Minerals and Rocks*, 2nd ed., Chapter on Titanium. (See especially pages 1054-6) AIME, New York, 1949.

[12] B. Gutenberg: Changes in Sea Level, Post Glacial Uplift, and Mobility of the Earth's Interior. *GSA Bull. 52*, 1941, pp. 721-772.

[13] E. L. Hamilton: Sunken Islands of the Mid-Pacific Mountains. GSA Memoir 64, 1956.

[14] H. H. Hess: Drowned Ancient Islands of the Pacific Basin. *American Journal of Science*, 1946, vol. 244, pp. 772-791.

[15] P. H. Kuenen: Origin and Classification of Submarine Canyons. *GSA Bull. 64*, November 1953, pp. 1295-1314.

[16] K. V. Landis: Our Shrinking Globe. *GSA Bull. 63*, 1952, pp. 225-240.

[17] L. E. Lynd, H. Sigurdson, C. H. North, W. W. Anderson: Characteristics of Titaniferous Concentrates. *AIME Trans.*, 1954, vol. 199, pp. 817-824.

[18] J. H. C. Martens: Beach Deposits of Ilmenite, Zircon and Rutile in Florida. *Fla. Geol. Surv. 19th Annual Report*, 1928, pp. 124-154.

[19] J. F. Murphy and R. S. Houston: Titanium-Bearing Black Sands of Wyoming, *Wyo. Geol. Assn. Guide Book*, 10th Annual Field Conf., 1955, pp. 190-196.

[20] R. J. Russell: Instability of Sea Level. *American Scientists*, 1957, vol. 45, pp. 414-430.

[21] F. P. Shepard: Composite Origin of Submarine Canyons. *Journal of Geology*, 1952, vol. 60, pp. 84-96.

[22] F. P. Shepard: *Submarine Geology*, 338 pp. Harper & Bros., New York, 1938.

[23] E. Stebinger: Titaniferous Magnetite Beds on the Blackfoot Indian Reservation, Montana. *USGS Bull. 540*, 1914, pp. 329-337.

[24] P. Viswanathan: Mining and Dressing of Titanium Minerals and Ores. *Eastern Metals Review*, 1954, vol. 7, pp. 940-942 and 958-959.

[25] P. Viswanathan: Studies on Beach Sands of Travancore. *Mining Magazine*, November 1957, pp. 313-315.

[26] N. L. Wimmler: Exploration of Choteau Titaniferous Magnetite Deposit, Teton County, Montana. *USBM R.I. 391*, 1946.

Discussion of this article sent (2 copies) to AIME before May 31, 1959, will be published in MINING ENGINEERING.

by A. M. GAUDIN, D. W. FUERSTENAU, and G. W. MAO

ACTIVATION AND DEACTIVATION STUDIES WITH COPPER ON SPHALERITE

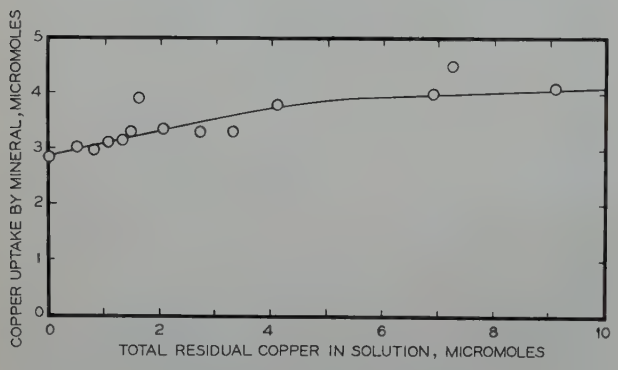

Fig. 1—The abstraction of copper (with 30 min agitation, 74 ml solution) by 5 g of 65/100-mesh sphalerite.

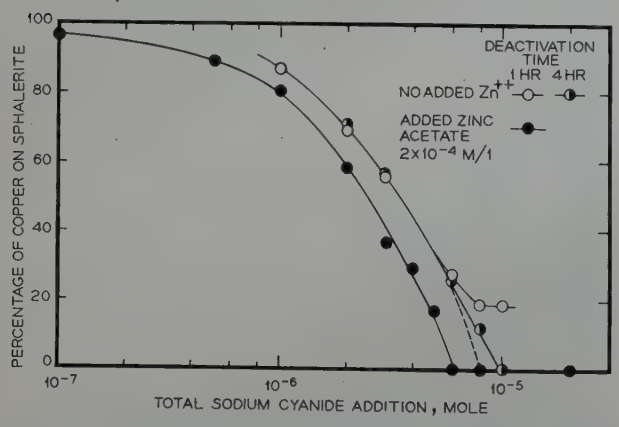
PERCENTAGE OF COPPER ON SPHALERITE
DEACTIVATION TIME
1 HR 4 HR
NO ADDED Zn++
ADDED ZINC ACETATE 2x10-4 M/1
TOTAL SODIUM CYANIDE ADDITION, MOLE

Fig. 3—Deactivation of Cu^{++}-activated sphalerite with sodium cyanide at pH 9.0 (5 g ZnS, 2μ moles Cu^{++}, 74 ml solution, preceded by 30 min activation. The dotted line represents the data for simultaneous agitation with $CuSO_4$ and NaCN for 1 hr and 4 hr.

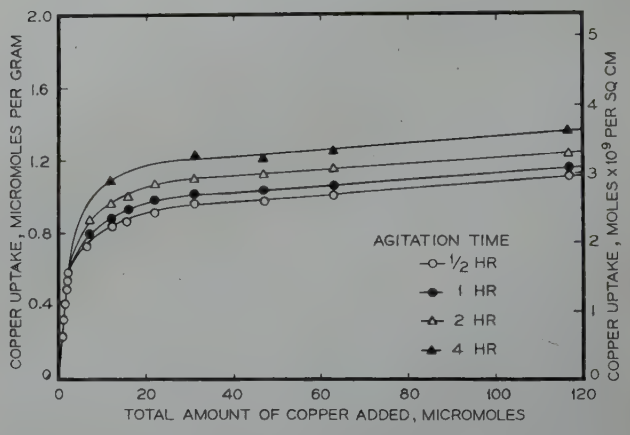

Fig. 2—Copper uptake shown as a function of the added copper and of agitation time.

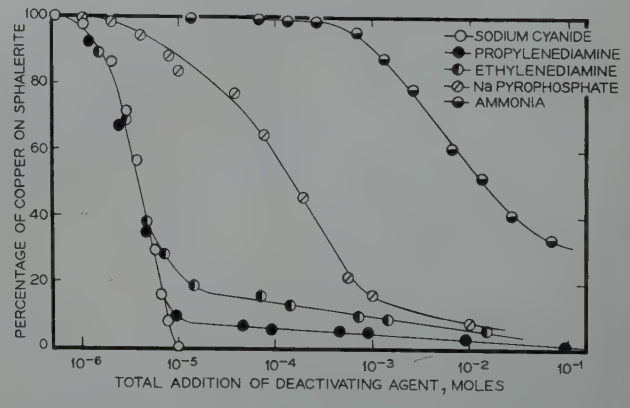

Fig. 4—Partition of copper between solution and sphalerite as a function of the addition of deactivating agent.

Experiments with Cu 64 indicate sphalerite activation to be a chemical exchange of Cu^{++} for Zn^{++} in the sphalerite lattice. This exchange is rapid until three layers of Zn^{++} have been replaced, after which the exchange is controlled by the parabolic rate law. Deactivation results from the sequestering of copper ions in solution. However, to approach the requisite value of $[Zn^{++}]/[Cu^{++}]$ or $[Zn^{++}]/[Cu^{+}]^2$ in solution, the copper complex must be considerably more stable than the corresponding zinc complex.

Activation of sphalerite with copper salts has long been thought of as a chemical reaction of the following form:

$$ZnS + Cu^{++} \rightleftharpoons CuS + Zn^{++} \qquad [1]$$

Early experimentation[1-3] showed that the reaction seemed to be stopped by the coating of insoluble copper sulfide, but since the analytical methods were crude, it was only surmised that the reaction could proceed by diffusion. Probably the most conclusive evidence for reaction (Eq. 1) was obtained by Cooke,[4] who found a stoichiometric replacement of Zn^{++} by Cu^{++} after 50 days' reaction at about 100°C. Cooke also found the sphalerite to be covered with a rather thick coating of covellite, which indicates that activation is a continuing replacement of Zn^{++} by Cu^{++} rather than diffusion of Cu^{++} throughout the sphalerite lattice. However, the occurrence of diffusion at high temperatures has been observed.[5, 6]

It was postulated that copper-activated sphalerite can be deactivated by removing the copper film from the sphalerite surface through the formation of the cupro-cyanide complex in solution,[1] but this hypothesis was never proved experimentally. Recent experimentation on the activation of sphalerite with Ag^{+} showed that uptake of Ag^{+} was controlled by a logarithmic rate law and that the cyanide ions prevented activation by controlling the ratio $[Zn^{++}]/[Ag^{+}]^2$ in solution.[7] Thus, for the copper-sphalerite system, deactivation or prevention of activation must depend on the effectiveness with which a complexing agent controls the ratio of $[Zn^{++}]/[Cu^{++}]$ in solution.

The general objective of this article is to present a study of the principles upon which the activation and deactivation of sphalerite depend. The experimental approach to this investigation was twofold: 1) the factors controlling the activation of sphalerite by copper ions were studied at room temperature, using Cu 64 as radio tracer; 2) the principles of the deactivation of copper-activated sphalerite with various complexing agents were investigated, using Cu 64 and C 14.

A. M. GAUDIN, Member AIME, is Richards Professor of Mineral Engineering, Massachusetts Institute of Technology, Cambridge, Mass. D. W. FUERSTENAU, Member AIME, is Manager of Mineral Engineering, Kaiser Aluminum & Chemical Corp., Permanente, Calif. G. W. MAO, Junior Member AIME, is Research Engineer, Foote Mineral Co., Philadelphia, Pa. TP 4786B. Manuscript, July 24, 1958. New York Meeting, February 1958. AIME Trans., Vol. 214, 1959.

EXPERIMENTAL MATERIALS AND METHOD

Materials: The 65/100-mesh fraction of crushed sphalerite from Ottawa County, Oklahoma, was cleaned with the Frantz isodynamic magnetic separator and the Haultain superpanner. After it had been leached with a 3 pct hydrogen peroxide solution, the sphalerite was washed repeatedly with distilled water and dried at room temperature under water-aspirator vacuum. Vacuum flotation tests confirmed that the mineral surface was free of oily contaminants. The specific surface of the product was found to be 370 ± 10 cm²/g, as measured by the krypton gas-adsorption apparatus. Chemical analysis of the sample gave the following results: 64.9 pct Zn, 32.4 pct S, 0.4 pct Fe, and 0.04 pct Cu.

Pure crystals of covellite (from Butte, Mont.) were wet-ground in a porcelain laboratory ball mill. The ground material, which was cleaned by repeated washing with distilled water, was found to have a specific area of 6100 ± 100 cm²/g.

For each series of experiments, Cu 64 was prepared from electrolytic copper sheet bombarded for 1 hr with deuterons in the MIT cyclotron. Cu 64, which has the relatively short half-life of 12.8 hr, decays with emission of 1.35 Mev gamma radiation.[8] Purification of the Cu 64 was accomplished by electrolysis in acid medium, resolution in sulfuric acid, and evaporation to dryness as copper sulfate.[9] The copper sulfate residue was then diluted with water to give a stock solution of known concentration. The purity of the radioactive copper was confirmed by measurements of its half-life.

Radioactive Zn 65, which has a half-life of 250 days, decays with emission of 1.11 Mev gamma radiation.[8] Marked zinc acetate solutions were prepared with the addition of a few drops of Zn 65 solution to inert zinc acetate. The amount of Zn 65 added was negligible compared to the inert zinc.

Sodium cyanide marked with C 14 was synthesized by Tracerlab Inc., Boston.

Reagent-grade chemical compounds and conductivity water were used for all solutions and tests. The water was deoxygenated by passing through pre-purified, pyrogallol-washed nitrogen for 12 hr.

Methods: For the experiments 5 g of 65/100-mesh sphalerite weighed to 0.1 mg were agitated in 74 ml of solution. The mixture was agitated in a specially prepared glass-stoppered pyrex cylinder having a

volume of about 75 ml at 26 rpm for periods ranging from 5 min to 64 hr. After agitation, the mixture was filtered and a portion of the solution was taken for radioanalysis and pH measurement. The treated mineral was dried before the radioanalysis for copper was made.

In the deactivation experiments, the mineral was first agitated with copper salt solution, the complexing agent was then added, and the cylinder was further agitated. To study the reversibility of the reaction, the complexing agent and copper were added simultaneously in duplicate tests. Total agitation time was 30 min unless otherwise specified. In each case, the total copper addition was 2 micromoles and the experiments were made under nitrogen.

In the experiments on the adsorption of Zn^{++} on covellite, 2 g of the finely ground covellite were mixed with various concentrations of zinc acetate for 30 min. The liquid sample was radioassayed by comparison with standards of known concentrations.

All measurements of Cu 64 and Zn 65 activities were made on scintillation counting equipment. Samples of mineral or samples of solution to be assayed were placed in 5-ml screw-top glass vials which fitted into the well in the top of the scintillation counter head. The liquid sample was 2 ml and the solid sample 5 g. Standard polarographic analysis of zinc was used to ascertain the amount of Zn^{++} displaced from the sphalerite surface during activation.

Sodium cyanide tagged with C 14 was first converted to silver cyanide precipitate and then measured on a beta-ray Q-gas counter. Details of the procedure are described elsewhere.[9]

ACTIVATION STUDIES

Effects of Quality of Copper Added and Reaction Time: Using the techniques described in the previous section, the uptake of Cu^{++} by sphalerite after 30-min agitation was determined for 14 different levels of copper addition. In Fig. 1 the Cu^{++} uptake is plotted as a function of the concentration of residual Cu^{++} in solution. These data show that where small additions of copper were made, all or substantially all of it was taken up by the mineral, whereas the uptake from solutions containing relatively large amounts of the metal was almost but not quite independent of the terminal copper content of the solution.

Similar experiments were made again over a range of copper additions, the time of reaction being increased to 1, 2, and 4 hr (Fig. 2). Great similarity is shown by the results, which suggest very fast surface reaction followed by a much slower subsequent phenomenon. In general, the fast reaction seems to require approximately 2.8 micromoles for 5 g of mineral or 0.57 micromole per gram.

To ascertain the effect of extended periods of agitation on Cu^{++} uptake, a series of experiments were performed in which the total copper in the system was maintained at 3 mg or 4.7×10^{-5} moles but the agitation time was varied from 5 min to 63 hr. The data, given in Table I, show that Cu^{++} continues to be abstracted by sphalerite as the activation time is increased.

Investigation of Factors Involving Exchange of Cu^{++} and Zn^{++}: In one case, as will be seen in Table II, the stoichiometric agreement is excellent; in the other, it differs by only 20 pct.

Table I. Copper Abstracted Per Gram of Sphalerite (65/100-Mesh) from Solutions Containing Excess Cu^{++} as a Function of Time of Agitation at Room Temperatures

Time	Abstraction, Micromoles Per Gram
5 min	0.58*
15 min	0.61*
30 min	0.94*
1 hr	0.98
2 hr	1.04
4 hr	1.17
8 hr	1.26
16 hr	1.42
32 hr	1.73
63 hr	2.14

* Average of two closely checking determinations.

Table II. Exchange of Copper for Zinc

Total Amount Cu^{++} Added, Micromoles	Total Amount Zn^{++} Detected in Solution, Micromoles	Zn^{++} Displaced, Micromoles	Cu^{++} Abstracted,* Micromoles
0	1.9	—	—
3.0	4.8	2.9	2.8
10.0	5.6	3.7	4.5

* Measured independently.

Because copper sulfide is 10^{10} times less soluble than zinc sulfide,[13] excess Zn^{++} should not affect activation in the absence of a copper-complexing agent. In several series of experiments, the initial copper sulfate concentration was varied from 4×10^{-8} to 3×10^{-4} molar and the zinc acetate concentration was systematically increased to a value greater than 0.1 molar. As predicted thermodynamically, in each case Zn failed to prevent Cu^{++} abstraction, although the rate was reduced slightly.[9]

If the large uptake of Cu^{++} by sphalerite is controlled by the relative solubility products of copper sulfide and zinc sulfide, it might be expected that abstraction of Zn^{++} by covellite would be low because this would merely be physical adsorption. Measurements of the equilibrium abstraction of Zn^{++} by covellite show that the actual Zn^{++} adsorption by covellite is 4×10^{-11} mole Zn^{++} per cm^2 at a concentration of 2.7×10^{-5} mole per liter and 1.9×10^{-10} mole per cm^2 at a concentration ten times greater. These data are similar to those obtained by Chang on the adsorption of Ba^{++} by quartz.[10] Thus it appears that the adsorption of Zn^{++} by covellite is analogous to the physical adsorption of Ba^{++} by quartz rather than to the chemical exchange of Cu^{++} for Zn^{++} by sphalerite, which involves a 30 to 70-fold greater uptake (see Fig. 2).

Exchange Between Radioactive Cu 64 and Inactive Cu 63: In one pair of experiments, 5 micromoles of radioactive copper were first agitated with 5 g of sphalerite for 30 min. Then 5 micromoles of inactive copper were added and the agitation was continued for an additional 2 hr. In a second set of experiments the order of adding active and inactive copper ions was reversed. After correction for radioactive decay, the activity on the sphalerite was 30,700 and 30,800 cpm in the two cases and that in the solution was 304,000 and 297,000 cpm, respectively. This shows

EQUATIONS 2 THROUGH 29

$ZnS \rightleftharpoons Zn^{++} + S^{=}$	$K = 7 \times 10^{-26}$	[2]
$CuS \rightleftharpoons Cu^{++} + S^{=}$	$K = 8 \times 10^{-37}$	[3]
$Cu_2S \rightleftharpoons 2Cu^{+} + S^{=}$	$K = 1 \times 10^{-49}$	[4]
$Cu^{++} + HCN \rightleftharpoons Cu^{+} + \frac{1}{2}C_2N_2 + H^{+}$	$K = 2.1 \times 10^{-4}$	[5]
$Cu(CN)_2^{-} \rightleftharpoons Cu^{+} + 2CN^{-}$	$K = 2.1 \times 10^{-24}$	[6]
$HCN \rightleftharpoons H^{+} + CN^{-}$	$K = 4 \times 10^{-10}$	[7]
$Zn(CN)_4^{=} \rightleftharpoons Zn^{++} + 4CN^{-}$	$K = 1.3 \times 10^{-17}$	[8]
$C_2N_2 + 2OH^{-} \rightleftharpoons CN^{-} + CNO^{-} + H_2O$	$K = 1.6 \times 10^{-25}$	[9]
$Cu(NH_3)^{++} \rightleftharpoons Cu^{++} + NH_{3(aq)}$	$K = 7.2 \times 10^{-5}$	[10]
$Cu(NH_3)_2^{++} \rightleftharpoons Cu^{++} + 2NH_{3(aq)}$	$K = 2.3 \times 10^{-8}$	[11]
$Cu(NH_3)_3^{++} \rightleftharpoons Cu^{++} + 3NH_{3(aq)}$	$K = 2.9 \times 10^{-11}$	[12]
$Cu(NH_3)_4^{++} \rightleftharpoons Cu^{++} + 4NH_{3(aq)}$	$K = 2.3 \times 10^{-13}$	[13]
$Cu(NH_3)_5^{++} \rightleftharpoons Cu(NH_3)_4^{++} + NH_{3(aq)}$	$K = 2.8$	[14]
$Zn(NH_3)_4^{++} \rightleftharpoons Zn^{++} + 4NH_{3(aq)}$	$K = 3.4 \times 10^{-10}$	[15]
$NH_4OH \rightleftharpoons NH_4^{+} + OH^{-}$	$K = 1.8 \times 10^{-5}$	[16]
$Cu(ED)_2^{++} \rightleftharpoons Cu^{++} + 2ED$	$K = 1.9 \times 10^{-20}$	[17]
$Cu(PD)_2^{++} \rightleftharpoons Cu^{++} + 2PD$	$K = 6.8 \times 10^{-21}$	[18]
$H_2ED^{++} \rightleftharpoons HED^{+} + H^{+}$	$K = 3.2 \times 10^{-8}$	[19]
$HED^{+} \rightleftharpoons ED + H^{+}$	$K = 6.8 \times 10^{-11}$	[20]
$H_2PD^{++} \rightleftharpoons HPD + H^{+}$	$K = 1.0 \times 10^{-7}$	[21]
$HPD^{+} \rightleftharpoons PD + H^{+}$	$K = 1.7 \times 10^{-10}$	[22]
$Zn(ED)_2^{++} \rightleftharpoons Zn^{++} + 2ED$	$K = 4.2 \times 10^{-11}$	[23]
$Zn(PD)_2^{++} \rightleftharpoons Zn^{++} + 2PD$	$K = 1.4 \times 10^{-11}$	[24]
$Cu(P_2O_7)_2^{\equiv\equiv} \rightleftharpoons Cu^{++} + 2P_2O_7^{==}$	$K = 3 \times 10^{-18}$	[25]
$Cu(HP_2O_7)_2^{==} \rightleftharpoons Cu^{++} + 2HP_2O_7^{\equiv}$	$K = 8 \times 10^{-11}$	[26]
$Zn(P_2O_7)_2^{\equiv\equiv} \rightleftharpoons Zn^{+} + 2P_2O_7^{==}$	$K = 10^{-7}$	[27]
$H_2P_2O_7^{=} \rightleftharpoons H^{+} + HP_2O_7^{\equiv}$	$K = 2.7 \times 10^{-7}$	[28]
$HP_2O_7^{\equiv} \rightleftharpoons H^{+} + P_2O_7^{==}$	$K = 2.4 \times 10^{-10}$	[29]

that in both cases complete exchange occurred between Cu 64 and Cu 63. Other experiments showed that this exchange takes place in less than an hour.

DEACTIVATION STUDIES

The equations that apply to the chemistry of the aqueous solutions with which this article is concerned are presented as Eqs. 2 to 29. Unless otherwise specified, equilibrium constants are those given by Latimer.[13]

Deactivation with Sodium Cyanide: In aqueous solutions, sodium cyanide, the most commonly used deactivator for sphalerite, reduces Cu^{++} (Eq. 5) with the formation of cyanogen. Cyanogen, produced during reduction of the copper, disproportionates (Eq. 9), but cyanogen hydrolyzes slowly compared to the rate of oxidation.[14] Cyanide ions then complex Cu^{+} in solution.[12]

In the first series of experiments using sodium cyanide as deactivator, sphalerite was activated with 2 micromoles of Cu^{++} for 30 min. Then the solution was replaced with one containing various amounts of sodium cyanide at pH 9.0 ± 0.2; the pulp was agitated for 1 hr and a similar sample for 4 hr. Another series of experiments were performed in which the copper-activated sphalerite was deactivated for 1 hr with a solution containing 2×10^{-4} M/l zinc acetate and varying amounts of sodium cyanide at pH 8.8 ± 0.1. These data are presented in Fig. 3. Four-hour deactivation with 10 micromoles of sodium cyanide is required for removal of 100 pct of the copper, if zinc salts are not added. In this case, part of the Cu^{++} coating on sphalerite is very readily removed, but removal of the remaining copper must be controlled by a slower step. In the presence of added zinc salts, however, the copper is completely removed by 6 micromoles of NaCN with 1-hr deactivation. In Fig. 3 a dotted line is drawn to represent data obtained by agitating sphalerite for both 1 hr and 4 hr when the copper sulfate and sodium cyanide were mixed together at pH 9.0. In this instance Cu^{++} is prevented from going to the sphalerite surface if 8 micromoles of NaCN have been added to the system.

The uptake of Cu^{++} by sphalerite from solutions containing both copper sulfate and sodium cyanide at pH 6.1 ± 0.1 was measured for ½, 1, 2, and 4-hr agitation. Since the system was found to be at equilibrium after 30-min agitation, only the data for 30-min agitation are presented in Fig. 4.

Several experiments were made in which the sphalerite was agitated for 1 hr with radioactively-marked $NaC^{14}N$. After agitation, the mineral and liquor were separated by filtration and the activity of the cake was measured, as well as its moisture content. In no case was there any activity on the mineral beyond background and that due to the moisture in the pores. Three experiments were also made in which copper sulfate and five to ten times as many equivalents of $NaC^{14}N$ in dilute aqueous solutions were added simultaneously to sphalerite. Again, activity on the solid was nil. Thus neither the adsorption of cyanide ion nor cuprocyanide ion can contribute to the deactivation of sphalerite.

Deactivation with Aqueous Ammonia: Since ammonia complexes Cu^{++}, it was thought that ammonia would perhaps provide a means of deactivating copper-activated sphalerite. Schwarzenbach[16] showed that five different copper-ammonia complexes exist in solution, none being dominant (Eqs. 10-14). Ammonia does not complex Cu^{++} as tightly as cyanide does Cu^{+} and, in addition, the stabilities of the Cu^{++} and Zn^{++} complexes do not differ greatly.

The effect of ammonia on preventing the activa-

tion of sphalerite was determined by measuring the uptake of Cu^{++} from solutions containing copper sulfate and ammonia mixed together. In these experiments the sphalerite was agitated for 30 min in the solutions. With the increasing ammonia additions, the pH of the solutions was found to increase[9] from 7 to 11.6. The data, plotted in Fig. 5, show that ammonia does not effectively prevent activation of sphalerite with Cu^{++}. Experimental data on removal of Cu^{++} from previously activated sphalerite was found similar to that presented in Fig. 5.[9]

Deactivation by Ethylenediamine and Propylenediamine: Both ethylenediamine (ED) and propylenediamine (PD) form very stable cupric chelate complexes[15] (Eqs. 17 to 24). The reaction between Cu^{++} and ethylenediamine (ED) is believed to be as follows:

$$Cu^{++} + 2(H_2N\text{-}CH_2\text{-}CH_2\text{-}NH_2) \rightleftharpoons \left[\begin{array}{c} H_2 \quad H_2 \quad H_2 \quad H_2 \\ C\text{-}N \quad\quad N\text{-}C \\ \quad\quad Cu \\ C\text{-}N \quad\quad N\text{-}C \\ H_2 \quad H_2 \quad H_2 \quad H_2 \end{array}\right]^{++} \quad [17a]$$

In the case of ethylenediamine, two series of tests were run. In the first series activation was allowed to proceed for 30 min, after which solutions containing ethylenediamine were added, and the container was again agitated for 1 hr. In these experiments the pH of the solutions ranged[9] from 6.6 to 11.9. The data obtained are plotted in Fig. 5, curve *A*. In the second series tests were run for 30 min with the simultaneous addition of Cu^{++} and ethylenediamine. The data are plotted as curve *B*, Fig. 5. Since curve *B* is slightly below and to the left of curve *A*, it seems that had enough deactivation time been allowed in the first series of tests, curve *A* might have coincided with curve *B*.

In the case of propylenediamine, copper uptake was measured only when Cu^{++} and propylenediamine solutions were added simultaneously and agitated for 30 min. In these experiments the pH ranged[9] from 6.6 to 12.1. The data obtained resemble those obtained with ethylenediamine, but the prevention of activation is somewhat more complete (Fig. 4).

Deactivation with Sodium Pyrophosphate: Since pyrophosphate forms several complexes with cupric copper,[3, 16, 17] it was thought that it could act as a deactivator for copper-activated sphalerite (Eqs. 25 to 29). Apparently the principal complex is the dipyrophosphatocuprate ion $Cu(P_2O_7)_2^{\equiv\equiv}$ when a slight excess of pyrophosphate is used, while acid or basic complexes are formed in acid and alkaline solutions. Pyrophosphate ions also complex Zn^{++} in solution[18] (Eq. 27).

Experiments were performed in which copper sulfate and sodium pyrophosphate were agitated with sphalerite for 30 min. In these experiments the pH increased from 6.5 to 9.8 with increasing sodium pyrophosphate. The data, presented in Fig. 4, indicate that the capacity of sodium pyrophosphate to prevent activation of quartz lies between that of ammonia and ethylenediamine.

DISCUSSION OF RESULTS

Activation: The experiments described in this work indicate that the uptake of Cu^{++} by sphalerite comprises a fast step followed by a slow one.

An indication of how much Cu^{++} is required to form a monolayer can be obtained from the crystal structure of sphalerite. Crushed sphalerite surface is composed mainly of dodecahedral cleavage faces (110), Fig. 6. A dodecahedral cleavage face has two cationic sites per unit of surface 5.42 x 7.66 Å, or two sites for each 41.6 A^2. If it is assumed that two surface zinc atoms are replaced by two copper atoms, the possible copper uptake is one ion for each 20.8 A^2.

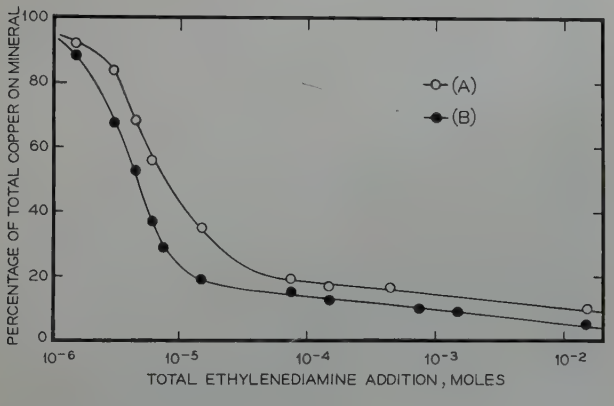

Fig. 5—Deactivation of Cu^{++}-activated sphalerite with ethylenediamine (5 g ZnS, 2μ moles Cu^{++}, 74 cc solution; curve A, 30 min activation followed by 1 hr deactivation; curve B, 30 min agitation with Cu^{++} and ethylenediamine mixed).

Table IV. Ratio of the Dissociation Constants for Zinc Complexes and Copper Complexes

Complexing Agent	K_{Zn} Complex/K_{Cu} Complex
Propylenediamine	2.2×10^9
Ethylenediamine	1.7×10^9
Sodium pyrophosphate	3×10^5
Ammonia	1.5×10^8

Table III. Evaluation of the Ratios $[Zn^{++}]/[Cu^{++}]$ and $[Zn^{++}]/[Cu^{+}]^2$ for Uptake of Cu^{++} by Sphalerite in Presence of NaCN

NaCN, Mole Per 74 Ml	Addition, Mole Per Liter	pH	Cu in Solution, Pct	Calculated Free Cu^{+}, Mole Per Liter	Calculated Free Cu^{++}, Mole Per Liter	Free Zn^{++}, Mole Per Liter	$\frac{[Zn^{++}]}{[Cu^{+}]^2}$	$\frac{[Zn^{++}]}{[Cu^{++}]}$
1×10^{-6}	1.4×10^{-5}	6.10	2.4	4.1×10^{-14}	7.5×10^{-15}	3.0×10^{-5}	2×10^{22}	4×10^9
2×10^{-6}	2.7×10^{-5}	6.15	12.9	8.2×10^{-14}	2.2×10^{-14}	3.4×10^{-5}	5×10^{21}	2×10^9
3×10^{-6}	4.0×10^{-5}	6.18	29.5	1.8×10^{-13}	7.1×10^{-14}	3.9×10^{-5}	1×10^{21}	6×10^8
4×10^{-6}	5.4×10^{-5}	6.19	42.9	1.8×10^{-13}	6.9×10^{-14}	4.3×10^{-5}	1×10^{21}	6×10^8
6×10^{-6}	8.1×10^{-5}	6.20	70.7	1.8×10^{-13}	6.8×10^{-14}	5.1×10^{-5}	2×10^{21}	8×10^8
7×10^{-6}	9.5×10^{-5}	6.21	84.0	1.7×10^{-13}	6.2×10^{-14}	5.5×10^{-5}	2×10^{21}	9×10^8
8×10^{-6}	1.08×10^{-4}	6.25	92.0	9.6×10^{-14}	2.7×10^{-14}	5.8×10^{-5}	6×10^{21}	2×10^9

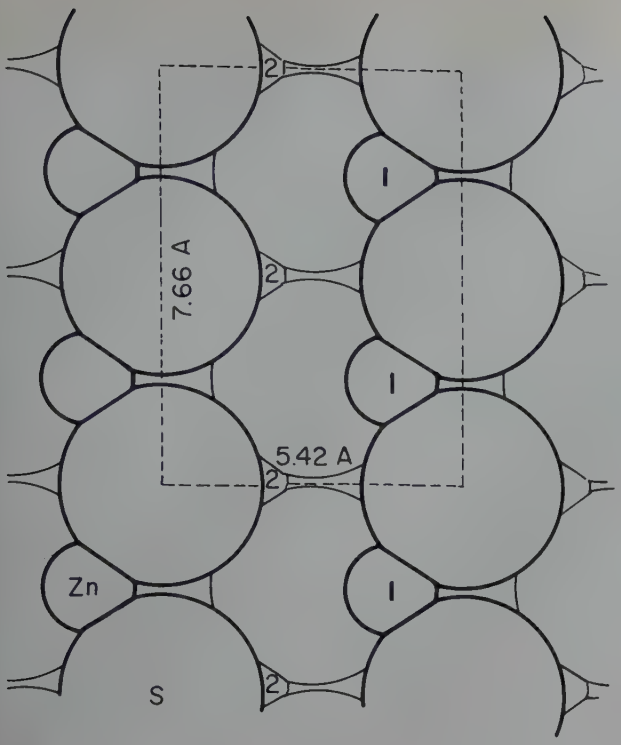

Fig. 6—The (110) plane of sphalerite. Unit area, 41.6 A². Zinc ions in the surface are designated by numeral 1 and zinc ions in the next lower layer by numeral 2.

Fig. 7—The copper abstraction by sphalerite as a function of the square root of the contact time (5 g sphalerite, 4.7 x 10^{-5} moles Cu^{++}, and 74 ml water).

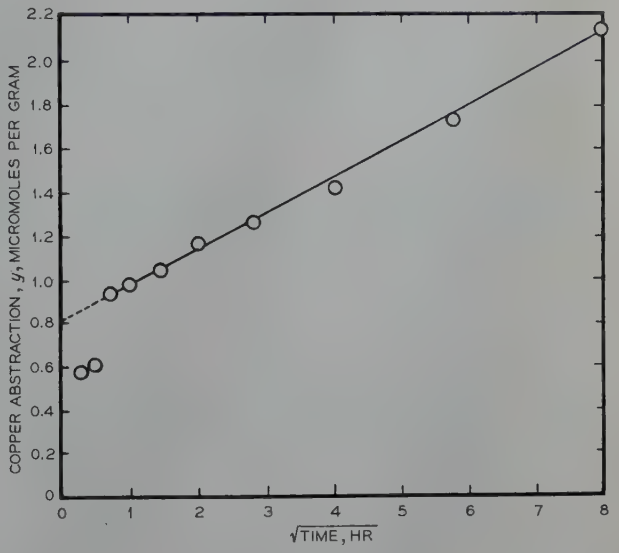

Therefore, the number of copper ions required to form a monolayer on one gram of this sphalerite will be 0.30 micromole. Table I, however, shows that the amount of copper involved in rapid uptake is 0.58 micromole, or almost exactly double this quantity. To reconcile these observations, it is the authors' view that Cu^{++} immediately replaces the surface zinc atoms at the sites labeled *1* in Fig. 6, and almost immediately after that, the partly buried zinc atoms at the sites labeled *2* also become involved in the exchange to involve a total of about 0.60 micromole per gram in the rapid reaction.

However, still another layer of zinc must be involved in a fairly rapid reaction. A straight line is obtained by plotting the quantity of Cu^{++} taken up by the sphalerite vs the square root of time; Fig. 7 reveals that a parabolic rate law is obeyed once the coating is three monolayers thick. More than 15 min but less than 30 min are required for the exchange of the third layer of zinc atoms; however, about 5 hr are required for the exchange of the fourth layer, and about 18 hr for the fifth layer. After three layers of zinc atoms have been exchanged, the uptake of Cu^{++}, y, in micromoles per gram is given as a function of time, t, in hours by Eq. 30.

$$y = 0.165\ t^{1/2} + 0.82 \qquad [30]$$

In the formation of the copper sulfide film on sphalerite, it may be thought that the large sulfide ions are practically devoid of movement while the small copper and zinc ions (0.70 and 0.74 A in radius) diffuse from lattice defect to lattice defect, one inward, the other outward. The two diffusions must be equal so that the net outward current of Zn^{++} equals the net inward current of Cu^{++}. If y is the thickness of the film and t the time, the rate of transfer inward of copper ions must be equal to the rate of growth in thickness in film, dy/dt. But this mass transfer must also be proportional to the gradient in copper-ion concentration across the film K/y (or to the gradient in zinc ion concentration with the sign changed). Hence

$$\frac{dy}{dt} = \frac{K}{y} \qquad [31]$$

which on integration gives the parabolic rate equation of the following form:

$$y^2 = K_1 t + K_2 \qquad [32]$$

The uptake of Ag^{+} by sphalerite has recently been demonstrated to follow the exponential function of time.[7] The authors briefly investigated the uptake of Ag^{+} and Cu^{++} by galena (unpublished data) and the experiments indicated that the uptake of Ag^{+} by galena follows the logarithmic rate law and that the uptake of Cu^{++} by galena follows the parabolic law. Thus the number of ions involved in the exchange affects the nature of the coating and, consequently, the rate. Actually the build-up of a copper sulfide film on sphalerite may be somewhat analogous to the build-up of oxide, sulfide, and halide films on certain metals, which follow several different rate laws, depending on the nature of the film.[19]

Deactivation: A difference apparently exists between the rate at which Cu^{++} goes onto sphalerite and the rate at which it can be removed (see Figs. 3 and 5). Actually, the copper added in the deactivation experiments was 2 micromoles, or 0.40 micromole per gram, which is more than the calculated monolayer but less than the double layer (Fig. 6). In Fig. 3, it may be a coincidence that the quantity of copper on the mineral where the two curves representing 1-hr and 4-hr deactivation diverge is equivalent to complete removal of the outer layer of Cu^{++}. The rest of the Cu^{++}, which occupies sites further inside the lattice, may be more difficult to remove unless the driving force is increased by addition of zinc salts to the solution.

Prevention of Activation: Eq. 1 indicates how the activation of sphalerite might be prevented.

According to this reaction, equilibrium should be reached when the following conditions are met:

$$ZnS + Cu^{++} \rightleftharpoons CuS + Zn^{++} \qquad [1b]$$

$$\frac{[Zn^{++}]}{[Cu^{++}]} = \frac{7 \times 10^{-26}}{8 \times 10^{-37}} = 9 \times 10^{10}$$

For this to be true, the liquid must be in equilbrium with the two solid phases, ZnS and CuS. Since most of the copper in solutions containing NaCN is reduced to the cuprous state, the following conditions must also be met:

$$ZnS + 2Cu^{+} \rightleftharpoons Cu_2S + Zn^{++} \qquad [1c]$$

$$\frac{[Zn^{++}]}{[Cu^{+}]^2} = \frac{7 \times 10^{-26}}{12 \times 10^{-49}} = 6 \times 10^{23}$$

The ratios $\frac{[Zn^{++}]}{[Cu^{++}]}$ and $\frac{[Zn^{++}]}{[Cu^{+}]^2}$ have been evaluated for solutions containing $CuSO_4$ and NaCN (data used in Fig. 4). The pertinent data and results of these calculations are presented in Table III. In view of the wide discrepancies in the values of the various dissociation constants, the agreement between the calculated ratios of $[Zn^{++}]/[Cu^{++}]$ and $[Zn^{++}]/[Cu^{+}]^2$ and the predicted values is quite good.

To show that deactivation does not depend merely on reducing the free Cu^{++} concentration in solution to a low value, the concentration of Cu^{++} was calculated for solutions to which 2.8×10^{-2} mole ammonia has been added. Under these conditions the concentration of free Cu^{++} was 2×10^{-16} and 4×10^{-18} mole per liter, respectively. Yet 31 and 23 pct of the total copper is on the sphalerite (Fig. 4). In the presence of sodium cyanide, copper can be prevented from going to the sphalerite surface when the free Cu^{++} concentration is much larger, 10^{-14} (Table III). But in this case, Zn^{++} is not complexed and its concentration is about 5×10^{-5} mole per liter, whereas in the two ammonia solutions cited above, the free Zn^{++} concentration is only 6×10^{-13} and 2×10^{-14} mole per liter respectively. This means the reaction given by Eq. 1 will proceed to the right.

To compare the effectiveness of different copper-complexing agents for preventing the activation of sphalerite, the results of experiments in which $CuSO_4$ and the complexing agent were agitated simultaneously with sphalerite are presented in Fig. 4. Observation of this figure shows that cyanide ions, ethylenediamine and propylenediamine, are essentially equally effective in preventing Cu^{++} from going to the sphalerite surface, at least at low concentrations, whereas sodium pyrophosphate is considerably less effective and ammonia even less so.

These data can be reconciled by comparing the effectiveness of the complexing agents in controlling the ratio $[Zn^{++}]/[Cu^{++}]$ in solution. Conditions with sodium cyanide present will not be discussed here because of the Cu^{++}—Cu^{+} complication.

By comparing the ratios of the dissociation constants of the zinc complexes and copper complexes, it is possible to observe the relative degree with which the requisite value of the ratio $[Zn^{++}]/[Cu^{++}]$ can be reached. For the case of ammonia, the copper-ammonia complex involving four ammonia molecules will be used for comparison with the zinc-ammonia complex. The ratios of the various dissociation constants are presented in Table IV. Observation of this table and Fig. 4 shows that the reagents follow the predicted order of effectiveness, but sodium pyrophosphate or ammonia should be unable to prevent the activation of sphalerite with Cu^{++} unless the concentration of Zn^{++} is exceedingly high. These two reagents are able to inhibit the uptake of Cu^{++}, but this may result from an actual leaching phenomenon that is not yet at equilibrium. Fig. 4 also shows that only NaCN can completely prevent activation. Propylenediamine and ethylenediamine prevent most of the Cu^{++} from going to the sphalerite surface, but the small amount of copper on the sphalerite at high ethylenediamine concentrations probably results from physical adsorption of the positively charged complex. In one experiment sphalerite was agitated for 30 min in a solution containing 2 micromoles $CuSO_4$, 10^{-2} molar ethylenediamine, and 10^{-3} molar zinc acetate at pH 10.5 and all the copper remained in solution. In this case, the excess zinc probably removes the adsorbed copper complex through competitive physical adsorption.

Summary: Experiments with radioactive Cu 64 indicate that sphalerite activation is a chemical reaction in which copper ions replace zinc ions at the sphalerite surface. This exchange is quite rapid until three layers of zinc ions have been replaced, after which the exchange is controlled by the parabolic rate law.

For deactivation, it was found that the copper complex should be much more stable than the zinc complex because deactivation does not depend merely on bringing the free Cu^{++} concentration to a low value but depends on the ratio of $[Zn^{++}]/[Cu^{++}]$ in solution. In the case of NaCN deactivation, the ratio $[Zn^{++}]/[Cu^{+}]^2$ is also important because most of the copper is in the cuprous state. Neither cyanide nor copper-cyanide complex is adsorbed and prevention of activation is not ascribable to adsorption of these ions.

The authors wish to acknowledge the interest of P. L. de Bruyn and Carl Wagner in this investigation, which was sponsored by the U. S. Atomic Energy Commission.

This presentation is condensed from a doctoral dissertation by G. W. Mao.

REFERENCES

1 A. M. Gaudin, C. B. Haynes, and E. C. Haas: *Flotation Fundamentals*, Part IV, Utah Eng. Experiment Station, *TP 7*, 1930.
2 A. M. Gaudin: *AIME Trans.*, 1930, vol. 87, pp. 417-428.
3 O. C. Ralston, C. R. King, and F. X. Tartaron: *AIME Trans.*, 1930, vol. 87, pp. 389-400.
4 S. R. B. Cooke: *Advances in Colloid Science*, 1950, vol. 3, p. 357.
5 G. Graue and N. Riehl: *Angeuante Chem.*, 1938, vol. 51, pp. 873-875.
6 N. Riehl and H. Ortman: *Zeit. für Phys. Chem.*, 1941, vol. 188, pp. 109-128.
7 A. M. Gaudin, D. W. Fuerstenau, and M. M. Turkanis: *AIME Trans.*, 1957, vol. 208, p. 65.
8 G. Friedlander and J. W. Kennedy: *Introduction to Radiochemistry*, pp. 164, 314. John Wiley & Sons Inc., New York, 1949.
9 G. W. Mao: *Activation and Deactivation Studies of Copper Sphalerite*. Doctor of Science thesis, Massachusetts Institute of Technology, 1956.
10 A. M. Gaudin and C. S. Chang: *AIME Trans.*, vol. 193, p. 193.
11 A. M. Gaudin: *Flotation*, sec. ed. McGraw-Hill Book Co., New York, 1957.
12 M. G. Vladimirova and I. A. Kakovsky: *Zhur. Priklad. Khim.*, 1950, vol. 23, pp. 580-598.
13 W. M. Latimer: *The Oxidation States of the Elements and Their Potentials in Aqueous Solutions*, sec. ed. Prentice-Hall Inc., New York, 1952.
14 F. R. Duke and W. G. Courtney: *Journal of Physical Chemistry*, 1952, vol. 56, p. 19.
15 H. A. Laitinen et al.: *Journal of the American Chemical Society*, 1949, vol. 71, p. 1550.
16 G. Schwarzenbach: *Analytica Chimica Acta*, 1952, vol. 7.
17 J. I. Waters and A. Aaron: *Journal of the American Chemical Society*, 1953, vol. 75, p. 611.
18 J. Vaid and T. L. Rama Char: *Current Science* (India), 1953, vol. 22, p. 170.
19 U. R. Evans: *Trans.* Electrochemical Society, 1943, vol. 83, p. 335.

Discussion of this article sent (2 copies) to AIME before May 31, 1959, will be published in MINING ENGINEERING.

THE 1959 JACKLING LECTURE

"A successful career in mining geology, consulting work and operation of substantial iron ore properties, and for his lecture, 'Economic History of the Lake Superior Iron District.' "—Citation of the Jackling Award Committee.

ECONOMIC HISTORY OF THE LAKE SUPERIOR IRON DISTRICT

by R. S. ARCHIBALD

The subject of this paper is particularly appropriate, since Daniel C. Jackling was active in early exploitation of taconites on the Mesabi Range and contributed greatly to their later economic development. After his success in developing the low grade porphyries in the West he looked for more worlds to conquer, and so undertook the concentration of low grade taconites, from which he hoped to produce commercial ore. Mesabi Iron Co., organized in 1919, actually did produce merchantable sinter from taconites in 1922. The enterprise did not prove commercial at the time, as cost of production was high and the surplus of iron ore in the Lake Superior District already contributed to a low market price, but this same property has since been developed by Reserve Mining Co. The work done by Jackling had much to do with the success of this later venture.

Iron ore was first discovered on the Marquette Range in Michigan in 1845. The first ore from this range came from the old Jackson mine in Negaunee in 1848. During these early years this property and others on the Marquette produced limited tonnages for transportation to Lower Lakes and for consumption by charcoal furnaces in the area, where a plentiful supply of hardwoods furnished the charcoal for iron smelting. The Marquette and other ranges tributary to Lake Superior did not produce much ore for transportation to Lower Lakes until the locks at Sault Ste. Marie were constructed, but from the time the first lock at the "Soo" was completed in 1855 these ores were transported through the locks to consumer centers in the East. The Marquette Range has a history of continuous production from 1848 to the present day.

In 1877 the Menominee Range was discovered at the location of the old Penn Mines near Vulcan, Mich. There were further discoveries of ore on the old Menominee Range and at Florence, Wis., in 1880 and at Iron River and Crystal Falls, Mich., in 1882. Penn Mines continued in operation from the date of their discovery until they were finally exhausted by Pickands-Mather in 1945, but operations still continue on the Menominee in the Crystal Falls and Iron River districts. Ore is shipped to a lake port at Escanaba, Mich.

R. S. ARCHIBALD is a Mining Geologist, Negaunee, Mich.
TP 59A91. Manuscript, Jan. 14, 1959. San Francisco Meeting, February 1959. AIME Trans., Vol. 214, 1959.

This page of AIME Transactions follows p. 436. The intervening non-Transactions pages appeared in MINING ENGINEERING.

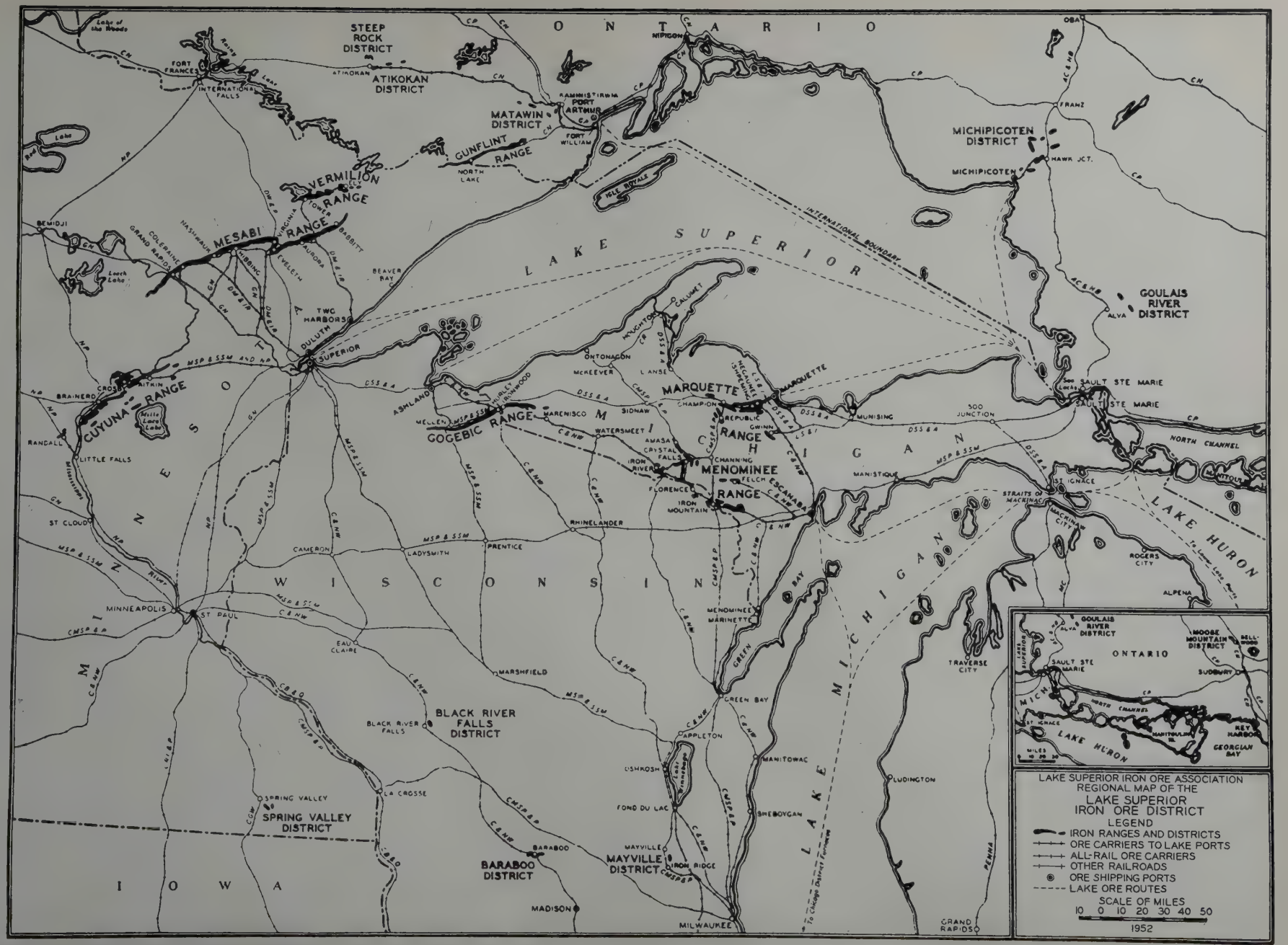
ONTARIO
LAKE SUPERIOR
MINNESOTA
WISCONSIN
MICHIGAN
IOWA
LAKE MICHIGAN
LAKE HURON
STEEP ROCK DISTRICT
ATIKOKAN DISTRICT
MATAWIN DISTRICT
GUNFLINT RANGE
VERMILION RANGE
MESABI RANGE
CUYUNA RANGE
GOGEBIC RANGE
MARQUETTE RANGE
MENOMINEE RANGE
MICHIPICOTEN DISTRICT
GOULAIS RIVER DISTRICT
BLACK RIVER FALLS DISTRICT
SPRING VALLEY DISTRICT
BARABOO DISTRICT
MAYVILLE DISTRICT
INTERNATIONAL BOUNDARY
LAKE SUPERIOR IRON ORE ASSOCIATION
REGIONAL MAP OF THE
LAKE SUPERIOR
IRON ORE DISTRICT
LEGEND
IRON RANGES AND DISTRICTS
ORE CARRIERS TO LAKE PORTS
ALL-RAIL ORE CARRIERS
OTHER RAILROADS
ORE SHIPPING PORTS
LAKE ORE ROUTES
SCALE OF MILES
10 0 10 20 30 40 50
1952

The Gogebic Range was discovered in 1884 at the location of the present Colby mine, and the first ore was shipped that same year by Joseph Sellwood. This ore was shipped all-rail to Milwaukee and thence loaded into vessels and transported to Cleveland, Ohio. The Gogebic Range extended from Gogebic County, Michigan, into Iron County, Wisconsin, and iron ore operations are being carried on in both Michigan and Wisconsin at the present time. This ore is shipped to a lake port at Ashland, Wis.

The Vermillion Range was discovered in 1882 at the Soudan mine at Tower, Minn., a property still in operation. Further discoveries were made on the Vermillion Range a little later, and two other mines on this range continue in production. The ore is shipped to a lake port at Two Harbors, Minn.

The Mesabi, discovered at Mountain Iron in 1890 by the Merritt brothers, began shipment in 1892. This range, developed for a length of some 80 miles, contains the largest reserve of iron ore in the U. S. The ore is shipped to lake ports at Duluth and Two Harbors, Minn., and Superior, Wis.

On the Cuyuna Range (1904) near Deerwood, Minn., the first mine was placed in operation in 1911. The range continues in operation to the present. Ore is shipped to a lake port at Superior, Wis.

In addition to these major iron ore ranges in the Lake Superior District, iron ore is being produced in Fillmore County, Minnesota. This is not a Lake Superior ore. It is shipped all-rail to consumer centers in the Middle West.

Iron ore was also found at Baraboo and Mayville, Wis. These ranges are sometimes classified in the Lake Superior District, but the geological occurrence is different from that of the Lake Superior ores. The mines on these ranges have been exhausted. From 1849 to 1928 a total of 3 million tons was shipped by rail to Chicago and other nearby consumer centers.

Michipicoten Range, northwest of Sault Ste. Marie in Canada, began producing ore in 1891 and has operated intermittently since then. The siderite from this range becomes a manganiferous iron ore of good quality when roasted and is classified as a Lake Superior ore. The ore is shipped all-rail to Sault Ste. Marie, Ont., and also to a lake port at Michipicoten Harbor on Lake Superior.

In 1945 production began at Ontario's Steep Rock Range, discovered in 1938. Steep Rock produces a true Lake Superior ore very similar to the ore of the Vermillion Range. It is shipped from the mine to Port Arthur, Ont., on Lake Superior. This property has operated continuously since 1945.

During the interval following discovery of the Mesabi and Cuyuna ranges, active development and exploration of these ranges was continued and by 1915 had progressed to the point where reasonable estimates of developed tonnage on all of the Lake Superior iron ranges were available. Likewise in the interval between 1900 and 1915 mergers of steel companies into large self-contained units were occurring. U. S. Steel Corp. was organized in 1901, and several other large integrated steel companies had either built or projected plants. A large and dependable source of iron ore was a necessity in organizing and financing these steel plants. Oliver Iron Mining Co., established by U. S. Steel as its iron ore subsidiary, proceeded to acquire large reserves on the Michigan and Minnesota ranges through purchases of existing corporations and leases of known ore reserves. Oliver carried on intensive exploration on the Mesabi Range to develop reserves for this corporation. In 1906 it acquired a lease on the extensive reserves owned by Great Northern Iron Ore Co.

Through these activities Oliver acquired large reserves on the Old Ranges—including the Marquette, Menominee, Gogebic, and Vermillion—and a large share of reserves on the Mesabi. Other steel corporations charged that they were being cut off from the sources of iron ore by the Oliver company, and there was talk in Washington of bringing an anti-trust suit to compel Oliver to release the Great Northern Ore properties. These properties were surrendered by the Oliver company in 1941 and were available to the open market and to other steel companies that were short of ore.

By 1915 the Mesabi and Cuyuna ranges had been rather thoroughly explored. The large discoveries on the Gogebic Range at Wakefield had been made, and reasonable estimates of tonnage were available on all the ranges:

Range	Tons
Marquette	82,547,000
Menominee	69,645,000
Gogebic	64,211,000
Mesabi	1,389,000,000
Vermillion	11,012,000
Cuyuna	72,403,000

This 1915 date was immediately before World War I and it will be noted that at that time there was a total tonnage of 1.689 billion developed in the Lake Superior District.

During an interval included by the two great wars the following tonnages were shipped from the Lake Superior District:

Period		Total, Millions of Tons	Yearly Average, Millions of Tons
Preceding World War I	1910 to 1914	207	41.4
During World War I	1915 to 1919	290	58
Preceding World War II	1920 to 1939	841	42
During World War II	1940 to 1945	485	81

By January 1946, at the end of World War II, developed reserves of iron ore in the Lake Superior District amounted to 1.183 billion tons. From the beginning of World War I to the end of World War II, that is, 1915 to 1945 inclusive, shipments from the Lake Superior District totaled 1.616 billion tons. The gain in reserves during this period in the Lake Superior District was about a billion tons—this in spite of the fact that the District was considered to be developed in 1915.

Factors Underlying Increase in Reserves: This gain in reserves occurred first because the deep mines on the Old Ranges continud to develop reserves in depth and there was little shrinkage in these reserves from year to year. Some new mines were discovered on the Old Ranges, but most of the increase in reserves resulted from extension of known orebodies either laterally or in depth. The great gain in reserves on the Mesabi Range was primarily due to change in mining methods and improvement in ore dressing.

Prior to 1926 all open pit mining was done by the railroad-type shovel loading to railway cars that were hauled out of the pit by steam locomotives. In 1926 the first revolving shovel was tried on the Mesabi by Oliver Iron Mining Co. In 1937 the first truck was used by E. P. Remer at the Leetonia mine in hauling ore from the pit to a loading ramp. Later

IRON ORE IN ONTARIO DURING 1957

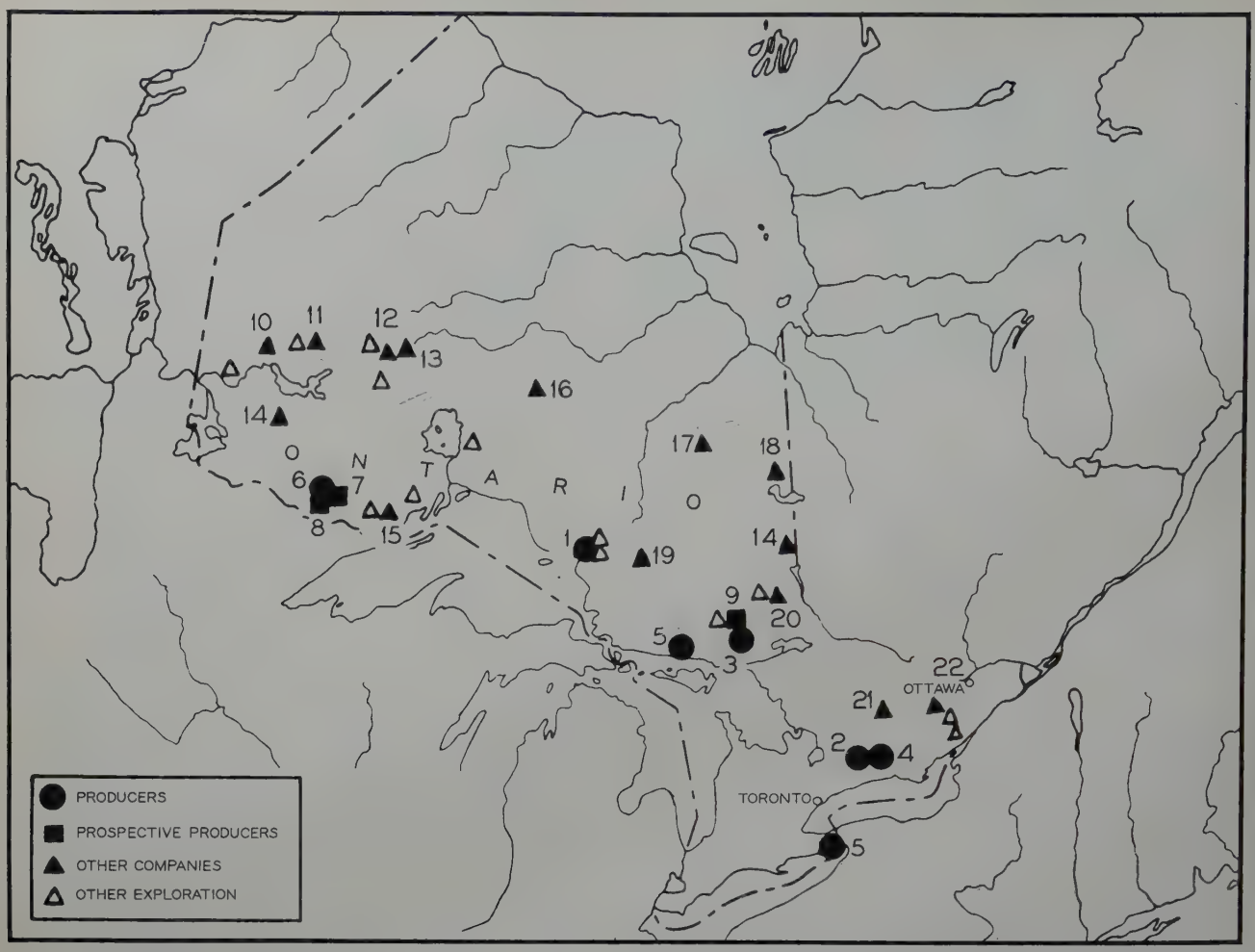

Producers of Iron Ore

1. Algoma Ore Properties Ltd.
2. Clarken Development Ltd.
3. International Nickel Co. of Canada Ltd.
4. Marmoraton Mining Co. Ltd.
5. Noranda Mines Ltd.
6. Steep Rock Iron Mines Ltd.

Prospective Producers with Announced Production Plans

7. Caland Ore Co. Ltd.
8. Canadian Charleson Ltd.
9. Lowphos Ore Ltd.

Some Exploration and Development Companies

10. Iron Bay Mines Ltd.
11. El Sol Gold Mines Ltd.
12. Lun-Echo Gold Mines
13. Steep Rock Iron Mines Ltd.
14. Jalore Mining Co. Ltd.
15. Monpre Mining Co. Ltd.
16. Anaconda Iron Ore (Ontario) Ltd.
17. Mattagami Mining Co. Ltd.
18. Triana Exploration Ltd.
19. Multi-Minerals Ltd.
20. North American Rare Metals Ltd.
21. Frobisher Ltd.
22. Algoma Ore Properties Ltd.

a belt conveyor was installed from the pit. Many of the pits on the Mesabi Range at this time were becoming too deep for economical mining by rail haulage, and many track benches were tied up and unavailable for mining because railroad haulage was used. The ore in many pits already abandoned for open pit mining was made available for mining by the introduction of revolving shovels and truck haulage. Likewise, much of the ore considered as underground reserves was developed for open pit mining because of these innovations.

Another factor that contributed largely to an increase in reserves, particularly on the Mesabi, was the development of iron ore concentration. The first concentrator, built by Oliver Iron Mining Co. at Trout Lake in 1910, made available very large tonnages of sandy wash ores, which could be readily concentrated into high grade ores. The progress in concentration has continued far beyond the original washing plant. In 1957 there were in use in Minnesota 15 straight washing plants, 35 washing and heavy density plants, and one fine ore concentration plant using flotation. There is one washing and sintering plant on the Cuyuna Range which is used in beneficiation of high-moisture low-grade ores. In 1910 610,000 tons of beneficiated ore were shipped and in 1957 24,418,000 tons.

In Michigan there are two heavy density plants and two flotation plants in operation. There is also a drying, screening, and heavy density plant and pellet plant. The pelletizing plant is operating on flotation concentrates.

During the years following the depression of 1929-1933 iron ore shipment from the Lake Superior District lagged, and it was the general opinion of the steel industry that the Michigan, Wisconsin, and Minnesota reserves would be ample for the forseeable future. An estimate made in 1936 by various representatives of the steel companies placed the expected average yearly consumption at 40 million tons. On the basis of reserves at that date—estimated at 1.42 billion tons—there was a life of 35 years for these reserves. During the ten-year period 1931 to 1940 the reserves decreased by only some 50 million tons, while 337,384,000 tons were shipped during this period. Accordingly there was a net

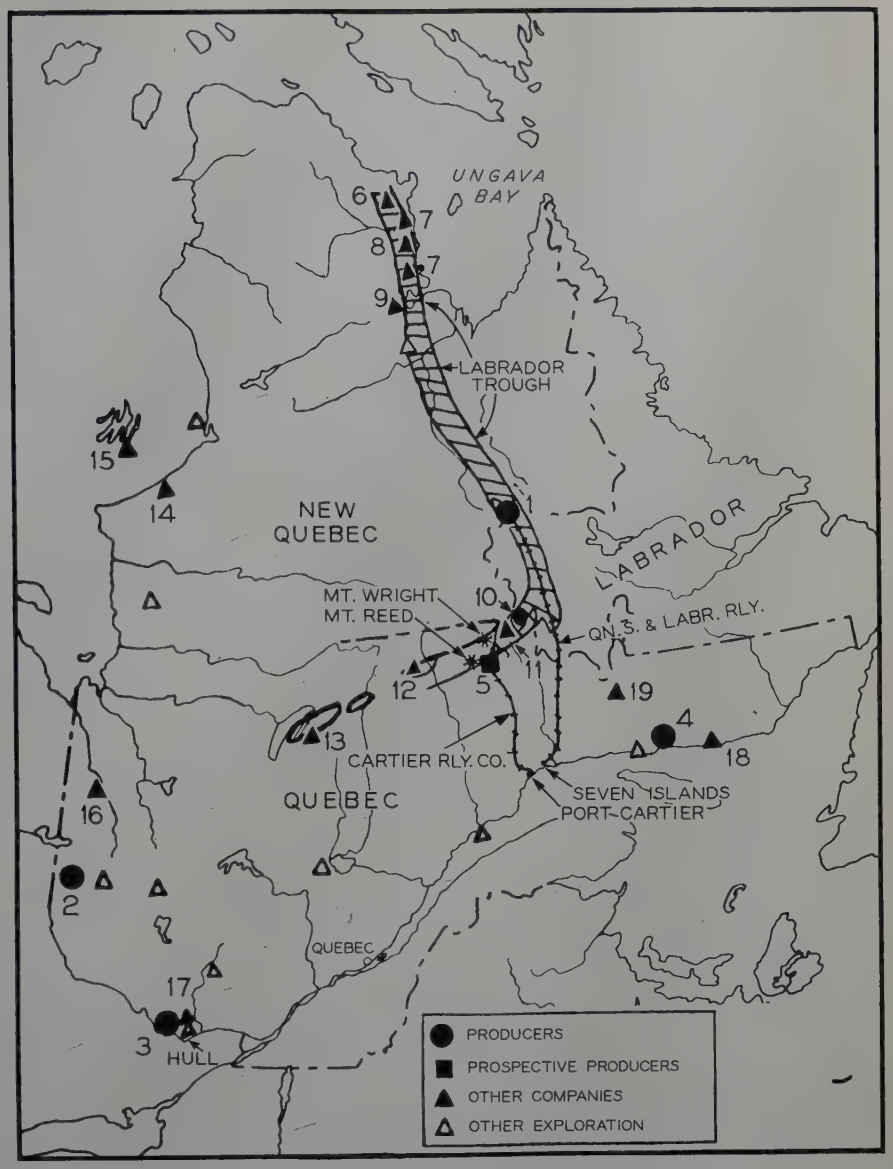

Producers of Iron Ore
1. Iron Ore Co. of Canada
2. Noranda Mines Ltd.
3. Quebec Iron & Titanium Corp.
4. The Hilton Mines

Prospective Producers with Announced Production Plans
5. Quebec Cartier Mining Co.

Some Exploration and Development Companies
6. Quebec Explorers Ltd.
7. Ungava Iron Ores Co. Ltd.
8. Oceanic Iron Ore Co. of Canada Ltd.
9. Consolidated Fenimore Iron Mines Ltd.
10. Wabash Lake Area:
    Canadian Javelin Ltd.
    Julian Iron Corp.
    Labrador Mining & Exploration Co. Ltd. and Iron Ore Co. Ltd.
    Wabash Iron Co., Ltd.
11. Mt. Wright Area:
    Bellechasse Mining Corp. Ltd.
    Holannah Mines Ltd.
    Jubilee Iron Corp.
    Quebec Cartier Mining Co.
    Quebec Cobalt & Exploration Ltd.
12. Pletipi Lake—Matonipi Lake Area:
    Consolidated Morrison Exploration Ltd.
    W. S. Moore & Co.
13. Albanel Minerals Ltd.
14. Great Whale Iron Mines Ltd.
15. Belcher Mining Corp. Ltd.
16. Atlin Ruffner Mines (B.C.) Ltd.
    Lambton Copper Mines Ltd.
17. Jalore Mining Co. Ltd.
18. Aconic Mining Corp.
    Olivier Iron & Steel Ltd.
19. Halmon Mining & Processing Ltd.

gain in the reserves in the ten-year period on account of further development of 287 million tons. On the basis of these figures, the steel industry considered that reserves of the Lake Superior District were good for at least 50 years and that there was no cause for concern.

Beginning with World War II a very large increase in consumption of Lake Superior ore began, and many blast furnaces were built at the expense of the Government and by private enterprise to increase iron and steel capacity. During 1940 to 1949 inclusive, 781 million tons were shipped, or a yearly average of 78 million, approximately double the consumption of ore anticipated in 1936.

This increased production has continued over the years, and the iron and steel industry began to realize that the Lake Superior District could not continue to supply its increased requirements for many years into the future. The industry began to look around for other sources of iron ore.

Bethlehem Steel Co. continued to import large tonnages of iron ore from Chile for its Eastern Seaboard furnaces and also initiated development of a property near the Orinoco River in Venezuela. U. S. Steel Corp. developed very large ore reserves in Venezuela. Republic Steel Corp. went to Liberia for part of its ore requirements. Substantial tonnages of iron ore were also imported from Brazil and Peru.

Intensive studies of iron and steel metallurgy made during the past five years indicate that improved structure of the iron ore going into blast furnaces will result in lower costs and greatly increased furnace capacity. These studies have indicated that a sized blast furnace feed with as high an iron content as possible is desired. The natural ores of the Lake Superior District as mined are unsized, range in structure from 3 in. down to —100 mesh, and average 51.50 natural in iron. Lake Superior operators are working to improve the structure and iron content of these ores, and large investments also have been made in concentrating and agglomerating low grade taconite.

Recent Plant Expansion: During this postwar period attention of the iron and steel industry was turned to the magnetic taconites, known to exist on

the Mesabi Range, that had been partially developed and operated by Jackling at Babbitt, Minn., in the early 1920's.

The original Jackling plant had been operated on an experimental basis. Reserve Mining Co., owned by Republic Steel Corp. and Armco, took over the plant and leases owned by the Jackling interests and about 1950 began development of a large taconite enterprise. A railroad was built from the mine to Silver Bay on Lake Superior, and concentrating and pelletizing plants were constructed on the lake. Magnetic taconites are now shipped from the mine and are concentrated and pelletized at Silver Bay. The Silver Bay plant, which began operating commercially in 1956, has a capacity of 5 to 6 million tons of high grade iron ore pellets per year.

Pickands-Mather, as agent for Bethlehem, Youngstown, and others, likewise proceeded to develop magnetic taconites west of those controlled by Reserve, first building an experimental plant on the range and then a large concentrating and pelletizing plant at Hoyt Lakes, Minn. Experimental pellets were produced by Erie from 1953 until 1958, when the large plant, rated at 8-million ton capacity, was placed in operation. Erie also built a railroad to Lake Superior and a harbor and power plant east of Silver Bay at Taconite Harbor. Combined capacity of these two plants is 12 to 15 million tons of pellets per year.

U. S. Steel's Oliver Iron Mining Div., which controls large reserves of magnetic taconite on the Mesabi Range, has carried on extensive experiments in magnetic concentration of taconites at its Pilotac plant at Mountain Iron. Fines from this plant and screened fines from direct-shipping ores on the Mesabi have been sent to Extaca, Oliver's experimental agglomerating plant near Virginia. Although these plants are experimental, they produce about 1 million tons of agglomerated material.

Marquette Iron Mining Co., operated by Cleveland-Cliffs, has built a pelletizing plant of 650 thousand-ton annual capacity on the Marquette Range to handle flotation concentrates from the Republic mine. Another pelletizing plant is projected for the Marquette Range to handle flotation concentrates from the Humboldt property. This property is controlled by Cleveland-Cliffs Iron Co. and Ford Motor Co. and has been shipping flotation concentrate to Ford Motor Co. for sintering. The plant will be able to handle about 640,000 tons per year.

M. A. Hanna Co. is developing a low grade property at Randville, Mich., which will also produce flotation concentrates. Some of these concentrates will be shipped to furnaces for sintering, but it is expected that facilities will also be built for agglomeration at the mine. Projected capacity of this plant is 500,000 tons of concentrates per year.

Problems in Treating Underground Reserves: Modern furnace practice will have an important effect on ore reserves of the Lake Superior District. Total reserves of direct-shipping and easily concentratable ore estimated for the District as of Jan. 1, 1957, were 952 million tons. Underground reserves included in this total were 388 million tons.

Early availability of these underground reserves is questionable. In order to prepare direct-shipping ore for blast furnace consumption it is proposed to screen the material at about ½ in., using the coarse fraction directly in the blast furnace and sintering the fine fraction, but there are serious difficulties involved in separating the coarse and fine fractions in the underground ores. As a general rule, ores that are mined underground contain 10 pct moisture or more, and to dry-screen then it will be necessary to drive off part of this moisture.

There is considerable variation in analysis of the coarse and fine fractions of ore screened. Generally the fine fraction contains a material of higher grade and removal of the fine material produces a lower grade coarse fraction. If this lower grade coarse fraction is to be used it must undergo beneficiation, which would probably involve a heavy density process. All in all, sizing and beneficiating underground ores is a complicated and expensive process, and it is questionable that the economics of the situation will permit such treatment.

Open Pit and Underground Costs Compared: With reference to this problem, comparison of the open pit and underground mining costs is illuminating. In 1955, when the last figures were available, average mining cost, not including royalty, was $1.50 per ton of open pit ore mined in the Lake Superior District and $5.32 per ton of underground ore mined in the District. Since 1955 increasing labor costs have further spread the differential between open pit and underground mining, and it is quite evident that even without the addition of any cost for beneficiating underground ores, they are not at present competitive with the open pit ores. The open pit ores as produced are comparatively free of moisture and can be dry-screened for sizing without serious difficulty.

In any calculation, therefore, of total reserves available for mining in the Lake Superior District at the present time, a large part of the Minnesota underground reserves should be eliminated. Currently there are only five underground mines operating in Minnesota out of a total number of 42 listed underground reserves. It is not expected that these underground reserves will be operated in the foreseeable future. Minnesota's estimated reserves total approximately 790 million tons, of which about 30 pct are underground. Accordingly, this reserve figure should be reduced to about 555 million tons.

With the exception of the low grade properties, all the mines in Wisconsin and Michigan are underground. These mines are already developed and represent large capital investment, they produce ore of superior quality, and their shipping facilities offer advantages in freight rates. It is expected that they will continue to operate.

Discussion has so far been concerned with the reserves of direct-shipping ore and concentrates from the Lake Superior District and has dwelt only briefly on the plants operating on magnetic taconites of the Mesabi Range and low grade ores in Michigan. The reserves of these ores have not been fully considered.

Low Grade Ore Reserves in U. S.: The magnetic taconites on the Mesabi extend from the extreme east end to about the center of the range west of Mountain Iron, Minn. On the extreme east end the whole formation is magnetic, but going westward the magnetic formation is located on the footwall and is known as the lower cherty formation. The upper part of the formation in this area is not magnetic. It has been estimated that there is a total reserve of open pit magnetic taconite ores of ap-

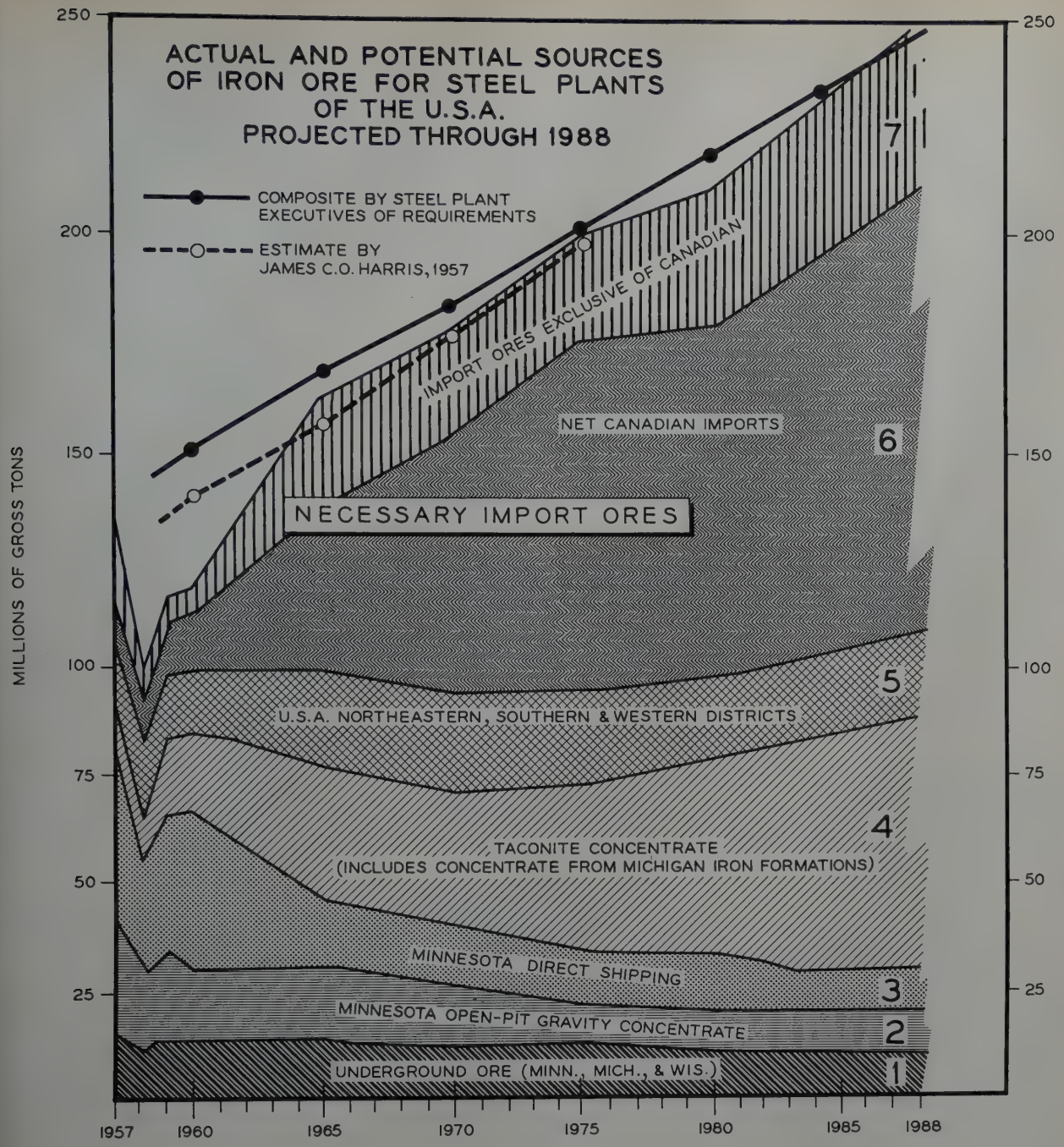

proximately 5 billion tons of crude, equivalent to 1.7 billion tons of concentrates. Two commercial operations, the Reserve and Erie plants, are now producing magnetic ore from taconites. It has been stated that these two plants have a combined capacity of 12 to 15 million tons per year. The cost of these plants—including rail connections, power plants, and housing—was approximately $40.00 per ton of annual capacity or in the neighborhood of $500 million.

Since Oliver has recently acquired large reserves of more easily concentratable material, it is generally believed that the company will postpone development of its magnetic taconites on the Mesabi, but these still remain a potential reserve in the Lake Superior District.

If additional ore is to be produced from the magnetic taconites, more plants must be built. With the very high capital investment involved it seems doubtful at this time that capacity will be increased in the near future. At the current rate of producing magnetic taconites, reserves of this ore will last for more than a hundred years.

The magnetic taconites as produced by Reserve Mining Co. during the past three years have become competitive with the underground ores in the Lake Superior District. During 1958, when consumption of Lake Superior ores decreased sharply, pellets from magnetic taconites were sold on the open market as a distress measure at the same price as the Old Range direct-shipping Lake Superior ores.

In addition to the Mesabi's magnetic taconites, there are known deposits of magnetic iron formation in Wisconsin which have been partially developed. These are quite similar to the magnetic taconites and are amenable to the same concentration and pelletizing process. Reserves of these ores are presently estimated at 263 million tons of concentrates.

There are also the low grade ores of the Marquette and Menominee ranges which are being developed at the present time. As mentioned pre-

viously, Marquette Iron Mining Co. is operating the Republic mine and a pelletizing plant on the Marquette Range and producing high grade pellets from concentrates. Likewise, the Humboldt mine has been developed to produce flotation concentrates heretofore used as sinter feed by the consumer. To pelletize these concentrates a plant will be constructed on the Marquette Range, where other deposits of treatable low grade ore are known to exist. A rough estimate of the present reserves of ore which can be concentrated by flotation on the Marquette and Menominee ranges is 300 million tons of concentrates.

Finally, there are large tonnages of lean ores in the Mesabi, Gogebic, Marquette, and Menominee ranges which are amenable to concentration by magnetic roasting and magnetic concentration. At present this process is not commercial, but if natural gas were available at reasonable cost, some of the lean ores of higher grade would immediately become merchantable by this magnetic roasting and magnetic concentration. Efforts have been made over the past 15 to 20 years to secure such supplies of natural gas for Michigan and Minnesota for concentration of these low grade ores. The tonnages that would be available are very large.

In the Lake Superior District the following reserves of iron ore would be available:

Estimated Reserves	Tons
Open pit ore	564,000,000
Underground ore	388,000,000
Total, direct-shipping or readily concentratable ores	952,000,000
Magnetic taconite concentrates	1,700,000,000
Wisconsin magnetic iron formation concentrates	263,000,000
Michigan low grade ore concentrates	300,000,000
Total	3,215,000,000

Future of Canadian Reserves: In recent years a constant and intensive search has been made for iron ore in Canada which could replace the dwindling reserves of the Lake Superior District and would not be subject to the hazard of shipping during war times.

Developments in Canada over the past 20 years have added to these reserves. The Michipicoten District, discovered many years ago, produced some direct-shipping ore from the Helen mine for Algoma Steel Corp. This direct-shipping ore was exhausted, but in 1936 active development of a large deposit of siderite at the Helen mine was begun. This property began shipments of a manganiferous sinter in 1939 and has continued from that date to the present. This mine, the Victoria property, and others in the area will no doubt continue to produce substantial tonnage of this ore in future years. No reserve estimate is available of the tonnage in these properties.

The year 1942 marked initial development of the Steep Rock mine near Atikokan, Ont. Placed in operation in 1945, the mine has been a substantial producer ever since. It is operated by Steep Rock Iron Mines Ltd. Part of this deposit has been leased to Inland Steel Co. (known as Caland in Canada), and it is expected that this company will begin producing iron ore in 1960. These two operations will be capable of producing 5 to 10 million tons per year, and reserves are estimated at 300 million tons.

In 1929 iron ore was discovered in the Labrador trough which straddles the boundary line of Quebec and Newfoundland. In 1949 the Iron Ore Co. of Canada was formed by the Hanna Coal & Ore Corp. with the participation of several American steel companies. This company, in association with Hollinger, proceeded to develop these direct-shipping orebodies, constructing a 360-mile railway to the properties from Sept Iles on the Gulf of St. Lawrence. An iron ore loading dock was built at Sept Iles and hydroelectric power was developed near the mines. The first iron ore was shipped from the properties in 1954 and large shipments have continued since that date. The total shipments in 1957 were 12,450,000 tons. Most of this ore goes to steel companies in the U. S., but some is exported to Europe. No estimate of ore reserves in these properties is available.

Development has now begun on many low grade properties discovered in Canada which will require concentration and agglomeration. Most of these properties are located in the extension of the Labrador trough both north and south of the discovery of high grade ore described above. To the extreme north developments have shown the presence of concentrating ore along Ungava Bay. South of the Iron Ore Co. of Canada holdings the Labrador trough turns to the southwest, and concentrating ore in large quantities has been discovered in this southwesterly extension. U. S. Steel Corp. has already undertaken development of a property at Mt. Reed on this extension, which contains a very large tonnage of concentrating ore. The property will go into operation within the next few years and is expected to produce 8 to 10 million tons of ore per year.

It is now believed that Canada can supply the loss of tonnage resulting from depletion of the Lake Superior District ores.

Accompanying this report is a chart showing estimated requirements of iron ore in the U. S. over a period of 30 years beginning with 1957, and the sources from which such requirements will be met. This chart was prepared by Verne D. Johnston of Oglebay Norton & Co. and the estimate of requirements has been made by several prominent steel executives. The chart shows a continued and rapid growth of the steel industry in the U. S. It will be noted that the underground production from the Lake Superior District continues almost in a horizontal line over this period. There is rapid depletion of the Minnesota open pit direct-shipping and gravity concentrates, and a rapid increase in production of taconite concentrates.

Cost per unit of plants for producing taconite concentrates is very high, and it is doubtful that taconite production will increase as rapidly as shown on the chart. The balance of reserves required for the steel industry will have to come from Canadian and other foreign imports. Recent developments in Canada indicate that reserves may be developed which will support this rapid growth of production. Iron ore is being very widely discovered both in Africa and South America, and no doubt the tonnages shown on the chart from imports, exclusive of Canada, can be met over the period. These imports, however, are subject to the hazards of shipping, which make them undependable in case of a national emergency.

Discussion of this article sent (2 copies) to AIME before June 30, 1959, will be published in MINING ENGINEERING.

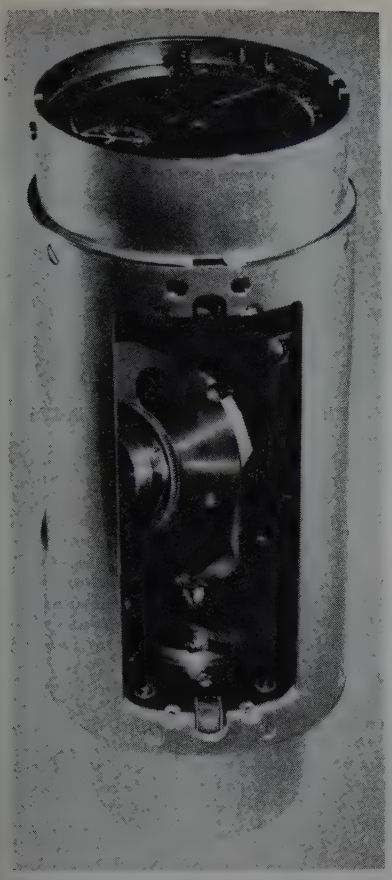

GYRO-COMPASS SURVEYS UNDERGROUND WORKINGS AND BOREHOLES

by EUGENE P. PFLEIDER and OTTO RELLENSMANN

For many years mine surveyors and exploration engineers have sought an accurate means of transferring meridian underground by using the gyro-compass. These efforts have generally failed, either because they were inaccurate or because the size and cost of the unit were prohibitive. During the past ten years, however, great strides have been made. Autonetics in California has developed a comparatively light-weight (100-lb) gyro-theodolite, and the Institute for Mine Surveying at Clausthal Mining Academy in Germany has developed an instrument that is accurate to within 20″ to 30″ of arc. Concurrently, Minneapolis-Honeywell has produced an astounding gyro, the size of a salt shaker, that weighs less than 0.5 lb and compares favorably in performance with the 50-lb gyros of conventional design. This unit, designed for missile guidance, should be adaptable for surveying small boreholes. Given the proper interest and approach from the engineering fraternity, excellent gyro-compasses could probably be available for accurate underground survey work at nominal cost within the next three years.

E. P. PFLEIDER, Member AIME, is Professor and Head, Division of Mineral Engineering, School of Mines and Metallurgy, University of Minnesota, Minneapolis. O. RELLENSMANN is Professor, Clausthal Mining Academy, Clausthal-Zellerfeld, West Germany. Manuscript, Dec. 8, 1958. TP 4798A. AIME Trans., Vol. 214, 1959.

Principles of the Gyro-Compass: The gyro-compass, used for 50 years as a navigational instrument in ships and aircraft, senses the turning axis of the earth and points out true polar north. It does this by employing the earth's rotation, the force of gravity, and the precession characteristics of a gyro. For further details the reader is referred to several excellent publications[1-8] covering the principles and application of the gyroscope.

The heart of the gyro-compass is the gyroscope, or rapidly spinning wheel, which rigidly maintains its angular orientation in inertial space. Free gyros employ universal joints to allow the wheel axle to maintain its rigid spatial orientation independent of base motion disturbances. Free gyros are independent of the earth's turning and are not north-seeking. Only as they might be initially oriented parallel to the earth's turning axis could any north indication be obtained. In practice, the free gyro tends to drift off its set position and lose its accuracy.

The Sperry-Sun Well Surveying Co. instrument (5½ in. O. D.) is of this free gyro type. It is counterbalanced, however, against the rotational effects of the earth, so that orientation of the spinning axis will be maintained throughout the survey.

Now, if a force is applied to one end of the spinning axis A-A′ in a direction parallel to C-C′, the primary response is the turning of the wheel assembly about axis C-C′. This effect, called *gyro-precession*, is explained by the mechanics of conservation of angular momentum. Conversely, turning rates around vertical axis C-C′ develop a proportional torque and angular deflection around axis B-B′. These angular deflections may be converted into electrical signals by a pick-off device, or a torquer or precession motor can be used to generate control torques on axis C-C′. The Honeywell gyro-compass, described later, employs this technique.

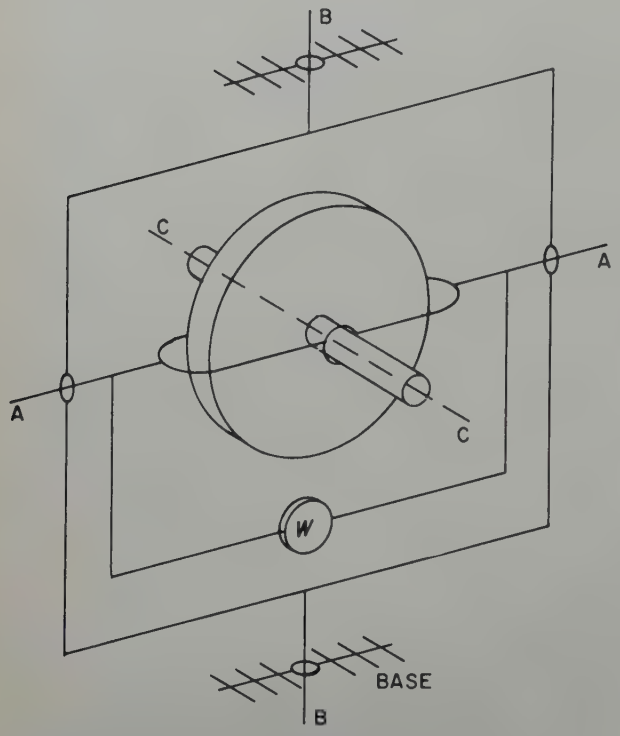

Fig. 1—The three-frame gyroscope with pendulous unbalance added to make it north-seeking. (After Lower).

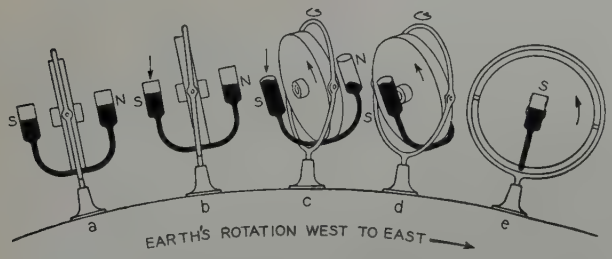

Fig. 2—Gyro-compass, mercury in U-tube. (Lower)

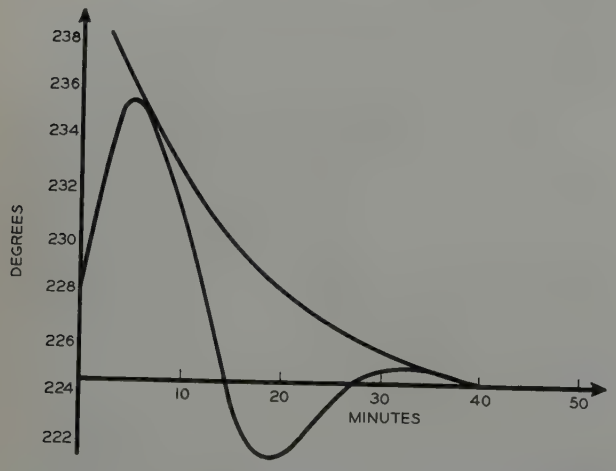

Fig. 3—The dampened swing cycle of the gyro-theodolite is shown on the above graph. (After Ludemann).

The mechanization of the conventional north-seeking gyro-compass departs from the free gyro concept and couples the earth-turning rate into the gyro. These earth rates precess the gyro and align its axle in a north-south direction. Lower[4] describes the gyro mechanization that will find north. He says, with reference to Fig. 1:

> Assuming the gyro axle to be at a random position off of north as it is started, the gyro rigidity in space will necessitate a tilting about axis A-A as the earth turns. But pendulous weight W tends to maintain the gyro axle in a horizontal orientation. This effect couples a spatial turning rate into the A-A axis and results in a precession of the assembly about axis B-B, in keeping with the basic principles of the gyro. This process will continue until the gyro axle is pointed north; at this unique orientation the earth's turning no longer results in tilting the gyro axle against the restoring pendulum. Fig. 2 serves to illustrate this process of a gyro-compass action using mercury in a U-tube as the pendulum.

The Clausthal gyro-theodolite employs this principle, using lead ballast as the pendulum.

Basic Factors: The accuracy and oscillatory characteristics of a gyro-compass in its seeking and holding of true north depend on several important factors:

1) The extremely low frictional restraint in all movements.

2) The magnitude of the meridian direction moment, R (or the torque developed around the vertical axis in its seeking of north direction).

This is dependent on the angular momentum of the gyro wheel, the earth's turning rate, and the latitude, as expressed by Eqs. 1-3:

$$K = I\,\omega\,\Omega \qquad [1]$$

$$R = \frac{K \cos \phi}{g} \cdot \sin \propto \qquad [2]$$

$$R = \frac{I\,\omega\,\Omega \cos \phi}{g} \cdot \sin \propto \qquad [3]$$

Where K = full directional torque developed by gyro at equator, dyne-cm.

R = meridian direction moment at latitude ϕ, gr-cm.

I = moment of inertia of gyro, gm-cm^2.

ω = angular velocity of gyro, radians per sec.

$I\,\omega$ = angular momentum of gyro, gm-cm^2 per sec.

Ω = angular rate of precession of gyro (or rate of turn) around horizontal axis, due to earth's revolving, radians per sec.

$$\frac{2\,\pi}{23.93 \times 60 \times 60} = 0.0000728 \text{ radians per sec.}$$

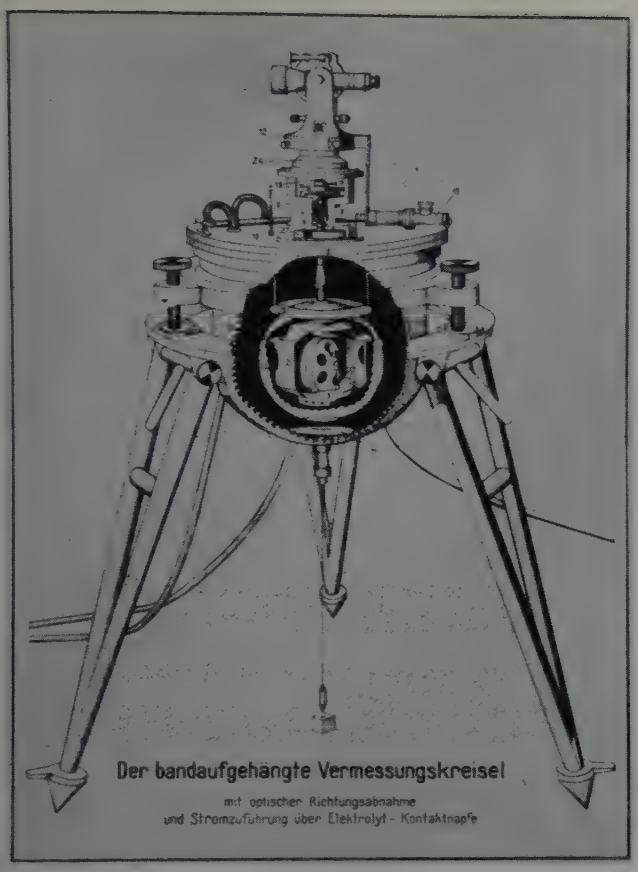
Der bandaufgehängte Vermessungskreisel
mit optischer Richtungsabnahme
und Stromzuführung über Elektrolyt - Kontaktnapfe

Fig. 4a—Insert shows the suspension of the gyro in earlier model of theodolite developed at Clausthal.

ϕ = latitude of observation, wherein only one half the available torque developed by the gyro would be applied at a latitude of 60° (cos 60° = 0.5).

g = acceleration of gravity, cm per sec^2, dependent on elevation and latitude. Equal to 980 cm per sec^2 at sea level and equator.

α = amplitude of precession from north, degrees.

3) The natural period of the compass, T, i.e., the time it takes to perform a complete oscillation of the gyro-compass about the meridian, as shown in Fig. 3.

This is dependent on the magnitude of the full directional torque, K, the weight of the pendulum, the latitude, and the metacentric height, as expressed by Eq. 4:

$$T = 2\pi \sqrt{\frac{K}{mga\ \Omega \cos \phi}} \qquad [4]$$

T = natural period of gyro-compass, sec

m = mass of pendulum, grams

a = metacentric height equal to distance between point of suspension and center of gravity, cm.

4) The proper damping of the oscillatory swings of the gyro-compass.

Various techniques are used to dampen the oscillatory swings on each side of the meridian. The Clausthal-designed instrument can achieve high accuracy after about 30 min warm-up and 9 reversals of 13.5 min each (for half pendulum time), or a total of 2.5 hr at latitude of Clausthal. Fig. 3 illustrates the damping characteristics of a compass having a 66 pct damping factor, i.e., from 30° to 10° to 3 1/3° to 1 1/9° for the first four half-oscillations.

5) The maintenance of a constant rotational speed of gyro and a constant temperature of the liquid in which the gyro sphere is floated.

These points are highlighted in Table I, a comparison of the basic design factors of the Clausthal precision gyro-theodolite, used for accurate surveying underground, and the Miniature Integrating Gyro of Honeywell, considered for borehole surveying.

CLAUSTHAL GYRO-THEODOLITE

The accurate meridian-indicator,[5-7] manufactured by the instrument firm of Otto Fennel-Söhne of Kassel in West Germany, was developed for underground surveying by Otto Rellensmann and his associates at Clausthal Mining Academy. A heavy version of the instrument is illustrated in Fig. 4a and a new smaller version in Fig. 4b. The latter weighs 76 lb: instrument, 28 lb; tripod, 16 lb; transistorized generator, 12 lb; and batteries, 10 lb.

Construction: Design of the instrument utilizes the gyro mounted in a sphere by a bracket. A mast passing through the sphere is attached to the bracket and has a mirror at its upper end. The motion of the mirror, which represents the horizontal pre-

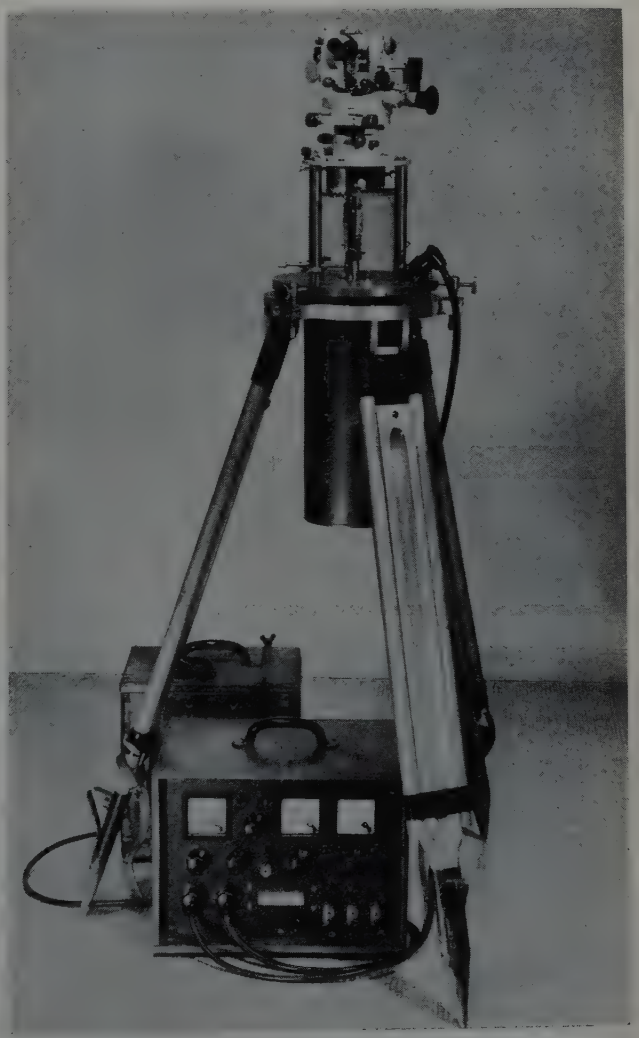

Fig. 4b—The Clausthal Academy KT-1 gyro-theodolite.

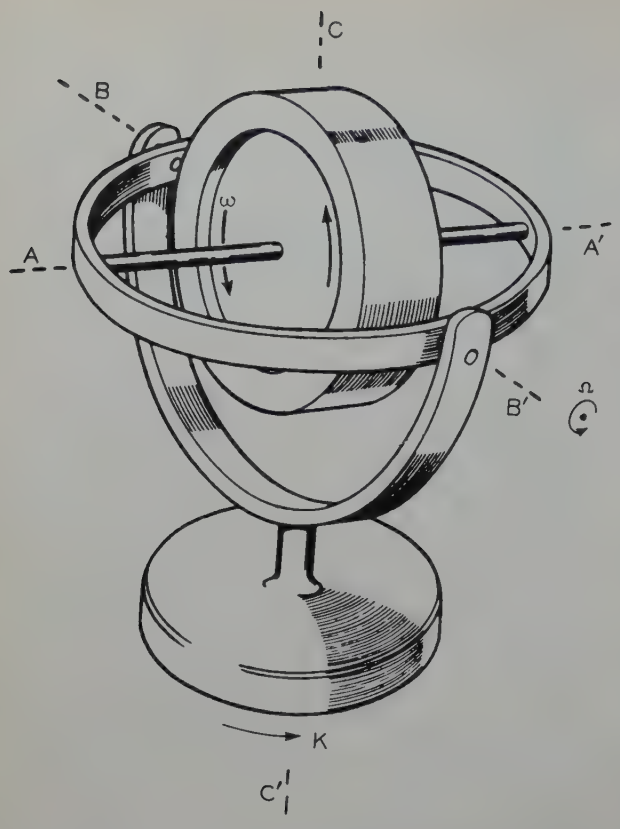

Fig. 5—A two-frame "rate" gyroscope showing relation between angular rate of precession, Ω, and resulting torque, K_p, as applied to gyro-compass. (Richardson).

cession of the gyro, is followed with an auto-collimation telescope attached rigidly to the alidade axis of the theodolite. The gyrosphere is hung by a metal band fastened to the end of the extended alidade axis. To reduce weight on the band to only 200 g, the gyrosphere floats in a water-filled gyro-container, a construction permitting the use of a fine metal band that has minimum torsional resistance to gyro swings. A sphere of Mu-metal on the inside of the container guards the gyro from influences of magnetic fields. The gyro wheel forms the rotor of a three-phase, 333-cycle asynchronous induction motor revolving at 20,000 rpm. Depending on availability or mine safety regulations, the generator providing the driving current may be powered by a 24-v, d-c battery-driven motor; a 220-v, a-c motor; or a compressed-air turbine unit. The instrument is transported in a special spring-mounted frame, with the gyrosphere clamped by two rings.

Table I. Fundamental Properties of the Clausthal Gyro-Theodolite and the Honeywell Miniature Gyro

		Gyro-Theodolite	Miniature Gyro
I =	Moment of inertia, gm-cm²	4.3×10^4	40
ω =	Angular velocity of gyro, rpm	20×10^3	24×10^3
	Angular velocity of gyro, rad./sec	2.1×10^3	2.5×10^3
$I\omega$ =	Angular momentum of gyro, gm per cm²/sec	9×10^7	10^5
K =	Torque, dyne-cm	6.5×10^3	7.5
R =	Meridian direction moment, gm per cm		
	at Clausthal, Germany—latitude 51° 19′	4.9	4.66×10^{-3}
	at Kiruna, Sweden—latitude 67° 42′	2.97	2.82×10^{-3}
T =	Natural period of gyro-compass, minutes		
	at Clausthal	27	
	at Kiruna	34.6	
W =	Weight of gyro assembly, lb	50±	0.5
D =	Diameter of gyro, in.	5.3	
	Diameter of gyro assembly, in.		1.75

Operation: After the instrument is centered and leveled, the swinging of the gyro is followed continuously by observing the mirror through the autocollimation telescope. At the same time, the torsion moment of the band is compensated by regulating the zero position. In this manner only the direction moment of the gyro is effective. At least three reversing points and probably more, depending on the accuracy desired, are read in order to calculate the north direction. The angle between the calculated north direction and the measured line is corrected by a constant of the instrument, which is determined by checking with the bearing of an accurate base line. If the base line is part of a geodetic system, the convergence of the meridians must be worked out and incorporated into the calculations. Generally, the constant of the instrument is checked by base line measurements both before and after an important series of observations.

Many checks have been made between well established base lines surveyed by astronomic methods and by the gyro-theodolite. The average error of an individual measurement is about 20″ of arc. An order of accuracy of 30″ can be assumed for most work.

Two gyro-theodolites in constant use in the Ruhr coal district are operated under the direction of the Gyro-Measuring Station of the Bochum Mining School at Bochum, Germany. Extensive measurements have also been made at the Kiruna iron mines and the Boliden base metal properties in northern Sweden with good results. Otto Fennel-Söhne manufactures the instruments now in use, copying the prototype developed at Clausthal.

Application: Since the gyro-theodolite measures angles from astronomic north, it is particularly useful for orienting underground surveys. Operating independently of other methods, it provides a check on previous surveys.

Accuracy of a conventional traverse decreases with the length and number of angles measured. The gyro-theodolite can be used to check the direction of any line in the traverse. Even in the case where the underground survey is connected with the surface traverse through two shafts, accuracy depends on distance between the shafts, length of traverse, and number of angles. The methods currently employed for transfer of directions from surface to underground depend on many local conditions, such as condition of shaft, depth, air currents, dripping water, magnetic influences, and hoisting operations. Many of these difficulties can be eliminated by suitable application of the meridian-indicator. Other uses for this instrument include surveys for geographers, cartographers, and geologists and inertial guidance for control of automatic mining machines.

AUTONETICS GYRO-THEODOLITE

A counterpart to the German theodolite has been produced by Autonetics, a division of North American Aviation, under the name of ABLE (Fig. 6). Weighing less than 100 lb, it is powered by either 115 v, single or three-phase current, at 60 or 400 cycles a-c, or by 28 v, d-c, at 125 w. Alignment time is 15 min at 30° latitude and 30 min at 60° to 70° latitude.

The ABLE system[8] consists of a high-quality

rate-measuring gyro coupled with an electromechanical arrangement for providing a signal proportional to the space rate of rotation of the gyro about its *input* axis. As the gyro tends to precess, a pick-off device senses a minute displacement and produces an electrical restraint or torque that prevents rotation and also indicates the magnitude of the required restraint. Internal bias torques are compensated for by the technique of completely reversing rotor rotation. Hence the resultant torque supplied by the electrical restraint is the only torque acting. This torque, shown by the indicator, is proportional to the input axis misalignment with respect to east-west.

In operation, the gyro is aligned by increments until the component of the earth rate lying along the gyro input axis is zero. At this point no restraint is required, the indicator shows null, and the north-south baseline is established.

All circuits for operation are transistorized, and plug-in cards provide for easy replacement of individual units. Provisions for rapid circuit checks are included so that marginal operation or malfunction is easily detected. The gyro and mirror

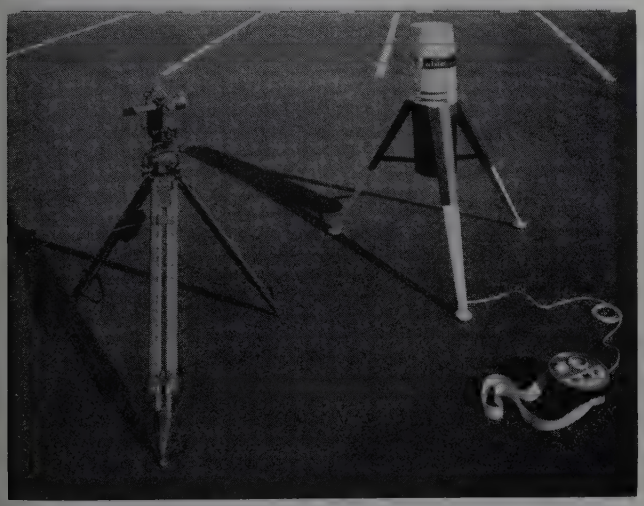

Fig. 6—The ABLE gyro-compass base line equipment.

assembly, or any of the plug-in cards, can be replaced in the field in a matter of minutes.

SURWEL GYRO-COMPASS FOR BOREHOLES

Boreholes having casings of 6⅝ in. O.D. or larger have been surveyed successfully for the past 25 years in both the mining and petroleum industries, using the Surwel well-surveying instrument equipped with a Sperry gyro. The instrument employs the free gyroscope," a plump bob type of angle unit, and a 16-mm camera. The protective casing is 5½ in. O.D. The free gyro is counterbalanced against the rotational effects of the earth, so that orientation of the spinning axis will be maintained throughout the course of the survey.

A gyroscopic direction indicator is attached to the top of the gyro's vertical axis, and a cross-hair plumb bob type of angle unit is mounted directly above the gyro to show the inclination of the hole. Directly under the gyro direction indicator is a tracer watch, which is synchronized with a surface watch. These three essential factors of direction, inclination, and time are superimposed on a background of concentric circles and recorded intermittently, at predetermined time intervals, on 16-mm

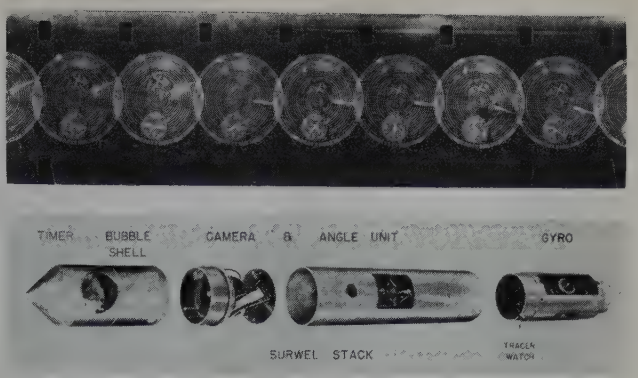

Fig. 7—Camera records of drillhole survey by Surwel. The Surwel multishot instrument is illustrated below.

continuous strip film. By using a time-depth log, the photographic reproduction of the time shown on the tracer watch indicates the depth at which each individual exposure is made. A group of photographic recordings is illustrated in Fig. 7.

Since orientation of the gyroscopic direction indicator is determined at the beginning of the survey, and is maintained throughout, the subtented angle between the direction indicator and a line drawn from the center of the inclination circles through the cross hairs gives the true bearing of the hole direction. The Surwel instrument is lowered on a wire line, and stop times of only half a minute are required for each record. Film capacity is sufficient to survey the deepest wells, both in lowering and with a check set of readings upon pulling out of the hole.

As to accuracy, the bottom hole coordinates of two gyroscopic surveys (one made going into the hole and the other coming out) generally will not vary more than 0.1 to 0.2 pct of the depth for the holes inclined less than 10° to 15° from the vertical. Comparable closures for holes of flatter inclination are likely to be greater.

HONEYWELL MINIATURE GYRO-COMPASS

Conventional gyro-compasses employ large gyro wheels, spinning at rapid rates, to obtain the gyro forces and torques required for performance accuracy. Relatively low frictional restraints are obtained by floating the gyro ball and using a system of small torsion wires. The result is an instrument weighing 50 lb or more, one far too large to fit into a small diamond drill hole. Further, the free gyro type of well-surveying equipment,

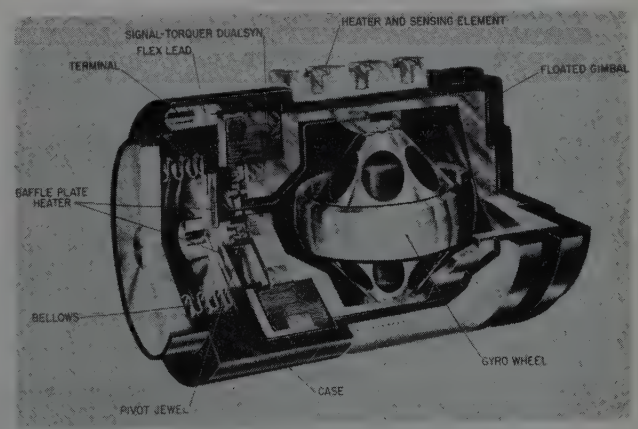

Fig. 8—Honeywell miniature integrating gyro. (Lower).

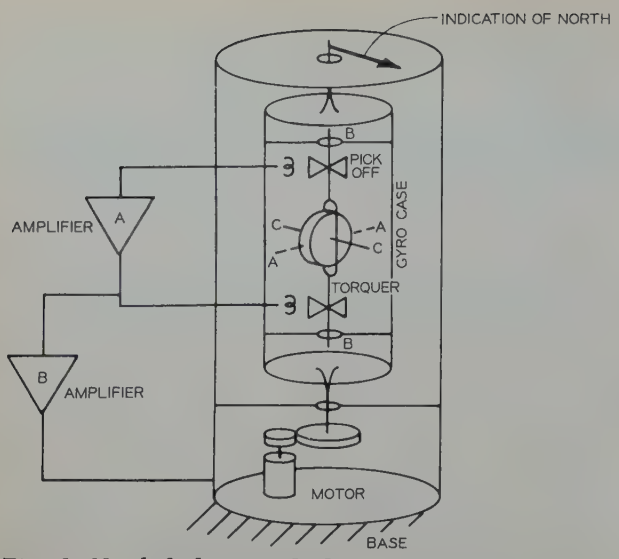

Fig. 9—North-finding method using Honeywell gyro.

such as the Surwel, is too large for use in small boreholes of 2 to 3 in. diam.

A new Honeywell miniature gyro with associated electro-mechanical equipment finds north by a technique somewhat different from that used in the conventional gyro-compass. As a consequence, it has promise of size reduction to 3 in. diam or less and may be a candidate for diamond drill hole exploration. The instrument, as described in detail by Lower,[4] is shown in Fig. 8. Although it is only 1.75 in. diam and 0.5 lb in weight, its sensitivity permits finding north to a fraction of a degree in most latitudes. This gyro sensitivity results from the greatly reduced frictional restraints realized by floating the gyro's moving element in a special heavy viscous fluid called Fluorolube. The gyro wheel (Fig. 8) spins in an inert gas within the floated gimbal, which is positioned by watchmaker-type pivots and jewels. Friction levels of about 0.01 dyne-cm are achieved. Since the gyro wheel momentum is 10^5 gm-cm^2 per sec, about 7.5 dyne-cm torque is developed for the earth's turning rates of 15° per hr. Hence high gyro-compass sensitivity has been made practical in a very small package. Furthermore, the distributed support afforded by the fluid makes for a very rugged instrument, capable of taking shocks and field use.

Fig. 9 illustrates the method of finding north. Any component of the earth's rate coupled into axis A-A will develop a torque about B-B and start to displace axis B-B relative to the gyro case. Such displacement causes the pick-off to generate a signal that is amplified by amplifier A to drive the torquer. Electrical input to the torquer is a measure of the earth's turning rate into axis A-A; when such rates are zero, axis A-A must have a unique east-west orientation. A second amplifier, B, would actuate a motor and gear train to turn the gyro case, thereby automatically making this rate settle out to zero. At this condition, the gyro case will be indicating polar north.

To log the direction and inclination of the drillhole, it will be necessary to correlate data from a pendulum or plumb-bob device to the gyro-compass data. Various solutions to this general problem are now in use, such as punching a disk by a plumb-bob tip. Possibly newer methods may be required to complement the miniature gyro-compass approach.

Accuracies to be expected from this new approach can only be surmised. As with the Surwel unit, it seems clear that the closures of surveys would be inversely proportional to departure of the hole from the vertical.

Summary: The gyro-compass is being perfected in accuracy, as well as miniaturized, to a point where mining and civil engineers should consider its application for certain phases of underground surveying. The gyro-theodolite, as developed at Clausthal Academy and now available both in Germany and the U. S., can determine or check bearings of lines to approximately 30″ of true direction when related to polar north. This is generally better than the accuracies obtained when bearings are taken underground by conventional wire methods through single shafts. Unfortunately the cost of the instrument is high, and only major companies operating several groups of underground mines could justify the purchase. In order that the smaller operator may have access to such a method for checking important surveys, it is suggested that the U. S. Bureau of Mines, or some mining supply or service company, have several gyro-theodolites available throughout the U. S. on a rental basis.

Relative to gyro well-surveying equipment, the Sperry-Sun Surwel unit has been doing a commendable job for years in both the oil and mining industries. However, the drillhole must have a casing size of 6⅝ in. O. D. or greater. This excludes the unit in surveys of diamond drill holes as used in mining, for which the NX hole at about 3 in. O.D. is the largest size employed. The magnetic compass is satisfactory for determining the direction of inclination if the hole is not cased or if rocks are nonmagnetic. Where this condition does not obtain, there is no satisfactory method of determining bottom coordinates, and there has been much interest in developing a gyro-compass package of 2 to 3 in. diam. The new Honeywell miniaturized gyro offers hope that a practical gyro-compass for small boreholes will be available.

Full development and use of these new surveying methods, employing the gyro-compass principle, are directly dependent on the interest of the world's mining and exploration drilling industries.

The authors thank Sperry-Sun Well Surveying Co., Autonetics, and particularly J. W. Lower, gyro section chief of Minneapolis-Honeywell, for their valuable contributions and permission to publish data on their respective instruments.

REFERENCES

[1] K. I. T. Richardson: *The Gyroscope Applied.* Philosophical Library Inc., New York, 1954.
[2] Sperry Gyroscope Co.: *Gyro-Compass and Gyro-Pilot Manual,* 1949.
[3] H. F. Banks: The Gyroscope in Mining. *Colliery Engineering,* London, October 1950, pp. 397-404, and November 1950, pp. 453-456.
[4] J. W. Lower: Gyro-Compass Principles and Possible Adaptation to Surveying of Small Bore Holes. *Proceedings,* Seventh Annual Exploration Drilling Symposium, University of Minnesota, 1957, pp. 100-104.
[5] O. von Rellensmann: Der Vermessungskreisel, heutinger Stand und Weiterentwicklung. *Freiberger Forshungshefte,* January 1957, pp. 5-13.
[6] J. von Ludemann: *Entwicklung sarbeiten zum bandaufgehangten Vermessungskreisel.* Thesis presentation, Clausthal Mining Academy.
[7] O. von Rellensmann and F. J. Oertgen: *Der Einstaz des bandaufgehangten Vermessungskreisels im nordschwedischen Erzbergbau.*
[8] M. E. Campbell: ABLE—A Portable High-Accuracy Gyrocompass. *Proceedings,* Second National Convention of Military Electronics, Institute of Radio Engineers, Washington, D. C., June 1958, p. 290.
[9] A. B. Palmer, Sperry-Sun Well Surveying Co.: Personal communication, June 18, 1957.

Discussion of this article sent (2 copies) to AIME before June 30, 1959, will be published in MINING ENGINEERING.

RECENT DEVELOPMENTS IN PEBBLE MILLING

by BUNTING S. CROCKER

Pebble grinding was used at Lake Shore Mines in 1949. A full description of experimental evidence and test plant results was published in 1952[1] and further operating details in 1954.[2] In more recent years the term *autogenous grinding* has been coined and is now frequently seen in the technical literature. Autogenous crushing and/or grinding covers any grinding mill in which the larger pieces of ore are made to grind the fine pieces; the crushing and grinding may be either dry or wet. This discussion deals only with wet autogenous grinding, and only in the fine grinding part of the circuit, i.e., from 6 mesh to 92 pct −325 mesh.

The term *pebble milling* could apply to fine autogenous grinding in which the pebbles are made from the ore itself, or it could also refer to grinding with pebbles, such as flint pebbles, from a source outside the mine.

The first mill to use *screened* ore to grind the ore (1949) was Lake Shore Mines, Kirkland Lake, Ont. Pebbles were screened from the jaw crusher discharge and used in 5x16-ft tube mills which had been converted to 6 ft 8 in. by 16-ft grate discharge pebble mills. The same general practice was adopted the following year by the Wright-Hargreaves Mine in Kirkland Lake. Shortly after that the Neptune Mines in Nicaragua started correspondence with the writer concerning the possibility of using screened ore for grinding in their plant. They first ran some plant-scale tests which confirmed the Lake Shore findings, with the ultimate result that their plant was successfully converted in 1956 to an autogenous grinding plant.

In 1957-1958 the writer was successful in converting the grinding plant of Renabie Mines in northern Ontario to autogenous grinding. In all these plants the existing grinding equipment was converted, usually by expanding the diameter of the shell to make the change from steel grinding to ore pebble grinding mills. In all the above plants primary grinding was done in either small rod mills or ball mills. These mills first reduced the pebble mill feed to about 6 mesh. The final grinding in the pebble mills varied from 75 pct −200 mesh to 92 pct −325 mesh. At Lake Shore three stages of pebble milling were used, with a different size pebble in each stage.

In other parts of the world interest was being shown in this form of grinding, and in March 1952 the writer had some correspondence with the mill staff at Outokumpu in Finland, with regard to the pebble system used at Lake Shore. At Stockholm in 1957 the account of the crushing and grinding system at Outokumpu was presented in a paper by H. Tanner and T. Heikkinen.[3] This is the only ore grinding plant that does not use grate discharges on its pebble mills; trunnion discharges equipped with heavy reverse spirals retain the pebble load.

The first new mill designed to use screened ore as a grinding medium was the Bicroft mill at Bancroft, Ont., which began operation in the fall of 1956. In 1957 this plant was followed by similar installations at Faraday Mines, also in the Bancroft area, and the North Rankin Nickel Mines in the North West Territories. In 1958 the Dyno Mill at Bancroft was converted, using the same type of grinding. Since all these plants, designed by Kilborn Engineering (1954) Ltd., were originally planned as pebble grinding mills, they were able to take full advantage of the latest design and technique. They are neat in appearance and very efficient and easy to operate.

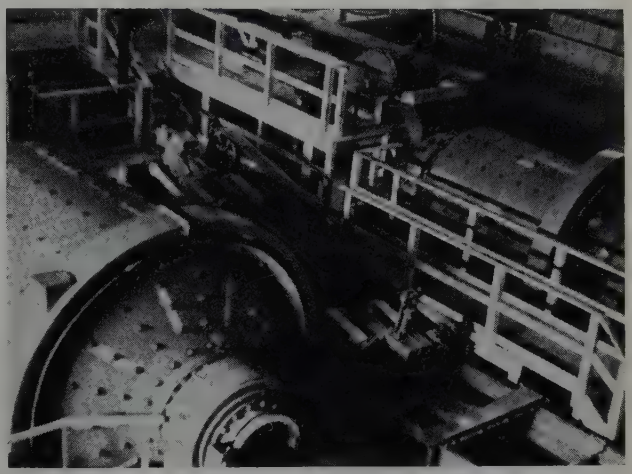

Fig. 1—One of the two grinding units at Bicroft Mines. The pebble mill is shown at left, the rod mill at right.

Effect of Ore Hardness: It is often commented that this type of autogenous grinding applies only to hard siliceous ores. Experience has shown that this is not so. In the past ten years the author has had an opportunity to test more than a dozen ores, several of which were quite soft. One of these was shale. The softer ores actually make better looking pebbles than the hard ores. These soft ores produced no particles in the intermediate size range which could not be ground by the largest pebbles in the mill charge. Slabby ores, such as shales, make a suitable pebble for the −6 mesh grinding. It is not generally recognized that for *fine grinding* a spherical medium is not essential or more efficient.

Another frequent objection to pebble grinding is the belief held by some operators that there is too much variation in the hardness of their particular ore to make it acceptable as a source of pebble media. Experience has also shown that this is not a serious problem at all. The variation in pebble load due to changes in the ore hardness is nothing like as great as most people would expect, and the method used for feeding the ore and controlling the the load in the mills is more than sufficient to take care of daily variations in ore hardness. This point

B. S. CROCKER, Member AIME, is Vice President and Director, Kilborn Engineering (1954) Ltd. TP 4801B. Manuscript, Oct. 6, 1958. AIME Rocky Mountain Minerals Conference, Salt Lake City, September 1958. AIME Trans., Vol. 214, 1959.

was well handled in a letter the author received from Rolland Merwin, mill superintendent of Neptune Mine, Nicaragua, with regard to wide variations in the hardness of the plant's mill feed. He reported no difficulty in maintaining smooth operation with normal supervision.[4]

Flint Pebbles: The use of hard pebbles for grinding ore is not a new metallurgical practice. Many operators in North America used either flint or Danish pebbles 30 or 40 years ago. These pebbles were either bought or mined from a local quarry and were usually fairly large in diameter, about the size of a man's fist. This resulted in somewhat inefficient operation, as the size of the pebble was frequently too large for the grinding job being done. At that time little thought was given to the importance of size of grinding media, which was governed to some extent by what was available on the market. The use of small grinding balls, and therefore small grinding pebbles, was actually introduced to the industry much later on. The contribution Lake Shore Mines made to autogenous grinding was to show a money-saving method of obtaining the pebbles (by screening them out of the jaw crusher discharge) with complete, quick, and easy control of pebble size. The grinding medium now represents a saving in the amount of ore that has to be crushed and at the same time represents an increase in the tons of ore milled per day. Under these circumstances, grinding with ore pebbles is more efficient and much more economical than grinding with steel balls. The Lake Shore test work and final plant operation clearly demonstrated that power used to grind the ore is exactly the same for ball milling as it is for grinding with the *correct* size of ore pebbles and under properly controlled conditions. The pebble mills are usually designed to be larger in diameter than the steel mills, and in this manner the same number of foot-pounds or the same amount of horsepower is developed.

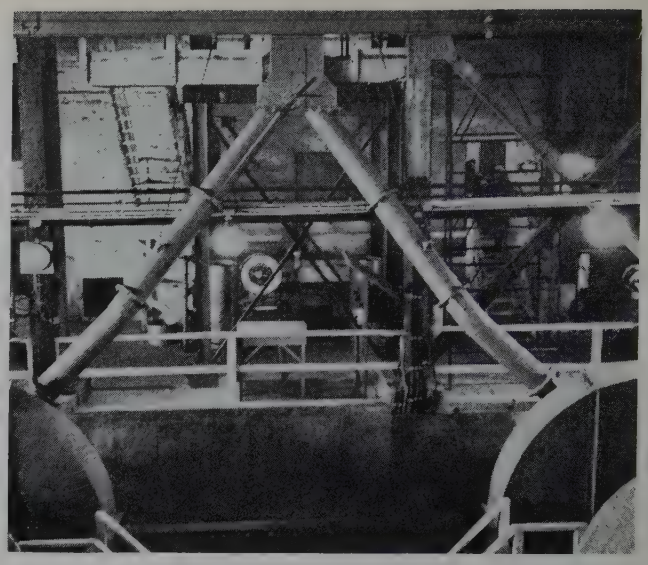

Fig. 2—Pebble feeding arrangement at Faraday Mines. Rock feed (pebbles) is drawn by a vibrating feeder, out of a storage bin shown at the top, weighed in a hopper and fed, at predetermined intervals, into the two pebble mills through the two rubber-lined pipes running to the combination feeders on the mills.

Table I. Diameter of Steel Balls and of Ore Having the Same Weight

Weight, Grams	Diameter of Steel Ball (7.8 Sp Gr)	Diameter of Ore Pebble (2.66 Sp Gr)
8.4	0.50	0.72
28.2	0.75	1.07
66.9	1.00	1.42
226	1.50	2.14
535	2.00	2.86
1807	3.00	4.27
4282	4.00	5.72
8364	5.00	7.17

Table II. Savings in Operating Costs at Lake Shore

	Savings Effected, $
Steel consumption 4.3 lb per ton @ $132.60	0.285
3.2 pct of the ore bypasses crusher and primary mills	0.016
Liner life saving	0.005
Primary agitation cuts through less iron in the grinding circuit, producing more oxygen in pebble mill discharge	0.013
Flotation tailing better, through stage grinding made possible by using several sizes of pebbles	0.028
Finer grind through more efficient small pebbles	0.030
Total	0.377

Table III. Savings in Operating Costs at Faraday

	Savings Effected, $
Steel consumption, 1.1 lb per ton	0.090
3.5 pct of the ore bypasses crusher and primary rod mills	0.015
Acid saved	0.025
Chlorate saved	0.030
Total	0.160

Pebble Size: The average pebble in the pebble load should be the *same weight* (not the same size) as the optimum size of steel balls. An empirical formula has been developed to relate the size of the screen used in sizing the rock feed to the size of pebble in the mill. At recent plants the rock feed has been screened in the crusher house through 2¾-in. or 3-in. square mesh screen and retained on 1½-in. square mesh screen. The −3+1½-in. screen combination gives a rock feed with a weighted mean size equivalent to a 2-in. pebble, after *rounding up* in the mill. The −2¾+1½-in. screen will give a weighted mean size equivalent to a 1½-in. pebble.[5] A 2-in. pebble is equivalent to a 1.4-in. steel ball and a 1½-in. pebble is equivalent to a 1.1-in steel ball.

As there are many factors other than screen openings which would affect the mean size of pebble in the mill, it is obvious that the proper procedure for any plant must be carefully studied to determine the best sizing combination to produce the correct pebble size for the sands being fed to any particular mill.

South African Practice: In South Africa, where autogenous grinding has been widely established for many years, cheap native labor is employed to hand-pick suitable pebbles—a situation that is not economical in many parts of the world. The natives pick the round pebbles and for convenience pick fairly large ones. The test run at Lake Shore Mines demonstrated that all of the screened ore could be used efficiently for fine grinding and not just the

round ones. Recent correspondence with Steve de Kok, who is metallurgical superintendent of Hartebeestfontein in the Union of South Africa, indicates that the South African mills are now using smaller pebbles and getting more efficient results.

"It is my view," writes de Kok, "that no ore is too soft to make it unsuitable for pebble milling." This has also been the author's opinion for a number of years, and it is interesting to find a similar view expressed by a metallurgist on another continent.

In South Africa the primary grinding is done in mills which are fed with large pebbles—about the size of a man's head—hand picked by natives and fed into the mill from a wheelbarrow. Up to the present time no completely satisfactory means of eliminating the wheelbarrow has been devised. The primary step, therefore, in all these grinding plants is to employ a small rod mill using 12 to 20 pct of total horsepower for wet grinding, to reduce the +¾ crusher product to about 6 mesh. These small rod mills are run in open circuit, and have proved very easy to operate.

Automatic Control: The new plants such as Bicroft, Faraday, and Dyno are almost completely automatic. When the pebble mill is started up the pebble feeding equipment is also started. The pebbles are automatically weighed in batch lots and fed into the mills at predetermined intervals. By watching the kilowatt demand meter used on these mills and varying the pebble feed rate, the operator can easily control the power being developed by the mill. This easily regulated power can also be used to vary the overall grind in the circuit. As a pebble load can be changed much more quickly than a steel load, there is a much greater degree of control available to the operators in these pebble grinding mills than in conventional ball mills. In South Africa Jack Williamson has recently proposed a control device in which the rate of feeding pebbles to the mill can be regulated to maintain a constant amount of power. This is a further improvement on the control of grinding in these circuits.

Flowsheet in Most Recent Plants: A brief discussion of the general arrangement of the plants in the Bancroft area will illustrate the grinding practice (Figs. 1 and 2). These plants are divided into two units, each handling about 600 tons of ore per day. A unit consists of a 6x8-ft primary rod mill operating at slow speed and drawing about 90 hp. The rod mill feed is —½-in. material and the rod mills are run in open circuit. The rod mill discharge passes to a classifier which is in closed circuit with a 9 x 11-ft grate discharge pebble mill, drawing from 240 to 260 hp, as required. The final grind over the classifier is 55 to 60 pct —200 mesh. These ores are of medium hardness, having a work index of 12. Rod consumption in the slow speed mills is ½ lb per ton and the two pebble mills consume a total of about 33 tons of ore per day. This 33 tons, representing about 3 pct of the rated tonnage of the plant, bypasses the fine crushing system and rod mill and is consumed in the pebble mills in grinding up the remainder of the ore. (Pebble consumption during the start-up period was considerably higher, averaging as much as 5 pct during the first six to eight weeks.) This represents a tonnage dividend over the rated capacity of the unit.

The ore pebbles are made by screening on scalping screens ahead of the secondary crusher. The pebbles pass through a 2¾-in. or 3-in. square mesh

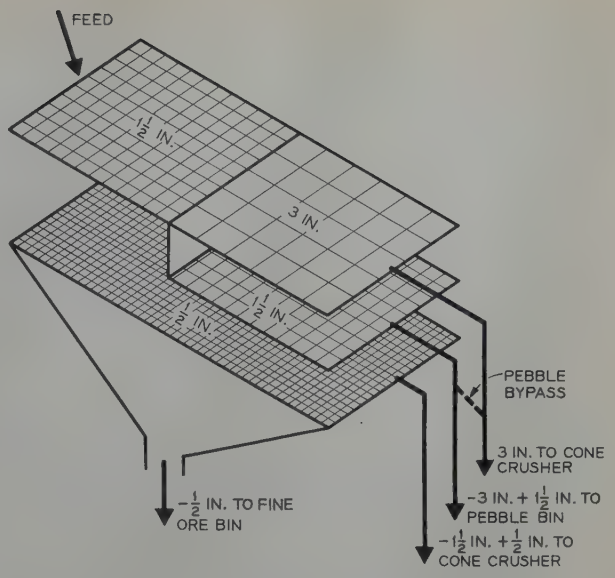

Fig. 3—Grinding pebble production.

and are retained on a 1½-in. square mesh screen. Ore of this size is sent directly to the pebble bins as required. Usually enough of the pebble medium can be made in two or three hours to furnish a day's supply. The screened rock feed is stored in a special pebble bin placed alongside the fine ore bins and is then automatically weighed and fed into the pebble mills. The pebble storage bin need not be particularly large. As soon as new ore is crushed there is a ready supply of pebbles. In South Africa some plants keep only about one shift's supply of pebbles ahead of the mill. On this continent, with the modern trend of celebrating holidays on Mondays, fine ore bins are usually designed for three days' capacity and the pebble bins, accordingly, are usually designed to hold the same relative amount. This is in sharp contrast to plants using steel balls where three to six months' supply of the grinding medium is considered necessary to service the mills properly. This of necessity results in a large inventory tie-up of steel ball.

Capital Cost of Autogenous Grinding Plants: Capital outlay for a modern pebble grinding plant of the type decribed above is only slightly higher than for an all-steel grinding plant, and further experience in design is continually lowering the cost. The chutes and the pebble feeding arrangements are extra for these plants. The pebble mills themselves are larger in diameter than steel mills of equal capacity, but they can be made of lighter materials, as the load is actually lighter. Also the steel mills must be supplied with an initial load of grinding balls. The steel mill, together with this initial ball load, costs about the same as the larger diameter pebble mill. When the cost of the customary four to six months' supply of grinding balls, together with storage bins and loading hoppers, is taken into account, the overall cost of the pebble grinding plant is not much greater than for the conventional steel plant.

On the conversion jobs, the capital cost of the conversion was realized out of the operating savings, in one or two years after the changeover was completed.

Operating Cost Savings: In 1957 the pebble grinding plants showed savings of 10¢ to 38¢ in operating costs per ton of ore milled. The greatest

savings were naturally made with ores which were ground the finest, and on which the greatest percentage of fine grinding equipment was converted to pebble milling. The savings shown in Tables II and III were taken from the Lake Shore Mines and the Faraday reports.[2, 6]

Pebble Grinding on Sulfide Ores: Of the plants listed above, all except the North Rankin Nickel Mines were grinding essentially siliceous ores. On these ores the specific gravity of the grinding medium is approximately 2.7. In autogenous grinding with sulfide ores allowances must be made for the heavier specific gravity of the ore. Experience has shown, however, that the more siliceous part of the ore is usually harder and therefore tends to build up in the pebble load, so that the final specific gravity of the grinding medium is often lower than that of the ore itself. This must be carefully evaluated in the test work, as the heavier the grinding medium the greater the capacity of a given mill. The chemical action within the grinding mill is also different from that experienced within the grinding mills using steel media. The action is usually less reducing. This is a very definite advantage in cyanide plants or uranium leach plants. It is not a disadvantage in flotation plants but may call for a slight change in the conditioning technique prior to flotation. It had no adverse effect on the nickel-copper float at North Rankin Nickel Mines. At Tennessee Copper, during pilot plant work on pebble grinding, this copper zinc ore was floated successfully after slight modifications of the usual practice. It is imperative, therefore, to run laboratory test work on flotation ores, using the ore pebbles in the laboratory grinding mills. This can be accomplished quite easily in any laboratory equipped to do flotation testing and it should be carried out during the preliminary test work so that the prospective client is free to choose any method of grinding with the assurance that the overall metallurgy will not be prejudiced.

Flexibility of Pebble Plants: Because these pebble plants are more flexible than the plants equipped with steel grinding balls, their efficiency is greater. For mills that are filled with steel balls, six to eight weeks are needed to change the ball size in the mill completely, to say nothing of the six months' supply of balls usually on hand, which would have to be used up before a new size of grinding ball could be introduced into the mill. Also, if the operator wished to change to a smaller size of grinding ball he would usually find that he had to pay a greater price for the smaller ball. These factors discourage most mill men from even attempting to change the grinding medium to suit changes in tonnage or changes in the plant's fineness of grind. In the pebble grinding layout, however, the operator can increase or decrease the size of grinding medium to suit conditions simply by changing one screen in the crusher house, and the pebble load is completely changed in two to four days. Here is a degree of control that opens up new fields in grinding efficiency.

Pebble Consumption: Table IV lists the pebble consumption, expressed as pounds per kilowatt-hour for a number of operating plants. Unlike steel consumption in grinding mills, the larger the pebble the greater the consumption. This is demonstrated in the Lake Shore results and in the results on the Rand. Generally the ores with a high Bond *work index* show a smaller consumption per kilowatt-hour than softer ores, as would be expected. The percent symbol under Pebble Consumption (column J) in Table IV refers to the percentage of total feed to the grinding circuit that is represented by the pebble feed.

High-Speed Mill Operation: Recently R. T. Hukki[9] called attention to the benefits to be derived from running autogenous fine grinding mills at supercritical speeds. Some interesting results have been obtained in Finland along these lines. Excessive steel consumption was one of the chief objections to running ball mills at high speeds. However, in autogenous grinding extra pebble consumption is an advantage rather than a disadvantage, and higher speeds are much more attractive. This is an interesting new field of operation which should be studied thoroughly.

REFERENCES

[1] B. S. Crocker: Screened Ore Used for Fine Grinding at Lake Shore Mines. *AIME Trans.*, 1952, vol. 193, pp. 449-508.
[2] B. S. Crocker: Fine Grinding with Screened Ore at Lake Shore Mines. *Trans., Canadian Institute of Mining and Metallurgy Bulletin*, 1954, vol. 57, pp. 115-128.
[3] H. Tanner and T. Heikkinen: Crushing and Grinding at Outokumpu. International Mineral Dressing Congress 1:4. Stockholm, 1957.
[4] B. S. Crocker: Pebble Grinding Gains Slowly in Canada. *Northern Miner* (Annual Review number), Nov. 28, 1957, p. 65.
[5] R. W. Merwin (Neptune Gold Mining Co., Bonanzo, Nicaragua): Private correspondence.
[6] R. J. Roach: Pebble Milling at Faraday Uranium Mines. 5817 AB.
[7] J. D. Bryce and J. M. Thompson: The Bicroft Uranium Mines Operation. 5820 Pl.
[8] *Hardinge Highlights*, October 1957, no. 45.
[9] R. T. Hukki: Fine Grinding at Supercritical Speeds. *AIME Trans.*, 1958, vol. 211, pp. 581-589.

Discussion of this article sent (2 copies) to AIME before June 30, 1959, will be published in MINING ENGINEERING.

Table IV. Pebble Consumption

	A	B	C	D	E	F	H	I	J	K	L
			Pebble Mill						Pebble Consumption		
Mine	Ore, Sp Gr	Ore Hardness (Wi.)	Size	Power, Kw	Tph	Pebbles, Lb per Hr	Theor. Pebble Size, In.	Kw-Hr per Ton	Pct	Lb per Ton	Lb per Kw-Hr
Lake Shore, Ontario	2.7	16	6 ft 8 in. x 16 ft	130	5.2	221	1.25	24.8	2.1	42	1.7
			6 ft 8 in. x 16 ft	130	5.2	329	1.75	24.8	3.2	63	2.5
Bicroft, Ontario	2.7	13	9x11 ft	210	23	1265	1.75+	9.1	2.75	55	6.0
Start-up									5.0	100	11.0
Faraday, Ontario	2.7	12	9x11 ft	194	25	1750	2	7.8	3.5	70	9.0
Start-up									7.0	140	18.0
Rand, South Africa	2.7	?	8x16 ft	218	44	2340	5.75	5.0	2.65	53	10.6
	2.7	?	8x16 ft	221	44	2000	3.4	5.0	2.3	46	9.2
	2.7	?	8x16 ft	179	44	918	1.8	4.1	1.05	21	5.1
Merriespruit, South Africa	2.7	?	8x16 ft	210	13.0	2660	2.3	16.1	10.0	200	12.4
Neptune, Nicaragua	2.7	?	5x10 ft								
			6x10 ft	212	30	918	2.3	7.1	1.5	31	4.4
			7x15 ft								
Renabie, Ontario	2.7	18	9x11 ft	194	11.2	945	1.9	17.3	4.2	84	4.8
Outokumpu, Finland	3.6	?	9x12 ft	150	25	2250	2	6.0	4.5	90	7.7

MIDNITE MINE
GEOLOGY AND DEVELOPMENT

by R. F. SHELDON

Aerial photo of southern section shows locally irregular granite-schist contact and six of the known orebodies.

Largest uranium deposit in the Northwest is Dawn Mining Co.'s Midnite mine on the Spokane Indian Reservation. The orebodies lie along the contact of granite and metamorphosed sedimentary rock and are controlled by faults and shear zones near the granite contact. In the oxidized zone the deposits consist mainly of the secondary uranium mineral meta-autunite; sooty uraninite and primary uranium minerals are known to occur at greater depths.

Elevations in the mine area range from 2500 to 3500 ft. The rolling hills and low, rounded mountains are covered with grass and evergreen trees.

R. F. SHELDON is a Geological Engineer with Newmont Exploration Ltd., Spokane, Wash. TP 4796I. Manuscript, May 26, 1958. Pacific Northwest Regional Conference, April 1958. AIME Trans., Vol. 214, 1959.

HISTORY AND DEVELOPMENT

Original showings were discovered with a geiger counter in the spring of 1954 by prospectors Jim and John LeBret. High radioactivity in several schist outcrops was found due to scaly coatings of a greenish-yellow, fluorescent mineral, later identified as meta-autunite. Prior to this time autunite was not known to occur in the state of Washington, and no significant uranium deposits had been found in the Pacific Northwest.

Outcrops in the area were few, and most of the ground was mantled with 2 to 10 ft of overburden, but three other radioactive zones were discovered by prospecting the ridge southward along the strike of the schist near its contact with granite for three quarters of a mile. Midnite Mines Inc. was formed

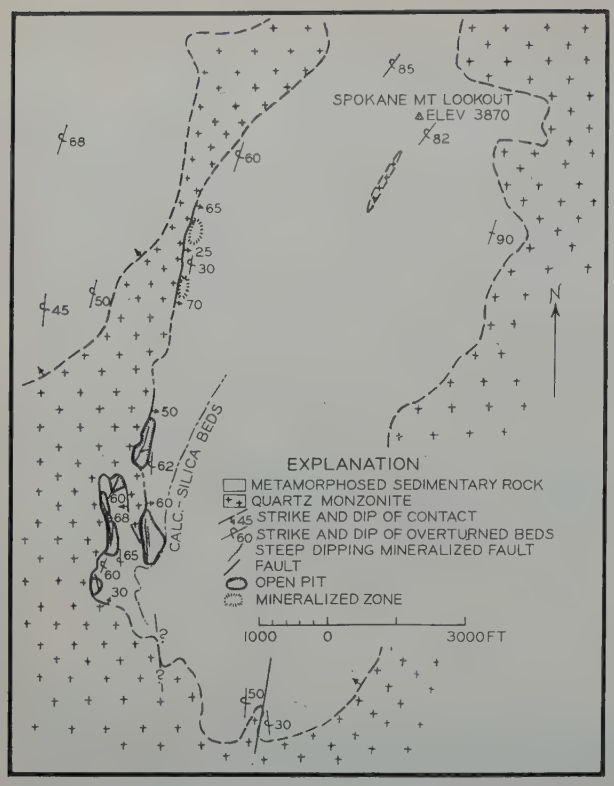

Fig. 1—Geological map shows location of orebodies.

to investigate these showings, which were trenched and opened up by bulldozer. It was soon apparent that ore occurred in economically mineable quantities, and late in 1954 a contract was obtained to ship 2400 tons to the AEC. To gain further structural and mineralogical information about this new deposit the AEC drilled 13 short diamond drill holes on the property, with generally encouraging results.

Dawn Mining Co., organized in the spring of 1955, is jointly owned by Newmont Mining Corp., which controls 51 pct, and Midnite Mines Inc. of Washington. During the summer of 1955 this newly organized company carried out an intensive development program, including 25,000 ft of wagon drilling, 550 ft of underground work, geological and radiometric mapping, bulldozer trenching, stripping of selected areas, and limited mining in three of the orebodies. Wagon drill holes as deep as 160 ft on a 50-ft grid pattern explored the granite-schist contact for a distance of a mile and a half. An adit was driven into one of the orebodies to check drilling results and gain a better idea of the physical nature of the ore and rock, while two other ore zones were developed by open pit mining. Bulk samples of the mined ore were taken for metallurgical tests.

This program indicated enough ore in six orebodies to justify building a mill, and a milling contract was negotiated with the AEC. The 440-tpd processing plant, approved in mid-1956, was completed by Western Knapp Eng. Co. in August 1957.

Open pits were designed from the drilling results, and stripping and mining, under contract to Isbell Construction Co., began in the fall of 1956. Equipment used in mining the 20-ft benches includes a Winter-Weiss rotary drill, a Gardner-Denver wagon drill, a 1-cu yd shovel for use in ore, a 2½-cu yd shovel for waste, and six 22-ton capacity Euclid trucks. As rock is loaded at the pit face, it is graded by a sampler using a shielded Babbel counter, which is calibrated in a high radiometric background to simulate pit conditions. This grade control has been most effective, usually within 0.02 pct U_3O_8 of chemical assays, as the ore is generally in balance radiometrically and chemically. About three tons of waste are removed to recover each ton of ore.

The mining and hauling, which depend on weather and road conditions, are carried on during May through January. In 1957, 592,000 tons of waste were stripped, 164,000 tons of ore mined and hauled to the mill, and 151,000 tons of low grade ore placed on the protore stockpile.

REGIONAL GEOLOGY

Midnite mine lies within the Turtle Lake Quadrangle currently being mapped by the USGS.[1] A series of Pre-Cambrian argillites, phyllites, quartzites, slates, and dolomites—separated by an erosional unconformity from Paleozoic quartzites, argillites, and dolomitic marble—form irregular, northerly-trending roof pendants surrounded by the Loon Lake granitic batholith, which consists of granodiorite, quartz monzonite, and alaskite believed to be of Cretaceous age.[1,2] The Pre-Cambrian and Paleozoic rocks are folded and overturned to the west into a north to northeast-trending series, the older rocks lying to the east. Remnants of Tertiary lava flows remain in some areas, and the terrain is modified by glacial action and the resulting deposition of silt and moraine. No individual faults of major magnitude have been recognized, though the area as a whole is laced by a series of northward-trending fractures.

The regional sequence of geologic events has been interpreted as follows:[3]

1) Deposition of a thick series of late Pre-Cambrian sediments believed to be part of the Belt group. The basal Togo formation alone appears to be more than 20,000 ft thick.

2) A long period of Pre-Cambrian erosion, but little deformation. The unconformity between the Pre-Cambrian and Paleozoic rocks represents about 8600 ft of erosion.

3) Deposition of Paleozoic sediments under relatively stable conditions.

4) Folding and faulting in the Mesozoic era. The source of pressure was from the east, resulting in northerly-striking anticlinal axes and overturning of the beds to the west.

5) The relatively quiescent batholithic intrusion of Cretaceous (?) granitic rocks.

6) Post-intrusive erosion of the order of 5000 ft.

7) Deposition of Tertiary lava flows that covered local areas.

8) Pleistocene glaciation.

9) Retreat of the glaciers, leaving moraines and silt-filled basins.

LOCAL GEOLOGY

Rock Types: The uranium deposits at the Midnite mine are found in a roof pendant of Pre-Cambrian Togo formation along its northerly-trending contact with the Loon Lake granitic batholith.

In the mining area the Togo formation consists of buff to dark gray, thin-bedded, silicious, argillite schist that has been locally altered by thermal metamorphism to phyllite, hornfels, and knotted schist for as much as 200 ft from the granite. Microscopic observations of thin sections show the development of the metamorphic minerals tremolite, andalusite, and wollastonite. The schistosity is parallel to the

bedding except for local deviations. Small seams and lenses of hematite have been noted in the argillite, and iron and manganese oxide stain is common. A few hundred feet east of the contact the lithology of the Togo changes to beds of buff-gray, impure, silicious, dolomitic limestone, locally called *calc-silica*, that contain diopside, epidote, feldspar, and garnet. Eastward these beds are progressively thicker and more limey.

The Loon Lake granite on the property is represented by a coarse-grained quartz monzonite with pegmatite facies. The feldspars are commonly slightly altered, rendering the rock much softer than normal. The granite is more easily weathered and eroded than the sedimentary rocks; hence the valleys are generally underlain by granite, whereas the more resistant metamorphosed sedimentary rocks form the ridges.

Structure: The Midnite mines property covers the western side of a south-pointing lobe of metamorphosed sedimentary rocks two miles long and three quarters of a mile wide, flanked and underlain by the granitic batholith (Fig. 1). In cross section the lobe is roughly saucer-shaped, with steeply dipping sides that rapidly flatten off to a rolling base (Fig. 2). Diamond drilling has shown depths of metamorphosed sedimentary rocks down to 500 ft before penetrating granite.

The drag-folded metasediments are the remaining portion of the western flank of a northerly-trending, overturned anticline. Marker beds within the more highly altered and broken contact area are lacking. The *calc-silica* horizon, however, is distinct, and exposures and drillholes along these beds indicate drag folds that plunge flatly north. In the mine area the general dip of the granite contact is to the east at angles from 30° to 70° parallel to the bedding. In detail, the contact is irregular, with apophyses of granite as noses, dikes, and sills intruding the schist along natural weaknesses formed by bedding planes, drag folds, and faults.

Faults: Steeply dipping faults are prevalent, especially in the metamorphosed sedimentary rocks, although no major displacements have been noted. Stress relief appears to have favored a great number of small displacements. Both pre-granite and post-granite faulting have occurred. In the mining area one fault shows a dip-slip of 15 ft on a granite-schist contact; all others observed to date show lesser movements. Most of the fracturing and shearing in the metasediments is due to pre-granite folding, whereas the faults within the granite are probably the result of differential cooling stresses. The stronger faults trend northerly and represent ruptures along fold axes. Bleaching and softening of the wall rocks is common to most of the faults and shear zones. A few late faults originating in the granite have provided the channelways for the hydrothermal uranium-bearing solutions. The sides of the mineralized faults in places show up to 15 ft of wall rock bleaching, accompanied by light pyritization and silicification.

Size and Shape of Deposits: Eight more or less separate orebodies are now known to occur on the property, strung out intermittently for one mile along the granite contact (Fig. 1). Two of these bodies had no surface expression and outcrops of the others gave generally scant evidence of their potential at depth.

Individual orebodies may be as much as 700 ft long, varying irregularly from a few feet to 200 ft wide. A typical generalized cross section of an orebody is shown in Fig. 2. In detail, however, the ore can be very irregular in the oxidized zone, where the shape is influenced by bedding and schistosity, faults, shear zones, slips, dikes, sills, and generally any factors affecting permeability of the rock. As the base of the oxidized zone is reached the ore gradually becomes more restricted to the environs of the mineralized faults. There is no sharp cutoff to the zone of oxidation, as it is dependent upon perched water tables in the schist.

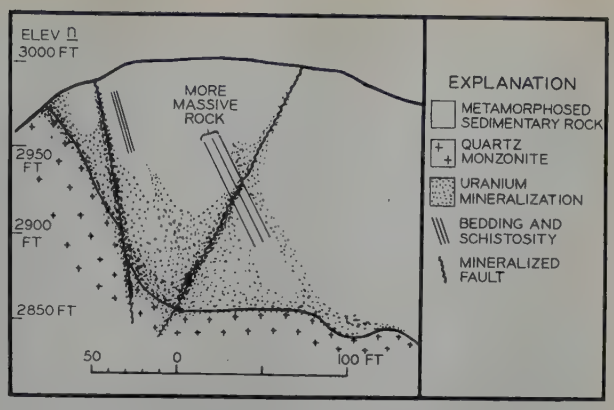

Fig. 2—Typical generalized cross section of an orebody at Midnite mine illustrates primary control of uranium mineralization along faults and the effect of rock permeability upon localization of secondary mineralization.

None of the orebodies to date have been mined to a depth completely devoid of oxidation effects, but drilling indicates that once the mineralized faults enter the granite the ore is restricted in width to only a few feet.

Mineralization of Deposits: The following uranium minerals have been identified from the Midnite mine:

Identification	Primary Minerals	Secondary Minerals	
Positive	Uraninite Coffinite	*Meta-autunite Zippeite Sklodowskite Sooty uraninite	Uranophane Phosphuranylite Liebigite
Tentative	Pitchblende	Torbernite Delvauxite	Gummite

* On drying or slight heating autunite passes reversibly to meta-autunite.

Most of the secondary uranium minerals are phosphates and silicates. The only metallic gangue mineral found in appreciable amounts is very fine-grained pyrite, which rarely exceeds 2 pct. Traces of molybdenite have been seen in drill cuttings and cores. A few erratic quartz veinlets a few inches to a foot wide occur but are barren of mineralization other than pyrite.

Meta-autunite, with lesser amounts of uranophane and sooty uraninite, has been the chief ore mineral mined to date. Three of the pits are now mined down to the semi-oxidized zone, where sooty uraninite is becoming predominant. The sooty uraninite is considered to represent the oxidation, essentially in place, of the primary uranium minerals, with only local movement and redeposition. It is expected that as mining progresses below the oxidized zone the primary mineralization found in drill cores and cuttings will appear.

There have been no age determinations received on the uranium. However, it is assumed that the

mineralization is a product of the granite intrusive and probably of Cretaceous age.

Ore Controls: Study of ore control at the Midnite mine involves factors affecting both primary emplacement of uranium and secondary redistribution of the mineralization by meteoric waters. A brief history of the formation of the uranium orebodies may be interpreted as follows:

Intrusion and cooling of the granitic batholith resulted in formation of fault fissures in the relatively brittle, thermally metamorphosed sedimentary rocks along the contact area and permitted the ascension of primary uranium solutions. Several thousand feet of erosion, accompanied by oxidation and ground water leaching of the primary uranium, permitted residual accumulation of the easily reprecipitated uranium as secondary mineral coatings in the fractured schist and, to a lesser extent, in the more impermeable granite. The sheeted nature of the schist, together with gougey transverse slips, caused perched water tables and a directional movement of ground waters tending to concentrate the redeposition of uranium in certain areas. The oxidized zone ranges from 40 ft to more than 150 ft below surface, depending on topography and the water table.

In the search for ore and for localization of ore in the area, the following features should be considered:

1) All the orebodies found to date lie in metasediments along the granite contact—preferably a steeply dipping contact. Locally, however, adjacent to ore zones in the schist, secondary uranium solutions have percolated into fractured zones in the granite or formed surface coatings around the kaolinized feldspar crystals.

2) The orebodies favor irregularities in the granite-schist such as noses, embayments, and changes of strike and dip.

3) The primary channelways of mineralization are northerly-trending, steep-dipping faults close to and roughly paralleling the granite contact. In the three orebodies that have been mined nearly down to the oxidized zone, one or two gougey, mineralized fault zones in each case contain sooty uraninite and appear to be the loci of the primary uranium solutions. Owing to leaching, the mineralized faults are often indistinguishable from unmineralized faults in the upper zone of oxidation. The mineralized faults seem to be those that were able to maintain themselves for an appreciable distance at some angle to the bedding and schistosity of the metamorphosed sedimentary rocks and remain open, thus allowing transport of ascending mineralizing solutions. None of these faults have been traced for more than a few hundred feet, however, as they tend to lose their identity either by aligning themselves with the bedding and schistosity or by gradually dying out in earlier formed shear zones.

4) Physical characteristics of the rocks have been important in ore localization. The brittleness and thin-bedded nature of the metasediments in the contact area have played a large part in both primary and secondary deposition of the ore.

The mineralized faults were able to persist in the competent rocks but were not able to maintain themselves in softer rock types. It is therefore believed that the dolomitic calc-silica beds lying next to the phyllites and argillite schists tended to flow or failed by weak shears under the confining rock pressures during the period of primary uranium mineralization, and any fissures that formed healed themselves. Ore does occur in the calc-silica beds, but only as a continuation of ore in the adjoining schist. It seems likely, however, that the calc-silica beds were important in buttressing the argillite schist, making it more competent and susceptible to fracturing.

The thin bedding in the metasediments has favored brecciation and permeability, resulting in wider zones of both primary and secondary mineralization. The concentration of secondary mineralization, to ore grade especially, requires the thin coating of a large number of rock faces. The more massive, thicker-bedded sections of argillite schist are therefore not generally favorable.

5) The directional permeability of the schist and the relative impermeability of the main granite body; granite dikes and sills; and numerous gougey faults, shears, and slips have resulted in the transport of the leached uranium by meteoric water to structural basins and traps, where redeposition has taken place and deposits of secondary ore have been formed. The main granite contact has been especially effective in containing the secondary solutions. The secondary ore zones are very erratic in places and are dependent upon the attitude and degree of permeability of the numerous slips, faults, and shear zones.

6) All the orebodies discovered to date occur either along the crests of ridges or on steeply sloping sidehills. There are probably at least two reasons for this: 1) The harder, easily fractured rocks favorable for uranium deposition are also the most resistant to weathering. 2) The effective concentration of uranium as secondary deposits of ore requires a seasonally fluctuating water table allowing the percolation and redeposition of uranium in structural traps.

Midnite's uranium orebodies, which are localized along the contact between granitic intrusive rocks and metamorphosed sedimentary rocks, constitute the largest known deposit of this type in America. It is anomalous that the site of the initial discoveries still represents the only appreciable deposit of its kind found in the surrounding region, despite extensive prospecting of the contact zone for many miles. There is a similar deposit now under development near Austin, Nev., and the Rum Jungle deposit in Australia[4] has been described as having several geological features common to the Midnite mine.

The writer wishes to thank members of the AEC and the USGS and the staff and management of Dawn Mining Co. and Midnite Mines for help in gathering some of the information presented in this article.

REFERENCES

[1] G. E. Becraft and P. L. Weis: Preliminary Geologic Map of the Turtle Lake Quadrangle, Lincoln and Stevens Counties, Washington. *USGS Survey Map MF135*, 1957.

[2] I. Campbell and J. S. Loofbourow, Jr.: *Preliminary Geologic Map and Section of the Magnesite Belt*, Stevens County, Washington, 1946.

[3] P. L. Weis: Personal communication.

[4] N. H. Fisher and C. J. Sullivan: Uranium Exploration by the Bureau of Mineral Resources, Geology and Geophysics in the Rum Jungle Province, Northern Territory, Australia. *Economic Geology*, 1954, vol. 49, no. 8, p. 828.

Discussion of this article sent (2 copies) to AIME before June 30, 1959, will be published in MINING ENGINEERING.

APPLICATION OF ELECTRON DIFFRACTION AND ELECTRON MICROSCOPY TO MINERAL ENGINEERING

by J. E. LAWVER and G. L. SAMSEL

The success of many mineral dressing processes, including froth flotation and electrical concentration, depends largely on knowledge of physical and chemical structures of the mineral surfaces involved. As a general rule solids have surface layers, usually invisible by optical tests, that differ from the substratum. To the mineral engineer, therefore, a knowledge of the surface structures of minerals is of paramount importance.

During the past decade one of the most powerful tools in the study of froth flotation mechanisms has been the use of radioactive tracers, but this technique usually cannot give definite information regarding the chemical changes that may or may not have occurred at the surface.

The electron microscope and electron diffraction camera can be particularly useful instruments in surface studies. An electron microscope permits much closer examination of surfaces than can be obtained with a petrographic microscope. In certain cases, it is possible to identify trace quantities formed by chemical reaction between flotation agents and mineral surfaces by the use of a single-crystal, reflection electron diffraction camera. This article describes several instances in which these instruments have been valuable guides in mineral dressing research at International Minerals & Chemical Corp.

One of the first applications of these techniques employed by International Minerals was in conjunction with the study of electrical concentration of potash ore. The first reasonably successful separation of potash ore was made by subjecting a sample of the ore to a methanol wash. Subsequent tests using tagged ${}_6C^{14}$ methanol showed that only a minute quantity of radioactivity was detectable after the methanol-washed sample had been dried and heated to about 300°F. It was concluded that although some methanol had been held to the surface by adsorption, this could not account for the improved electrification because there was no evidence of methanol selectivity with respect to NaCl or KCl. Consequently there must have been some other change in the surface.

Carbon replicas* of the mineral grains were made before and after the methanol wash. The replicas were separated from the minerals by dissolving in water. This extraction replica technique is particularly attractive because the specimen can first be used with the electron microscope to observe the general structure of the surface and can be re-used as a specimen for electron-diffraction studies to identify any solvent insoluble material present on the mineral surface.* Fig. 1 shows the general

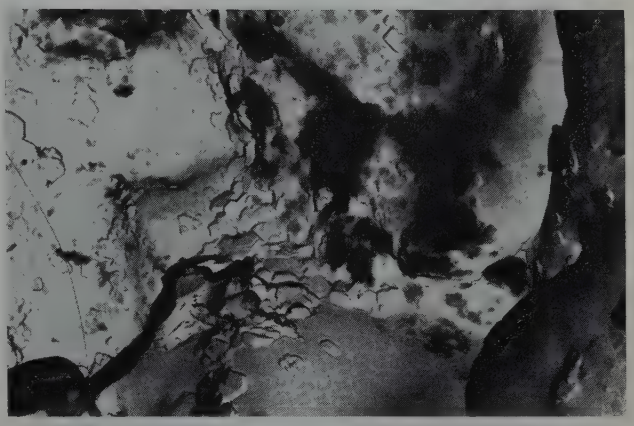

Fig. 1—Raw sylvite. X9800.

Fig. 2—Methanol-washed sylvite. X17,800.

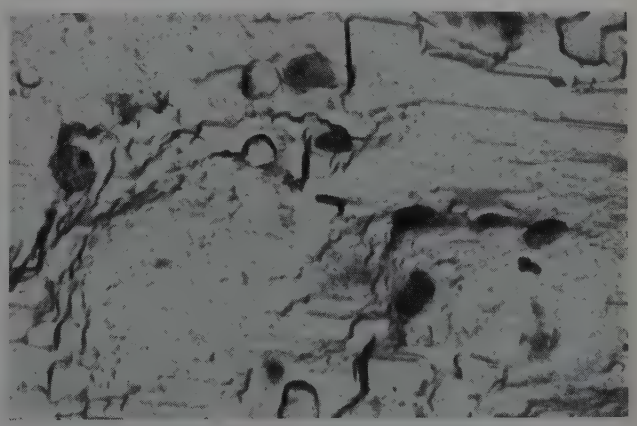

Fig. 3—Sylvite heated to about 510°C. X7300.

* For details of preparing surface replicas see Refs. 1 and 2.

* Many electron microscopes are equipped with a selected area diffraction attachment so that the experimenter can often identify trace materials present in a selected area of the replica.

J. E. LAWVER, Member AIME, is Research Specialist and G. L. SAMSEL is Senior Research Chemist, Mineral Processing Dept., International Minerals & Chemical Corp., Mulberry, Fla. TP 4803B.
Manuscript, June 9, 1958. AIME Trans., Vol. 214, 1959.

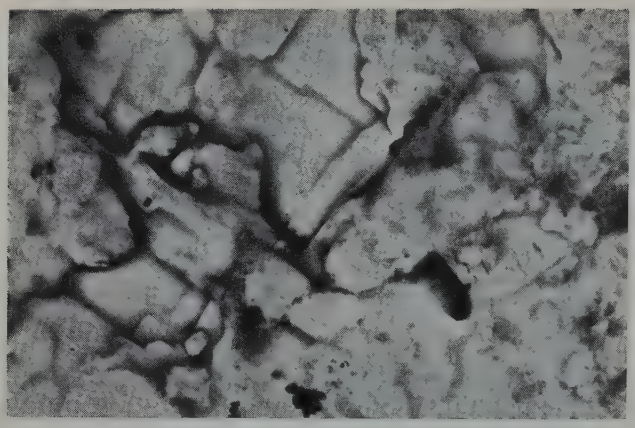

Fig. 4—Halite heated to about 510°C. X7300.

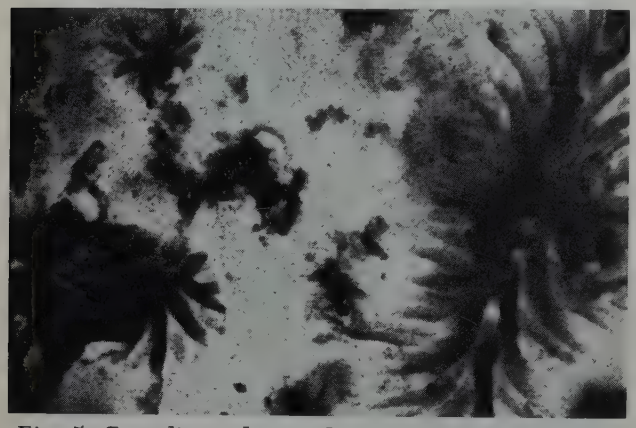

Fig. 5—Caprylic acid spreading over slime-coated sylvite. White area is true mineral surface. X9800.

appearance of the surface (as observed with an electron microscope at 11,000 X) before the methanol wash. The black areas are water-insoluble complex slimes identified by the electron diffraction pattern.

Fig. 2 is an electron micrograph of the methanol-washed sample. Note that the surface has been etched and that most of the water-insoluble slime has been removed. Although the surface appeared clean, electrostatic tests on the methanol-washed ore gave results which, on analysis, indicated that other factors were operating. Further examination of single particles using reflection-diffraction techniques indicated that many particles were covered with a film of both NaCl and KCl, probably due to the slight but finite solubility of both salts in methanol. The presence of this film tended to lower the selectivity of electrification of the two minerals. At a later date it was found that satisfactory electrical concentration of this ore (without solvent treatment) could also be made by heat treatment.[3] Although the effect of heat treatment is complex and cannot be completely explained by electron micrographs, the change in surface structure due to heating is intriguing. Fig. 3 is an electron micrograph of a sylvite grain that has been heated to a temperature between 480°C and 540°C. Fig. 4 is a corresponding micrograph for a halite grain. (Note that new surfaces have formed.) These fresh slime-free surfaces apparently are the reason that potash ore can be electrically concentrated after heat treatment.

Another application of these techniques employed by International Minerals has been in the study of interactions between surface-active agents and mineral surfaces. The study of surface-active agents by electron diffraction and electron microscopy is limited to substances that do not completely volatilize under high vacuum. Fortunately, many surface-active agents of interest to the metallurgist do not volatilize; hence the technique is very useful in this area of research. For example, Fig. 5 is a micrograph showing the spreading action of caprylic acid over a slime-coated section of potash ore. The slime is gray, whereas the caprylic acid is black, and the white area is the true mineral surface. Note the selectivity of the spreading action of the surface-active agent. Reagent covering of the clay surface apparently improves the amenability of the particles to beneficiation.

Although the micrographs accompanying this article give considerable insight as to surface properties of minerals, it is important to note that it is not posssible to deduce directly the exact surface state in a flotation pulp by observing electron micrographs obtained using a dry system under vacuum. These few examples have shown, however, the usefulness of the electron diffraction and electron microscope as an aid to better understanding of surface phenomena.

REFERENCES

[1] C. E. Hall: *Introduction to Electron Microscopy.* McGraw-Hill Book Co., New York, 1953.
[2] R. B. Fischer: *Applied Electron Microscopy.* Indiana University Press, 1954.
[3] J. E. Lawver: U. S. Patent 2,805,768.

Discussion of this article sent (2 copies) to AIME before June 30, 1959, will be published in MINING ENGINEERING.

Discussion

GRINDING BALL SIZE SELECTION

by F. C. BOND

(MINING ENGINEERING, page 592, May 1958, AIME Trans., Vol. 211)

B. H. Bergstrom *(Allis-Chalmers Mfg. Co., Milwaukee)*—In reading this article, it was difficult to follow through the example given as a starting point in the derivation of the theoretical equation which relates ball size to feed size. A discussion with F. C. Bond led to the following clarification:

Bond postulates that "the breaking force exerted by a ball varies . . . as the cube of its diameter . . ." and that the force in pounds per square inch required to break a particle varies . . . as its diameter squared." He concludes: "It follows that when a 1-in. ball breaks a 1-mm particle, a 2-in. ball will break a 4-mm particle, and a 3-in. ball a 9-mm particle." The above example can be true only for a different set of assumptions. Since the first assumption is apparently true, it is the second that must be revised. The second assumption should read that the breaking force required to break a particle varies as its diameter to the 3/2 power. This relationship was derived in the next paragraph of the article.

ROCK BREAKAGE WITH CONFINED CONCENTRATED CHARGES

by WILBUR I. DUVALL and THOMAS C. ATCHISON

Over the past ten years a series of investigations have been conducted to determine some of the physical processes involved in breaking rock with confined concentrated charges. Detailed discussions of many of these investigations have been published elsewhere.[1-6]

Laboratory experiments made by other investigators using Hopkinson pressure-bar techniques have shown that solid materials are fractured in tension by the reflection of an incident compressive stress pulse at a free surface.[7-12] In these tests a small charge of explosive is placed in contact with one end of a bar. Detonation produces some plastic flow and crushing of the bar near the charge and generates a compressive stress pulse that travels along the length of the bar. At the free end of the bar the compressive stress pulse is reflected back into the bar as a tensile stress pulse. If the tensile strength of the bar is exceeded during this reflection process, a tensile fracture normal to the length of the bar is produced, and the broken end of the bar moves forward with a constant velocity equal to the average particle velocity trapped in the broken fragment. The new surface formed by the fracture becomes the new free end of the bar that reflects the remaining portion of the incident compressive stress pulse. This process is repeated any number of times until all of the incident stress pulse is reflected.

Hino has demonstrated this kind of breakage for three rock types—marble, granite, and sandstone.[8] He has defined a blastibility coefficient, B, as the ratio of compressive strength, C, to tensile strength, T, thus:

$$B = \frac{C}{T} \qquad [1]$$

The quantity B is the maximum number of slabs that can be produced by reflection breakage. Normally fewer slabs are produced because of loss of energy as the stress pulse travels through the rock.

Fig. 1 illustrates reflection-type fracture for a triangular compressive stress pulse. The number of slabs produced by the reflection breakage process is the first whole number less than the ratio of the peak stress of the incident pulse to the tensile breaking stress of the solid. Thus the number of slabs is given by

$$N = \frac{S}{T} = \frac{F}{2h}, \qquad [2]$$

the thickness of each slab is given by

$$h = \frac{FT}{2S} = \frac{F}{2N}, \qquad [3]$$

and the total length of rock broken is given by

$$D = hN = \frac{F}{2}, \qquad [4]$$

N = number of slabs
S = peak stress in incident pulse
T = tensile strength of the rock
F = fall length of incident stress pulse
h = thickness of each slab
D = total length of rock broken

During the reflection process the particle velocity at the free surface is twice the particle velocity in the incident stress pulse. Thus the velocity with which the broken fragments move forward is given by

$$v_f = 2\,\bar{v} \qquad [5]$$

where

v_f = velocity of broken fragment, and

$\bar{v}$ = average particle velocity contained in that portion of the incident pulse trapped in the broken fragment.

Results of these laboratory experiments cannot be applied directly to rock blasting where the explosive charge is placed in a drillhole. In laboratory tests the charge is unconfined and in contact with the rock in only one direction. In a drillhole additional confinement is offered by the rock surrounding the charge and by the stemming placed above it. This additional confinement may be enough to allow the explosive gases to do additional work on the rock during their expansion. Other writers have discussed possible effects of gas expansion on rock breakage.[13-16] However, very few experimental data are available to determine to what extent expansion of the gases is responsible for rock fragmentation.

The USBM has studied the physical processes involved in breaking rock with confined concentrated charges by using simple crater tests breaking to one free surface. Crater tests have been performed in four rock types: granite, sandstone, marlstone, and chalk. Table I gives some physical properties of these rocks. Fig. 2 shows plan and section drawings of two typical crater tests and illustrates some of the test variables measured. For these tests the charge was placed at the bottom of the drillhole and primed with an electric cap. The hole was stemmed to the collar with sand and the charge detonated. Size and shape of the crater were measured after it was cleared of broken rock.

As a given charge size was buried deeper in a drillhole, the crater depth usually was equal to or

W. I. DUVALL and T. C. ATCHISON are Supervisory Physicists, Applied Physics Laboratory, U. S. Bureau of Mines, Region V, College Park, Md. TP 4810A. Manuscript, June 4, 1958. AIME Trans., Vol. 214, 1959.

This page of Mining Transactions AIME follows p. 536. The intervening non-Transactions pages appeared in MINING ENGINEERING.

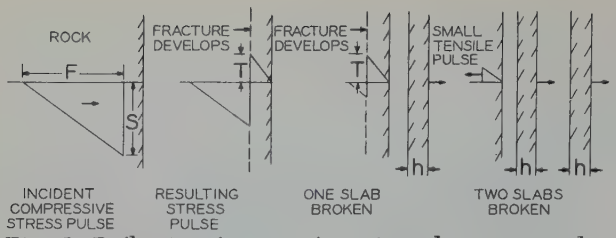

Fig. 1—Reflection fracture for triangular stress pulse. F = fall length of stress pulse, T = tensile-breaking stress, S = rock compressive stress, h = slab thickness.

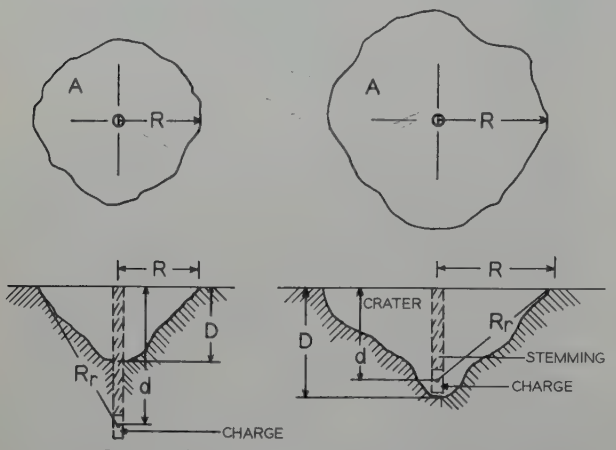

Fig. 2—Plan and section drawings for crater tests. A is the crater area; D, crater depth; R, crater radius; d, the charge depth; and R_r, the radius of rupture.

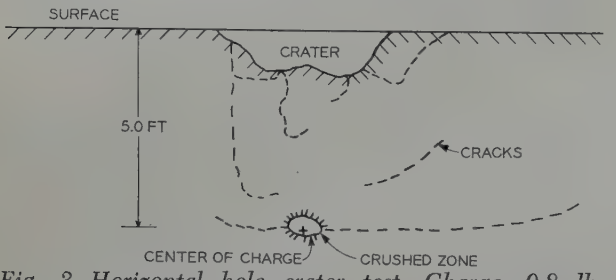

Fig. 3—Horizontal hole crater test. Charge, 0.8 lb; charge depth, 5.0 ft; scaled charge depth, 5.4 ft/$\sqrt[3]{lb}$.

slightly greater than the charge depth until a critical charge depth was reached; thereafter the crater depth became less than charge depth. A crater with a depth less than charge depth, as illustrated on the left in Fig. 2, indicates that energy has been transmitted from the charge point to the crater zone without causing damage to the intervening rock. Because the presence of the drillhole allows for the possibility that expanding gases may transmit this energy, long horizontal holes drilled from a vertical face were substituted for the drillhole in the crater zone. The length of hole was much greater than the depth of hole below the horizontal surface. A small charge of proper size to produce a crater depth less than the charge depth was placed at the back of the hole and the hole stemmed to the collar with sand. After detonation a vertical saw cut was made through the crater and shot point so that damage to the rock could be observed. Fig. 3 shows a crater produced by this type of test in chalk. Notice that there is a crater at the horizontal surface, a crushed zone around the charge point, and some additional cracking of the rock. As there is solid rock between the shot point and the crater zone, no gases were in the crater zone. Craters formed in this manner give convincing evidence that some form of wave motion transmits energy from the shot points to the free surface where damage to the rock occurs.

To study the wave motion generated when a charge is detonated in rock, the USBM developed a strain gage that could be cemented in drillholes in rock.[5] Fig. 4 shows the various parts of this gage and the completed assembly. The active element is an SR-4 strain gage, *B*, cemented into a brass cup, *C*, that previously had been cemented to a piece of drill core, *D*. The cup is covered by a lid, *A*, which provides a cable connection and a means of orienting the gage. A centering ring, *E*, is fastened to the core, and the whole assembly is cemented into a drillhole with a high-strength gypsum cement. Usually gages were placed in drillholes at various distances from the shot point, at the depth of the charge, and oriented to measure radial strain.

Outputs of the gages were recorded by high-speed oscilloscope drum cameras housed in the USBM mobile laboratory, which has 16 channels, each of which records on a 67-cm length of 35-mm film moving at 1000 or 2000 cm per sec. Photographic records obtained with this equipment are strain vs time plots. Enlarged drawings of typical strain records are shown in Fig. 5, which also illustrates and defines the measurements made on these records. Compressive strain is a deflection below the baseline and tensile strain a deflection above the baseline, and time increases left to right.

Typical strain records for granite and sandstone are presented in Fig. 6. Strain waves near the shot point are characterized by a single compressive pulse having a fast rise time and a slower decay time. As the strain pulse travels away from the

Table I. Physical Properties of Rock Types

Rock Type	Lithonia Granite	Green River Marlstone	Kanawha Sandstone	Niobrara Chalk
Formation Member	Lithonia Belt	Parachute Creek	Homewood	Smoky Hill-Fort Hays
Description	Gneissic	Kerogenaceous, dolomitic limestone (oil shale)	Coarse-grained	Chalky limestone
Apparent specific gravity	2.6	2.1	2.2	2.0
Compressive strength, lb per sq in.	30,000	10,000	10,000	2,000
Tensile strength, lb per sq in.	450	Not measured	70	Not measured
Tensile breaking strain, μin. per in.*	280	Not measured	500	Not measured
Modulus of rupture, lb per sq in.	2,000	400	400	300
Scleroscope hardness, units	85	45	30	10
Dynamic Young's Modulus, lb per sq in.	3.0×10^6	1.2×10^6	1.0×10^6	0.75×10^6
Modulus of rigidity, lb per sq in.	1.5×10^6	0.5×10^6	0.5×10^6	0.5×10^6
Longitudinal bar velocity, fps	9,000	6,000	5,000	5,000
Longitudinal field velocity, fps	18,500	13,000	5,000	7,500

* Microinch per inch = 10^{-6} in. per in.

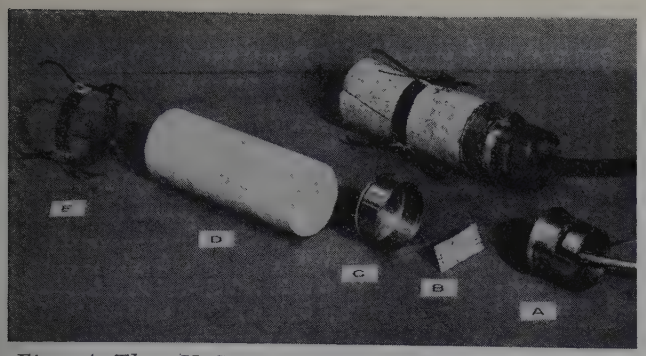

Fig. 4—The U. S. Bureau of Mines strain gage.

shot point its amplitude decays rapidly, and the pulse broadens and develops a small tensile phase. The rock type affects strongly the size and shape of the strain pulse, as is shown by comparison of strain records for granite and sandstone in Fig. 6. The type of explosive used mainly affected the amplitude of the strain pulse. Rise and fall times were not appreciably changed by the different explosives. Fig. 7 shows typical strain records in granite for three different explosives.

Strain-wave records were obtained at several distances for various charge sizes in the same rock types and with the same explosives employed in the crater tests. Measurements were made of peak strain, fall strain, rise time, and fall time. To eliminate the effect of charge size these data were scaled and plotted as functions of scaled travel distance. Distance is scaled to the charge size by dividing distance in feet by the cube root of the charge size in pounds. Time is scaled by dividing time in seconds by the cube root of the charge weight in pounds. Thus a scaled time multiplied by a propagation velocity in feet per second gives a scaled distance. Fig. 8 gives an example for granite.

A detailed study of reflected strain pulses shows that a conical crater should be produced above a concentrated charge buried below the surface. The depth of this crater should equal half the fall length of the strain pulse provided that half the fall length of the strain pulse is less than charge depth and provided that the fall strain is several times larger than the breaking strain of the rock.

If half the fall length of the strain pulse is greater than charge depth, reflected tensile breakage will occur only from the free surface back to the crushed zone. Reflected tensile breakage below the crushed zone is not possible in a simple crater test because of the geometry involved and the fact that the amount of tension developed during reflection decreases as the angle of incidence increases.

If the fall strain is only slightly greater than the tensile breaking strain of the rock, a crater is formed with a depth less than half the fall length of the strain pulse. Consider the case when the fall

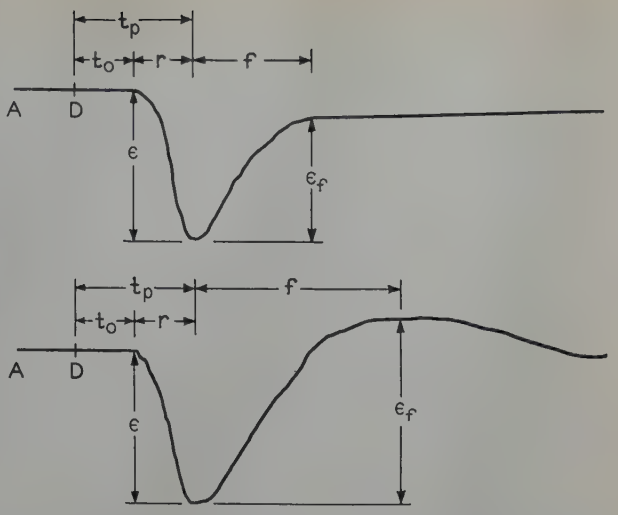

Fig. 5—Strain records showing the measurements made.
A = start of trace
D = time of detonation
ϵ = peak compressive strain
$ϵ_f$ = fall strain
t_o = arrival time for start of pulse
r = rise time
f = fall time
t_p = arrival time for peak strain

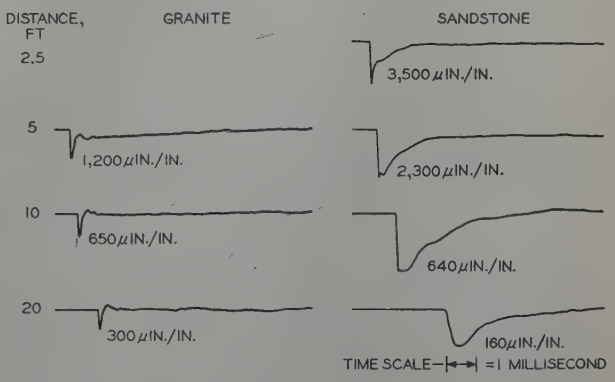

Fig. 6—Granite, sandstone strain records; 8-lb charge.

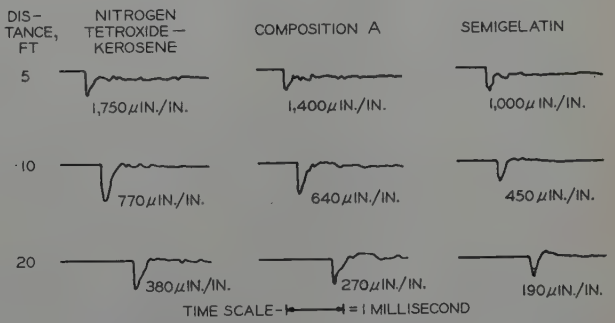

Fig. 7—Comparison of the strain records for different explosives. Rock type, granite. Charge weight, 8 lb.

Table II. Comparison of Dynamic and Static Tensile Breaking Strain of Rock

Rock Type	Maximum Scaled Crater Depth $D/\sqrt[3]{W}$ Ft/$\sqrt[3]{Lb}$	Scaled Charge Depth $d/\sqrt[3]{W}$ Ft/$\sqrt[3]{Lb}$	Scaled Travel Distance $L/\sqrt[3]{W}$ Ft/$\sqrt[3]{Lb}$	Fall Strain μ In. per In.	Dynamic Tensile Breaking Strain μ In. per In.	Static Tensile Breaking Strain μ In. per In.
Granite	0.8	1.9	2.7	720	360	280
Sandstone	1.6	1.5	3.1	1,100	550	500
Marlstone	2.2	2.3	4.5	620	310	—
Chalk	3.7	3.1	6.8	600	300	—

strain is exactly twice the breaking strain. In this instance just two slabs are produced, the bottom of the second slab occurring at a depth equal to half the fall length of the strain pulse. Next consider the case where the fall strain is slightly less than twice the breaking strain. Here only one slab is produced. The thickness of this slab is less than half the fall length.

The fall length of the strain pulse, F, is the fall time, f, multiplied by the propagation velocity, c, thus:

$$F = cf \qquad [6]$$

The distance traveled by the strain pulse during the reflection process of fracture, L, is the sum of the depth of the charge, d, and the depth of the crater, D, thus:

$$L = d + D. \qquad [7]$$

Therefore, the scaled equations for predicting crater depths for any charge size, W, from strain pulse data are:

$$\frac{D}{\sqrt[3]{W}} = \frac{1}{2}\,\frac{cf}{\sqrt[3]{W}} \quad \text{if} \quad \frac{cf}{2\sqrt[3]{W}} < \frac{d}{\sqrt[3]{W}}, \qquad [8]$$

$$\frac{D}{\sqrt[3]{W}} = \frac{d}{\sqrt[3]{W}} \quad \text{if} \quad \frac{cf}{2\sqrt[3]{W}} > \frac{d}{\sqrt[3]{W}}, \qquad [9]$$

$$\frac{d}{\sqrt[3]{W}} = \frac{L}{\sqrt[3]{W}} - \frac{D}{\sqrt[3]{W}}. \qquad [10]$$

The above equations are good only if the fall strain is greater than twice the breaking strain of the rock. Thus there is an upper limit on the value of $\frac{L}{\sqrt[3]{W}}$ that can be used to compute charge depth and crater depth. This upper limit can be specified for any rock type for which the dynamic breaking strain and the fall strain as a function of scaled travel distance are known.

Eqs. 8-10 have been used to calculate scaled crater depths for different scaled charge depths in the four rock types tested, using the scaled fall-time data given in Fig. 9. Results of these calculations are presented in Fig. 10 as a solid line showing the relation between scaled crater depth and scaled charge depth. The experimental crater data are shown as plotted points. For small scaled charge depths the experimental data and the calculated curves agree closely. For large scaled charge depths the experimental data lie below the calculated curves. This result is expected if the fall strain available in the strain pulse is less than twice the breaking strain of the rock. When this condition exists, one-slab craters are produced and the thickness of the slab is less than half the fall length of the strain pulse. Typical examples of these one-slab craters are shown in Fig. 11.

The dynamic breaking strain of rock can be estimated from crater and strain-pulse data. Maximum crater depth is produced by a strain pulse with a fall strain just twice the breaking strain of the rock. This strain pulse has traveled a scaled distance equal to the sum of the maximum scaled crater depth and the corresponding scaled charge depth. These experimental values can be read from Fig. 10. The fall strain corresponding to this scaled distance is determined from Fig. 12. One half the fall strain is the estimated dynamic tensile breaking strain of the rock. The results of these calculations,

Table III. Predicted and Measured Time of Breaking in Sandstone

Charge Depth, Ft	Horizontal Distance to Foil Strip, Ft	Arrival Time for Peak, M-Sec	Arrival Time for Peak Plus One Half Fall Time, M-Sec	Measured Break Time, M-Sec
0.4	1.0	0.14	0.96	0.39
	2.5	0.29	1.23	0.87
	5.0	0.63	1.75	1.05
0.9	1.0	0.17	1.02	0.27
	2.5	0.33	1.27	0.46
	5.0	0.66	1.80	1.05
1.8	1.0	0.25	1.15	0.38
	2.5	0.36	1.33	0.58
	5.0	0.68	1.83	1.30
2.5	1.0	0.32	1.31	0.57
	2.5	0.42	1.41	1.40
	5.0	0.74	1.94	2.60
2.9	1.0	0.36	1.33	0.62
	2.5	0.45	1.46	1.15
	5.0	0.77	1.93	2.50
3.9	1.0	0.48	1.50	1.33
	2.5	0.56	1.64	2.10
	5.0	0.84	2.14	4.02
4.7	1.0	0.61	1.72	1.23
	2.5	0.68	1.92	1.35
	5.0	0.95	2.37	3.50

Table IV. Velocities Determined from High-Speed Movies of Crater Tests in Sandstone, Charge Size 8 Lb.

Type of Explosive	Charge Depth, Ft	Stemming Velocity, Fps	Gas Velocity, Fps	Velocity of Rocks in Gas Stream, Fps	Rock Dome Velocity, Fps	Calculated Velocity of Rock Dome, Fps
Ammonia dynamite	0.44	2800	2800	360	—*	—**
Ammonia dynamite	0.44	3400	3400	240	—*	—**
Semigelatin	0.42	3000	3000	320	—*	—**
Semigelatin	0.42	4400	4400	180	—*	—**
Semigelatin	0.90	1800	1800	200	210	—**
Gelatin	1.80	1240	1800	180	120	—**
Semigelatin	2.4	900	1900	—†	80	74
Semigelatin	2.4	420	560	330	90	74
Gelatin	2.5	550	1600	105	70	72
Semigelatin	2.9	380	910	106	70	60
Gelatin	2.9	700	1050	210	50	60
Semigelatin	3.9	300	—‡	125	13	42
Gelatin	3.9	440	620	190	19	42
Semigelatin	4.7	82	—‡	51	9	32
Gelatin	4.9	105	—‡	—§	—§	30
Semigelatin	6.8	140	260	73	—§	16
Semigelatin	6.9	350	—‡	20	—§	16
Gelatin	7.0	27	—‡	—†	—§	15
Semigelatin	10.0	—§§	—‡	—†	—§	7

* No rock dome visible in picture.
** No strain data available for these distances.
† No pieces of rock observed in gas stream.
‡ No gas observed expanding out of hole.
§ No crater produced.
§§ Stemming did not come out of hole.

see Table II, show that the estimated dynamic tensile breaking strains are slightly greater than laboratory-determined static tensile breaking strains.

For some of the sandstone crater tests, strips of conducting foil were cemented to the rock surface in concentric circles around the charge hole in the expected crater area. These strips of foil were connected to circuits that generated a voltage pip when the foil strips were broken by cracking of the rock surface. Thus the time of rock cracking was determined by recording these voltage pips. These times are compared in Table III with the arrival times of the strain pulse at the break circuit. Specifically it is shown that breaking of the foil strips occurred after the arrival of the peak of the strain pulse and usually before half the fall time had elapsed. Four breaks occurred after half the fall time had elapsed. These late breaks occurred for the deeper charge depths and for the foil strips at the greater horizontal distances from the charge hole; they may result from a small time delay between the cracking of the rock and the breaking of the foil strips, because the rock is moving slowly at these larger distances.

High-speed movies of the explosions in sandstone were made with an Eastman high-speed camera capable of taking 3000 pictures a second. From these movies various phenomena during rock breakage were observed (Figs. 13-15).

For crater shots in sandstone having a scaled charge depth greater than 2.5 ft/$\sqrt[3]{\text{lb}}$, craters were seldom produced. High-speed movies of these tests show the sand stemming moving vertically upward with a constant velocity. Any loose rocks on the surface near the shot hole bounce upward before the top of the sand moves. Thus the seismic wave in the solid rock travels faster than it does in the sand stemming. However, the gases push the stemming out of the charge hole at a velocity higher than that of rocks bounced off the surface.

High-speed movies for crater shots in sandstone having a scaled charge depth less than 2.5 but greater than 0.5 ft/$\sqrt[3]{\text{lb}}$ show different phenomena. The sand stemming moves upward out of the charge hole followed by the explosion gases. There is an acceleration present in this motion. Cracks appear on the surface, and the broken rock moves upward, forming an almost perfect hemispherical dome underneath the gas cloud (Fig. 14). Little or no gas is observed issuing from the cracks in the rock dome. Out of the top there is a rush of gas and rock which appears as a conical funnel above the dome. Rock coming from the center is fragmented more than that forming the dome. Rock forming the dome has a constant velocity, with virtually no horizontal component, whereas the rock coming out of the top has a greater velocity, with both a horizontal and vertical component. Individual fragments can be observed as they separate because of the differences in their velocity. Rock near the center of the crater area has a higher vertical velocity than rock from the edges, and the surface fragments have higher velocity than those formed below the surface. The absence of a large horizontal component of velocity in the rock dome is convincing evidence that broken rock is not pushed out by expanding gas.

High-speed movies for crater tests having a scaled charge depth of 0.5 ft/$\sqrt[3]{\text{lb}}$ or less show no hemispherical dome of broken rock. Sand and gas expand out of the charge hole, followed by a rush

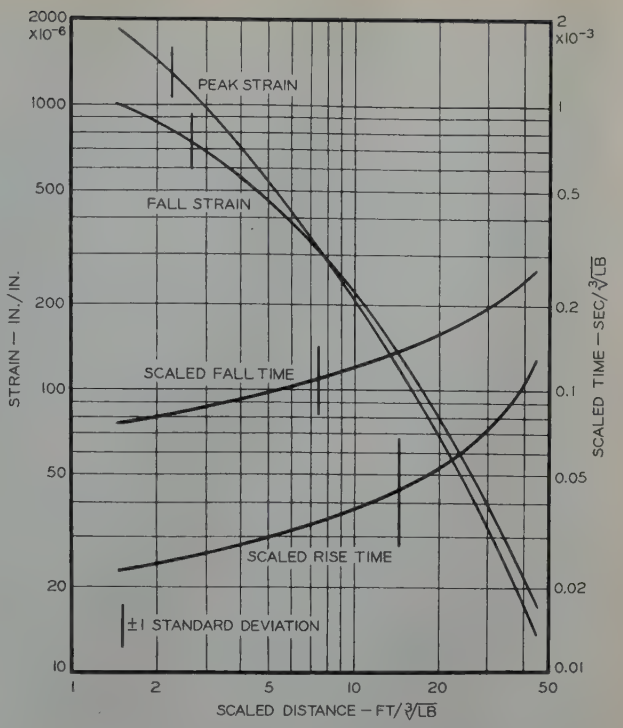

Fig. 8—Granite strain pulse data.

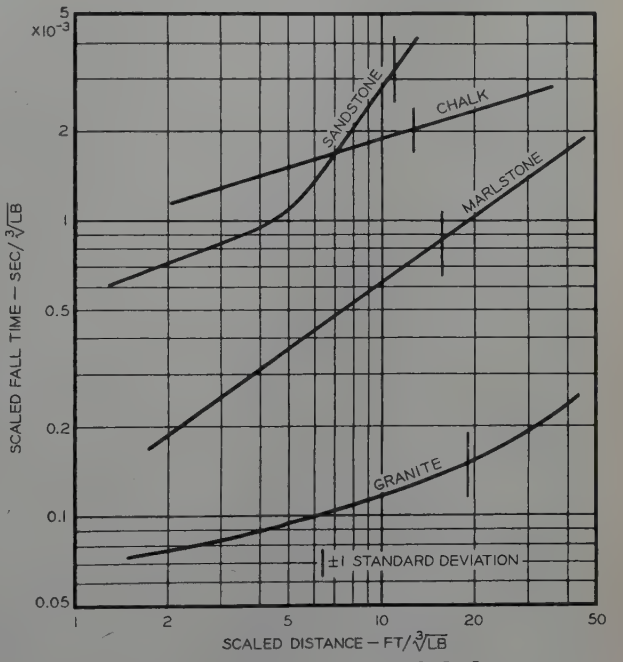

Fig. 9—Scaled fall time vs scaled distance.

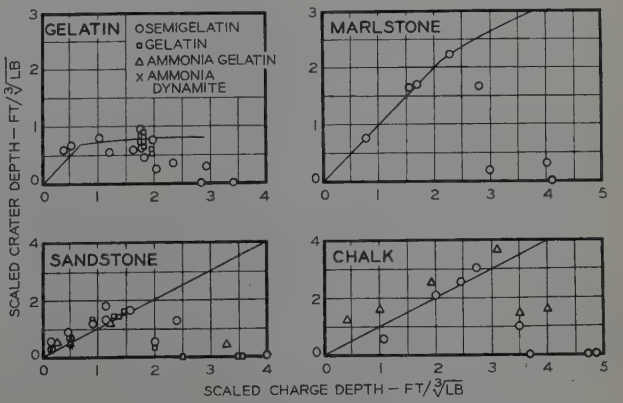

Fig. 10—Experimental, calculated scaled crater depths.

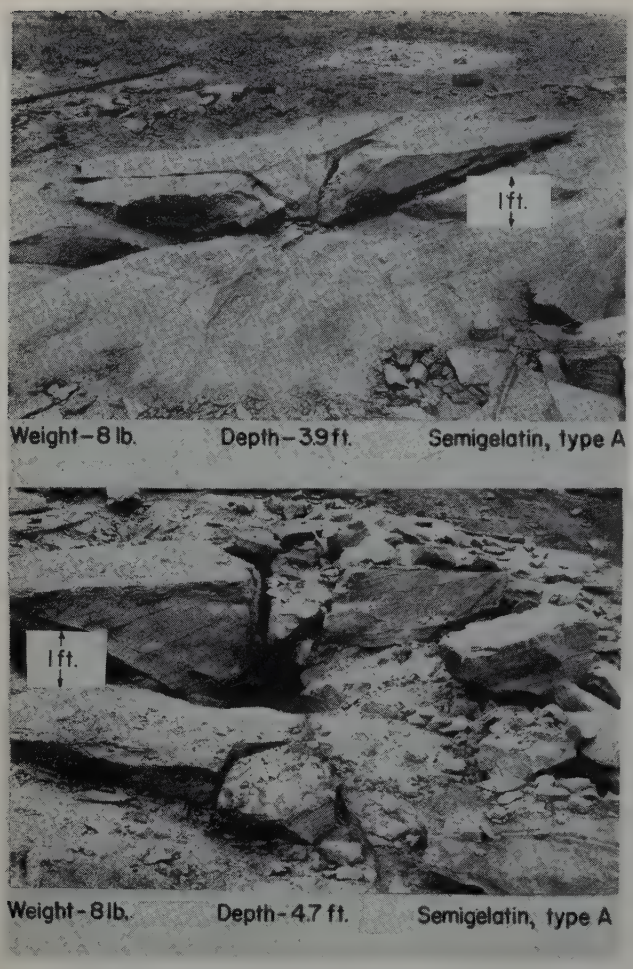

Fig. 11–Sandstone craters showing fragmentation.

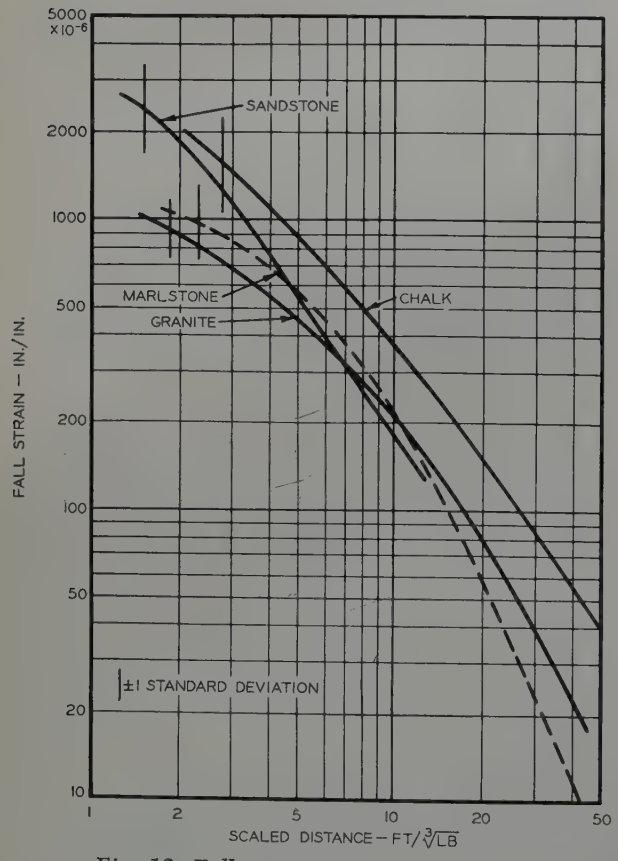

Fig. 12–Fall strain vs scaled distance.

of rock and gas out of the crater zone. This mass of broken rock and gas moves outward in all directions, forming an inverted cone above the crater. The rock is very finely fragmented and shows some acceleration.

The velocities of various motions observed in the high-speed movies were measured and are summarized in Table IV, where they may be compared with fly rock velocities calculated from peak strain data. These fly rock velocities were obtained by using Eq. 5 and the relation

$$v = c\epsilon \qquad [11]$$

where v = particle velocity, c = propagation velocity, and ϵ = peak strain.

Table IV shows that in general velocities of the various motions decrease as depth of charge increases. The expanding gases had the highest velocities; sand stemming velocities were lower than these except for the smallest charge depths, where there was so little sand on top of the charge that the gas and sand could not be distinguished from each other. Velocities of the rock dome are of the same order of magnitude as the calculated rock dome velocities, except for the larger charge depths. For large charge depths the first slabs broken are relatively thick; thus the velocity of these slabs is the average particle velocity trapped in the slab, whereas the calculated value was based upon peak values of particle velocity. Velocities of the rocks caught in the gas stream are greater than the rock dome velocities. This is to be expected, as the expanding gases have accelerated these rocks. Since most of the broken rock is contained in the dome that moves upward underneath the gas cloud, and since the velocity of this rock can be accounted for by the particle velocity associated with the strain pulse, it is evident that most of the rock fragmentation is a result of the strain pulse reflecting from the free surface.

REFERENCES

[1] T. C. Atchison, W. I. Duvall, and L. Obert: Mobile Laboratory for Recording Blasting and Other Transient Phenomena. *USBM R.I. 5197*, 1956, 22 pp.
[2] B. E. Blair and W. I. Duvall: Evaluation of Gages for Measuring Displacement, Velocity, and Acceleration of Seismic Waves. *USBM R.I. 5073*, 21 pp.
[3] W. I. Duvall and T. C. Atchison: Vibration Associated with a Spherical Cavity in an Elastic Medium. *USBM R.I. 4714*, 1950, 29 pp.
[4] W. I. Duvall and T. C. Atchison: Rock Breakage by Explosives. *USBM R.I. 5356*, 1957, 52 pp.
[5] L. Obert and W. I. Duvall: A Gage and Recording Equipment for Measuring Dynamic Strain in Rock. *USBM R.I. 4581*, 1949, 12 pp.
[6] L. Obert and W. I. Duvall: Generation and Propagation of Strain Waves in Rock—Part I. *USBM R.I. 4683*, 1950, 19 pp.
[7] K. B. Broberg: Studies in Scabbing of Solids Under Explosive Attack. *Journal of Applied Mechanics*, 1955, vol. 22, no. 3, pp. 317-323.
[8] K. Hino: Theory of Blasting with Concentrated Charge. *Journal of the Industrial Explosives Society*, Japan, 1956, vol. 15, no. 4, pp. 233-249.
[9] H. Kolsky and A. C. Sherman: Investigation of Fractures Produced by Transient Stress Waves. *Research Supplement*, 1949, vol. 2, no. 8, pp. 384-389.
[10] J. W. Landon and H. Quinney: Experiments with the Hopkins Pressure Bar. *Proceedings Royal Society*, 1923, vol. 130, pp. 622-643.
[11] J. S. Rinehart: Some Quantitative Data Bearing on the Scabbing of Metals Under Explosive Attack. *Journal of Applied Physics*, 1951, vol. 22, no. 5, pp. 555-560.
[12] J. S. Rinehart: Scabbing of Metals Under Explosive Attack—Multiple Scabbing. *Journal of Applied Physics*, 1952, vol. 23, no. 11, pp. 1229-1233.
[13] C. H. Johansson and U. Langefors: Short Delay Blasting in Sweden. *Mine and Quarry Engineering*, September 1951, pp. 287-293.
[14] G. E. Pearce: Rock Blasting—Some Aspects of the Theory and Practice. *Mine and Quarry Engineering*, January 1955, pp. 25-30.
[15] G. A. Teichmann and J. Hancock: Recent Trends in Short Delay Blasting. *Mine and Quarry Engineering*, October 1952, pp. 305-312.
[16] K. Hino: Fragmentation of Rock Through Blasting. *Journal of the Explosives Society*, Japan, 1954, vol. 17, no. 1, pp. 1-11.
[17] T. C. Atchison and W. E. Tournay: Comparative Studies of Explosives in Granite. *USBM Report of Investigation*, in preparation.

Discussion of this article sent (2 copies) to AIME before July 31, 1959, will be published in MINING ENGINEERING.

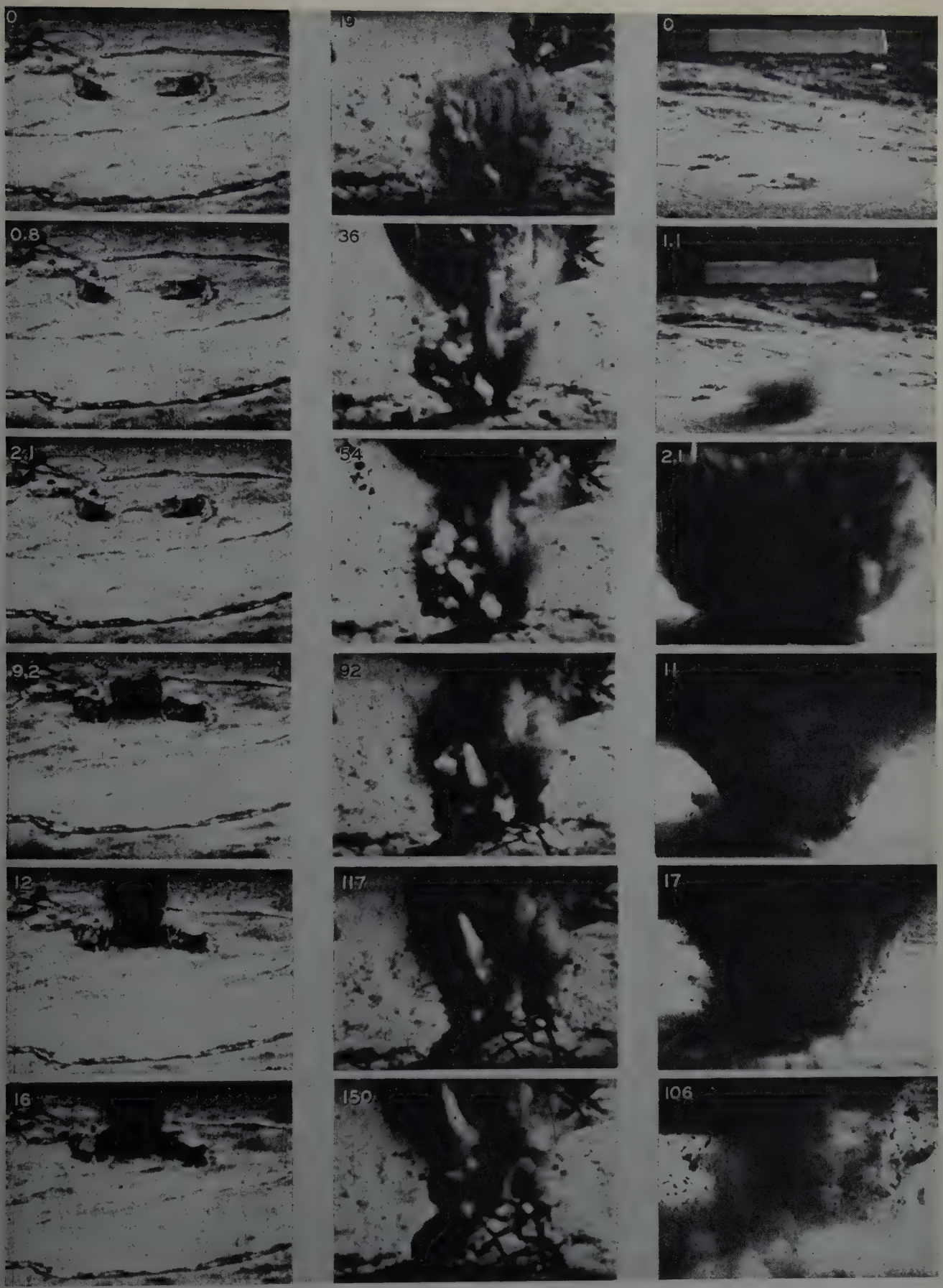

Figs. 13, 14, 15 (three columns, left to right)—High-speed pictures at different times after detonation of charge. Sandstone crater tests with scaled charge depths = 3.4 ft/$\sqrt[3]{lb}$, 1.45 ft/$\sqrt[3]{lb}$, and 0.25 ft/$\sqrt[3]{lb}$, respectively. Fig. 13—Charge, 8 lb semigelatin, type A; depth, 6.8 ft. Fig. 14—Charge, 8 lb gelatin, type A; depth, 2.9 ft. Fig. 15—Charge, 8 lb ammonia dynamite; depth, 0.5 ft. Millisecond numbers are given in the upper left of the photographs.

DISCUSSION

LINEAMENT TECTONICS AND SOME ORE DISTRICTS OF THE SOUTHWEST

by E. B. MAYO

(MINING ENGINEERING, page 1169, November 1958, AIME Trans., vol. 214)

David LeCount Evans (*Consulting Petroleum and Mining Geologist, Wichita, Kans.*)—Not only E. B. Mayo but also W. C. Lacy, who apparently urged the preparation of this analysis, is to be commended. Regional thinking of this type is needed to assure future success in the never-ending search for new mineralized and petroliferous districts.

As is usually the case, here is a regional study that will be read by the mining geologist alone. It is ironic that several of the trends established in this study have suggested themselves in northern mid-continent, detailed, and regional studies. These, where established, have offered new keys to petroleum exploration and have provided a possible basis for unraveling a number of broad generalities. The oil geologists, active in Colorado, Kansas, and Oklahoma, would find much food for thought in Mr. Mayo's projections.

To be more specific:

1) The parallelism between E. B. Mayo's Texas Lineament and the Amarillo Uplift, the Wichita Complex and the Arbuckle Complex of the Texas Panhandle and Southern Oklahoma is viewed with interest and appears especially significant when compared with the similar northwest trend of the Central Kansas Uplift, a major trend of production.

2) Considering the various northeast zones of Fig. 2, and with particular reference to Mayo's C-C, the Jemez Zone is on direct line with one of several northeast-southwest controls which the present writer has been using with some success in Kansas subsurface correlations. Considering zones of shearing, with no apparent vertical displacement, but suggesting strike-slip movement, because of the *staggered* effect on other features which cross such trends, Mayo's philosophy presents regional possibilities for lines of weakness, considered to this time of only local significance.

3) And, finally, in an area as distant from the Southwest as central Kansas, the north-south trends of the Fiarport-Ruggles anticline, the Voshel-Hollow Nikkel-Burrton structures, the Dayton to Stutgart trend, the north, slightly east trend of the Nemaha structural complex, and others all seem to approach the north-south alignments, *a* through *f*, of Mayo's Fig. 3.

Mayo's employment of structural intersections to pinpoint crustal weakness, to localize igneous activity and its accompanying mineralization is not, perhaps, a new concept, but it is a 1958 model, produced by tools improved from the ever-increasing accumulation of geological observations.

The use of intersecting trends in petroleum geology is not a new idea, since much production in earlier days was encountered via the straight line projections of established trends to centers of intersection.

A tragedy in this age of specialization is that *iron curtains* have been raised between groups, all seeking raw materials, all acolytes at the altar of structural geology, but all smugly content in and protected by the ivory towers of petroleum geology, engineering geology, mining geology, and geophysics.

Mayo presents basic ideas which can stimulate mid-continent structural thinking and, in the case of central Kansas, he provides a key to replace the broad and overworked simple monoclinal, sinkhole-dotted, Karst topography credo, which is not finding its share of new oil in a state where the declining discovery ratio is disconcerting.

The American Association of Petroleum Geologists would do well to add E. B. Mayo to its list of Distinguished Lecturers.

Evans B. Mayo (*author's reply*)—In reply to David LeCount Evans' comments, it is pleasing to learn that some of the elements discussed in my paper may interest petroleum geologists as well as mining geologists. This should not be surprising, however, because the lineaments make up the framework of the continent, and the oil-bearing sediments must reflect to varying degrees adjustments of basement blocks along their boundaries. A further possibility that petroleum geologists must have considered is that the slow escape of heat from buried lineaments and their intersections has aided the separation of oil from the sediments and started the migration into traps.

Regarding the specific points listed by Evans, the following are suggested:

1) The branch of Texas Lineament marked 1′ (Fig. 3) is thought to extend eastward through the Capitan Mts., New Mexico, through the long Tertiary dikes east of Roswell, and beyond via the Matador and Electra ranges of the Red River Uplift, Texas. Its further continuation might be the eastern flank of the Ouachita Fold Belt. The Amarillo-Wichita-Arbuckle zone of uplifts appears to continue east-southeastward the Spanish Peaks belt (3-5, Fig. 3). The northwest-trending Central Kansas Uplift would not belong to the above set, except insofar as the Central Kansas Uplift is traversed by west-northwest folds, possible continuations of the Uinta belt (5-5, Fig. 3).

2) The possible continuations into Kansas of the Jemez zone are new to me and are most welcome suggestions.

3) Most of the nearly north-south Kansan structures mentioned by Evans are unfamiliar to me, but the Nemaha Uplift itself appears to be part of a very pronounced structure traceable from the Cerralvo Fault Zone, south of the Rio Grande, through the Bend Arch, Texas, and the Nemaha Uplift, into the Pre-Cambrian of Minnesota (?). This nearly meridional zone is crossed and broken by the Rio Grande Embayment and by the Red River-Wichita Syntaxis. Petroleum geologists realize the economic importance of these features.

Perhaps it is inevitable that some papers of general interest be *buried* in the journals of specialized groups. Moreover, papers dealing with regional, or lineament, tectonics and its applications to exploration for economic mineral deposits are as yet few in the American literature. The opportunity to advance this field is open to all those who are not ultra-conservative and who have a lively curiosity, plenty of patience, and not too many business restrictions.

In conclusion, much appreciation is extended to D. L. Evans for his comments.

EFFECT OF PULP DEPTH AND INITIAL PULP DENSITY IN BATCH THICKENING

by A. M. GAUDIN, M. C. FUERSTENAU, and S. R. MITCHELL

The two principal attributes of a thickener pulp are its settling rate and the ultimate pulp density of the thickened mud. Testing for evaluation of thickening attributes of a pulp has usually been done batch-wise by placing the pulp in a one-liter glass graduated cylinder and noting the position of the boundary between clear liquor and mud as a function of time. Refinements in testing have included repulping a thickened mud to various dilutions and evaluating the settling rate on these various repulped muds. This is considered to make possible an estimate of the settling rate as a function of pulp density and therefore to pinpoint the slowest settling pulp which ought to be critical from the standpoint of thickener plant design. Finally, tests are sometimes made with model-size continuous thickeners of arbitrary size.

In batch tests it is generally accepted that the behavior of a pulp is described by a curve such as the one shown in Fig. 1, in which the position of the boundary between clear liquor and mud (the mudline) is plotted against time. It has also been assumed that the initial settling rate (the slope of the line segment *AB*) is descriptive of the pulp and independent of the size and shape of the container. Where the settling rate is slower and clearly a function of time (portion *CD* of the settling curve), it has been assumed that the data are not of much use because of the intrusion of compacting phenomena. The next important datum is the height, *PE*, which is a measure of the so-called *ultimate pulp density*. This quantity is assumed to be characteristic of the pulp and independent of the container.

When actual data are recorded, results are rarely exactly according to this theory and numerous deviations may be noted. For example, some pulps seem to require an appreciable delay before beginning to settle, as in line *AF*. This is spoken of as representing the need for an *induction time* for flocculation.

It has seemed desirable to explore thickener data with a more sensitive charting tool than is afforded by the coordinates of Fig. 1. Instead of relating the position of the mudline to time, it has seemed desirable to relate the rate of descent of the mudline to time. This, in effect, amounts to charting the slope of the line in Fig. 1, or the derivative of its ordinates, against the same abscissas. Fig. 2 shows the new chart for the curve *ABCDE* of Fig. 1.

When this new tool was applied to data obtained, for example, with sized clay pulps, astonishing differences appeared. Apparently the traditional tool conceals differences instead of revealing them, whereas the new method emphasizes them. It seems, also, that both charting methods have their uses.

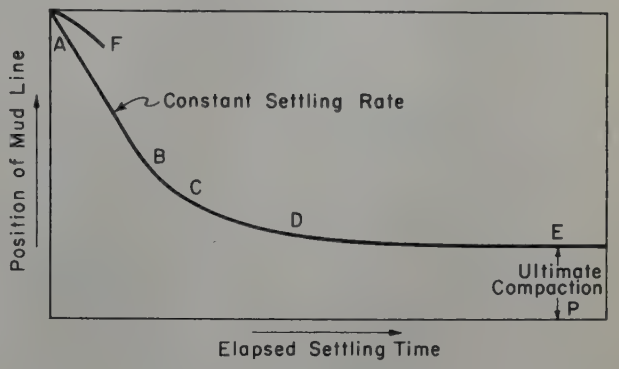

Fig. 1—Normal settling curve.

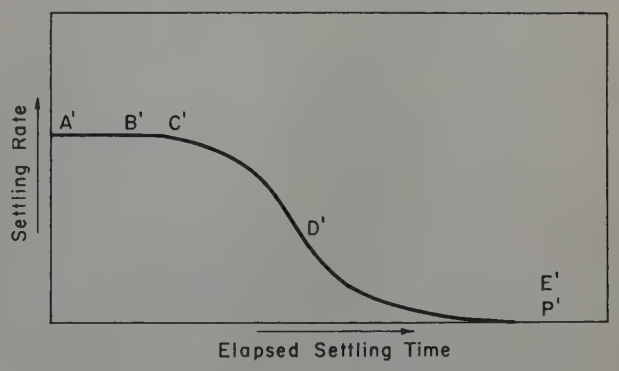

Fig. 2—Differential curve for data of Fig. 1.

In this article attention is focused on the effects of pulp density and container height as they affect the settling behavior of flocculated suspensions of a sized kaolin. The thesis by M. C. Fuerstenau[1] gives more details than this summary, as well as some information about the effect of other variables.

Sized fractions of kaolin were used, supplied through the courtesy of S. C. Lyons of the Georgia Kaolin Co. Large batches were made by agitation in a flotation machine and in a glass jar equipped with a mixer. The settling vessels were 2, 4, and 6-in. diam glass cylinders of various heights.

Pulp Dilution: The effects of pulp dilution on sedimentation behavior are shown in Figs. 3, 4, and 5. Fig. 3 shows data on pulps ranging from 2.44 to 16.7 pct solids initial pulp density, flocculated with Separan and charted in the traditional manner. At least two of the lines appear nearly straight in their early sections, but neither of the others does. Each of the curves in this figure includes a region labeled

A. M. GAUDIN, Member AIME, is Richards Professor of Mineral Engineering; M. C. FUERSTENAU, Student Member AIME, is Research Assistant; and S. R. MITCHELL is Senior Technician, Massachusetts Institute of Technology, Cambridge, Mass. TP 4806B.
Manuscript, Jan. 2, 1959. AIME Trans., Vol. 214, 1959.

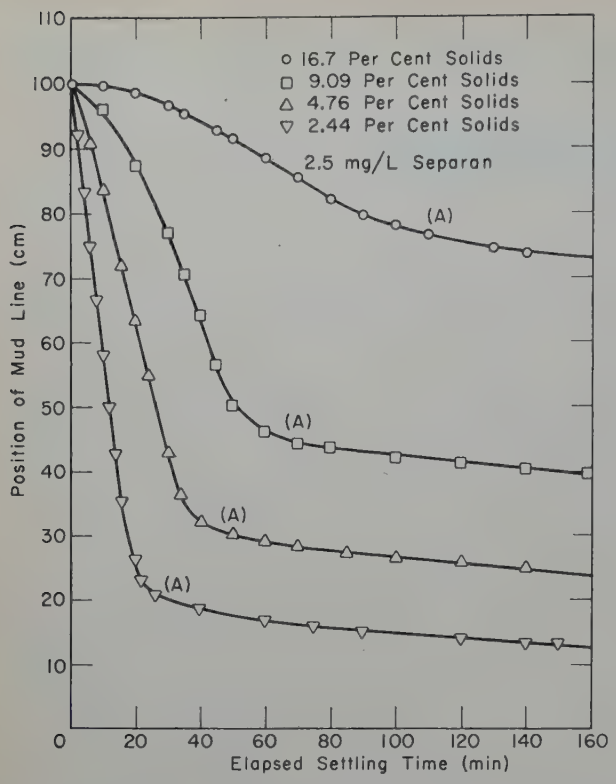

Fig. 3—Relation between position of mudline and elapsed time at various pulp dilutions (kaolin 2 to 20μ).

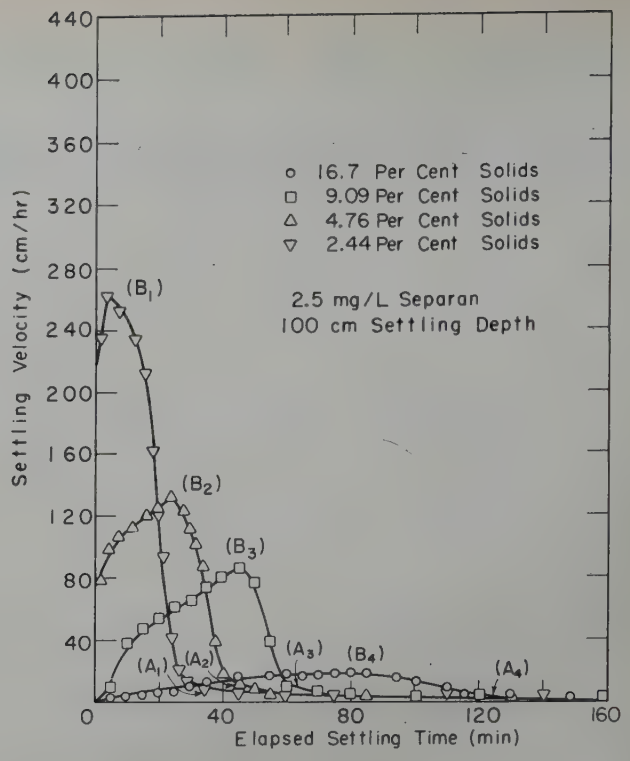

Fig. 4—Relation between settling velocity and elapsed settling time, various pulp dilutions (kaolin 2 to 20μ).

(*A*) in which the settling changes radically, becoming relatively slow. Fig. 4 is a plot of the same data, charted in terms of settling velocity vs time. It is clear that no horizontal section is shown in any of the curves and, therefore, that the conclusion of linearity for the early part of two of the curves in Fig. 3 is in error. The curves in Fig. 4 were drawn from the numerical data from which Fig. 3 was drawn, each of the points for the curves of Fig. 4 having as ordinate the difference of two numbers representing the mudline position at succeeding time intervals.

Fig. 5 shows data on similar pulps flocculated with lime instead of Separan, the data being charted as in Fig. 4. The purpose of Fig. 5 is to show that the behavior represented by Fig. 4 is not ascribable to the new flocculant, since similar results are obtained with the traditional lime.

As the concentration of solids in the feed pulp is decreased, maximal settling velocity increases and is attained sooner (points *B*, for example, in Figs. 4 and 5). At great feed-pulp dilution, maximal settling velocity is obtained at the very beginning of settling, but with thicker pulps more or less time must elapse before maximal mudline settling velocity is attained.

The time required for condition *A* to appear (Figs. 3 and 4) is shortened as the pulp is made thinner. The appearance of condition *A* is marked by formation of *volcanoes* at the mudline from which small flocs erupt, as noted by Coe and Clevenger.[2]

Settling Depth: Settling depth has heretofore not been regarded as a factor in the behavior of batch-settling thickener pulps. The writers found it to be of major importance. Tall settling columns (100 and 200 cm in height) as well as settling columns of more usual height (25 and 50 cm) were used in this study.

When dilute pulps are under consideration, as shown in Fig. 6, maximal settling velocity is substantially independent of settling depth (points *B*). Also, maximal settling velocity is attained early in the sedimentation period and occurs at almost the same time for all settling depths. The shorter the settling depth, the more rapid the rate at which settling velocity decreases after the maximum is attained. In fact, if the settling velocity is plotted against the ratio of settling time to initial depth, the data from all the tests fall on about the same line (Fig. 8A). Thus the decay in settling velocity with *relative time* seems the same in all cases. No doubt the decrease in settling velocity as settling proceeds is due to the increased pulp density, and this increase occurs more slowly when tall vessels are used.

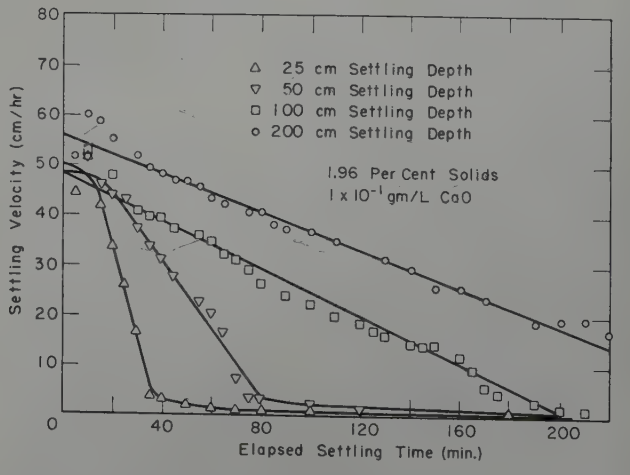
△ 25 cm Settling Depth
▽ 50 cm Settling Depth
□ 100 cm Settling Depth
o 200 cm Settling Depth
1.96 Per Cent Solids
1 x 10⁻¹ gm/L CaO
Settling Velocity (cm/hr)
Elapsed Settling Time (min.)

Fig. 6—Showing the relationship between the settling velocity and the elapsed settling time for various settling depths at high pulp dilution (kaolin 0 to 2μ).

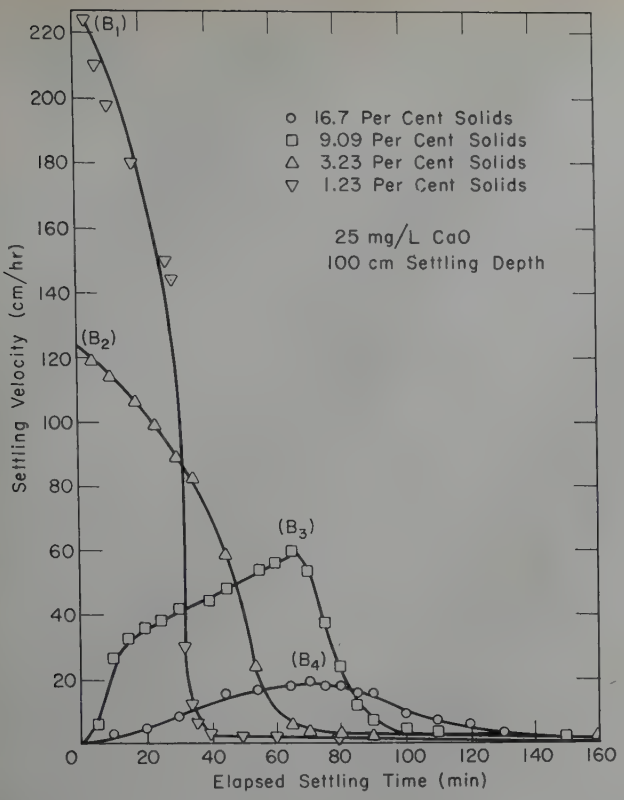

Fig. 5—Relation between settling velocity and elapsed settling time, various pulp dilutions (kaolin 2 to 2μ).

When thicker pulps are settling, e.g., 10 pct kaolin by weight, a profound difference in maximal settling velocity exists between pulps settling in shorter vessels and those settling in taller vessels, as shown in Fig. 7. Also, the time to attain condition *A* is greater for greater settling depth. If a plot is made of settling velocity vs relative time, the data for vessels of various depths do not fall on the same line, wherein they differ from the data obtained with dilute pulps. This is brought out clearly by Fig. 8, which is composed of four parts that show data for the settling of pulps of the same kaolin made up to various dilutions and placed in vessels of various heights. The vessels used were 25, 50, 100, and 200 cm in height and the pulp dilutions were 50 parts of water to one of solids, 30:1, 15:1,

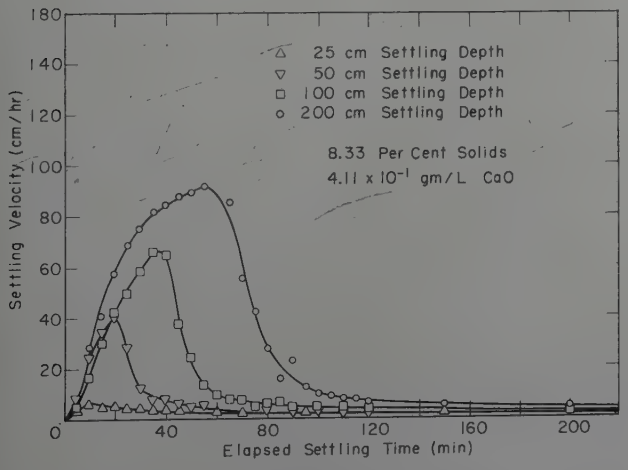
△ 25 cm Settling Depth
▽ 50 cm Settling Depth
□ 100 cm Settling Depth
o 200 cm Settling Depth
8.33 Per Cent Solids
4.11 x 10⁻¹ gm/L CaO
Settling Velocity (cm/hr)
Elapsed Settling Time (min)

Fig. 7—Showing the relationship between the settling velocity and the elapsed settling time for various settling depths at lower pulp dilution (kaolin 0 to 2μ).

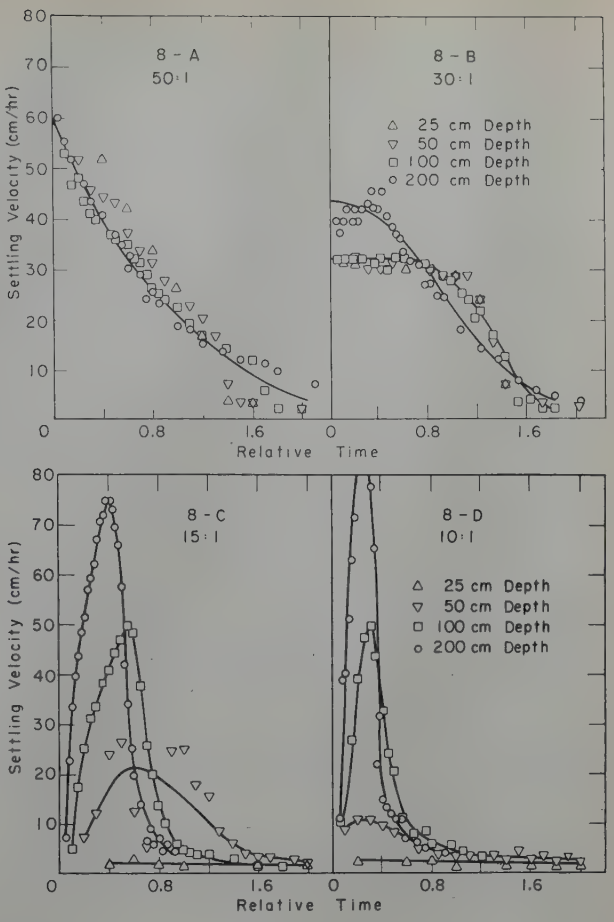

Figs. 8A through 8D—The relationship between the settling velocity and the relative time for various settling depths at various pulp dilutions (kaolin 0 to 2μ).

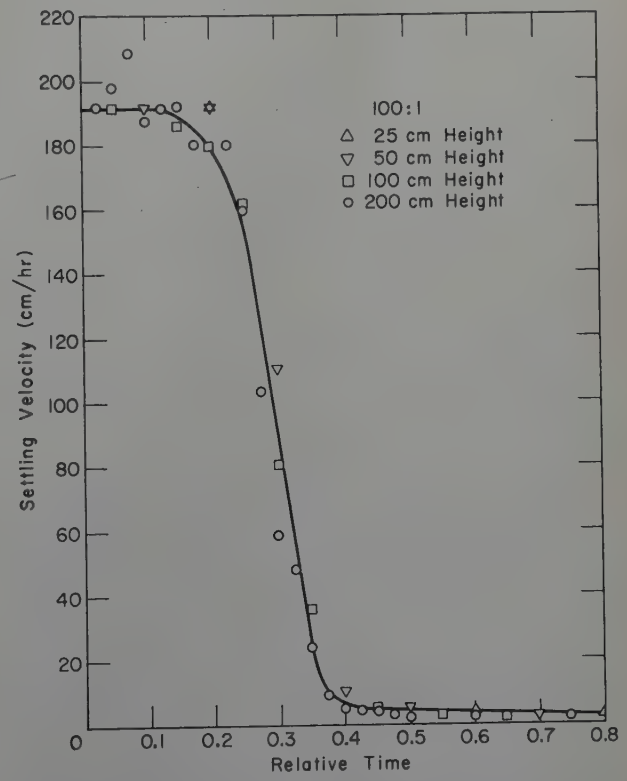

Fig. 9—Relationship between settling velocity and relative time at very high pulp dilution (kaolin 0 to 2μ).

and 10:1. In all cases the pulps were flocculated with lime. The amounts were different if rated on the liquid but the same if rated on the solids. Additional experiments made with other pulp dilutions are omitted for the sake of brevity; these experiments were made at 100:1, 40:1, 20:1, 12:1, and 8:1. They tell the same story.

The experiments made at 100:1 provide the one instance approximately constant settling rate was attained at the beginning of settling. Otherwise, they are the only experiments that accord with the accepted theory of settlement of flocculated suspensions. For the record, a chart of settling velocity vs relative time is included in Fig. 9. (Note that the scale of ordinates is much condensed from those in Fig. 8, while the scale of abscissas is expanded.)

Discussion: It has generally been thought that in a settling column of pulp that is initially of uniform pulp density throughout its height, two zones form shortly after the start of the settling process. The lower zone was thought to consist of compacting sediment and the upper zone of relatively fast-settling flocs. It was believed that this upper zone did not change in pulp density from top to bottom, or in time, but merely in the extent of its vertical dimension.

Since the settling of the mudline is so strongly dependent on the height of pulp initially placed in the batch thickener, it may well be suspected that the above ideas—while correct in respect to the existence of two zones and the time-and-position variability in pulp density of the lower zone—are incorrect in respect to the homogeneity of the upper zone.

This reasoning has led to construction of a device for measuring pulp density continuously as a function of time and position and without disturbance. This device, the Transviewer, has already been described, and work with it is actively in progress.[3] The phenomena described here explain why it is believed the Transviewer will serve a useful purpose in the development of thickening theory.

The authors are grateful for the financial support provided by Crucible Steel Co.; Duval Sulfur & Potash Co.; Engineering Foundation, Georgia Kaolin Co.; and the U. S. Atomic Energy Commission.

REFERENCES

[1] M. C. Fuerstenau: Master of Science Thesis, *The Sedimentation of Clay Pulps.* Massachusetts Institute of Technology, 1957.
[2] H. S. Coe and G. H. Clevenger: Methods for Determining the Capacities of Slime-Settling Tanks: *AIME Trans.*, 1916, vol. 55, pp. 356-384.
[3] A. M. Gaudin and M. C. Fuerstenau: The Transviewer—X-Rays to Measure Suspended Solids Concentration. *Engineering and Mining Journal*, 1958, vol. 159, no. 9, pp. 110-112.

Discussion of this article sent (2 copies) to AIME before July 31, 1959, will be published in MINING ENGINEERING.

DISCUSSION

SCALE-UP RELATIONSHIPS IN SPODUMENE FLOTATION

by W. E. HORST

(MINING ENGINEERING, page 1182, November 1958, AIME Trans., vol. 214)

John Dasher (*Central Research Laboratory, Crucible Steel Co. of America, Pittsburgh, Pa.*)—Getting spodumene to float quickly and cleanly can be a problem. The author has presented an excellent account of a valid and useful approach to the scale-up of such problem floats. This indicated advantages for doubling retention time, i.e., buying another set of flotation cells.

The author states that 21 pct of the spodumene floated in 2 min in the laboratory cell, that the grade of the rougher was about 75 pct spodumene, and that the final tailing contained 4 to 12 pct spodumene in different sizes with the present cells and 1 to 9 pct spodumene with twice as many cells.

About 20 years ago, this writer obtained in the laboratory the flotation of over 90 pct of this spodumene in a King's Mountain sample in 1 min at a grade of 90 pct spodumene in the rougher and a final tailing that contained only 1 pct spodumene. The methods of Norman, Ralston,[6] and Gieseke[7] were used, which teach that spodumene floats quickly and cleanly if its surfaces have been properly conditioned chemically and/or mechanically prior to flotation.

Although feed preparation is not discussed, the results reported indicate that it is inadequate. This writer suggests that improvements in this area might be more effective than doubling the number of cells.

W. E. Horst (*author's reply*)—Dasher's comments are appreciated by the author and require some clarification. He suggests that improved spodumene flotation performance may be obtained by feed preparation techniques rather than increased retention time in flotation. Certainly flotation performance is dependent on feed preparation and this is an important feature in the flotation process. It is true that certain types of spodumene ores, particularly weathered ores, require more complicated feed preparation processing than clean ores to achieve the desired flotation results. It was not implied that current feed preparation techniques are the same as experienced during the scale-up investigations.

Although discussion of feed preparation was omitted from the article on scale-up relationships, the important feature was that pre-treatment processing was the same for each level of operation investigated—laboratory, pilot plant, and plant scale. Under these similar conditions large differences existed in recovery for comparable time intervals in each scale of operation. It is highly probable that feed preparation techniques could be modified and thereby increase the flotation rate for each scale or all scales of operation discussed. However, modifications would have to be justified on an economic basis.

REFERENCES

[6] J. E. Norman and O. C. Ralston: Conditioning Surfaces for Froth Flotation. *AIME TP 1074B*, 1939, p. 85.
[7] J. E. Norman and E. W. Gieseke: Beneficiation of Spodumene Rock by Froth Flotation. *AIME TP 1161B*, 1940.

DRILL CORE SCANNER PROVED IN FIELD

Solid phosphor core scanner offers rapid and reliable method of checking radioactivity as drill core is moved automatically through high-sensitivity chamber. Continuous graph of radiation intensity is plotted.

by W. W. VAUGHN, R. H. BARNETT, and E. E. WILSON

Soon after the search for uranium ores on the Colorado Plateau began in earnest, thousands of feet of drill core ranging from 1⅛ to 2⅛ in. diam became available for study. Although significant advances had been made in the technique of quantitative gamma-ray borehole logging, instrumentation was in the development stage, and complete reliance could not be placed on gamma-ray logs alone to interpret quantitatively the meaning of radioactivity in a drillhole. A method that would be faster than chemical analysis and still give reproducible and reliable results for various drill core sizes was desirable to provide additional information on the enormous footage of drill core being accumulated.

A solid phosphor scintillation drill core scanner was designed and constructed. Basically the instrument was developed to measure radiation from a drill core which would not be clearly recorded by a gamma-ray logger using a Geiger tube as the sensitive element. Such data would be beneficial in constructing isorad maps to delineate ore-bearing zones. A calibration in the range 0.01 to 0.1 pct eU_3O_8 was provided; above 0.1 pct eU_3O_8 gamma-ray logs were available and were being used to calculate grade and tonnage of ore reserves. The core scanner, however, has been used to estimate equivalent uranium content of ore-grade materials containing as much as 2.2 pct eU_3O_8 with an accuracy of ± 10 pct, the sample being in the form of a BX drill core. Actually, an apparent calibration of eU_3O_8 vs counts per unit time is a straight line with a slope that is a function of the sensitive element and the geometry of the counting assembly. A true calibration that will show the expected departure from a straight line is due principally to the random nature of the pulse from a radiation source and the nonlinearity of the electron circuitry.

Design and Construction: Three methods of detecting radioactivity were considered and applied in developing the core scanner now in use: 1) the Geiger tube, 2) liquid scintillation phosphors, and 3) solid scintillation phosphors. The desired sensitivity and long-term drift characteristics needed for this operation could be attained only by using solid scintillation phosphors. All three methods are discussed.

Before scintillation counters were common, nine beta-gamma sensitive Geiger tubes ⅞ in. diam by 12 in. long were used, arranged to surround the drill core with tube axes parallel to the axis of the core. This arrangement of Geiger tubes was enclosed in a lead shield 1 in. thick, and provision was made to slide a 6-ft length of drill core manually into the counting chamber, one foot at a time. A count for each segment was taken with a scaler while the core remained stationary. The equivalent uranium content of the different sections of drill core could then be estimated with the aid of a calibration curve of counts per unit time vs percent equivalent uranium (eU). In rare cases the effects of the radioactivity concentrated in small areas within the core introduced errors in the readings made with the Geiger tube arrangement owing to the geometry of the measurement. The variability of counting rate due to a localized concentration of radioactivity in a spot in the wall of a drill core is illustrated in Fig. 1. This effect and the inherent low efficiency of the Geiger tube were considered major disadvantages of this counting arrangement.

When liquid scintillation phosphors became available the core scanner in Fig. 2 was constructed to make a more accurate measurement of the equivalent uranium content of a sample. This instrument contains about 4 liters of liquid phosphor in a stainless steel coaxial cylinder 1 ft long, with inner and outer walls 0.060 in. and 0.125 in. thick, respectively. Four end-window type photomultiplier tube with cathodes of 2 in. diam, immersed in the solution at right angles to the axis of the core, were used to observe light flashes in the phosphor. The liquid phosphor offered equal sensitivity to radiation originating at any point in the enclosure and represented geometrically the optimum in design. However, providing a semi-permanent leak-proof seal between the glass envelope of the phototube and the metal walls of the container proved to be a serious problem in constructing the equipment. The most effective seals were especially machined O-rings from sections of large tygon tubing. The tygon took a permanent set owing to cold flow characteristics and in most cases sealed completely. The light absorption characteristics of the liquid phosphor changed gradually with time, and after one month the counting rate had decreased to half the original value. The most sensitive liquid phosphor tested proved to be a solution containing 4 g of 2.5-diphenyloxazole and 0.01 g of 2-(1-naphthyl)-5-phenyloxazole per liter of toluene. With fresh solution in the chamber and with all photomultiplier tubes operating in parallel, the counting rate contributed by any one of the four photomultiplier tubes was about 85 pct of the counting rate from a single tube operated individually. From these observations it was concluded that owing to coincident loss and light attenuation within the liquid phosphor, the apparent sensitivity could not have been materially increased by additional phototubes. However, this approach to core

W. W. VAUGHN, Chief, R. H. BARNETT, and E. E. WILSON are with the Electronics Laboratory, Geophysics Branch, U. S. Geological Survey, Denver. TP 4802I. Manuscript, Sept. 29, 1958. AIME Trans., Vol. 214, 1959.

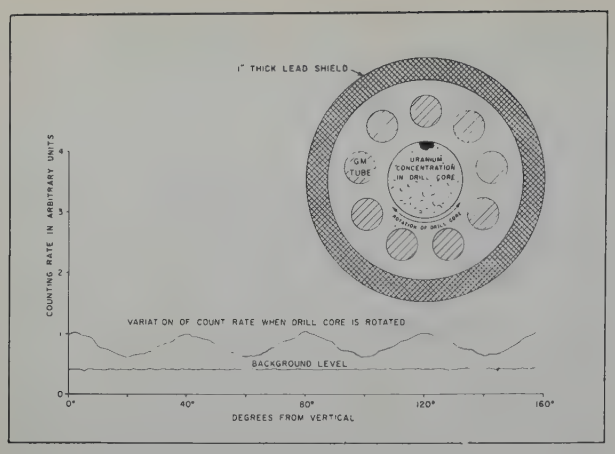

Fig. 1—Idealized counting geometry, GM tube scanner.

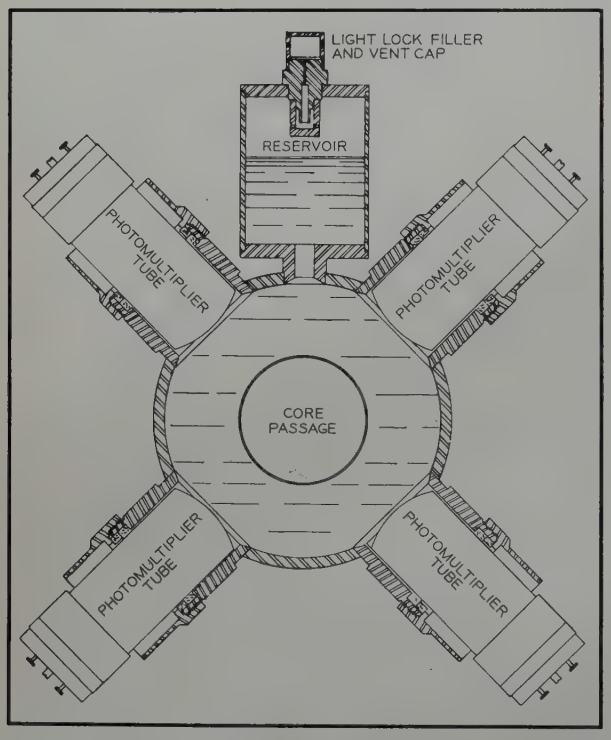

Fig. 2—Liquid scintillator core scanner. Section through reservoir and photomultiplier tube holders.

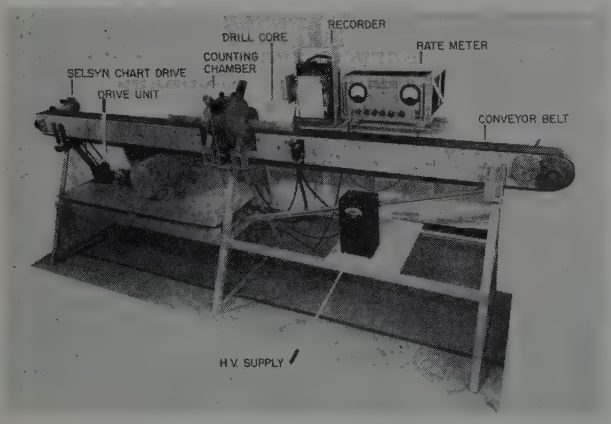

Fig. 3—Solid phosphor detector scanner.

scanning was abandoned because of long-term drift characteristics which were caused by gradual discoloration of the solution and the subsequent increased attenuation to light transmission in the range of 4000 to 6000Å.

Because of the greater sensitivity per unit volume and the long-term stability of light output from sodium iodide crystals immersed in the higher-viscosity silicone fluids, a core scanner with this type of phosphor was developed (Fig. 3). A thickness of about 2 in. of lead is used to shield the sensitive area except for the openings of the photomultiplier tubes and the passageway for the drill core. Four sodium iodide crystals 2 in. diam by 2 in. long, mounted individually in spun aluminum cups of 0.032-in. wall thickness, are spaced radially at right angles around the drill core. Approximately 3 π geometry is obtained in the counting chamber with this arrangement. Each crystal is immersed in silicone compound of 200,000 centistokes viscosity and coupled optically with the same silicone compound to the 2-in. diam cathode of an end-window type of photomultiplier tube.

The crystals and phototubes were selected individually from stock for uniformity of spectral response, resolution, and low microphonics, and the amplification factors were matched when possible. The resistor divider system for the dynodes of the phototubes used 5-megohm, ¼-watt resistors between all dynodes except 5, 6, and 7. A 5-megohm potentiometer and two 2½-megohm, ¼-watt fixed resistors connected between dynodes 5 and 7 of each phototube (with the arm of the potentiometer connected to dynode 6) control the amplification of the photomultiplier tubes (Fig. 4). The divider system, including the 5-megohm potentiometer, is molded in a silicone rubber compound called 3M Dielectric sealer EC-1120-PC. Two leads for the high voltage connection were brought out external to each mold and the four tubes were connected in parallel. Since the amplification factor of the phototube varies roughly as the fourth power of the dynode voltage, it is desirable to have the voltage across the dynode resistance change as little as possible with counting rate. The secondary emission electrons flowing internally from dynode to dynode within the phototube fluctuate wih the radiation impinging on the sodium iodide crystal. The end result of this fluctuation of phototube current is the effect of varying resistance in parallel with a fixed resistance, the external dynode resistor divider system. The current, particularly between dynodes

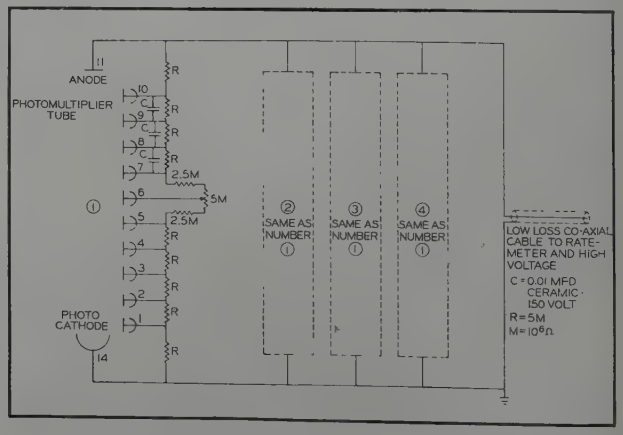

Fig. 4—Solid phosphor detector assembly.

8 through 10, is considerable at high counting rates. The voltage decreases due to the decrease in resistance resulting from the shunting effect of the high-density current may be as much as 10 v on these dynodes. Since the overall voltage across the divider system remains constant, other dynode potentials will rise as a result of this redistribution of current. This fluctuation of voltage may be minimized in two ways: a glow discharge type of voltage regulator tube may be used between dynodes in the divider system, or the value of the fixed resistors may be decreased (providing the high voltage supply will stand the additional current drain).

The latter choice was made, and the high voltage supply (Fig. 5) separate from the rate meter was constructed to supply the load presented by the four phototubes in parallel. The high voltage supply is a series-parallel type with a regulation of 0.001 pct change in line voltage. A 7A4 vacuum tube in series with a bleeder resistor controls the high voltage. A 6AG5 vacuum tube in parallel with the bleeder resistor compares a sample of the output voltage with a reference voltage obtained from the cascaded voltage-regulator tubes (VR 150 and VR 105) and amplifies the difference in voltage. This amplified error voltage appears at the grid of the series regulator tube, effecting control by varying the conductance and voltage drop across this tube. When the high voltage output decreases, the grid of the 6AG5 tube becomes less positive, the plate and the grid of the 7A4 tube less negative. The increased conductance in the 7A4 tube causes less voltage drop. The four phototubes have a common load resistor where a voltage pulse is developed and fed to the rate meter circuit. A commercially available rate meter, EK Cole Model 522, and a 1-ma graphic recorder are used to count and record results.

Physical Assembly: The frame for the core scanner, constructed of 1½-in. angle iron, is approximately 12 ft long and stands 3 ft high. The 4-in. wide conveyor belt, which can accommodate 6-ft lengths of core, is driven through a variable-speed pulley arrangement by a reversible motor. Manual adjustments to set the tension and angle of belt travel are provided at each end. Wooden guide rails, which can be changed for drill cores of various diameters, tend to cup the ¼-in. thick conveyor belt before it enters the counting chamber. The chart drive in the recorder, which has five interchangeable gear ratios, is driven by a selsyn and gear box from the pulley system moving the belt. The depth to which the phototubes may be inserted into the lead-

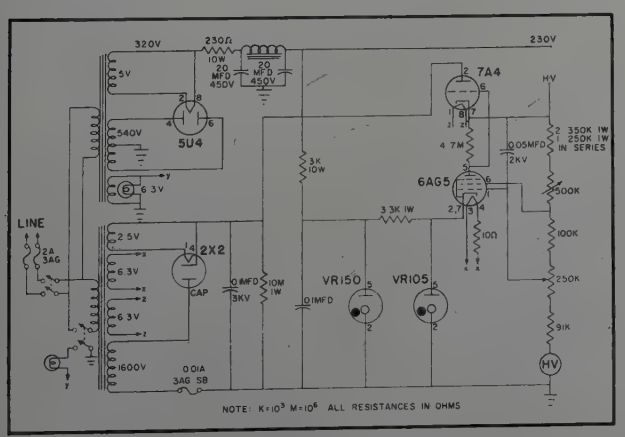

Fig. 5—High voltage supply for solid phosphor scanner.

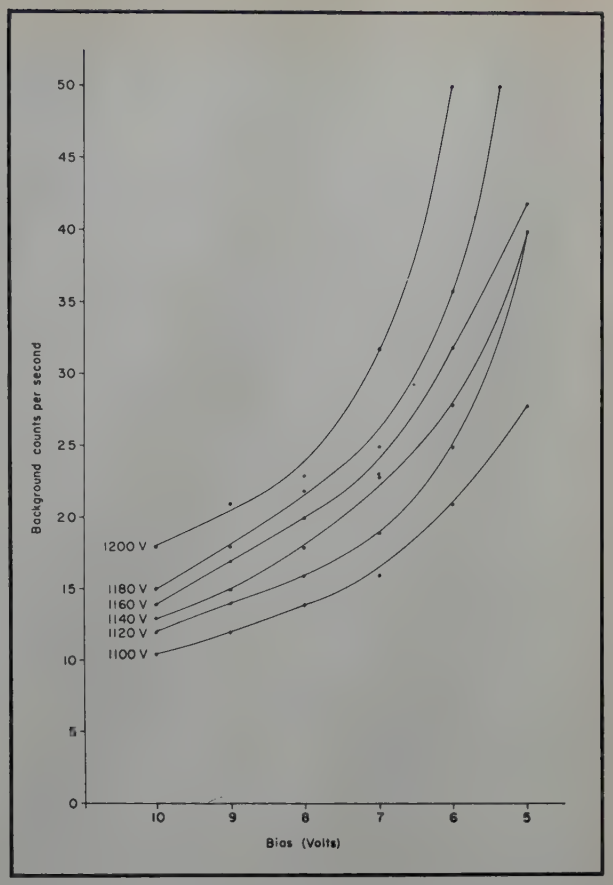

Fig. 6—Graph showing the fluctuations in background with bias level at different high voltage settings.

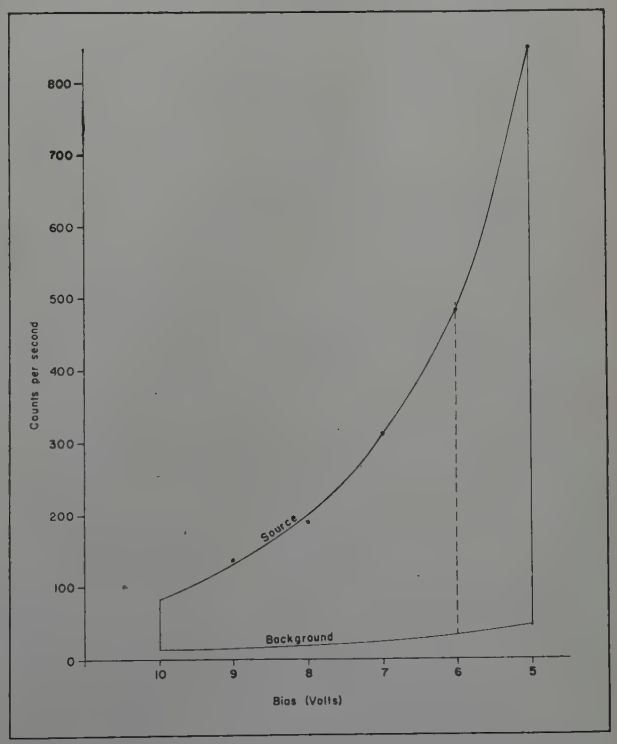

Fig. 7—Graph showing source to background relationships at different bias settings of the rate meter.

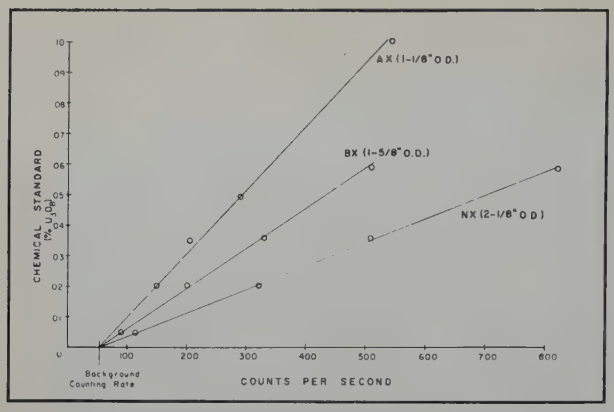

Fig. 8—Calibration curve, solid phosphor core scanner.

shielded chamber and the spacing between the surface of the drill core and crystal face are adjustable. Overall sensitivity is affected when the position of the scintillation head is altered and a new calibration must be established. In practice the sensitivity is adequate for the minimum activity in the smallest core studied and the position of the detecting element is usually maintained constant even though core diameters vary.

Calibration: There are many interpretations of sensitivity and calibration as applied to radiation-detecting equipment for geologic application. Spectral response, conversion efficiency from quanta to electrical energy of the sensitive element, signal-to-noise ratio and statistical fluctuation of counting rate are factors to be considered. Probably the most useful convention is an expression of counts per unit time ratio to a background or a standard counting rate, with source material and instrumentation specified. Such was the logic of calibrating the core scanner.

First a series of tests was made to determine how the combination of high voltage and discriminator bias affected the background counting rate of a given phototube and crystal assembly (Fig. 6). It is generally desirable to operate a photomultiplier tube at a voltage just below the dark current threshold for a given bias setting. In this case the operating voltage of 1160 v was selected. At higher voltages operation of the photomultiplier tube became erratic. Similar tests were made with a source located centrally in the counter chamber and the results were compared to the background counting rate to determine the bias setting for a particular high voltage (Fig. 7). Since an estimation of percent eU was made from the recorded results, operating conditions offering the greatest source to background count ratio were considered optimum. A bias setting of 6 v has been used with this equipment. Undesirable long-term drift characteristics in the input system of the rate meter ruled out lower bias voltages.

Artificial drill core samples of 1⅛, 1⅝, and 2⅛ in. diam corresponding in size to AX, BX, and NX drill core were molded. A chemically analyzed pitchblende sample containing 64.5 pct U_3O_8, whose uranium was in equilibrium with its daughter products, was ground to 100-mesh size and mixed in different proportions with potters clay. Each mixture was split four times and water added to bring the mixture to a paste consistency. Samples 1 ft long were cast in plastic molds and allowed to harden. A second chemical analysis for uranium content was made after the samples were removed from the molds. A plot of percent U_3O_8 vs counting rate for each drill core size is shown in Fig. 8. These curves deviate from a linear function by ± 6 pct, which is within the operational error expected from experience with similar equipment. The range of percent equivalent uranium indicated is for subgrade ore material; however, any curve may be extended to include ore-grade materials containing as much as 10 pct eU_3O_8 and yet lie within the operational linearity of the equipment. Linearity depends primarily on the range of counting rate selected to indicate the equivalent uranium content. Chemically analyzed samples containing 1 pct U_3O_8 and no other radioactive constitutents are within the linearity stated when the high voltage and bias settings for data in Fig. 8 were used. For high grade ore of 1 to 10 pct eU_3O_8 a different high voltage and bias setting to reduce the overall counting rate should be selected. It should be pointed out that unless the equilibrium condition as well as the radioactive constituents other than uranium are known, a calibration in terms of uranium content is meaningless. Where equilibrium conditions, or other radioactive constituents, are not known results should be expressed in eU or eU_3O_8, which will be valid regardless of the state of equilibrium.

In addition to providing a fast semi-quantitative means of scanning drill core to determine the equivalent uranium content, the instrument has a practical use in other radiometric analysis. Crushed grab samples of drill cuttings may be sealed in pint-size cardboard containers equally spaced on the conveyor belt and run through the chamber to obtain readings of equivalent uranium content. Semi-quantitative results are achieved in this way with sample containing as little as 0.005 pct eU_3O_8

Conclusions: A reliable and rapid method of scanning large amounts of drill core for radioactivity was constructed and proven in field operation. The drill core is scanned as it is automatically moved through a high-sensitivity chamber and a continuous graph of radiation intensity along the length of the core is plotted. Advantages of the equipment are simple and automatic operation, high sensitivity, and low long-term drift characteristics.

The authors are indebted to H. Faul and J. Rosholt of the U. S. Geological Survey, who gave freely of their time in technical discussions, and to J. Ohm and D. Hough of the USGS for mechanically constructing the instrument and assisting in experimental work.

The work reported here is part of an investigation carried on by the USGS on behalf of the Division of Raw Materials of the U. S. Atomic Energy Commission.

REFERENCES

P. R. Bell, R. C. Davis, and W. Bernstein: Pulse-Height Variation in Scintillation Counters. *Review of Scientific Instruments*, 1955, vol. 26, p. 726.

J. B. Birks: *Scintillation Counters*. McGraw-Hill Book Co. Inc., New York, 1953.

S. C. Curran: *Luminescence and the Scintillation Counter*. New York Academic Press, New York, 1953.

F. B. Harrison: Large Area Scintillation Counters. *Nucleonics*, June 1952, vol. 10, pp. 40-45.

F. N. Hayes, D. G. Ott, V. N. Kerr, and B. S. Rogers: Pulse Height Comparison of Primary Solutes. *Nucleonics*, December 1955, vol. 13, pp. 38-41.

R. Hofstadter: Detection of Slow Neutrons. *Physical Review*, 1951, vol. 82, p. 749.

W. A. Schneider, J. Hershkowitz, and N. Kallmann: Properties of Long Columns of Scintillating Liquids. *Nucleonics*, December 1953, vol. 11, p. 46.

Discussion of this article sent (2 copies) to AIME before July 31, 1959, will be published in MINING ENGINEERING.

THE GEM STOCKS AND ADJACENT OREBODIES, COEUR D'ALENE DISTRICT, IDAHO

by GARTH M. CROSBY

Seven mines with important production records in the Coeur d'Alene lie adjacent to the Gem stocks —the Frisco (Gem), Hercules, Interstate, Rex (Sixteen to One), Success (Granite), Sunset, and Tamarack. Old records are incomplete, but available data given in Table I show these mines have produced 10,550,721 tons of ore containing more than 50 million oz of silver, more than 1.5 billion lb of lead, and about 1 billion lb of zinc (approximately 1.25 million tons of lead and zinc combined). Average ore grade is 4.8 oz of silver per ton, 7.2 pct Pb, and 4.6 pct Zn.

This impressive production represents about 12 pct of the District's yield. At present metal prices, with modern beneficiation, the gross value would be more than $400 million.

THE GEM STOCKS

The Gem stocks, considered to be outliers of the Idaho batholith of Late Cretaceous age, are located in the northern half of the Mullan quadrangle, and extend from the town of Gem, Idaho, along a strike of N30°E for a distance of approximately five miles. They occur as two major masses of monzonitic rocks commonly referred to as the North stock, which covers an area of 1.1 sq miles, and the South stock, which covers 2.6 sq miles. The areal pattern is roughly club-shaped, the North stock representing the handle and the South stock the head of the club. Two and a half miles west and five miles northeast are two groups of smaller stocks, isolated from the main masses but of the same general rock type. This discussion is limited for the most part to the North and South stocks.

GARTH M. CROSBY is Chief Geologist, Day Mines Inc., Wallace, Idaho. TP 4810I. Manuscript, Dec. 19, 1958. Pacific Northwest Regional Conference, Spokane, Wash., April 1958. AIME Trans., Vol. 214, 1959.

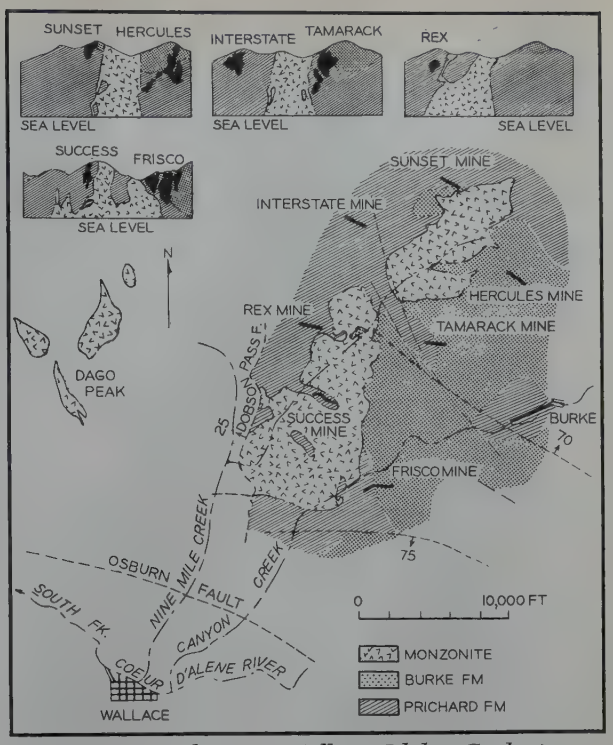

Fig. 1—Gem stocks area, Wallace, Idaho. Geologic map and generalized longitudinal sections of the oreshoots.

At the north end, where the intrusion is about 3200 ft wide, the walls are about parallel and dip very steeply west. At the south end, where the mass is about 7000 ft wide at surface, the walls dip away from each other at moderately steep angles. An aeromagnetic survey[1] detects and outlines with surprising accuracy the two main stocks, as illustrated on the magnetic contour map (Fig. 2). Of particular interest is the location and shape of the magnetic anomaly representing the South stock. The anomaly is centered over the south end of the outcrop, and a westerly extension joins it with a smaller anomaly over the Dago Peak stocks. The latter anomaly, likewise, is located over the south end of the isolated stocks. This pattern suggests the intrusion has greater extent at depth to the south and west. Though correlation between the Dago Peak stocks and the larger masses is suggested, the controversial aspects of the Dobson Pass fault, which separates the two areas, casts doubt on a correlation.

Topographically the monzonite stocks are ignored by the drainage pattern indicating these rocks, and the invaded rocks of the Lower Belt Series react similarly to erosion. The drainage patterns of Nine Mile and Canyon creeks cut indiscriminately across the monzonite-Belt contact, resulting in both valleys and ridges in the southern end of the intrusion. Nine Mile Creek traverses diagonally the entire five-mile length of the stocks.

The monzonite rocks of the intrusion are referred to locally as *granite,* but granite is rare and the rocks comprise a wide variety of types. Their characteristics, described in detail by F. L. Ransome and F. C. Calkins,[2] are summarized by P. J. Shenon.[3] The principal rock type is coarse-grained, light gray, porphoritic monzonite containing black crystals of hornblende. Pyroxene, epidote, and titanite

This page of Mining Transactions AIME follows p. 620. The intervening non-Transactions pages appeared in MINING ENGINEERING.

are seen commonly in the hand specimen, and quartz is usually less than 5 pct of the rock. Phenocrysts of microcline and microperthite occur in a ground mass of smaller equidimensional plagioclase crystals. Carlsbad twinning is seen commonly in the phenocrysts, and albite twinning can be seen in some of the groundmass. Rocks in the smaller Dago Peak stocks differ from the main masses, chiefly in grain size. Phenocrysts are smaller and the groundmass commonly is so fine-grained the minerals cannot be identified with the unaided eye. Classification of the rocks is governed by the relative abundance of the phenocrysts; with an increase of phenocrysts the classification approaches syenite, and with a decrease it approaches diorite.

THE INVADED ROCKS

The ore deposits around the stocks occur in the Burke, Upper Prichard, and Prichard formations of the Lower Belt Series of Algonkian age. The rocks of the Burke Formation are chiefly medium to thin-bedded, gray argillaceous quartzites, becoming progressively more argillaceous toward the older Prichard rocks. The Upper Prichard Formation, 1800 ft thick, contains massive and thick-bedded relatively pure quartzites interlayered with black argillites. Argillite is the dominant rock of the Lower Prichard Formation.

CONTACT METAMORPHISM

A thesis study by A. M. Piper[4] discloses that the intruded rocks are metamorphosed in an irregular rim extending 50 to 100 ft away from the monzonite. Within the argillaceous rocks of this zone magnetite, garnet, pyroxene, biotite, and epidote have been developed, as well as some andalusite. The relatively pure quartzites contain a few of these minerals in only small amounts but they have been recrystallized generally, which gives them a brilliant, sparkling appearance. The various rocks resulting from these changes are classified as hornfels.

Ransome and Calkins (Ref. 2, p. 72) mention the absence of schistosity and cleavage in the invaded rocks and the absence of arching in the vicinity as evidence that high pressures were not present during emplacement. Stoping of the invaded rocks by the magma is suggested as the dominant process of intrusion. Embayments and tongues of country rock and several isolated remnants of the Burke and Prichard formations in the monzonite support the theory. The most certain evidence for the argument is a stope block of the Wallace Formation located near the north end of the South stock. The nearest exposures of the Wallace Formation are at least several miles away, and this Wallace remnant must have settled through the magma several thousand feet to occupy its present position.

The mines adjacent to the Gem stocks can be divided into two geographical groups (Fig. 1). Three important mines, the Hercules, Tamarack, and Frisco, are located on the east margin of the intrusion and four others, the Sunset, Interstate, Rex, and Success, are on the west side. Within these mines 29 productive veins occur. Average strike is 75° W and dips are moderately steep to vertical. Veins dip both north and south. Stoped widths range from less than 5 ft to several tens of feet, but the average is estimated to be about 10 ft. Viewed in vertical longitudinal projection the oreshoots display the characteristic shape found in the Coeur d'Alene district, that is, a greater vertical than horizontal dimension. These mines are recognized as members of three or four extensive mineral belts along which other important mines are located. Consideration of these belts, now under study, is not within the scope of this paper. It should be pointed out, however, that the orebodies adjacent to the stocks represent their respective mineral belts at the margin of the stock.

Types of Deposit: The orebodies located around the stock are classified as hypothermal replacement veins. They are characterized by tabular shapes and shearing, with the exception of those in the Success mine. Here shapes are very irregular, and it is usually difficult to find fractures leading away from the ends of ore shoots. The Success orebodies, then, are classified as contact metamorphic. J. B. Umpleby and E. L. Jones[5] consider the orebodies of the Frisco, Rex, and Sunset mines closely related in origin to typical contact deposits, since these contain silicates and magnetite intimately associated with metallic sulfides. The orebodies of the Hercules, Tamarack, and Interstate mines also contain high-temperature minerals and can be included in the contact group.

Mineralogy: Gangue minerals common to the deposits are quartz, pyrite, siderite or ankerite, and magnetite. Stringham, Galbraith, and Crosby[6] report pyrrhotite, biotite, garnet, chlorite, hematite, and grunerite as major constituents of the veins in the Hercules and Tamarack mines. A study of paragenesis of minerals in the Hercules mine suggests *five* stages of mineralization. In the first stage, known as the Silicate stage, biotite, andradite, grunerite, and chlorite were formed. In the second, the Carbonate stage, siderite was formed and in the third, the Oxide stage, magnetite was formed. The fourth stage, known as the Sulfide stage, is subdivided into the Early and Late substages. During the Early Sulfide substage pyrrhotite and pyrite with some chalcopyrite and arsenopyrite were formed. Galena, sphalerite, and some jamesonite were formed during the Late Sulfide substage. Grunerite and siderite occur in roughly reversed proportions from top to bottom in the mine, siderite being the

Table I. Production from Mines Adjacent to Gem Stocks

Mine	Tons	Ag, Oz	Pb, Pct	Zn, Pct	Silver, Oz	Lead, Lb	Zinc, Lb
Frisco	2,000,000	2.9	4.8	2.4	5,800,000	192,000,000	96,000,000
Hercules	3,482,023	8.7	11.0	1.3	30,293,600	766,045,060	90,532,598
Interstate	950,000	2.0	5.2	17.4	1,900,000	98,800,000	330,600,000
Rex	169,762	1.4	3.2	3.2	237,667	10,864,768	10,864,768
Success	783,975	1.3	2.0	7.4	1,019,168	31,359,000	116,028,300
Sunset	307,429*	2.1	4.1	6.1	645,601	25,209,178	37,506,338
Tamarack	2,857,532	3.6	6.9	5.0	10,287,115	394,339,416	285,753,200
Total	10,550,721	4.8	7.2	4.6	50,183,151	1,518,617,422	967,285,204

* These tonnages are based on relatively incomplete records but are thought to be minimum reports.

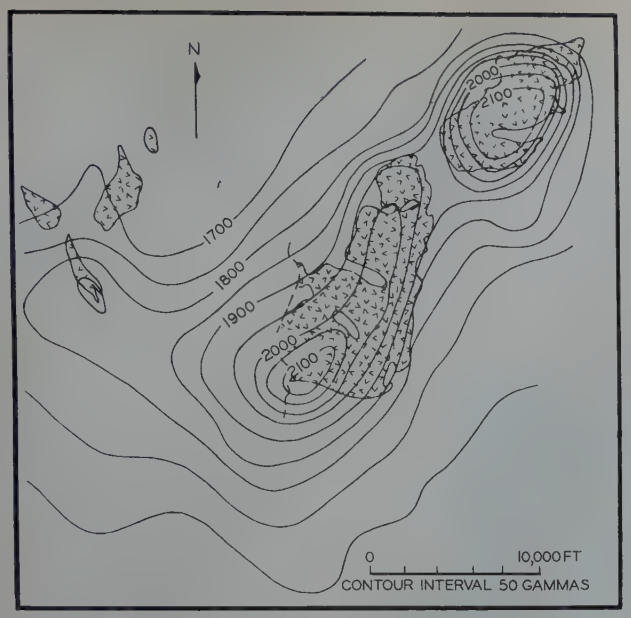

Fig. 2—A magnetic contour map of the Gem stocks area.

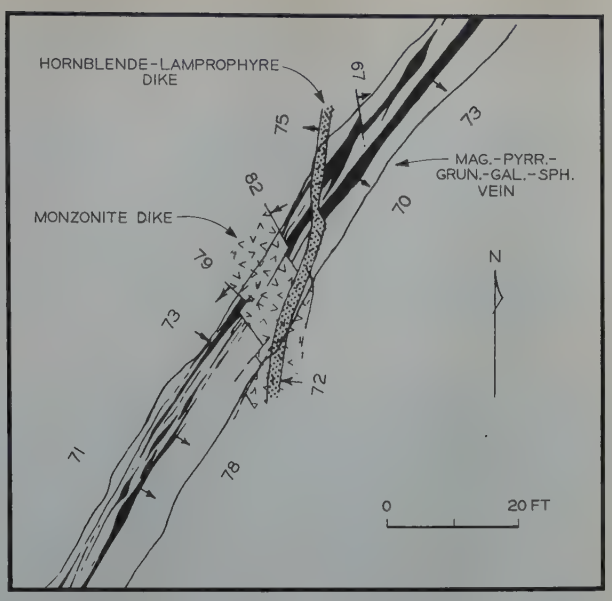

Fig. 3—Relationship of dikes to ore, 1900 level, drift west, as revealed by recent exposure in Hercules mine.

more abundant mineral toward the top of the orebody. In the lower part of the mine a transition zone is recognized above which the predominant iron sulfide is pyrite and below which it is pyrrhotite.

Mineral Zoning: Other observers have reported mineral zoning in the veins near the Gem stocks. At the Interstate mine there was some decrease in the amount of lead with depth, but no increase in the amount of zinc. In the Success mine Ransome and Calkins (Ref. 2, p. 184) point out an increasing amount of zinc on the 330 level, the ore having been primarily lead in the levels above. It was noted that lead oreshoots contained increasing proportions of sphalerite at their outer margins and that pyrite was the principal constituent where the vein graded out into country rock. The Hercules mine also contains a higher proportion of lead to zinc in the upper levels. In the Hercules there is an excellent example of zoning in the gangue minerals, with quartz, pyrite, and siderite on the upper part of the mine passing through the transition zone into the higher temperature minerals pyrrhotite and grunerite. West of the Sunset mine a magnetometer survey shows an increase in the size of the anomaly found over the veins as the monzonite stock is approached, indicating a corresponding increase in the amounts of pyrrhotite and magnetite occurring in the veins.

Wallrock Alteration: Wallrock alteration is not as noticeable near these orebodies as in many orebodies of the Coeur d'Alene mining district where sericitization or *bleaching* has been the major alteration process. In contrast, the rocks are harder and often darker than their original counterparts. The most intensely altered wall rocks occur in the Success mine, where the siliceous rocks of the Upper Prichard Formation have been changed to dark micaceous recrystallized quartzites—some colored green containing pyroxene and some pink containing garnet. Quartz schists are developed locally. An unusual rock worthy of note is a narrow though persistent biotite schist found near the ore throughout the mine. It probably corresponds to an original argillaceous layer of the Upper Prichard Formation. With the exception of the biotite schist, alteration has produced fine-grained, hard, tough rocks which grade into each other and into monzonite. The entire Success pendant has been altered in this manner, and the intensity of the alteration here is to be considered very great as compared to that found elsewhere in the area. Chief differences in alteration of wall rocks found in the other mines lie in the abundance and variety of contact metamorphic minerals developed. These minerals occur very irregularly in patches and confined altered zones along the veins. Normally the intensity of alteration decreases as distance from the stock increases, and at some points the wall rock is quite fresh and unaltered.

RELATIONSHIP TO INTRUSIVE ROCKS

In considering the relative ages of the monzonite and the orebodies nearby, it is helpful to observe the more common relationship of ore with dike rocks encountered in the mines. The rocks are classified as monzonite, diabase, and lamprophyre dikes. The monzonite dikes are light-colored, relatively coarse-grained rocks of about the same composition as the main stocks. The diabase dikes are gray-green to black rocks containing feldspar laths in a groundmass of pyroxene too fine-grained to be identified by the unaided eye. The lamprophyre dikes are characteristically dark, containing an abundance of well formed hornblende crystals or biotite plates in a fine-grained groundmass of plagioclase. The light-colored monzonite rocks are referred to locally as *acid* dikes, and all the dark rocks are loosely termed *basic* dikes. On surface the basic dikes are seen to be later than the main mass of the stocks and usually occur as deeply weathered zones containing decomposed rock and mud. The acid dikes do not react differently to erosion, and the relationships to the enclosing rocks are not evident. Underground both acid and basic dikes are seen in relation to ore, but to date there is no clear example of the relationship between the main mass of the monzonite and the acid dikes. This particular relationship might be difficult to determine because of the irregular apophyses of monzonite rocks at the margins of the stocks.

Underground the acid dikes are seen in contact with ore in the Success, Interstate, and Hercules mines. With respect to the Success mine Umpleby and Jones (Ref. 5, p. 5) state:

> The monzonite apophyses are traversed by the ore as is clearly shown . . . where a 10 foot dike nearly at right angles to the course of the ore body is exposed in opposite sides of the stope at a point where ore was extracted to a width of about 12 feet. Another equally clear example of ore formed subsequently to the monzonite appears . . . where an offshoot from the main ore body replaces a four foot dike and extends into the quartzite beyond.
>
> On the 100-foot level . . . the ore body, retaining its width of 3½ to 5 feet, crosses a southwestward-dipping monzonite dike. This relation continues for 60 feet below the level, but lower down no ore was found in the monzonite, although ore has been mined in the adjacent quartzite for more than 100 feet farther down. Above the level the stope continues between granite walls for 40 feet without diminution in width. As there is notably less fracturing within the dike than beyond it, the relationships are interpreted as indicating this sequence—1. shearing, 2. intrusion of the dike, and 3. renewed shearing accompanied or followed by replacement of wall rock, whether quartzite or monzonite by ore.

In the Interstate mine, several hundred feet from the main stocks, a relatively large monzonite dike occurs. Umpleby and Jones (Ref. 5, p. 94) state that galena and sphalerite replace the monzonite here and that both ore and dike are offset by post-ore faulting.

Recent observations in the Success mine made during lessee activity suggest the ore pre-dates the monzonite. On the 1200 level ore in a stope 30 ft wide and 150 ft long is abruptly terminated at its northwest end by monzonite, which the ore abuts directly. In the southeast end of the same stope there are lenses or stringers of monzonitic material within the vein, suggesting contemporaneous ages for the monzonite and ore.

In the Hercules mine at least two acid dikes cross the vein in typical push-apart fashion. Vein material abuts the wall of the dike and shows a slight crowding against it. In a few places a very small amount of galena and sphalerite extend into the monzonite a matter of inches. The vein structure, however, does not persist into the monzonite, and the short sulfide prongs are interpreted as post-sulfide adjustments. It has been noted that these occurrences are located where small offsets in the monzonite are opposite galena or sphalerite in the vein.

The basic dikes are known to be post-ore in several mines adjacent to the Gem stocks but otherwise are undated. Some consider relationship with the Tertiary extrusives to the west not unlikely. A remarkable exposure made recently in the Hercules mine showing the relationship of basic dike, acid dike, and ore is illustrated by the map of the 1900 level (Fig. 3). The relationship of ore to the basic dike, a hornblende-lamprophyre, is similar to the previously described relationship of ore to the younger acid dike, except that no prongs of sulfides or any other vein material extend into it. The lamprophyre is younger than the acid dike and shows a very weak selvage at the contact. Where the lamprophyre crosses the vein there is a characteristic increase in the angle between the vein and dike as viewed in plan. The same relationship is often seen between the vein and transverse faults, and it appears that the lamprophyre dike occurs along one of these structures and has simply pushed apart the vein and the monzonite alike.

In conclusion, the orebodies adjacent to the Gem stocks are classified as contact metamorphic and hypothermal. The Success deposit is the best example of the contact metamorphic type. The orebodies occurring in the other mines are distinguished from those of the Success by their association with fissuring. At the west end of the Hercules 1000 level the deposit becomes very irregular in plan, resembling the contorted shapes of ore found in the Success mine. There is, also, a marked lack of shearing and fissuring in this part of the Hercules mine. These features, together with the mineral associations typical of contact metamorphic deposits, identify this portion of the Hercules deposit as contact metamorphic. Shearing increases progressively toward the east end and top where the deposit assumes the shape of a typical lode and can be classified as a hypothermal replacement vein. The Hercules, therefore, is an example of a contact metamorphic deposit grading into a hypothermal vein deposit.

Because ore in the Sucess mine is seen to be later than the main mass of the monzonite in some places and earlier in other places, it is considered to be very closely related in time to the monzonite. Closer dating of the ore depends on the relative ages of the monzonite dikes and the main stocks. Though this relationship has not been observed to date, their ages are assumed to be nearly the same. The fact that the same minerals are found in the altered rocks around the stocks and in the altered rocks along and in the veins suggests that the veins are very closely related to the monzonite intrusion.

The author expresses gratitude to the management of Day Mines Inc. for permission to publish this article and especially thanks H. L. Day and R. Farmin for their encouragement and valuable assistance. The cooperation of the mining companies throughout the district has been of inestimable value, and the courtesies extended by their staff members are very much appreciated. Discussions with J. C. Kieffer, P. I. Conley, S. N. Kesten, H. E. Harper, M. W. Hutchinson, J. B. Colson, R. McConnel, and M. C. Brown have enlightened many of the problems encountered.

REFERENCES

[1] W. J. Dempsey, J. R. Reese, and F. E. Moore: Aeromagnetic Survey of Wallace and Vicinity and Mullan and Vicinity Quadrangles. *USGS Open File Report*, Spokane, Wash., 1950.

[2] F. L. Ransome and F. C. Calkins: The Geology and Ore Deposits of the Coeur d'Alene District, Idaho. *USGS Prof. Paper 62*, 1908, pp. 45-49.

[3] P. J. Shenon: Geology and Ore Deposits Near Murray, Idaho. *Pamphlet 47*, Idaho Bureau of Mines and Geology, October 1938, pp. 7-9.

[4] A. M. Piper: *Paragenesis of Some Primary Ores from the Rex and Success Mines, Coeur d'Alene District, Idaho*. Master of Science thesis, University of Idaho, 1925.

[5] J. B. Umpleby and E. L. Jones, Jr.: Geology and Ore Deposits of Shoshone County, Idaho. *USGS Bull. 732*, 1923, p. 33.

[6] B. Stringham, F. M. Galbraith, and G. M. Crosby: Mineralization and Hydrothermal Alteration in the Hercules Mine, Burke, Idaho. *AIME Trans.*, 1953, vol. 196, pp. 1278-1282.

[7] H. E. McKinstry and R. H. Svendsen: Unpublished report, 1938.

[8] W. R. Wagner: The Geology of Part of the South Slope of the St. Joe Mountains, Shoshone County, Idaho, *Pamphlet 82*, Idaho Bureau of Mines and Geology, 1949.

[9] G. M. Crosby: Geology of the Hercules Mine, Burke, Idaho. *Mining Congress Journal*, June 1956, pp. 43-45 and 82.

Discussion of this article sent (2 copies) to AIME before Aug. 31, 1959, will be published in MINING ENGINEERING.

CASE HISTORY IN PILLAR RECOVERY

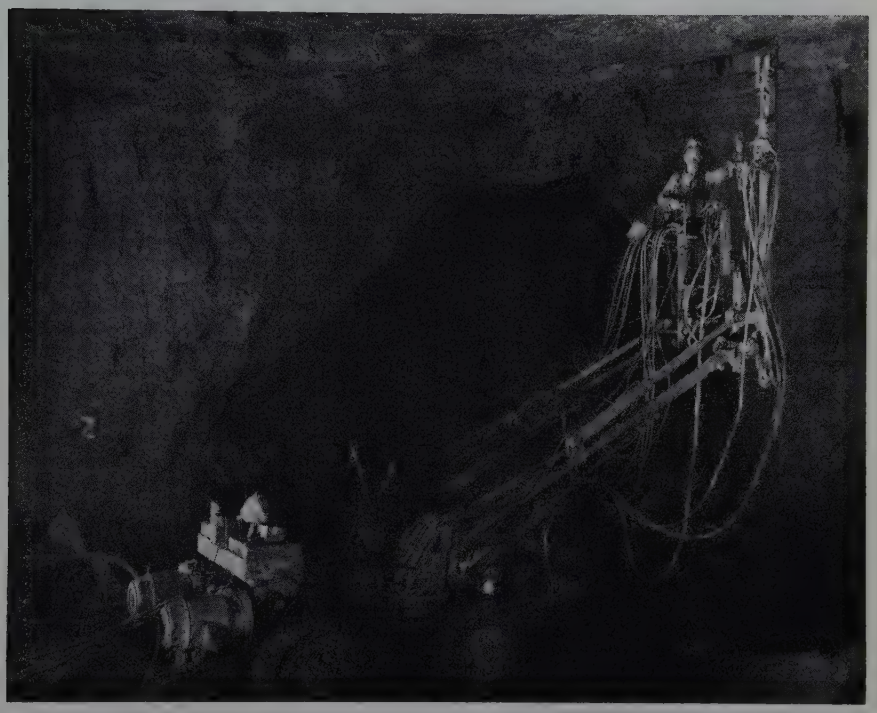

Fig. 2—Drillmobile modified for roof bolting.

by JOHN J. REED

The mines of southeast Missouri's Lead Belt have been in operation since 1864, almost 100 years. During this period about 10 pct of the total ore available has been left in place as pillars, and this now represents the best ore reserve left to the older mines.

St. Joseph Lead Co. has been investigating various plans of pillar recovery for several years. The example to be described is only one possible approach under a specific set of conditions. Conditions vary greatly in the different areas within the Lead Belt, and the same approach would be entirely inadequate in certain other areas, but there are important sections where this system is clearly applicable.

Horizon mining is practiced in the Lead Belt, and stopes may vary from 10 ft to well over 100 ft high. Fig. 1 is a plan view of 6100 stope, the area to be discussed. For these mines this is a small stope, only 10 to 12 ft high.

J. J. REED, Member AIME, is Head Mine Research Engineer, St. Joseph Lead Co., Bonne Terre, Mo. TP 4811A. Manuscript, Dec. 10, 1958. Mid-America Minerals Conference, St. Louis, October 1958. AIME Trans., Vol. 214, 1959.

Before any plans were drawn up for pillar recovery, three independent estimates of the pillar grades were made by the mine superintendent, the mine captain, and the mine geologist. After these results were averaged, pillars indicated to be of economic grade were marked for removal as shown. At this stage several alternatives were considered: 1) retreat with caving, 2) concrete replacement pillars, and 3) systematic bolting and retreat.

A retreating system with caving was not chosen because the roof was known to be too bad even to permit loading a blasted pillar before caving would begin. Concrete replacement pillars would have been too costly and would have required a large crew, bulky materials, and unwieldy equipment. Systematic bolting was chosen as being most acceptable for the following reasons:

1) Limited area and spans were involved.

2) Only minor modifications to the jumbo would be required for bolting.

3) Only a two-man bolting crew would be needed.

4) Only compact bolting materials would be required.

5) The bolting plan could be modified to allow

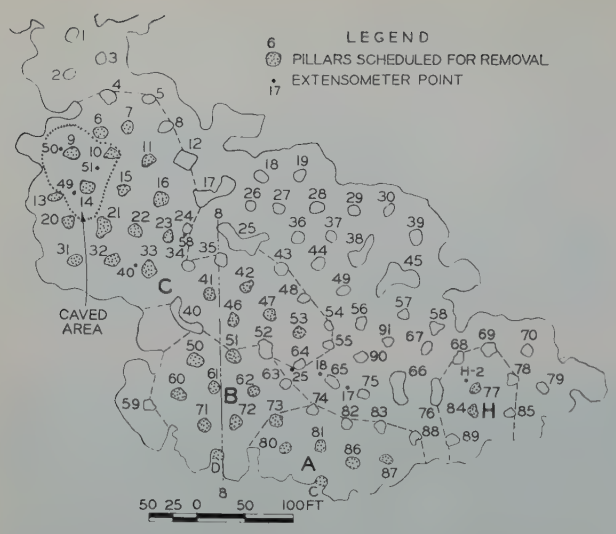

Fig. 1—Baker 6100 stope. Plan view of pillar removal.

for varying roof conditions and degrees of permanence in bolted roof.

EQUIPMENT

The only unusual equipment needed for this project was a roof-bolting jumbo. A rubber-tired, electric stope jumbo was modified as shown in Fig. 2. With this unit, now capable of bolting roof 25 ft high, two men can place about thirty 7-ft bolts per shift. Headed, ¾-in. high-strength bolts were used with an expansion shell anchorage. The holes were drilled with a pneumatic drill and the bolts tightened with a pneumatic impact wrench that has an automatic cutoff at any desired torque. The wrench is mounted on an air cylinder feed which pushes the bolt up into the hole and holds the wrench while tightening. Drill and wrench are mounted on one boom of the jumbo, and an operator's basket is mounted on the second boom. A standard torque wrench with a range of 0 to 350 lb-ft was used to spot check a few bolts periodically.

The pillars were drilled with the same jumbo used for bolting and blasted with millisecond delays. A Joy loader was used to load into a shuttle car, which transferred the rock to rail cars. A diesel bulldozer was used for clean-ups.

INSTRUMENTATION

Because this pillar removal was an experiment, and no past experience could give assurance as to what might be expected, quantitative measurements in the area affected were very important as safety indicators. The instruments used in making these measurements will be described here, because they are not widely used in the mining industry.

Convergence Extensometer: Two types of extensometers have been developed to measure total convergence in a vertical direction. The tube extensometer (Fig. 3) consists of two telescoping tubes of stainless steel with a dial gage at the top which measures convergence directly to 0.001 in. This unit will measure in stope heights from 9 to 16 ft. It has two basic limitations: 1) Because the dial gage is at the top, a ladder is required for accurate readings above 10 or 12 ft. 2) The tubes are unwieldy and inaccurate above 16 to 18 ft. For these reasons, the tape extensometer shown in Fig. 4 has been developed. On this instrument enough steel tape is stored on a reel to reach any desired height. This tape is drilled with small index holes at intervals of 0.3 ft and is rigidly pinned where desired. The entire *constant* weight of the instrument tensions this upper tape. The lower tape is a fixed length that will place the instrument at eye level. This tape is hooked in a floor station, passes through a guide slot and over a pulley, and is rigidly pinned to the square central sliding frame, which is further counterweighted with two lead blocks as shown. Thus the lower tape is also under a *constant* tension, with no springs involved. The relative motion between the main frame and the sliding frame is equal to the total convergence and is read on a dial gage with a range of 4 in. Indicated accuracy of this instrument is ±0.003 in., since it is inherently less precise than the tube extensometer in the low ranges. However, the accuracy is adequate for the actual convergences of 0.050 to 1.000 in. being measured. These extensometers are the most useful instruments in the collection. In all, about 70 extensometer stations were placed and measured in 6100 stope. Probably 30 would be sufficient for operating purposes only.

Warning Lights: These lights (see Fig. 5) immediately warn of any convergence in a working area. They consist of two spring-loaded telescoping tubes, a micro-switch, and a flashlight. The tubes are adjustable in various stope heights, and the microswitch can be adjusted so that a convergence of only a few thousandths of an inch is enough to turn on the light. Several of these warning lights were always placed around the stope during noisy activities such as drilling or loading.

Seismetron: This device consists of a very sensitive borehole type of geophone connected to a powerful amplifier. The theory of the equipment, and the detection of microseismic noises in connection with predicting rock failure, were developed by the USBM's Applied Physics Branch under Leonard Obert.[1,2] Most miners can recall the audi-

Table I. Physical Properties of Rock, Baker 6100 Stope

Sample	Compressive Strength, Psi,* (1⅛x2¾-In. Core)	Young's Modulus, Psi	Tensile Strength, Psi*
1	23,400	5,000,000	1,240
2	—	—	890
3	26,050	5,000,000	1,590
4	43,800	6,000,000	1,410

* Average of three samples each.

Table II. Pillar Recovery Results in Baker 6100 Stope

	Baker Mine, 1957 Average	Area A	Area B	Area C	Area B + C
Ore loaded, tons		707	725	2,988	3,713
Grade, assay*	1	2.4	2.8	2.7	2.75
Cost per ton*†	1	3.66	2.22	2.08	2.09
Cost per lb lead*†	1	1.58	0.82	0.79	0.79
Area bolted, sq ft		12,125	12,950	43,550	56,500
Area bolted per ton		17.2	17.9	14.6	15.2
Estimated tons				2,824	
Explosive consumption, lb per ton	0.49§			0.33	

* All these values have been reduced to ratios in order to reduce the Baker mine figures to unity.
† These are costs of ore on the ground, but not loaded.
§ Consumption for first six months of 1958.

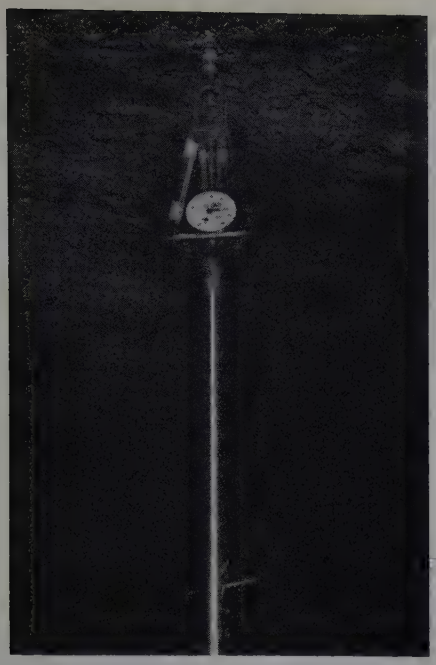

Fig. 3—Tube extensometer.

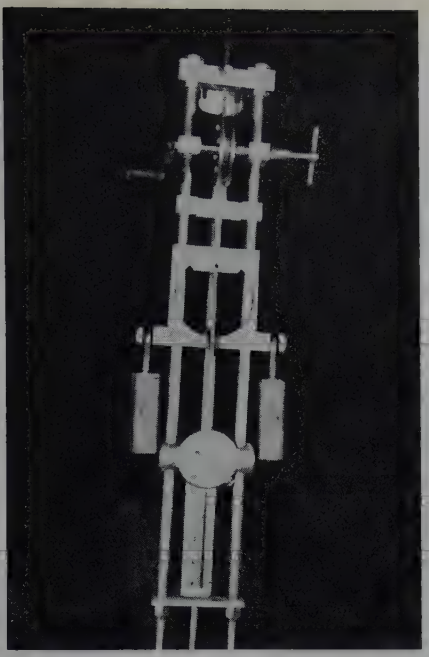

Fig. 4—Tape extensometer.

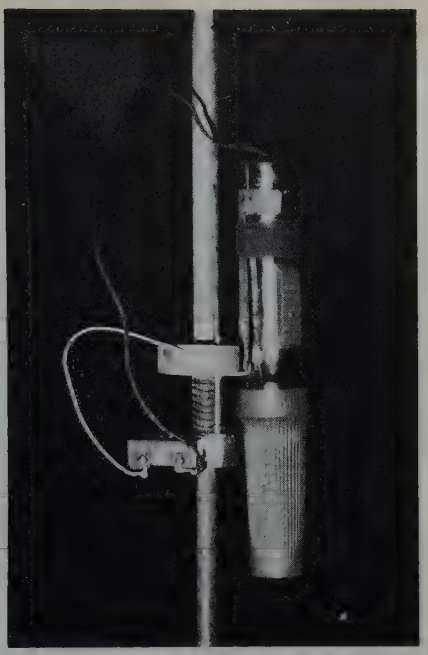

Fig. 5—Convergence warning light.

ble pops and cracks produced by the *working* of heavy ground. There is also a preliminary period during which sub-audible noises are emitted at an increasing rate as the load is applied. The seismetron[3] permits these noises to be heard and recorded at so many counts per minute.

Whittemore Strain Gage: The standard mechanical strain gage, used regularly by civil and mechanical engineers, has a gage length of either 2 or 10 in. The gage used by St. Joseph Lead has a length of 20 in. to straddle more of the inconsistencies of the rock being measured for strain. Stainless steel reference points are placed in countersunk holes as shown in Fig. 6, and the Whittemore gage measures the relative motion between the points to the nearest 0.0001 in. Its dependability and value are limited when measuring the compression in a rough rock pillar, because the reference points are anchored in a surface layer of rock which is probably loose and stress-relieved.

Roof Bolt Compression Pads: These devices, made by Goodyear Rubber, consist of two steel plates ⅜ in. thick with ⅜ in. of rubber vulcanized between them. They have a hole through the center to take the bolt, and in use they replace the normal bearing plate under the head of the bolt. Under load the rubber squeezes out between the plates, and its circumference is measured with a calibrated gage.

PLAN OF THE EXPERIMENT

To refer again to Fig. 1, it was decided to test-bolt in a small preliminary area before determining what to do in the rest of the stope. Area *A*, of limited span, was to be bolted very conservatively on 4-ft centers with 8-ft bolts, the most common length used in the mines. Before bolting began, 17 bolt-pulling tests were made in the same area to establish optimum installation specifications. Consistent results indicated that best anchorage would be obtained by the highest possible initial torque, which was set at 250 ± 25 lb-ft for all bolting in this stope. These pull tests were later substantiated by pulling 11 more bolts in the other end of the stope.

Theoretically, this torque corresponds to a bolt tension of about 16,000 lb, but the average initial tension indicated by 15 roof bolt compression pads was about 9000 lb. This discrepancy is believed due to galling of the bolt ears in the base of the shell, torque and spring in the unusually long bolts, and perhaps a tendency to bounce and kick back in the pad itself. This problem will be investigated further.

RESULTS

Pillars 80, 81, 86, 87 of area *A* and breast pillar *C* in Fig. 1 were removed after the area was completely bolted with 7 and 8-ft bolts on 4-ft centers. The maximum convergence measured in the center of the area was 0.142 in. The microseismic count increased to 20 to 30 cpm for a few hours after blasting but within 24 hr returned to the normal background level of 1 to 5 cpm. Fifteen roof bolt compression pads installed between pillars 86, 87,

Fig. 6—Whittemore strain gage.

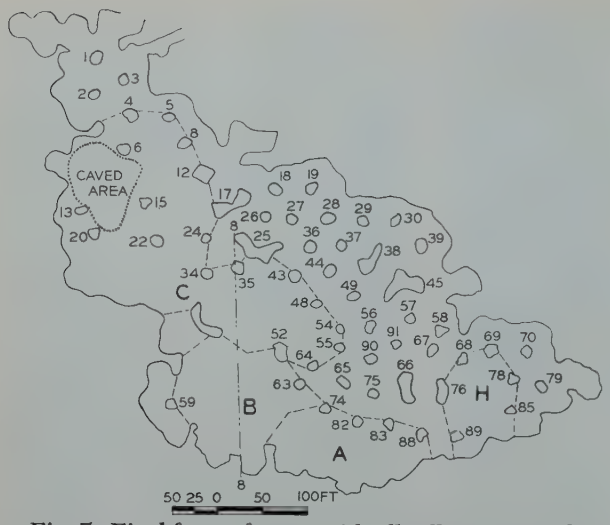

Fig. 7—Final form of stope with all pillars removed.

and 88 showed an average increase in load of 410 lb per bolt after one week and 720 lb per bolt after 7 weeks. When the entire 6100 stope project was completed about seven months after the first pillars in area *A* were removed, average indicated bolt load was 1220 lb per bolt above the installation load of about 9000 lb.

After the pillars were removed in area *A*, pillars 77 and 84 were blasted in area *H* without any preliminary bolting to give a basis of comparison. Extensometer station *H-2*, adjacent to pillar 77, showed a convergence of 0.212 in. 24 hr after blasting and 0.232 in. at 48 hr. The roof was too loose and dangerous to work under, so the rock from these two pillars was never loaded. During the 10 months since these pillars were blasted, 2 to 3 ft of roof have fallen over most of area *H*.

In view of the good results, area *B* was bolted on 5-ft centers. The first pillars blasted in this area were numbers 61, 71, 72, and *D*, which caused a convergence of about 0.081 in. in area *B* but had little effect on area *A*. However, when the two areas were joined by blasting pillars 62 and 73, maximum convergence amounted to 0.166 in. in area *A* and 0.118 in area *B* and the convergence spread outward beyond the barrier pillars 63, 74, and 82. Four hours after pillars 62 and 73 were blasted, the microseismic count was 50 to 60 per min and 24 hr later was still 35 to 45 per min. During this period boundary pillars 63, 74, 82, 64, and 65 showed signs of failure, with cracks and small slabs popping off. After four days the pillar activity had ceased, and the microseismic count was down to 10 to 15 per min. After eight days all activity had stopped, and the count was down to a normal background level of 1 to 5 per min. It is significant to note that during this period of pillar compression, extensometer stations 17, 18, and 25, in the *second row* of barrier pillars, showed convergences of 0.010 in., 0.019 in., and 0.015 in.

With the experience gained in areas *A* and *B*, it was decided to bolt the remainder, area *C*, on 5-ft centers and remove all the rest of the pillars in as rapid and continuous an operation as possible. It took a two-man crew about three months to bolt area *C* and drill the pillars, which were then blasted and loaded in about three weeks.

In discussing convergence as measured and reported here, it is important to note that what is observed is *total* convergence, which actually consists of three parts: 1) roof sag, 2) floor heaving, and 3) compression in the remaining pillars.

Roof sag is probably the largest component and certainly the one of most concern. Pillar compression can also be appreciable, as evidenced by some of the data available here. Average maximum convergence at stations 17, 18, and 25, which presumably was largely pillar compression, was 0.046 in., approximately 13 pct of average convergence measured in adjacent areas of pillar recovery (about 0.360 in.). Also, station 58 was placed only 1 ft from pillar 24 and showed a convergence of 0.127 in., or 42 pct of the total convergence of 0.301 in. measured at station 40.

Bolting in area C was planned to permit progressive pillar removal until there was failure due to excessive unsupported spans. This finally was caused by locally jointed ground and very poor bolt

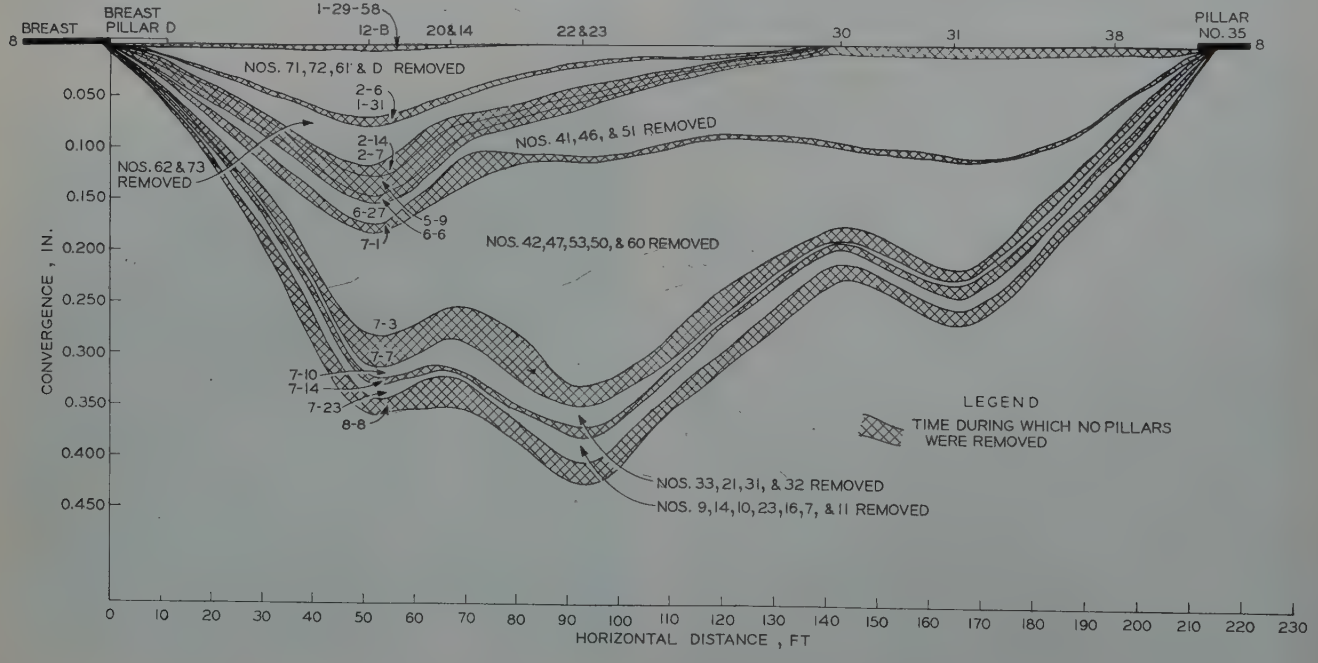

Fig. 8—Vertical section 8-8 showing convergence due to pillar removal compared with that due to time alone.

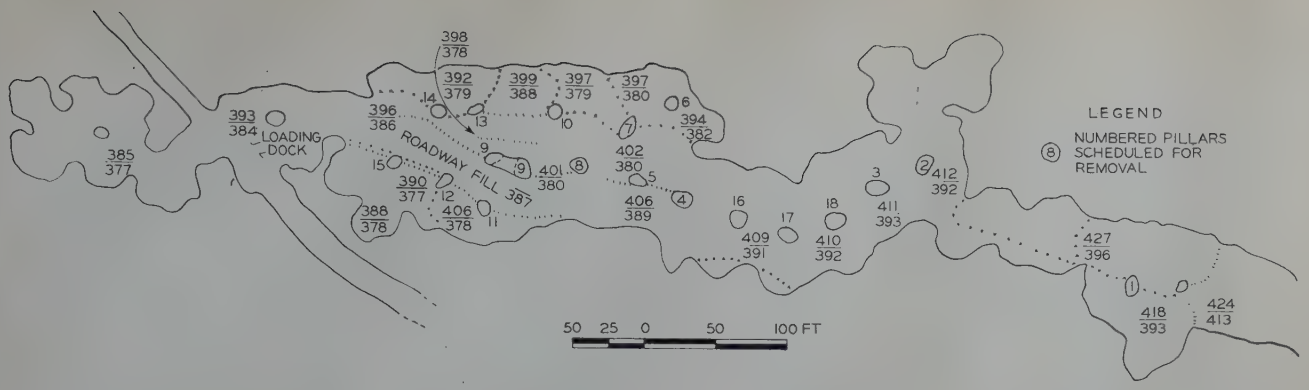

Fig. 9—Portion of stope 40L400, Leadwood South mine. Stope configuration adapted to pillar recovery by roof bolting.

anchorage in the area of pillars 9, 10, and 14, as indicated in Fig. 1. Pillars 31, 32, 33, and 21 had been removed when pillars 9 and 14 were blasted. There were no visible signs of failure at this time, and no audible sounds of the roof or pillars working, but during the two days which followed, when no further blasting was done, instruments showed that failure was imminent. Stations 50, 51, and 49 showed 0.385 in., 0.485 in., and 0.849 in. of initial convergence, which continued at about 0.005 in. per hr. Warning lights in the area turned on about every 15 min, and a microseismic count taken with the probe in pillar 10 gave about 30 cpm, with extra-strong continuous background noise. Immediately after pillar 10 was blasted, at the end of the second day, the microseismic noise became almost continuous, and there were frequent loud sounds of rock failure. Within 16 hr the area indicated in Fig. 1 had caved over the 8-ft bolts to a height of some 15 ft. This meant that most of the rock from pillars 9 and 10 was not recovered, and to limit the caving pillars 6, 15, 22, 13, and 20 were not blasted. Fig. 7 shows the final form of the stope with all the pillars removed.

Fig. 8 is a typical vertical section marked 8-8 in Figs. 1 and 7. This section shows the effect of time on stope convergence after pillar removal and emphasizes the importance of moving through an area and out of it as rapidly as possible once pillar removal has begun.

Table I gives the results of a few tests made to determine physical properties of the rock from Baker 6100 stope, and Table II summarizes final results of the experiment in pillar recovery in this stope. In Table II the value for "area bolted per ton" can be further refined to give "area bolted per lb lead." This figure is a valuable characteristic of any specific stope area and is constant regardless of cost price of lead. It can be used for comparisons, therefore, in deciding which stope should be most profitable for pillar recovery. At any time this value can be multiplied by the *current* cost of bolting and the result compared with the *current* price of lead to determine whether or not pillar recovery in a specific area can be profitable.

CONCLUSIONS

1) Systematic roof bolting will safely permit pillar removal in limited areas.

2) Although the cost of pillar ore produced in this way is relatively high, when the method is applied to the better grade pillars the cost of lead produced is still lower than that of the average new ore now available.

3) High-strength, ¾-in. headed bolts with expansion shells are equal or superior to presently used 1-in. slotted bolts, and much cheaper.

4) Roof bolting with a relatively simple bolting jumbo can raise the efficiency of present bolting efforts about five times.

5) Reasonable stope convergence and pillar loading can be detected and measured dependably by means of the extensometer, seismetron, and warning lights. General instability of the mine structure is quickly detectable by any or all of these instruments, although they are no substitute for experience and a scaling bar on small local areas of loose roof.

FUTURE PLANS

Fig. 9 shows the stope configuration specifically adapted to this type of pillar recovery by roof bolting. In this stope the ratio of area bolted to pillar ore (estimated) is 14.4 sq ft per ton. Systematic bolting also facilitates removing a limited number of high grade pillars in any large area, but the method is definitely limited and is not the answer to 100 pct recovery over large areas.

In the Lead Belt's very large pillar areas, some recovery method on the retreat with caving appears the only logical approach. But the roof rocks are not, in general, the type that will cave gradually or predictably, and it is thought that a form of induced caving to periodic lines of roof bolts might be employed. The situation is further complicated by towns on the surface only 200 to 500 ft over many of the mine areas. In these cases, delayed sand fill after initial caving has been considered as a possible means to control surface subsidence.

The author expresses appreciation to the St. Joseph Lead Co. for permission to publish this article, and to R. L. Bullock, J. J. Yancik, C. D. Mann, and Lee Bilheimer of the mine research department for the field work and preparation of drawings.

REFERENCES

[1] L. Obert and W. I. Duvall: The Microseismic Method of Predicting Rock Failure in Underground Mining. Part I. General Method. *USBM R.I. 3797*, 1945.
[2] L. Obert and W. I. Duvall: The Microseismic Method of Predicting Rock Failure in Underground Mining. Part II. Laboratory Experiments. *USBM R.I. 3803*, 1945.
[3] How You Can Predict Rock Falls. *Engineering and Mining Journal*, December 1955.
[4] R. H. Merrill: Design of Underground Mine Openings, Oil-Shale Mine, Rifle, Colo. *USBM R.I. 5089*, 1954.
[5] R. H. Merrill: Roof-Span Studies in Limestone. *USBM R.I. 5348*, 1957.
[6] R. H. Merrill and T. A. Morgan: Method of Determining the Strength of a Mine Roof. *USBM R.I. 5406*, 1958.
[7] C & H Develops New Uranium Mine Through Long Flat Incline. *Mining World*, April 1958.

Discussion of this article sent (2 copies) to AIME before Aug. 31, 1959, will be published in MINING ENGINEERING.

METEOROLOGICAL INFLUENCE ON RADON CONCENTRATION IN DRILLHOLES

by ALLAN B. TANNER

The effects of radon in drillholes on gamma-ray logs have been described by L. S. Hilpert and C. M. Bunker.[1] Since these effects may cause drastic error in the evaluation of uranium deposits, it is useful to know the conditions under which significant amounts of radon tend to accumulate in drillholes. In the studies described here, atmospheric conditions were found to dominate in the control of the behavior of radon in drillholes in the vicinity of a uranium orebody.

The site of the investigation was in McKinley County, New Mexico, about 12 miles north of Grants. Drillholes of 4¼-in. diam, on 25-ft and 100-ft centers, penetrate ore in dry rock at a depth of about 100 ft. A geologic log of the drillhole of primary interest is shown in Fig. 1. Gamma-ray logs revealed three zones of ore-grade mineralization in the Todilto limestone. A 6-ft zone, the lowest of the three, assayed 0.20 pct U_3O_8 by chemical analysis. The limestone ores in this area contain disseminated uraninite and some yellow and orange secondary minerals.

Only radon^{222}, a member of the uranium^{238} series, was measured in this investigation. Radon is one of the chemically inert noble gases and is radioactive by alpha particle emission with a half life of about four days. In this discussion, amounts of radon are expressed in microcuries (1 microcurie equals 37,000 disintegrations per sec) and concentrations of radon are expressed in microcuries per liter of drillhole air.

Samples of air were obtained by lowering a sampling device (Fig. 2) into a drillhole and actuating the device at the desired depth. It was then raised to the surface and the sample was transferred to a storage tube. Within two days the sample was transferred to an ionization chamber, and the activity of radon and its short-lived daughter products was measured at radioactive equilibrium with a vibrating-reed electrometer. The measurements were corrected back to the time of collection and involve errors estimated generally not to exceed +5 pct to −15 pct.

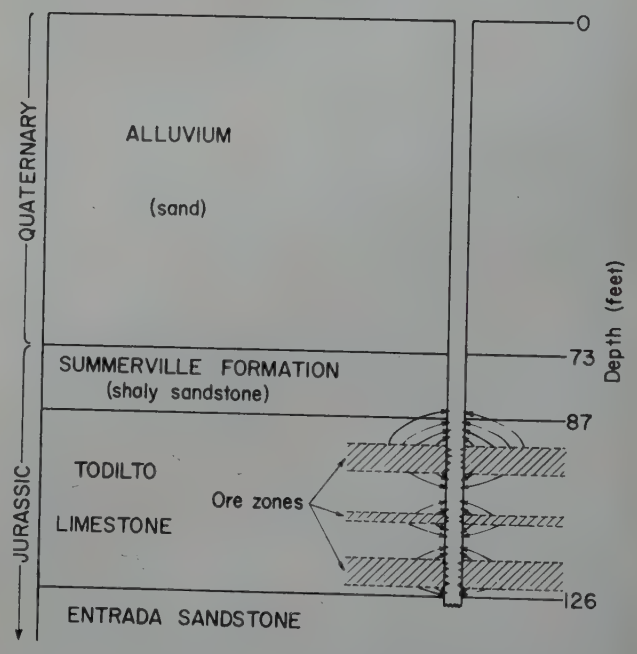

Fig. 1—Probable paths of radon movement in drillhole.

Radon Behavior in a Covered Hole: Fig. 3, a typical log of radon concentration vs depth in the covered drillhole, was made by using values of radon concentration at discrete depths. Continuous logs of alpha-particle radiation in the drillholes showed that such radon logs depict the continuous variation of radon concentration with depth quite accurately. Three features of radon logs were noted: 1) maximum

A. B. TANNER is a Geophysicist with the Geophysics Branch of the U. S. Geological Survey, Salt Lake City. TP 4804L. Manuscript, Nov. 28, 1958. New York Meeting, February 1958. AIME Trans., Vol. 214, 1959.

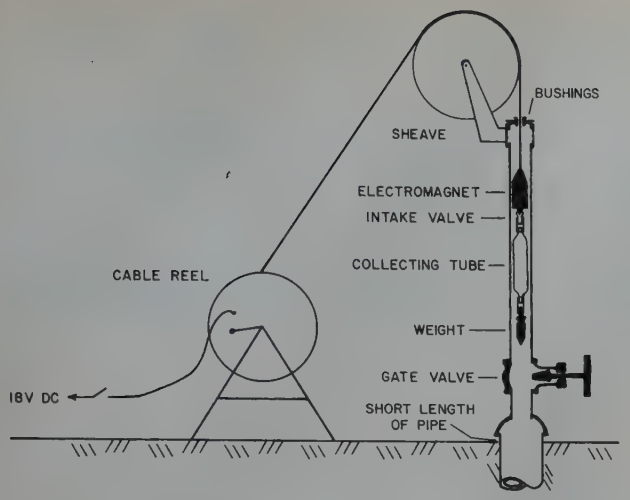

Fig. 2—System for sampling air in drillholes.

concentration, 2) depth corresponding to the maximum concentration, and 3) total amount of radon in the hole. Maximum concentration and its corresponding depth were found by inspection of the log. Total amount of radon in the hole was found by making a graphical summation of the area under the curve of radon concentration vs depth and making the appropriate dimensional conversion. All three features changed considerably from day to day.

Fig. 4 is a plot of atmospheric pressure and the total radon content of the covered hole vs time. Cross hatching marks two periods when the cover was removed in order to determine the effect of moderate wind on the radon content of the hole. For several months before and during the other parts of the 20-day investigation of this hole it was covered. The meterological data for the period were obtained from continuous-recording instruments housed only a few feet away.

Symmetry is evident between the curve of atmospheric pressure vs time and the curve of total radon content vs time. The total radon-content curve appears to be approximately a mirror image of the pressure curve, suggesting an inverse relation between the two quantities. After inversion and scale change, the total radon-content curve has the shape of the upper dashed line on Fig. 4. To facilitate comparison of the curves the lower dashed line has been drawn, showing the relative pressure changes between series of radon measurements. The curves closely parallel each other for eight of the nine intervals between measurements.

Although the results in Fig. 4 show a fairly consistent relation between changes in atmospheric pressure and changes in total radon content of the hole, it must be noted that strict inverse proportionality between pressure and total radon content was not observed. At four different times when the atmospheric pressure was 601 mm of mercury, the values for total radon content were 129, 103, 86, and 148 microcuries. The inferences drawn from these data seem to be valid for day to day changes only.

During the periods shown by cross hatching on Fig. 4, the covering system was removed. The first period was 1 hr, during which 26 miles of air passed the wind-measuring instrument at a height of 6 ft. Analyses of air from the hole before and after the exposure to wind indicated a drop in total radon con-

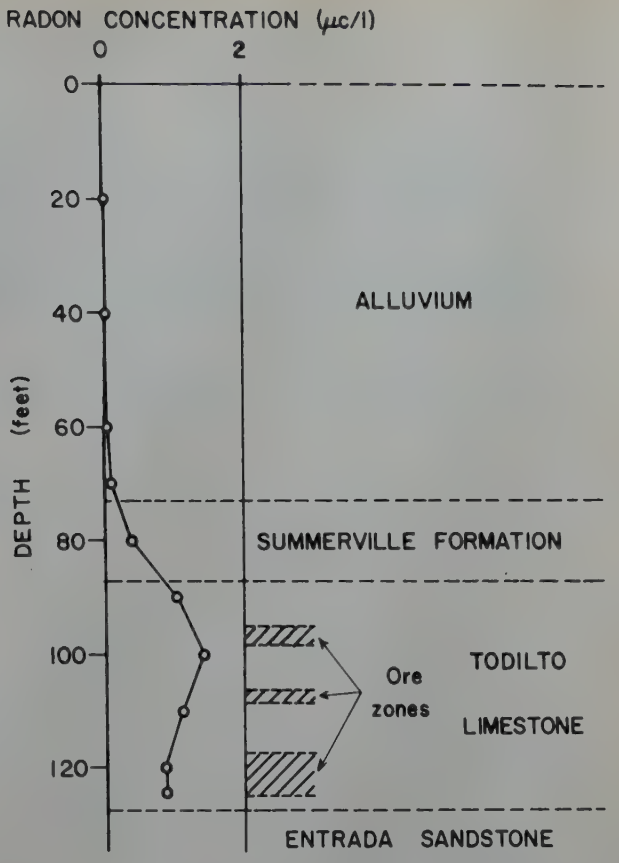

Fig. 3.—Typical log of radon concentration.

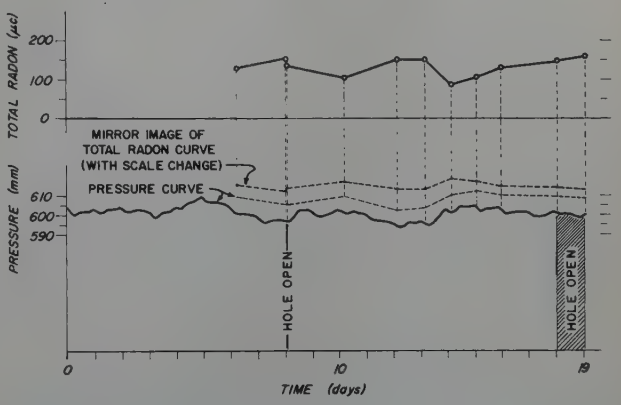

Fig. 4. Radon variation in covered hole.

tent from 153 to 134 microcuries. The second period was 24 hr, during which 118 miles of air passed the wind-measuring instrument, the wind speed averaging 14 miles per hr for the last 4 hr. During this latter period the wind did not greatly affect the total radon content, which increased from 148 to 160 microcuries, coincident with a drop in atmospheric pressure. There was marked reduction in radon concentrations to a depth of 60 ft as a result of the wind. Radon concentrations at depths of 80 ft and greater were not diminished.

No relation was observed between surface temperature or wind direction and any of the characteristics of the radon logs. Because wind velocity and temperature extremes were relatable, days on which only temperature characteristics varied were not found. Calculation shows that the maximum

effect of temperature change upon radon concentration through thermal expansion or contraction could not have been more than 8 pct, however, and probably not more than a few percent, in contrast with the changes by factors of two or more that were actually observed.

Mechanism of Radon Migration: Experimental evidence and theoretical treatment of the migration of radon have led to the conclusion that diffusion is not the mechanism whereby large amounts of radon migrated from uraniferous rock into drillholes. The observations of radon behavior in the covered hole indicate that surface temperature and light to moderate winds did not affect significantly the amount or the distribution of radon in the hole but that decreasing atmospheric pressure tended to cause an increase in the amount of radon in the hole, and conversely. If this relation is true, the mechanism whereby radon tended to migrate into and out of the drillhole is easy to deduce. The ore-bearing limestone undoubtedly has some minor porosity, some of which is interconnecting. In addition to this minor porosity and permeability of the unfractured rock, numerous fractures and silty layers are known to exist in the rock and may be assumed to add appreciably to its overall permeability and porosity. There should be, then, an air reservoir in the ore-bearing rock, into which radon is emanated at a constant rate from its radium parent in the ore. Under the influence of decreasing atmospheric pressure, transmitted through the drillhole and along paths of greatest permeability, the air in the reservoir should expand, moving into the hole and carrying radon with it. Once in the hole, the influent air should mix with the air already in the hole and produce a larger amount of air with a lower radon concentration. An increase in atmospheric pressure should result in the movement of air—with only part of the undecayed radon in the hole—back into the rock. A similar phenomenon, the movement of air from rock into tunnels, has been observed in mines and has been called earth breathing. The path of movement of air to the drillholes is not definitely known, but the characteristics of variation in radon concentration suggest the flow paths shown in Fig. 1. The relative stability of radon concentration from the lower part of the ore horizon downward indicates most of the flow to be in the upper part of the ore horizon or from the upper surface of the ore into the overlying Summerville formation and thence into the drillhole. The path cannot be uniquely resolved from the evidence available.

Radon Behavior in an Open Hole: Several other drillholes were investigated. A more limited series of analyses was made on air samples from one of these holes, which was always open. There was much greater variation in radon behavior in this hole than in the one first described. Radon concentrations at given depths in the hole varied by as much as 4½ orders of magnitude. The depth corresponding to the maximum concentration was sometimes at surface and sometimes at the ore horizon. Total radon in the hole varied between 220 microcuries and 0.5 microcurie. Wind speed and atmospheric pressure both appear to have had important effects on the behavior of radon in the hole. The most noticeable of these effects was a great reduction in the amount of radon in the hole on a day of strong wind—in one day the amount of radon decreased from about 200 microcuries to 0.5 microcurie. Assuming that the relation between total radon and atmospheric pressure inferred for the covered hole was true for the open hole also, part of the decrease in total radon was probably due to an observed rise in atmospheric pressure. It is unlikely that pressure change alone was responsible for the decrease, as a similar rise in atmospheric pressure on another day was not accompanied by such a great decrease in total radon. It is believed that the wind, blowing over the open hole from 4 to 6 hr at 25 to 35 mph, was more effective than the increase in pressure in reducing the total amount of radon in the hole by the observed factor of about 400.

Three possible mechanisms are suggested for the reduction in radon content of the hole by strong wind. The first of these is that this drillhole, combined with underground flow channels and other drillholes, acted as a venturi tube system of some sort and that minor pressure differentials arose because of the relief of the ground into which the holes were drilled and over which the wind was moving. Considering the relative planeness of the ground, this possibility does not seem likely. The second possibility is that the strong wind caused turbulence in the drillhole that accelerated dilution of the drillhole air by air from the surface. The third possibility is that the wind was strong enough to excite the air column in the hole as in a closed organ pipe having a fundamental frequency of two to three cycles per second. Considerable turbulence would arise with such oscillations in an irregular drillhole and would promote diffusion of radon through the air in the hole more rapidly than under quiescent conditions.

Since the wind speed was appreciably higher at the open hole on the windy day than during the 24-hr period when the covered hole was uncovered, the lack of evidence of great reduction in total radon in the covered hole during that period does not necessarily contradict the inference that strong winds were capable of greatly reducing the radon content of drillholes. Light and moderate winds do not appear to have had much influence on radon concentrations in the open hole, even near surface, as the maximum concentration, seven orders of magnitude greater than that usually found in the atmosphere, was observed at the surface over a hole on a day when winds were 5 to 10 mph. As with the covered hole, no relation was noted between surface temperature and radon behavior in the open hole.

Acknowledgment is made to F. O. Manol and I. Rapaport of Four Corners Exploration Co. and to E. B. Butts, A. W. Callahan, and P. Melancon of Holly Minerals Corp. for furnishing information about the drillholes. The Grants Airway Communications Station of the Civil Aeronautics Administration, Department of Commerce, furnished some of the meteorological data. R. H. Barnett, of the USGS, developed the apparatus used to obtain continuous logs of alpha-particle radiation in the holes. This work was performed by the USGS in behalf of the Division of Research of the U. S. Atomic Energy Commission.

REFERENCE

[1] L. S. Hilpert and C. M. Bunker: Effects of Radon in Drill Holes on Gamma-Ray Logs: *Economic Geology*, 1957, vol. 52, pp. 438-455.

Discussion of this article sent (2 copies) to AIME before Aug. 31, 1959, will be published in MINING ENGINEERING.

THORIUM AND URANIUM RESOURCES IN MONAZITE PLACERS OF THE WESTERN PIEDMONT, NORTH AND SOUTH CAROLINA

by WILLIAM C. OVERSTREET, PAUL K. THEOBALD, JR., and JESSE W. WHITLOW

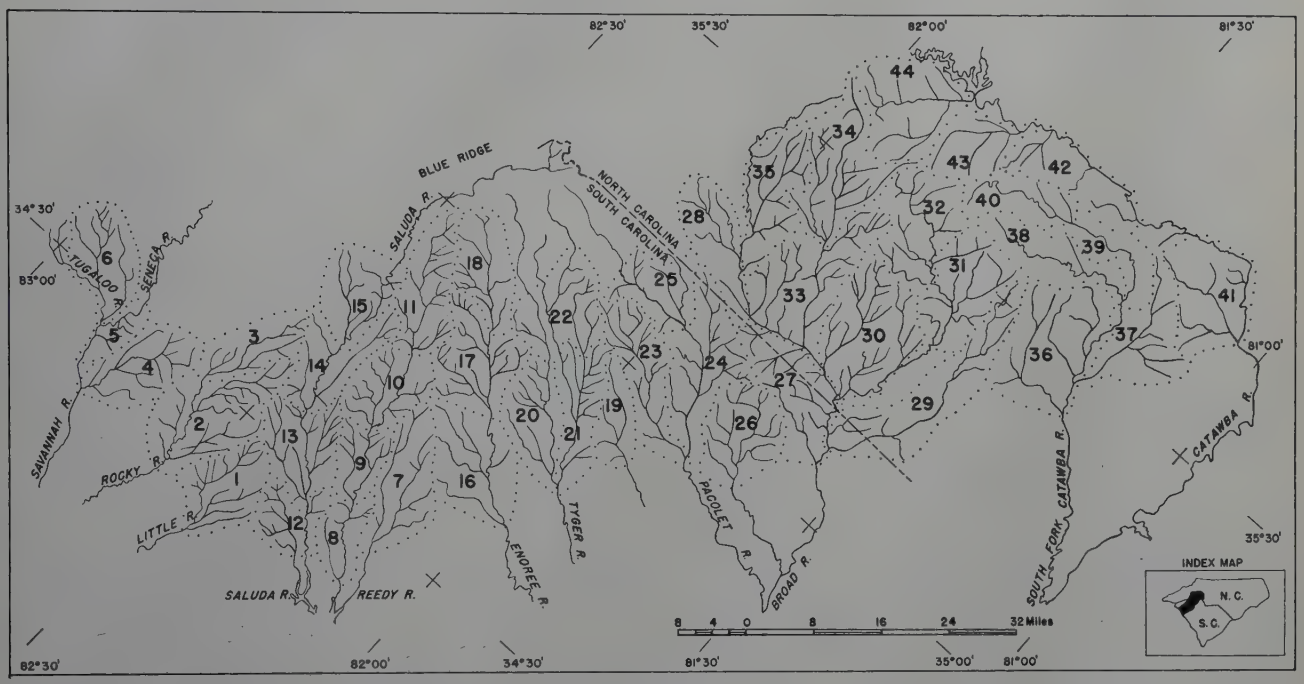

Fig. 1—Locations of the 44 drainage basins appraised for placer monazite between the Savannah and Catawba rivers, S. C. and N. C. Numbers in outlined areas correspond to those preceding drainage basins in Tables IA-ID.

Monazite placers in a region of the Carolinas explored in 1951-1954 by the USGS are estimated to contain at least 53,000 short tons of thorium and 4600 short tons of uranium. None of these deposits is being mined.

The 5200-sq mile area investigated extends northeast along the western Piedmont from the Savannah River in South Carolina to the Catawba River in North Carolina. Much of the region is 700 to 1100 ft above sea level. Gentle hills and broad interfluves give a local relief of 100 to 200 ft. This increases to 1700 ft at the west margin of the area where the east flank of the Blue Ridge is approached in South Carolina and the South Mts. are entered in North Carolina.

This report is restricted to placers in the Piedmont. Monazite deposits in the Blue Ridge and coastal plain were not covered by the investigation.

W. C. OVERSTREET; P. K. THEOBALD, JR.; and J. W. WHITLOW are, respectively, with the U. S. Geological Survey in Beltsville, Md.; Denver, Colo.; and Knoxville, Tenn. TP 4807H. Manuscript, July 10, 1958. AIME Trans., Vol. 214, 1959.

Monazite Mining in the Carolina Piedmont: Discovered in 1879 by W. E. Hidden,[1] the monazite placers in the Carolina Piedmont were first mined in 1886. The area was a major world source for thorium and the lanthanides until 1895, when Brazilian monazite entered the trade. Total output from the Carolina Piedmont has been nearly 5500 tons of monazite,[2] but the placers have been idle since 1911, except for 48 tons produced between 1915 and 1917.

Monazite mining was revived in the Carolinas in 1954 when a dredge operated by the Heavy Minerals Co. opened a fluviatile placer along Horse Creek in the coastal plain near Aiken, S. C.

Geology and Mineralogy: Two recent papers[3, 4] have described the geology of the monazite placer district in the Piedmont between the Savannah and Catawba rivers; the general geology of the region has been reviewed by P. B. King.[5] These reports show that the placers are in locally derived alluvial sediments that cover the floors of shallow, narrow valleys in an area underlain by monazite-

Table I. Volume, Composition, and Tenor of Alluvium and Resources in Monazite in Tributary Drainage Basins

IA River Basins	Estimated Volume of Sediment Explored, Million Cu Yd				Tenor, Lb per Cu Yd				Estimated Resources in Monazite, Million Lb			
	Clay	Silt and Sand	Gravel	Total	Clay	Silt and Sand	Gravel	Weighted Average	Clay	Silt and Sand	Gravel	Total
Savannah River, S. C. (Appraised by D. W. Caldwell, 1952-1953)												
1. Hogskin Creek and other tributaries to Little River, Anderson and Abbeville counties, S. C.	9.15	13.56	2.30	25.01	0.3	1.5	2.8	1.2	3.24	20.93	6.36	30.53
2. Broadway Creek and other streams entering Rocky River, Anderson County, S. C.	20.92	35.47	5.94	62.33	0.1	0.6	0.8	0.5	2.72	22.49	4.96	30.17
3. Big Beaverdam Creek, Anderson County, S. C.	19.77	27.43	3.19	50.39	0.01	0.2	0.2	0.1	0.28	4.54	0.75	5.57
4. Big Generostee Creek, Anderson County, S. C.	8.38	32.38	3.65	44.41	0.1	0.5	1.1	0.5	1.06	17.62	4.06	22.74
5. Saddler Creek and small tributaries to Savannah and Seneca Rivers, Anderson County, S. C.	0.99	2.26	0.57	3.82	0.6	2.2	3.7	2.0	0.59	5.07	2.12	7.78
6. Big Beaverdam and Little Beaverdam Creeks, Anderson and Oconee counties, S. C	17.15	28.28	4.79	50.22	0.2	0.6	1.3	0.5	2.64	17.49	6.00	26.13
Totals and averages, basins tributary to Savannah River	76.36	139.38	20.44	236.18	0.1	0.6	1.2	0.5	10.53	88.14	24.25	122.92
Saluda River (Appraised by D. W. Caldwell, 1952-1953)												
7. Rabon Creek, Greenville and Laurens counties, S. C.	20.08	35.57	5.30	60.95	0.1	0.5	0.9	0.4	2.19	18.17	4.80	25.16
8. Walnut Creek and other tributaries to Reedy River, Laurens County, S. C.	1.80	4.02	0.98	6.80	0.1	0.5	1.1	0.5	0.25	2.20	1.05	3.50
9. Horse Creek and neighboring streams joining Reedy River, Greenville and Laurens counties, S. C.	7.18	12.49	1.96	21.63	0.1	0.3	0.8	0.3	0.76	3.59	1.62	5.97
10. Huff Creek and other streams entering Reedy River, Greenville County, S. C.	3.71	11.03	2.19	16.93	0.5	2.3	3.8	2.1	1.93	25.58	8.33	35.84
11. Laurel Creek and adjoining tributaries to Reedy River, Greenville County, S. C.	8.68	17.14	3.71	29.53	0.2	1.0	1.6	0.8	1.87	17.74	5.76	25.37
12. Turkey Creek and other tributaries to Saluda River, Anderson, Abbeville, and Laurens counties, S. C.	4.39	8.68	1.51	14.58	0.2	0.7	1.4	0.6	0.77	6.18	2.08	9.03
13. Broad Mouth Creek and nearby streams entering Saluda River, Anderson, Greenville, Abbeville, and Laurens counties, S. C.	10.56	20.21	3.38	34.15	0.2	1.0	1.8	0.8	2.46	19.97	6.26	28.69
14. Grove Creek and other tributaries to Saluda River, Anderson and Greenville counties, S. C.	10.91	20.37	3.65	34.93	0.07	0.4	0.7	0.3	0.75	7.69	2.66	11.10
15. Big Brushy Creek and adjoining streams tributary to Saluda River, Anderson and Greenville counties, S. C.	8.23	14.37	2.50	25.10	0.02	0.2	0.3	0.2	0.16	2.84	0.85	3.85
Totals and averages, basins tributary to Saluda River	75.54	143.88	25.18	244.60	0.1	0.7	1.3	0.6	11.14	103.96	33.41	148.51

IB River Basins												
Enoree River, S. C. (Appraised by N. P. Cuppels, 1952-1953)												
16. Durbin Creek and other tributaries to Enoree River, Laurens, Spartanburg, and Greenville counties, S. C.	14.41	37.73	3.32	55.46	0.1	0.3	0.6	0.3	1.63	10.76	2.11	14.50
17. Gilder Creek and adjoining streams tributary to Enoree River, Spartanburg, Greenville, and Laurens counties, S. C.	11.27	33.22	4.48	48.97	0.3	1.3	2.5	1.2	3.51	43.97	11.11	58.59
18. Mountain Creek and adjacent streams entering Enoree River, Greenville County, S. C.	6.18	13.74	2.64	22.56	0.1	0.5	1.0	0.4	0.85	6.79	2.68	10.32
Totals and averages, basins tributary to Enoree River	31.86	84.69	10.44	126.99	0.2	0.7	1.5	0.7	5.99	61.52	15.90	83.41
Tyger River, S. C. (Appraised by N. P. Cuppels, 1952-1953)												
19. Beaverdam Creek and other tributaries to Fairforest Creek, Spartanburg County, S. C.	8.07	20.43	3.07	31.57	0.2	0.6	1.1	0.5	1.30	11.26	3.26	15.82
20. Ferguson Creek and other streams tributary to South Tyger River, Spartanburg County, S. C.	13.18	34.10	3.00	50.28	0.1	0.4	0.9	0.4	1.50	14.42	2.83	18.75
21. Junction of North Tyger River, Middle Tyger River, and adjoining streams, Spartanburg County, S. C.	26.82	48.51	3.88	79.21	0.1	0.6	1.1	0.4	3.16	28.26	4.19	35.61
22. Parts of North Tyger River, Middle Tyger River, South Tyger River, and tributaries, Spartanburg and Greenville counties, S. C.	16.13	27.36	2.94	46.43	0.1	0.5	0.8	0.4	1.74	14.55	2.21	18.50
Totals and averages, basins tributary to the Tyger River	64.20	130.40	12.89	207.49	0.1	0.5	1.0	0.4	7.70	68.49	12.49	88.68
Pacolet River, S. C. (Appraised by N. P. Cuppels, 1952-1953)												
23. Lawson Fork Creek, Spartanburg County, S. C.	11.13	31.21	4.03	46.37	0.2	0.8	1.6	0.7	2.35	26.04	6.33	34.72
24. Buck Creek and other tributaries to Pacolet River, Spartanburg and Cherokee counties, S. C.	14.25	47.78	7.27	69.30	0.5	1.4	3.1	1.4	6.75	66.83	22.59	96.17
25. Junction of North Pacolet River, South Pacolet River, and adjoining streams, Spartanburg County, S. C.	20.80	46.05	8.13	74.98	0.08	0.4	0.8	0.4	1.69	19.54	6.47	27.70
Totals and averages, basins tributary to Pacolet River	46.18	125.04	19.43	190.65	0.2	0.9	1.8	0.8	10.79	112.41	35.39	158.59

Table I. Volume, Composition, and Tenor of Alluvium and Resources in Monazite in Tributary Drainage Basins (Continued)

IC River Basins	Estimated Volume of Sediment Explored, Million Cu Yd				Tenor, Lb per Cu Yd				Estimated Resources in Monazite, Million Lb			
	Clay	Silt and Sand	Gravel	Total	Clay	Silt and Sand	Gravel	Weighted Average	Clay	Silt and Sand	Gravel	Total
Broad River, S. C.-N. C. (Appraised by P. K. Theobald, Jr., A. M. White, J. W. Whitlow, and W. C. Overstreet, 1951-1953)												
26. Thicketty Creek, Cherokee and Spartanburg counties, S. C.	21.96	32.20	4.88	59.04	0.3	1.1	2.5	0.9	5.84	36.30	12.40	54.54
27. Cherokee Creek and other tributaries to Broad River, Spartanburg and Cherokee counties, S. C.; Rutherford and Cleveland counties, N. C.	9.28	18.33	2.75	120.03	0.4	2.1	3.3	0.7	4.24	38.04	9.19	85.57
	(a)	(a)	(a)	(b)	(c)	(c)	(c)	(d)	(a)	(a)	(a)	(b)
28. McKinney Creek and other southern tributaries to Broad River, Polk and Rutherford counties, N. C.	2.92	11.20	1.26	15.38	0.07	0.4	0.7	0.5	0.21	4.20	0.89	7.20
					(c)	(c)	(c)	(d)	(a)	(a)	(a)	(e)
29. Buffalo Creek and Boween River, Cleveland and Lincoln counties, N. C.; Cherokee County, S. C.	17.23	70.31	13.47	101.01	0.3	0.9	1.8	0.9	4.92	61.52	24.04	90.48
30. Sandy Run, Brushy Creek, and Beaverdam Creek, Cleveland and Rutherford counties, N. C.	18.04	41.00	6.79	82.20	0.5	2.0	4.1	1.6	8.23	83.82	28.11	132.76
	(a)	(a)	(a)	(f)	(c)	(c)	(c)	(d)	(a)	(a)	(a)	(f)
31. Knob Creek and other tributaries to First Broad River, Cleveland County, N. C.	8.69	23.04	6.71	43.85	0.4	2.4	4.1	2.1	3.78	54.80	27.64	90.02
	(a)	(a)	(a)	(g)	(c)	(c)	(c)	(d)	(a)	(a)	(a)	(g)
32. Hinton Creek and adjacent streams entering First Broad River, Rutherford and Cleveland counties, N. C.	7.72	37.91	12.73	58.36	0.3	1.3	2.2	1.3	2.43	48.44	27.51	78.38
33. Floyds Creek and neighboring tributaries to Broad River, Rutherford County, N. C.	12.19	36.76	7.01	75.92	0.4	1.3	2.6	1.1	4.97	47.40	18.44	85.45
	(a)	(a)	(a)	(h)	(c)	(c)	(c)	(d)	(a)	(a)	(a)	(h)
34. Catheys Creek and adjoining streams tributary to Second Broad River, Rutherford and McDowell counties, N. C.	19.57	61.93	14.62	105.04	0.2	0.8	1.2	0.7	3.82	48.18	18.18	73.78
	(a)	(a)	(a)	(i)	(c)	(c)	(c)	(d)	(a)	(a)	(a)	(i)
35. Mountain Creek and other tributaries to Broad River, Rutherford County, N. C.	5.27	21.60	2.36	29.23	0.1	0.5	0.9	0.5	0.51	11.02	2.10	13.63
Totals and averages, basins tributary to Broad River	121.04	346.40	71.41	690.06	0.3	1.3	2.4	1.0	38.95	433.72	168.50	711.81
	(a)	(a)	(a)		(c)	(c)	(c)	(d)	(a)	(a)	(a)	(c)

(a) Incomplete sum.
(b) Includes 89,670,000 cu yd of undifferentiated sediment containing 34.1 million lb of monazite along Broad River.
(c) Tenor for part of total alluvium.
(d) Tenor for total alluvium.
(e) Includes 1.9 million lb of monazite in 3,830,000 cu yd of sediment for which the tenor was not calculated for kind of sediment.
(f) Includes 16,370,000 cu yd of undifferentiated sediment having 12.6 million lb of monazite along First Broad River.
(g) Includes 5,410,000 cu yd of undifferentiated sediment containing 3.8 million lb of monazite along First Broad River.
(h) Includes 19,960,000 cu yd of undifferentiated alluvium having 14.64 million lb of monazite along Second Broad River and Broad River.
(i) Includes 8,920,000 cu yd of sediment with 3.60 million lb of monazite along Second Broad River.

ID River Basins												
Catawba River, N. C. (Appraised by A. M. White, 1952-1953)												
36. Indian Creek and other tributaries to the South Fork Catawba River, Lincoln, Catawba, and Gaston counties, N. C.	16.79	44.97	6.39	128.15	0.3	1.2	2.2	0.8	4.44	54.67	13.95	103.06
	(a)	(a)	(a)	(b)	(c)	(c)	(c)	(d)	(a)	(a)	(a)	(b)
37. Clark Creek, Catawba and Lincoln counties, N. C.	9.33	39.43	4.31	53.07	0.1	0.4	0.8	0.4	1.03	17.54	3.43	22.00
38. Jacob Fork and adjoining streams, Burke, Catawba, Cleveland, and Lincoln counties, N. C.	6.94	19.76	4.28	30.98	0.1	0.9	1.9	0.8	1.03	17.21	8.15	26.39
39. Downstream part of Henry Fork, Burke and Catawba counties, N. C.	6.36	19.50	2.80	28.66	0.2	1.1	1.9	1.0	1.37	20.84	5.19	27.40
40. Laurel Creek and neighboring tributaries to Henry Fork, Burke County, N. C.	1.03	5.63	0.62	7.28	0.2	0.7	1.1	0.6	0.16	3.75	0.66	4.57
41. Lyle Creek and adjacent streams entering Catawba River, Catawba County, N. C.	8.44	39.06	4.83	52.33	0.08	0.3	0.5	0.4	0.66	10.56	2.22	22.70
					(c)	(c)	(c)	(d)	(a)	(a)	(a)	(e)
42. Hunting Creek and other tributaries to Catawba River, Burke County, N. C.	3.14	10.35	1.46	14.95	0.2	0.8	1.3	0.7	0.53	8.62	1.94	11.09
43. Silver Creek, Burke County, N. C.	11.44	24.87	3.10	39.41	0.2	1.0	1.7	0.8	2.35	25.70	5.37	33.42
44. Muddy Creek and Shadrick Creek, McDowell County, N. C.	14.38	37.53	6.46	58.37	0.1	0.7	1.1	0.6	2.11	24.49	6.93	37.03
					(c)	(c)	(c)	(d)	(a)	(a)	(a)	(f)
Totals and averages, basins tributary to Catawba River	77.85	241.10	34.25	413.20	0.2	0.8	1.4	0.7	13.68	183.38	47.84	287.66
	(a)	(a)	(a)		(c)	(c)	(c)	(d)	(a)	(a)	(a)	

(a) Incomplete sum.
(b) Includes 60,000,000 cu yd of alluvium with 30.0 million lb of monazite along South Fork Catawba River.
(c) Tenor for part of total alluvium.
(d) Tenor for total alluvium.
(e) Includes 9.26 million lb of monazite in 23,990,000 cu yd of sediment for which tenor was not calculated for kind of sediment.
(f) Includes 3.50 million lb of monazite in 8,730,000 cu yd of sediment for which tenor was not calculated for kind of sediment.

Table II. Comparison of Tenors in Monazite Estimated by Reconnaissance and by Churn Drilling

Flood Plain	Reconnaissance Appraisal by USGS	Exploration with Churn Drill by USBM		
	Resources, Lb Per Cu Yd	Inferred, Lb Per Cu Yd	Indicated, Lb Per Cu Yd	Reference Number
Knob Creek, N. C.	2.0	—	1.67	6
Buffalo Creek, N. C.	1.1	—	1.25	7
South Muddy Creek, N. C.	0.8	0.6	0.64	9
Silver Creek, N.C.	1.0	0.6	0.83	9
North Tyger and Middle Tyger Rivers, S. C.	0.3	0.4	—	11
Hinton Creek, N. C.	1.2	0.72	—	10
Wards Creek, N. C.	1.2	0.72	—	10

bearing metamorphic and igneous rocks. The monazite-bearing metamorphic rocks are a stratigraphic sequence of unknown age which was metamorphosed to biotite gneiss and sillimanite-almandine schist in Ordovician time. Intruded into these metamorphic rocks are monazite-bearing conformable masses of quartz monzonite and pegmatite and cross-cutting bodies of monazite-free quartz monozite, pegmatite, and diabase.

The stream sediments are well bedded, poorly graded, and unconsolidated and of similar stratigraphy from the Savannah to the Catawba rivers. They are deposited on deeply weathered flat valley floors in successive sheetlike layers of differing lithology. The lowermost layer is quartz-pebble gravel with a matrix of sandy clay. Overlying the gravel, or resting on bedrock where gravel is absent, is dense gray clay. Quartz pebbles and fragments of carbonized wood are scattered through the clay, which grades locally into peat or muck. Above the clay is coarse to fine-grained gray, buff, or brown sand overlain by buff, brown, or gray clayey silt. The uppermost sediment is red to brown sandy silt. Average thickness of the sediments is 14.6 ft. The layer of gravel at the bottom of the deposits averages 1.5 ft thick, the layer of clay is about 3.6 ft, and the sand and silt about 9.5 ft thick. The deposits are of Recent age, except for small areas of pre-Wisconsin sediment in the heads of some streams. The uppermost red to brown sandy silt has been deposited since the region was cleared for agriculture in the nineteenth century.

Table III. Resources of Monazite and Zircon in the Forty-Four Drainage Basins Between the Savannah and Catawba Rivers

Drainage Basin	Volume of Sediment Explored, Million Cubic Yards	Estimated Average Tenor, Lb Per Cu Yd		Estimated Resources, 1000 Short Tons	
		Monazite*	Zircon	Monazite*	Zircon
Savannah River (in South Carolina)	236.2	0.5	0.4	59	47
Saluda River	244.6	0.6	0.2	73	24
Enoree River	127.0	0.7	0.1	44	6
Tyger River	207.5	0.4	0.6	42	62
Pacolet River	190.6	0.8	0.4	76	38
Broad River	690.1	1.0	0.4	345	138
Catawba River (southern tributaries)	413.2	0.7	0.4	145	83
	2,109.2	0.8	0.4	784	398

* Includes xenotime.

Individual flood plains in the Piedmont monazite district are rarely more than 2 or 3 miles long. Each is separated from the next upstream or downstream flood plain by short narrows, shoals, or rocky ledges. These flood plains are 10 ft to 2500 ft wide and range in area from several thousand square yards to 7 million sq yd. In about half the valleys they reach 200 to 800 ft in width and exceed 1 million sq yd in area. However, the small flood plains at the extreme heads of creeks, which were the traditional sites of monazite mining, are only a few hundred to about 200,000 sq yd in area, and the volume of sediment in the smallest of these is no greater than a few hundred to a few thousand cubic yards. The largest flood plain in the area contains 60 million cu yd of sediment. Average is about 7 million cu yd. Among the hundreds of individual flood plains in the area the USGS classed 84 as monazite placers. Eight of these contain less than a million cubic yards of sediment, 39 have between 1 and 5 million cu yd, 19 have from 5 to 10 million cu yd, and 18 more than 10 million cu yd. Average volume of fill in these 84 flood plains is 6.8 million cu yd of sediment.

Tenors of the flood plain sediments range from less than 0.1 lb to 50 lb of monazite per cu yd and less than 0.1 lb to 30 lb of zircon per cu yd. Average tenor throughout the area is 0.8 lb of monazite and 0.4 lb of zircon per cu yd of sediment. Among the 84 flood plains classed as placers the average tenor is 1.3 lb of monazite and 0.6 lb of zircon per cu yd of sediment.

Highest tenors are in the coarsest-grained, lowest sediments in the flood plains and are in the smallest headwater deposits.

Monazite, the chief thorium-bearing and uranium-bearing mineral in the deposits, ranges in abundance from 1 to 80 pct of the concentrate and commonly makes up 10 to 30 pct. Monazite from placers in North and South Carolina and Georgia was shown by John B. Mertie, Jr.,[2] to average 5.67 pct ThO_2 and 0.38 pct U_3O_8 in 53 samples. Similar percentages were reported by the USBM[6-13] in analyses of 19 samples of placer monazite from North and South Carolina. Average values for thorium and uranium in placer monazite in the drainage basins from the Savannah to the Catawba rivers are:

River Basin	Number of Analyses	ThO_2, Pct	U_3O_8, Pct
Savannah (in South Carolina)	1	4.21	0.44
Saluda	8	5.96	0.39
Enoree	1	5.56	0.55
Tyger	2	5.77	0.70
Pacolet	4	5.04	0.52
Broad	47	5.94	0.41
Catawba (southern tributaries)	6	4.39	0.39

Other thorium-bearing and uranium-bearing minerals noted in the concentrates include zircon, xenotime, sphene, and unidentified radioactive opaque minerals. Zircon, found in about 65 pct of the samples of alluvium, makes up 1 to 50 pct of the concentrate and ordinarily constitutes 1 to 10 pct of the heavy minerals. It is concluded from study of 1200 heavy-mineral concentrates from crystalline rocks in the region that zircon in the placers is derived chiefly from the schists, but that possibly 20 pct comes from granitic rocks and pegmatite. Laboratory studies of zircon from this area[14] suggest that the placer zircon contains about 0.01 pct ThO_2 and 0.04 pct U_3O_8.

Xenotime is not abundant. It constitutes 20 pct of the heavy minerals in two samples and 1 pct of the concentrates from samples in 27 small areas. Elsewhere it is present but is less than 1 pct of the concentrate. Xenotime from a tributary to the Catawba River is reported[15] to contain a trace of thorium and 4.26 pct U_3O_8, and xenotime from a tributary to the Broad River has 0.20 pct ThO_2 and 1.40 pct U_3O_8.

Sphene, which in some specimens contains thorium and uranium, was found in concentrates from nine localites. At no place did it make up more than 3 pct of the concentrate; hence it is not a source of thorium or uranium in this region. The largest sphene-bearing area is a zone a mile wide and 12 miles long crossed by tributaries to the Catawba River in the extreme northeastern part of the region.

Unidentified radioactive opaque minerals make up less than 0.1 pct of the heavy minerals in tributaries to the Catawba River[9] and in several tributaries to the Broad River.[10, 13] Minor amounts of fergusonite, gadolinite, and euxenite have been detected in concentrates from the monazite placers and reported in older literature,[1, 16] but they are mineralogical curiosities and contribute practically nothing to the amount of thorium and uranium in the placers.

RESOURCES

Monazite and Zircon: The resources of monazite and zircon in the stream sediments were appraised by reconnaissance methods. For the appraisal the streams were grouped into 44 drainage basins (Fig. 1). Margins of individual flood plains in each drainage basin were interpreted stereoscopically on 1:20,000 scale aerial photographs, which were compiled into uncontrolled mosiacs. After field check of the interpretation the areas of the flood plains were measured by polar planimeter. At a scale of 1:20,000 a deviation of 0.03 sq in. in the measured area represents an error of 10,000 sq yd in the estimated area of the flood plain. Accuracy of planimetry within 5 pct of the area was achieved for flood plains having an area of 200,000 sq yd. Accuracy of planimetry equal to 1 pct of the area was achieved for flood plains having an area of 1 million sq yd. Nearly half of the flood plains exceed 1 million sq yd in area. A comparison between areas of three flood plains mapped by photo interpretation and the same flood plains mapped by plane table and telescopic alidade showed differences in area, assuming the plane table map to be the more accurate and the planimetry to be the same, of −7.5 pct, +6.1 pct, and +4.2 pct.

Average depth of alluvium in each flood plain was estimated from stratigraphic measurements of exposed flood plain sediments and from holes made with a jeep-mounted auger drill. Sediments were classed as clay, silt and sand, and gravel. A weighted average thickness of each class of sediment was allocated to every flood plain. The weighted average thickness of a class of sediment in a flood plain was estimated by assigning areas of influence to auger holes and stratigraphic measurements and weighting the individual thicknesses by the area factor. In a check of 51 flood plains where geologists estimated thickness of flood plain sediments by stratigraphic measurements and where the flood plains were subsequently augered, it was found that two estimates were in error by 67 pct and that the algebraic average error was an overestimate of slightly less than 10 pct.

The amount of monazite and other heavy minerals in the sediment was estimated by the USGS party from microscopic study of heavy minerals panned from 2672 samples of sediment. The samples, totaling nearly 110,000 lb, were distributed among all the classes of sediment and were taken between the top and bottom of the flood plain at intervals controlled by changes in lithology. A weighted average tenor for each class of sediment in every flood plain was calculated by attributing areas of influence to the samples. The weighted average tenor of each class of sediment multiplied by the volume of that class gave the estimated weight of monazite in that class of sediment in the flood plain. The sum of the weights of monazite in each class of sediment gave the amount of monazite in the flood plain. The estimated volume of sediment and weight of monazite in one drainage basin are the sums of the values for the individual flood plains in the basin.

A study made of the recovery of heavy minerals by panning was reported by Theobald,[17] who showed that average recovery of monazite was 84 pct and of zircon 72 pct of the amount in the sample of sediment. Recovery ranged from a low of 35 pct of the monazite and 12 pct of the zircon in some samples of clay and silt to a high of 94 pct of the monazite and 100 pct of the zircon in some samples of gravel.

Table IV. Resources of Thorium and Uranium in Explored Alluvial Monazite Deposits Between Savannah and Catawba Rivers, S. C.-N. C.

Drainage Basin	Monazite*					Zircon				
		ThO_2		U_3O_8			ThO_2		U_3O_8	
	Short Tons	Pct	Short Tons	Pct	Short Tons	Short Tons	Pct	Short Tons	Pct	Short Tons
Savannah River (in South Carolina)	59,000	4.21	2,000	0.44	300	47,000	Estimated 0.01	4.7	Estimated 0.04	18.8
Saluda River	73,000	5.96	4,000	0.39	300	24,000		2.4		9.6
Enoree River	44,000	5.56	2,000	0.55	200	6,000		0.6		2.4
Tyger River	42,000	5.77	2,000	0.70	300	62,000		6.2		24.8
Pacolet River	76,000	5.04	4,000	0.52	400	38,000		3.8		15.2
Broad River	345,000	5.94	20,000	0.41	1,400	138,000		13.8		55.2
Catawba River (southern tributaries)	145,000	4.39	6,000	0.39	600	83,000		8.3		33.2
Total	784,000		40,000		3,500	398,000		39.8		159.2

* Includes traces of xenotime.

The panned concentrates were examined mineralogically in the USGS laboratories by a staff directed by Jerome Stone, who devised the routine followed in the laboratory.[18] The panned concentrates, without processing in heavy liquids, were sized into three to five sieve fractions. The sieve fractions were weighed and a split of 100 to 150 mineral grains was made from each fraction. The grains were identified microscopically and counted. For one concentrate the total number of grains counted ranged from 300 to 750 and averaged 400. Numerical frequencies of each mineral in each sieve fraction were converted to weight percents by appropriate specific gravity factors. The weight percent of each mineral in the separate sieve fractions from one concentrate was recalculated according to the weight of each sieve fraction to give the weight percent of each mineral in the concentrate. The estimated weight of monazite or zircon in a concentrate was its weight percent times the weight of the concentrate.

The estimated tenor of a cubic yard of flood plain sediment in this reconnaissance appraisal was the weight of the mineral in the concentrate multiplied by appropriate factors for the original volume of the sample corrected for swell. No corrections were made for losses in panning.

The volume and tenor of the alluvium, and the resources in monazite in the 44 drainage basins outlined in Fig. 1, are estimated in Tables IA through ID. Numbers assigned to the drainage in Tables IA through ID match the numbers in Fig. 1. Columns headed "Estimated Volume of Sediment Explored" contain sums of the volumes of the separate classes of sediment estimated to be in the individual flood plain in each basin. The columns headed "Estimated Resources in Monazite" contain the sums of the weights of monazite estimated to be in each class of sediment in the individual flood plains in each basin. Columns headed "Tenor" were compiled by dividing the volume of sediment into the resources in monazite. No check is available for these tenors, but checks are available for the average tenor in monazite of several individual flood plains appraised by the Survey and subsequently drilled by the USBM (Table II). These comparisons suggest that the tenors listed in Table I are of the proper order of magnitude.

The resources in monazite shown in Tables IA through ID are summarized in Table III, which gives an estimate of the resources in zircon.

Thorium and Uranium: The resources in thorium and uranium in the alluvial monazite deposits listed in Tables IA through ID amount to 40,000 short tons of thorium and 3700 short tons of uranium (Table IV). The small contribution to these resources made by the hundreds of thousands of tons of zircon in the deposits shows that this mineral is not a source for thorium and uranium in this area.

Small deposits at the extreme heads of the creeks, some of which were the former sites of monazite mining in the Piedmont, are not included in the estimates of resources given in the tables. Despite their small size the vast number of these deposits, combined with high average tenor, reported by Mertie[2] to be 8.4 lb of monazite per cu yd and observed by the writers to be about 4 lb of monazite per cu yd of sediment, provide substantial resources of thorium and uranium. In the area covered by Fig. 1 the small deposits are estimated to contain 250,000 short tons of monazite. On the average this monazite contains 5.4 pct ThO_2 and 0.44 pct U_3O_8. Thus these small deposits contain an estimated 13,000 short tons of thorium and 1100 short tons of uranium.

Conclusions: The resources of thorium and uranium in deposits of alluvial monazite in the western Piedmont of North and South Carolina between the Savannah and Catawba rivers are estimated to be 53,000 tons of thorium and 4600 tons of uranium in more than 2 billion cu yd of material. None of these deposits are mineable at 1958 prices.

The work leading to this report was sponsored by the Division of Raw Materials of the U. S. Atomic Energy Commission and was conducted by the U. S. Geological Survey between July 1951 and June 1954. The choice of area examined and many ideas related to methods were influenced by previous investigations made by J. B. Mertie, Jr.[2] in North and South Carolina, Georgia, Alabama, and Virginia. A. M. White, N. P. Cuppels, and D. W Caldwell of the USGS did much of the field work upon which this report is based, and J. Stone supervised the mineralogical examination of the samples collected by the field party. R. F. Griffith and L. A. Hansen of the U. S Bureau of Mines directed the drilling of 12 deposits in the area.[6-13]

REFERENCES

[1] J. H. Pratt: Zircon, Monazite and Other Minerals Used in the Production of Chemical Compounds Employed in the Manufacture of Lighting Apparatus. North Carolina Geological and Economic Survey, Raleigh, N. C., *Bull. 25*, 1916, pp. 1-120.

[2] J. B. Mertie, Jr.: Monazite Deposits of the Southeastern Atlantic States. *USGS Circ. 237*, 1953, pp. 1-31.

[3] W. C. Overstreet, N. P. Cuppels, and A. M. White: Monazite in Southeastern United States. In *USGS Prof. Paper 300*, 1956, pp. 597-601. (Contributions to the geology of uranium and thorium by U. S. Geological Survey and Atomic Energy Commission for the United Nations International Conference on Peaceful Uses of Atomic Energy, Geneva, Switzerland, 1955, compiled by L. R. Page, H. E. Stocking, and H. B. Smith, 739 pp.).

[4] W. C. Overstreet and W. R. Griffitts: Inner Piedmont Belt. In R. J. Russell's *Guides to Southeastern Geology*, Geol. Soc. Amer., 1955, pp. 549-577.

[5] P. B. King: A Geologic Section Across the Southern Appalachians: an Outline of the Geology in the Segment in Tennessee, North Carolina, and South Carolina. In R. J. Russell's *Guides to Southeastern Geology*. Geol. Soc. Amer., 1955, pp. 332-373.

[6] R. F. Griffith and W. C. Overstreet: Knob Creek Monazite Placer, Cleveland County, North Carolina. U. S. Atomic Energy Commission, *RME—3112*, Oak Ridge, Tenn., January 1953, p. 1130.

[7] R. F. Griffith and W. C. Overstreet: Buffalo Creek Monazite Placer, Cleveland and Lincoln Countries, North Carolina. U. S. Atomic Energy Commission, *RME—3113*, Oak Ridge, Tenn., January 1953, pp. 1-17.

[8] R. F. Griffith and W. C. Overstreet: Sandy Run Creek Monazite Placer, Rutherford County, North Carolina. U. S. Atomic Energy Commission, *RME—3114*, Oak Ridge, Tenn., January 1953, pp. 1-27.

[9] L. A. Hansen and A. M. White: Monazite Placers on South Muddy Creek, McDowell County and Silver Creek, Burke County, North Carolina. U. S. Atomic Energy Commission, *RME—3115*, March 1954, pp. 1-27.

[10] L. A. Hansen and N. P. Cuppels: Monazite Placer on the First Broad River and Its Tributaries, Cleveland County, North Carolina. U. S. Atomic Energy Commission, *RME—3116*, Oak Ridge, Tenn., July 1954, pp. 1-27.

[11] L. A. Hansen and N. P. Cuppels: Monazite Placer at the Junction of the North Tyger River with the Middle Tyger River, Spartanburg County, South Carolina. U. S. Atomic Energy Commission, *RME—3117*, January 1955, pp. 1-22.

[12] L. A. Hansen and D. W. Caldwell: Monazite Placers on Rabon Creek, Laurens County, and Big Generostee Creek, Anderson County, South Carolina. U. S. Atomic Energy Commission, *RME—3118*, Oak Ridge, Tenn., February 1955, pp. 1-25.

[13] L. A. Hansen and P. K. Theobald, Jr.: Monazite Placers of the Broad River and Thicketty Creek, Cherokee County, South Carolina. U. S. Atomic Energy Commission, *RME—3126*, May 1955, pp. 1-29.

[14] H. Jaffe: Personal communication, 1957.

[15] C. Palache, H. Berman, and C. Frondel: *The System of Mineralogy of James Dwight Dana and Edward Salisbury Dana, Yale University 1837-1892*, 7th ed., vol. 2, pp. 1-1124. John Wiley & Sons, Inc., New York, 1951.

[16] E. Sloan: Catalogue of the Mineral Localities of South Carolina. South Carolina Geological Survey, *Ser. 4, Bull. 2*, 1908, pp. 1-505.

[17] P. K. Theobald, Jr.: The Gold Pan as a Quantitative Geologic Tool. *USGS Bull. 1071-A*, 1957, pp. 1-54.

[18] W. C. Overstreet, P. K. Theobald, Jr., J. W. Whitlow, and J. Stone: Heavy-Mineral Prospecting. In *USGS Prof. Paper 300*, 1956, pp. 647-650.

Discussion of this article sent (2 copies) to AIME before Aug. 31, 1959, will be published in MINING ENGINEERING.

LABORATORY INVESTIGATION —

FLOCCULATION TO IMPROVE COAL SLURRY FILTRATION

by M. R. GEER, P. S. JACOBSEN, and H. F. YANCEY

Two growing problems confront the preparation engineer—still further restrictions on stream pollution and a greater proportion of fine coal as more and more continuous miners come into use. The dewatering screens, centrifuges, and settling ponds that sufficed a few years ago must often be supplemented by more effective equipment, and in some instances the finest solids are now being recovered by vacuum filtration, once considered too costly in many coal washeries. Unfortunately not all slurries can be readily filtered. Some are virtually unfilterable, and others do not permit the high cake rates needed to hold costs within reason. Often, however, these difficult slurries can be rendered filterable by flocculation.

Starch and lime have long increased settling rate in thickeners and can also aid filtration. More recently there have been other flocculants, primarily synthetic polymers or gums. Reports of their great effectiveness prompted the U. S. Bureau of Mines to test their use in filtration as part of its program on recovering and cleaning fine coal. The object of the present work was to compare some of the newer flocculants with starch and lime and to test the reaction of different types of slurries to flocculation. Three natural slurries, three synthetic coal-clay mixtures, and five flocculants were tested, all with a laboratory filter leaf.

Slurries and Flocculants Tested: First of the slurries was the thickener feed from the washed coal section of the Michel colliery of Crow's Nest Pass Co. Ltd., Michel, B.C.

As shown by the screen and ash analyses in Table I, practically all this slurry was finer than 28 mesh, and about half the solids were finer than 200. Substantially all material coarser than 200 mesh was clean coal, but the ash content of 20.7 pct in the finest size indicates a moderate amount of impurity. This coal is medium-volatile bituminous in rank.

Slurry was also obtained from the Black Diamond washery of Palmer Coking Coal Co., King County, Wash. This underflow of a ½-mm vibrating slurry screen is a waste product discharged to a settling pond. As shown by the data in Table I it contained about 20 pct material finer than 200 mesh, which analyzed 77.5 pct ash, indicating a high proportion of clay. The coarser sizes were also high in ash content because of the presence of bone and shale. Black Diamond coal is on the dividing line between bituminous and subbituminous rank.

The third slurry, from the washery of Roslyn-Cascade Coal Co. in Kittitas County, Wash., was the underflow of a battery of 8-in. cyclones that is wasted with the coarser refuse from the plant. In both size and ash content this slurry was similar to the Black Diamond, but since it was a cyclone-underflow product, the fraction finer than 200 mesh undoubtedly contained a much smaller proportion of finely divided clay than was present in the Black Diamond slurry. The Roslyn-Cascade coal is high-volatile A bituminous in rank.

Initially the slurry samples were stored in the laboratory at a concentration of 40 pct solids. A progressive change in filtration and flocculation characteristics during storage was noted, however, presumably because of progressive disintegration of the clay. After careful testing demonstrated that the slurry solids could be dried and then repulped without changing the original filtration characteristics, this procedure was adopted.

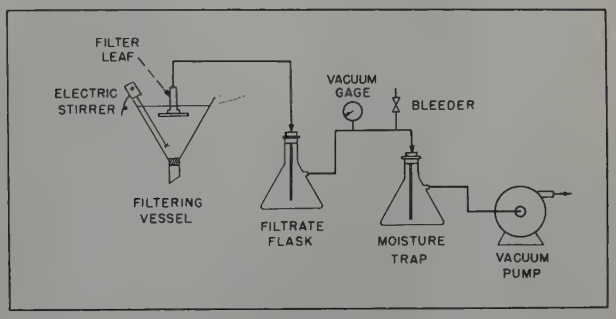

Fig. 1—Test leaf filtration apparatus.

The flocculants used were Separan 2610, Kylo 27, Jaguar MD-A, Idaho potato starch, and lime. The lime was used as a slurry, the Separan 2610 as a 0.10 pct aqueous solution, and the other flocculants as 0.50 pct aqueous solutions. The starch was causticized with sodium hydroxide before use. As some of the flocculants are reported to deteriorate on storage, new batches of flocculants were prepared every two days.

Test Procedure: Fig. 1 diagrams the filter leaf apparatus employed. This consists of a test leaf having an effective area of 0.10 sq ft., a 60°, 8½-in. diam cone to hold the slurry sample, a variable-speed electric stirrer, vacuum gage, bleed line for controlling vacuum, filtrate flask, moisture trap, and vacuum pump.

Two filter cloths were selected—Saran SA 603, a monofilament, coarse-weave cloth, and polyethylene PO-801 HF, a monofilament, fine-weave cloth. The Saran was selected to provide maximum cake rate without regard to clarity of filtrate and the polyethylene to provide the best quality of filtrate without regard to cake rate.

The test charge for the filtering vessel consisted of 800 g of solids (previously soaked for 24 hr) and

H. F. YANCEY and M. R. GEER, Members AIME, and P. S. JACOBSEN are, respectively, Chief, Supervising Mining Engineer, and Chemist, Division of Solid Fuels Technology, Region I, U. S. Bureau of Mines, Seattle, Wash. TP 59F34. Manuscript, Oct. 14, 1958. San Francisco Meeting, February 1959. AIME Trans., Vol. 214, 1959.

Table I. Size and Ash Content of Slurry Solids

Slurry	Over 28	28 to 48	48 to 100	100 to 200	Under 200	Total
Crow's Nest Pass						
Screen analysis, pct	1.3	3.5	20.7	25.5	49.0	100.0
Ash, pct	12.2	8.2	8.9	11.3	20.7	15.3
Black Diamond						
Screen analysis, pct	6.3	25.8	31.7	16.3	19.9	100.0
Ash, pct	15.9	18.9	31.1	53.6	77.5	39.9
Roslyn-Cascade						
Screen analysis, pct	8.7	17.4	31.8	18.4	23.7	100.0
Ash, pct	19.3	29.5	36.8	43.3	73.1	43.8

1200 g of water, giving a standard solids concentration of 40 pct. The desired amount of flocculant was added and the mixture stirred for 2 min. The vacuum was then turned on and the test leaf immersed in the funnel so that the leaf face was just covered. As filtration commenced, the vacuum was adjusted and maintained at 25 in. of mercury. The filtration cycle consisted of 0.80 min form time followed by 1.10 min drying.

The two filter runs made are designated trials 1 and 2. Trial 2 was obtained by returning the cake and filtrate of trial 1 to the funnel, remixing, and refiltering without adding more flocculant. In tests of the Crow's Nest Pass slurry the cloth was cleaned between trials, but with other slurries it was not. Comparative tests showed that reduction in cake rate generally obtained on the second trial was much the same whether or not the cloth was cleaned between trials; consequently the cleaning step was omitted for the Black Diamond and Roslyn-Cascade slurries. The wet cake weight was determined after each trial, and the moisture content of the cake and percentage of solids in the filtrate was determined after the second trial. The purpose of the second trial was to provide a measure of floc strength, that is, to evaluate the extent of floc destruction caused by remixing.

With a readily filterable slurry, one giving a dry cake rate exceeding 165 lb per sq ft, the entire usable volume of slurry in the vessel was exhausted in less than the standard 0.80 min form time; also, the standard vacuum could not be attained. With such slurries an adaptation of a formula advanced by Silverblatt and Dahlstrom[1] was used to convert the data to the same basis as that for less filterable slurries. The equation is as follows:

$$R = 5720\ (TV)^{-1/2} \qquad [1]$$

where R = dry filter rate, lb per hr per sq ft
T = time required to filter charge, sec
V = vacuum attained during time T, in. of Hg.

The cake rates obtained with this test procedure probably cannot be translated directly into rates for a commercial filter, but they provide useful comparative values for judging the effectiveness of flocculation.

Results of Filtration Tests: Results obtained with the test leaf are presented in Tables II through V, in terms of cake rate, moisture in cake, and percentage of solids in filtrate.

In untreated form the Crow's Nest Pass slurry gave cake rates of 50 and 68 lb per hr per sq ft, respectively, with the fine and coarse cloths, which classes it as being filterable but providing only a moderate cake rate. Separan, Kylo, and Jaguar all behaved quite similarly with this slurry. All three increased the cake rate three to fourfold, were nearly as effective with the minimum flocculant concentration of 0.025 lb per ton as with the maximum, provided nearly as high cake rates with the fine cloth as with the coarse, and showed little reduction in cake rate between the first and second trials. All three flocculants slightly increased the moisture content of the cake obtained with the fine cloth, but no more than would be expected with the increased thickness of cake. All three reduced the percentage of solids in the filtrate to about the same level—0.04 to 0.07 with the fine cloth and 0.59 to 1.67 with the coarse cloth. The figures representing quality of filtrate are the only data showing any influence of increasing flocculant concentration. With all three flocculants each increase in concentration distinctly improved the quality of filtrate obtained with the coarse cloth.

The amount of Crow's Nest Pass slurry available did not permit testing lime and starch at the low concentrations employed for the other flocculants; they were used at concentrations from 0.10 to 4.0 lb per ton, as shown in Table V. Lime was not a particularly effective reagent with this slurry. Even when used at 4 lb per ton it increased the cake rate only twofold. Starch, on the other hand, when used at 0.4 lb per ton, provided cake rates fully as great as those obtained with the newer flocculants, and equaled these flocculants in terms of cake moisture and filtration quality.

In natural form the Black Diamond slurry could not be filtered with either the coarse or fine cloth. Cake rates exceeding 11 lb per hr per sq ft could not be obtained, the cakes analyzed up to 50 pct moisture, and the filtrates were dirty. But the same concentrations of flocculant used with the Crow's Nest Pass slurry strikingly improved filtration. Separan, Kylo, and Jaguar all were effective. Separan gave the highest cake rates obtained—390 lb. These flocculants reduced the solids in the filtrate to 0.05 pct with the fine cloth and 0.18 to 0.49 pct with the coarse cloth, as well as cutting cake moisture content in half. Lime was ineffective at the concentration shown in the tables and even when used at 4.5 lb per ton was distinctly inferior to the other flocculants. At 0.025 lb per ton starch was a fairly good flocculant, and when employed at 1 lb per ton it gave cake rates exceeding those obtained with all the flocculants except Separan. With this slurry the cake rates obtained with the coarse cloth were only moderately higher than those provided by the fine cloth, and the coarse cloth provided filtrate of better quality than was obtained with either of the other two slurries.

In raw form the Roslyn-Cascade slurry could not be filtered at all with the fine cloth but gave cake rates of 119 to 89 lb per hr per sq ft with the coarse cloth. Because of the high cake rate obtained with the coarse cloth the concentration of flocculant used with this slurry was reduced to a range of 0.00625 to 0.025 lb per ton. At 0.00625 lb per ton, however, there was virtually no improvement in filtration with the fine cloth and only a moderate increase in cake rate with the coarse cloth. Increasing the dosage improved the results obtained with Separan, Kylo and Jaguar, Separan providing the highest rate. The fact that each increase in flocculant concentration substantially increased the cake rate for these reagents suggests that the optimum level of concentration was not obtained, even at the maximum dosage.

Table II. Cake Rates Obtained With Various Flocculants

Slurry	Flocculant*	Cake Rate, Lb Per Hr Per Sq Ft, Dry							
		Fine Filter Medium				Coarse Filter Medium			
		0	0.025	0.05	0.10	0	0.025	0.05	0.10
Crow's Nest Pass**	None								
	Trial 1	50	—	—	—	67	—	—	—
	Trial 2	50	—	—	—	68	—	—	—
	Separan 2610								
	Trial 1	—	143	181	210	—	170	242	247
	Trial 2	—	140	168	197	—	140	207	218
	Kylo 27								
	Trial 1	—	139	149	156	—	149	180	198
	Trial 2	—	150	156	162	—	139	174	198
	Jaguar MD-A								
	Trial 1	—	134	155	203	—	157	181	218
	Trial 2	—	119	147	169	—	142	132	204
Black Diamond	None								
	Trial 1	4	—	—	—	11	—	—	—
	Trial 2	1	—	—	—	6	—	—	—
	Separan 2610								
	Trial 1	—	322	390	467	—	322	425	491
	Trial 2	—	56	265	390	—	210	343	390
	Kylo 27								
	Trial 1	—	156	216	244	—	239	322	390
	Trial 2	—	26	149	167	—	175	250	277
	Jaguar MD-A								
	Trial 1	—	229	306	343	—	265	322	365
	Trial 2	—	125	216	256	—	199	277	343
	Starch								
	Trial 1	—	3	66	167	—	42	123	229
	Trial 2	—	2	3	25	—	20	37	127
	Lime								
	Trial 1	—	4	4	4	—	11	11	11
	Trial 2	—	1	1	1	—	6	6	6
	Flocculant*	**0**	**0.00625**	**0.0125**	**0.025**	**0**	**0.00625**	**0.0125**	**0.025**
Roslyn-Cascade	None								
	Trial 1	1	—	—	—	119	—	—	—
	Trial 2	1	—	—	—	89	—	—	—
	Separan 2610								
	Trial 1	—	4	116	343	—	164	390	491
	Trial 2	—	1	5	188	—	146	169	365
	Kylo 27								
	Trial 1	—	5	98	145	—	203	234	256
	Trial 2	—	5	103	145	—	203	239	292
	Jaguar MD-A								
	Trial 1	—	4	24	256	—	156	224	390
	Trial 2	—	1	1	177	—	105	186	322
	Starch								
	Trial 1	—	1	2	2	—	145	159	229
	Trial 2	—	1	1	1	—	109	101	93
	Lime								
	Trial 1	—	1	1	1	—	119	121	120
	Trial 2	—	1	1	1	—	89	91	93

* Pound per ton of solids.
** See Table V for lime and starch results.

Table III. Moisture Content of Cakes Obtained With Various Flocculants

Slurry	Flocculant*	Moisture in Cake, Pct							
		Fine Filter Medium				Coarse Filter Medium			
		0	0.025	0.05	0.10	0	0.025	0.05	0.10
Crow's Nest Pass**	None	22.4	—	—	—	27.7	—	—	—
	Separan 2610	—	24.6	25.3	26.1	—	28.5	30.5	30.6
	Kylo 27	—	24.8	25.3	25.2	—	26.9	28.4	32.2
	Jaguar MD-A	—	23.9	25.1	24.5	—	26.1	26.7	26.4
Black Diamond	None	50.0	—	—	—	42.0	—	—	—
	Separan 2610	—	23.4	22.7	23.2	—	23.5	23.8	24.8
	Kylo 27	—	24.5	25.0	24.6	—	24.1	25.4	24.1
	Jaguar MD-A	—	23.5	24.8	21.0	—	24.1	24.3	24.3
	Starch	—	50.0	39.6	21.4	—	29.6	22.3	23.3
	Lime	—	50.0	50.0	50.0	—	42.0	42.0	42.0
	Flocculant*	**0**	**0.00625**	**0.0125**	**0.025**	**0**	**0.00625**	**0.0125**	**0.025**
Roslyn-Cascade	None	40.0	—	—	—	23.9	—	—	—
	Separan 2610	—	40.0	21.7	21.3	—	21.1	19.6	19.5
	Kylo 27	—	27.8	20.4	20.4	—	21.8	20.6	20.9
	Jaguar MD-A	—	32.6	35.0	19.9	—	22.5	21.2	20.6
	Starch	—	40.0	40.0	40.0	—	22.0	22.0	20.9
	Lime	—	40.0	40.0	40.0	—	23.9	23.6	23.6

* Pound per ton of solids.
** See Table V for lime and starch results.

Table IV. Solids in Filtrate Obtained With Various Flocculants

Slurry	Flocculant*	Solids in Filtrate, Pct							
		Fine Filter Medium				Coarse Filter Medium			
		0	0.025	0.05	0.10	0	0.025	0.05	0.10
Crow's Nest Pass**	None	0.18	—	—	—	4.00	—	—	—
	Separan 2610	—	0.07	0.05	0.04	—	1.33	0.81	0.59
	Kylo 27	—	0.06	0.06	0.06	—	1.40	1.18	0.98
	Jaguar MD-A	—	0.07	0.05	0.04	—	1.67	1.33	0.92
Black Diamond	None	0.24	—	—	—	2.44	—	—	—
	Separan 2610	—	0.06	0.05	0.05	—	0.33	0.27	0.18
	Kylo 27	—	0.06	0.05	0.05	—	0.39	0.45	0.41
	Jaguar MD-A	—	0.06	0.05	0.05	—	0.49	0.47	0.23
	Starch	—	0.11	0.08	0.08	—	1.90	1.40	0.69
	Lime	—	0.24	0.24	0.24	—	2.44	2.40	2.40
	Flocculant*	**0**	**0.00625**	**0.0125**	**0.025**	**0**	**0.00625**	**0.0125**	**0.025**
Roslyn-Cascade	None	0.49	—	—	—	1.59	—	—	—
	Separan 2610	—	0.21	0.10	0.06	—	0.93	0.75	0.65
	Kylo 27	—	0.11	0.08	0.06	—	0.73	0.65	0.58
	Jaguar MD-A	—	0.49	0.12	0.07	—	1.28	0.79	0.51
	Starch	—	0.49	0.22	0.14	—	1.13	1.08	0.95
	Lime	—	0.49	0.41	0.34	—	1.59	1.50	1.51

* Pound per ton of solids.
** See Table V for lime and starch results.

Table V. Filtration Data of Crow's Nest Pass Slurry Flocculated with Lime and Starch

Flocculant*	Fine Filter Medium						Coarse Filter Medium					
	0.10	0.20	0.40	1.0	2.0	4.0	0.10	0.20	0.40	1.0	2.0	4.0
Lime												
Cake rate, lb per hr per sq ft, dry												
Trial 1	—	—	—	82	105	110	—	—	—	75	103	114
Trial 2	—	—	—	69	90	90	—	—	—	69	99	93
Moisture in cake, pct	—	—	—	21.6	22.5	22.5	—	—	—	25.8	25.5	24.6
Solids in filtrate, pct	—	—	—	0.11	0.07	0.08	—	—	—	4.29	2.69	2.54
Starch												
Cake rate, lb per hr per sq ft, dry												
Trial 1	125	168	197	—	—	—	130	207	251	—	—	—
Trial 2	122	157	155	—	—	—	134	146	202	—	—	—
Moisture in cake, pct	25.3	24.4	24.2	—	—	—	28.2	24.9	26.2	—	—	—
Solids in filtrate, pct	0.08	0.05	0.04	—	—	—	1.55	1.21	0.97	—	—	—

* Pound per ton of solids.

Table VI. Cake Rates Obtained From a Synthetic Slurry Contaminated With Various Clays

Flocculant*	Filter Rate, Lb Per Hr Per Sq Ft, Dry											
	Kaolinite				Calcium Montmorillonite				Sodium Montmorillonite			
	0.00	0.025	0.05	0.10	0.00	0.025	0.05	0.10	0.00	0.025	0.05	0.10
None												
Trial 1	51	—	—	—	48	—	—	—	50	—	—	—
Trial 2	51	—	—	—	44	—	—	—	40	—	—	—
Jaguar MD-A												
Trial 1	—	60	60	64	—	69	136	160	—	99	125	210
Trial 2	—	58	59	61	—	49	105	156	—	82	105	163
Kylo 27												
Trial 1	—	123	159	189	—	110	144	165	—	179	196	249
Trial 2	—	107	155	170	—	95	138	155	—	174	179	237
Separan 2610												
Trial 1	—	55	69	177	—	58	95	177	—	170	229	234
Trial 2	—	54	54	154	—	52	77	166	—	154	191	215
Flocculant*	**0.00**	**0.750**	**1.50**	**2.0**	**0.00**	**0.750**	**1.50**	**2.0**	**0.00**	**0.750**	**1.50**	**2.0**
Lime												
Trial 1	—	69	107	113	—	57	78	120	—	155	196	218
Trial 2	—	59	93	102	—	50	53	99	—	144	167	206
Flocculant*	**0.00**	**0.0750**	**0.150**	**0.30**	**0.00**	**0.0750**	**0.150**	**0.30**	**0.00**	**0.0750**	**0.150**	**0.30**
Starch												
Trial 1	—	51	64	82	—	98	138	157	—	159	192	278
Trial 2	—	51	52	63	—	56	97	118	—	95	135	257

* Pounds per ton of dry solids.

With this slurry the influence of floc strength is evident. At a concentration of 0.0125 lb per ton the first trial with Separan gave a rate of 116 lb, but in the second trial the rate fell to 5 lb, indicating that the flocs were too weak to withstand agitation of slurry between runs. On the other hand, Kylo gave substantially the same results in the first and second trials, indicating a much stronger floc.

With all flocculants, as with the raw slurry, much higher cake rates were obtained with coarse cloth than with fine, but the increase was accompanied by deterioration in the quality of filtrate, as revealed in Table IV.

At the concentration shown in Table II, neither lime nor starch provided any improved filtration with the fine cloth, but the maximum concentration of starch nearly doubled the initial cake rate obtained with the coarse cloth. However, the starch flocs were very weak, and cake rate on the second trial was not significantly improved over that for the raw slurry. At still higher concentration of flocculant the results obtained with lime were improved but never equaled those for Separan, Kylo, or Jaguar. In contrast, starch at 0.2 lb per ton provided cake rates of 368 to 285 lb with the fine cloth and 495 to 451 lb with the coarse. At this higher concentration, therefore, the cake rates with starch were higher than those obtained with Separan at the lower dosage in which it was used.

Experiments with Synthetic Slurries: Filterability of a slurry is related to the amount and nature of extreme fines present.[1] Clay generally impedes filtration, and since individual types of clay often behave quite differently, the influence of clay on filtration and flocculation was investigated. A synthetic slurry matching the size composition of the Black Diamond slurry shown in Table I was prepared by grinding a clean bituminous coal from Utah to required fineness. This slurry gave a cake rate of 391 lb per hr per sq ft with the coarse cloth. Then admixtures of three different clays were made. One clay was a bentonite containing principally sodium montmorillonite, the second a bentonite in which the predominant clay mineral was calcium montmorillonite, and the third a kaolinitic clay. The first step was to determine how much of each clay was required to reduce the test-leaf filtration rate to an arbitrary level of 50 lb. The following percentages were required: sodium montmorillonite, 0.8 pct; calcium montmorillonite, 7.5 pct; and kaolinite, 16.2 pct. Thus it is evident that the type of clay contaminating a slurry has a major bearing on filtration properties.

Samples of the synthetic slurry contaminated with the amounts of individual clays required to reduce cake rate to 50 lb were flocculated and filtered according to the same test procedures employed for the natural slurries previously described, except that only the coarse filter cloth was used. Results of these tests are shown in Table VI.

With the kaolinite-contaminated slurry neither Jaguar nor starch was effective. Kylo was the best flocculant, followed closely by Separan. Lime, which had proved ineffective with the three natural slurries, was better than smaller amounts of either starch or Jaguar.

With the slurry containing calcium montmorillonite Jaguar, Kylo, and Separan were about equally effective, and starch at a concentration of 0.3 lb per ton was nearly as effective as the three better flocculants at 0.10 lb. With the slurry containing sodium montmorillonite clay all five flocculants were about equally effective when used at their maximum concentration, each of them increasing the cake rate four or fivefold.

Conclusions: Experimental results appear to support two principal conclusions: First, three natural and three synthetic slurries tested exhibited individual filtration characteristics and individual flocculation properties; moreover, their behavior was not related directly either to size composition or to ash content. Thus each slurry must be evaluated individually for possible benefits of flocculation to be predicted. Substantially the same conclusion was reached by Meerman,[2] whose investigation was on a full plant scale.

Second, some of the newer flocculants are so effective that only a few thousandths of a pound per ton are needed, but with the slurries examined the performance obtained did not exceed that possible with greater amounts of starch.

The work described in this report is part of a continuous program of coal preparation research sponsored jointly by the Northwest Experiment Station of the U. S. Bureau of Mines and the School of Mineral Engineering of the University of Washington.

REFERENCES

[1] C. E. Silverblatt and D. A. Dahlstrom: Theory and Practice of Continuous Filtration of Fine Coal and Slimes. Contribution A IV 14, *Proceedings*, Second International Coal Preparation Congress, 1954.

[2] P. G. Meerman: Interface-Active Chemicals in Coal Preparation —Practical Experience at the Dutch State Mines. Paper No. 10, Symposium on Coal Preparation, University of Leeds, England, 1957.

Discussion of this article sent (2 copies) to AIME before Aug. 31, 1959, will be published in MINING ENGINEERING.

Discussion

J. G. John (*Preparation Engineer, Crow's Nest Pass Coal Co. Ltd., Michel, B.C.*)—This excellent paper by Geer, Jacobsen, and Yancey was particularly interesting to our company, as we have just placed in operation a slimes recovery plant at our Michel colliery. The slurry recovered, by means of flocculation, thickening, and filtration, is one of the three natural slurries used in the described investigation.

From Tables II and IV of the paper it is noted that rate of cake formation and filtrate clarity improve with increase in flocculant concentration. In our operation the flocculant concentration is primarily controlled by the settling character of our slurry in the thickener rather than by filterability of the thickener underflow going to the filter.

With our particular slurry we found it advantageous to use a dry synthetic starch manufactured in England. Flocculant concentration required is 30 ppm of slurry or 0.3 lb per ton of dry coal recovered. The concentration is considerably greater than those concentrations used in the described investigation, namely 0.025 to 0.10 lb per ton.

With concentrations in excess of 60 ppm we noted a deterioration in the settling rate characteristics.

It is our experience, too, that flocculation requirements of a slurry cannot be solely predetermined from consideration of the coal slurry's sizing and ash content. The advent of the new synthetic flocculants gives the coal preparation personnel additional opportunity in this lucrative field of coal recovery.

ADVANCING THROUGH CAVED GROUND WITH YIELDABLE ARCHES

by JAMES QUIGLEY

As the outcrop mines in the West developed into underground operations, systems of ground support were gradually evolved. In the early coal mines there was little need for support except near the dirt line in portals, where stone masonry was common. Where the top was shaley or broken, native pine props with light cross bars and legs furnished enough support even in Utah's 25-ft coal seams. As depth of workings increased, roofs and backs of the same general nature as those near the surface became more and more unstable and required more and more support. Some coal airways show this tendency very clearly. From the surface down the same type of roof shows deterioration which an experienced eye can translate into a measure of depth under surface rather than change in rock characteristics.

Rock bolts, developed by various companies and by the U. S. Bureau of Mines, have become an effective substitute for timber in sections of some metal and nonmetal mines formerly requiring excessive timber support, and further use of war surplus landing mats, chain link fencing, and a new punched channel developed by one of the steel companies has enabled other mines to operate deposits where costs of timber and lack of clearance for timber support would have prohibited mining. The block caving mines have made extensive use of reinforced concrete underground to achieve similar ends under difficult conditions. Steel sets are standard in many Bureau of Reclamation projects, although these are usually covered in with concrete to make the permanent structures the Bureau's reclamation projects require. But the use of steel in mining operations is limited and has been confined principally to the iron ore mines of Michigan, Wisconsin, and Minnesota. Some mines have installed used rail as posts, caps, and crossbars, but a rail section is not suited for load carrying, and used rails are generally brittle, having a tendency to fail without warning when overloaded.

European mines were the first to reach the size of worked out areas and depths of cover resulting in major roof problems. The Europeans resorted to pack walls and masonry walls, in conjunction with timber arched sets, rail arches, and combination timber and rail and steel arches. The *give* in these pack walls and wooden blocking was supplemented by a hinge in the center of the arch. This design is called an *articulated arch*. Through various refinements of this principle of the support giving gradually with the load, Toussaint-Heintzmann developed the *yielding* or *sliding* arches, in which yield is accomplished by friction in the overlapping joints of the arch. This type has gained widespread acceptance in the Ruhr and Lorraine Basin and is being manufactured by Bethlehem Steel for sale in this country. In North America the anthracite mines in Pennsylvania, followed by certain iron ore mines in upper Michigan and Canada, were the first to employ these arches to any extent. The practice was later adopted by Kennecott at Ruth, Nev., and by others. Despite high initial cost, the use of these arches is growing in many parts of the country because of their suitability in heavy ground.

In its present form of manufacture the yieldable arch consists of open U-shaped rolled section with heavy beads on the edge. The open edge of the U is placed toward the wall. The section nests in another section of the same dimensions, and an arch can be built up from rolled radii and tangents of various weights and lengths. Sections are fastened together by U bolts and saddles. The lap on the joint varies from 12 to 24 in., and ordinarily the bolts are tightened with a 1-in. drive air wrench. The arches are spaced with channel struts held by J bolts and saddles. Sections can also be obtained that are composed of various combinations of radii and tangents and true circles. The joints can be placed to bear against anticipated loads and asymmetrical loads imposed by dipping strata. In the arches now being manufactured clearance widths up to 19 ft are obtainable in weights of sections from 9 to 30 lb per ft. The circular cross sections are available in the same weights ranging from 8 to 16 ft diam. At present most of the arches sold are supplied only in carload lots. It is hoped that demand will grow so that distributors can stock various weights and sections to give small operators a chance to try this new type of rock support under their own particular conditions.

Several excellent papers have discussed the properties of various sections now manufactured, the dimensions of the sets obtainable, and their application under widely differing conditions. The present article will describe the methods and results of a special use of the arches at Kaiser Steel mine No. 3, Sunnyside, Utah.

Problem at Mine No. 3: In 1953 Kaiser Steel Corp. laid out Sunnyside mine No. 3 to recover coking coal left by the previous operator, Utah Fuel Co., below workings that had been abandoned in 1928. Two seams had been worked, the upper and lower, separated by 30 to 42 ft of rock. Approximately 10 million tons of coal had been extracted from this area some 3000 ft down the pitch from the outcrop to a 1500-ft depth of cover. The mine had been opened by slopes in both upper and lower seams. Sometime in the late 1920's the lower slope

J. QUIGLEY, Member AIME, is Vice President, Centennial Development Co., Eureka, Utah. TP 4812F. Manuscript, Oct. 3, 1958. Rocky Mountain Minerals Conference, Salt Lake City, September 1958. AIME Trans., Vol. 214, 1959.

caved about 3000 ft from the portal. Utah Fuel cleaned up this cave and retimbered the slope, but weight induced by depth of cover and by mined out areas on the sides of the slope rapidly crushed this timber and enlarged the original cave. After one more attempt at reopening, using timber which again failed, the mine was abandoned and allowed to fill with water.

Concrete the First Solution Attempted: Because it was necessary to integrate this mine with the surface plant serving all three mines, Kaiser reopened No. 3 through the old caved slope. The upper portion was regraded to a pitch from 10 pct at the top to 7 pct near the cave. Pumps were installed at the cave to handle water, and rock bolts and landing mats held the walls and roof while the walls were lined with 12-in. concrete, reinforced with 1½-in. bars on 12-in. centers. The caved material was gobbed over the top of this concrete as mining advanced. This cave was found to be up to 25 ft wide and 55 ft high, breaking into and above the upper seam in places.

Shortly after this work was completed, while drop-ins were being prepared for mining entries below the cave, evidence of tremendous weight became apparent. In old entries and slopes adjacent to the main slope the same intense pressure developed, making it impossible to hold the drop-ins with normal timber, bolting, and landing mat and rib support. Although entries above the cave continued to produce coal, it was impossible to commence mining in the entries below. Roofs and ribs deteriorated rapidly, and six months after the major project of cleaning up and concreting on the main slope was completed, the necessary drop-ins and air courses became a problem more serious than the original cave that had forced abandonment in the 1920's. Cracks developed in the concrete walls, opening up as much as 4 in., and the lower portion of the walls pushed in as much as 5 in. Eventually the concrete cracking reached a limit and the ground appeared to be stabilized, but the loads seemed to shift to the adjacent openings needed for haulage and ventilation. It seemed inevitable that this pressure would increase as the entries above the cave were worked out, throwing more and more load on the slope pillars and on the virgin ground below.

Since concrete support had proved inadequate, the Kaiser management reverted to the possibility of using steel arches, originally considered for the clean-up job in the cave. When a bolted aircourse parallel to the main slope showed signs of failure it was buttressed by 15 ft-per-lb section yieldable arches. These arches, 16 ft wide at the base and 9 ft high in the center, were first placed on 4-ft centers and later on 2-ft centers.

Following a severe bounce in the Kaiser No. 1 mine in January 1957, other arches were installed on 2-ft centers in the main slope through a heavy area near a major fault that was believed to be the axis of loads related to tectonic movement. The early arches were placed by cleaning up the rock and standing an arch, then cribbing with 6x8 timber to the roof as in an ordinary timber set. The original arches paralleling the concrete-lined cave have stood up under heavy loads, some joints yielding as much as 8 in., but timber cribbing is slow and hazardous and difficult to block to achieve an even load distribution. Some of the loads seemed to

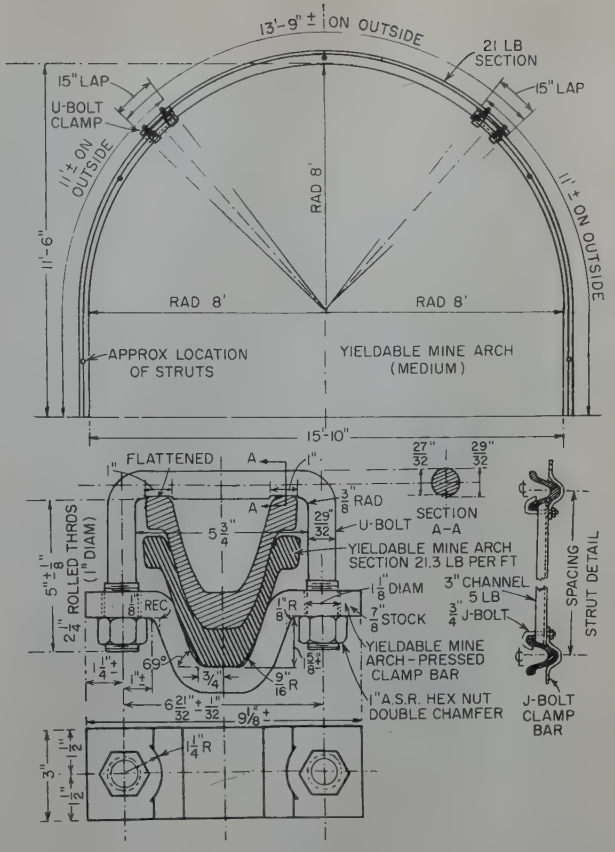

Fig. 1—Arch used at Kaiser Steel Mines, Sunnyside, Utah.

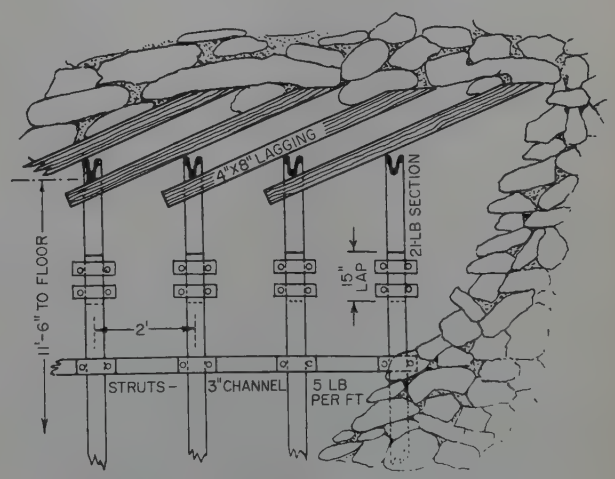

Fig. 2—Plank spiling driven over standard arches.

be horizontal and might be movement related to the mined out areas on either side of the supported areas, and some of the load evidently resulted from the dead weight of the crushed rock mass lying above the arch. A third source of load impingement comes from pillars in the mined out upper seam bearing directly on the roof of the lower seam 30 ft below.

Resort to Spiling: To provide additional coking coal for Kaiser's Fourth Blast Furnace expansion program it was necessary to continue reopening mine No. 3 beyond the limits of the mining entries at the bottom of the concrete. The old development slopes driven by Utah Fuel were certain to be caved. Because the arches in the No. 1 mine slope and in the aircourse paralleling the concrete had

proved successful, is was decided to advance by spiling, or forepoling using arches as support.

As the caves to be penetrated were under water, their extent was unknown. In appearance they are tightly packed masses of slabby shale with some admixture of coal. The coal and rock in the walls of the old entries have flowed inward as much as 2 ft, leaving a face consisting of packed crushed rock and coal with solid rock and coal on the ribs.

Work with the yieldable arches has been in progress for more than a year, and it is clear that reopening caved areas by removing as little rock as possible results in a much more stable permanent opening. The problems of sealing between air courses and gobs, which necessitated cleaning up many of the crosscuts and then rebolting, can be overcome by pumping fill into the voids in the crosscuts. It is also obvious that the crushed rock around the spiling forms a protective cushion that distributes the load evenly, and although the arches have yielded up to 4 in. in some sections, there is very little distortion.

From an operating standpoint spiling is simple. The first two sets must be blocked accurately, after which 4x8 planks 6½ ft long, with a 6-in. taper on one end, are driven out under the rear set and over the leading set. When the planking on roof and sides has sealed off the loose rock, the caved material in the face is loaded out and the next set erected. Perhaps the ultimate would be to substitute a steel channel for the plank, but at present treated plank is the most economical.

Various systems of jacks and come-alongs have been used to raise the center sections of the arch, but the best method is also the easiest. A 3-in. pipe is laid sloping up to the caved face just under the end of the 4x8 spiling, the bottom end resting on the floor. The miners push the center section of the arch up the pipe, and one man holds it in place while the legs are bolted on with air wrenches.

In coal mining all openings must be driven in pairs for ventilation. This gives a four-man crew a chance to split their duties. While two men are loading rock from one entry with a loader and shuttle car, the other two can drive spiling, drill, or block the arch to the walls in the other places. All join together to stand the set when the spiling has been installed. The holes necessary to break the large slabs in the face and overhang on the ribs are shot, and the loading crew returns to remove the rock from under the spiling.

Many of the problems in advance in spiling are normal to any type of rock advance in any mining operation. Waste haulage and materials delivery are necessarily intermittent; transportation of waste rock over the mine haulage depends on haulage of the mineral being mined, and arches and spiling must be brought in during normal material supply train schedules to avoid breaks in production. As opposed to cleaning up and cribbing, the lesser amounts of rock to be removed and material needed for spiling are important benefits.

Best performances, including the pumping of 250 gpm of water, are six sets per day on 2-ft centers, carried out on a two-shift basis with four men and a foreman on each shift. Where ventilation clears smoke from the shots readily, normal progress is two sets per shift, or 4 ft. If ground conditions permit 3 or 4-ft spacing, the work of driving the spiling is correspondingly easier and the advance in feet can be increased proportionately, but problems of removing the waste rock remain the same.

Few tools are required. Air wrenches are a great help in tightening the nuts, although spud wrenches are needed to line up the holes and place the nuts. In driving spiling various methods have been used. Where the ground is soft a sheeting driver is suspended by a chain from the third arch from the face and swung into position behind each plank. In many cases, however, the caved material is coarse and slabby, and it is possible to advance the spiling by poking the loose rock ahead with a bar and tapping the plank with a double jack.

Kaiser mine No. 3 may be a special instance of weight coming on after the opening has been made. Other mines may require more elaborate mechanisms for driving the spiling. In one case in the No. 3 mine the caved material was exceptionally heavy and the crushed rock ran around the spiling, filling the face and preventing the standing of the next arch. Here conventional breast boards were blocked against the leading arch and the advance was continued, although it was slowed to one set per shift on 2-ft centers.

As ground support problems increase, spiling over yieldable arches should have wide application in mines of all types. Where it is not economical to use maximum support throughout the length of haulageways and airways, it must be anticipated that caves will develop at unsuspected pressure points during the useful life of the opening. Spiling by means of yieldable arches offers a quick and economical method of reopening these workings. Any loading method can be used. Since the cross sectional area of the steel arch is small compared to timber, less hand digging is necessary along the rib, and there is less rock to load out. The plank drives well over the steel with little friction, the angle of driving spiling is less than over timber sets, giving more effective length to each plank, and the great strength of the arch compared to that of timber insures low maintenance costs against loads of all natures. Doubling up is easy compared with timbering and is accomplished with little loss of clearance. If it is necessary to seal off the sides of the opening for purposes of ventilation, low pressure grouting is effective.

Steel manufacturers continue to develop different sizes and sections of arches, and a variety of dimensions and shapes offer uniform, dependable support, easily installed and maintained.

The authors acknowledges the cooperation of the officials of Kaiser Steel Co.; J. Peperakis, manager of mines at Sunnyside; and J. Taylor, chief engineer.

REFERENCES

Institut National de l'Industrie Charbonniere, International Conference on Rock Pressure and Support in the Workings, Liege, Belgium, April 1951. (English text available.)

C. S. Kuebler: Arches in the Anthracite District. *Coal Age*, April 1954.

R. W. Sleeman: Yieldable Arches for Roof Support. (Cornwall, Pa.) *Mining Congress Journal*, November 1955.

G. P. Mahood: Yieldable Arches for Underground Roof Control. Lake Superior Mines Safety Conference.

R. C. Nispel: Yieldable Steel Arches for Roof Support. (Ruth, Nev.) *Mining Congress Journal*, July 1956.

R. W. Edwards: Ground Support in Bulk Mining. (Lake Superior) *Mining Congress Journal*, June 1956.

G. M. Huck: How Yieldable Steel Sets in Heavy Ground Save Money at Western Mines. *Mining World*, June 1958.

W. W. Wirth and W. L. Dennen: Development and Application of Concrete and Steel Roof Support on Haulageways, Pump Rooms, and Main Openings in the Anthracite Mines of Pennsylvania. *AIME TP 1193*, 1940.

Discussion of this article sent (2 copies) to AIME before Aug. 31, 1959, will be published in MINING ENGINEERING.

PRECISION SURVEY FOR TUNNEL CONTROL

by DOUGLAS D. DONALD

(*MINING ENGINEERING, page 977, September 1958, AIME Trans., vol. 214*)

C. J. Barber (*U. S. Smelting Refining & Mining Co., Salt Lake City*)—In his paper Donald describes how New Jersey Zinc Co. made surveys for a connection between the Ivanhoe and Van Mater shafts at Austinville, Va. Except to say that the two faces had to meet "accurately" on line and grade, Donald does not indicate the required precision.

Assuming that there were 24 angles in the 1½-mile traverse and 15 in the one-mile traverse, it can be shown that if the average error in plumbing each shaft was ±30″ and the average error in measuring each traverse angle was ±10″, then the average error at the point of connection would have been about ±1.9 ft normal to the line between the shafts. This calculation assumes that any errors in the triangulation would be negligible compared with the errors in the plumbings and traverses, and it also neglects taping errors. With no constant errors or blunders, the latter would be important only in lines normal to the line between the shafts.

To make the average error at the connection less than 1.9 ft would, therefore, require either reducing the error in the plumbings to less than ±30″, or that in the traverse angles to less than ±10″, or fewer stations, or a combination of these.

Referring briefly to the triangulation, because of the problem of fitting a new triangulation into older surveys of the district the orientation deserved some mention, even though the connection could have been made with an assumed bearing. It would be interesting to know how many triangles were required and what the average summation error was before making any adjustments and without considering the algebraic signs. Perhaps this is referred to indirectly in the statement that the maximum angular error distributed was 2″.

Turning to the shaft plumbings, it would be helpful to know how many men were employed and how long each shaft was in use. Donald says that the surface positions of W-2 and W-3 were carefully surveyed from the collar position of W-1, without indicating how this was done. The length of the backsight would be particularly important.

There must have been some error in setting W-1 vertically below the stations in the headframes. How immovable were the headframes, especially the Van Mater, which appears higher than the Ivanhoe and subject to more vibration because of skip hoisting?

Donald does not say whether the plumbing wires had been previously restraightened to minimize spinning (otherwise they behave like weak helical springs). The use of light steel weights is most surprising because there seem to be excellent reasons for using heavier, nonmagnetic weights. Did the shafts contain no steel sets, pipes, power cables, etc., which might attract steel?

The plumbing method described by Donald was designed for deep shafts in South Africa but differed from the South African practice in two important respects. As described by Browne,[6] in South Africa the line between the wires was made parallel to the long axis of the shaft, whereas in the Ivanhoe shaft the lines between the wires were diagonally across the shaft. The main reason given for the South African practice is to insure that the gravitational attraction between the wires and the rock walls is the same on both wires, and therefore does not affect the bearing of the line between them. It seems probable, however, that the effect of air currents might be minimized in the South African procedure, and might be serious with the wires in the diagonal position at the Ivanhoe shaft.

In the South African case cited by Donald the wires were swinging freely (although the plumb bobs were sheltered from air currents) but in the Ivanhoe case they were dampened with the plumb bobs set in water. In the discussion of Browne's paper R. St. J. Rowland said:[7]

> It has been the practice for a long time to damp the oscillations by immersing the bobs in oil or water. The time per oscillation is thus increased, thereby extending the time taken to complete the work. The longer the suspended wire the less there is to recommend the practice . . .

The theoretical time for one swing of a simple pendulum 1050 ft long is approximately 36 sec, which would be increased by dampening the plumb bob in water. Hence very few complete swings would be observed in the 5 min intervals used at the Ivanhoe shaft. In the two South African cases described by Browne, the length of plumb line in one shaft was 5425 ft, the calculated period of swing was 81.6 sec, the average actual period was 76.6 sec, and 94 complete swings were observed in 2 hr. In the other case the length of plumb line was 3116 ft, the calculated period of swing was 61.8 sec, the average period was 63.5 sec, and 86 complete swings were observed in 1 hr 31 min. Browne concluded that observations of more than 30 swings are not likely to result in sufficient gain in accuracy to be justified.

Returning to the Ivanhoe and Van Mater plumbings, an objection to the method used is that all four azimuths were taken from fixed points instead of swinging wires, and that each pair of observations would—barring blunders— check closely, and so perhaps give a false feeling of security. In fact, it seems that only two azimuths were obtained from one plumbing, and not four as stated by Donald. Nevertheless, the tying in of each pair of wires from both sides of the shaft has much to commend it.

Donald's description leaves the impression that if each shaft was plumbed only once, the engineers were fortunate indeed if the average error in the underground orientation was as little as 30″. Because the survey was done over a period of three years, it seems likely that the plumbings were repeated, perhaps more than once.

The underground traverse angles were measured by conventional methods, but because the number of angles in the overlapping traverses was not given, the angular closure given by Donald does not indicate the accuracy with which this was done.

Donald's description of a method of taping lines of irregular length is welcome. The literature on taping is usually confined to lines of about one tape length, generally 100 ft. Such lines are rare in metal mining because the time, trouble, and cost of setting points at 100-ft distances underground are not warranted. (Nevertheless civil engineers may go to this expense

in tunneling projects.) Was the base line measured in 100-ft drafts?

Unfortunately Donald did not give a sketch or photograph of the device by which the two men did all the taping.

Because one of the permanent rails was directly under the survey stations, it would seem to have been easier to tape USGS style along the rail, and to correct for inclination, than to have leveled each tape length. Perhaps the track was brought to final line and grade after the connection.

If the triangulation base were, say, 1200 ft higher than the 1100 level, and if no correction were made for elevation, then the calculated underground distance between the shafts would be about 0.75 ft longer than the taped distance.

Donald says that the precision obtained was considerably in excess of the requirements, but gives neither the requirements nor the actual closing error. If each shaft were plumbed only once, the engineers appear to have been very fortunate in this outcome.

Methods of improving the accuracy of the survey might have included:

1) Using an etched glass theodolite of European design, which would have many advantages over an American mining transit.

2) Reading the outside angles at all triangulation, plumbing, and traverse stations, so as to close on 360°.

3) Using re-straightened wire and heavier, nonmagnetic plumb bobs.

4) Repeating the plumbing with the wires parallel to the long axis of the shaft, or at least with the wires in different positions in the shaft. If air currents were a serious problem perhaps a simplification of the Roberts' method[8-10] might have been tried.

Reading Donald's interesting paper raises another question. When will mine surveys be oriented cheaply and conveniently by gyroscopic, electronic, or similar devices?

Douglas D. Donald *(author's reply)*— In response to C. J. Barber's discussion of my paper, I regret to state that to my knowledge, no final closure of the survey was carried out. I understand that when the tunnel faces were within about 200 ft of each other a diamond drill hole was put through. This hole cut the other face within a foot of centerline, but 2 or 3 ft above dead center. The joy occasioned by this holing through turned to consternation, for as the face advanced on line and grade the drillhole wandered upward and eventually disappeared in the back. As the tunnel drive continued, the hole wandered back into the face so that by the time the last round was taken it was approximately in its proper position in the advancing face. For practical purposes, the tunnel closed perfectly on line, although between 1 and 2 ft off on grade.

The article neglected to mention that check angles were turned on the long straight reaches of the tunnel and the sights on these shots were occasionally greater than 1000 ft. The new triangulation net used as its initial coordinates the original coordinates of one of the old stations and assumed an original bearing from the station. As I recall, nine triangles were used and the average summation error would be about 1".

In establishing W-2 and W-3 from W-1 positions, it was arranged so that the backsight was a station in the triangulation net and its length was between 40 and 50 ft. Angles were turned at W-1 from the backsight to WO2 and to W-3. The internal angle W2-W1-W3 was also turned and these results were compared with results obtained by subtraction. All hoisting operations were suspended while W-1 in each headframe was occupied by a transit and while the point was being transferred to collar elevations. In fact, a platform was arranged for the engineer to stand on while turning angles from W-1 in the headframe so his moving around the transit would not in any way disturb the set-up.

The spinning effect Barber refers to was minimized by inserting several small fishing tackle swivels in the plumbing line at widely spaced intervals. We take exception to the old theory that a plumbing wire must have no splices in it. Kinks, of course should be cut out and the wire fastened together by means of interlocking small open loops on a small swivel. The rigidity of the wire was sufficient to prevent closure of these loops when the heavier plumb bob was attached. I feel that mass effect on plumbing lines is generally overrated, especially since the greatest effect would be on the plumb bob itself, and this is usually located in a shaft station where the rock has been excavated for quite a distance in all directions around the bob.

Theoretically the resultant of mass effect on the wires may be determined by the distance of the midpoint of the line between the wires from the center of gravity of the shaft section. Should the midpoint of this line coincide with the center of gravity, it becomes obvious that each wire would be displaced so as to affect only the distance between the wires, but not the azimuth. The distance between the center of gravity and the midpoint of lines W1-W2-and W1-W3 was only about 1 ft. Thus mass effect would have negligible effect on azimuth.

We felt that our plumb lines did not act as a simple pendulum because of the three or four splices and swivels that occurred in the wire at irregular intervals. This was fully proved first by actually plotting the wire observations to see if there was a constant trend of the mean point between pairs of observations and, second, by the mean position of the second set of reading, which corresponded almost precisely with the results of the first set. Maximum permissible limits were ½ of a scale division (0.017 in.) and usually the averages checked to 0.2 of a scale division or better.

It is granted that fundamentally two independent sets of azimuths were taken off underground. However, the accuracy of each set is increased by using two groups of observations to arrive at each set.

Barber is entirely correct about repeated plumbings. Since the Ivanhoe was not a production shaft, our methods were initially worked out in that shaft. The Ivanhoe shaft was plumbed twice before acceptable results were obtained. The first plumbing of the Van Mater shaft appeared to be satisfactory, but a fatal blunder was made in not transferring the control to enough points in the shaft station. Several days after doing the job, a development crew shot out most of the control, so the plumbing had to be repeated. Each time the plumbing was carried out on a weekend and was completed in less than 16 hr so as not to interfere with production. Five engineers and a couple of helpers usually worked on the job.

Taped traverse distances were usually 105 to 110 ft long, but by using our calibration curve, we could accurately tape any distance up to 200 ft. The base line was taped with a 100-ft standardized tape, so each draft was 100-ft long plus or minus a few tenths of a foot.

Concerning Barber's concluding suggestions, I concur wholeheartedly about the benefits of a 1" theodolite. I neglected to state in the paper that all angles were turned first to the right and then to the left, thus closing to 360° on the plate.

REFERENCES

[6] L. D. Browne: Movement of Freely Swinging Plumb Lines in Deep Vertical Shafts, *Journal of the Chemical, Metallurgical & Mining Society of South Africa*, vol. 49, no. 11, May 1949, pp. 445-450.

[7] The above paper also appeared in *The Journal of the Institute of Mine Surveyors of South Africa*, vol. 6, no. 1, March 1950, pp. 11-24. The quotation from Mr. Rowland's contribution to the discussion is from p. 22.

[8] F. G. A. Roberts: Deep Level Shaft Plumbing on the Far East Rand. *Journal of the Institute of Mine Surveyors of South Africa*, vol. 2, January 1929, pp. 10-12.

[9] Eric R. Wykes: Plumbing No. 2 Shaft, East Geduld Mines Ltd., Springs, Transvaal. *Canadian Mining & Metallurgy Bulletin*, no. 297, January 1937, pp. 17-24.

[10] F. Winniberg: *Metalliferous Mine Surveying*, 4th ed. Mining Publications Ltd., London, 1957, pp. 221-226.

BAUXITIZATION IN THE POCOS DE CALDAS DISTRICT, BRAZIL

by BENJAMIN N. WEBBER

During World War II the Pocos de Caldas bauxite deposits of Minas Gerais in Brazil yielded some 60,000 tons. Since then they have maintained a small but almost continuous production. Known for many years, the deposits have been reconnoitered by a number of geologists,[1-4] but no dimensional study has been possible because there have not been enough exposures to show clearly the depth, bedrock, and habit of occurrence.

The deposits are somewhat unorthodox in their occurrence mainly on steep slopes of mountainous terrain. Although the parent rocks are a sequence of alkalic intrusions that bauxitize readily under the proper conditions, bauxitization has not been the dominant weathering process in the area. It is limited to certain localities where important volumes of bauxite have formed by laterization of several rock types, each yielding a distinctive type of bauxite. Bauxitization may be observed in several stages and in both direct and indirect cycles of formation. The deposits are unique in being of demonstrably recent age, so that the conditions under which the bauxite formed are essentially those of the present time. The bauxitization sequence is postulated in Fig. 1.

Pocos de Caldas district is situated at approximately 21° 50′ south latitude and 46° 30′ west longitude in southwestern Minas Gerais, near its boundary with the state of São Paulo. It lies within the Eastern Plateau physiographic province of Brazil, occupying a prominent highland area that rises some 2000 ft above the surrounding country. The central portion of the Pocos de Caldas highland is characterized by gently undulating topography, with generally sluggish drainage, and is surrounded by a rim of hills rising above 1000 ft above it. In cross section the highland resembles a truncated cone with a depressed central area. The rim has been sculptured into a more prominent and abrupt topographic pattern than the central area, and streams that are of low to moderate gradient in the central plateau plunge over the rim in a spectacular series of cascades and falls.

B. N. WEBBER, Member AIME, is Chief Geologist, Mineração Hannaco Ltda., Belo Horizonte, Brazil, TP 4805 I. Manuscript, Jan. 9, 1959. AIME Trans., Vol. 214, 1959.

GEOLOGIC SETTING

The Pocos de Caldas highland owes its physiographic expression mainly to the differential erosion of a complex intrusion of alkalic rocks into gneiss and sandstone. Erosion was guided somewhat by faulting. The highland is almost circular, and its limits, except in one locality, coincide with the periphery of the intrusion. The alkalic intrusions largely control its shape and extent, aided by some subsidence through faulting of the central portion. The mountainous rim of chilled phase, the later intrusions, and the indurated intruded rocks have resisted erosion more effectively than the central portion of the intrusion, which is composed of more coarsely crystalline alkalic rocks that form a central basin in the highland. Gneiss and sandstone are found coincident in elevation with the topographically highest intrusions.

BAUXITE TYPES

Most of the bauxite, which varies in physical type, is on the top and steep slopes of the northern rim. The only alumina mineral is gibbsite, definitely crystalline but iron-stained unless of secondary origin. Clay particles occurring with the bauxite are kaolinite.

Some types of bauxite are an index to their origin. There are four general physical types of bauxite or bauxite laterite:

1) Surface Rubble: This partly nodular and partly fragmented type, usually less than 3 ft thick, results from surface weathering of massive bauxite or may form by superficial enrichment of nodular bauxite with a clay matrix when the interstitial clay is removed by surface runoff.

This page of Mining Transactions AIME follows p. 724. The intervening non-Transactions pages appeared in MINING ENGINEERING.

2) Massive Bauxite: This is light yellow, porous, cellular, and massive but friable. If it is derived by direct bauxitization of the country rock, it may show a phantom joint pattern inherited from the parent rock. The cells are reticulate and often show alignment similar to limonite silica boxwork in iron gossan; near the surface they may be lined with secondary crystals of gibbsite. This type of bauxite consists almost entirely of slightly iron-stained gibbsite with a small amount of residual kaolinite.

3) Nodular Bauxite in Clay Matrix: This consists of nodules, perdigon, and irregular aggregates of bauxite, some of which show a cylindrical stem-like form. These are disseminated through a matrix of kaolinic clay. The bauxite fragments usually contain entrained clay or may be relatively pure gibbsite. The bauxite nodules may be accompanied by nodules of hard kaolin.

4) Replacement Pattern Bauxite: This type of occurrence consists of irregular aggregates of massive bauxite in a clay matrix. Both bauxite and clay aggregates may be several feet across and are highly erratic in distribution. This occurence suggests incomplete bauxitization of clay, with the bauxitization process spreading from replacement nuclei.

PARENT ROCKS

The alkalic intrusive rocks are consanguineous, with slightly variant mineralogy, including some unusual species. They have a notable range in texture—from dense, compact, aphanitic rocks to coarsely crystalline in which the crystals approach pegmatitic size. The range in crystal size suggests intrusion at different pressures and cooling rates. There probably was an important hiatus in time, particularly between the older and younger groups. The older intrusions are more coarsely crystalline and more intensely zeolitized than the younger group.

The following alkalic rock facies associated with bauxite were recognized. No regional study was made and these observations are confined to areas where commercial bauxite occurred. In order of increasing age, the younger group is as follows:

1) Phonolite: This is either an extrusion rock or a near-surface intrusion. It has a fine-grained aphanitic texture with a tendency toward layering which may represent flow structure. Its occurrence as observed is already limited, but it could be an important unit elsewhere in the highland. It is not lateritized and it overlies phonolite porphyry.

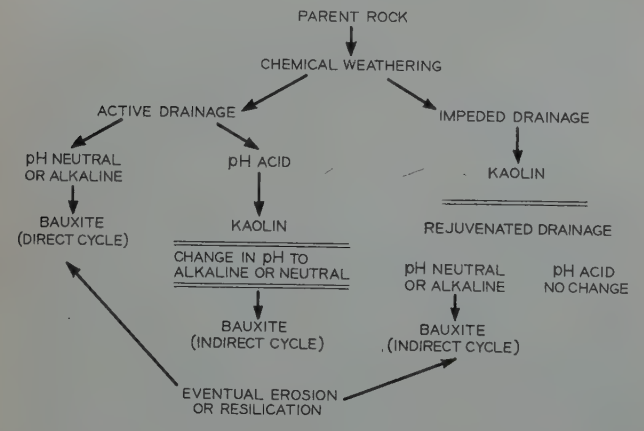

Fig. 1—Bauxitization cycles, Pocos de Caldas, Brazil.

2) Phonolite Porphyry: This is intruded in an irregular pattern into older alkalic rocks as well as the gneiss and sandstone. Parent rock of fully half the bauxite, it is characterized by abundant nephelite and alkalic feldspars. Femic accessories are mainly pyroxene with subordinate amphibole. No zeolitization was observed. Phonolite porphyry was the last intrusive phase of the alkalic rocks; it cuts all the other facies and penetrates the Botucatu' sandstone of Triassic age which unconformably overlies the Pre-Cambrian gneiss. This dates the last intrusion as post-Triassic, probably Cretaceous.

3) Nephelite Syenite: An important parent rock of bauxite, nephelite syenite contains the same minerals as the phonolite porphyry in about the same proportions. It preceded the phonolite porphyry, which cuts it with a sharp intrusive contact.

4) Nephelite Cancrinite Syenite: This consists of nephelite and alkalic feldspars in large crystals up to 3 in. long; it contains appreciable cancrinite in places and apatite and acmite as rare accessories. Occasionally a crystal of pyrite occurs. Zeolitization is apparent but not intense. Nephelite may be partly altered to analcite. This syenite is older than the phonolite porphyry that penetrates it. Its intrusive relation to the nephelite syenite was not encountered. It lateritizes readily to a low iron bauxite.

The older group of rocks is as follows:

1) Eudialyte Nephelite Syenite: This is a moderately coarse-textured intrusive rock consisting mainly of nephelite and alkalic feldspars and pyroxenes. Amphibole is less abundant than pyroxene. Eudialyte, euhedral zircon, and sphene are common accessories. The rock bauxitizes readily, yielding a product high in iron owing to the abundance of pyroxenes. The phonolite porphyry penetrates this intrusive, but the relation of this syenite to the other members of the alkalic group was not apparent in the limited area studied.

2) Gneissoid Eudialyte Nephelite Syenite: Essentially nephelite and feldspar, with abundant pyroxenes and considerable green amphibole, this rock has developed gneissic banding by parallel arrangement of tabular feldspars. Abundant femic minerals constitute about half the rock, generally occurring as augen around the feldspars. Eudialyte is usually a common accessory but in some localities is one of the principal minerals. Zircon and sphene are common accessories. Zeolitization is widespread. Zeolites developed are analcite and natrolite. Lack of metamorphic minerals other than zeolite belies the gneissic banding. Possibly the parallel arrangement of feldspars in augen of femic minerals results from crystallization under conditions of stress, so that the crystals tended to grow along lines of least stress. The rock lateritizes readily, with almost complete removal of silica except that contained in the zircon. Zircon remains inert to lateritization process and zircon crystals may be found in the laterite. Eudialyte breaks down completely, leaving residues of iron and manganese oxides. The lateritic end point of this rock is a ferralite or high-iron bauxite.

The rocks which have been intruded by the alkalic complex are an orthogneiss of granitic parentage and the Botucatu' sandstone. The gneiss forms bauxite on lateritization, but the free silica is unaffected; quartz crystals remain in the laterite.

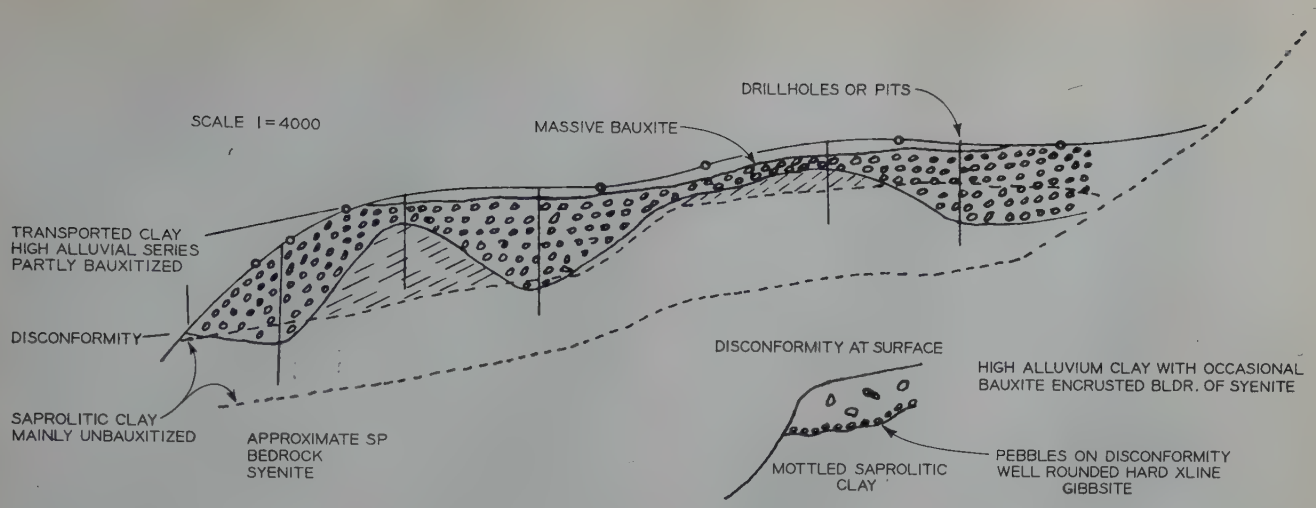

Fig. 2—Section along the disconformity between the high alluvials and the saprolitic clay. The inset at lower right shows the relation of bauxitization to disconformity between the high alluvium and the older saprolitic clay.

There is evidence that the alkalic intrusions have not been deeply truncated. Exposure is barely below the hood of the intrusive.

In addition to the igneous and metamorphic rocks that have yielded bauxite on lateritization, a very recent sediment has lateritized, which gives an index to the age of the bauxite. This is a high alluvium with a limited occurrence on stream terraces. It is composed of roughly stratified clay with small lenses of gravel and contains a lense of black clay whose color is due to particles of fixed carbon which ignite and burn at calcination temperature. This clay probably marks a local paludal condition at the time of deposition. The alluvium contains local accretions of outwash gravel and clay from the steel adjacent slopes. The drainage that deposited the bulk of the high alluvium is now entrenched about 50 meters below its former level. Drainage is entirely within the alkalic rocks and the sediments were all derived from the drainage basin. The high alluvium rests on saprolitic clay derived from alkalic syenite and in a few instances rests directly on the syenite. A disconformity between the saprolitic clay and high alluvium is a well-marked undulating surface with pockets and lenses of smooth water-worn pebbles consisting largely of hard crystalline gibbsite. The disconformity can usually be located in drillholes by an increase in bauxite due to the basal layer of gibbsite pebbles, followed by a change to saprolitic clay (Fig. 2).

AGE OF DEPOSITS

The significance of lateritization of the high alluvium is an index to the age of lateritization. The pebbles of gibbsite on the disconformity show that bauxite had formed and had been eroded before the high alluvials were deposited. Bauxitization of the high alluvials probably began when stream entrenchment reached a level where the terraces were well drained. The degree of lateritization of the high alluvials compares with that of several areas where igneous rocks or their saprolitic clays have lateritized.

Most lateritization in the district appears to have taken place after the drainage had been subjected to some rejuvenation and had been lowered to almost its present level. This is geologically recent and bauxitization is in process in some localities at the present time. The recent age makes it unnecessary to infer the conditions at the time of bauxitization. They are essentially those now existent in the region, with the exception of the foremost cover.

FEATURES CONDITIONING BAUXITIZATION

Climate: The alternate wetting and drying favorable to bauxitization are characteristic of this area, not only seasonally as evidenced by the distribution of rainfall (Fig. 3), but also because there are steep slopes and rapid drainage after every storm. Annual precipitation is 90.87 in. Rainfall on the highland rim is believed to be appreciably higher than that shown but is subject to the same periodicity. Masses of moisture-laden air collide with the highland rim and drop a considerable portion of their moisture before reaching Pocos de Caldas, and it is the higher elevations of the peripheral hills that are most extensively bauxitized.

Climate throughout the year is temperate, bordering on the subtropic. The following record for 1957 was obtained through the courtesy of the Ministry of Agriculture, Meteorologic Service:

Average Monthly Daytime Temperatures, °F, 1957

Jan.	Feb.	Mar.	Apr.	May	June	July	Aug.	Sept.	Oct.	Nov.	Dec.
69.8	68.8	68.0	65.0	60.0	59.0	57.2	62.8	64.1	69.4	67.8	70.7

Minimum recorded 46°; maximum recorded 79.9°.

Average Monthly Humidity, Pct, 1957

Jan.	Feb.	Mar.	Apr.	May	June	July	Aug.	Sept.	Oct.	Nov.	Dec.
80.7	82.1	80.7	81.9	77.8	77.7	78.4	71.8	77.4	76.1	79.5	80.3

These climatic conditions favor chemical reactions and bacterial activity.

Permeability: Porosity of the aphanitic phonolite porphyry is low. The syenites have a somewhat higher penetrability, owing to the size of the crystals of silicate minerals. Both are about equally jointed and rock joints are the major points of attack for pluvial water. Along occasional faults where the rocks were shattered there is a great increase in permeability. The footwall of one noted fault is unbauxitized, whereas the hanging wall side is bauxitized to a depth of 30 ft.

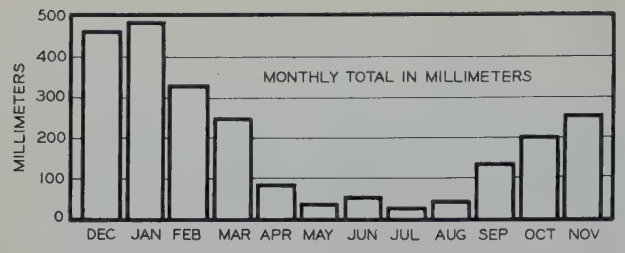

Fig. 3—The quantity and frequency of precipitation in the Pocos de Caldas district of Brazil as observed over a period of 19 years. (Servico Meteorologico Paulista).

Vegetation: Undoubtedly human occupancy has altered the vegetation pattern, which is highly variable. Heavy forest remains in some localities, mostly on steep slopes; others are open grass land. In the areas now occupied by forests there is some accumulation of humus, but the balance between micro-flora and macro-flora usually does not permit more than a foot of humus to accumulate. On the steep slopes, where most of the bauxitization has occurred, there is enough rainfall to flush most of the soluble humic compounds into the drainage.

Drainage and Erosion: Topographic relief of the bauxite deposits is pronounced, with elevations from 4000 ft at the base of the mountain rim to 5500 ft at its crest—a variation of 1500 ft in less than a mile. The steepness of slopes which have been bauxitized is notable; statistics show a minimum of 5° and a maximum of 27°. The average slope of bauxitized terrain is 18°, far from the near-peneplain conditions or topographic maturity of most laterite formation.

Topographic relief and rapidity of drainage apparently favor bauxite formation, but the critical factor is preservation of bauxite rather than its formation.

The physiographic surface is gradually being modified, a process that probably began when the alkalic rocks were first exposed. In some localities erosion has kept pace with bauxitization, but in many places it has proceeded more slowly. On the higher slopes where most of the bauxite occurs, runoff is partially impeded by vegetation. Much of it seeps through that portion of the bauxite that is highly porous, but only after saturation has been reached. This lessens erosion by rainfall and facilitates removal of the soluble products of rock decay.

The depth of secular decay is highly variable over the area of bauxitization, ranging from nothing over rock outcrops to a maximum of 65 ft and averaging 33 ft. Out on the central plateau where erosion is less active and drainage more sluggish, hydrolization to kaolinic minerals is the dominant process, although alkalic rocks predominate and rock decay has extended to greater depths, often approaching 100 ft.

Influence of Parent Rocks: The parent rocks have already been briefly described. Most of the bauxite has been derived from phonolite porphyry and nephelite syenite, and there is little difference in the chemical character of the bauxite from these two rocks. Each of the other five units from which appreciable amounts have been derived yields a distinctive bauxite that is a chemical reflection of the mineral components of its parent. The eudialyte rocks yield a high-iron bauxite, which indicates the relative abundance of femic minerals in these rocks. The titania content reflects the appreciable sphene, and the low iron content of the bauxite derived from the cancrinite-bearing nephelite syenite reflects the sparsity of femic minerals. The bauxite derived from high alluvials reflects the origin of the high alluvials, which were in turn derived from phonolite porphyry and nephelite syenite. The bauxite derived from gneiss was incompletely analyzed but reflects the free silica of the component gneiss (see Table I).

BAUXITIZATION

Bauxitization has been accomplished by a direct and an indirect cycle. The direct cycle is bauxitization of country rock with no intermediate stage. The indirect cycle shows an intermediate clay stage, during which the country rock was kaolinized and the kaolin later desilicated to form bauxite. In chemical character there is little difference between bauxite derived directly from the parent rock and that which went through a saprolitic clay stage before bauxitization.

Statistics from a large number of exploration openings show that 65 pct of these openings bottom on clay underlying bauxite and 35 pct on rock. These figures are considered a good index to the relative amount of bauxite which went through a preliminary clay stage and indicate that only about one third of the bauxite was directly derived from country rocks.

Evidence of direct bauxitization may be found in many exploration openings where bauxite with practically no clay content bottoms on bedrock and bauxitization extends into the joints of the bedrock, making a microscopically sharp contact of bauxite to rock. As shown in Fig. 4, these exploration exposures have a typical chemical profile from top to bottom, with practically no variation in bauxite or clay content to suggest that a clay stage ever existed.

Indirect bauxitization is evidenced by a larger number of openings which show a downward transition from massive bauxite at the top to a mixture of bauxite aggregates in clay, the clay content in-

Table I. Comparison of Bauxite Derived from Various Rock Units

Percent	Phonolite Porphyry	Syenite	Eudialyte Nephelite Syenite	Gneissoid Eudialyte Nephelite Syenite	Cancrinite Nephelite Syenite	High Alluvium	Ortho-Gneiss
LOI	27.08	27.55	25.00	24.05	29.18	27.68	—
Insol.	3.92	4.46	4.9	5.39	5.50	6.55	12.00*
Fe_2O_3	8.62	8.81	16.4	21.43	6.60	8.00	9.00
TiO_2	0.86	0.88	1.7	1.63	0.60	0.80	—
Al_2O_3	58.59	58.36	49.5	47.83	57.90	57.10	50.34

* Approximately 6 pct free SiO_2.

creasing and the bauxite content decreasing downward through bauxitic clay to clay bedrock. In some of these holes, bedrock was reached that is hydrolizing to clay minerals. The chemical profile of the hole shows a distinct relation of clay to bauxite which varies directly with depth. Kaolinization, apparently the first process, is still under way. In the upper and better drained portion of the profile bauxitization has proceeded to completion by desilication of clay and is advancing downward as a function of time and drainage, its intensity varying inversely with depth. A few instances were noted in which the clay gradient indicated changes from the usual profile. The profile in the upper portion of the hole indicated desilication of clay and in the lower portion direct bauxitization of country rock. Statistically only 4.2 pct of the exploration openings reveals an abnormal chemical profile differing essentially from those illustrated. Where clay has been desilicated to bauxite, the process of bauxitization is almost invariably more complete near surface (Fig. 4).

No instances were noted in which direct bauxitization of country rock had changed to kaolinization, though conceivably this would happen if an active drainage became rapidly stagnated.

The many iron analyses of bauxite plotted against depth show no appreciable variation in iron content with depth. This lack of iron mobility during bauxitization is attributed to a neutral or alkaline environment with an abundant supply of oxygen, conditions under which ferrous compounds are rapidly oxidized and become relatively fixed as sesquioxides.

Those changes in the bauxite which have taken place after bauxitization was completed are of minor volumetric importance and are best observed in massive bauxite. There is evidence of some solution, migration, and reprecipitation of alumina, and in certain instances tiny veinlets of hard crystalline gibbsite reticulate massive bauxite. These show a tendency to follow the phantom jointing of the bauxite, which is a partial preservation of the original jointing of the parent rock. The cells in porous cellular bauxite often contain secondary gibbsite crystals. In the surface rubble overlying massive bauxite, concretions of almost pure, hard, crystalline gibbsite occur which tend toward a turnip shape with a hole or other evidence of a central conduit on the long axis. In place, they always point downward. Some of these are intricately plicated, showing growth by accretion.

Resilication of bauxite is suggested by clay veinlets cutting massive bauxite. Like the secondary gibbsite veinlets, these tend to follow the phantom jointing, though not invariably. Replacement of bauxite by clay may spread from the phantom joints, leaving unreplaced massive bauxite in the center of the phantom joint block.

Chemical weathering predominates over mechanical weathering throughout most of the district. Hydrolization of rocks to kaolinic products is the predominating process. Direct bauxitization and kaolinization are both in progress, occasionally in the same general locality.

Drainage is an observable control, both in direct bauxitization of country rock and bauxitization of clay. In an environment of impeded drainage the weathering product is always clay. Under conditions of active drainage, either kaolinization or direct bauxitization of country rock may occur. Direct

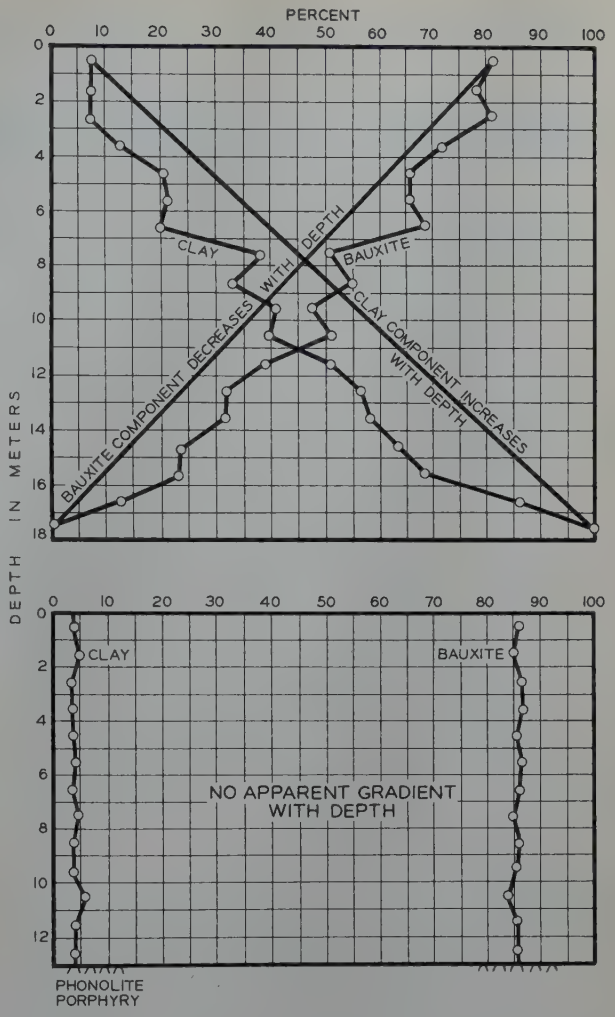

Fig. 4—Typical bauxite and clay variation with depth. Clay and bauxite calculated from analyses. ABOVE: Bauxite which is derived from the desilication of clay. BELOW: Bauxite derived directly from parent rock.

bauxitization is here considered to result from a favorable pH. A slight increase in acidity results in kaolinizaton. The role of pH may be oversimplified, since the conditions under which alumina and silica react to form clays are subject to complicated controls. The conditions under which silica may remain in solution and be removed, though unsual in nature, appear to be chemically simpler. Kaolin once formed under the existing climatic controls is subject to bauxitization, if the drainage remains or becomes active. Bauxite, regardless of direct or indirect origin, is subject to both enrichment by secondary gibbsite and resilication to clay. Both processes can be observed but are considered volumetrically unimportant.

The writer is indebted to J. K. Gustafson, vice president and director of exploration of Hanna Mining Co., for permission to publish data obtained during exploration of these deposits.

REFERENCES

[1] E. C. Harder: Examples of Bauxite Deposits Illustrating Variations in Origin. *AIME Trans.*, 1951, vol. 193.
[2] E. C. Harder: Stratigraphy and Origin of Bauxite Deposits. *65A*, 1949, vol. 60.
[3] M. de S. Pinto: Bauxite em Pocos de Caldad. *Bull. 22*, 1938, Dept. Nacional de Producao Mineral.
[4] T. de S. Santos: Contribuicao da Congr. Sul. Amar. de Chem. Inst. Pengrica. *Bull 17*, 1937.

Discussion of this article sent (2 copies) to AIME before Sept. 30, 1959, will be published in MINING ENGINEERING.

FERROGRADE CONCENTRATES FROM ARKANSAS MANGANIFEROUS LIMESTONE

by M. M. FINE

Normally the U. S. produces less than 10 pct of its annual manganese requirement. About 95 pct of domestic consumption is used by the steel industry.[1] The strategic and critical nature of manganese has been recognized by its inclusion in the national stockpile and by intensified research directed toward cataloging and evaluating domestic manganiferous deposits.

The USBM has participated in these activities for many years with field and laboratory studies to assess the extent and potential utilization of domestic manganese ores. One area of particular interest is in the vinicity of Batesville, Ark., where deposits have been mined since 1849 for both manganese and ferruginous manganese ores. Production is centered in Independence County, but deposits are also found in Sharp, Izard, and Stone counties in north-central Arkansas. Miser has described the geology and manganese mineralization in some detail.[2, 3] The rocks of the area are sedimentary, consisting of sandstone, limestone, shale, and chert. The two formations of greatest importance,[4] Fernvale limestone and Cason shale, are host rocks of the primary manganese mineralization.

Through 1955 the district produced some 230,000 long tons of manganese ore (35 pct Mn or more) and 236,000 tons of ferruginous manganese (10 to 35 pct Mn).[5] Most of the ore has been mined from deposits of manganese oxides in residual clays resulting from weathering of the two formations noted above. Concentration methods have been primitive, consisting for the most part of washing, hand picking, and jigging.

A significant accomplishment in the district in recent years was the USBM recognition and investigation of the huge manganese potential represented by unaltered Fernvale limestone. Systematic reconnaissance of manganiferous limestone and other occurrences has been in progress since 1953 to delineate the extent and tonnage of manganiferous materials. Results of that survey have appeared in two recent publications,[4, 5] which ascribe to the district an inferred reserve of 166 million long dry tons at a grade of 5 to 6 pct Mn. Most of this was manganiferous limestone with an estimated content of 5 pct Mn.

Specifications: Beneficiation was carried out on a group of manganiferous limestones to develop a way to recover commercial-grade concentrate from this extensive resource. The following chemical specifications were established by the GSA for metallurgical manganese ore acceptable for delivery to the national stockpile:

Constituent	Percent by Weight, Dry Basis
Mn	40.00 minimum
Fe	16.00 maximum
SiO_2 plus Al_2O_3	*
P	0.30 maximum
Cu plus Pb plus Zn	1.00 maximum**

* No limit specified, but material over 15 pct will be purchased in exceptional cases only.
** Of which not more than 0.25 pct may be copper.

Size specifications were not considered, as it was assumed that the concentrates could be pelletized or sintered.

Manganiferous Limestones: Of the 11 samples tested to date, six were taken by cutting vertical channels across beds of limestone outcrops. Diamond drilling through overlying barren chert into unexposed limestone provided four samples, and the last was a churn drill sample. In general, the samples were dark, fossiliferous limestone containing small amounts of braunite, hausmannite, rhodochrosite, massive and micaceous iron and manganese silicates, quartz, barite, and glauconite. The braunite and other manganese oxides partly to completely replaced some of the calcite and fossil material. The calcite was generously stained with mangenese and iron oxides. Phosphorus was present in all samples as collophanite grains, calcium phosphate fossil replacements, or an unidentified manganese-bearing carbonate.

The difficulty in separating this complex array of minerals was further complicated by a very intimate association. Although some manganese grains as large as ⅛ in. were noted, grinding to subsieve sizes would have been necessary to liberate the components. Figs. 1 and 2 are micrographs, at X100, of typical polished sections in which white areas are manganese, gray is gangue, and black areas are surface depressions. By comparison with the 100 mesh opening, it is seen that some of the grains are coarse enough to respond, perhaps to tabling or flotation, but many are obviously beyond the scope of physical processing.

Partial chemical analyses of the eight samples that were ultimately amenable to concentration are presented in Table I.

BENEFICIATION RESEARCH

Tabling: To take advantage of the presence of sand-size grains, both jigging and tabling were considered at the outset. Jigging was largely ineffective, but tabling achieved a partial recovery from most samples. As an example, the surface material from Baxter Hill was crushed to —28 mesh, hydraulically classified, and the coarsest spigot fraction was tabled to yield a concentrate, middling, and tailing. The latter two were reground to pass 48 mesh, combined with the primary fines, reclassified, and retabled. The middling and tailing were again ground, this time to pass 150 mesh, and deslimed at 20μ in a 3-in. hydraulic cyclone. The cyclone underflow was returned to the table to reclaim a small amount of high-grade manganese.

An interesting facet of the gravity concentration developed on certain samples in which braunite was the principal manganese constituent. Since braunite has a Mohs hardness of 6 to 6.5, while the host rock, limestone, is only 3, a differential size reduction took place during crushing, and the

M. M. FINE, Member AIME, is Supervising Extractive Metallurgist, Region IV, U. S. Bureau of Mines, Rolla, Mo. TP 5982S. Manuscript, Oct. 14, 1958. San Francisco Meeting, February 1959. AIME Trans., Vol. 214, 1959.

coarsest fraction became enriched in manganese. However, at this the size (about 28 to 48 mesh) many manganese grains were still locked and on subsequent tabling reported in the middling along with finer gangue. Screening this middling on 40 to 48 mesh, it was found, recovered up to 15 pct of the total manganese. The screen product was of lower grade than the conventional concentrate, but the two could usually be blended.

Table II presents the results of tabling the Baxter Hill surface ore. More than 40 pct of the manganese was recovered in a product acceptable in all respects other than phosphorus.

Flotation: Flotation was included in the flowsheet as a scavenging operation to capture some of the fine manganese remaining in the cyclone overflow and table rejects, which still accounted for 59.1 pct of the total manganese at a grade of 3.5 pct Mn. It was recognized that much of this, in the form of dustlike inclusions in limestone, was unrecoverable manganese.

A double-flotation scheme was devised which recovered about one third of the remaining manganese at a usable grade. The combined table rejects were pulped with zeolite-softened water, charged to a flotation cell, and conditioned with caustic soda to disperse the slime and with corn dextrin to retard flotation of the braunite. Most of the limestone was then floated with a tall oil fatty acid and cleaned once. The cleaner and rougher tailing were combined, settled, and deslimed at 10μ by decantation. The settled sand was then refloated to reject most of the remaining limestone, leaving the manganese as the nonfloat product.

Table III details the results typical of floating Baxter Hill table rejects. Note that 34.0 pct of the manganese in the feed was recovered at a grade of 25.3 pct Mn. Though low, this was adequate, as will be shown later. For reasons already discussed, the flotation step is inefficient from a metallurgical standpoint. From an economic standpoint flotation of the gangue rather than the manganese minerals is also undersirable, as it is necessary to bring about 90 pct of the bulk into the froth to recover the much smaller amount of manganese. However, many experiments failed to indicate a satisfactory method for reversing the procedure. Quebracho, under other circumstances a potent depressant for calcite, in this instance had very little effect on the limestone but did retard manganese flotation. Other reagents like sodium silicate and soda ash will depress manganese oxides in the presence of limestone, but starch products seem best for this purpose.

Leaching: At this stage, combining the table and flotation manganese products had achieved a recovery of 61.0 pct at a grade of 34.4 pct Mn, 9.9 pct Fe, 11.3 pct acid insoluble, and 0.53 pct P, but the product was still submarginal. Final upgrading was effected by a dilute-acid leach that removed enough phosphorus and limestone to raise the manganese to an acceptable value. Leaching was conducted with 2.5 pct sulfuric acid for 1 to 2 hr at room temperature. The leached product was washed twice with 25 to 50 volumes of water, dried, and ignited.

SUMMARY AND CONCLUSIONS

An extensive low-grade occurrence of manganiferous limestone in Arkansas has been studied by the U. S. Bureau of Mines as a possible source of manganese ore. Laboratory research on samples from surface exposures and churn and diamond drill cores developed a beneficiation process comprising tabling, flotation, and leaching applicable to 8 of the 11 samples studied. From feed materials analyzing less than 5.0 pct Mn, ferrograde concentrates of 41.7 to 49.5 pct Mn were achieved at 48.2 to 66.0 pct recoveries.

In view of these results, Arkansas manganiferous limestone is considered a potential source of metallurgical manganese ore. The following conclusions are guides to examination and treatment of manganiferous limestone:

1) Grade is much less important than mineralogical composition.

2) Samples containing substantial amounts of rhodochrosite, in addition to manganese oxides, are unlikely to respond to processing.

3) Soft manganese oxides and those in which iron constitutes an appreciable content of the mineral are not easily separable from limestone gangue, and resulting concentrates will be submarginal.

4) Ores in which braunite and/or hausmannite are the principal manganese minerals are likely to be concentratable.

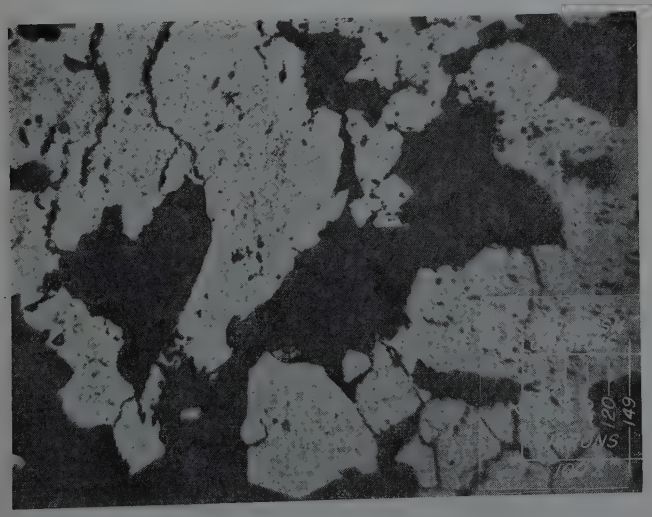

Fig. 1—Manganiferous limestone showing coarser manganese. X100. Reduced about one fourth for reproduction.

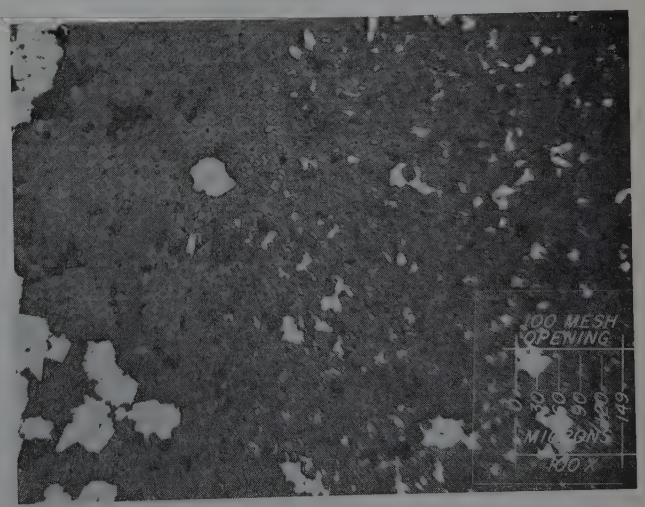

Fig. 2—Manganiferous limestone showing fine manganese. X100. Reduced approximately one fourth for reproduction.

The final product analyzed 42.4 pct Mn, 12.1 pct Fe, 12.5 pct SiO_2, 2.0 pct Al_2O_3, 0.21 pct P, and 0.36 pct S, which meets the specifications given earlier. Less than 2 pct Mn was lost by solution, so final recovery amounted to 59.2 pct. Acid consumption came to 0.15 lb of H_2SO_4 per pound of concentrate or 22.7 lb per ton of crude ore. These figures would fluctuate with efficiency of limestone rejection in both tabling and flotation. Although the exact wash water requirements were not determined, much water would be needed, since calcium sulfate is the principal reaction product in leaching.

Residual sulfur in the concentrate is partly accounted for by the limited solubility of calcium sulfate and partly by the presence of barite in the ore which must concentrate to some extent with the manganese. Gangue sulfates are not uncommon in manganese ores,[6, 7] and small amounts of barite are tolerated in metallurgical ore.[8] Hence minor quantities of barite and calcium sulfate in the products of this investigation are not expected to lessen their potenial value as metallurgical manganese ore.

Other Samples: The experimental procedure detailed above is the maximum processing accorded any sample. Table IV summarizes respective concentrate grades and recoveries of all samples, analyses of which are given in Table I.

Although the basic flowsheet described above was followed, differences in mineralization and improvements in technique permitted simplifications. For example, certain table tailings and cyclone slimes (either or both) from samples 2, 3, 6, and 8 were discarded immediately without being routed to flotation. Sample 8 was tabled at −20 mesh, and clean tailings were rejected at that size. Sample 4 yielded concentrates low enough in phosphorus so that leaching was unnecessary.

The three samples not amenable to concentration were a drill core sample from Reeves Hill, a surface sample from Miller-Rhinehart property, and churn drill cuttings from Greenfield Hill, all in Independence County, Ark. All contained 5.0 to 5.7 pct Mn, but the mineralization was such that satisfactory beneficiation by mechanical processes was impossible.

Byproduct: A considerable amount of crushed Fernvale limestone is sold in the Batesville area for agricultural purposes, so it is possible that table and flotation tailings similar to those created in this investigation may have potential value. The limestone is a high-calcium type, as shown in the Table V analyses of two random products.

Table I. Manganiferous Limestone Head Samples

Sample No.	Property	Type of Sample	Analysis, Pct			
			Mn	Fe	Insol	P
1	Baxter Hill	Surface	5.4	2.7	2.4	0.31
2	Baxter Hill	Cores	3.5	2.9	2.2	0.39
3	Chinn	Surface	4.5	1.2	2.0	0.22
4	Chinn	Cores	3.6	4.6	1.9	0.24
5	Adler	Surface	7.7	1.9	2.1	0.32
6	Vanemburg	Surface	5.2	1.3	3.9	0.24
7	Thompson	Surface	4.6	2.0	1.6	0.26
8	Arkansas Mining & Exploration Corp.	Cores	4.5	2.5	2.2	0.25

Table II. Results of Tabling Baxter Hill Surface Ore

Product	Weight, Pct	Analysis, Pct				Percent of Total Mn
		Mn	Fe	Insol	P	
Concentrate	5.5	41.5	7.7	6.5	0.50	40.9
Middling	6.6	7.2	3.4	2.0	0.50	8.5
Tailing	53.2	3.0	1.8	1.6	0.21	28.2
Slime	34.7	3.6	2.4	2.4	0.29	22.4
Composite	100.0	5.6	2.4	2.1	0.27	100.0

Table III. Flotation of Baxter Hill Table Rejects

Metallurgical Data

Product	Weight, Pct	Analysis, Pct				Percent of Total Mn
		Mn	Fe	Insol	P	
Limestone 1	85.5	1.6				40.0
Limestone 2	5.0	8.3				12.1
Manganese	4.6	25.3	12.6	17.4	0.58	34.0
Slime	4.9	9.7				13.9
Composite	100.0	3.4				100.0

Operating Data

Reagent	Pounds Per Ton of Feed						
	Conditioner		Rougher	Cleaner	Conditioner		Rougher
	1	2	1		3	4	2
Caustic soda	2.5						
Dextrin 152*	1.0			0.5	0.125		
Aliphat 44E**		0.32					
Soda ash							
Sodium oleate						0.20	
pH		10.1				9.2	
Time, min	5	5	8	6	5	5	8

* Corn Products Refining Co.
** General Mills Inc.

Table IV. Concentrates and Recoveries

Sample No.	Analysis of Concentrate, Pct				Recovery, Pct Mn
	Mn	Fe	SiO_2	P	
1	42.4	12.1	12.5	0.21	59.2
2	42.9	9.7	12.5	0.09	48.2
3	45.2	5.0	14.0	0.15	60.6
4	45.7	5.5	6.9	0.26	56.1
5	45.5	7.0	5.3	0.11	58.9
6	49.5	2.9	12.2	0.08	62.3
7	41.7	9.0	8.1	0.11	66.0
8	46.0	8.1	9.1	0.14	51.4

Table V. Analysis of Limestone Products

Product	Analysis, Pct					
	CaO	MgO	SiO_2	P	Fe	Mn
Table	51.9	0.22	0.56	0.16	1.2	1.3
Flotation	45.9	1.4	2.0	0.33	3.5	1.6

REFERENCES

[1] G. L. DeHuff: Manganese, a Chapter from Mineral Facts and Problems. *USBM Bull. 556*, pp. 493-509, 1956.
[2] H. D. Miser: Deposits of Manganese Ore in the Batesville District, Ark. *USGS Bull. 734*, 1922, 273 pp.
[3] H. D. Miser: Manganese Carbonate in the Batesville District, Ark. *USGS Bull. 921A*, 1941, 97 pp.
[4] H. D. Kline and J. P. Ryan: Manganese Resources of the Batesville District, Ark. Interim Report I, *USBM R. I. 5206*, 1955, 40 pp.
[5] H. D. Kline and W. F. Brown: Manganese Resources of the Batesville District, Ark. Part II of three parts, *USBM R. I. 5411*, 1958, 46 pp.
[6] A. M. Bateman: *Economic Mineral Deposits*, 2nd ed., p. 581. John Wiley & Sons Inc., New York, 1950.
[7] S. J. McCarroll: Upgrading Manganese Ore. *AIME Trans.*, 1954, vol. 199, p. 289.
[8] *Materials Survey—Manganese*, chap. 1, p. 12. USBM and USGS, October 1952.

Discussion of this article sent (2 copies) to AIME before Sept. 30, 1959, will be published in MINING ENGINEERING.

MARKET TRENDS FOR MINERAL FILLERS IN WESTERN STATES

by WALDEMAR F. DIETRICH

Mineral fillers are relatively inert chemically under the conditions of use but have physical properties* that modify those of the materials in which they are incorporated.

* The properties, uses, and other data on 15 classes of important fillers are listed in the second edition of *Industrial Minerals and Rocks*.[1] A third edition of this reference is in preparation.

The mineral fillers considered in this article are asbestos, barite, clays, diatomite, crushed limestone, limestone whiting and lime, mica, silica, talc and soapstone, and pyrophyllite. Slate and stone, other than limestone and its derivatives, are excluded because, even though used in large quantities, they are exceptionally low-cost materials generally produced close to the area where they are used.

Carbon black is excluded because it is manufactured from natural gas and more than 90 pct of the output is used in rubber; hence the factors for estimating requirements are easily evaluated.

OVERALL GROWTH FACTORS

Table I gives the population, retail sales, and value added by manufactures in the U. S. and in the eleven western states in 1954. These data are rough guides to the proportionate part of total U. S. markets for products containing mineral fillers that may be expected in a given area. For example, the population of the eight Mountain states in 1954 was 3.6 pct, and retail sales in these states were 3.8 pct of the U. S. total, but the value added by manufactures was only 1.3 pct of the U. S. total. On the other hand, the three Pacific Coast states, with 10.3 pct of the total population, had 12.0 pct of the retail sales and produced 9.6 pct of the value added by manufactures.

On an industry-by-industry basis the correlation between the three guideposts will not be as close as shown in the 1954 data for the Pacific Coast states, but in the long-term view the continuing rapid population growth in the western states is certain to result in expanded industrial production at an even more accelerated pace, which will shorten the gap between local consumption and production in most major groups of manufactured consumer goods. Of course, there will always remain favorable areas for production of specific products. Such special situations must be individually analyzed.

Fig. 1 compares the population trends in the U. S., the western states, and California with Real Gross National Product from 1910 to 1957, with forecasts to 1970.

It is estimated[2] that the U. S. Real Gross National Product, as measured by the value of goods and

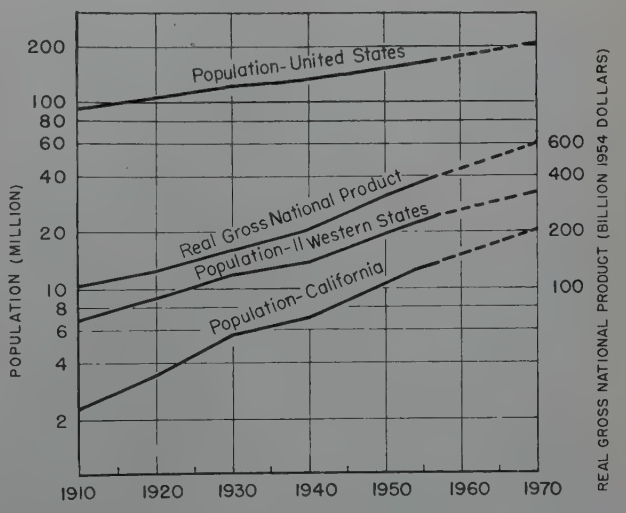

Fig. 1—Population of U. S., 11 western states, and California, and Real Gross National Product (1954 dollars), 1910-1957. Forecasts to 1970. (Dept. of Commerce.)

W. F. DIETRICH, Member AIME, is Chief, Division of Mineral Resources II, U. S. Bureau of Mines, San Francisco. TP 59H89. Manuscript, Feb. 16, 1959. San Francisco Meeting, February 1959. AIME Trans., Vol. 214, 1959.

Table I. Population, Retail Sales, and Value Added By Manufactures in U. S. and in Eleven Western States in 1954

States	Population		Retail Sales		Value Added by Manufactures	
	Thousands	Percent of U. S. Total	Billion Dollars	Percent of U. S. Total	Billion Dollars	Percent of U. S. Total
United States	161,200	100.0	170.0	100.0	116.9	100.0
11 Western States	22,400	13.9	26.8	15.8	12.7	10.9
Pacific Coast	16,683	10.3	20.4	12.0	11.2	9.6
California	12,254	7.6	15.6	9.2	8.6	7.4
Oregon	1,648	1.1	1.9	1.1	1.0	0.8
Washington	2,527	1.6	2.9	1.7	1.6	1.4
Mountain States	5,680	3.5	6.4	3.8	1.5	1.3
Arizona	930	0.6	1.0	0.6	0.20	0.17
Colorado	1,492	0.9	1.7	1.0	0.47	0.40
Idaho	598	0.4	0.67	0.39	0.18	0.15
Montana	619	0.4	0.78	0.46	0.14	0.12
Nevada	212	0.1	0.33	0.19	0.06	0.05
New Mexico	769	0.5	0.73	0.42	0.13	0.11
Utah	762	0.5	0.73	0.42	0.28	0.24
Wyoming	298	0.2	0.38	0.22	0.05	0.04

Source: U. S. Bureau of Census.

services produced, will increase at the rate of about 3.2 pct a year, compounded, over the period 1954-1970.

At this rate the Real Gross National Product would double every 22 years. Although this is slightly higher than the historic rate of the past 100 years, it is still the conservative view. Many economists predict more rapid growth. The annual growth of the value added by manufactures is assumed to be 3 pct, compounded during the 1954-1970 period. This is slightly less than the assumed growth of the Gross National Product which probably will reflect an increasing proportion of services.

On the basis of these assumptions and on U. S. Bureau of Census projections of population, the value added by manufactures in the U. S., the 11 western states, and California were calculated for 1970 (Table II). Overall requirements for mineral fillers in the U. S. should follow rather closely the *value-added* trend but, of course, the market trend for individual minerals will deviate more widely from the manufacturing growth owing to changes in technology and in the relative availability of specific materials and acceptable substitutes on a cost-quality basis. The overall regional trends in demand for mineral fillers also will tend to follow the pattern of industrial growth, again as influenced by technologic and cost factors. Individual commodities, however, probably will show some striking anomalies on a regional basis.

Table II. Population Trend and Value Added by Manufactures in U. S., Eleven Western States, and California, 1929-1954, with Forecasts for 1954-1970

		U. S.	Eleven Western States	California
Population				
Annual increase, pct	1929-1954*	1.14	2.64	3.25
	1954-1970**	1.54	2.67	3.21
Value Added by Manufacture				
Billion 1954 dollars	1954†	116.9	12.7	8.6
	1970‡	187.6	30.0	18.5
Annual increase, pct	1929-1954†	6.2	8.5	9.1
	1954-1970	3.0	5.5	4.9

* Calculated from U.S. Bureau of Census midyear estimates for 1929 and 1954.

** Calculated from U.S. Bureau of Census *Illustrative Projections of the Population by States, 1960, 1965, and 1970.*

† U.S. Bureau of Census, *Census of Manufactures, 1954.* (1929 data converted to 1954 dollars by use of GNP deflators.)

‡ Based on assumed national increase at 3.0 pct per year and calculated values for the western states and California, correlated with population projections and adjusted by the author for estimated per capita value added by manufactures in 1970.

CURRENT PRODUCTION AND CONSUMPTION OF SELECTED FILLERS

Table III shows the estimated percentage of total apparent supply of mineral fillers produced in the U. S., in the western states, and in the principal producing states.

Of the materials listed in Table III, production from the western states is adequate to supply the requirements in those states except for asbestos, barite, kaolin, mica, and ground silica. Consumer preferences provide a market for small quantities of eastern talc and pyrophyllite, yet California and Montana are important suppliers of talc to consumers outside the western states, especially for paper and paint uses. California, Nevada, and Oregon supply practically all of the diatomite used for all purposes in the U. S., and exports of processed diatomite to foreign countries are substantial. Asbestos is the only material listed in Table III in which U. S. production is far behind requirements—about 94 pct of the apparent U. S. consumption is imported, mostly from Canada. Barite imports, largely from Mexico and Canada, are currently at a high level, although in 1948-1952 imports averaged only 7 pct of U. S. consumption.

Table III. Distribution of U. S. Production of Selected Minerals Used as Fillers in 1957

	Estimated Percent of Total Apparent Supply		
	U. S.	Eleven Western States	Principal Producing States
Asbestos	6	1*	Vermont
Barite	61	15	Arkansas, Missouri, Georgia
Clays:			
Kaolin	97	3	Georgia, South Carolina
Fuller's earth	100	4	Florida, Georgia, Tennessee
Diatomite	100	100	California, Nevada, Oregon
Limestone and products	100	8	Ohio, Missouri, Pennsylvania
Mica (grinders scrap and flake)	92	5	North Carolina
Silica (ground sand)	100	1*	Illinois, West Virginia, New Jersey
Talc and soapstone	100	28	New York, California, Georgia
Pyrophyllite	100	10	North Carolina

Source: U.S. Bureau of Mines.
* Less than 1 pct.

The estimated quantity and value of the 1957 consumption as fillers of the selected minerals in the U. S. are shown in Table IV.

GROWTH TRENDS OF PRINCIPAL FILLER-CONSUMING INDUSTRIES

As shown in Table V, five industries consumed 88 pct of the value of the selected mineral fillers used in the U. S. in 1957: paper, rubber, asphalt, insecticide, and paint.

The pulp, paper, and paper-products industries of

the U. S. grew at the rate of 5 pct annually from 1929 to 1954, as measured by the value added by manufacture in constant dollars. This growth is somewhat more rapid than that of the Real Gross National Product. In 1954 production of the paper industries of the western states in proportion to the entire continental U. S. was comparable to other manufacturing industries in those states.

The 11 western states produced about 16 pct of the U. S. paper pulp in 1954 but only about 7 pct of the paper, paperboard, and building paper and board and 5 pct of the coated and glazed paper. On the other hand, nearly 8 pct of the paper and paperboard used in manufacturing paper products in the U. S. was consumed in the western states. Since total retail sales in the western states in 1954 were nearly 16 pct of the U. S. total retail sales, consumption of coated and glazed paper in the western states probably was at least 15 pct of the U. S. total, or three times production in the western states.

The value added by the manufacture of rubber products in the U. S. from 1929 to 1954 increased at about the same rate as the Real Gross National Product. The proportion of the entire industry located in the 11 western states in 1954 was 9.7 pct, compared with 10.9 pct of all manufacturing industries. However, there was then and even now virtually no white-rubber production in the western states; hence the market for white-rubber fillers in these states is negligible.

Data on the insecticide and fungicide-producing industries were not reported separately by the U. S. Bureau of Census before 1939. The growth rate of of the industry from 1939 to 1954, as measured by the value added by manufactures, was 15 pct annually, more than three times the growth of Gross National Product and about two and a half times the growth of the value added by all manufactures in the same period. In 1954 the 11 western states contributed 35.4 pct of the U. S. total of the value added by manufacture of insecticides and fungicides. In the same year sales for use in insecticides and fungicides of talc, soapstone, and pyrophyllite by producers in the western states were 32 pct of the U. S. total sales of these materials for the same uses.

The value added by manufacture of paint and allied products in the U. S. increased 3.0 pct annually from 1929 to 1954, the same as the increase in Real Gross National Product. Although as yet the 11 western states probably produce only about half as much of these products as is consumed in the area, California production, if all were used in the state, nearly balances consumption.

Table IV. Estimated Quantity and Value of Consumption as Fillers of Selected Minerals in U. S. in 1957

Commodity	Use	Quantity, Thousand Short Tons	Subtotals	Value, Thousand Dollars
Asbestos	Asphalt tile and other	*175*	175	7,000
Barite	Paint	16		
	Rubber	*22*		
Total			38	1,400
Clays:				
Kaolin	Paper Coating	659		
	Paper filling	528		
	Rubber	301		
	Insecticide and fungicide	39		
	Paint	35		
	Fertilizer, plastics, other	*78*		
Total			1,640	41,000
Fuller's earth	Mostly insecticide and fungicide	*70*	70	1,200
Other clays	Insecticide and fungicide	20		
	Linoleum and oilcloth	12		
	Other	*11*		
Total			43	500
Diatomite	Wide range of uses	*101**	101*	3,800*
Limestone and Products:				
Limestone, crushed	Asphalt	2,054		
	Fertilizer	345		
	Other	*541*		
Total			2,940	8,200
Limestone whiting	Paint, rubber, caulking compound, other	*809*	809	6,000
Lime, quick	Insecticide, fungicide, disinfectant	15		
	Paint and other	*15*		
Total			30	700
Lime, hydrated	Insecticide, fungicide, disinfectant	48		
	Paint and other	*26*		
Total			74	1,400
Mica, Ground	Roofing	30		
	Paint	23		
	Joint cement	13		
	Rubber, wallpaper, plastics	*12*		
Total			78	5,000
Silica, Ground Sand	Rubber, plastics, other	*134*	134	1,200
Talc and Soapstone	Paint	120		
	Insecticide	45		
	Roofing	39		
	Rubber	29		
	Asphalt filler	19		
	Paper	16		
	Other	*72*		
Total			340	9,000
Pyrophyllite	Insecticide	42		
	Asphalt, paint, rubber, other	*56*		
Total			98	1,400
Grand total			6,527	87,300

Source: U.S. Bureau of Mines.
* 1954-1956 average.

SUPPLY-DEMAND STATUS OF SELECTED MINERAL FILLERS

Asbestos: Most of the asbestos of Canadian group 7 or equivalent consumed in the U. S. is used for boiler and roofing cements and as filler in asphalt floor tile and various other products. In 1957 the apparent supply of group 7 asbestos, mostly from Canada, was about 350,000 short tons, valued at about $15 million. It is estimated that 150,000 to 200,000 tons were consumed for filler uses. Small quantities of other grades of asbestos, especially group 8, also are used for fillers.

Less than 1 pct of the U. S. supply of asbestos is produced in the western states, and the chance of substantially improving the supply appears remote. Current (1958) consumption of asbestos fillers in the western states is believed to be about 4 pct of the national total, although consumption of products containing asbestos fillers probably is at least twice as great. Hence, while there appears to be room for expansion of the asbestos-filler consuming industries in the West, the asbestos supply will continue to be obtained largely from Canada and Vermont.

Barite

Only about 2 pct of the barite consumption in the U. S. is used as filler—mostly in rubber and paint. Although nearly 40 pct of the crude barite requirements of the U. S. is imported, about 15 pct of the total domestic supply is produced in the western states. However, only a small part of the western production is of filler grade.

Clays

Kaolin: Kaolin acounts for about one fourth the tonnage and half the value of the domestic mineral-filler consumption; three fourths of the domestic kaolin consumption is used as fillers. The three major filler uses are paper coating, paper filling, and rubber.

From 1947 to 1957 U. S. consumption of kaolin fillers increased at the rate of 4.5 pct annually, reflecting the growth of the consuming industries.

Most of the filler-grade kaolin used in the western states is obtained from Georgia and South Carolina. The freight on kaolin from Georgia to Los Angeles is $21.80 per ton; hence, Georgia paper clays sell at $33 to $40 per ton, f.o.b. Los Angeles. The freight from Georgia to the Pacific Northwest is about $26 per ton.

The high cost of kaolin fillers delivered to West Coast industrial areas has been a major factor in retarding the growth of the white paper and white food-carton industries in this area and probably has also had an adverse effect on establishment of plants for making various other products requiring high-grade fillers. The first major breakthrough in establishing a western supply of paper clays may be the beneficiation plant of the J. R. Simplot Co. at Bovill, Idaho, now (February 1959) under construction. On the basis of cooperative studies by the U. S. Bureau of Mines, it is believed that high-grade paper filling and coating clay can be produced from the Bovill clays. Although the dominant mineral in these clays is halloysite, little difficulty is anticipated in introducing the beneficiated clay in a wide range of products in the Pacific Northwest at somewhat lower cost than Georgia kaolin on a delivered basis.

Fuller's Earth: The principal use of fuller's earth as a filler is in insecticides and fungicides. Production in the western states is small, and most filler requirements are met by regionally available substitutes, especially pyrophyllite.

Other Clays: Small quantities of ball clay, fire clay, and miscellaneous clay are used as fillers in special applications where price and availability are favorable.

Diatomite

The use of diatomite fillers increased about 7 pct annually from 1949 to 1956, more rapidly than for any other major mineral filler. About 25 pct of the domestic diatomite consumption is used as a filler in paper, paint, varnish, and many other items. All of the domestic production is in California, Nevada, Oregon, and Washington. The diatomite filler market in the Pacific Coast states probably is somewhat higher in proportion to total industrial activity than elsewhere in the U. S.

Limestone and Products

Crushed Limestone: The western market for crushed limestone for use as a filler in asphalt, fertilizer, and other products is approximately proportionate to the level of manufacturing and construction activity, compared with the entire U. S. Adequate raw material supplies and production facilities serve the metropolitan areas in the West. Since crushed limestone used as a filler has low-unit value ($2 to $4 per ton, f.o.b. plant), there is little movement of crushed limestone far from the sources of production.

Limestone Whiting: Limestone whiting and precipitated calcium carbonate have almost entirely replaced imported chalk whiting, which dominated the market before World War I. Limestone whiting has a variety of filler uses, as in rubber, calcimine paint, caulking compound, putty, and asphalt. The western market is approximately in balance with supply from western sources, although higher prices widen the competitive marketing area compared with crushed limestone. Prices delivered in the Los Angeles metropolitan area range from $8.70 per ton for asphalt filler to $13.50 for 180 mesh putty-grade material, $16.50 for 400 mesh paint filler, and $35 for extremely fine-ground, low-micron paint fillers.

Lime: Both quicklime and hydrated lime have minor uses as fillers in insecticide, fungicide, disinfectant, paint, glue, medicines and drugs, rubber, and soap. The western supply-demand position is in balance.

Mica

About 80 pct of the ground mica sold by producers in the U. S. in 1957 was used as filler, principally in roofing, paint, joint cement, rubber, wallpaper, and plastics. From 1947 to 1957 the consumption of ground-mica fillers increased about 4 pct annually.

Table V. Estimated Value of Selected Mineral Fillers Used in U. S. in 1957, by Consuming Industries

Consuming Industry	Value, Million Dollars	Percent of Total
Paper	30.1	34.5
Rubber	15.7	18.0
Asphalt	15.7	18.0
Insecticide	7.9	9.0
Paint	7.5	8.6
Other	10.4	11.9
Total	87.3	100.0

Source: U.S. Bureau of Mines.

It is estimated that mica-filler consumption in the western states is at least double the current supply from those states. Shipments from mica-grinding plants in the Southeast to California alone are believed to exceed 3000 tons annually, valued at $200,000.

Silica

Silica, in the form of ground sand, is used extensively as a filler in rubber and plastics. Development of raw-material resources and plant facilities keeps pace with industrial demand in most geographic areas, but demand in most western states thus far greatly exceeds the local supply.

Talc and Soapstone

Consumption of talc, soapstone, and pyrophyllite fillers increased about 4 pct annually from 1947 to 1957. Separate data for pyrophyllite for this period are not available.

The western states produce about twice as much talc as is consumed by western industries. Even so, the proximity of California talc deposits to southern California industries, together with extensive technological and marketing research and the lack of western sources of kaolin fillers, has resulted in establishing a market for talc in California at somewhat higher than the proportionate level of manufacturing elsewhere in the U. S.

In 1957 filler uses accounted for 64 pct of the talc and soapstone production in the U. S. Chief among these were paints—second only to ceramics—insecticides, roofing, and rubber.

Prices of California filler talc and soapstone delivered in the Los Angeles area range from less than $20 to more than $70, depending on quality and particle size. The softness and high gloss of the best qualities of California talc give it a favored status as a paint and textile filler. Continued research on the properties and processing of western talcs, notably those from California, Nevada, and Montana, is expected to extend the range of consumer acceptance, especially in the paper and rubber industries.

Pyrophyllite

Over 60 pct of the U. S. pyrophyllite consumption in 1957 was used as filler, principally in insecticide, asphalt, paint, and rubber. For most filler uses, pyrophyllite and talc of equivalent particle size distribution and whiteness are interchangeable, and the choice depends primarily on price. Western pyrophyllite, however, is usually too dark in color to be acceptable as a white paint filler and is used mainly for insecticides. In the Los Angeles area insecticide-grade pyrophyllite sells for about $18 per ton, compared with about $25 per ton for insecticide-grade talc.

The supply of western pyrophyllite keeps pace with requirements in the western states. Interregional shipments are negligible.

REFERENCES

[1] A. B. Cummins: Mineral Fillers: In *Industrial Minerals and Rocks*, 2nd ed., pp. 570-578 (Table I). AIME, New York, 1949.
[2] U. S. Bureau of Mines: Office of the Chief Economist.

Discussion of this article sent (2 copies) to AIME before Sept. 30, 1959, will be published in MINING ENGINEERING.

AIRBORNE GRAVITY METER

DESCRIPTION AND PRELIMINARY RESULTS

by HANS T. LUNDBERG and JOHN H. RATCLIFFE

In airborne gravity surveys effects of acceleration and irregular movements of the aircraft must be balanced out or overcome. The gradient of vertical gravity is recorded, therefore, by using two masses instead of one. As the amplitude variations are infinitesimal and difficult to measure accurately, at present it is enough to determine whether variation of gradient during flight is positive or negative. The positive portions of the pattern can then be indicated and contoured. Even with these simplifications, the source of energy must be exceptionally stable.

General Principles: In the conventional gravimeter the weight of a standard mass is determined at a number of selected points within the survey area. In most systems weight is determined by comparing the gravity pull with extension or torque

H. T. LUNDBERG, Member AIME, is President and J. H. Ratcliffe, Chief Geophysicist, Lundberg Explorations Ltd., Toronto, Canada. TP 4815L. Manuscript, June 16, 1958. New York Meeting, February 1958.

produced in a wire spring. The instruments employed are sensitive to the slightest movement; they cannot be used on a moving platform unless velocity is kept strictly uniform.

Assume, however, that two similar masses are suspended from each end of a very short linking beam, one mass lower than the other. At center point the beam is suspended from a supporting platform by a frictionless pivot. A fixed plate close to the plane surface of one mass acts as a variable condenser. Displacement of the mass in respect to the fixed plate can be electronically determined.

When the beam is made to stay horizontal on neutral ground the vertical distance between the two masses equals the difference in length of the two supporting filaments. When the system is moved into a field of increasing gravity, the lower mass is attracted downward slightly more than the upper one. The lower mass will thus move downward and the upper mass upward until equilibrium is reached. This displacement can be observed by the change in capacity between the mass and the fixed plate.

If the balance system is suspended from a moving platform, forces due to acceleration in any direction will then be applied equally to each mass, provided the acceleration remains constant. If acceleration varies, as in an aircraft bump, differential forces may be applied to the mass, causing a short-term, small-amplitude *hash* to be superimposed on the output signal. However, as these changes in acceleration are generally of short duration compared with the gravity anomalies, this disturbance can be filtered out electrically.*

* Certain long-time changes caused by the aircraft flying an arc of large radius rather than a straight line may slightly displace the datum, but the local anomalies superimposed on it will still be in their correct position.

Theoretical Considerations: Consider the actual magnitude of the forces involved. For example, at a point 1000 ft vertically above the uppermost surface of a sphere of 2500-ft radius having a density contrast of 1 over its surroundings, a gravity anomaly of about 10 milligals, or 10^{-2} C.G.S. units, will result. The first vertical derivative of gravity at this point will then be about 2×10^{-7} C.G.S. units or 200 Eötvös units, while the second vertical derivative anomaly will be only about 6×10^{-12} C.G.S. units. Obviously it is preferable to work with either the vertical component or the first vertical derivative of gravity, as the higher derivative necessitates measuring such extremely minute quantities.

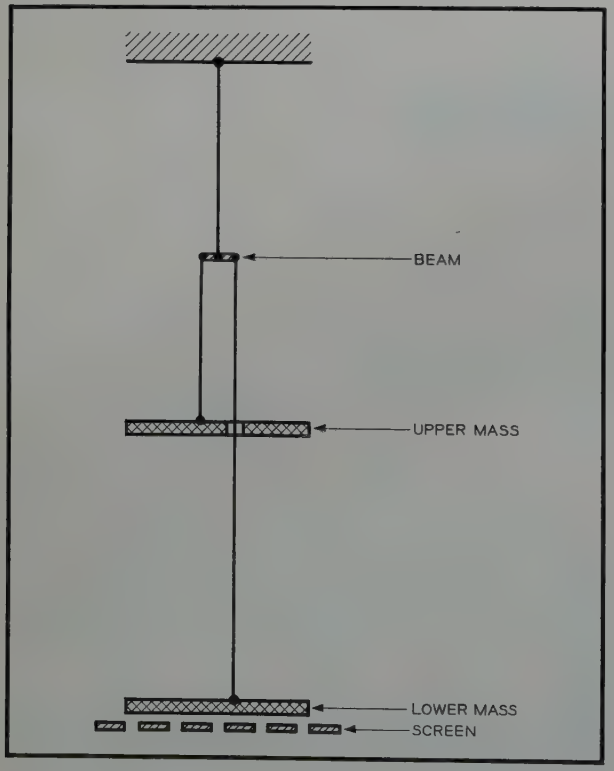

Fig. 1—Diagram of the moving system of the gravity gradiometer. Scale is highly distorted and enlarged.

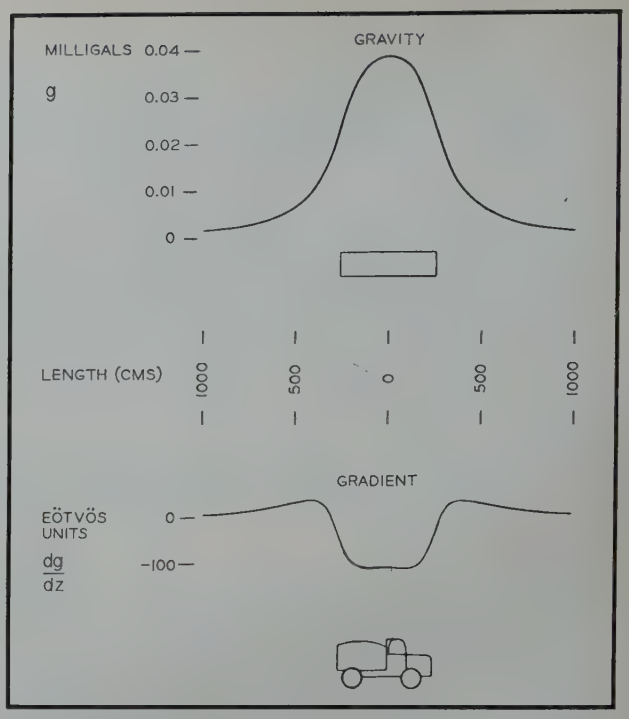

Fig. 2—Calculated gravity gradient anomaly over moving sand truck. This comparison is simplified in Fig. 3.

The conventional gravimeter measures variations in the gravity field of the order of 0.01 milligals or 10^{-5} C.G.S. units. Helmer Hedstrom (1938)[1] describes a gravimeter in which the mass displacement is determined by measuring variations in electric capacity. He states that in the Boliden gravity meter a 1-milligal anomaly would cause a deflection of the moving system of about 5.5×10^{-7} cm. As the instrument could register movements of the order of 3.5×10^{-9} cm, or 0.35 Angstrom units, it was theoretically possible to detect gravity anomalies of the order of 0.01 milligals. Although this sensitivity was never reached in the field, it is interesting to note that under controlled conditions a sensitivity of this order could be obtained with electronic devices that would now be considered obsolete.

It has been shown that anomalies in the first vertical derivative are much smaller in magnitude than those of the equivalent gravity. The question is, therefore, can the airborne instrument detect anomalies in the first vertical derivative? The equations of motion for the system have been developed, and it is found that the first vertical derivative of gravity is proportional to the displacement of either mass (the constant of proportionality being about 0.5). Thus a change of 1 Eötvös unit in the first vertical derivative will cause a mass displacement of 0.2 Å.

The 0.35 Å movement that can be detected by the

Boliden gravity meter corresponds to a sensitivity of 2 Eötvös units. Although this figure is theoretically plausible, it may be somewhat optimistic. By actual observations it is known, however, that the present instrument described here is capable of detecting a movement of 5 Å, that is, a change of about 25 Eötvös units in the first vertical derivative of gravity.

To reach this sensitivity all components of the gravity gradiometer must function with perfect precision. Power packs, oscillators, and amplifiers must have linear characteristics over the operational range, and to hold temperature effects to a minimum, materials with low coefficients of expansion must be used. These and similar design problems have persistently dogged the writers' development program.

Instrumental Details: The complete instrument comprises an ultra-stable power supply feeding a timing device that in turn controls operation of the moving balance system in the head unit. Changes in relative position of the two masses within the head unit are relayed by a capacity bridge circuit, which feeds through an amplifier into a recording device.

In the early models the recording apparatus consisted merely of a set of head phones. By detecting changes in signal tone it was possible to map changes in the gravity field. It is obvious, however, that for survey work automatic data recording is essential. In their present models the writers are using a standard automatic recording milliammeter.

The timing mechanism regulating movements of the masses in the head unit requires a 60-cps power source not generally available in aircraft, so the instrument is operated from a d-c supply. The output of vibrator systems and rotary converters was found too unstable for linear operation of the timing device, but a crystal-controlled, frequency-divided, voltage-regulated power supply has proved eminently satisfactory.

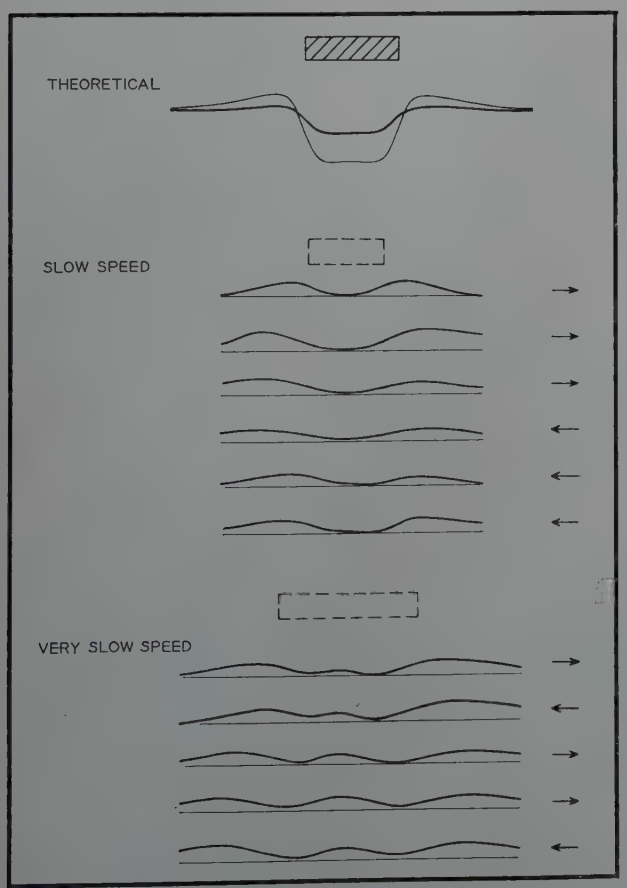

Fig. 3—Gravity gradient anomaly over moving sand truck.

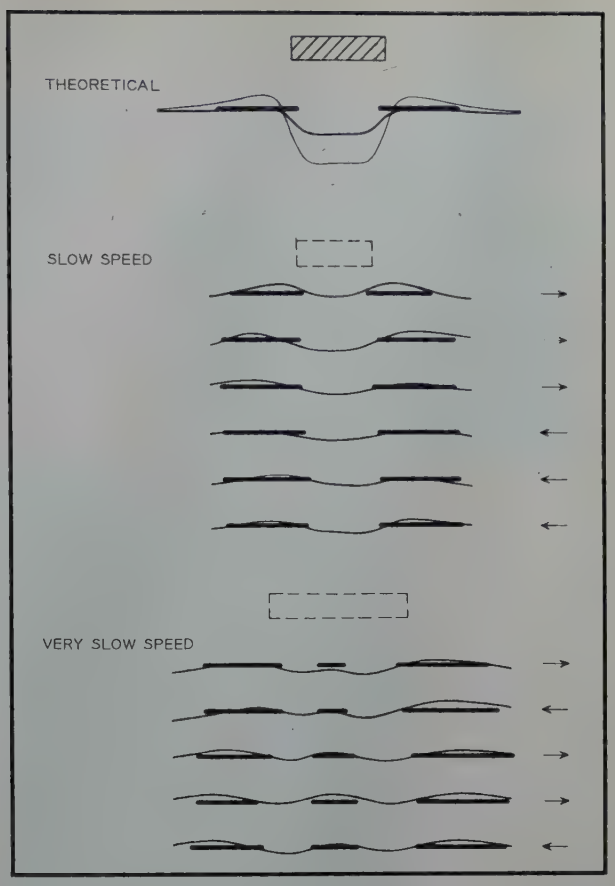

Fig. 4—Gravity gradient anomaly over the moving sand truck. The positive portion of the gradient is indicated.

The frequency-controlled timing unit locks the two masses in a central position in their housing while the distance between one of the masses and the fixed plate is measured by means of the capacity bridge. The masses are then freed and the cycle is repeated. Each cycle thus consists of two periods: 1) During the static period a strong electrostatic charge returns the masses laterally to a central position in their housing without disturbing their relative vertical position and then permits the capacity between one mass and the fixed condenser to be compared with a known capacity in the bridge circuit. 2) During the dynamic period the two masses are free to seek a new position of equilibrium under the influence of differential gravity forces acting upon them.

The cycling speed of the timing device can be altered by external controls. It is therefore possible to synchronize the dynamic period of the instrument with a fraction of the natural period of vibration of the mechanical system, so that the two masses, which have been under restraint during the static period, will tend to move toward a new equilibium point. If they were allowed to oscillate freely, they would continue about the new equilibrium point *ad infinitum* in the absence of damping, the amplitude of oscillation being a function of the original restraining force. But during this period accelerations applied to the moving platform might cause the masses to become misaligned. For this reason they must be locked periodically. The best time to

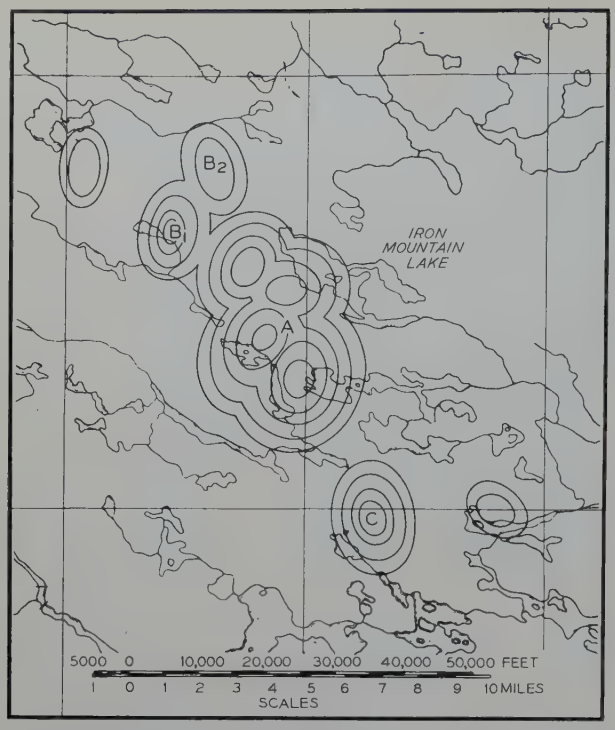

Fig. 5—Results of airborne gradiometer survey over the Iron Mountain lake area, New Quebec. Altitude 1000 ft. North-south east-west flight directions are combined.

impose the locking system, of course, is at a point equal to one quarter or three quarters of the natural frequency of the oscillating beam system.

Tests and Trials: In early tests of the instrument, carried out on the ground, traverses were made on foot over a narrow lead vein. Later the instrument was mounted in a station wagon and driven back and forth over a straight, flat stretch of highway which crossed a known gravity anomaly. When good results were finally obtained, the instrument was placed in an aircraft and flown over the same route. Naturally transposition from a ground to an airborne device created additional problems. Many of these are still being sorted out, but the goal is rapidly being attained.

An interesting test was recently made by running a heavy truck loaded with gravel under the instrument, which was mounted stationary above the roadway. Recordings of gravity gradient variations were made in the usual way. To obtain proper records the truck had to move at a speed too slow to be read on the speedometer. This caused the engine to heat up so that toward the end of the testing period it was difficult to drive the truck at even speed. Even so, the recorded runs showed very interesting results. By way of comparison, Fig. 2 shows the calculated gradient for a 15.8-ton block measuring 17x4x7 ft, corresponding approximately to the gravity effect of the truck loaded with gravel. In Fig. 3 the amplitude scale of the calculated variations has been considerably reduced, for easier comparison with the recorded profiles.

For the moderately slow runs the recorded profiles look very similar to the calculated curve but, as might be expected, for very slow runs the character of the profiles changes, showing a pronounced bump over the gravel truck owing to the change in scale factor.

Interpretation: It is still an art to interpret the data. As the system is very sensitive to the relation between the timing cycle and the natural frequency of the moving beam, exact synchronization of the two cannot be accomplished with the present equipment, so that no true values are recorded, but only the changes in vertical gradient of gravity. It is possible, however, to indicate where the gravity gradient is positive and where it is negative.

To prepare data for interpretation the record tapes are transcribed into constant scale and corrected for curvilinear coordinates. The transcribed records are traced onto flight line maps in profile form. The positions of positive gravity gradient zones are marked off on the profiles (see Fig. 4) and the zones are then joined, by contouring, into a series of concentric rings which surround the mass causing the anomalous gravity field (see Fig. 5).

At first lines were flown in two directions perpendicular to each other at two different altitudes. After four maps had been produced and contoured independently, the results were matched. Where anomaly centers coincided, existence of a gravity anomaly could be postulated. Although this conservative approach has been costly, it has built up a safe interpretation technique that is in the best interest of the client.

Future Development: The airborne gravity gradiometer is still in its infancy. Three types of power supply have been tried, different moving beam systems have been incorporated into the head unit, various amplifiers have been designed and tested, and two systems of data recording have been used. The writers consider the present unit vastly superior to its predecessors, but there is still much room for improvement. The authors hope to have, in the near future, an instrument that can record the true value of the gravity gradient, permitting a more accurate contour pattern and a mathematical analysis of results.

Conclusions and Present Results: In an earlier article[2] the authors showed examples of surveys over salt domes and bodies of magnetite. Although these results should speak for themselves, many professionals have inferred that they are useless because no exact value of a definite function is included in a discussion. Certainly an exact value would be desirable, but the writers are convinced that contour mapping of a function which indicates an anomalous gravity center should be of value in any exploration program.*

* Flat to moderate topographic relief has little or no effect on the recordings because of the relatively high flight altitude (1000 to 2000 ft). In more rugged terrain actual comparisons between topography and the gravity gradient anomalies provide an empirical method of rating the gravity results.

The method has been applied in many parts of the world and the originators have to their credit the discovery of a large, relatively nonmagnetic hematite orebody in West Africa. Salt domes and structures have been successfully outlined in Europe and Canada, and recently a very large iron ore deposit was outlined by this method in Canada (Fig. 5). Tests over bodies of sulfides and manganese have been made, but final results are not yet available.

REFERENCES

[1] H. Hedstrom: *AIME TP 953*, 1938.
[2] H. Lundberg: *Transactions*, Canadian Institute of Mining and Metallurgy, 1957, vol. 60, pp. 251-259.

Discussion of this article sent (2 copies) to AIME before Sept. 30, 1959, will be published in MINING ENGINEERING.

ECONOMY THROUGH DESIGN

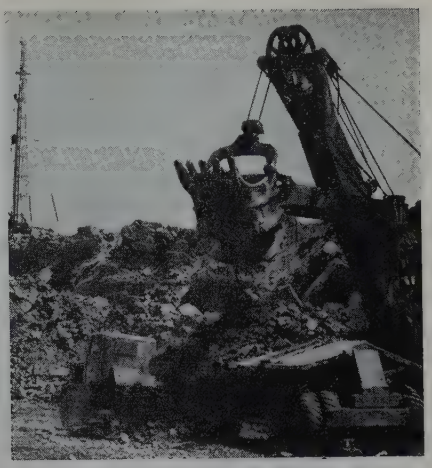

Building a beneficiation plant? Plan it right the first time. Operating and maintenance improvements in a large taconite plant were faster, easier, and less costly because initial engineering was sound.

by ROBERT J. LINNEY

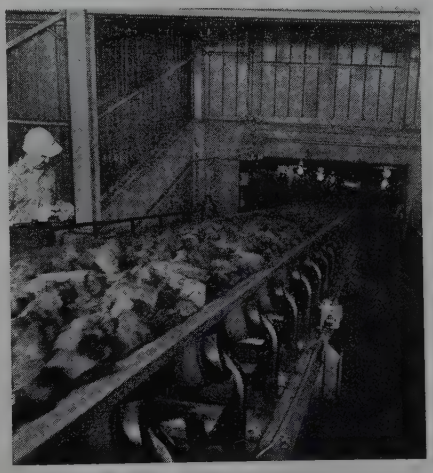

Reserve Mining Co. produces 5 million tons of iron ore pellets per year. The finished product runs about 65.50 pct Fe, with 7.75 to 8.00 pct SiO_2. Less than 12 pct arrives at the blast furnaces smaller than 3/8 in.

This plant was originally designed to produce 3.75 tons annually—not 5 million. To handle the increased tonnage a fifth fine crushing line was added, and some very minor changes were made.

When production can be stepped up 33 1/3 pct without extensive additions or changes—within the short period of a year—basic engineering has been sound. Operators of the plant consider it the best design job they have seen or heard of, and competent authorities have said that start-up was quicker and easier than for any previous large-scale minerals beneficiation plant.

One big advantage is the elbow room allowed. Generally speaking, there is an eternal conflict between operator and designer over space. The designer has his costs per cubic foot, and he is keenly aware that if he permits the number of cubic feet to rise unnecessarily, total costs will be too high.

But this was a new operation, and on a large scale. There were no proven standards to go by. Realizing this, Reserve's engineers provided ample and efficient access to machinery, allowing extra space for unanticipated situations. In three years of production this planning has paid off handsomely.

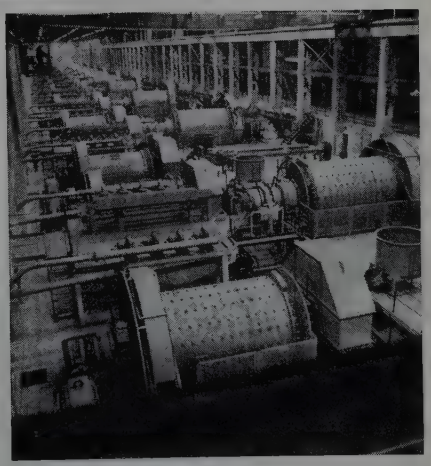

Gravity Flow Saves Time and Money: This plant is on a rocky hillside, the car dumper about 270 ft above Lake Superior. In locating buildings and placing machinery the designers made good use of gravity flow, at considerable financial savings. In the concentrator building from rod mills to filters, gravity carries the material between all stages of the operation except one—the closed circuit pumping of concentrate between cone classifiers and ball mills. Since no machine is located directly above any other, an observer can stand on the truck ramp adjacent to the offices and laboratory and see practically every phase of activity in the huge building.

The first mill section started in August 1955. After a day's run several modifications were made on auxiliary chutes and launders where spillage had occurred. This procedure was followed for the first

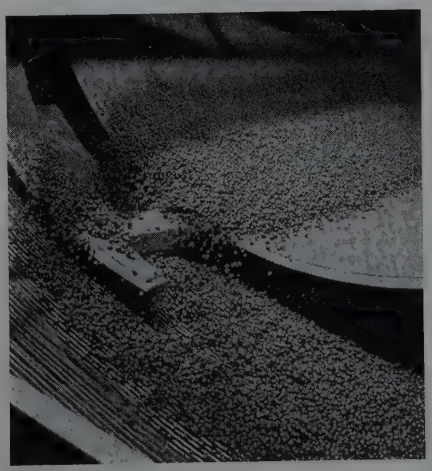

R. J. LINNEY, Member AIME, is Executive Vice President, Reserve Mining Co., Silver Bay, Minn. TP 59B68. Manuscript, Jan. 28, 1959. San Francisco Meeting, 1959. AIME Trans., Vol. 214, 1959.

This page of Mining Transactions AIME follows p. 820. The intervening non-Transactions pages appeared in MINING ENGINEERING.

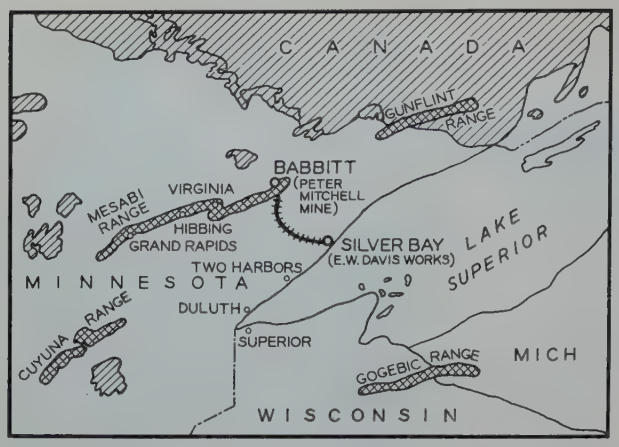

Reserve's Peter Mitchell mine is a deposit of magnetic taconite approximately 9 miles long, 3000 ft wide, and 175 ft deep at the thickest point. The deposit is virtually free of glacial overburden and can be mined by open pit methods. It contains more than 1.5 billion tons of taconite, with approximately 25 pct recoverable iron.

week, and the corrective measures proved out on the No. 1 section were incorporated throughout the mill. When the remaining 11 sections were ready, they were started up almost without a hitch.

Design Improvements in Coarse Crushing Plant: As operations progressed, difficulties not specifically accounted for in the basic plans were ironed out in consultations between the operating staff and plant designers. One of their early problems turned up in the coarse crushing plant at Babbitt. Originally it was not uncommon to see pieces of taconite the size of a piano being dumped into this crusher. Needless to say, the manganese mantle liner and concaves took a severe beating. These wear liners were supposed to crush well over a million tons of rock, but at 600,000 tons the lower part of the mantle had stretched so badly it became loose on the head center. The mantle was of three-piece design with a self-tightening head nut, but the upper third had not stretched as much as the lower third and the self-tightener could not work. The concaves, too, had grown so severely that the strain had stretched the main frame bolts, even though the concave joints had been scarfed every week to relieve the growth.

Cooperative studies by the engineers and operators and the equipment manufacturer's technicians solved this problem. A two-piece mantle was substituted for the earlier design. The concaves were stepped out slightly, in effect lengthening the crushing zone to help distribute the stresses more evenly over the entire surface of both mantle and concaves. The lower concaves were scarfed more often. After these adjustments had been made, the set of liners gave a good performance of 1.2 million tons.

Improved blasting in the pit produced better fragmentation, eliminating the piano-sized chunks. This, of course, prolonged the life of the crusher liners. Mantle life is now about 1.8 million tons and concave life about 1.9 million tons.

The first reline job back in 1955 took more than 120 hr. Too long. Too expensive. So the mechanical maintenance department set up work analysis sheets right on the job. A study of these led to better coordination of the various steps and pointed up the need for special tools, many of which were designed and built in the well equipped shops near the crusher. With better tools and better planning, progress was steady. Today a reline job averages not 120 hr but only 38 hr. The record, so far, is 36 hr. Further, the maintenance department recently completed more than a million manhours without a lost time accident.

This remarkable improvement was facilitated by the countless sessions the designers had held, with the operators, in planning adequate space for storage and maintenance. There is an exact spot for every tool, and each is in the proper sequence for most efficient use.

Unloading at 40°F Blow Zero: No winter freeze-up problems had been encountered in Reserve's earlier experience, and none were anticipated. Taconite is hard and dense and not susceptible to freezing; it was expected the ore would be kept moving. But when winter struck northern Minnesota in 1955, some 80 ore cars in the yard at Silver Bay became giant ice cubes almost overnight. A spare boiler was rigged up to steam them, but this was a costly, drawn-out arrangement. Even after steaming, great frozen chunks lodged in the dumper pocket and bin openings. A temporary grizzly of railroad rails was hurriedly installed in the dumper pocket to screen out the larger blocks, but delays resulted from breakdowns, and heavy maintenance was needed on the rails.

At the two big loading bins in Babbitt there were freeze-up problems too, despite the use of steam and hot torches. Then a solution of calcium chloride was pumped into the tops of the frozen bins, and bags of it were hand-sumped into the railroad cars. Before long the cars were cleaned out and the bins running freely.

Now a permanent feeder set-up at the 60-in. crusher adds a pre-determined amount of calcium chloride to the ore stream as each mine-haul truck is dumped. Here again, installation was simple because the designers had left enough room. One pound of calcium chloride per ton of ore prevents freeze-up problems all down the line, even in 40°F below zero.

Better Mileage for Rail Cars: After about six months, wear on the railroad car wheels became noticeable. At nine months, under the company's wheel inspection program, the first wheels began to show up in the machine shop for *turning*. In 15 months the problem reached major proportions when 350 wheels were turned in a single month. This work could not have been handled except for the shop layout and equipment provided in the original planning; the automatic double-wheel lathe, in particular, proved to be a life-saver.

Earlier investigations had revealed the reasons for this rapid wear: loading was heavier than designers had specified, mileage rates were high, and only half the wheels were the heat-treated type. Eliminating overloading was a major factor in reducing wear. But turning the cars end-for-end—running them loaded in one direction for a time and then in the other direction—compensated for differential flange wear, spring set, and coupler loadings due to one-side rotation during dumping. Gradual replacement with rim-treated wheels will further reduce the wear rate.

By January 1959 116,000 miles had been accumulated on the original ore cars. Car mileage per month now averages 3000, and only two sets of original wheels have been scrapped because of tread wear.

Reserve Mining Co.

Mining–Concentrating–Pelletizing

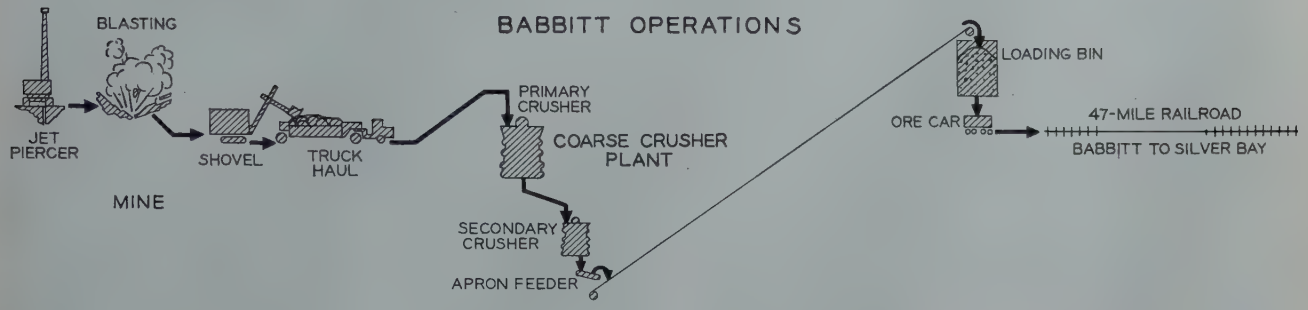

After four jet piercers have sunk the 40-ft blastholes, up to a million tons of crude material are shot at one time. Four shovels load the hard, abrasive rock into specially designed 45-ton side-dump trucks, which carry the taconite to the 60-in. primary crusher. Here it is crushed to a maximum 8 in. This product is fed to three 30x70-in. gyratorys, which further reduce the rock to a maximum 3½ in. A 60-in., 1000-ft conveyor belt running beneath the crusher carries the taconite to the top of two storage bins holding about 10,000 tons. The custom-designed 86-ton railroad cars passing beneath these bins are loaded without stopping. Trains are made up of some 110 cars, which carry the taconite along a 47-mile railroad from the mine and crusher to the E. W. Davis Works.

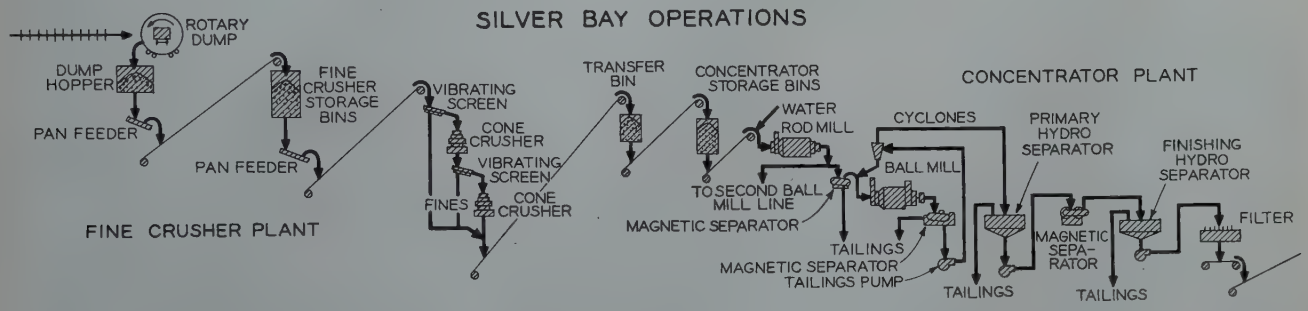

At Silver Bay, high on a cliff above Lake Superior, the cars move into a rotary dumper, where they are turned over and dumped without uncoupling and without the air hose being disconnected. This is a one-man operation, the controller viewing his work on closed-circuit TV cameras. Here, at the fine crusher plant, taconite is carried by a 60-in. conveyor belt to five storage bins, each furnishing crude ore to one of the five fine crushing sections in the building. Each line consists of a primary screen and crusher and a secondary screen and crusher in open circuit series grinding. Here the final product runs about 90 pct —¾ in. It is carried by conveyor belt to 24 concrete storage bins next to the concentrator building. Two bins supply the crushed ore to each of the 12 sections of the concentrator. In the concentrator building water is introduced as the taconite enters the rod mill. The discharge is split, flowing to two magnetic separators. The cobber concentrate goes to the two ball mills in each of the 12 sections for further grinding; the discharge is split to each of four belt-type rougher magnetic separators. The concentrate is then pumped to the cone classifiers. The rougher overflow is laundered to the rougher hydro separators, and the underflow is laundered back to the ball mills. Concentrate from the rougher hydro goes to the finishing magnetic separators, then to the finishing hydro separators for a final washing before it reaches the filters. Tailings from each step of the operation flow by gravity from the plant. The concentrate is carried by conveyor belt to the pelletizing department.

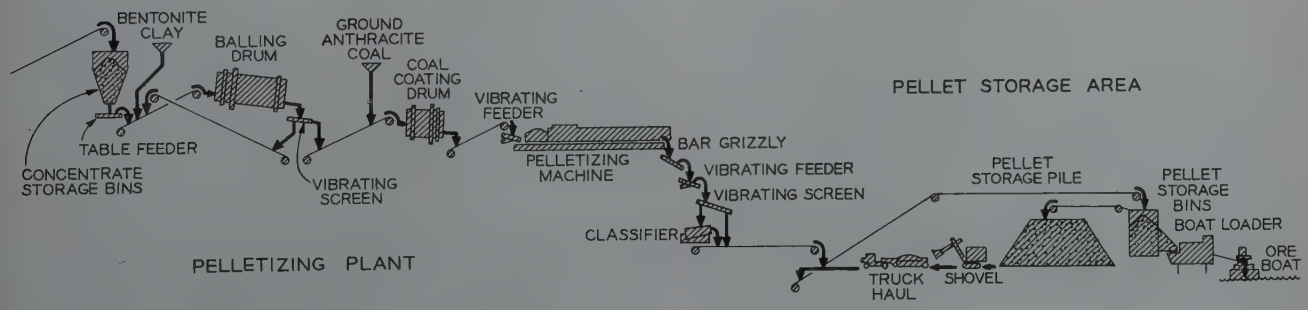

At each of six furnaces in the pelletizing department the bed of pellets is 12 x 14 in. deep. When finished pellets are discharged at the end of the machines, they are carried by belt conveyor to the storage yard or directly to the ship-loading facilities for shipment down the lake to Armco and Republic Steel, joint owners of Reserve.

Crude material is carried by 45-ton trucks to the primary crusher and side-dumped into pocket shown here.

Loaded car in foreground carries 86 tons of crushed taconite to this rotary dump at fine crusher plant.

Under initial wear rates the entire installation of some 2000 untreated wheels, costing more than $275,000, and a large number of the rim-treated wheels would now have been replaced.

Combating Abrasion: The abrasiveness of Reserve's taconite is a constant source of trouble. Dipper teeth on shovels have to be replaced after only 8 hr. The taconite chews up truck bodies, truck tires, in fact, everything it touches. Although real progress has been made in securing abrasion-resistant materials, the problem is so serious that a full-time metallurgist is employed to study, test, upgrade, and control the materials used in mill and crusher liners, grate bars, pallets, and railroad wheels.

In early stages of operation serious maintenance trouble developed with the screen decks in the fine crushing plant. These decks were made up of ⅜-in. diam rods, 2 ft 9 in. long, in panels 1 ft wide. They were held in place by steel clamps and a rubber locking device. The design was chosen because the screen deck would be easy to renew and because tough-alloy abrasion-resistant rods could be used.

But experience demonstrated that alloy rods were not tough enough; in the early days two crusher lines were sometimes down for screen repairs at the same time. Punch plate and wire mesh were tried but were ruled out by low tonnage life and the cost of hard surfacing. Finally a new upper deck was made from rugged bulb angles covered with sections of cast manganese grizzly bars. This turned the trick. Delays are now hardly noticeable, and screening costs, once 7¢ per ton, are down to a few mills.

This was another benefit of having the original plant engineers work right along with the operations group, taking advantage of knowledge that could be gained only in large-scale operation.

Time Cut on Liner Change: At the fine crusher a set of liners is changed about every 1.8 days. At first this required 12 hr. Then a spare bowl and shaft and head center were obtained so that the manganese steel liners could be zinced in place before the change-out. This cut the time in half. As in the coarse crusher change, careful studies were made to see where time could be gained and equipment and tools improved. The time was cut from 12 to 2 hr, then to 1 hr. Today it is being done in 38 min.

This has been possible only because each piece of equipment is readily accessible to the crane. When a crusher must be relined, the crane can lift the bowl mantle and head center without first having to remove other auxiliary equipment.

Magnetizing Speeds Up Settling Action: To obtain a high-grade concentrate with a satisfactory silica it is necessary to discard a middling product containing some magnetic iron. This middling cannot be brought up to grade no matter how fine it is ground. As tonnages were increased on the mills it was found that some of this middling product which should have been washed out in the rougher hydro separators was retained in the concentrates, lowering the grade.

Several changes were made in attempts to improve the washing action. The final solution was further magnetization of the hydro feed to speed up the settling action so that more water could be added. After magnetizing coils were installed around the pipes feeding the hydros, excellent washing was obtained and concentrate grade was raised even at maximum mill tonnage without any loss of concentratable ore in the tailings.

All this required more pumps. Fortunately space had been provided in the pumping station for just such contingencies.

What Was Done to Increase Efficiency of Cobbers: Cobbers consisted of two 36 x 48-in. magnetic drums in series, originally two machines for each of the 12 mill sections. Since about 35 pct of the total load of rod mill discharge is thrown off as tailings here, it is highly important that these machines function efficiently. Here again it was discovered that at maximum tonnages the machines did not perform satisfactorily. It was concluded that the drums were handling too much tonnage per foot, so a second machine was installed, in parallel with the first, and the feed was divided between them. But there was no improvement. Then a third drum was tried in series with the original two-drum machine, with a repulping box between the first and second drum. Improvement in the cobber concentrate was clearly visible and later confirmed by test data. Further, a higher tonnage of clean tailings was consistently thrown out by the three-drum cobber. All 24 cobbers have been modified in this way.

Some of the magnetic separators, hydro separators, and filters in the concentrator building. Rod mills are on upper level and ball mills just below. Plenty of space has been allowed for ease of operation and maintenance.

It could not have been anticipated that this problem would arise when production levels exceeded original capacity. The solution was relatively simple, but only because the designers had not crammed in the equipment.

Liner Wear Costs: In the first year of operation (1955-1956) Reserve's primary crusher alone used up 2,066,650 lb of liners, more than $600,000 worth. The fine crushing plant consumed more than 2 million lb of liners, almost $800,000 worth! Rods and balls accounted for nearly 25 million lb of steel, about $2 million. Replacement of mill shell and end liners called for another 2.4 million lb, worth about $600,000. The staggering total was 31,038,000 lb of material, with a price tag of $4 million.

The 24 ball mills and 12 rod mills furnished an excellent opportunity for quick evaluation of different materials and designs in shell liners. Practically every design that was thought to have a chance of survival was installed in one or another of the 36 mills—single-wave liners, with waves 2½ to 3½ in. high, on top of a 3-in. base; lifter-bar liners; and double-wave liners. The materials included chrome-moly alloys, chrome-moly with nickel, rolled plate with hardened lifters, and manganese and nickel alloys. The NiHard liner with the 3½-in. single wave showed up best in both rod and ball mills. Final life of these liners in the rod mills is about 2.5 million tons. In the ball mills the original Nihard sets have not yet been changed. This is a vast improvement over one type of rod mill liner that had to be changed at about 350,000 tons.

Progress in Pelletizing: Pelletizing is the newest development in Reserve's process. The choice of horizontal rather than vertical shaft furnaces was, in fact, the last major engineering decision made; consequently it has given rise to many problems that are important in terms of cost. Nowhere else have the advantages of cooperation between operators and designers been more evident than in the pelletizing of concentrates.

The six horizontal pelletizing machines at the E. W. Davis Works are the traveling-grate type, similar to a sintering machine, with 28 6x6-ft wind boxes. Pelletizing and sintering processes, however, are quite different.

Green pellets from the balling drums are almost completely dried in the first nine wind boxes; they are preheated, ignited, and burned over the next nine wind boxes and air-cooled to about 400°C in the last ten. In the drying, preheat, and ignition sections as much high-temperature air as possible is

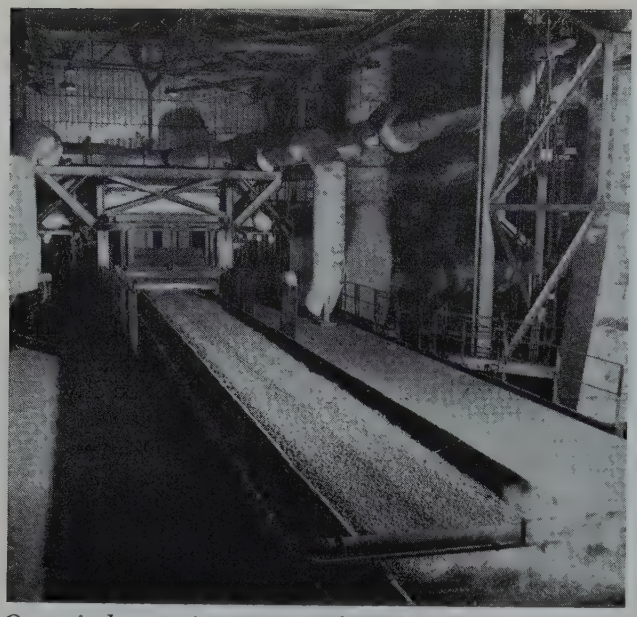

One of the six furnaces in the Silver Bay pelletizing plant. Bed of pellets shown is 12 to 14 in. deep.

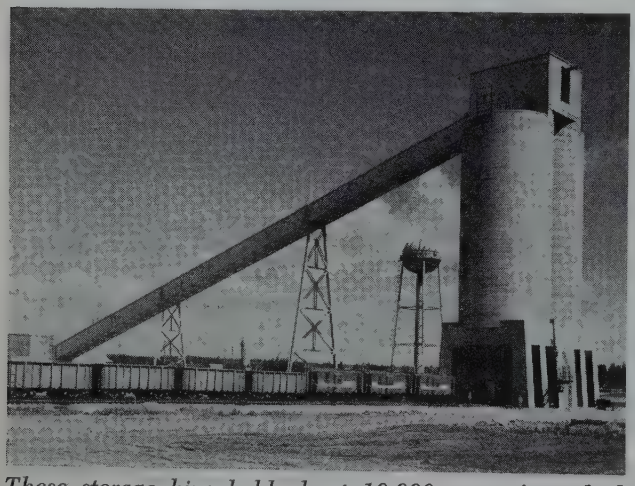

These storage bins hold about 10,000 tons of crushed taconite. Cars below are loaded without stopping.

re-used from the burning and cooling wind boxes. Owing to this heat recuperation the fuel requirements are substantially lower than for sintering.

During the early start-up period each of the three types of screens used in pelletizing caused excessive delays. For the green pellet screens balling drum delays averaged 343 hr per month. This was corrected by replacing all 18 screen bodies with heavier equipment and arranging for a complete spare screen so that each screen could be taken out of service for a complete overhaul as required.

Delays for repair of furnace feeder screens, originally 32 hr per month, have been cut to less than 6 hr. This improvement was brought about in several ways. New and better-designed cross members and side plates were used. Failure of mounting rubber due to excess heat was corrected by installing turbo blowers to air-cool the rubber, a job greatly simplified by the provision of ample building space. Bearing life has been prolonged from about two months to more than a year by an extensive program carried out in collaboration with the screen manufacturer, bearing and lubrication suppliers, and manufacturers of automatic lubrication equipment. It is expected that screen bearing life will be increased to approximately two years as study with designers and specialists continues.

With the finished pellet screens about 90 hr per month were lost because of short deck life and bearing troubles. Today the average is only 2 hr monthly. Deck life has been prolonged by improved design, and the installation of water-cooled housings has forestalled further trouble with the bearings.

Some of the heat problems were caused by higher than anticipated temperatures throughout the pelletizing machines. For example, there were frequent failures of grate bars, pallet frames, and breechings and downcomers in the recuperation air-handling system. First-year replacements of grate bars for the pelletizing furnaces amounted to $251,000. Pallet frame replacements that year alone came to $185,000. In 1958 the company spent $385,000 for grate bars, $98,000 for pallet frames, and $215,000 for pelletizing screens.

A seemingly endless number of grate bars were specially made for the pelletizing machines. Different designs, analyses, and casting practices were tried. In the beginning grate bars lasted only two months. Average life is now 12 months, and engineers and operators are still working at it. At the earlier rate, grate bar replacements would have approached $900,000 annually.

To date the best answer to pallet frame breakage has been a split pallet frame, bolted together at the center. Average life has increased from 60 to 300 days.

In the recuperation area of the machines the 1250° to 1300°C air temperatures caused failure of ducts and breechings carrying hot air from the wind boxes to the fans. Originally the ducts and breechings were of steel plate insulated on the outside. About a third of these have been replaced by others of new design with refractory linings, and eventually all of them will be changed. This has already been a major job calling for 155 tons of fabricated steel and 562 tons of refractory at a cost of about $180,000 installed to date. Here again, there was plenty of space for truck cranes and other heavy mobile equipment to operate between the pelletizing machines, and changes have been carried out with minimum delay in production.

To overcome the many problems of high temperature, a new investigation-development program has been instituted on one of the pelletizing machines, calling for updraft instead of downdraft cooling on the last six wind boxes. Equipment has been added and rearranged without the necessity of extending the building.

This updraft system has solved the pallet frame problem. It also recuperates more high-temperature air, which is used to improve quality, increase production, and lower fuel consumption. In fact, on this machine the use of coal-coating drums has been completely eliminated, saving costs on installation and operation and maintenance and part of the cost of anthracite fines. Somewhat more oil is used to supply the needed Btu's, partially offsetting the apparent saving in coal costs.

Now that the plant has been running for three full years, still further significant improvements in maintenance and operation are expected. They will be easier, quicker, and less costly because they can be incorporated in a sound, flexible engineering design.

Discussion of this article sent (2 copies) to AIME before Oct. 31, 1959 will be published in MINING ENGINEERING.

GEOLOGY OF THE ROSS-ADAMS URANIUM-THORIUM DEPOSIT, ALASKA

by E. M. MacKEVETT, JR.

The only source of uranium ore in Alaska that has been mined commercially is the Ross-Adams deposit, a gently inclined, fusiform orebody in alkali granite in which uranothorite and uranoan thorianite are the chief ore minerals. In mode of occurrence, apparent genetic association with the granite, and to a lesser extent in mineralogy, this type of deposit is uncommon.

The mine is in the southern part of Prince of Wales Island (Fig. 1) at an altitude of about 950 ft on the southeast flank of Bokan Mountain. A steep unpaved road 1¾ miles long leads to the dock on the West Arm of Kendrick Bay, which can be reached by boat or seaplane from Ketchikan, some 35 miles to the northeast.

The southern section of Prince of Wales Island is covered by dense forests interspersed with swampy tracts of muskeg. Most of the higher peaks support only sparse vegetation, and in areas underlain by alkali granite bare rocky slopes prevail to as low as 800 ft. Numerous fiord-like embayments penetrate this part of the island, and their shorelines provide near-continuous rock exposures. Rainfall is heavy, about 150 in. annually. Throughout the year the climate is relatively mild.

History and Production: In May 1955 two members of a Ketchikan prospecting group, Don Ross and his wife, found the deposit while working with an airborne geiger counter. Later they confirmed their discovery by ground investigations. During the summer Climax Molybdenum acquired controlling interest in the property and started exploratory diamond drilling, resuming the drilling on a larger scale in the summer and fall of 1956. Climax began mining in July 1957, shipping the ore by barge and train to the Dawn Mining Co. mill at Ford, Wash.

The open pit workings, about 370 ft long, between 25 and 75 ft wide, and 25 ft deep (shown in Fig. 2) were shut down in October 1957. As of September 1958 the pit was still inactive, although a small tonnage of known reserves remains in the southern part. The operators believe the 15,000 tons of uranium ore already produced will average 0.80 pct.

E. M. MacKEVETT, JR., Member AIME, is a Geologist with the U. S. Geological Survey, Menlo Park, Calif. TP 591200. Manuscript, Jan. 2, 1959. Pacific Northwest Minerals Conference, Spokane, Wash., April 1958. AIME Trans., Vol. 214, 1959.

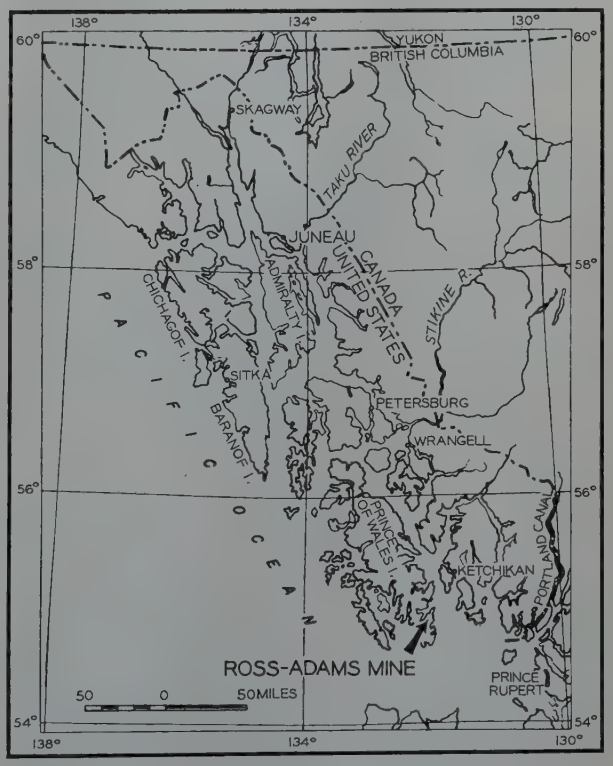

Fig. 1—Site of Ross-Adams mine in southeastern Alaska.

GEOLOGY

The Ross-Adams mine is within a small stock or boss of alkali granite, about 1000 ft from the southeast margin of the granite (Fig. 3). The area around the boss is underlain chiefly by plutonic rocks of intermediate composition and by metamorphosed sedimentary and volcanic rocks.

The oldest rocks in the area probably are the metamorphosed volcanic rocks that are well exposed adjacent to the South Arm of Moira Sound. They are considered by Buddington and Chapin[1] to be of Devonian age. These light gray to dark gray rocks mainly represent a layered volcanic sequence. They are commonly porphyritic with plagioclase phenocrysts in an altered, fine-grained groundmass. The

minerals of the groundmass are commonly altered to chlorite, epidote, and clay minerals. These rocks are chiefly of intermediate composition, probably ranging from quartz latite to andesite.

Another rock of Paleozoic age, consisting largely of black slate and hornfels, forms a crudely arcuate outcrop in the area. These rocks are locally chiastolite-bearing and in places graphitic.

A heterogeneous dioritic assemblage probably represents the oldest Cretaceous(?) rocks in the area. Rocks of this type crop out abundantly near the West Arm of Kendrick Bay and less extensively elsewhere. They comprise chiefly hornblende quartz diorite, hornblende diorite, and amphibolite, which range from fine to coarse-grained and generally are altered to chlorite, epidote, clinozoisite, calcite, and clay minerals.

The next younger rocks are the dominant intrusive rocks in the area shown in Fig. 3. These consist of altered medium-grained quartz monzonite and granodiorite, both of which commonly contain less than 5 pct mafic minerals, chiefly biotite. Salients of these rocks cut the dioritic unit.

Aplite and alaskite as much as 500 ft thick locally intervene between the quartz monzonite and the alkali granite.

The youngest intrusive rock, excluding that of the dikes, is alkali granite, probably of Late Cretaceous or early Tertiary age. Almost all the uranium-thorium deposits in the district are within or near the alkali granite and are believed genetically related to it. The alkali granite forms a small stock or boss, about 3 sq miles in area, that is centered near Bokan Mountain. The rock ranges from fine to coarse-grained and is characterized by diverse textures including hypidiomorphic granular, porphyritic, seriate porphyritic, and cataclastic. Predominant minerals of the alkali granite are quartz and varieties of K-feldspar. Albite, commonly An_{5}, forms between 5 and 15 pct of the rock and acmite and riebeckite each constitute between 1 and 12 pct of the alkali granite. Minor accessory minerals, which commonly form less than 1 pct of the granite, consist chiefly of zircon with less abundant uranothorite, pyrite, zenotime, fluorite, and magnetite. The granite apparently has had a complex history, as indicated by its variety of textures and two stages of formation of its constituent quartz and K-feldspar. Late-stage quartz locally cuts and embays older quartz, and sodian adularia in places embays and replaces grid-twinned K-feldspar. The alkali granite contains abnormal quantities of certain minor elements, notably uranium, thorium, yttrium, lanthanum, niobium, and cerium and other rare earths. Results of semiquantitative spectrographic analyses and analyses for equivalent and chemical uranium of seven samples of the alkali granite are shown in Table I.

Dikes, mainly fine-grained intermediate to mafic types, are abundant, particularly in the diorite. They apparently were intruded at several different times, but their precise age relationships are unknown. Most of the pegmatite and aplite dikes are late-stage affiliates of the alkali granite. They occur chiefly within the granite and in the adjacent rocks as small irregular masses generally less than 200 ft long and 2 ft thick. Commonly they contain the suite of rare elements that is typical of the alkali granite.

Structure: The rocks of the area are cut by numerous joints and faults. Only the strongest faults are shown in Fig. 3. They occur principally in two steep-dipping sets, one striking near east and the other near north. A few of the faults are breccia zones as much as 100 ft thick, but most are narrow iron-stained shear zones a few feet thick.

ORE DEPOSIT

The dominant ore minerals are uranothorite and uranoan thorianite. The deposit is reddish-brown in color, owing largely to its constituent hematite, and therefore contrasts markedly with its nearly white alkali granite host. The orebody, which is crudely fusiform and trends northward, had surface exposures over a length of about 180 ft. Average width was 40 ft and its maximum vertical dimension about 50 ft (Figs. 2, 4, and 5). The longitudinal dimension of the orebody as revealed by diamond drilling is at least 350 ft. Fig. 4 shows the mine area prior to mining, and Fig. 2 the open pit as it was in September 1957, during the latter stages of mining. Scabs of ore are shown on the walls of the pit in Fig. 2, and minor amounts of ore are beneath the rubble that covers the bottom of the pit. The concealed extent of the orebody is inferred from diamond drill hole data and subsequent mine excavations.

A steep fault that strikes N 70° W cuts another steep fault that strikes N 80° E where the faults are exposed in the southern part of the pit (Fig. 2). Both faults cut the orebody, causing its southern part to be downthrown, but the amount of displacement could not be accurately determined. A small amount of fractured and iron-stained andesite(?) is exposed locally along the faults. South of the faults the orebody has only one small outcrop. A few other faults are exposed in the open pit (Fig. 2) where they locally cut remnants of the orebody.

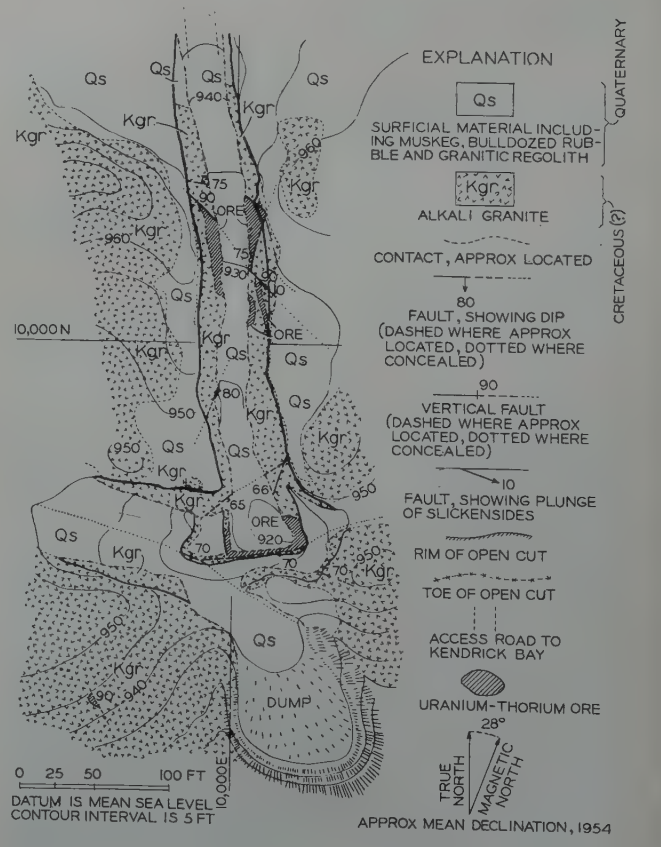

Fig. 2—Geologic map of the Ross-Adams open pit.

Table I. Results of Semiquantitative Spectrographic Analyses and Uranium Analyses of Seven Samples of the Alkali Granite Near Bokan Mountain*†

Sample No.	Percent eU	Percent U	>10	10	3	1	0.3	0.1	0.03	0.01	0.003	0.001
1	0.004	0.0024	Si	Al	Fe, Na, K		Zr	Ti, Ce	Ca, Mn, La	Ga, Nb, Nd, Sn	Mg, Ba, Cr, Cu, Ni, Y, Yb, U, Th	Pb, Sc
159	0.005	0.0038	Si	Al	Fe, Na, K		Zr	Ti	Ca, Mn, Ba, Ce	Mg, La, Nb, Y	Cr, Ga, Ni, Sn, Yb, U, Th	Be, Cu, Pb, Sc, Sr
168	0.005	0.0017	Si	Al	Fe, Na, K			Ti	Ca, Mn, Ce, Zr	Mg, Ga, La, Nb, Y, Zn	Ba, Cr, Sn, Th	Cu, Ni, Pb, Yb, U
219	0.005	0.003	Si	Al	Fe, Na, K		Ce	Ca, Ti, Zr	Mn, La, Nb, Nd, Y	Mg, Ba, Cu, Dy, Er, Pb, Zn	Be, Ga, Ni, Sn, Sr, Yb, U	Cr, Th
225	0.002	0.002	Si		Al, Fe, Na	K		Zr	Ca, Ti, Mn		Nb, Ni, Y, U	Ba, Cr, Cu, Ga, Yb
233	0.020	0.005	Si	Al	Fe, Na, K		Ca	Ti, Ce, Th, Y	Mn, La, Nb, Nd, Zr, U	Mg, Ba, Dy, Er, Sr, Yb	Pb, Sn, Zn	Be, Cr, Cu, Ga, Ni
234	0.009	0.008	Si	Al	Fe, Na, K			Ti, Ce, Zr	Mn, Y	Ca, Ba, La, Nb, Nd, U	Mg, Cu, Ni, Yb	Cr, Ga, Pb, Sr, Th

* Nearest percent in the series 10, 3, 1, 0.3, 0.1, 0.03, 0.01, 0.003, 0.001.
† Spectrographic analyses by Joseph Haffty, USGS. Raidometric and chemical analyses by B. A. McCall, Roosevelt Moore, Erma Campbell, and Joseph Budinsky, USGS.

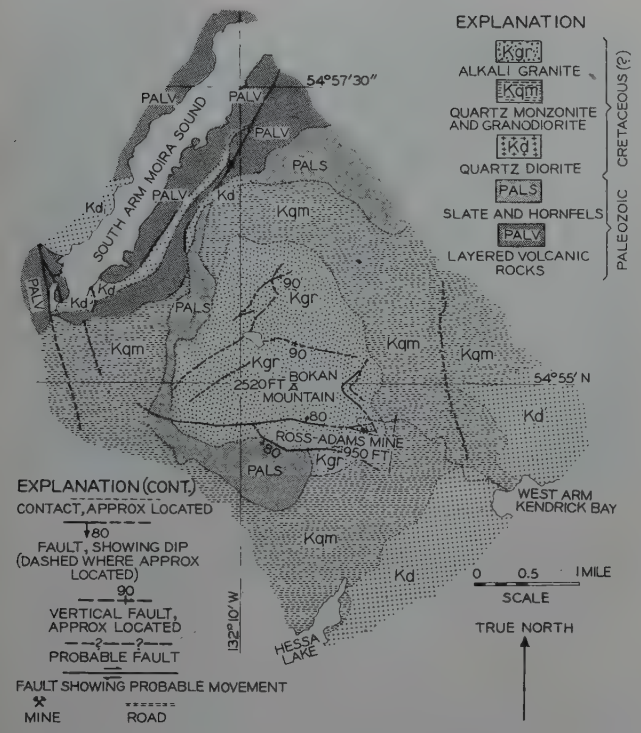

Fig. 3—Generalized geologic map of area near the mine.

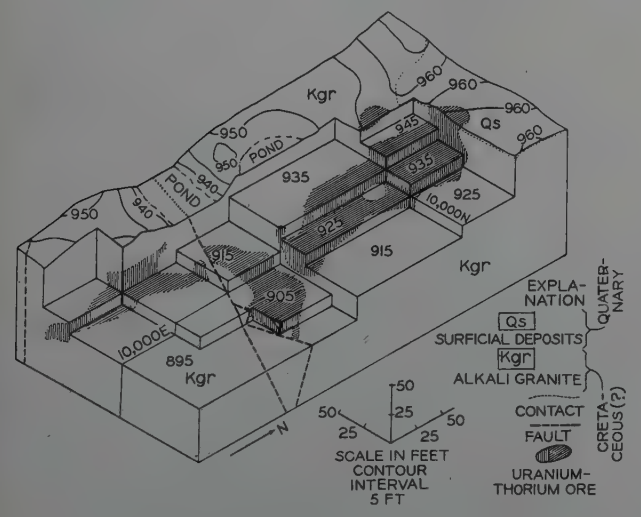

Fig. 5—Isometric block diagram of Ross-Adams deposit.

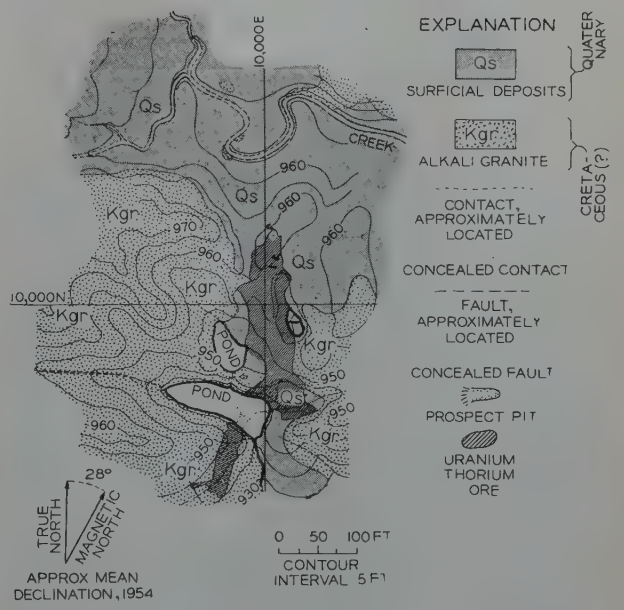

Fig. 4—Geologic map of the Ross-Adams mine area.

Most of the orebody has a gentle southerly plunge, which increases to 35° near the faults that cut the southern part of the deposit. This local steeper plunge is probably largely a drag effect of faulting. The size and shape of most of the orebody have been fairly well established by the surface exposures, mining, and diamond drilling, but south of the two crosscutting faults exploration consists only of scattered diamond drill holes—not enough to delineate the orebody thoroughly. Other orebodies may exist beneath the known one, but this possibility has not been tested by deep drilling.

MINERALOGY AND COMPOSITION

In general, the Ross-Adams orebody consists of a core of high grade ore that contains greater than 0.05 pct U_3O_8 enveloped by a uraniferous zone 2 to 20 ft thick that contains less than 0.50 pct U_3O_8. There are a few small pods of low grade ore and locally barren rock within the high grade ore. Texturally, the ore resembles its alkali granite host rock. It consists of numerous ore-bearing veinlets between 0.1 and 0.8 mm thick and scattered uranium-thorium minerals throughout the alkali granite. Almost all of the primary uranium-thorium

minerals are in the metamict state. Commonly iron-stained fractures emanate from the radioactive minerals; in places the fractures form reticulating iron-stained veinlets along cleavage planes in feldspars.

Fig. 6 and 7 are micrographs showing scattered uranium-thorium minerals accompanied by iron-stained fractures in the alkali granite.

The dominant ore minerals, uranothorite and uranoan thorianite, occur both in the veinlets and scattered throughout the alkali granite of the lode. Jerome Stern, Alan King, Daphne Riska, and Betsy Levin of the USGS have identified uranothorite and uranoan thorianite in several specimens by X-ray diffraction after heating. By X-ray diffraction methods King has also identified coffinite, which occurs in minor amounts in the ore.

Besides the uranium-thorium minerals the veinlets contain abundant hematite and lesser amounts of calcite, fluorite, pyrite, galena, quartz, and chlorite. Pyrite and galena are locally abundant in the veinlets near the crosscutting faults. Fluorite in the veinlets is deep purple. Micrographs of some of the typical vein minerals are shown with uranoan thorianite (?) in Figs. 8 and 9.

Secondary uranium minerals occur in minor amounts in near-surface environments at the deposit. They include gummite, sklodowskite, beta-uranophane, bassetite, and novacekite, all originally identified by Alan King of the USGS by X-ray diffraction methods. Most identifications have subsequently been confirmed by the writer.

Composition of the ore is indicated by Table II, which shows the results of semiquantitative spectrographic analyses for 69 elements and chemical analyses for uranium and thorium.

Although there is general similarity in composition between the ore and the alkali granite, several differences are apparent from studying Tables I and II. Notable among these are the increase of uranium and thorium in the ore and its lack of potassium. The ore also differs from the alkali granite in generally containing more iron, lead, and aluminum, slightly more zirconium, titanium, magnesium, calcium, manganese, and arsenic, and less cerium.

Most of the deposit is out of radioactive equilibrium in such a way that the radioactivity of the thorium daughter products combines with that of the uranium daughter products to give an effect of apparent equilibrium and most equivalent uranium and chemical uranium analyses of the same samples are nearly equal (Table II) despite the presence of abundant thorium. Throughout most of the deposit there is slightly more thorium than uranium, but the few analyses available on diamond drill cores from the southernmost known parts of the orebody indicate thorium-uranium ratios of as much as 7:1.

PROBABLE GENESIS

Formation of the Ross-Adams deposit is believed attributable to two processes, a local concentration of probably late-stage accessory uranothorite and uranoan thorianite in the alkali granite, followed by the emplacement of numerous uranium-bearing and thorium-bearing veinlets at the site of the lode. Possibly the uranium and thorium minerals in the veinlets were derived from reworking the earlier accessory uranium-thorium minerals. The causes of the local concentration of the accessory uranium-thorium minerals are not well understood. Except for the quantity of the uranium-thorium minerals, the numerous veinlets, and the lack of potassium, the properties of the host alkali granite of the lode are similar to its unmineralized counterparts. There are no recognizable structural features that would favor accumulation of the accessory uranium-thorium minerals at the site of the deposit.

One or both of the crosscutting faults may have acted as channelways from which the ore-bearing veinlets emanated. It is postulated that these faults

Table II. Results of Semiquantitative Spectrographic Analyses and Analyses for Uranium and Thorium of Twelve Samples of Ore from Ross-Adams Deposit*†

Sample No.	Percent eU	Percent U	Percent Th	>10	10	3	1	0.3	0.1	0.03	0.01	0.003	0.001
36-2	0.61	0.64	0.74	Si, Al, Fe		Na	Th, U, Zr	Ti	Mg, Ca, Mn, Y	Ba, Dy, Er, Pb, Yb	As, La, Nb, Nd, Sr	Co, Cr, Ga, Sn	Be, Cu
40-1	0.38	0.38	‡	Si, Al, Fe		Na	Th, Zr	Ti, U	Y	Mg, Ca, Mn, Dy, Er, La, Nd, Yb	As, Ce, Nb, Pb	Ba, Cr, Ga, Sn	Be, Co, Cu, Sr
40-3	0.53	0.56	‡	Si, Al, Fe		Na	Th, Zr	Ti, U	Y	Mg, Ca, Mn, Dy, Er, Pb, Yb	As, Ba, Nb	Cr, Ga, Sn	Be, Co, Cu, Sr
41-1	0.20	0.18	‡	Si, Al, Fe		Na		Ti, Th	U, Zr	Mg, Ca, Mn, Nb, Y	As, Ba, Pb	Cr, Ga, Sn, Yb	Co, Cu, Sr
42-2	0.40	0.36	‡	Si, Al	Fe	Na	Th	U, Zr	Mg, Ti, Mn, Y	Ca, Dy, Er, Pb	As, Ba, La, Nb, Nd	Co, Ga, Sn	Be, Cr, Cu, Sr
42-4	0.69	0.60	‡	Si, Al	Fe	Na	Th, U		Mg, Ca, Ti, Mn	Pb, Y, Zr	As, Ba, Dy, Nb, Nd	Co, Ga, Mo, Sn, Yb	Be, Cr, Cu, Sr
43-1	1.6	1.8	2.20	Si, Al	Fe	Na, Th, U		Zr	Ca, Ti, Pb, Y	Mg, Mn, Ba, Dy, Er, Nd, Yb	As, Cu, La	Co, Ga, Mo, Sn, Sr	Be, Cr
43-3	0.63	0.55	‡	Si, Al	Fe	Na	Th	U, Zr	Ti	Mg. Ca, Mn, Pb, Y	Ba, Dy, La, Nb, Nd, Yb	Ga, Sn	Be, Co, Cr. Sr
44	4.4	3.2	5.66	Si		Al, Fe, Th, U, Na		Ca, Ti, Pb	Mn, Ce, Y, Zr	Mg, Ba, Dy, Er, La, Nd	Nb, Sr, Yb	Ga, V	Cr, Cu
45	2.3	2.8	2.32	Si		Al,Fe, Na, Th, U		Ti, Pb, Zr	Ca, Mn, Y	Mg, Ba, Dy, Er, Sr	Nb, Yb	Cu, Ga	Cr, V
46	1.6	1.3	1.62	Si	Al, Fe	Na, Th	Mg, U	Ca, Hn, Zr	Ti, Ba, Pb, Y	Dy, Er, Sr	As, Yb	Co, Ga, Mo, Sn	Be, Cr, Cu, V
50	3.1	0.60	3.34	Si		Al, Fe, Na, Th	U	Pb, Zr	Mg, Ca, Ti, Mn, Y	Ba, Dy, Er	Nb, Sr, Yb	Ga	Be, Cr, Cu, V

* Nearest percent in the series 10, 3, 1, 0.3, 0.1, 0.03, 0.01, 0.003, 0.001.
† Spectrographic analyses by Joseph Haffty, radiometric analyses by B. A. McCall, chemical analyses for uranium and thorium by Roosevelt Moore and for thorium by Erma Campbell, and X-ray fluorescence analyses for thorium by Isadore Adler, all of USGS.
‡ Thorium not analyzed by chemical or X-ray fluorescent methods.

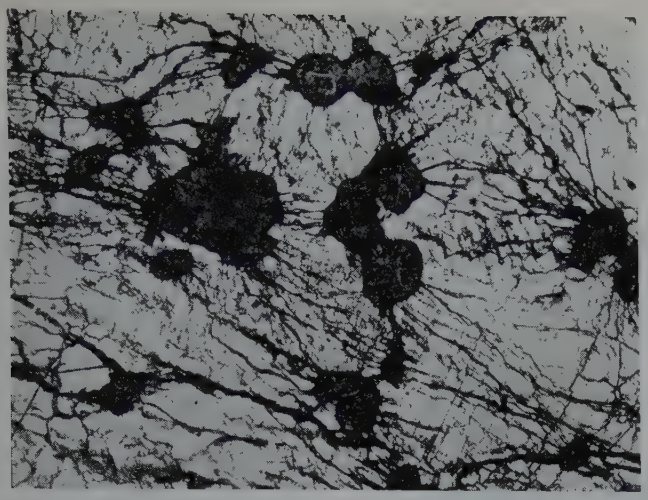

Fig. 6—Uranium-thorium minerals in alkali granite host. Iron-stained veinlets emanate from the radioactive minerals. Ordinary light, X20. Reduced about one third.

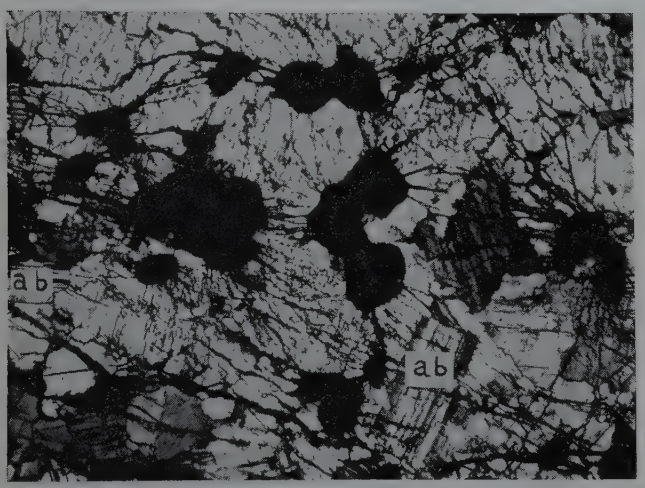

Fig. 7—Same field as Fig. 6. The isotropic uranium-thorium minerals probably include both uranothorite and uranoan thorianite. ab is albite, An_4. Rest of field consists mainly of quartz and sodian adularia. Polarized light, X20. Micrograph reduced approximately one third.

had at least two periods of activity and that they were open channels when the hydrothermal solutions that formed the ore-bearing veinlets were active. Later movements on them offset the orebody. Indications that these faults may have been channelways are that the ore deposit attains its widest dimension near the faults (Fig. 4); finely crushed ore and vein minerals are found along them; and local small deposits of uranium-thorium minerals, fluorite, hematite, and rare earths occur along similar faults nearby.

CONCLUSIONS

This small deposit represents an uncommon type of uranium-thorium deposit both in shape and mineralogy. Its origin seems to be linked with a late fractionization in the alkali granite of uranium, thorium, other rare elements, and sodium; first uranium-thorium-bearing accessory minerals were locally concentrated in the granite, and subsequently numerous ore-bearing veinlets were emplaced.

This report is based in part on field investigations in the south of Prince of Wales Island during the summers of 1956 and 1957, during which time the writer was capably assisted by A. L. Kimball. The author also gratefully acknowledges assistance in the field studies from personnel of the Kendrick Bay Mining Co. and Climax Molybdenum Co., particularly R. J. O'Hara and H. Wright, as well as several Ketchikan residents. Permission to publish data on early mine production was granted by Climax Molybdenum Co.

This work is part of a program conducted by the U. S. Geological Survey on behalf of the Division of Raw Materials of the U. S. Atomic Energy Commission.

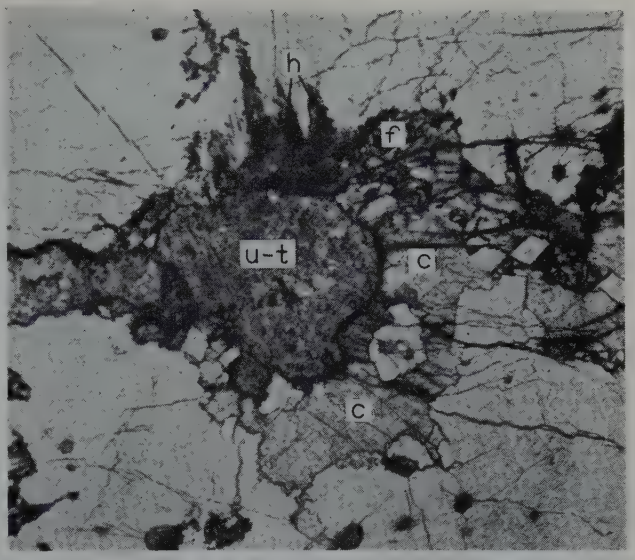

Fig. 8—Details of uranium-thorium-bearing veinlet at the Ross-Adams deposit showing uranoan thorianite (?) (U-t), calcite (c), hematite (h), and fluorite (f). Iron-stained fractures emanating from the uranoan thorianite (?) cut the other vein minerals and the alkali granite host. Ordinary light, X50. Reduced about one fourth.

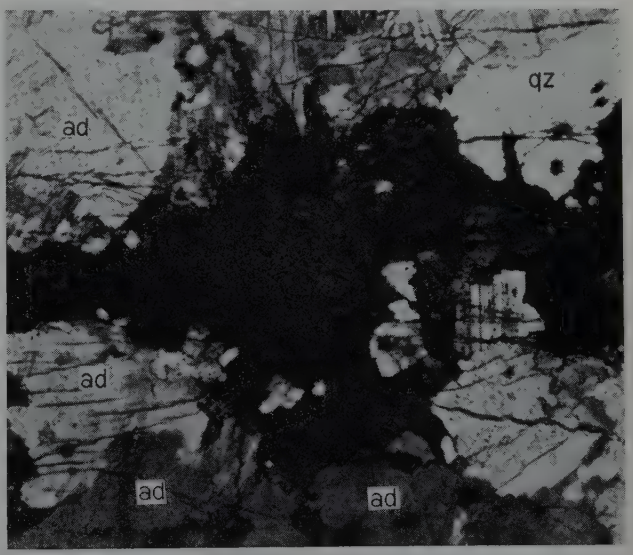

Fig. 9—Same field as Fig. 8, showing the albite (ab), An_5; sodian adularia (ad), and quartz (qz) of alkali granite host. Crossed nicols, X50. Reduced one fourth.

REFERENCE

A. F. Buddington and T. Chapin: Geology and Mineral Deposits of Southeastern Alaska, *USGA Bull 800*, 1929.

Discussion of this article sent (2 copies) to AIME before Oct. 31, 1959, will be published in MINING ENGINEERING.

EFFECTS OF STRUCTURE AND UNSATURATION OF COLLECTOR ON SOAP FLOTATION OF IRON ORES

by STRATHMORE R. B. COOKE, IWAO IWASAKI, and HYUNG SUP CHOI

Oleic acid is the chief ingredient of fatty acids used as collectors in nonsulfide flotation. With a few notable exceptions, the various quantities of saturated and other unsaturated acids comprising the remainder are usually unspecified. There have been occasional investigations to determine the collecting ability of these other acids and their effect on collection with oleic acid, but much remains to be done in this field. Hukki and Vartiainen, on the basis of tests using palmitic, oleic, and linoleic acids and an impure linolenic acid, concluded: "The collecting power of fatty acids used in flotation increases with increasing unsaturation of the hydrocarbon chain." [1] Their work was concerned mainly with the response of ilmenite to the foregoing collectors, although tests were also made with magnetite, pyrite, hematite, and rutile. Cooke and Nummela, employing an almost identical technical procedure to evaluate flotation of hematite, magnetite, and goethite with various fatty acids, including oleic, linoleic, and linolenic acids of the highest purity obtainable, found: "The effectiveness of 18-carbon unsaturated fatty acids, as collectors for hematite, decreases with increase in the number of non-conjugated double bonds." [2] In the foregoing investigations, collector efficacy was measured on the basis of reagent addition in moles per liter.

S. R. B. COOKE, Member AIME, is Professor and Head, School of Mines and Metallurgy, University of Minnesota. I. IWASAKI, Junior Member AIME, is Assistant Professor of Metallurgical Engineering, University of Minnesota. H. S. CHOI, Junior Member AIME, formerly U. S. Fish and Wildlife Fellow, University of Minnesota, is now Metallurgist, U. S. Fish and Wildlife Service.
TP 59B203. Manuscript, Jan. 26, 1959. AIME Trans., Vol. 214, 1959.

Sources of fatty acids which may be used as collectors are legion, but provided the oleic acid content is high enough, cost is normally the determining factor. Usually this restricts severely the purity of the collector in terms of its oleic acid content. Within the past year or so users of crude oleic acid have become somewhat more discriminating, apparently realizing that some of the organic acid impurities may exert deleterious effects upon certain separations.

Marine fish oils have been used as collecting agents, particularly in the earlier days of froth flotation. Currently their use is restricted in this field to relatively minor applications, although they are cheap sources of fatty acids. In an effort to increase the range of uses for fish oils, the U. S. Fish and Wildlife Service has awarded contracts to study these materials as sources of new products suitable for commercial development. Funds for these investigations were provided by the Saltonstall-Kennedy Act of 1954. One such contract was awarded to the University of Minnesota School of Mines and Metallurgy for the purpose of investigating the use of fish oil fatty acids and their derivatives in ore flotation.

Besides the esters of various saturated aliphatic acids and of palmitoleic and oleic acids, fish oil also contains esters of monoethenoid and polyethenoid acids with 20, 22, and 2 carbon atoms. The basic purpose of the investigation was to determine whether the longer-chained unsaturated acids possess collective properties superior to those of the C_{18} monoethenoid oleic acid, the C_{16} monoethenoid palmitoleic acid, or the saturated C_{18} stearic acid and its shorter chain homologues; whether highly unsaturated acids have merit as collectors; whether rela-

tively simple and inexpensive fractionation of fish-oil fatty acids would yield products that could function as well as other fatty acid collectors (including relatively pure reagents) or better; and whether certain derivatives of fish-oil fatty acids could serve as special flotation reagents.

This article reports the findings with regard to anionic flotation of either the iron oxides or the silica of ores in which the principal iron minerals are hematite and goethite and the principal gangue mineral is quartz.

REAGENTS

Most of the fatty acids used have been listed in Table I, together with pertinent information. Acids *A* through *I* were of relatively high purity, but some were available only in very limited quantities. The position of the double bond or bonds of these acids is given as numbered from the carboxyl (-COOH) carbon. The iodine value (I.V.) is a measure of the unsaturation of the acid.

Acids *J* through *O* are relatively impure commercial oleic acids or fractions or derivatives thereof. Although acids *J* through *N* are mixtures of saturated acids and of C_{16} and C_{18} monoethenoid and polyethenoid acids, they contain considerably more oleic acid than the oleic acid used for most flotation purposes.

Reagents *P* through *X* are mixtures of highly unsaturated fatty acids, for which the sources are indicated. In some instances the bulk mixture was separated into fractions of higher and lower degree of unsaturation by crystallization from acetone at low temperature. Tuna and menhaden fish oils were fractionated at the Hormel Institute by the urea method.[3] The corresponding fatty acids are listed in Table I as *HO-2*, etc., together with their iodine values and other information provided by the Institute.

Acids *1*, *2*, and *3* are relatively pure saturated acids, each containing 18 carbon atoms in the chain. Stearic acid is solid at room temperature; the other two are liquid.

The relationship between acids with cis- and trans- configurations is represented by the two following planar formulas:

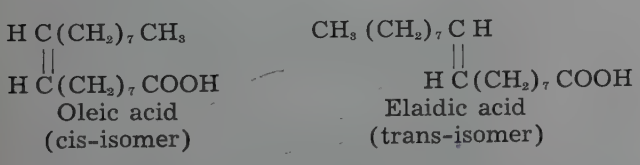

In the case of the unsaturated acids, samples were stored under nitrogen in a refrigerator. Except in certain special tests in which liquid free acids were added directly to the conditioning beaker, all were converted, under nitrogen, to the corresponding sodium soap by neutralization with 150 pct of the stoichiometric requirement of 0.1N carbonate-free NaOH.

Reagent consumption is expressed throughout in pounds per short ton of original slime-containing ore, i.e., on the basis of 500-gm nondeslimed head samples. Soap collectors, inorganic acid, alkali, Quebracho, and Marasperse C were measured volumetrically from standard solutions. In certain confirmatory tests, liquid fatty acids were accurately weighed and added directly to the conditioner. No tests were made below pH 5 because of the poor frothing properties of the fatty acids below this value.

ORE OPERATION AND PROCEDURE

Most of the flotation tests were made in a Fagergren laboratory cell using wash ore tailings from the Mesabi Range, but from time to time confirmatory tests were made on other iron ores. Most of the information presented here was provided by tests made on two wash ore tailings: ore *A* was used primarily for the flotation of contained iron oxide minerals and ore *B* for the flotation of siliceous minerals. Since the supply of ore *A* was exhausted before all the silica flotation tests were completed, it was later necessary to substitute two somewhat different ores. Enough silica flotation tests were made on ore *A*, however, to prove that the same principles applied to both ores *A* and *B* when essentially the same procedure was used.

Preparation of Ore A for Floatation of Iron Oxide Minerals: Ore *A* contained about 20 pct Fe as hematite, goethite, a very minor amount of magnetite, and about 70 pct insoluble, consisting of quartz and chert. A screen analysis of the dry ore, as received, is given in Table II.

After thorough mixing, the ore was divided into 500-gm samples. Each sample was ground with 5 lb H_2SO_4 per ton for 3 min at 60 pct solids. The grind was filtered to remove soluble salts, placed in the flotation cell, and diluted to 19 pct solids. After Quebracho was added (0.1 lb per ton) and NaOH (0.32 lb per ton) the pulp was agitated for 3 min. Agitation was then stopped and all plus 20μ quartz was allowed to settle. The supernatant slimes were removed by siphoning, and agitation without further reagent addition was resumed for 3 min. This cycle of agitation, sedimentation, and siphoning was repeated four times for each sample. As shown by the consistency in weights and in iron and insoluble contents of products, reproducibility of the desliming operation was excellent. The weight of -20μ slimes removed amounted to some 8 pct of the ore and contained an average of 36 pct Fe and 31 pct insoluble, or about 13 pct and 3 pct respectively of those constituents in the head sample.

Following desliming, the sands were transferred to a 1000-ml beaker, diluted to 60 pct solids, and conditioned for 5 min after the addition of Marasperse C (0.05 lb per ton) and the desired amount of collector. The pH during conditioning was not controlled and ranged only from 6.8 to 7.1 as measured at the end of conditioning. The conditioned pulp was immediately transferred to the flotation cell and diluted; the pH was readjusted and a rougher froth removed. This was cleaned twice in the same cell. The rougher tailing, the second cleaner concentrate, and the combined middlings from the two cleaning stages were then analyzed for iron and insoluble contents.

Preparation of Ore B for Flotation of Silica: Ore B assayed about 37 pct Fe as hematite, goethite, a small quantity of magnetite, and about 45 pct insoluble as quartz and chert, so that mineralogically it was qualitatively similar to ore *A*. Table III gives a screen analysis.

In tests made to determine the response of this ore to anionic flotation of its silica, it was processed down to the conditioning stage in the same way as ore *A*, with the two following exceptions: 1) the 500-gm sample was ground considerably finer (through 150 mesh) in the Abbé mill, because it is the writers' experience that a finer grind is necessary

in floating silica than in floating iron oxides, and 2) five stages of sedimentation were used to remove -20μ slimes rather than the four employed in preparing ore *A*. In each test about 20 pct of the original 500-gm charge was removed as slimes and assayed about 37.5 pct Fe and 40 pct insoluble.

The deslimed ore was transferred to a 1000-ml beaker. After dilution to 60 pct solids the pulp was conditioned for successive 5-min intervals with $CaCl_2 \cdot 2H_2O$ (1.0 to 1.5 lb per ton) and NaOH (to the desired pH, usually 11.5), with Gum 9072 (0.3 to 0.5 lb per ton) and finally with the equivalent of 1.0 lb of fatty acid, or a total of 15 min conditioning time. The pulp was immediately transferred to the flotation cell and diluted to volume; the pH was readjusted to 11.5 by addition of NaOH, and flotation commenced. After the silica-bearing froth had been removed, the iron oxides remaining in the cell were scavenged once using $CaCl_2 \cdot 2H_2O$ (1.0 lb per ton), Gum 9072 (0.2 lb per ton), and collector (0.5 lb per ton). This operation is summarized in the accompanying flowsheet (Fig. 1).

Ca^{++} AND Mg^{++} EFFECT ON IRON OXIDE FLOTATION

It is known that both Ca^{++} and Mg^{++} are adsorbed by quartz, particularly in the pH range more alkaline than pH 5, and may function as activating ions in the presence of fatty acids or soaps.[4] Laboratory tap water at the University of Minnesota averages 18 and 6.8 ppm of Ca^{++} and Mg^{++}, respectively. Under these conditions both the iron oxide minerals and substantial quantities of quartz are collected, with deleterious effects on selectivity. Even though distilled water was used throughout the flotation experiment to avoid introducing these activating cations, it was noted that the rougher concentrates obtained by floating the iron oxides were consistently low-grade and large in bulk. Two or three stages of cleaning, however, invariably gave a high-grade product, most of the quartz dropping back to the middling.

The rougher and cleaner middlings were found to consist chiefly of clean quartz particles, with few true middling grains. As the froths were consistently good, with no undue toughness that might cause excessive mechanical entrapment, it was concluded that the clean quartz was being activated either by a slime coating of iron oxides or by traces of Ca^{++} and Mg^{++} liberated from the ore itself. To check these points the following experiments were made.

A series of simplified flotation tests were made on clean quartz, using demineralized distilled water containing a suspension of either very finely ground hematite or goethite, and oleic, elaidic, and linoleic acids as collectors. The quartz did not float, so that under the specified conditions it seems improbable that either hematite or goethite slimes can activate this mineral.

Ten grams of ore *A*, containing its slimes, were thoroughly agitated with 50 ml of demineralized distilled water in a pyrex container, then centrifuged at 10,000 rpm for 1 hr. The clarified supernatant fluid obtained was used as the liquid phase in a series of vacuum flotation tests made with clean quartz, employing pure sodium oleate, elaidate, and linoleate, each at an equivalent acid concentration of

Table I. Fatty Acids Used in Flotation Tests

Designation	Name	Position of Double Bond	Iodine Value	Remarks
A	Oleic	9, 10	89.8	m.p. = 13.4° Cis-isomer
B	Elaidic	9, 10	80.6	m.p. = 43.7° Trans-isomer
C	Linoleic	9, 10, 12, 13	181.0	m.p. = −5.0° to −5.2° Non-conjugated cis-isomer
D	Linoelaidic	9, 10, 12, 13	—	m.p. = 28° to 29° Non-conjugated trans-isomer
E	Conjugated linoleic	9, 10, 11, 12	—	m.p. = 54° Conjugated cis-isomer
F	Conjugated linoleic	10, 11, 12, 13	—	m.p. = 57° Conjugated trans-isomer
G	Linolenic	9, 10, 12, 13, 15, 16	273.0	m.p. = −11° to −11.3° Non-conjugated cis-isomer
H	α-elaeostearic	9, 10, 11, 12, 13, 14	—	m.p. = 48° to 49° Conjugated cis-isomer
I	β-elaeostearic	9, 10, 11, 12, 13, 14	—	m.p. = 71° to 72° Conjugated trans-isomer
J	Oleic (technical)	—	88.2	93 pct C_{18} monoethenoid acid
K	—	—	93.5	A less saturated fraction prepared from J
L	—	—	75.0	A more saturated fraction prepared from J
M	Oleic (commercial)	—	85.1	15.9 pct saturated, 79.9 pct monoethenoid, 4.2 pct diethenoid acids
N	Oleic (commercial)	—	95.0	—
O	Elaidic (impure)	—	80.9	Prepared by selenium isomerization of J. 56.5 pct monoethenoid, 13.5 pct diethenoid acids
P	Marine fatty acid	—	219.2	From menhaden oil. 1.9 pct C_{18} di-, 10 pct C_{20} tetra-, 14.9 pct C_{20} pentaethenoid, 27 pct C_{22} acids
Q	Marine fatty acid	—	271.0	Unsaturated fraction prepared from P
R	Marine fatty acid	—	266.2	Unsaturated fraction prepared from P
S	Marine fatty acid	—	116.0	More saturated fraction prepared from P
T	Marine fatty acid	—	218.5	Bulk fatty acid from salmon egg oil
U	Marine fatty acid	—	255.0	Unsaturated fraction prepared from T
V	Marine fatty acid	—	230.0	Bulk fatty acid from salmon egg oil
W	Marine fatty acid	—	247.0	Unsaturated fraction prepared from V
X	Marine fatty acid	—	255.2	Less saturated fraction prepared from P
HO-2	Marine fatty acid	—	144.0	Palmitic acid with appreciable quantities of palmitoleic and polyethenoid acids
HO-3	Marine fatty acid	—	181.2	Palmitic and stearic acids with appreciable oleic and polyethenoid acids
HO-5	Marine fatty acid	—	67.6	Mixture of palmitoleic and palmitic acids
HO-6	Marine fatty acid	—	109.7	High content of palmitoleic acid
HO-10	Marine fatty acid	—	196.5	Mixture of C_{20} and C_{22} mono- to hexaethenoid acids
HO-12	Marine fatty acid	—	202.2	Mixture of C_{20} and C_{22} mono- to hexaethenoid acids
HO-13	Marine fatty acid	—	111.1	Largely C_{20} mono- and diethenoid acids
HO-15	Marine fatty acid	—	115.8	Complex mixture of stearic, oleic and polyethenoid acids
HO-16	Marine fatty acid	—	197.4	Largely C_{16} and C_{18} di- to tetraethenoid acids
HO-18	Marine fatty acid	—	71.4	C_{16} and C_{18} saturated and monoethenoid acids
HO-19	Marine fatty acid	—	109.4	Primarily palmitoleic and oleic acids
HO-25	Marine fatty acid	—	149.8	Mainly C_{20} mono-, di-, and polyethenoid acids
HO-26	Marine fatty acid	—	69.7	Mainly C_{20} monoethenoid acid
1	Stearic	Saturated	—	m.p. 69.6°
2	Phenylstearic	Saturated	—	m.p. below −15°. 96 to 98 pct pure, obtained commercially
3	Chlorocarbonated oleic	Saturated	—	Prepared by Hormel Institute

Table II. Dry Screen Analysis of Ore *A*

Mesh	Weight, Pct	Percent Assay	
		Fe	Insoluble
+48	0.68	21.63	67.09
48 to 65	4.68	16.65	73.46
65 to 100	16.71	16.81	73.82
100 to 150	26.92	20.59	68.75
150 to 200	22.74	21.64	67.07
200 to 270	17.66	21.32	67.35
270 to 400	8.45	20.93	68.64
−400	2.16	11.34	81.19
Total	100.00	19.98	69.44

Table III. Dry Screen Analysis of Ore *B*

Mesh	Weight, Pct	Percent Assay	
		Fe	Insoluble
+48	3.70	30.09	53.87
48 to 65	13.61	36.60	45.19
65 to 100	20.92	44.01	34.42
100 to 150	20.52	42.16	37.11
150 to 200	15.72	39.34	41.73
−200	25.53	26.15	60.74
Total	100.00	36.81	45.03

Table IV. Selectivity Indexes Obtained with Synthetic Mixtures of Pure C_{18} Aliphatic Acids

Acid Mixture No.	Constituents	Percent of Constituent	Iodine Value of Mixture	Selectivity Index
M-1	Stearic acid	45	101.7	4.03
	Linoleic acid	55		
M-2	Stearic acid	60	106.5	8.40
	Linolenic acid	40		
M-3	Oleic acid	92	107.2	10.05
	Linolenic acid	8		
M-4	Stearic acid	50	113.3	6.72
	Linoleic acid	25		
	Linolenic acid	25		
M-5	Stearic acid	40	112.0	8.16
	Oleic acid	20		
	Linoleic acid	20		
	Linolenic acid	20		
M-6	Oleic acid	85	104.3	9.93
	Linoleic acid	15		
M-7	Oleic acid	90	102.5	8.85
	Linoleic acid	5		
	Linolenic acid	5		

Table VI. Flotation of Undeslimed Ore *A* at pH 11 with Three Acids of High Unsaturation

Collector	Percent Assay of Cleaner Concentrate		Percent Recovery, Fe	Selectivity Index
	Fe	Insol.		
Linoleic acid	63.64	3.64	62.64	13.5
Linolenic acid	63.70	3.48	73.62	16.5
Acid *R*	61.86	6.82	51.59	8.4

10^{-4} M per liter. At pH 8.8 the quartz floated with linoleate but not with oleate or elaidate. At pH 10.5 the quartz floated with oleate, but only slightly with elaidate.

A further test consisted of agitating 10 and 20 gm of the whole ore in 50 ml of demineralized distilled water, centrifuging as before, and determining spectrograpically the ion content of the clarified supernatant liquid. A similar procedure was applied to 50 ml of the supernatant liquid from a flotation pulp of the same ore, after it had been deslimed by the procedure described on page 921. The averaged alkaline earth metal contents so determined were respectively 17, 23, and 7 mg of calcium per liter and 0.5, 0.5, and 0.1 mg of magnesium per liter.

This shows conclusively that enough ions are liberated from the ore itself to activate quartz and that the relatively large quantity of quartz floated in the rougher concentrate can be attributed to this factor. It is also significant that a single stage of cleaning, performed by diluting the rougher concentrate with water free of calcium and magnesium, can depress a major quantity of the included quartz. It is logical to presume that the dilution causes desorption of the activating ions. Experimentally the same end result can be obtained by using calcium and magnesium complexing reagents in either the rougher or cleaning stages, but to avoid introducing another variable these reagents were not used in obtaining the results presented here.

PRESENTATION OF RESULTS

To circumvent the usual difficulty in evaluating flotation separation, selectivity index[5] has been preferred over any other single-number criterion. In a three-product separation (concentrate, middling, tailing) there is a question of what to do with the middling. The writers have followed the uniform practice of including any middling product with the tailing in computing selectivity index, although they are fully aware that this penalizes the reagent because of the increased iron content of the tailing in the case of iron oxide flotation and of the siliceous froth product in the case of quartz flotation. Selectivity index has been calculated from the expression:

$$SI = \sqrt{\frac{M}{m} \cdot \frac{n}{N}}$$

in which:

M = percent Fe in the second cleaner concentrate, when iron oxides were floated, or percent Fe in the final cell residue when silica was floated.

m = percent Fe in the composite consisting of combined rougher tailings and the two middlings, when iron oxides were floated, or percent Fe in the composited siliceous tailing of Fig. 1 when silica was floated.

Table V. Performance of Some Isomers of C_{18} Aliphatic Acids as Collectors for Iron Oxide Minerals at pH 6.0

Acid	Name	Configuration	Selectivity Index		Percent Insoluble in Second Cleaner Concentrate	
			25°	70°	25°	70°
C	Linoleic	Non-conjugated, cis-cis	4.46	10.30	42.85	20.52
D	Linoelaidic	Non-conjugated, trans-trans	8.03	11.58	16.55	5.50
E	Linoleic	Conjugated, cis-cis	8.38	9.32	13.45	4.39
F	Linoleic	Conjugated, trans-trans	6.47	16.85	13.14	3.05
G	Linolenic	Non-conjugated, cis-cis-cis	5.68	8.85	37.55	18.34
H	α-eleostearic	Conjugated, cis-cis-cis	—	1.00	—	All ore floated
I	β-eleostearic	Conjugated, trans-trans-trans	—	1.00	—	All ore floated

N = percent insoluble in the iron oxide concentrates, whichever process was employed.

n = percent insoluble in the respective composite products listed under m above.

On the basis of a large number of systematic tests it was determined that, among other factors, the pH of the pulp, the degree of unsaturation of the fatty acid collector, the structure of the fatty acid collector, the pulp density during conditioning, and the temperature of conditioning and flotation were of critical importance in obtaining high selectivity indexes. The effects of the first three listed factors are described in this article. Conditioning at 60 pct solids was adopted because this gave markedly superior results compared with those obtained at lower pulp consistencies. Insufficient ore for the large number of tests required prevented flotation at higher pulp consistencies than the 19 pct solids adopted, although other tests have clearly demonstrated that superior results can be so obtained. Conditioning and flotation for all tests reported in this article were performed at room temperature (25°C ± 1°), unless otherwise specified.

In all but two of the accompanying illustrations pH is plotted as the abscissa and selectivity index as the ordinate, and each curve represents the results obtained with a particular collector, labeled in conformity with its listing in Table I. Because the grade of iron ore concentrates is important, the insoluble content of these is indicated for each point shown on the pH-selectivity index curves.

In the two illustrations excepted, the iodine value of the collector is plotted against the corresponding selectivity index as obtained at flotation pH of 6.0 or 11.5.

SELECTIVE FLOTATION OF IRON OXIDES WITH FATTY ACIDS

Flotation with Pure and Impure Oleic Acids: Oleic acid is a commonly used collector because it is cheap and readily available. The commercial acid is a very impure mixture only roughly approximating a C_{18} monoethenoid acid. Four *oleic* acids were used (*A, J, M,* and *N* of Table I), one (*A*) being 99.8 pct oleic acid, hereafter referred to as *pure* oleic acid. The addition level for all collectors was 0.5 lb per ton of original (nondeslimed) ore, and tests were made at pH values for 5.0 through 9.0.

Fig. 2 gives the results, which show that selectivity index rises to a maximum between pH 6 and some value above 7 for all four collectors. At pH 8 the selectivity index decreases to unity (i.e., all the ore floated), except for pure oleic acid, for which it decreases to unity at pH 9. It will be noted that *optimum grade* of concentrate was obtained with acids *M* and *N* at pH 6, and with acids *A* and *J* at pH 7. From other work, it seems probable that the linoleic and linolenic acids in *J* are partly or wholly responsible for its relatively poor selectivity. Results in Fig. 2 show that selective flotation of the ore investigated depends on pH of the pulp and that only through a narrow pH range are the iron oxide minerals floated selectively from quartz. Tests on other iron ores gave results that agreed remarkably with these.

Effect of Degree of Unsaturation of the Fatty Acid on Selectivity: Tests were made with 22 fractions of fish-oil fatty acids of various degrees of unsaturation, and with other acids or mixtures of acids. All tests were made at pH 6 using 0.5 lb of fatty acid per ton. Fig. 3 gives the results of plotting selectivity index against the iodine value of the collector.

All available evidence indicates that highly unsaturated acids are unsatisfactory collectors in floating iron oxides from quartz. Omitting the apparently anomalous behavior of acids *HO-18* and *HO-26*, best results were obtained with fatty acids of less than 110 I.V. Acid *HO-5*, a mixture of palmitoleic acid (C_{16}, with one double bond) and palmitic acid (C_{16}, saturated), gave moderately superior selectivity. Acids *HO-6* and *HO-19* are oustandingly good collectors, both strictly comparable with pure oleic acid in ability to give high selectivity index, high grade

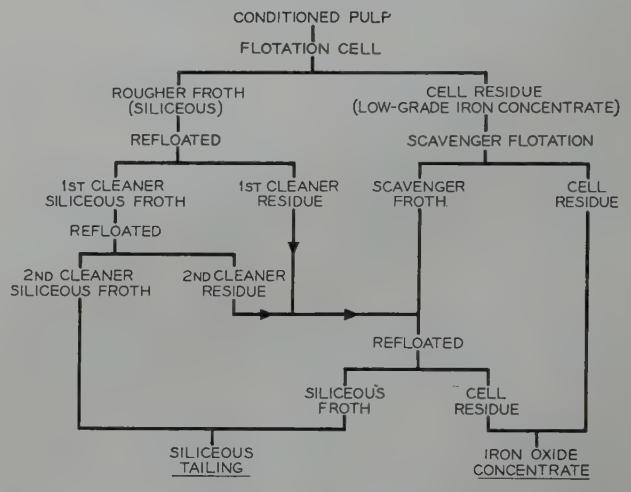

Fig. 1—Anionic flotation, silica from wash ore tailing.

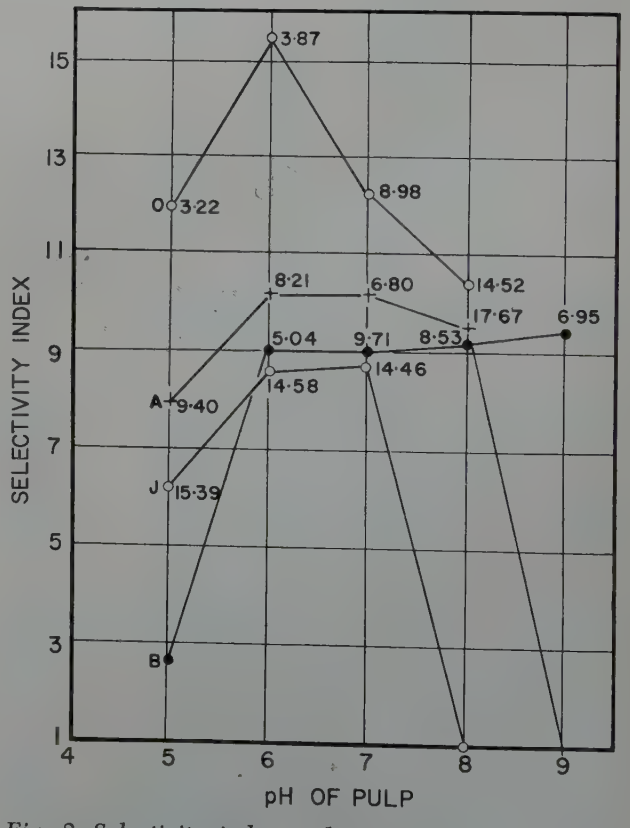

Fig. 2—Selectivity indexes obtained on wash ore tailing (ore A) with four grades of oleic acid. Numbers give percent insoluble in each second cleaner concentrate. Fatty acid added, 0.5 lb per ton original feed.

of second cleaner concentrate, low grade of tailing, and high recovery of iron. *HO-6* has a high content of palmitoleic acid, and *HO-19* consists primarily of palmitoleic and oleic acids.

Fig. 3 shows that a pure acid (*A*) or a mixture of essentially monoethenoid acids (*HO-6, HO-19*), of limited unsaturation, gives high selectivity. To determine whether mixtures of saturated and unsaturated acids having about the same iodine values would serve the same purpose, a number of synthetic mixtures of pure fatty acids were prepared. Composition of the mixtures is given in Table IV, and flotation results are plotted in Fig. 3 under the *M*-designation used in the table. The selectivity indexes agree well with the curve of Fig. 3. Some of the synthetic mixtures were semi-solid at room temperature, and for the sake of uniformity all were converted to the sodium soaps and added to the conditioner as such.

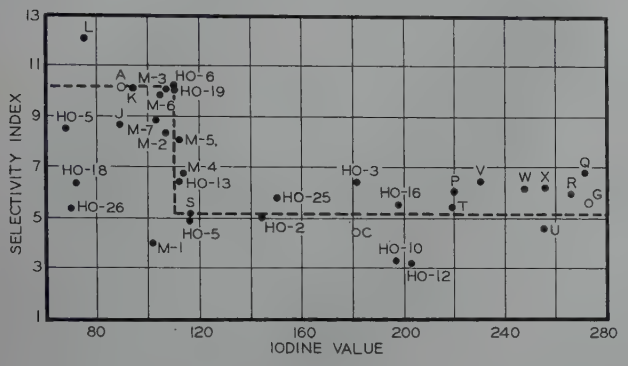

Fig. 3—Selectivity indexes on flotation of iron oxide minerals from wash ore tailing (ore A) with pure C_{18} saturated acids (open circles) and with fish-oil fatty acids and mixtures of pure C_{18} acids (see Table I).

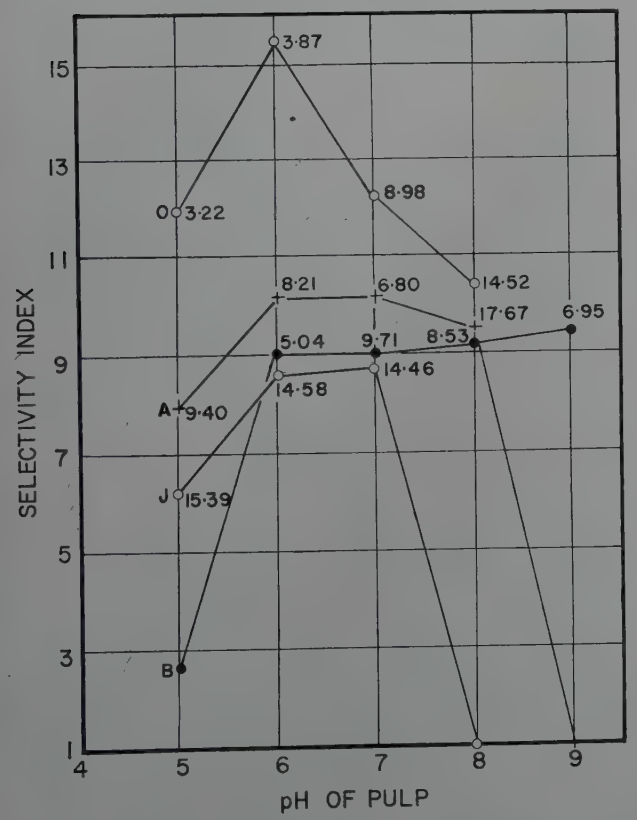

Fig. 4—The selectivity indexes obtained on wash ore tailing (ore A) with a technical grade of oleic acid (J), with an impure elaidic acid (O) prepared from J, with pure oleic acid (A), and with a pure elaidic acid (B). Fatty acid addition was 0.5 lb per ton of ore.

Effect of Fatty Acid Structure on Collection: Under the requisite conditions, palmitoleic and oleic acids are highly effective collectors in floating iron oxides from quartz. Palmitic acid, the sixteen-carbon saturated analogue of palmitoleic acid, has been shown by Keck[6] to be a moderately good collector for hematite. Stearic acid is a solid at room temperature, and the free acid is so slightly soluble in water that it is completely ineffective as a collector. Above pH 7 sodium stearate is a moderately selective collector for iron oxides but seems considerably less effective than sodium oleate, either in selectivity or in level of addition to give a desired recovery.

In view of the marked difference in performance between stearic and oleic acids and their soaps, it is valid to inquire if there is a difference in collecting ability between oleic and elaidic acids, the cis- and the trans-isomer, respectively, of $\Delta^{9,10}$-octadecenoic acid.

Initially no elaidic acid was available, so acid *J* (Table I) was isomerized with selenium.[6] Separation of reaction products from the equilibrium mixture was effected in methyl alcohol at low temperature, giving a 66 pct yield of a high melting point product, presumably containing the trans-isomer, and a 34 pct yield of low melting point material, in accord with anticipated yield. The melting point of the former, however, was only 26°C, compared with about 45°C for pure elaidic acid, and it is probable that it was an impure mixture of elaidic, linoelaidic, linolenelaidic, and oleic acids.

The sodium soap of the high melting point fraction so obtained was used as a collector for deslimed ore *A* in a series of flotation tests over the pH range 5 to 8. It will be noted from the results (Fig. 4) that selectivity index was exceptionally high over the given pH range, with a maximum at pH 6. The high grades of the second cleaner concentrates at pH 5 and 6 (3.22 and 3.87 pct insoluble, respectively) should also be noted. Results differ markedly from those obtained (curve *J*, Fig. 4) with the oleic acid from which the impure elaidic acid was prepared.

Later work with pure elaidic acid gave the results shown in curve *B*, Fig. 4. In comparing selectivity indexes and grades of concentrates obtained with the impure and the pure elaidic acids, it will be seen that results obtained with the former are much superior over the pH range 5 to 7. However, selectivity indexes given by the pure acid remain relatively constant over the pH range 6 through 9, and the concentrates range in grade only from 5.04 to 9.71 pct insoluble. At pH 8 the grade given by pure elaidic acid is markedly superior to that obtained with pure oleic acid at almost identical selectivity index. At pH 9 all the ore floated with pure oleic acid, but selection remained excellent with elaidic acid.

Reasons for the differences in performance between the impure and pure elaidic acids are obscure. From observation during testing it does not seem that these variations in performance can be attributed to differences in frothing characteristics. It is possible that they are partly due to the presence of linoelaidic acid derived from the technical grade of

oleic acid used in preparing the impure elaidic acid.

From work that will be presented in detail in another paper it has been determined that, at equivalent additions, elaidic acid is only slightly less effective than oleic acid as a collector for hematite over the pH range 4 to 8 but is markedly superior from 8 to 9.5. Elaidic and oleic acids are excellent and equally effective collectors for goethite over the pH range 3 to 10. Conversely, at any pH above 8, elaidic acid is inferior to oleic acid as a collector for calcium-activated and magnesium-activated quartz. These results offer an empirical explanation for the superior grades and selectivities obtained with pure elaidic acid between pH 8 and 9, as shown in Fig. 4.

In an attempt to extend the foregoing work, a number of flotation tests were made on ore *A* at pH 6, using various structural isomers of linoleic and linolenic acids at 25°C and 70°C (Table V). Scope of the tests was limited because only a small amount of each isomer was available.

At 25°C neither nonconjugated linoleic nor nonconjugated linolenic acids are particularly selective collectors for iron oxides, and both give undesirably fine-bubbled froths that occlude much gangue. At 70°C selectivity improves, more so for linoleic than for linolenic acid. At 25°C linoelaidic acid is markedly more selective than its cis-isomer, but at 70°C the difference is much less marked. Conjugated trans-trans linoleic acid gave intermediate selectivity at 25°C, but at 70°C selectivity was much enhanced and gave a concentrate containing only 3.05 pct insoluble. It is noteworthy that at pH 6, neither α- nor β- eleostearic acids (both positional isomers of linolenic acid) function as selective collectors.

Because the tests were limited to a single pH, the information provided is perhaps too meager to permit drawing specific conclusions, but the generalization may be made that selectivity depends on configuration of the acid used as a collector.

SELECTIVE FLOTATION OF QUARTZ WITH FATTY ACIDS

It has long been known that quartz can be floated with fatty acids provided that a multivalent metal cation is available for activation and that the pH is adjusted to an optimum value for the cation used. The availability of a large number of fatty acids led to an investigation of their applicability to flotation of calcium-activated quartz.

Preliminary tests were made on ore *A* after it had been ground through 100 mesh, deslimed at 20μ and conditioned at 60 pct solids with the reagents and addition levels given above. (See Preparation of Ore *B* for Flotation of Silica.) One pound of oleic, linoleic, and linolenic acids was used per ton of ore. Results at pH 10, 11, and 12 are given in Fig. 5.

Selectivity with linoleic and linolenic acids is low at pH 10 but is greatly enhanced at higher alkalinities. In comparison, oleic acid is a very poor collector for calcium-activated quartz over the pH range shown. At pH 11 and above, the quartz was heavily flocculated when linoleic and linolenic acids were used in collecting, but not when oleic acid was used. Addition of small quantities of a hydrocarbon oil markedly decreased this flocculation and tended to inhibit flotation.

It is relevant to present the results of another series of tests in which ore *A* was ground through 100 mesh with the usual addition of H_2SO_4. The grind was filtered and washed and, *retaining its complement of slimes,* was conditioned at 60 pct solids for silica flotation. In separate tests one pound of linoleic and linolenic acids, and fish-oil acid *R* (Table I), per ton of ore was used in collecting. The results of three such tests made at pH 11 are given in abbreviated form in Table VI. Both linolenic and linoleic acids gave excellent results, producing concentrates with almost the same iron content (63 + pct Fe) as those obtained by floating the deslimed ore. Acid *R,* a mixture of highly unsaturated fish-oil fatty acids, was less effective than the foregoing pure acids but gave a selectivity and grade of concentrate comparable to those obtained with pure oleic acid when iron oxides were floated from the deslimed ore (Fig. 2). Under no conditions could the iron oxides be floated from their ores unless the slimes had been removed.

Effect of Degree of Unsaturation upon Selectivity: Tests were made on ore *B,* ground through 150 mesh, deslimed, and conditioned as described previously. Pure oleic, linoleic, and linolenic acids and 19 acids derived from fish-oils were used as collectors. In Fig. 6 a dotted line is drawn through the points representing results with the pure acids.

It will be noted that in general the results are the converse of those obtained when iron oxides are floated from the silica, i.e., the greater the degree of unsaturation of the collector the higher the selectivity index.

Acids *J, M,* and *N* (impure oleic acids) gave higher selectivity indexes than pure oleic acid (*A*) presumably because of the content of polyethenoid acids.

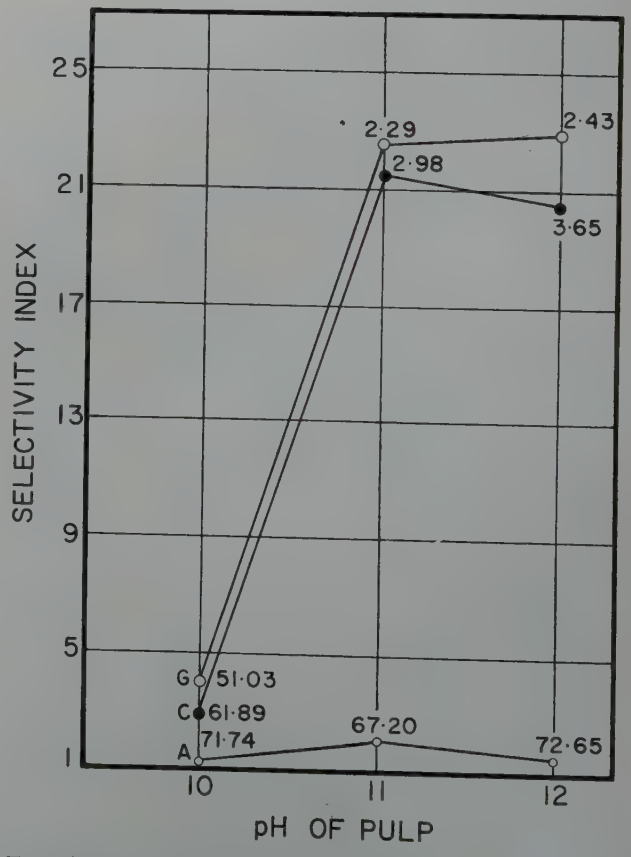

Fig. 5—The selectivity indexes and grades of concentrates (percent insoluble) that were obtained by floating the silica from wash ore tailing (ore A) with oleic acid (A), linoleic acid (C), and linolenic acid (G).

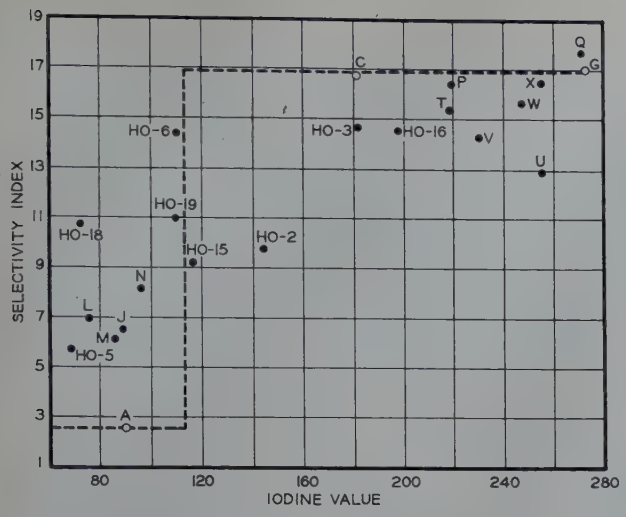

Fig. 6—Selectivity indexes on flotation of silica from wash ore (B) tailing with C_{18} unsaturated acids (open circles) and with marine-oil fatty acids (Table I).

The results given by acids *L* and *HO-18* seem to be anomalous. The former is a fraction prepared from acid *J* and from its iodine value should contain the more saturated constituents. Acid *HO-18* gave a low selectivity when iron oxides were floated (Fig. 3) and a high index when silica was floated. The reasons for these apparent anomalies are unknown. It is worth noting that acids containing relatively large quantities of palmitoleic acid (*HO-6* and *HO-19*) gave high selectivity indexes.

A less extensive investigation of silica flotation from ore *A* gave essentially the same distribution of selectivity index *vs* iodine value as that shown in Fig. 6.

On a laboratory scale there is one noteworthy difference between floating the iron oxides and floating the silica. For iron oxide, flotation time is rarely less than 4 to 5 min. With silica, flotation is extremely rapid, and most of the silica, the major component of the ores tested, is removed from the cell in less than a minute. This difference in flotation rates may be related to the much lower froth stability at pH 5 than at pH 11, and enhancement of flotation at the former pH may be affected by addition of froth-modifying reagents.

SUMMARY

Standardized flotation tests were made on iron wash ore tailings containing hematite, goethite, quartz, and chert, using fatty acid collectors of various degrees of unsaturation and of different structure. Some of the collectors were nearly pure, others were mixtures of fatty acids which had been carefully fractionated from several types of fish oils. Separation was effected either by floating the iron oxide minerals from the siliceous gangue or by activating the gangue and floating it from the iron oxides. The primary variable was pH.

Results of the tests led to the following conclusions:

1) With all the collectors tested, and under the conditions specified, there is a sharply defined correlation of pH with selectivity index. This is true for the flotation of either the iron oxide minerals or of the calcium-activated siliceous gangue.

2) When the iron oxide minerals are floated, the selectivity index obtained depends on the structure of the fatty acid collector. Acids with the trans-configuration give a higher selectivity than those with the cis-configuration.

3) Fatty acids of less than 110 I.V. give satisfactory separation of iron oxides from siliceous gangue within a narrow pH range, usually from 6 to 7.

4) Fatty acids of greater than 110 I.V. are unsatisfactory for floating iron oxides from siliceous gangue, irrespective of the pH.

5) Oxidized iron ores release appreciable quantities of calcium and magnesium to the aqueous phase. The evidence shows that this is responsible for the activation of quartz and chert when iron oxides are floated from those minerals and that this leads to a marked decrease in selectivity. This is particularly true of collecting with fatty acids of high degree of unsaturation.

6) Fatty acids of greater than 110 I.V. are powerful and selective collectors for calcium-activated quartz and chert when these minerals are floated from iron oxides, and the rate of flotation is very rapid. For maximum selectivity in this process the pH must be higher than 11.

7) Some evidence is presented that quartz and chert may be floated from slime-containing iron ore. The slimes completely inhibit the inverse process of floating the iron oxides from the same ore.

8) The more saturated fractions of fish oil fatty acids show technical promise in floating iron oxide minerals from siliceous gangue. Conversely, the highly unsaturated fractions are effective collectors for calcium-activated quartz and chert.

This article is condensed from a thesis submitted by H. S. Choi in partial fulfillment of the requirements for the degree of Doctor of Philosophy at the University of Minnesota. The project was initiated by M. Stansby, chief, Pacific Coast Technological Research, Bureau of Commercial Fisheries, Fish and Wildlife Service, U. S. Department of the Interior. To him and to his staff grateful acknowledgment is made for technical assistance and continuing interest. The scope of the work was greatly extended by the availability of various high-purity aliphatic acids and fish-oil acids furnished by Hormel Institute, University of Minnesota, to whose director, W. O. Lundberg, and staff the writers owe thanks for advice and for many courtesies. Particular thanks are due H. H. Wade, director, and V. E. Bye, chemical engineer, of the Mines Experiment Station, University of Minnesota, for providing the necessarily large number of chemical analyses. K. V. Batro also assisted in some of the experimental work.

REFERENCES

[1] R. T. Hukki and O. Vartianen: An Investigation of the Collecting Effects of Fatty Acids in Tall Oil on Oxide Minerals, Particularly on Ilmenite. *AIME Trans.*, 1953, vol. 196, pp. 818-820.

[2] S. R. B. Cooke and W. Nummela: Fatty and Resin Acids as Collectors for Iron Oxides. To be published as a U. S. Bureau of Mines *Report of Investigations.*

[3] C. Domart, D. T. Miyauchi, and W. N. Sumerwell: The Fractionation of Marine Oil Fatty Acids with Urea. *Journal of the American Oil Chemists' Society*, 1955, vol. 32, pp. 481-483.

[4] H. Glover: Flotation of Some Oxide and Silicate Minerals. Flotation Fundamentals, Part I, Section E, *Utah Engineering Experiment Station, TP 1*, 1928, pp. 77-101.

[5] A. M. Gaudin: Selectivity Index: a Yardstick of the Segregation Accomplished by Concentrating Operations. *AIME Trans.*, 1930, vol. 87, pp. 483-487.

[6] S. H. Bertram. Elaidization of Oleic Acid and the Cis-trans Isomerism. *Chem. Weekblad.*, 1936, vol. 33, pp. 3-5.

Discussion of this article sent (2 copies) to AIME before Oct. 31, 1959, will be published in MINING ENGINEERING.

FACE VENTILATION FOR CONTINUOUS MINERS

by JOHN D. KALASKY

Continuous mining has revolutionized the coal industry but intensified the problems of earlier mechanization. From the installation of the first miner, it was recognized that face ventilation would be one of these problems.

To establish an efficient work cycle for the equipment being used, conventional mechanized mining provides four or more development faces. Continuous mining, relying on a single machine, requires only one face, although more than one can be driven alternately by the same machine. In gaseous areas mined by the older methods, the intermittent rate of exposure allows time for the face to bleed off or be cleared, and the width obtained with conventional units makes it possible to hang a brattice line almost to the face. Continuous mining increases the ventilation hazards; there is no margin of time, and very limited space.

For all practical purposes, continuous miners available today can be grouped into two major types, *rippers* and *borers*. The two can be further classified, respectively, as flexible and rigid.

Both types have been in operation in U. S. coal mines for the past five to ten years in a number of seams, under various conditions ranging from slightly gaseous to very gaseous. Common methods of face ventilation utilizing jute or plastic brattice material for line curtains, stoppings, and checks have so far met with success. Air volumes to operating sections are greater than for conventional mining, and specific instructions have been given to section crews stressing the precautions needed in dealing with a steady rate of gas emission and the importance of maintaining reasonably air-tight brattice to direct a good steady flow toward the face at all times.

J. D. KALASKY is Ventilation Engineer, Eastern Gas & Fuel Associates, Pittsburgh, Pa. TP 4809F. Manuscript, Oct. 2, 1958. Spring Meeting, Central Appalachian and Coal Division, Lexington, Ky., June 1958. AIME Trans., Vol. 214, 1959.

Operators of continuous miners, as well as the foreman on each section, are equipped with an approved safety lamp for gas testing. When the miner is in steady operation, tests for gas at the face are made at 15 to 30-min intervals, depending on the

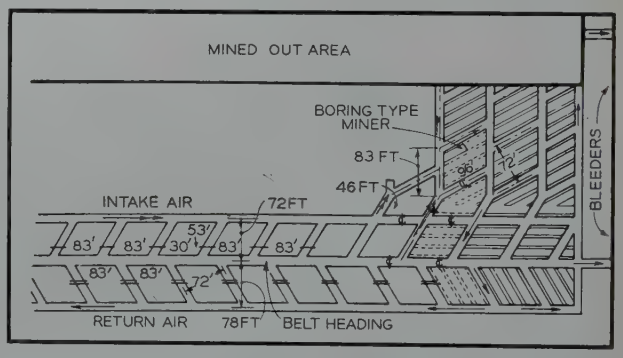

Fig. 1—Mining plan, Pittsburgh seam, boring-type miner.

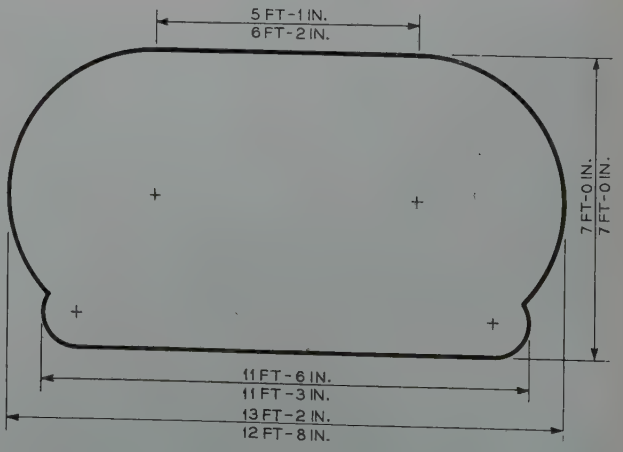

Fig. 2—Pittsburgh seam, face pattern and cross-sectional dimensions of entries driven by two models of borer.

rules set up by the particular mine in which the machine is being used. In some cases the operator can test for gas directly behind the head of the machine while it is working. When the miner loads directly into shuttle cars, tests are made between car changes.

Company standards require that ventilation on an active section be improved if air immediately returning from the split contains more than 0.50 pct methane. To comply with this standard, approved methane detectors are used by safety officials and others to make daily checks in the working areas, and weekly atmosphere analyses are made on return air samples taken from the sections and tested in the laboratory.

To maintain the methane content below the 0.50 pct standard, air volume requirements per split for a section employing a boring type of miner in the Pittsburgh seam average 20,000 cfm; for a ripper type in the Pocahontas No. 3 seam, 18,000 cfm; and for a butt heading set-up utilizing both ripper and borer simultaneously in development and retreat in the Lower Kittanning seam, 18,000 cfm. These are requirements in three particular mines and are not necessarily representative for other mines in the same coal seams.

Boring-Type Miner, Pittsburgh Seam: Fig. 1 shows the plan for the Pittsburgh seam where a boring-type miner is used. Methane liberation for this mine in a 24-hr period is approximately 3 million cu ft. Fig. 2 shows the face pattern and cross-sectional dimensions of entries driven by the two models of the boring miner in operation.

Butts are driven (Fig. 1) with three entries on 72-ft and 78-ft centers. Breakthroughs are driven on an angle of 60° and staggered by 30 ft. Breakthrough centers measured along the center line of the entry are 83 ft.

The miner drives the middle entry (No. 2) about 30 ft, then drops back and drives a break through to the right to entry No. 3 and drives entry No. 3 ahead 85 ft. The unit is then moved back through the breakthrough to its initial starting point in the middle entry. The miner drives about 55 ft in the No. 2 entry, drops back and drives the breakthrough to the left, and continues driving No 1 entry approximately 85 ft. As the miner advances, the brattice man brings up the canvas directly behind the machine.

Air is brought up the No. 1 entry (Fig. 1) when rooms are to be driven off to the left and up the No. 3 entry when they are to be driven to the right. This directs it first to the solid workings and then to the pillars and worked out areas. The bleeder system and the main return from the butt maintains positive air pressure on the gob.

In development, an adequate and continuous flow of air is provided at the face by a line brattice hung on the rib of the entry and maintained at all times to within 16 ft of the face or up to the position of the miner operator.

The brattice material, 7-ft wide canvas, is held snugly against the top and sides of the entry by nails stuck through the canvas edges and holes located in case-hardened spads driven into the coal top and rib. Easily handled lengths of canvas, folded and placed on the miner, are extended as it advances. An overlap of about 12 in. is allowed at the joints. The spads for hanging the canvas are driven beyond the end of the brattice line, sometimes to within 5 or 6 ft of the face. All there is to extending the canvas is to stretch it and pin it to the spads, which are spaced on 2-ft centers in the direction of advance.

Canvas hung in this manner gives a cross section of about 10 sq ft, with smooth sides offering little resistance to air flow. This type of brattice has

Fig. 3—As miner advances, brattice man brings up canvas.

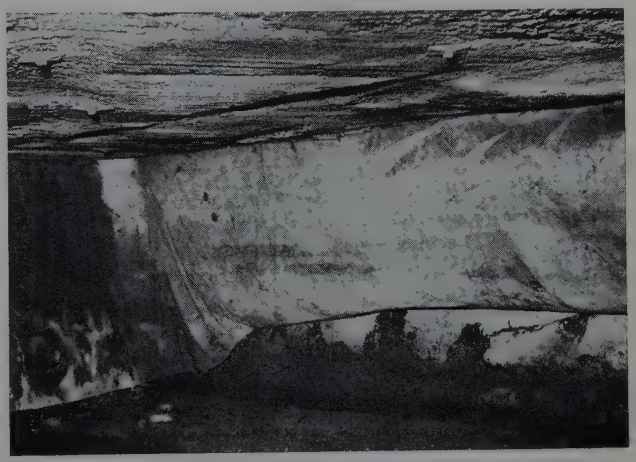

Fig. 4—The view above shows how the canvas is held up off bottom to allow the loading machine to pick up coal that is dropped to the mine floor by continuous miner.

Fig. 5—Photograph shows the installed brattice line in the entry after the continuous miner has been moved out.

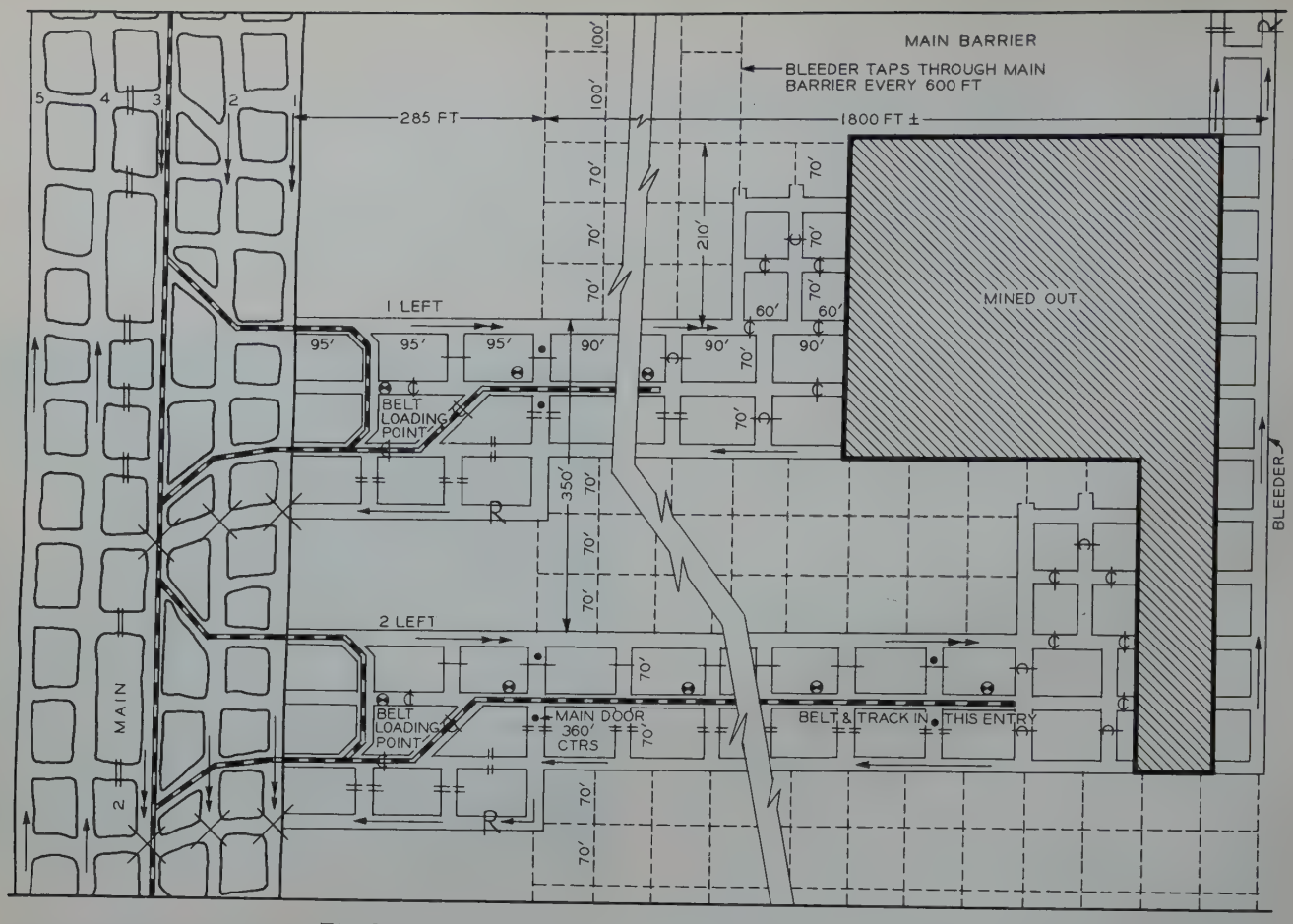

Fig. 6—Projection plan for mining with the continuous miner.

proved very successful in conducting intake to the face, as air pressure inflates the canvas to its maximum surface. It would not be satisfactory in conducting return from the face, since pressure would slacken the canvas unless other more expensive methods of holding it open were used.

When the line brattice, installed as described, is used for intake, air arriving at the end of the canvas has ample velocity. It is also directed by the motor blower, the revolving arms of the machine, and the body of the machine itself. With this set-up it has been possible to conduct an effective volume of 6000 cfm to the end of a 70-ft brattice line, starting with approximately 12,000 cfm outby the point where the air is checked and directed into the brattice areas. Under present conditions in the mine, it is believed that 4000 cfm at the end of the brattice would amply handle the job.

One of the objectionable features of this system is the dust problem that arises when water sprays are not functioning properly, but this can be minimized by dual controls on the machine to allow the operator to handle it from the intake side at all times. One machine has been equipped with these controls.

Another way to prevent dust passing over equipment operators is to conduct the air to the face on the wide side of the line brattice and return it on the narrow side. It is assumed in this case that the miner operator is on the intake side of the split. The disadvantage here is that the lowered velocity in the air stream reaching the end of the line brattice would appreciably reduce the effectiveness of face ventilation. To impart the same sweeping velocity to the air as that obtained in the intake brattice system would require considerably more air on the section and consequently in the main ventilation system.

Rooms on 83-ft centers, with breakthroughs on 83-ft centers, are driven to the gob made by a previously mined out butt (Fig. 1). Room pillars are then retreated in lifts, leaving a 4 to 5-ft fender between each lift. Brattice is maintained in the same way it is used in the butt headings, except that after the pillars are formed canvas checks in the room breakthroughs are enough to insure adequate ventilation in the pillar lifts.

Ripper-Type Miner, Pocahontas No. 3 Seam: The mining plan used with a modified ripper in the Pocahontas No. 3 seam is shown in Fig. 6. The mine liberates 1.5 cu ft of methane daily.

Three butt headings, approximately 17 ft wide on 70-ft centers, are driven with right angle breakthroughs on 90-ft centers. Development is cyclical, as the miner can open a width of only 8 ft 6 in. and requires two passes to develop the entry desired.

The miner advances the face 6 ft in one penetration before moving over to widen the entry and bring up the face. Advance has been set at 6 ft primarily because it has proved difficult in this mine to remove gas from the pocket formed.

With each 4-ft advance of face, production is stopped long enough for temporary installation of a 4 in. x 8 in. x 14-ft header on roof jacks and wood posts so the miner operator will be protected at all times. The pre-drilled headers are bolted to the roof

when the miner moves out. As each header is set, the canvas brattice line is extended.

The immediate top is a treacherous draw slate with kettle bottoms, horsebacks, and slips which limit the amount of top that can be temporarily supported. Consequently the miner must move out after advancing the entry about 32 ft to allow the bolting machine to bolt the headers.

When the butt entry is developed to the back end, rooms on 60-ft centers with breakthroughs on 70-ft centers are driven to the gob. Room pillars are split once in the middle and lifts taken open-ended from the split in the direction of the gob.

Canvas face ventilation facilities are used throughout, even in the pillar splits, to provide adequate air flow to the miner face (Fig. 7). When nailed to the headers and posts, the 6-ft wide canvas makes an air brattice of about 3x4½ ft, or 12 sq ft, between coal rib and canvas. Effective volumes of 3000 to 4000 cfm are maintained at the end of the brattice lines.

Ripper and Boring-Type Miners, Lower Kittanning Seam: The mining plan used in low coal in the Lower Kittanning seam is shown in Fig. 10. One million cubic feet of methane is liberated from this seam mine in 24 hr. Two miners, one a ripper and the other a low coal boring type, develop eight entries on 80-ft centers after three entries are driven through the main entry barrier. Breakthroughs also are on 80-ft centers, forming pillars about 63 ft square. When the butt heading is advanced to the back end, the pillars formed are retreated on a flat pillar line by the two miners. The boring machine mines the center entry and the area to the left while the ripper mines the area to the right.

The boring-type miner, capable of driving an entry 9 ft wide in one pass, requires two passes to develop entries and breakthroughs 18 ft wide. Gas and roof conditions permit a 12-ft advance, sump cut, before the face reaches its required width. As each 4 ft of face is evened up, 5x8-in. 14-ft headers are set on posts. At the same time, a plastic brattice line 48 in. wide is nailed to the posts and ends of headers which are set to one side of the entry. An area of about 3 ft by 3 ft 4 in. is available behind the brattice line to conduct air to the miner face.

The ripper-type miner drives entries 16 ft wide. Since the shallow sump cut makes it possible to advance almost a full face width at all times, the brattice line is advanced as headers are set. The area provided by the brattice in this case is about 2 ft by 3 ft 4 in., or 6.5 sq ft.

Air volumes at the miner faces are 8000 cfm for the borer and 7000 cfm for the ripper. Brattice lines on this section are used to exhaust and intake with equal effectiveness at each of the miner faces, since the plastic brattice, nailed to posts and headers, is firmly supported and the full face width is developed on the ripper section where the exhaust brattice is used.

Plastic brattice stoppings and checks, as shown on the plan, together with brattice lines as near the face as miner width allows, provide facilities for an air lock system that confines air flow along the working places, whether in development or along pillar lines. The successful ventilation of continuous miner faces under this program can be attributed to good face control and to the entire air distribution and control system. This system minimizes the possibility of interruption and insures a constant flow of air, however small, across the pillar line to the bleeder and away from the men and equipment. The alertness and care of the mining crews have been essential in carrying out this program.

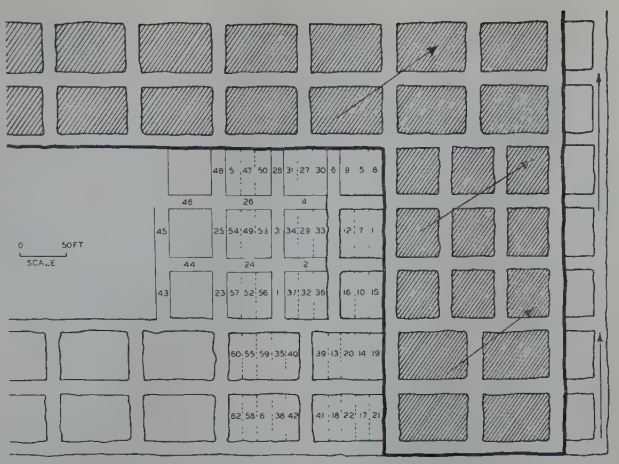

Fig. 7—Schedule of pillar extraction with miner. Canvas face ventilation facilities are used here also.

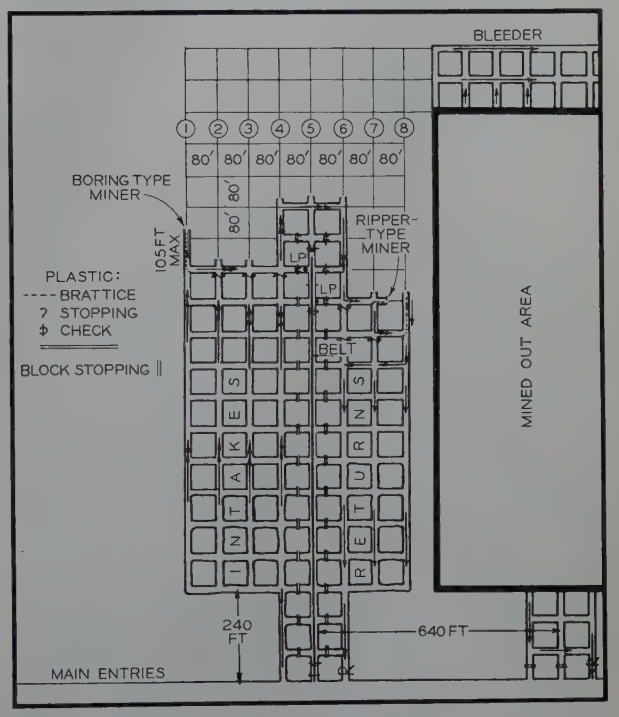

Fig. 8—Plan for low coal in Lower Kittanning seam.

Other methods of face ventilation for continuous miners have been suggested on the basis of data collected for many more installations than the few described in this article. Those discussed here are examples of systems now in use and are not intended to be the last word in this important phase of mining.

It is anticipated that face ventilation for continuous miners will present greater problems when extremely gaseous, virgin coal areas are developed. Only through research and development and open-minded consideration of results can a practical solution be attained.

Discussion of this article sent (2 copies) to AIME before Oct. 31, 1959, will be published in MINING ENGINEERING.

SCANDINAVIAN ELECTROMAGNETIC PROSPECTING

by FRANK C. FRISCHKNECHT

Most early development and application of electromagnetic prospecting methods took place in Scandinavia, where geological conditions favor their use. In other parts of the world these methods have aroused cycles of interest, but in Scandinavia they have been used continuously and successfully since the 1920's.

Electromagnetic methods may be classified into two general groups. One group includes methods in which the source of the electromagnetic field remains stationary while the receivers are moved about to explore the area. The other includes procedures in which the energizing and receiving systems are moved together. Other classifications could be based on the size of the energizing source, the particular components of the electromagnetic field which are measured, or the mode of transporting the equipment. The difference between fixed-source and moving-source methods, however, is of such great fundamental importance that it will be emphasized in this discussion.

FIXED-SOURCE METHODS

Essentially, a fixed-source method consists of the measurement of electromagnetic fields about the source. The mutual coupling between the source and the earth is constant, but the mutual coupling between the receiver and the earth (unless the earth is homogeneous) and also between the source and the receiver changes at each station. The results are usually normalized by relating the field data to the calculated free space or primary field.

Turam and Radio Reference Signal Methods: The turam or *two-frame** (see Fig. 1A) is probably the most common fixed-source method. The energizing source is an insulated cable grounded at both ends or formed into a large rectangular loop. Measurements are taken along a traverse at 5 to 50-meter intervals using two small receiving coils, the lagging coil being placed at the position previously occupied by the leading coil. The complex ratio (i.e., inphase and out-of-phase ratios) of the voltages induced in the two coils is measured. Operating frequency range is about 100 to 800 cps.

* Turam means two-coil.

In a typical turam survey a straight, grounded cable several kilometers long is laid out parallel to the probable strike of the ore deposits or conducting strata being sought. An area extending 1 or 2 km on each side of the cable, and within 1 or 2 km of the ends of the cable, is surveyed. Measurements are made at stations 5 to 25 m apart along traverses perpendicular to the cable. Measurements may be made along lines parallel to the cable to serve as base lines for the traverses or for other special purposes. Commonly the receiving coils are oriented with their planes horizontal so that only the vertical component of the field is measured. If additional information is required, one of the horizontal components may also be measured by orienting the coils with their planes vertical.

In a modified turam technique developed recently for both ground and airborne measurements (Fig. 1B) the amplitude of the complex voltage induced in a single receiving coil is measured and its phase compared with that of a reference signal transmitted from the energizing system by a radio frequency carrier. Thus the un-normalized field is obtained directly, whereas with the turam method it is obtained by calculation from the ratios.

The turam method and its modifications have a greater working depth than the other electromagnetic procedures used in ore prospecting. Under favorable conditions conductors have been located at depths of 200 to 300 m. A modified turam method with one of the electrodes grounded in the upper end of a plunging orebody was used to follow the extension of this body to a depth of 200 m beneath a layer of conducting schists.

Straight grounded cables are usually preferred to insulated loops because they are easier to lay out and because they often make the method more sensitive. The greater sensitivity of a grounded cable is a result of ground return currents which may flow in the orebodies in addition to the eddy currents caused by induction from the current in the cable. Anomalies in the vertical field due to eddy currents are characterized by a correspondence between high values for the inphase component and positive out-of-phase components and/or low values for the inphase component and negative out-of-phase components. Also the inphase component may approach zero, but it does not become negative. In very long continuous conductors that are parallel to a grounded cable the effect of ground return currents may far exceed the effect of eddy currents. These ground return currents cause a lack of correspondence between the inphase and out-of-phase components and may cause negative inphase or anti-phase components. It becomes difficult to carry out the measurements and often difficult to interpret the results. Such results immediately suggest the presence of graphitic strata, however, since ore deposits are rarely extensive enough to accumulate sufficient ground return current to cause these results. A cable laid out perpendicular to the strike or an insulated loop is sometimes used in areas where graphitic schists and slates are present. Anomalies are then completely or almost entirely due to eddy currents and are easier to interpret.

The measured voltage ratios are normalized by either subtracting or dividing by normal field ratios calculated from free space considerations. The normalized ratios are then plotted as individual profiles. When significant anomalies occur in the ratio measurements, the actual normalized fields are calculated by beginning with a measured or an assumed value for the field at a point near the cable and successively multiplying this value by the normalized ratios. There is a similarity between this process and a numerical integration of the ratio curve. Conversely, in many respects the ratio curve is similar to the first derivative of the field curve.

F. C. FRISCHKNECHT is a Geophysicist with the U. S. Geological Survey, Denver. TP 4808L. Manuscript, Feb. 27, 1959. AIME Trans., Vol. 214, 1959.

For example, a simple maximum in the field curve becomes a combination of a maximum and a minimum in the ratio curve. Because it has fewer maxima and minima the field curve is usually easier to interpret than the ratio curve.

The attitude and depth of a conductor are usually determined from the normalized field anomalies. Some simple rules based upon single current concentrations and results of scale-model studies are combined with a wealth of previous experience in making interpretations. Under conditions of favorable terrain and regular-shaped orebodies, the error in locating the horizontal position of the top of an orebody may be only a few percent of its depth of burial and the error in the depth estimate may be only 10 pct. Usually the direction of dip can be determined.

In most cases the horizontal position of the conductor is determined from the location of the inphase anomaly. Comparison of the inphase and out-of-phase anomalies often gives additional valuable information, such as the relative conductivity of the body. Sometimes a difference in position of the inphase current concentration and the out-of-phase current concentration may be used to indicate the direction of dip of the body. In areas of great topographic relief corrections must be applied to inphase anomalies; out-of-phase anomalies seldom require corrections.

Compensator Technique: The compensator method (Fig. 1C) employs large energizing layouts similar to those used with the turam method. The voltage induced in a single receiving coil is measured relative to a reference signal carried by a cable from the energizing source. Usually both the vertical and a horizontal component of the field are measured at each station at two or more frequencies in the range from 10 to 300 cps. Interpretative procedures make it possible to estimate depth to conducting horizons.

The compensator method is used chiefly to map horizons in sedimentary rocks, although it is sometimes employed in searching for flat-lying metallic ore deposits. It is used in Scandinavia in searching for coal and similar economic resources of sedimentary origin. The method is well described in the literature and will not be discussed further here.

Cross-Ring Method: The cross-ring method (Fig. 1D) utilizes a small portable energizing loop oriented with its plane roughly parallel to the ground. Two identical receiving coils are fastened together in a perpendicular arrangement, one oriented so that it is in the plane of the energizing coil. The complex ratio of the voltages induced in the two receiving coils is measured and the data are plotted directly in profile form without preliminary calculations. Short profiles (up to 100 m long) can be measured by moving the receiving coils and holding the energizing coil in fixed position. Usual frequency is 3500 cps.

Depth range of the cross-ring equipment now in use is limited to some tens of meters. In making detailed surveys over shallow conductors the method is extremely useful; the transmitter may be positioned easily to minimize the effects of certain conductors and to accentuate the effects of others. But an important drawback is the difficulty of orienting the coils properly in hilly or heavily wooded areas.

Borehole Methods: Borehole electromagnetic methods have not been used widely in Scandinavia, but limited applications have been successful and additional work is planned by various organizations.

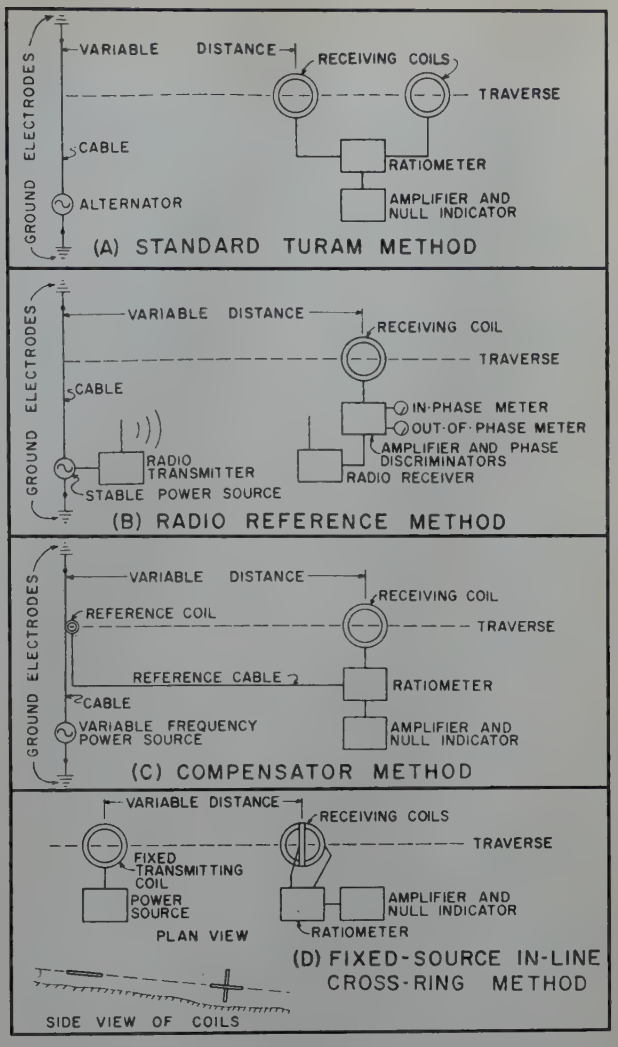

Fig. 1—Scandinavian fixed-source methods.

A combination surface-inhole method uses a single coil in the borehole as a receiver and a large low-frequency energizing loop or grounded cable placed on the surface of the ground. The complex ratio of the voltage induced in the receiving coil to the current in the energizing source is measured.

MOVING-SOURCE METHODS

In a moving-source method, changes in the mutual coupling between source and receiver are measured. The coupling between both the source and receiver and the earth (unless the earth is homogeneous) changes at each station, but the free space coupling between source and receiver remains constant. Usually results are normalized in the instrument by relating the readings to the free space coupling.

Slingram Method: The most common moving source method is the slingram or *loop frame.** (Fig. 2A), which utilizes a small portable energizing coil and one receiving coil. A reference voltage is brought from the energizing coil to the receiving coil by a cable. The ratio of the mutual impedance between the two coils in the presence of the earth to their mutual impedance in free space is measured by finding the complex ratio between the voltage induced in the receiving coil and the reference voltage. The coil spacing, held constant for each series of measurements, may range from 20 to

* Slingram means a sending and receiving coil.

100 m. Usually the coils are oriented so that they are coplanar and horizontal or (on steep slopes) parallel to the ground; however, in techniques used less frequently, the coils are held in perpendicular positions or in vertical coaxial or coplanar positions. Operating frequency ranges from 500 to 3600 cps. The complex mutual impedance ratios are presented in the form of individual profiles or contour maps without preliminary calculations.

Modifications of the slingram method incorporating automatic recording systems are the ones most commonly used for mobile operations. In a unit designed for surface operations during winter, one of the coils is placed on a track-laying vehicle and the other on a sled that is connected rigidly to the vehicle by a long boom. A simple airborne system uses a large horizontal transmitting loop attached to the aircraft and a vertical receiving loop in a *bird* which is towed some 30° to 40° below the plane of the energizing loop. Such a system is successful only in relatively quiet air; changes in orientation and position of the bird relative to the aircraft introduce large errors in the magnitude of the mutual coupling.

Various systems have been devised to minimize the errors introduced by motion of the bird relative to the aircraft. One such system uses two similar and coincident energizing coils, one of which is excited by a suitable operating frequency and the other by a much lower frequency. Two selective receiving coils and amplifiers are used, and the ratio of their outputs is recorded. In the absence of conducting material, the motions of the bird relative to the airplane affect the mutual couplings at the two frequencies in exactly the same way, and the ratio of the two couplings remains constant. However, the presence of a conductor in the vicinity of the system has a much larger effect on the coupling at the principal frequency than at the lower frequency. Thus the ratio of the couplings changes when conductors are nearby. Changes in the phase angle of the coupling at the principal frequency are measured by comparing the principal signal with a reference signal transmitted by a radio frequency carrier.

The maximum working depth for the slingram method using two horizontal coils is equal roughly to the coil spacing. The greatest depth at which a poorly conducting vertical orebody will cause a significant anomaly may be less than one half the coil spacing, but a large, horizontal, highly conductive body at a depth of twice the coil spacing may give a significant anomaly. The working depth for using a perpendicular coil arrangement is about the same or a little greater than with two horizontal coils, but with vertical coils it may be only half as great.

The greatest coil spacing that can be used with existing equipment is about 120 m for ground measurements and somewhat more for airborne surveys. *Geological noise* (minor anomalies which rapidly attenuate with distance) is less troublesome in airborne than in surface work and thus it is feasible to design airborne equipment with greater sensitivity than surface equipment. However, when the height of the aircraft above the ground is taken into consideration airborne slingram methods are restricted, in effect, to a working depth below surface of 100 m or less, which is comparable to or less than the depth obtained with surface equipment.

Slingram data are usually presented in the form of mutual impedance ratio contours, often with little attempt to locate conductor axes or to define precisely the limits of individual bodies. If the field data suggest a simple arrangement of conductors at moderate depths, model results can sometimes be used in predicting their number, position, and shape.

Comparison between inphase and out-of-phase ratios is of value in distinguishing good conductors from poor conductors. When flat-lying bodies are encountered and horizontal coil orientations are used, the signs of the anomalies directly over the body may be either negative or positive depending on the conductivity and depth of burial. Over a good conductor at a shallow depth the sign of both the inphase and out-of-phase anomalies is negative. For good conductors at depths greater than about 0.4 of the coil spacing the signs of both anomalies are positive. For poor conductors the signs become positive at shallow depths, the sign of the real component being the first to become positive. Reliable depth estimates often can be made over a large flat-lying conductor by determining the coil spacing at which the anomaly over the middle of the body disappears. On the other hand, this change in sign with depth may only complicate the interpretation of results when bodies occur at different depths. This is especially true when magnetic bodies are present because they give rise to positive anomalies. Vertical coil arrangements which always give positive anomalies over conducting bodies are sometimes used to resolve a number of these ambiguities.

Cross-Ring Technique: Cross-ring equipment is sometimes used in a moving-source technique simply by maintaining a fixed distance between energizing and receiving loops. The coil spacing used may range from 20 to 80 m.

Rotating Field Method: An airborne system having some similarity to the cross-ring method uses two perpendicular energizing coils whose planes are parallel to the axis of the aircraft. Two receiving coils are oriented in similar directions to the transmitting coils and are towed in a bird, which is positioned as closely as possible along the axis of the aircraft. A relatively large source-to-receiver distance of 200 m or more is sometimes obtained by towing the bird in a second aircraft. The energizing coils are excited by two voltages of the same frequency but 90° out-of-phase with respect to each other, thereby creating a rotating or circularly polarized free space or primary field. The complex ratio of the voltages induced in the receiving coils is measured. In the absence of conducting material this ratio is independent of the distance between aircraft and bird, axial rotation of the bird, and to a considerable extent other misorientations of the bird.

Borehole System: A moving-source method is used in conductivity logging of boreholes. Frequencies in the order of 20,000 cps are used in a sonde having a coaxial slingram arrangement. The coil spacing is some tens of centimeters; hence the radius of investigation is quite small.

Comparison of Methods: Before discussing certain aspects of various specific methods it is desirable to point out some of the relative merits of fixed-source and moving-source methods. With a fixed-source method, two identical disturbing

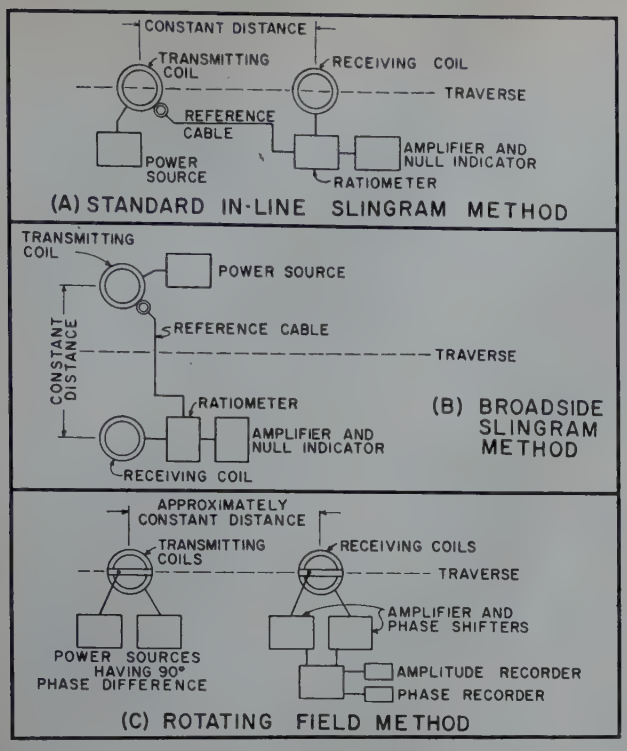

Fig. 2—Scandinavian moving-source methods.

bodies do not, in general, give rise to equal anomalies because the free space coupling between source and receiver (and hence the depth of penetration, the normal fields, and other factors) is unequal at successive stations. The shapes of the anomalies obtained with fixed-source methods, however, are relatively simple; the anomalies tend to be similar in shape to magnetic anomalies.

When a moving-source technique is used, the free space coupling between source and receiver is constant; therefore, two identical disturbing bodies give rise to equal anomalies. In general, however, anomalies obtained with a moving-source method are somewhat complicated because the coupling between the source and the conductors varies. An anomaly obtained with a moving-source method usually has more maxima and minima than one obtained with a fixed-source method. The additional maxima and minima in moving-source anomalies are sometimes referred to as edge effects because they occur near the edges of conductors.

Usually several conducting bodies in proximity are most easily located and defined by fixed-source methods because of their relative freedom from edge effects. When moving-source techniques are employed the occurrence of more than one shallow conducting body within a distance equal to or less than the source-to-receiver distance results in data that are very difficult to interpret correctly.

When edge effects are not too troublesome, moving-source methods are often superior to fixed-source methods, since the importance of one anomaly compared to another is more easily evaluated. Edge effects are not too troublesome: 1) if the horizontal extent of the conducting units is somewhat larger than the source to receiver distance, 2) if depth of burial and separation between units is great, 3) or if the boundary between units of different conductivities is not abrupt.

With a moving-source method, if vegetation and terrain do not interfere with lines of sight or connecting cables, the source and receiver may be placed *broad-side* (Fig. 2B) rather than *in-line* (Fig. 2A) to the traverse. Edge effects are thereby reduced and, if the traverse is perpendicular to the strike, individual conductors among a group of several parallel linear conductors may be resolved more easily.

In areas that are very complex geologically, especially when graphitic schists and slates are involved, the horizontal range of fixed-source equipment may be limited greatly by high attenuation of the normal field and the results may be complicated by the mutual coupling between adjacent conductors. Measurements with a fixed-source method become very laborious, and in interpreting the results it may be impossible to resolve all the separate conductors as distinct units. In such areas a contour map prepared from moving-source data may give the interpreter the most useful information. This is especially true when the purpose of the survey is to map geological trends rather than to locate individual ore deposits.

Among the fixed-source methods the radio-reference-signal system requires the fewest men to make the measurements. It offers an advantage over the turam method in obtaining the fields directly instead of by calculation. These measured values are often more accurate than those obtained by calculation, especially in regions where the field is near zero and the ratios may approach zero or infinity.

However, the ratio curve is more sensitive to small features than the field curve. By considering the ratios, therefore, it is possible to detect weaker conductors with the turam method than with the radio-reference-signal system. Also, since the magnitude of a field anomaly depends on the position of the disturbing body with respect to the cable and to other bodies, a field anomaly cannot be evaluated on the basis of its magnitude alone. Ratio anomalies, however, depend on the shape, and not on magnitude, of the field anomaly. Thus it may be advantageous to have the ratios as well as the fields.

The depth range and speed of operation of the cross-ring method are inferior to those of the turam and radio-reference signal, but the cross-ring is sometimes the most useful for working out details of a group of shallow conductors in proximity to each other.

When a moving source is used, cross-ring equipment has an advantage over slingram because it does not require a cable connection from transmitting to receiving coil. Also, the maintenance of a constant distance between the two coils is not critical unless response from the overburden is great. Results are not as easily interpreted as those obtained by the slingram method because, in general, anomalies occur simultaneously in both the horizontal and vertical fields and thus the data are not related to any fixed reference.

Slingram methods, either ground or airborne, are probably less expensive per traverse kilometer than their counterparts in other systems. Slingram is especially adaptable to reconnaissance work because no large energizing layouts are necessary. When a sizable area is to be surveyed in detail by ground work the radio-reference signal may be nearly as inexpensive as the slingram method, since the expense of laying out cables is partially offset by the fact that each set of measuring apparatus can be operated by less than one man. For detailed

work over areas of particular interest it may be advisable to use the method that yields the most information regardless of cost. In such cases one of the fixed-source methods will usually be chosen because of its greater sensitivity, depth of penetration, and resolving power. The variety of problems in prospecting is so great that any one of the systems discussed may be the best in a particular instance.

EQUIPMENT

The usual set of equipment for ground electromagnetic work consists of four major components or groups of components: 1) energizing and receiving coils and cables, 2) a source of energizing current, 3) an alternating current potentiometer or ratiometer, and 4) an amplifier used as a null detector. In mobile operations, electronic phase discriminators supplement or replace the ordinary ratiometer, and various additional components such as automatic recorders are necessary.

Older types of turam, slingram, and cross-ring equipment were designed to be carried by a crew of four men. The ratiometer is carried as a back-pack by one man and operated by a second man. Each of the other two men carries a coil; for the slingram and cross-ring methods, one of these men also carries the source of energizing current. Newer types of equipment are designed for a two-man operation, one man carrying both the receiving coil and the ratiometer in such a way that he is able to operate the ratiometer.

Coils and Cables: Air-core coils are usually wound on circular forms having a diameter of perhaps 50 to 120 cm. Turns of wire may range from 100 to 1500, and the wire weight from 2 to 10 kg for copper wire and half that for aluminum wire. A single turn of aluminum tubing with appropriate matching transformers is used in the cross-ring equipment. Coils for turam and low-frequency slingram work have more turns than those for high-frequency slingram work.

Coils must always be shielded from electric fields. At low frequencies an aluminum tube bent into the form of a loop serves as both the winding form and the shield. At higher frequencies plywood forms enclosed by brass screening or very thin tin foil are used. The windings are impregnated with wax or other compounds, and the entire unit is made watertight. Level bubbles are usually attached to the coils so that they may be oriented accurately in either horizontal or vertical positions.

Ferrite core coils are used in some of the newest equipment. The core may be about 80 cm long and 2 or 3 cm diam, and the weight of wire used is about the same as for an equivalent air-core coil. At low frequencies the performance of ferrite core coils is probably superior to that of air-core coils of the same weight, but at high frequencies they are inferior. Ferrite core coils are often more convenient to handle. In most work they may easily be suspended so as to be self-orienting. A disadvantage of ferrite core coils is that they may be noisy when subjected to vibrations such as are caused by wind.

At their operating frequencies, typical coils have Q values from as low as 15 to as high as perhaps 60. Both energizing and receiving coils are tuned to the operating frequency by means of a series or a shunt-connected capacitor.

Large layouts for the energizing source are formed from a single length or loop of flexible rubber-covered cable.

Energizing Current Sources: Long grounded wires and large loops are usually excited by an alternator driven by a portable gasoline engine. Usually, with an exciting voltage of 200 to 300 v, about 1 amp is supplied to a grounded cable and perhaps 3 or 4 amp to an insulated loop. Larger currents may be required for airborne and other special work. With usual cables and grounding resistances the power factor is nearly unity for a grounded cable, but it may be somewhat less for an insulated loop.

Mechanical engine governors are generally adequate for controlling frequency, and fluctuations in current do not affect ratio measurements. However, frequency and current stability requirements are severe when the direct method of measuring fields using a radio-reference signal is employed. A vacuum tube oscillator and a stabilized power amplifier powered by an engine generator are then used.

The slingram and cross-ring methods use small battery-powered vacuum tube or transistor oscillators and amplifiers as sources of energy. Typical tube amplifiers deliver about 2 w of power to the coil. If interference from power lines and other sources of extraneous fields is not too severe, slingram equipment can operate on much less than 2 w at moderate spacings and frequencies. Equipment now being developed will use a 250-milliwatt transistor oscillator. Tuning the energizing coil causes it to be highly selective to the operating frequency; hence the power amplifier can be operated class C with resulting high efficiencies and long battery life.

Some equipment uses a tuned load single-stage tube or transistor oscillator driving a one-stage push-pull amplifier. In other equipment two tubes or transistors serve as both oscillator and amplifier, and the coil and tuning capacitor are the tuned load controlling the frequency of oscillation.

For airborne work vacuum tube oscillators and power amplifiers are preferred, although alternators have been used. Power requirements may range from 50 to 300 w for each energizing coil.

Ratiometers: Some alternating current potentiometers or ratiometers are designed to measure in polar form, i.e., amplitude ratios and phase angles, while others are designed to measure in cartesian form, i.e., inphase and out-of-phase ratios. Amplitude and phase measurements are the easiest to use in turam work in calculating field curves from the ratio data, but data are often most conveniently interpreted in terms of inphase and out-of-phase quantities. Also it is probably easier to design ratiometers that measure inphase and out-of-phase ratios than ratiometers that measure amplitude ratios and phase angles.

In a typical ratiometer the reference signal is applied to an RC phase-splitting network. Voltages are developed across two linear potentiometers; one voltage is inphase with the current in the energizing coil and one is out-of-phase. The two sliding contacts on the potentiometers are connected to the receiving coil with the input of the amplifier placed in series or coupled into the circuit through a transformer. The potentiometers are adjusted until the amplifier indicates a minimum and the ratios are read from dials connected to the potentiometers.

Either RC or RL phase-splitting networks may be used in ratiometers, but the RC networks are the most stable and easiest to construct. Also, when inductances are used great care must be taken that voltages are not induced directly into the inductances. The variable components are preferably linear potentiometers. Ratiometers used for turam work are usually designed with two nearly identical arms, each connected to a coil. This design greatly reduces errors due to frequency and temperature variations and other disturbances.

A frequency independent ratiometer that measures amplitude ratios and phase angles, using only two linear potentiometers and scales and only RC networks, is reported but details of the circuit are not available.

Amplifiers: Principal requirements for the amplifiers used in null detectors are low noise level, moderately good band pass characteristics at the operating frequency, and durability and portability. Typical values of grain are 80 decibels for a slingram amplifier and 100 decibels for a turam amplifier; this is easily obtained with a three-stage vacuum tube amplifier. Usually at least two of the stages are tuned. Some of the amplifiers designed for high-frequency (3600 cps) work use a frequency converter requiring two extra stages.

Transistor amplifiers and combination transistor-vacuum tube amplifiers are used in some of the newer equipment. During their initial development straight transistor amplifiers generated more noise than the best vacuum tube amplifiers and for certain applications it was necessary to use a tube in at least the first stage of the amplifier. Recently developed transistor amplifiers are less noisy than vacuum tube amplifiers, but in some cases their lower input impedance is a disadvantage. Headphones and rectifier-galvanometer combinations are used as null indicators. A galvanometer is usually more pleasant to work with, but lower signal-to-noise ratios can be tolerated when earphones are used because of the selective power of the ear. Instrumentation for the radio-reference signal system places greater demand on the amplifier than the ordinary turam method. Reliable amplitude information cannot easily be transmitted by radio; hence a comparison method cannot be used and actual amplitudes have to be measured requiring that the gain of the amplifier connected to the receiving coil be constant. Difficulties have been encountered with varying phase shifts in the radio receiver amplifiers.

Radio-Reference Signals and Continuous Recording Systems: A reference signal from the cable is used to modulate the radio transmitter placed near the energizing layout. The voltage demodulated in a radio receiver located in the measuring apparatus is sent to a phase splitter and then applied as the reference voltage to each of two diode-transformer phase discriminators. The voltage induced in the receiving coil is amplified by a calibrated amplifier and fed to the phase discriminators. D-C meters connected to the outputs of the phase discriminators then give the inphase and out-of-phase components of the magnetic field at the receiver relative to the current in the energizing cable.

One of the airborne electromagnetic methods using ground energization utilizes essentially this same system, but with the output of the phase discriminators fed to two continuously recording meters.

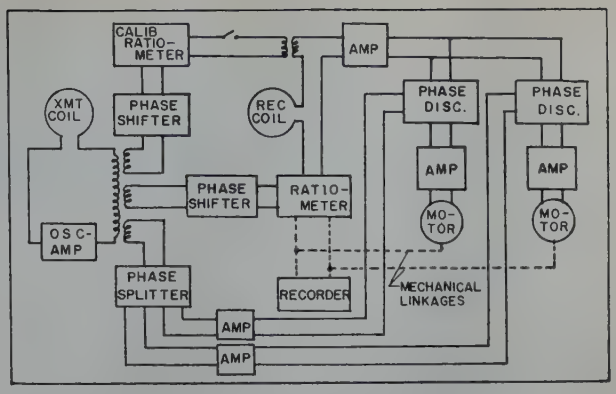

Fig. 3—Diagram of mobile slingram system.

A simple airborne slingram arrangement also uses this measuring system, except that the reference voltage is sometimes transmitted by a wire connection. Also, the normal or primary signal from the receiver is compensated for by a reference voltage, so that in the absence of conductors there is no signal voltage applied to the phase discriminators.

The block diagram of a more elaborate mobile slingram system is shown in Fig. 3. Reference and signal voltages are supplied to a ratiometer. The unbalanced signal from the ratiometer is amplified and fed to two phase discriminators. A second reference voltage is passed through a phase splitter, and the resulting voltages are applied as reference to the phase discriminators. Output of the phase discriminators is amplified and fed to each of two d-c motors, which in turn are mechanically coupled to the sliders in the potentiometers of a two-pen recorder. Any unbalanced voltage from the potentiometer causes the appropriate motor to reposition the slider until a new balance position is found.

This discussion by no means covers all the equipment now used in Scandinavia. It does illustrate, however, some representative measuring systems.

Most of the material for this discussion was acquired during a stay at Geofysisk Malmleting in Norway and at the conference of Scandinavian mining geophysicists held in Boliden, Sweden, during November 1956. The author wishes to acknowledge the help and information given him by the people attending the conference and by the personnel of Geofysisk Malmleting. He also wishes to thank AB Elektrisk Malmletning and Sveriges Geologiska Undersokning for permission to publish certain portions of this article.

SELECTED BIBLIOGRAPHY

H. Hedström: Phase Measurements in Electrical Prospecting. *AIME Trans.*, 1940, vol. 138, pp. 456-472.

H. Hedström and D. Parasnis: Some Model Experiments Relating to Electromagnetic Prospecting with Special Reference to Airborne Work. *Geophysical Prospecting*, 1958, vol. 6, no. 4, pp. 322-341.

M. Puranen and A. A. Kahma: Method for Inductive Prospecting. U. S. Patent 2,642,477 (1953).

L. B. Slichter: Geophysics Applied to Prospecting for Ores. *Economic Geology*, 50th Anniversary Volume, Part II, pp. 885-969.

K. Sundberg and H. Hedström: *Structural Investigations by Electromagnetic Methods.* World Petroleum Congress, London, 1933.

G. Törneqvist: Some Practical Results of Airborne Electromagnetic Prospecting in Sweden. *Geophysical Prospecting*, 1958, vol. 6, no. 2, pp. 112-126.

J. R. Wait: Mutual Electromagnetic Coupling of Loops over a Homogeneous Ground. *Geophysics*, 1955, vol. 20, no. 3, pp. 630-637.

J. R. Wait: The Fields of a Line Source of Current over a Stratified Conductor. *Applied Scientific Research*, 1953, section B, vol. 3, pp. 279-292.

Discussion of this article sent (2 copies) to AIME before Oct. 31, 1959, will be published in MINING ENGINEERING.

NUCLEAR DETECTOR FOR BERYLLIUM MINERALS

by T. CANTWELL, H. E. HAWKES, and N. C. RASMUSSEN

Beryl is a mineral that may be difficult to distinguish from quartz by casual field inspection. The easily recognized green color and hexagonal crystal form of coarse-grained beryl are by no means universal, even in beryl from pegmatitic deposits. If it occurred as a fine-grained accessory mineral in an igneous rock, it would almost certainly escape detection unless samples were submitted for petrographic or chemical analysis. There may be substantial deposits of some beryllium mineral, other than beryl, that has been overlooked because that mineral also closely resembles the common rock-forming minerals.

A reliable and simple method of identifying beryllium minerals and determining the beryllium content of a rock would be helpful in exploration. This article describes preliminary experiments in applying nuclear reaction to the qualitative identification of beryl and to the semiquantitative determination of the beryllium content of rock samples.

Gaudin,[1, 2] the first to apply a nuclear reaction in detecting beryllium minerals, developed a method that irradiates the sample with gamma rays, which react with beryllium nuclei to produce neutrons. The neutrons are then measured with standard equipment. The cross section for this reaction is about 1 millibarn. The cross section is a measure of the probability that a reaction will take place, for example, between a beryllium nucleus and an incident gamma ray or alpha particles.[3–5] At 1-millibarn cross section for the reaction, satisfactory performance required a source strength of the order of 1 curie (3.7×10^{10} disintegrations per sec, where each disintegration releases one or more gamma rays). The reactions will not take place if the gamma radiation is below a minimum energy, in this case 1.63 mev. The size of the source and the energy of the radiation made heavy shielding necessary for these experiments, both to reduce the background count of the neutron counter and to safeguard personnel.

The original discovery of the neutron by Chadwick in 1932 resulted from experiments with another nuclear reaction, induced by bombarding beryllium with alpha particles in which the products are carbon-12 and neutrons. The equation for this reaction is as follows:[4, 5]

$$ {}_4Be^9 + {}_2He^4 \rightarrow {}_6C^{12} + {}_0n^1 \qquad [1] $$

α-particle neutron

In the above nuclear equation (Eq. 1), the subscript number indicates the number of protons in the nucleus (the atomic number) and the superscript the total number of neutrons and protons (approximately the atomic mass). For the alpha-neutron reaction the cross section is about 250 millibarns, or 250 times that of the gamma-neutron reaction used by Gaudin. The positively charged alpha particle is repelled by the positive charge of the beryllium nucleus; it must, therefore, have a certain minimum energy in order to approach close enough to the beryllium nucleus to react. For reaction with the beryllium nucleus, the lower limit of the alpha-particle energy is 3.7 mev.

The alpha-neutron reaction, with polonium-210 as an alpha source, was selected for the present experiments. Alpha particles are emitted by polonium-210 at 5.30 mev, which is adequate for the reaction with beryllium. Furthermore, this isotope of polonium emits alpha particles with negligible associated gamma radiation, thus eliminating the necessity of shielding. The half-life of polonium-210 is 138 days.

Inasmuch as alpha particles carry a possible charge and are large compared with most nuclear particles, their energy is rapidly dissipated in passing through matter. Their range in standard air is 3.66 cm,[3] and they penetrate only a few tens of microns into a mineral sample. The short range in air can be minimized by preparation of a flat sample surface that can be brought very close to the alpha source during analysis. On the other hand, short range of alpha particles in air lessens the radiological health hazard and makes it possible to use this method without shielding. It must be emphasized, however, that the alpha emitters are potentially very dangerous if they enter the human body. Polonium must be handled with extreme caution.

The literature has reported experiments on the yield of neutrons from reaction of alpha particles with beryllium nuclei. Feld[6] reports that in intimate mixtures of polonium and beryllium, 3×10^6 neutrons per sec are produced per curie of polonium. Elsewhere in the same reference it is stated that a sandwich-type source yields about one third as many neutrons as an intimate mixture. A table of neutron yields for full energy polonium alpha-particles on thick targets as reported by Anderson[7] is the basis of Table I.

From Table I it can be deduced that the elements most likely to interfere, i.e., those that also produce neutrons when bombarded by alpha particles, are boron and fluorine. These data also show that it will probably not be possible to determine very small quantities of beryllium in rocks because of the masking effects of the major elements, sodium, magnesium, and aluminum.

The neutrons emitted in the alpha reaction are detected by another nuclear reaction. Either of the

T. CANTWELL is with the Department of Geology and Geophysics and H. E. HAWKES, Member AIME, with the Department of Mineral Technology, University of California, Berkeley, Calif. N. C. RASMUSSEN is with the Department of Nuclear Engineering, Massachusetts Institute of Technology. TP 4813I. Manuscript, Oct. 22, 1958. New York Meeting, February 1958. AIME Trans., Vol. 214, 1959.

two common neutron detectors, boron trifluoride counters and fission counters, depends on a count of the amplified impulses resulting from nuclear capture of neutrons. The energy of neutrons emitted by reaction of alpha particles with beryllium nuclei is very high, in the mev range. Since the capture cross section of neutrons increases as their energy decreases, it is desirable to slow them down, or *moderate* them, before they enter the counter tube. This may be done by surrounding the experiment with a hydrogenous material such as paraffin, as the impact of neutrons with hydrogen atoms rapidly dissipates their initial energy of motion.

Experimental Work: The experimental work was carried out by bombarding samples of beryl and of metallic beryllium with alpha particles from a polonium-plated silver foil.

For the present experiments, 30 millicuries of Po-210 were purchased from the Mound Laboratory of Monsanto Chemical Co. at Miamisburg, Ohio. This polonium was supplied in dry form as polonium nitrate. It was redissolved and plated on one side of a 2x4-in. silver foil by slight modification of standard techniques.[8] The foil was mounted on a plastic plate. The active foil surface was then protected by a sheet of rubber hyrdochloride 0.00017 in. thick, which is thin enough to allow alpha particle penetration. The experimental setup is illustrated in Figs. 1 and 2.

The method of preparing the mineral sample was dictated by the need to get a large amount of the sample at a uniform distance from the polonium source. Therefore the mineral sample, usually a piece of beryl several centimeters in size, was pulverized by hand and sprinkled over a glue-coated surface, which was then allowed to dry. The polonium foil was placed within 0.5 cm of the test sample. Foil and sample were completely surrounded by paraffin to moderate the emitted neutrons and increase thermal neutron concentration close to the source. The neutrons were detected with a BF_3 counter tube, also surrounded by paraffin.

Preparation of the sample is an important step in the analysis, as it is in any mineral analysis. Assuming that a representative sample has been obtained in pulverized form, it must be mounted so that a nearly plane surface is presented to the source of radiation. With a pulverized sample this is best approximated by fine pulverization (about 100 mesh) and uniform depth of mounting. One method of accomplishing this was used by the present investigators.

Detection was carried out with a Radiation Counter Laboratory $B^{10}F_3$ tube connected to an Atomic Instrument scaler No. 1085 through an Atomic Instrument amplifier No. 218 and amplifier No. 255.

Results: The results show that the proposed scheme of detection is feasible, but interpretation is complicated by the fact that no exact analyses of the beryl ores are available; they can only be compared to pure beryllium metal. Standard mineralogy references[9] give the BeO content of beryl as 14 pct, equivalent to a Be content of 5 pct.

In the time available it was not possible to vary all the parameters of the system. It was possible to run several different ore samples and one pegmatite gangue sample, and further work is planned.

The results are shown in Table II. The error in the total counts is the standard deviation computed by taking the square root of the number of counts.

The results show that pure beryl containing in the order of 5 pct Be can easily be detected qualitatively with the alpha-neutron reaction described here. Indications are that lower concentrations of beryllium could also be detected in this experiment.

For a quantitative determination of the beryllium content of a sample, it might be possible to compare the count rate from a mineral sample with the count rate from pure beryllium. This method is

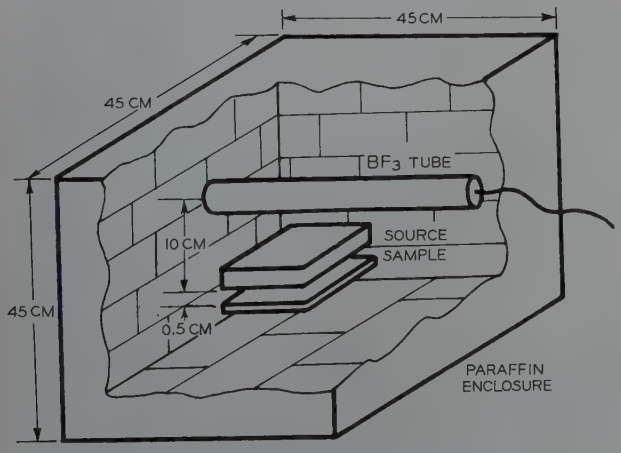

Fig. 1—Experimental arrangement.

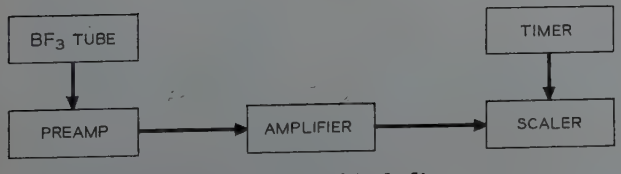

Fig. 2—Instrument block diagram.

Table I. Neutron Yield in Alpha-Neutron Reactions

Element	Yield of Neutrons Per 10^6 Alphas	Element	Yield of Neutrons Per 10^6 Alphas
Be	80	A	0.38
B	24	Si	0.16
F	12	C	0.11
Li	2.6	Cl	0.11
Na	1.5	O	0.07
Mg	1.4	N	0.01
Al	0.74		

Table II. Results of Experiments

Sample Number	Sample Description	Run Number	Total Counts	Count Time, Min
A	Background measurement, no sample ore present	0	10± 3.2	10
B	Pure Be metal disk, 3.4-in. diam	1	3910±62.5	10
1	Crushed beryl sample, 1½x2-in. rectangle	1	120±11	10
		2	114±10.7	10
2	Crushed beryl sample, 3.4-in. diam disk	1	182±13.5	10
		2	200±14.1	10
3	Crushed beryl sample 3.4-in. diam disk	1	116±10.8*	10
		2	147±12.1	10
4	Crushed muscovite-quartz-feldspar sample, 3.4-in. diam disk	1	3± 1.7	2

* Sample was placed about 1 cm away from source and moved closer for run 2.

subject to difficulties, since the small penetration of alpha particles means that only the exposed area of the sample is being measured. A direct ratio of the observed data on mineral samples to the data on pure beryllium shows 3 to 5 pct of beryllium in the beryl tested, a figure in reasonable agreement with published analyses of pure beryl.[9]

Summary and Conclusion: The work reported here is preliminary. The conclusions are as follows:

1) An instrument to detect beryllium in mineral assemblies down to 1 pct contained beryllium is possible. With a stronger alpha particle source and more careful experimental techniques, it may be possible to extend this lower detection limit to 0.1 pct contained beryllium.

2) Semiquantitative analysis of mineral specimens may be possible by comparison of count rates on an unknown sample with the count rate from a standard sample.

3) Experience with the method in the laboratory indicates that no serious obstacles to the construction of a field instrument need be anticipated.

REFERENCES

[1] A. M. Gaudin, J. Dasher, J. H. Pannell, and W. L. Freyberger: Use of an Induced Nuclear Reaction for the Concentration of Beryl. *AIME Trans.*, 1950, vol. 187, pp. 495-498.

[2] A. M. Gaudin and J. H. Pannell: Determination of Beryllium by Photodistintegration. *Analytical Chemistry*, 1951, vol. 23, pp. 1261-1265.

[3] R. D. Evans: *The Atomic Nucleus.* McGraw-Hill Book Co., New York, 1955.

[4] R. E. Lapp and H. L. Andrews: *Nuclear Radiation Physics.* Prentice-Hall Publishing Co., New York, 1954.

[5] E. C. Pollard and W. L. Davidson: *Applied Nuclear Physics.* John Wiley & Sons Inc., New York, 1957.

[6] E. Segre: *Experimental Nuclear Physics*, Vol. II, pp. 363-366. John Wiley & Sons Inc., New York, 1953.

[7] H. L. Anderson: Neutrons from Alpha Emitters. *Preliminary Report No. 3, Nuclear Science Series*, pp. 1-4. National Research Council, 1948.

[8] R. M. Fink: Biological Studies with Polonium, Radium and Plutonium. McGraw-Hill Book Co., New York, 1950.

[9] C. S. Hurlbut: *Dana's Manual of Mineralogy*, pp. 376-378. John Wiley & Sons Inc., New York, 1955.

Discussion of this article sent (2 copies) to AIME before Oct. 31, 1959, will be published in MINING ENGINEERING.

Technical Note

GEOCHEMICAL STUDY OF Pb-Ag-Zn ORE FROM THE DARWIN MINE, INYO COUNTY, CALIFORNIA

by **WAYNE E. HALL**

The Darwin mining district of California, 160 miles north of Los Angeles, has yielded an estimated $45 million in lead, silver, zinc, and copper since 1875. The deposits are in silicated limestone of Pennsylvanian and Permian age close to a stock of hornblende-biotite-quartz monzonite. Steep left-lateral strike-slip faults that strike N 50° 70° E served as feeder channels for the ore solutions, and minor folds, favorable beds, and faults close to the feeder channels localized the orebodies.

The orebodies are irregular, steep, pipe-like replacements that cut across bedding, bedding replacements, and fissure fillings in a calc-silicate country rock consisting mainly of wollastonite, grossularite-andradite garnet, idocrase, and diopside. Near surface the ore consists of a soft, crumbly mass of cerussite, hemimorphite, jarosite, limonite, and some secondary copper minerals. The primary ore consists of galena, sphalerite, pyrite, pyrrhotite, and chalcopyrite with smaller amounts of andorite, matildite, scheelite, tetrahedrite, and a high silver-lead-bismuth-selenium-bearing galena.

Preliminary X-ray fluorescence study of the primary ore has indicated unusually high concentrations of bismuth, selenium, and silver in galena from certain parts of the mine. One phase of this study concerns the distribution of these elements. Twenty-two samples of galena and thirty of sphalerite have been purified and analyzed or are being analyzed.

The selenium in 21 samples of galena ranges from 0.0045 to 2.11 pct; four contain more than 1 pct. These four samples were collected from the Essex orebody, where most of the selenium is concentrated. Three are from high-grade, near-surface ore, and one is from the 700 level. Four of the seven analyzed galena samples from the Thompson workings immediately north of the Essex orebody contain 0.29 to 0.74 pct Se; the others show less than 0.05 pct. Galena from the Defiance workings about 2000 ft south of the Essex has less than 0.03 pct Se.

The selenium-bearing galena also contains concentrations of bismuth and silver. Preliminary spectographic analyses indicate as much as 3 pct Bi and more than 1 pct Ag in galena with high selenium content. Antimony is the only other minor element present in galena in amounts greater than 0.02 pct; most galena contains between 0.1 and 0.2 pct and the maximum is 0.72 pct.

A second phase of the study is an attempt to determine the temperature range of the formation of the ore. The iron content of sphalerite deposited in equilibrium with pyrrhotite is being used as a geologic thermometer as it is a function of the temperature of deposition of the ore.[1] Preliminary results indicate temperature range from 430°C in replacement orebodies in the Defiance workings to 180°C in shallow fissure fillings.

W. E. HALL is with the Mineral Deposits Branch of the U. S. Geological Survey, Menlo Park, Calif. TN 59147.

Manuscript, Jan. 17, 1959. San Francisco Meeting, February 1959. AIME Trans., Vol. 214, 1959.

REFERENCE

[1] G. Kullerud: The FeS-ZnS System—A Geological Thermometer. *Norsk geol. tidsskr*, 1953, vol. 32, pp. 62-147.

DEFLECTION OF MINE ROOF SUPPORTS

by LAWRENCE ADLER

Any design of a mine roof in bedded deposits which ignores differential deflections at the supports can quickly lead to dangerous overstressing. As illustrated by the typical case presented on page 1029, if one support deflects only 0.1 in. more than its neighbor, stresses 50 pct higher than anticipated will result.

Previous studies[1-3] have assumed that the mine roof acts like a beam clamped at both ends, with no deflection or slope[4] at the supports (Fig. 1). Essentially this assumes:[5,6] $\theta_A = \theta_B = 0$ and $d_A = d_B = 0$.

However, a host of conditions can cause differential sag or deflection at one support, and even an apparently trivial deviation can have major consequences in the beam: variations in spacing, size, and material of supports; local settlement due to floor heaving or lower mine openings; non-uniformity in wedging or bolt tensioning.[8] In one particular instance concrete pillars, poured in place, shrank away from the roof upon setting.[9]

When understood and controlled, differential sag becomes a definite advantage, permitting the transfer of loads from one support to another. Where one support is a bolt or prop and the other a pillar or rib, the load on the former can be reduced while the load on the pillar or rib is increased. This means two things: 1) savings can be effected by using smaller artificial supports such as props and bolts and 2) loads can be increased in the rib to induce eventual failure for longwall caving. In this last respect, another factor underlying coal bumps becomes understandable.

The design of a mine roof by beam theory assumes that when a bedded formation is homogeneous, isotropic, and elastic, it will act like a uniformly loaded beam, fixed or clamped at both ends,[6] as in Fig. 1.[10] These are important assumptions.

The uniform load is the weight of the beam itself or its body load. For a beam of unit width, this load becomes per foot: $w = \gamma h b$.

w = uniform load
γ = specific weight, lb per ft^3
h = depth or thickness of beam, ft
b = width of beam, ft

Since $b = 1$,

$$w = \gamma h \qquad [1]$$

A beam fixed at both supports is statically indeterminate to the second degree, that is, two equations in addition to those for static equilibrium are required to determine the reactions at the supports. These equations result from the geometry.

From statistics:

$$\Sigma F_y = 0\ ;\ R_A + R_B - wL = 0 \qquad [2]$$

$$\Sigma M_o = 0\ ;\ M_B + \frac{wL^2}{2} - M_A - R_B L = 0 \qquad [3]$$

Using superposition in which the left support is kept intact and the right one resolved into an active force and moment, we obtain from Fig. 2:[11]

$$\theta_B = \theta_{B1} + \theta_{B2} + \theta_{B3} = 0$$

$$\theta_B = \left(\frac{wL^2}{6} + M_B - \frac{R_B L}{2}\right)\frac{L}{EI} = 0 \qquad [4]$$

$$d_B = d_{B1} + d_{B2} + d_{B3}$$

$$d_B = \left(\frac{wL^2}{8} + \frac{M_B}{2} - \frac{R_B L}{3}\right)\frac{L^2}{EI} \qquad [5]$$

Where: Subscripts refer to position on axis of beam

R = force, lb
M = moment, ft-lb
w = uniformly distributed load, lb per ft
L = span, ft
θ = slope, radians
d = deflection, ft
E = Young's Modulus, lb per ft^2
I = Moment of inertia about the neutral axis, ft^4

Solving Eqs. 2 through 5 for the four unknown reactions, we obtain:

$$M_A = \frac{wL^2}{12} + \frac{6EI}{L^2}d_B \qquad [6]$$

$$M_B = \frac{wL^2}{12} - \frac{6EI}{L^2}d_B \qquad [7]$$

$$R_A = \frac{wL}{2} + \frac{12EI}{L^3}d_B \qquad [8]$$

$$R_B = \frac{wL}{2} - \frac{12EI}{L^3} \qquad [9]$$

Fig. 3 is obtained by plotting M_A and M_B vs d_B and then plotting R_A and R_B vs d_B and adjusting their scales to coincide with M_A and M_B vs d_B. It should be noted in Eqs. 6 and 7 that as d_B increases, M_A increases the same amount that M_B decreases. Eqs. 8 and 9 show a similar relationship between R_A and R_B.

Proof that M_A is the maximum absolute moment occurring in the beam is as follows:

$$+\circlearrowleft \Sigma M_x = 0$$

$$R_A x - M_A - \frac{wx^2}{2} + M_x = 0$$

where M_x = moment at x

$$M_x = -R_A x + M_A + \frac{wx^2}{2}$$

$$\frac{dM_x}{dx} = -R_A + wx$$

When

$$\frac{dM_x}{dx} = 0;\ x = \frac{R_A}{w}$$

$$\therefore M_x = M_{max} = M_A - \frac{R_A^2}{2w}$$

where M_{max} = maximum positive moment

Eqs. 6 and 8 into above:

$$M_{max} = -\frac{wL^2}{24} - \frac{72E^2I^2}{wL^6}d_B \qquad [10]$$

For small d_B: $M_A > M_{max}$

L. ADLER, Member AIME, is Assistant Professor of Mining Engineering, Michigan College of Mining and Technology, Houghton.
TP 4816A. Manuscript, Nov. 20, 1958. AIME Trans., Vol. 214, 1959.

The absolute value of M_A is greater than the absolute value of M_{max}; consequently, M_A will be the basis of design, and M_{max} can be checked.

Comparison of the actual stresses, S, due to deflection with the assumed stresses, S_r (allowable modulus of rupture), for zero deflection is necessary.

$$M_A = \frac{wL^2}{12} + \frac{6EI}{L^2} d_B \qquad [6]$$

If $d_B = 0$: M_{A0} = maximum moment @ $d_B = 0$

$$M_{A0} = \frac{wL^2}{12} \quad \text{and} \quad L^2 = \frac{12\, M_{A0}}{w} \qquad [11]$$

Eq. 11 into Eq. 6:

$$M_A = M_{A0} + \frac{EIw}{2M_{A0}} d_B$$

$$\frac{M_A}{M_{A0}} = 1 + \frac{EIw}{2M_{A0}^2} d_B \qquad [12]$$

Since

$$S = \frac{Mc}{I} \text{ and } I = \frac{bh^3}{12} = \frac{h^3}{12}, c = \frac{h}{2}$$

$$S = \frac{6M}{h^2}$$

$$\therefore M = \frac{Sh^2}{6}$$

$$M_A = \frac{Sh^2}{6}; \; M_{A0} = \frac{S_r h^2}{6} \qquad [13]$$

Eqs. 1 and 13 into Eq. 12:

$$\frac{S}{S_r} = 1 + \frac{1.5E}{S_r^2} \gamma\, d_B \qquad [14]$$

That is: If the design is made on the basis of zero deflection, the ratio of actual stress to allowable stress is given by Eq. 14.

By substituting typical values into Eq. 14, the order of magnitude of S/S_r can be estimated.[12]

For sandstone:

$$E = 1.3 \times 10^6 \text{ psi}$$

$$\gamma = 0.0761 \text{ lb per in.}^3$$

$$S_r = \frac{640}{4} = 160 \text{ psi}$$

$$\frac{S}{S_r} = 1 + \frac{1.5 \times 1.3 \times 10^6 \times 0.0761}{160^2} d_B$$

$$\frac{S}{S_r} = 1 + 5.8\, d_B \qquad [15]$$

The S/S_r ratio is very high for even trivial values of d_B.

If $d_B = 0.1$ in. into Eq. 15,

$$\frac{S}{S_r} = 1.58$$

The actual stress is over 50 pct more than the allowable, a very significant increase.

This means that whenever deflection can not be calculated, it is best to strive for zero deflection. All supports should be kept as uniform as possible in size, material, and spacing. Where this can not be done, as when supports are adjacent to ribs and pillars, these variables should be adjusted to minimize the differential deflections. Where there are lower workings, supports should be aligned directly above one another. Floor heave should be carefully observed to prevent unsafe conditions in the roof. Maximum and uniform pre-stressing of bolts and props is necessary and must be maintained.

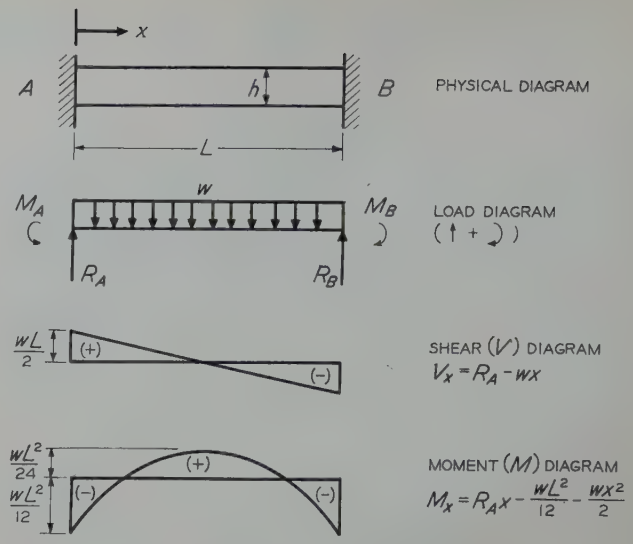

Fig. 1—Properties of a beam with both ends built in.

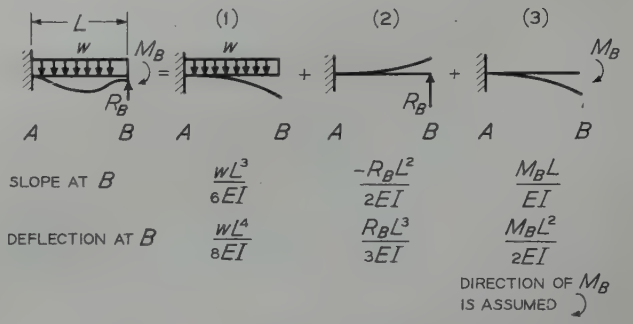

Fig. 2—Components of deformation.

When a deflection d_B is known to occur, the roof span L should be calculated on the basis of Eq. 6 and checked by Eq. 10.

An advantage can be obtained in certain cases by permitting controlled deflection through the use of crush blocks. In coal mining, no attempt is made to support the main roof by props;[13] the roof is permitted to deflect and crush the blocking without impairing the structural integrity of the props and their ability to support the immediate roof. When the immediate roof itself is still not loaded to its allowable stress, additional deflection of the crush blocks will reduce the load on the props while increasing the stress in the roof. (See Eqs. 6 through 10). If the span is predetermined, and is less than the allowable span, the problem is most easily solved by use of Fig. 3, which is accompanied here by a sample problem. When more than one adjacent support deflects, the solution must be repeated from span to span.

Conversely, as R_B decreases R_A increases. Sufficient increase in R_A can lead to conditions suitable for longwall caving by stressing the face toward failure as applied to coal mining. The particular situation should be analyzed with reference to the procedure presented here, rather than by blind use of the equation, since they themselves contain the assumed restriction $\theta_B = 0$. Fig. 4 illustrates this roof action.

Conclusion: When a mine roof is designed for maximum safe span, it is usually assumed that the

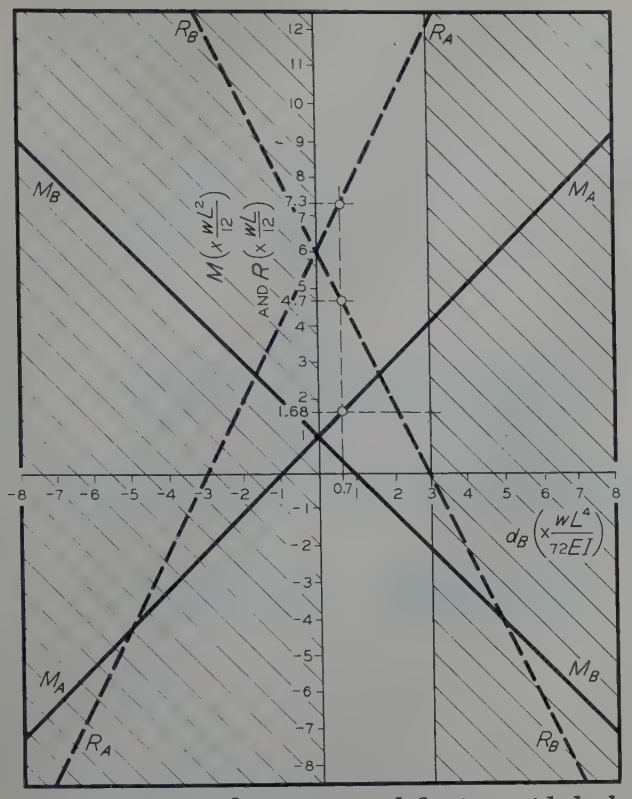

Fig. 3—Moment and reaction vs deflection, with both ends built in. Since $d_{B-}>O$ and $R_{B-}>O$, values cannot exist in shaded areas. Sample problem at right.

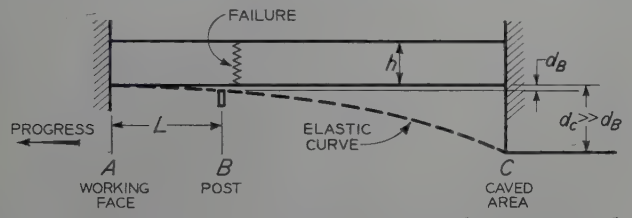

Fig. 4—Elements of roof during longwall caving. Both supports B and C deflect, but since $d_c>>d_B$, roof failure will occur as illustrated above. Working face A is loaded by wL/2 and additionally by the deflection at B.

differential deflection of the supports is zero. However, should an apparently insignificant deflection exist, stresses in the roof can quickly exceed the allowables. Consequently, where these deflections are indeterminate, strong measures should be taken to minimize them and if possible to make them zero.

When a mine roof is designed for some convenient lesser span, controlled, permissive deflection will result in lower loads on the props or bolts.

A corollary action increases the load on the other support. If this is the rib, conditions favorable to longwall caving can be induced in the working face.

REFERENCES

[1] F. Wright and P. B. Bucky: Determination of Roof and Pillar Dimensions of the Oil-Shale Mine at Rifle, Colo. *AIME Trans.*, 1949, vol. 181, pp. 352-359.

[2] R. H. Merrill: Design of Underground Mine Openings, Oil-Shale Mine, Rifle, Colo. *USBM R. I. 5089*, December 1954.

[3] R. H. Merrill: Roof Span Studies in Limestone. *USBM R. I. 5348*, July 1957.

[4] P. B. Bucky: Use of Models for the Study of Mining Problems. *AIME TP 425*, February 1931.

[5] S. Boshkov: Some Mathematical and Model Guides in the Analysis of Underground Mine Stress Problems. Canadian Institute of Mining and Metallurgy *Bulletin*, June 1956.

[6] R. D. Caudle and G. B. Clark: Stresses around Mine Openings in Some Simple Geologic Structures. University of Illinois, *Bull. No. 430*.

[7] C. T. Holland: Cause and Occurrence of Coal Mine Bumps. *AIME Trans.*, 1958, vol. 211, p. 1001.

[8] L. A. Panek: Principles of Reinforcing Bedded Mine Roof with Bolts. *USBM R. I. 5156*, March 1956.

[9] J. J. Reed, R. L. Bullock, and J. J. Yancik: How St. Joe Uses Mining Research. *Engineering & Mining Journal*, May 1958, p. 86.

SAMPLE PROBLEM

$E = 1.3 \times 10^6$ psi
$\gamma = 0.0761$ lb per in.^{3} } Sandstone

$$S_r = \frac{640}{S.F.} = \frac{640}{4} = 160 \text{ psi}$$

$S.F.$ = Safety factor = 4
h = bed thickness = 3 ft
L = existing roof span = 25 ft
$w = \gamma h$
M_{all} = allowable moment in roof
M_{ex} = existing moment in roof

$$S_r = \frac{M_{all}\,C}{I} \; ; M_{all} = \frac{Sr\,I}{C} = \frac{160 \times 144}{1.5}\left(\frac{3^3}{12}\right)$$

$$= 1728 \times 20 \text{ ft-lb}$$

$$M_{ex} = \frac{wL^2}{12} = \frac{0.0761 \times 1728 \times 3 \times 625}{12} = 1728 \times 11.9 \text{ ft-lb}$$

$$\frac{M_{all}}{M_{ex}} = \frac{20}{11.9} = 1.68$$

$$M_{all} = 1.68\, M_{ex} = 1.68\left(\frac{wL^2}{12}\right)$$

Through

$$M = 1.68\left(\frac{wL^2}{12}\right)$$

draw a horizontal line as shown. Any moment below this value is permissible. If it is desired to load the roof up to the allowable moment, draw a vertical line at the intersection of this horizontal line and M_A. Its abscissa of 0.7 $\left(\frac{wL^4}{72EI}\right)$ gives the permissive differential deflection of support B or d_B. The intersection of this vertical line $d_B = 0.7\left(\frac{wL^4}{72EI}\right)$ with R_A, and R_B, represents the load at these supports, in this case 7.3 $\left(\frac{wL}{12}\right)$ and 4.7 $\left(\frac{wL}{12}\right)$ respectively.

Therefore:

$$d_B = 0.7\left(\frac{wL^4}{72EI}\right) = 0.7\left[\frac{0.0761 \times 1728 \times 3 \times 25^4}{72 \times 1.3 \times 10^6 \times 144\left(\frac{3^3}{12}\right)}\right] = 0.00356 \text{ ft}$$

$$d_B = 0.0428 \text{ in.}$$

$$R_A = 7.3\left(\frac{wL}{12}\right) = 4.7\left(\frac{0.0761 \times 1728 \times 3 \times 25}{12}\right) = 6000 \text{ lb}$$

$$R_B = 4.7\left(\frac{wL}{12}\right) = 7.3\left(\frac{0.0761 \times 1728 \times 3 \times 25}{12}\right) = 3880 \text{ lb}$$

With

$d_B = 0$:

$$R_A = R_B = \frac{wL}{2} = \frac{0.0761 \times 1728 \times 3 \times 25}{2} = 4940 \text{ lb}$$

which not only gives the load transferred from B to A, but also checks the result, since: $4940 = \frac{6000 + 3880}{2}$.

[10] R. Peele: *Mining Engineers' Handbook*, 3rd ed., pp. 43-44. John Wiley & Sons, New York, 1941.

[11] S. Timoshenko and G. H. MacCullough: *Elements of Strength of Materials*, 3rd ed., pp. 182-184. D. Van Nostrand Co., 1949, pp. 182-184.

[12] S. L. Windes: Physical Properties of Mine Rock, Parts I and II. *USBM R. I. 4459* and *4727*, 1949 and 1950.

[13] E. N. Zern: *Coal Miner's Pocketbook*, p. 704. McGraw-Hill Book Co. Inc., New York, 1928.

Discussion of this article sent (2 copies) to AIME before Nov. 30, 1959, will be published in MINING ENGINEERING.

RELATION OF LAND SUBSIDENCE TO GROUND-WATER WITHDRAWALS IN THE UPPER GULF COAST REGION, TEXAS

by A. G. WINSLOW and LEONARD A. WOOD

Subsidence has occurred in several areas of the upper Gulf Coast region of Texas, although in most cases this is not evident without precise instrumental leveling.

As referred to in this report, the region comprises about 7200 sq miles of the Gulf Coastal Plain and includes all or parts of the following counties: Harris, Fort Bend, Waller, Brazoria, Galveston, Liberty, Chambers, Orange, and Jefferson (Fig. 1). Topographic relief is low, ranging from sea level at the Gulf of Mexico to 300 ft or more in northwestern Harris County.

In this upper Gulf Coast region, which embraces the most heavily populated and industrialized parts of Texas, industrial and municipal water supply is obtained chiefly from wells. Largest center of ground-water withdrawal is the Houston-Baytown area, where about 200 million gallons per day was pumped in 1956 for municipal and industrial use. Other large centers of ground-water withdrawal include the Alta Loma sector and the heavily industrialized Texas City area in Galveston County, where about 23 mgd was pumped in 1956. In the Freeport area in Brazoria County about 6 mgd was pumped in 1956 for city and industrial supply.

In addition to withdrawals in metropolitan districts, great quantities of ground water are supplied by irrigation wells to thousands of acres of rice. These wells are widely dispersed over many miles, principally in Harris, Waller, Fort Bend, Brazoria, and Liberty counties, and effects of pumping are not so readily noticed as in the industrial and metropolitan sectors.

Subsidence: Starting with the 1905-1906 line from Smithville, Tex., to Galveston, the U. S. Coast and Geodetic Survey has extended a network of first and second-order level lines throughout the upper Gulf Coast region. In 1918, when a line was run from Sinton, Tex., to New Orleans, La., a tie was made to the 1905 leveling at Houston. In 1932-1933 a line was run from Palestine, Tex., to Houston, and a good deal of leveling was carried out in the vicinity of Houston. At this time the entire network was adjusted to the Sea Level Datum of 1929.

In 1935-1936 and 1942-1943 several new lines were run and considerable releveling was performed. Supplementary adjustments were made after both the 1936 and 1943 levelings in order to reduce the elevations to the Sea Level Datum of 1929. These adjustments probably masked some of the subsidence that had occurred up to that time, although a certain amount of subsidence was noticed in the 1943 leveling.

When several lines in the vicinity of Houston and Galveston were releveled in 1951, the regional nature of the subsidence became apparent.[1] Direct comparison with the 1943 leveling was possible because the datum was not changed. Comparisons with prior leveling were unreliable because of differences in the early and subsequent datums.

In 1953-1954 many lines in the region were releveled and in 1957 the entire network, including the elevations previously determined, was readjusted to determine the changes in elevations as indicated by various levelings between 1905 and 1953-1954. In this instance the adjusted elevations were held fixed near the boundaries of the region where the bench marks seem to have remained stable. The only sea-level connection held fixed was the connection of the 1905 leveling to the 1903-1906 tidal series at Galveston.

Almost the entire region has been at least slightly affected by the subsidence, some areas to a great extent. The profiles of subsidence (Fig. 2) and the map showing the contours (Fig. 3) illustrate both regional and local changes.

A large area of subsidence is centered in the Houston-Baytown district, where the maximum recorded is about 2.7 ft between 1905 and 1954. This probably falls short of the actual maximum, since land surface subsided as much as 2.5 ft in the industrial section alone between 1943 and 1954. Sub-

A. G. WINSLOW and L. A. WOOD are with the U. S. Geological Survey, Austin, Tex. TP 59H2. Manuscript, Feb. 20, 1959. San Francisco Meeting, February 1959. AIME Trans., Vol. 214, 1959.

sidence in the Houston-Baytown area as a whole has been on a rather broad scale; in only a few localities do great variations occur within short distances. For this reason there is little visible surface evidence. In several places, however, particularly in the industrial section, certain features can be attributed to subsidence. In some instances deep-set well casings protrude from the ground where the land surface has subsided. In others there is surface evidence of faulting which may be related to subsidence.

The Texas City area has experienced more local subsidence than the Houston-Baytown vicinity (Figs. 2 and 3); both profile and contour map reveal great differences in the amount that has occurred within short horizontal distances. This differential subsidence has had visible results in the immediate vicinity of Texas City—protruding well casings, clogged sewers, and broken pipelines. Maximum subsidence along the line of profile (Fig. 2) has been about 3.5 ft between 1905 and 1954, but this line does not run through the industrial section, where even greater amounts have occurred. Industrial representatives in the area report a total of more than 4 ft.

Another subsidence center in the upper Gulf Coast region appears to be the Beaumont-Port Arthur-Orange area, where there is a concentration of industry. The total here is probably not as great as in the Houston-Baytown or Texas City sectors; however, there is a rather large area in which the land surface has subsided at least 0.25 ft in the years 1918 to 1954. During the same period about 1 ft of local subsidence took place in this area in the immediate vicinity of Spindletop oil field.

Another small area is centered at Freeport, where there is a concentration of industry and groundwater withdrawal from shallow sands. Subsidence here has been on a small scale; a maximum of about 0.5 ft was recorded during the perid 1943-1951. Record of earlier subsidence at Freeport is not available.

Geology and Hydrology: The upper Gulf Coast region of Texas is underlain by a thick sequence of unconsolidated fresh-water-bearing sands, sandy clays, and clays. Geological formations comprising the aquifers include the Lagarto clay of Miocene (?) age, the Goliad sand of Pliocene age, the Willis sand of Pliocene (?) age, the Lissie formation and the Beaumont clay, both of Pleistocene age. The formations consist largely of alternating beds of sand and clay; most individual beds are lenticular and not persistent over great distances.

Some of the formations consist predominantly of sand, others predominantly of clay. The Lagarto is principally clay but contains layers of sand, mostly fine to medium-grained.

The Goliad and Willis sands and the Lissie formation are not distinguished in the subsurface and are generally referred to locally as *Lissie*. The so-called *Lissie* is largely sand, which occurs primarily as discontinuous lenses interbedded with clay. The *Lissie* is the principal aquifer in the Houston area.

The Beaumont clay is composed of two members —the *Alta Loma* member and the upper member. The Alta Loma is primarily a massive sand bed,

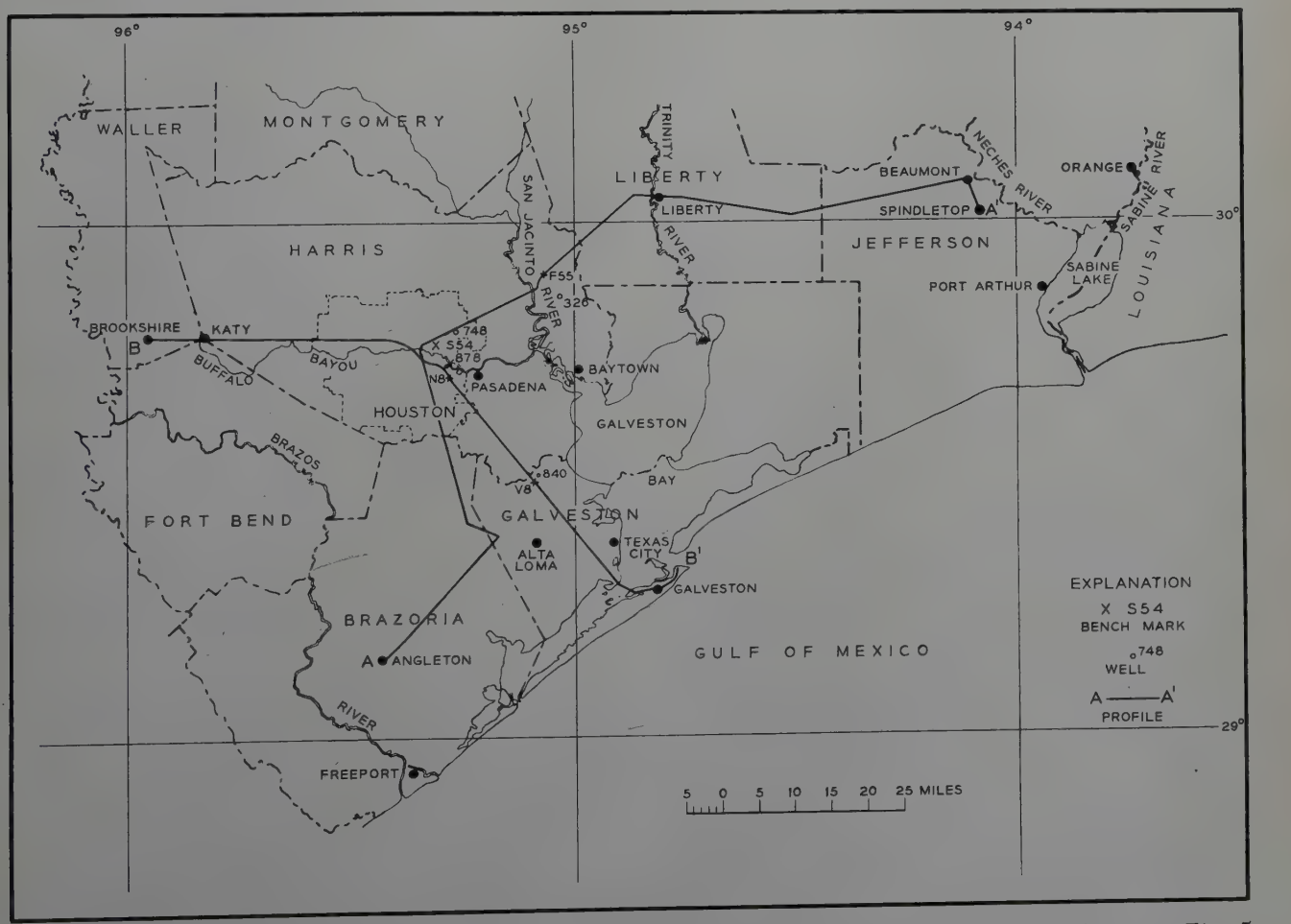

Fig. 1—Map of the upper Gulf Coast region, Texas. Subsidence of selected bench marks is shown in Fig. 5.

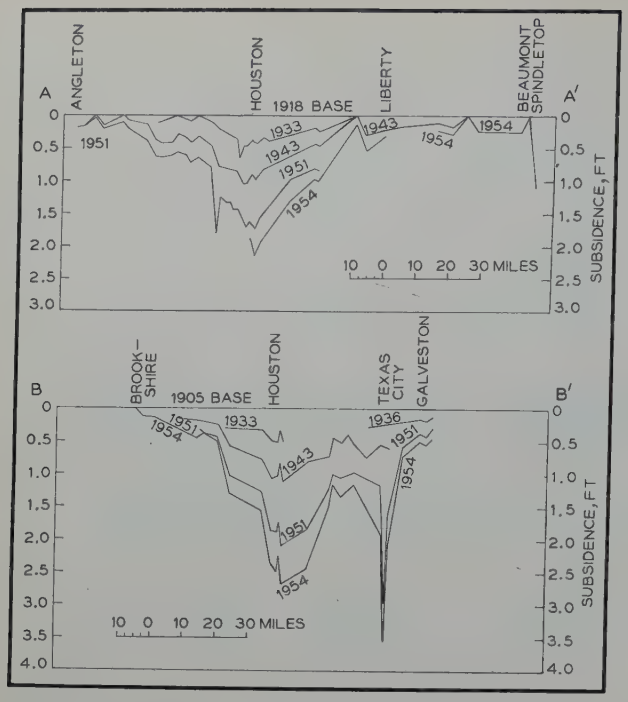

Fig. 2—Subsidence of the land surface along the lines A-A′ and B-B′ in the upper Gulf Coast region of Texas, 1953-1954. Locations of profiles are shown in Fig. 1.

though it does have a few clay layers. The most persistent single sand bed in the region, it can be traced from Freeport to the Louisiana line. It is the main aquifier in Galveston County, southeastern Harris County, and Orange County.

The upper member of the Beaumont clay consists chiefly of clay but contains thin lenticular beds of sand, most of it fine-grained. This member supplies comparatively large quantities of water to municipal and industrial wells in the Texas City area.

Geologic structure of the region is relatively simple. The formations crop out in bands roughly parallel to the coast and dip gently toward it. The older water-bearing beds dip 20 to 30 ft per mile; the younger ones may dip less than 10 ft per mile. The beds are disrupted locally by salt domes, some more than a mile in diameter, which nearly reach the surface in several places. No large-scale faulting has been observed in the younger beds, but there are many small-scale faults.

Although the principal water-producing zones in the upper Gulf Coast region are more or less distinct locally, they are all in hydraulic connection and regionally may be considered as a unit. Movement of water through the aquifer before groundwater withdrawals began has been described as follows (Ref. 2, p. 388): "Water moves from the intake areas down the dip of the beds, and when it passes beneath a confining layer (bed of lower permeability) artesian conditions are established. As soon

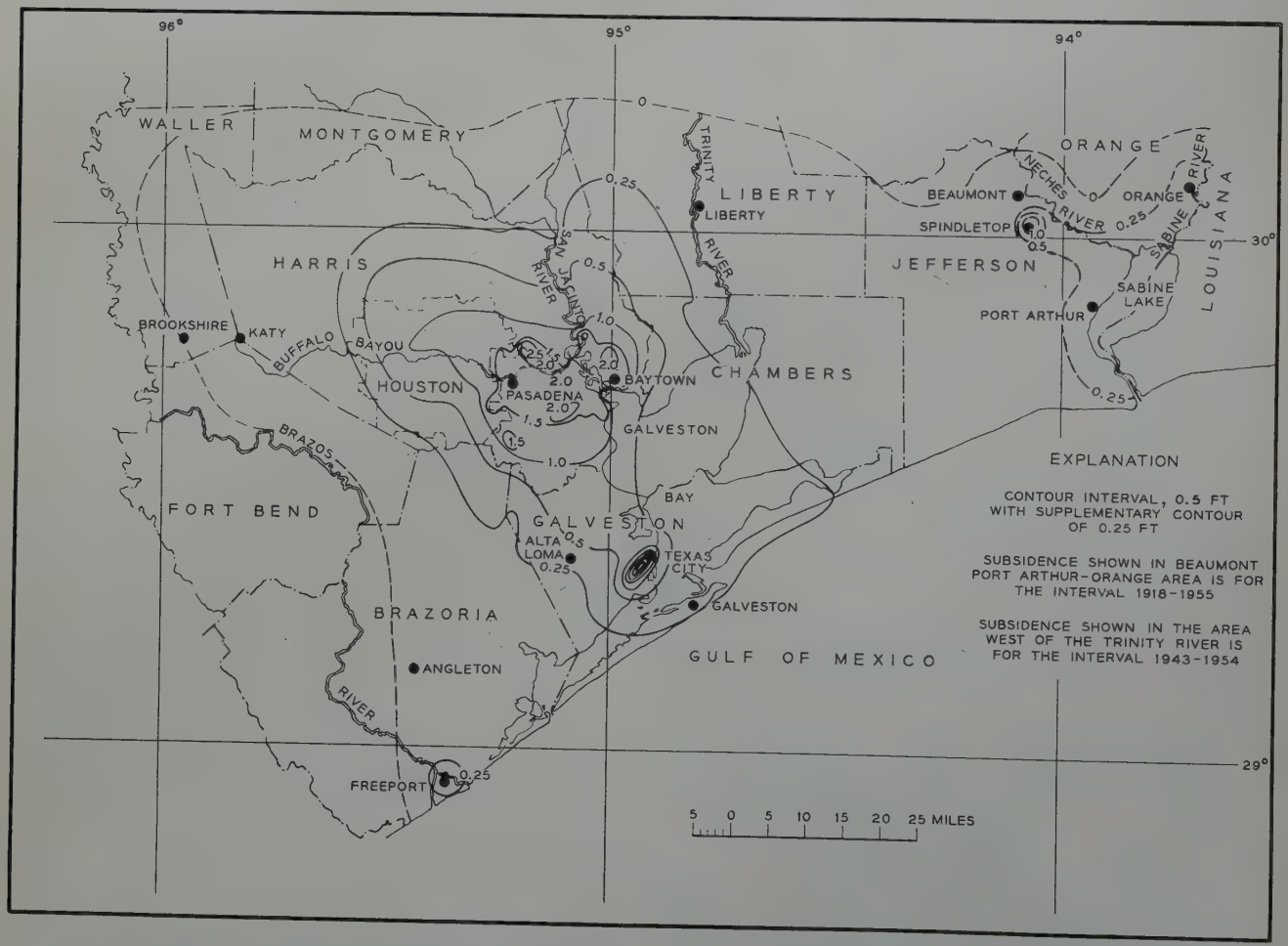

Fig. 3—Subsidence of the land surface in the upper Gulf Coast region of Texas during the period 1943-1954.

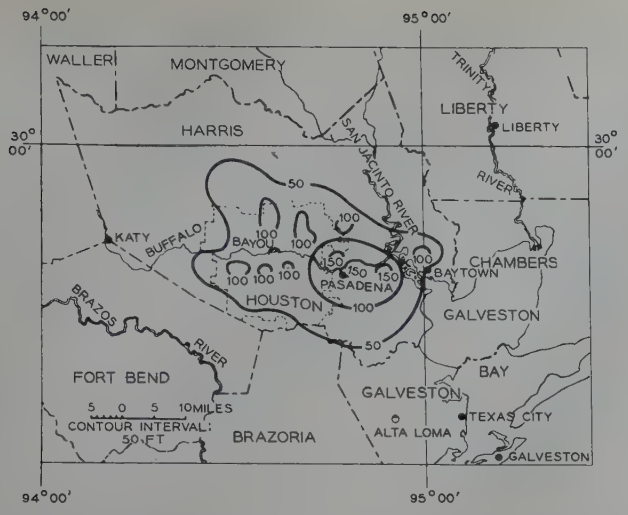

Fig. 4—Decline of artesian pressure head in the Katy-Houston-Pasadena-Baytown area of Texas, 1943-1954.

as these conditions occur, water will move upward through the clays (or beds of lower permeability) as well as laterally through the sands although . . . the vertical movement will be at a much lower rate than the lateral movement." Under such conditions both a vertical and lateral pressure gradient will be established and water will ultimately be discharged at land surface. The artesian pressure provides a buoyant effect that helps to support the aquifer (Ref. 3, p. 458).

Development of large ground-water supplies and consequent lowering of artesian pressure in the upper Gulf Coast region has disturbed the natural hydraulic gradients in the aquifer. Some sands have been pumped more heavily than others, and because of differences in permeability and the remoteness of hydraulic connection, pressure heads in different sands now vary greatly with depth. Fig. 4 shows the decline in artesian pressure head in the most heavily pumped sands in the Houston-Baytown area during the period 1943-1954; this is a composite of the decline in many individual sands, as most of the observation wells are screened in several.

Ground-water withdrawals in Harris County have been concentrated in three districts: 1) the Pasadena-Baytown area, where the water has been used mostly for industry; 2) the Houston area, where it is used chiefly for municipal purposes; and 3) the Katy rice-irrigation sector. In the Pasadena-Baytown district industrial demands have led to the concentration of wells within short distances, causing excessive water-level declines—especially in the vicinity of Pasadena, as shown in Fig. 4. In the Houston sector withdrawals have been largely from Houston's municipal wells, which are fairly well distributed throughout the city. This has resulted in more widespread and uniform decline of water levels than in the Pasadena-Baytown area. In the Katy rice-irrigation area the wells are even more widely dispersed and declines are less.

Although most ground-water withdrawals in Harris County have been from the *Lissie,* in the Baytown area and southeastern part of the county and in Galveston County the principal aquifer is the Alta Loma sand member of the Beaumont clay. In the Alta Loma area of Galveston County the development was started in 1898. Since that time water levels have declined some 150 ft, mostly prior to 1945.

In the Texas City area the principal aquifer is now the upper part of the Beaumont clay, but before 1948 larger quantities of water were pumped from the Alta Loma sand member. Problems relating to encroachment of salt water and the land-surface subsidence in the Texas City area resulted in partial abandonment of the Alta Loma as an aquifer in that locality when surface water was made available in 1948. This raised the Alta Loma water levels, which previously had dropped considerably. Continued withdrawals from the upper member of the Beaumont clay have lowered levels in that part of the aquifer, but in recent years the rate of decline has been very slow.

Withdrawals in the Beaumont-Port Arthur-Orange area have been concentrated largely in the Alta Loma sand, but declines in water levels have not been great. Considerable amounts were formerly withdrawn from the Beaumont-Port Arthur sector, but practically all the wells in that vicinity have been abandoned because of the encroachment of salt water. Most of the ground-water withdrawal at present is in the Orange district.

Causes of Subsidence: Land-surface subsidence caused by removal of ground water or other fluids has been observed in many places, and the mechanics of the processes involved have been investigated. Meinzer (Ref. 4, p. 90-93) states that in an artesian system the artesian pressure helps support the framework of the aquifer and that when the artesian pressure is lowered water is released from storage in the aquifer and the beds are compacted. He says also (Ref. 3, p. 458) that most of the compression takes place in the finer-grained materials. Tolman (Ref. 5, pp. 328-329) states that where an aquifer is confined by slightly permeable beds, the reduction in pressure heads in the sands will create a hydraulic gradient from the confining beds toward the sand and water will move slowly from the slightly permeable beds into the sand.

Poland and Davis (Ref. 6, pp. 294-295) have summarized possible causes of subsidence as follows: 1) loading at land surface, 2) vibrations at or near land surface, 3) compaction due to irrigation and farming, 4) solution due to irrigation, 5) drying out and shrinking of deposits, 6) oxidation of organic

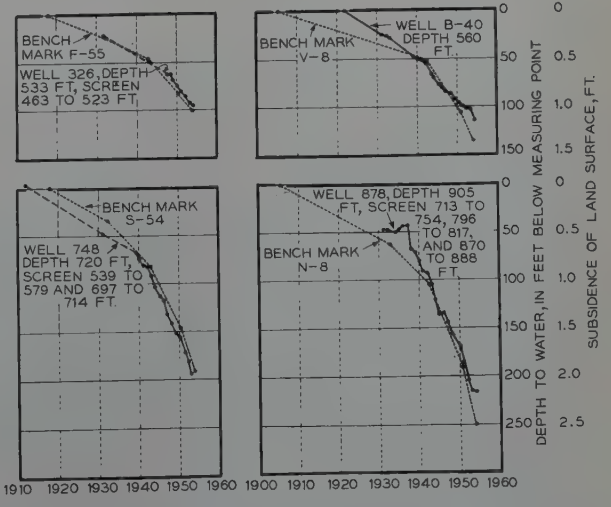
BENCH MARK F-55
WELL 326, DEPTH 533 FT, SCREEN 463 TO 523 FT.
BENCH MARK V-8
WELL B-40 DEPTH 560 FT.
BENCH MARK S-54
WELL 748 DEPTH 720 FT, SCREEN 539 TO 579 AND 697 TO 714 FT.
BENCH MARK N-8
WELL 878, DEPTH 905 FT, SCREEN 713 TO 754, 796 TO 817, AND 870 TO 888 FT.
DEPTH TO WATER, IN FEET BELOW MEASURING POINT
SUBSIDENCE OF LAND SURFACE, FT.
1910 1920 1930 1940 1950 1960
1900 1910 1920 1930 1940 1950 1960

Fig. 5—The subsidence of selected bench marks compared with the decline of artesian pressure head in nearby wells, upper Gulf Coast region of Texas. The locations of wells and bench marks are shown in Fig. 1.

material, 7) lowering of water table, 8) decline of pressure head in confined aquifers, 9) decline of pressure in oil zones due to removal of oil and gas, and 10) tectonic movement.

The first six of these possible causes of subsidence probably do not apply in the upper Gulf Coast region of Texas. Lowering of the water table is quite possibly one of the contributing causes of subsidence in the region, but direct evidence of this is lacking. An obvious case of subsidence caused by decline of pressure in oil zones due to removal of oil and gas is furnished by the profile at Spindletop (Fig. 2). Land-surface subsidence has been observed in other oil fields in the region, and subsidence in the Goose Creek field in eastern Harris County has been described by Pratt and Johnson.[7]

Tectonic movement may be a cause of subsidence, since obvious displacement has been noted along some of the many small faults known to exist in the region. It is not clear, however, whether the displacement is the result of strictly tectonic movements or whether the faulting is related to subsidence in the region due to removal of ground water or other fluids.

The principal and certainly most obvious cause of subsidence in the upper Gulf Coast region of Texas is the decline of artesian pressure head. Fig. 5 shows a remarkable coincidence between graphs of subsidence of individual bench marks and graphs of decline in water levels (artesian pressure head) in nearby wells. In the Houston area the ratio of approximately 1 ft of subsidence to 100 ft of decline of artesian pressure head has remained fairly constant throughout the period of record. In the Texas City area the ratio is greater.

Further evidence of relation between subsidence and decline of artesian pressure head is afforded by comparison of Figs. 3 and 4. Resemblance of the two maps is apparent. Subsidence has centered in the industrial area near Pasadena where the artesian pressure head has declined the most, becoming less at great distances from the area of large pressure declines in the industrial sector.

Relation of Volume of Subsidence to Volume of Ground Water Withdrawn: When the fine-grained materials in the fresh-water-bearing section compact, the volume of pore space lost by compaction is equal to the volume of subsidence. The volume of water yielded from storage in the clays can be determined by computing the volume of subsidence (1 ft of subsidence yields 1 ft of water). The data needed to compute accurately the volume of subsidence in the upper Gulf Coast region are not available; however, an approximate volume for part of the region can be determined from the subsidence contours in Fig. 3. An estimated 3.4×10^{10} cu ft of subsidence took place between 1943 and 1954 in that part of the region influenced by ground-water withdrawals in the Katy-Houston-Pasadena-Baytown areas. During the same period about 114×10^{10} gal was withdrawn from wells in the same area. Converting the volume of subsidence to gallons of water (3.4×10^{10} cu ft $= 25.4 \times 10^{10}$ gal), it can be seen that 25.4 or about 22 pct of the water pumped in the

$$\frac{}{114}$$

Katy-Houston-Pasadena-Baytown area represents water that had been stored in the fine-grained materials. Quality and quantity of data preclude an exact answer, but 22 pct is believed to be of the correct order of magnitude.

Effects of Subsidence: Continued land-surface subsidence in the region has had and will have certain undesirable effects. In the Texas City area structural difficulties have already occurred—protruding well casings, broken pipelines, reversed flow in sewage lines, and cracked foundations. In the Houston-Baytown area, where the process has been more on a regional scale, there have been comparatively few problems of this kind that can be attributed definitely to subsidence of the land surface, but in places where well casings have failed and foundations and highways have cracked, subsidence may have been the cause. The threat to structures throughout the area has been a matter of concern to industry, and plans for construction have been modified acordingly.

Another effect of subsidence has been lowering of land in the coastal areas. Part of the Baytown district once used for grazing is now tideland. In the Texas City area some of the land formerly believed high enough above sea level to be safe from hurricane tides is now subject to inundation during hurricanes.

The few effects that might be considered beneficial should be mentioned. About one fifth of the water made available to wells in the region has been freed from the fine-grained materials as the land subsided, obviating the need for greater pumping lifts. Furthermore, subsidence has centered in the Houston ship channel area, deepening the channel so that less dredging is required.

The question of first importance in any discussion of the subject is what is going to happen in this region in the future. Subsidence will probably continue indefinitely even if ground-water withdrawals are not increased, because the head in the shallow sands will continue to decline as it adjusts to the lower heads in the deeper sands. Reasonably accurate quantitative predictions of the future of subsidence in the region will require a much better knowledge of the causes and mechanics and the actual details of what is happening in the region. More research and collection of basic data are needed. The U. S. Coast and Geodetic Survey has proposed releveling every five years in this region, but the most important lines should be releveled more often, and additional level lines should be installed.

This report is based on data obtained during ground-water investigations made by the U. S. Geological Survey in cooperation with the Texas Board of Water Engineers and the cities of Houston and Galveston.

REFERENCES

[1] A. G. Winslow and W. W. Doyel: Land-Surface Subsidence and Its Relation to the Withdrawal of Ground Water in the Houston-Galveston Region, Texas. *Economic Geology*, 1954, vol. 49, no. 4, pp. 413-422.

[2] A. G. Winslow, W. W. Doyel, and L. A. Wood: Salt Water and Its Relation to Fresh Ground Water in Harris County, Texas. *USGS Water-Supply Paper 1360-F*, 1957, pp. 375-405.

[3] O. E. Meinzer and L. K. Wenzel: Occurrence, Origin, and Discharge of Ground Water. National Research Council: Physics of the Earth, vol. 9, chap. 10 in *Hydrology*, pp. 385-477. McGraw-Hill Book Co. Inc., New York, 1942.

[4] O. E. Meinzer: The Artesian-Water Supply of the Dakota Sandstone in North Dakota. *USGS Water-Supply Paper 520-E*, 1925, pp. 73-95.

[5] C. F. Tolman: *Ground Water*, 593 pp. McGraw-Hill Book Co. Inc., New York, 1937.

[6] J. F. Poland and G. H. Davis: Subsidence of the Land Surface in the Tulare-Wasco (Delano) and Los Banos-Kettleman City Areas, San Joaquin Valley, California. American Geophysical Union, *Trans.*, 1956, vol. 37, no. 3, pp. 287-296.

[7] W. E. Pratt and D. W. Johnson: Local Subsidence of the Goose Creek Oil Field. *Journal of Geology*, 1926, vol. 34, pp. 577-590.

Discussion of this article sent (2 copies) to AIME before Nov. 30, 1959, will be published in MINING ENGINEERING.

THE ELECTRONIC COMPUTER AND STATISTICS FOR PREDICTING ORE RECOVERY

by ROBERT F. SHURTZ

The author proposes a method used with some success on a magnesite deposit at Gabbs, Nev. He believes this procedure to be more sound than the blind practice of assigning uniform quality to large, sometimes vast blocks or ore on the basis of analyses made of a small number of samples.

When an ore deposit is evaluated on the basis of core sampling, questions always arise as to how much weight should be given the various sample grades and how the deposit should be divided into specific volumes assigned to corresponding grades. For a tabular deposit it is customary to use the so-called *zone-of-influence*. This zone is usually defined as the polygon in the plane of the deposit having corners halfway between a given core drill intersection and each of the nearest neighboring intersections. The volume of the ore in this polygon is assigned the analysis obtained from the drill core taken at the intersection. In massive or irregular deposits, volumes of various shapes may be defined with respect to the locations of drill core samples. These volumes may be regarded as three-dimensional zones-of-influence; the theory involved in assigning the values of the central analyses to the ore in the volumes is the same as that used in the case of a tabular deposit.

The zone-of-influence method was used in evaluating one of the magnesite deposits at Gabbs, Nev.[1-8]

R. F. SHURTZ, Member AIME, is Assistant to the Vice President, Basic Inc., Cleveland, Ohio. TP 4817 I. Manuscript, Aug. 13, 1959. AIME Trans., Vol. 214, 1959.

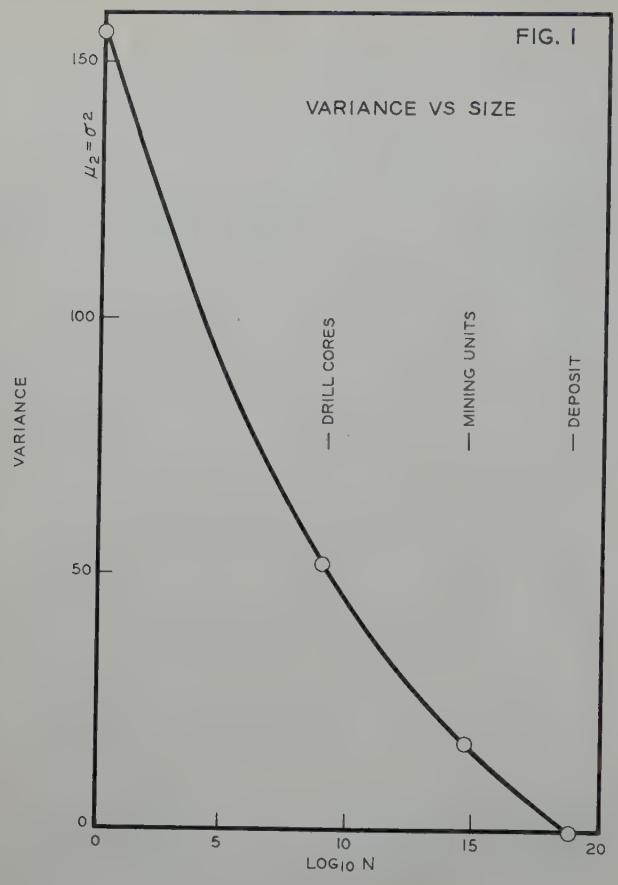

Original estimates of ore tonnages falling in the various ranges of quality were based on almost 5000 analyses of core samples from about 100 core drillholes. On the basis of this drilling a pit was designed for mining as much of the magnesite as possible without removing an excessive amount of the dolomite irregularly surrounding the deposit. The pit was then divided into horizontal benches 10 ft thick for mining. Each bench was subdivided into 100-ft squares and each square assigned the average grade of the drill intersection it contained. There were one to four intersections in each square, usually less than four. The concentrations of both lime and silica were considered in making the early estimates, although later experience has shown that control of the silica is relatively easy. For this reason the following discussion will be limited to the problem of lime concentrations.

Early experience in mining this deposit selectively showed that recovery of high-grade magnesite ore was substantially less than the proportion of high-grade ore calculated from the core-drilling results. Since it was known that this reduced recovery could not be attributed to poor operation in the quarry, a method was sought that would correct the estimates of ore tonnages falling within the desired ranges of quality.

At first a correction was made by calculating an experience factor equal to the ratio between the amount of each grade of ore recovered and the amount of the corresponding grade of ore estimated from the core drilling results. However, it was believed that the factors so derived could not be applied with confidence to the whole deposit, since their values must certainly depend heavily on the grade and distribution of ore in the first portion removed by mining. That portion happened to be of substantially lower grade than the average estimated for the whole deposit. It was suspected, therefore, that the experience factor for high-grade ore was smaller than it should be and that if this factor were applied to the whole deposit the total proportion of high-grade ore would be seriously underestimated.

Alternative methods of estimating the distribution of reserves in the deposit were carefully investigated. Almost from the start, it was clear that the difficulty lay in the great variability of magnesite ore quality over short distances in the deposit. The vertical core drillholes, for the most part spaced roughly on a 100-ft square lattice, were obviously too far apart to provide accurate direct information on the proportion of ore falling within various ranges of quality. The blastholes, drilled on 6.5-ft centers, provided accurate data on this point, but this information differed radically from that obtained from the core drillholes. This divergence is believed due to the fact that sampling is systematic with both kinds of drillhole and therefore heavily dependent on the interrelation between drillhole spacing and distances in the deposit over which quasi-periodic variations of quality may occur.[4] Preliminary consideration of various methods showed that accurate correlation of the two sets of drillhole data, though possible in principle, would be highly complicated and expensive to compute.

The most forthright attack on this problem, and one that illustrates the principles involved, would be a two-dimensional harmonic analysis of variation in the quality of each horizontal bench in the ore deposit, based on analyses of drill cores taken from that bench. However, such an analysis would necessitate simultaneous solution of a set of equations containing as many variables as there are drillholes through the bench. Since the number of holes is about 100 and the proposed quarry contains more than 40 benches, it is readily seen that a truly formidable amount of computation would be involved.

Harmonic analysis would contemplate the variations in quality as being due to periodic variations above and below the average quality of ore in a particular bench, and it is instructive to consider how the analyses from holes at large spacings are related to analyses from holes at smaller spacings in such a model of the quality variations. The periodic variations are regarded as sine and cosine waves of various lengths and amplitudes so oriented on a given bench that the positive and negative contributions of all these waves at any point added algebraically to the average lime concentration will approximate the lime concentration at that point on the bench. As the lengths of these waves are rational fractions of the linear dimensions of the bench, they do not require evaluation, that is, waves having lengths of 1/2, 1/3, 1/4, etc. of the linear dimensions of the bench must be considered. The number of these waves which can be summed together in a harmonic analysis is, therefore, equal to the number of observations of lime concentration made in the bench in question, that is, as great as the number of holes intersecting the bench in question. Although in the present instance this number is high enough to offer an appalling computation problem, it still is not sufficient to represent accurately the amplitude of the short waves when the initial long-period terms of the series are evaluated by the use of assays from the coreholes, which are spaced for the most part on 100-ft centers. However, analyses

from these holes could be used to evaluate an arbitrary group of the short-period terms selected as being most important on the basis of geologic considerations such as the spacing of joints, etc. In view of the uncertainties involved this was not carried out, even though it would have been interesting to see how the results came out.

Attention was also given the possible use of auto-correlation coefficients between successive analyses along the vertical lengths of the drillholes, a scheme resembling the one proposed and employed by H. J. de Wijs.[5] If auto-correlation could be found in the cores over vertical distances of some substantial number of feet, it might be reasonable to assume that high-grade ore extended for about an equal distance from the location of an intersection. This plan, and modifications of the same idea, was abandoned because geologic considerations showed that variation in quality over vertical distances in the deposit bears little or no resemblance to the variation over horizontal distances.

Consideration of the interdependence between sample sizes and the distribution of samples into quality ranges led finally to development and application of the procedure detailed in this article. To summarize briefly in advance, it may be pointed out that samples of individual mineral grains from the deposit would distribute themselves into only two classes of quality represented by the pure minerals magnesite and dolomite, since dolomite is the principal lime-bearing mineral involved. On the other hand, samples comparable in size to the size of the deposit itself would necessarily cluster very closely around the average lime concentration for the whole deposit, which is about 6.5 pct CaO. Therefore, as the size of the samples is continuously increased, there should be a transition from a bi-modal frequency distribution having all samples clustered at the ends of the range of quality between magnesite and dolomite to the uni-modal distribution with all samples clustered closely around the average. Discontinuities in this clustering tendency will be present because the samples are assumed to contain integral numbers of mineral grains. However, when samples containing as many as several hundred grains are considered, it is legitimate to treat the frequency distribution of samples over this range—from 0 to 30.4 pct lime—as being substantially continuous. Therefore, in discussing the interrelations between quality distributions in samples of drill core and in larger samples, it seems reasonable to regard the tendency toward clustering as being continuous.

It will be argued in the following discussion that this tendency is closely related to the clustering that would be observed in averaging the lime concentrations in groups containing equal numbers of drill core samples drawn at random from all the core samples actually taken from the deposit. In some respects this is similar to the relation between the probability of drawing a single ace in a poker hand and the probability of drawing 2, 3, or 4 aces, which is much less than that of drawing a single ace. A method will be proposed for evaluating this reduced probability of finding high-grade ore. That is to say, using the analogy of aces, it will be determined whether the probability relationship between a high-grade piece of drill core and a mineable unit of ore is most like the corresponding relationship between one ace and two, one ace and three, or one ace and four. An empirical method for determining this relationship using an electronic computer will be described, as well as an analytical method using procedures available from the theory of statistics.

It is of considerable incidental interest to note that a quantitative measure can be placed on the reduced probability and that the reciprocal of this measure can be used to indicate the efficiency of the selective mining procedures employed. This reciprocal can serve as a sort of precision constant for evaluating the effect of changes in mining practice.

Reducing the Variance: The foregoing comments have all been of a general and qualitative nature. We now proceed to illustrate quantitatively how the clustering effect described above can be expected to take place as the size of samples is increased and how this effect can be evaluated.

A reasonable quantitative measure for this clustering tendency must be selected. The variance, s^2, of a group of samples is often used for this purpose; for reasons that will soon be apparent it is also convenient to use it here. The variance for a group of analyses is computed by finding the average lime concentration for the group and then finding all the differences between this average and the concentrations of lime in the individual samples. The sum of the squares of these differences is the variance. It may readily be seen that all the differences, and the hence the variance, will be small when the concentrations of lime fall closely around the average concentration, whereas the differences and variance will both be large when the concentrations of lime differ greatly from the average. With reference to an earlier statement that the distribution of lime analyses from individual grains would consist of two groups of values at 0 pct and 30.4 pct lime, whereas the distribution of lime analyses from very large samples would cluster near the average value of 6.5 pct, it becomes plain that the variance must undergo an overall decrease as the size of the samples increases.

When a great many analyses are available, it is customary to group them into grade intervals in order to simplify calculation of both the average, m, and the variance. Standard texts[6, 7] on statistics give short cuts for accomplishing this, so only the fundamental formulas need be given here:

$$m = \frac{1}{n} \sum_{1}^{n} f_i x_i \qquad [1]$$

Table I. Observed Frequencies

Grade Interval	Range, Percent CaO	Designed Pit	Mined Ore
0	0 to 2	134	89
1	2 to 4	66	73
2	4 to 6	38	43
3	6 to 8	30	24
4	8 to 10	17	10
5	10 to 12	20	25
6	12 to 14	14	13
7	14 to 16	10	14
8	16 to 18	8	14
9	18 to 20	6	3
10	20 to 22	2	8
11	22 to 24	8	6
12	24 to 26	6	4
13	26 to 28	6	7
14	28 to 30	12	23
15	30 to 32	7	18

$$s^2 = \frac{1}{n} \sum_{i}^{n} f_i (x_i - m)^2 \qquad [2]$$

In these equations x_i is the value of the lime concentration at the midpoint of a grade interval and f_i the number of concentrations falling in that particular interval. The mean or average value for the lime concentration is represented in Eq. 1 by m and the variance in Eq. 2 by s^2.

It is of interest to calculate the means and variances to be expected in the distributions of lime concentrations from hypothetical samples of extreme sizes taken from the deposit in question. The value for the average lime concentration, m, has been determined to be very close to 6.5 pct. In the extreme case in which samples are taken consisting of the whole deposit less one grain of mineral, there are as many possible samples as there are grains in the deposit and all these samples will show lime concentrations exceedingly close to 6.5 pct. Whatever number of samples might be taken, the values of $x_i - m$ in Eq. 2 are so small as to make the value of s^2 come out at zero for practical purposes.

On the other hand, in samples consisting of single grains of mineral, these grains must, as already mentioned, be either of dolomite or magnesite. Since 78.6 pct of the deposit consists of magnesite and 21.4 pct of dolomite (excluding for present purposes the presence of other minerals), for any single grain picked at random the probability will be 0.214 that it is dolomite and 0.786 that it is magnesite. In 1000 such samples the expected numbers of dolomite and magnesite grains will be 214 and 786 respectively. The mean of this distribution can be verified by calculation with Eq. 1 as follows:

$$m = \frac{1}{1.00} [(0.214 \times 30.4) + (0.786 \times 0.00)] \qquad [3]$$

$$m = 6.5 \text{ pct CaO}$$

The variance comes out as:

$$s^2 = \frac{1}{1.00} [(0.214 \times 23.9^2) + (0.786 \times 6.5^2)]$$

$$s^2 = 155.4 \qquad [4]$$

Column 3 of Table I lists 384 lime analyses selected from the total of several thousand by a random procedure to be described later. Substituting the values from Table I for the f_i in Eq. 2 and using the percentages of lime at the midpoints of the grade intervals for the x_i, the variance of this frequency distribution may be calculated to be 51.9.

The three values just calculated for the expected variances of the distributions for examples of various sizes may be related to the sizes themselves. For this purpose, size of sample may be expressed in terms of the number of mineral grains it contains. Thus for samples of size 1, the variance is 155.4. The whole deposit is estimated to contain 5.95×10^{18} grains averaging 150 mesh, and the expected variance for samples approaching this size is 0. The core samples differ somewhat in size, but the average may be taken as a 5-ft cylinder of 2⅛-in. diam containing about 1.27×10^9 grains. The variance for the lime concentration in samples of this size is 51.9. In Fig. 1 these three pairs of values are plotted as a curve showing the variance of expected distribution as a function of the logarithm of sample size.

Taking into account the methods adopted for the quarry at Gabbs, it can be estimated roughly that a 30x30x10-ft ore block is the smallest size that can be mined selectively. Such a block contains about 4.19×10^{14} mineral grains. When this point is also plotted in Fig. 1, it is observed that the variance of distribution of the lime concentrations in samples of this size may be expected to be about 17. The ratio between the variance expected from drill core samples and the variance expected from mineable units is therefore approximately 3.1. This value is only a rough estimate, but because the abscissa is on a logarithmic scale it is not very sensitive to variations in the estimated size of the mineable unit.

It is now in order to show how the distributions of samples of different sizes may be related to one another in a wider sense. If, in the case of the magnesite deposit under consideration, it had been determined in advance that the mining method would not be capable of selecting units of ore smaller than 30x30x10 ft, a sampling system for evaluating the proportion of blocks of this size in various ranges of quality could have been used. A reasonable way to have done this would have been to select areas 30 ft square either at random or systematically in the area covered by the deposit and to sample each of these areas with a cluster of n drillholes. Quality of the 30x30x10-ft blocks stacked under each of the sample areas could have been evaluated by averaging the analyses of the drill cores from each sample block. The blocks in the stacks could then have been taken as a sample representing the total population of blocks of this size forming the deposit. However, the totality of core samples taken in this manner would be expected to have a quality distribution very like the one observed from the holes that were in fact drilled, i.e., the distribution of Table I. The expected relation between this distribution and the distribution of averages for the blocks described above will now be discussed.

In the first extreme case, the deposit may be regarded as comprised of core-sized pieces distributed at random. The distribution of the averages of n analyses of cores taken from each block can then be visualized easily by using a card-drawing model. Assume that an ace represents a core containing 1 pct lime, a deuce represents a core containing 2 pct lime, and so on. If n (in the previous paragraph) were equal to 3, a 30x30x10-ft block having 1 pct lime would be represented by a drawing of three aces. A block containing 2 pct lime would be represented by draws of ace-deuce-three or ace-ace-four with either combination in any order. These events are much less likely than the drawing of single aces or deuces. Statistics provide an exact method for handling such computations by use of characteristic functions.[8] It will suffice here to note that the characteristic function for the distribution of averages from the n analyses of our example is the nth power of the characteristic function for the distribution of the individual analyses.

$$\phi_n(t) = [\phi(t)]^n \qquad [5]$$

The variance of the distribution of the averages, $\frac{S_n^2}{n}$, is:

$$\text{Var}\left(\frac{S_n^2}{n}\right) = \frac{s_n^2}{n} \qquad [6]$$

Other higher order moments of the distribution of averages are obtained by similar simple equations.

On the other hand, if the core analyses from a volume as small as an individual block are not independent of one another this simplicity disappears. If, however, there is perfect correlation among the lime concentrations in the cores from each block, a new type of simplicity appears. Mathematically perfect correlation requires that the correlation coefficients, r_{jk}, between all possible pairs of lime concentrations taken from a group of n cores in a 30x30x10-ft volume in the deposit are all equal to 1. In this ideal second extreme case, all the cores from each block would have the same lime concentrations and the distribution of the lime concentrations for the blocks would be identical with that for the cores. The characteristic function of the distribution of the blocks is then identical with that of the distribution of cores to the first power instead of the nth power and the variance of the former distribution is equal to that of the latter divided by 1 instead of n as in Eq. 6.

The latter case can also be represented by a card-drawing model in which we imagine a sequence of 13 packs of cards each consisting entirely of cards of a single denomination with the packs arranged in order of the denominations and a fourteenth pack which is normal. The first card of the desired group of n cards is drawn from the normal pack and the remaining n-1 cards are drawn from the mth deck of the 13 stacked decks where m is the denomination of the first card drawn from the normal pack. Obviously the distribution of groups in this case will be identical with the distribution of single cards in the normal deck, just as the lime concentrations from the cores and the blocks in the hypothetical example were identically distributed.

It is here assumed that the relation in any actual ore deposit will fall somewhere between the extremes just described.

The essential idea is that the characteristic function of the distribution of blocks is estimated to be equal to some power of the characteristic function of the distribution of cores. For the moment, we are assuming that we know nothing about the characteristic function or the distribution function beyond the observed frequencies shown in Table I. However, for any n we can find the distribution function corresponding to the nth power of the characteristic function by drawing enough groups of n samples from the distributions of Table I to form a new distribution of average lime analyses for the n-fold groups. This is what was actually done for 1000 groups of 2, 3, 4, and 5 members each for core distributions from the mined portion of the deposit and from the deposit as a whole. Comparison of the amount of high-grade ore as mined with the amounts shown on the distributions derived for the mined ore for various values of n permitted interpolating a value for n. This value was used to interpolate between the derived distributions for the deposit as a whole in order to find an estimated distribution of mineable units in the deposit.

Before any further discussion of this estimate, details of the sampling procedure will be given.

Data Selection and Reduction: In view of the labor involved in making other statistical investigations not dealt with in this article, it was desired to reduce the number of analyses used. Therefore, 414 analyses were selected from the several thousand available by a random procedure to be described. The drawing was made in two groups of 207 samples each. The frequency distributions of lime analyses for these two groups were compared by means of the chi-squared test. Without giving details of this comparison, it can be stated that agreement was satisfactory. Both groups of analyses were then combined for further work. As was expected, some of the core locations selected at random fell in areas where rhyolite dikes or other types of intrusive rocks were found. These samples were rejected, leaving a total of 384 samples.

Table II. Derived Frequency Distributions Designed Pit

Grade Interval	Percent CaO	Cum. Freq.	Individual Frequency				
			$n = 1$	$n = 2$	$n = 3$	$n = 4$	$n = 5$
0	0 to 2	360	360	216	126	85	38
1	2 to 4	538	178	196	245	221	192
2	4 to 6	641	103	176	203	198	263
3	6 to 8	721	80	123	147	181	220
4	8 to 10	767	46	83	90	156	147
5	10 to 12	821	54	60	89	70	77
6	12 to 14	858	37	58	36	39	31
7	14 to 16	885	27	44	33	35	19
8	16 to 18	906	21	18	14	11	7
9	18 to 20	923	17	8	10	2	3
10	20 to 22	929	6	5	6	1	1
11	22 to 24	950	21	3	—	—	1
12	24 to 26	967	17	3	—	—	—
13	26 to 28	983	16	1	—	—	—
14	28 to 30	994	11	3	—	—	—
15	30 to 32	1000	6	2	—	—	—

Even though the samples were selected at random from the population of drill cores available, the locations of the core drillholes themselves are not at random. To avoid over-representation of certain portions of the deposit in which the drillholes are systematically more closely spaced, the area of the deposit was divided into sub-areas each 100 ft square; when there was more than one core drillhole in a square, one of the holes was selected at random to represent it.

The depths of the core drillholes from the surface to their intersection with the wall or bottom of the planned pit were divided by 50 and the integer nearest the result of this division was used as a weighting factor for that particular hole to assure that samples from that hole would have a probability of being drawn in rough proportion to the depth. In order for this to be done, a table of the numbers of the holes was prepared in which each number was entered a number of times equal to the weighting factor. This produced a table having 241 entries, which were assigned serial numbers from 0 to 240, 250 to 490, 500 to 740, and 750 to 990. Each entry had four numbers; for example, 1, 251, 501, and 751 all corresponded to the second entry in the table.

A table of six-digit random numbers was used to select entries from the table of drillhole numbers and to select simultaneously a depth from the corresponding drillhole. To do this, the first three digits of the six-digit number were used to select the entry in the table of drillhole numbers. If these first three digits comprised a number not entered in the table, e.g., 247, that random number was discarded and the next random number used.

The depth in the drillhole so selected at which the analysis should be taken was determined by the last three digits in the six-digit random number. If these last three digits formed a number greater than the depth of the hole within the designed pit, then

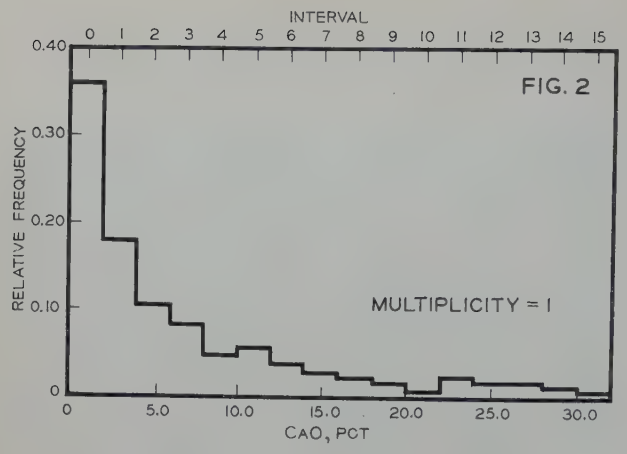

FIG. 2

the depth of the hole was divided into the last three digits and the remainder was used as the depth from which the core sample was selected. Many other ways can be proposed for carrying out the selection process although, in spite of the apparent complexity, the writer and his assistant required only one afternoon to select and tabulate the 414 analyses.

Many of these same core drillholes passed through a portion of the deposit from which well over a million tons of rock had already been mined. The magnesitic core drill samples from this portion of the deposit numbered 374. In view of this small number, the whole population of core samples for the quarried portion was used.

Table I shows the distribution into grade intervals of the two groups of samples thus far described. It will be observed that there is a marked tendency toward the appearance of a second maximum in the range from 28 to 31 pct lime. This secondary maximum is caused by the incursion into the pit of substantially pure dolomite which can easily be discarded during mining. Therefore, when the frequency distributions were recalculated to a base of 1000 samples, the secondary maxima at the dolomitic end of the range were eliminated by extrapolation of the smooth curves through this range of concentrations. In the actual calculation of reserves, the total tonnage of rock to which the derived frequency distribution was finally applied was reduced in proportion to the number of samples discarded by this smoothing process. The result of these operations is shown in Table II in the fourth column under $n=1$.

Computation of Derived Distributions: The cumulative frequencies of Table II were all punched in each of a group of 1000 Remington-Rand cards in preparation for computing the derived distributions. The lime concentrations at the midpoints of the grade intervals were wired on the plug boards for the Univac-60 on which the programs were run. A lead card containing a random number having eight digits was sent through the computer at the beginning of each run. A total of eight runs was required to produce the twofold, threefold, fourfold, and fivefold averages for each of the two distributions of samples. A different random number was used, of course, on each of the eight lead cards.

The computer was programmed to develop its own random numbers using Lehmer's method,[9] starting from the number on the lead card for a given program. The cumulative frequencies punched on each of the program cards were range-tested by subtraction from the first three digits of the random number then in storage in the computer. When a negative result was found, the percentage of lime appropriate to that range of cumulative frequencies was accumulated in the storage for lime percentages and the number 1 was accumulated in the cycle-counting storage. The computer then range-tested the accumulated number in the cycle-counting storage to determine whether the multiplicity for that program, 2, 3, 4, or 5, had been reached. If it had not, the computer calculated another random number, selected the approximate range of frequencies, accumulated the number corresponding to the percentage of lime, accumulated another unit in the cycle-counting storage, and range-tested again for multiplicity. When the desired multiplicity had been reached, the accumulated percentage value for lime from the several steps was divided by the number of cycles to produce an average. The average was punched in the card and then in the computer, and the whole operation was repeated on the next card. The averages for all four multiplicities were punched in each card by changing the location of the punch output between programs.

For the high multiplicities as many as 160 separate steps were required on a single card, so the computer worked much more slowly than usual. Even so, only about one working day of computer time was necessary. Some additional time was required on the tabulating machine to assemble the averages from the cards.

There is nothing novel about this procedure, which is a common variation of the class called *Monte Carlo methods*. The computer program has been discussed here only to demonstrate the principle involved and to assist those who may wish to attack similar problems. It is obvious, for example, that with a probability of 1 in 1000, the first three digits of a truly random number may be any number between 000 and 999. To illustrate the computation procedure described, the 538 to 641 frequency range (Table II) corresponding to the number of analyses in the grade interval between 4 and 6 pct lime will have 103 chances in 1000 of being selected in any given cycle. This is equal to the probability of finding in the deposit a core sample having a lime concentration between 4 and 6 pct. The average lime concentration in this range is very near 5 pct. Thus, during the programs, the computer was in effect drawing random groups of n lime concentrations with the same probability that the concentrations occur in drill cores.

The same result would be obtained by writing 5 *pct* on 103 slips of paper and the other average lime concentrations on the numbers of slips shown

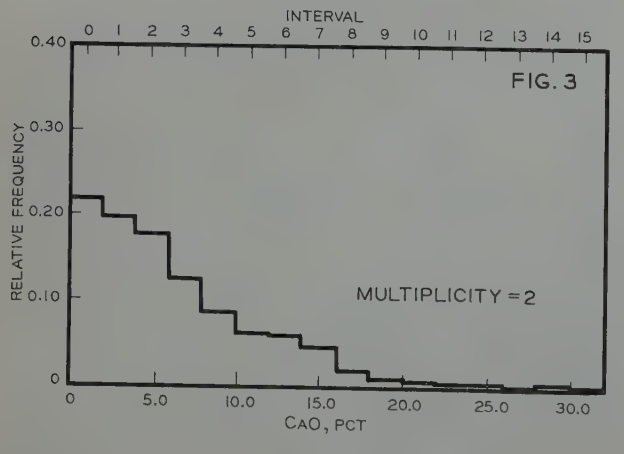

FIG. 3

opposite the corresponding ranges in Table II under $n=1$. The total number of slips would then be 1000. All of these could be shuffled together and dealt, for example, into piles of five slips each. The numbers on the slips could then be averaged. When 1000 such averages had been obtained in this way, the distribution of these averages would be very like that shown for $n=5$ in Table II. This procedure would be unpleasantly time-consuming but by no means an impractical substitute when a computer is not available.

The derived distributions for the several multiplicities, which are all based on the observed distribution for the designed pit, are shown in Table II under appropriate values of n. In Figs. 2-6, the histograms representing these distributions, the gradual tendency toward increased clustering around the average lime concentration at 6.5 pct is obvious. Variances for the distributions for n (multiplicity) = 1, 2, 3, 4, and 5 are 51.96, 25.88, 17.84, 14.12, and 11.12 respectively. These should be 51.96, 25.98, 17.32, 13.24, and 10.39 in strict accord with the inverse relation to n set forth in Eq. 6.

The derived distributions based on the observed distribution for the mined portion of the deposit are

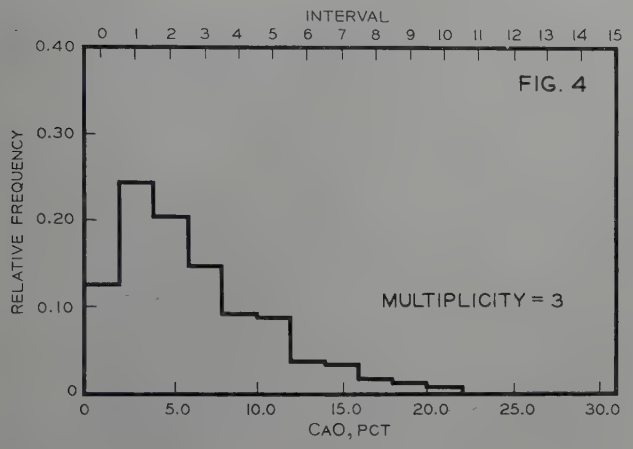

not detailed here. The only use made of these consisted of calculating from them the expected proportions of ore averaging 2 pct lime. An accurate record of the proportion of ore of this grade which was actually recovered was available for comparison with the proportions on the derived distributions in order to determine the estimated value for n.

The lower portion of Fig. 7 shows how n was determined graphically. The curve labeled *Pit 9-1-56* is drawn through the five points showing the relative frequencies of samples from the observed distribution ($n=1$) and from the derived distributions ($n=2$, 3, 4, or 5) for ore mined before Sept. 1, 1956. The points are for the 0th grade interval, which includes lime concentrations from 0 to 2 pct. The upper curve labeled *Designed Pit* is drawn through the relative frequencies for this interval taken from Table II. The rapid decrease in the frequency of averages in this interval with increasing n strikingly illustrates the main argument being made here. The smoothing practiced is deemed warranted by the random fluctuations that appear as a result of the limited number of samples drawn by the computer and the irregularities in the observed distributions. The proportion of ore averaging 2 pct lime is taken as being double the proportion averaging 1 pct lime, which is that ore falling

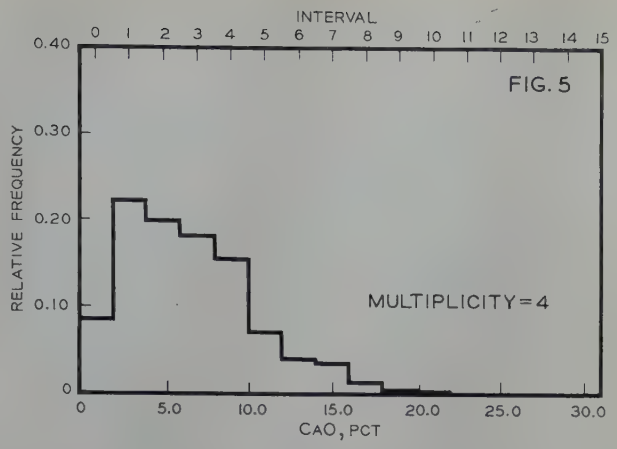

in the 0th interval. This statement is not true for $n=1$ because there is not an equal or larger amount of ore averaging 3 pct lime to average with the higher-grade ore in this case. However, discussion in the present instance will not be concerned with values of n near 1.

The proportion of ore actually mined in which the lime concentration averaged 2 pct was 0.14. Therefore, a value for the multiplicity should be selected which will yield a proportion of 0.07 of ore in the 0th interval for the derived distribution for mined ore. When this is done as shown in Fig. 7, the estimated multiplicity turns out to be 3.2, in good agreement with the crude value previously obtained by much more general reasoning. This suggests that the crude approach described under *Reducing the Variance* may be useful in the absence of other data, although more experience with its use and a liberal application of good judgment are desirable.

Turning now to the other grade intervals, the variations of the estimated proportions of ore in these intervals are shown in Figs. 7, 8, and 9. In each case, the average lime concentration is equal to twice the interval number plus 1, a convention needed for later discussion. The estimated proportion of ore in the 3 pct lime grade interval remains fairly constant over the range of multiplicities investigated, while the proportions for the intervals from that for 3 pct lime up to that for 13 pct lime increase with multiplicity as an expression of the tendency to group around the average. Still higher intervals show the decreases to be expected at the ends of the range of concentrations. By taking the ordinates of these curves at $n = 3.2$, it is possible to find the final interpolated derived distribution for the deposit. This is shown in Fig. 10 as a cumula-

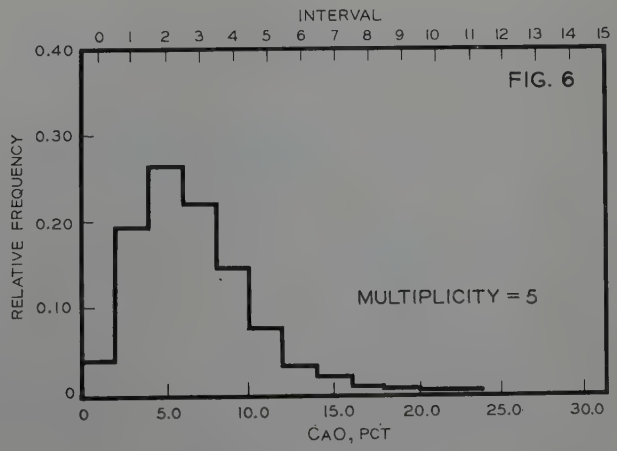

tive curve for ore of lower grades than the high-grade direct mining ore containing 2 pct lime.

This completes the task of distributing the ore in this deposit into ranges of quality by a method that is believed to be more realistic and theoretically more sound than the commonly used zone-of-influence methods. It is time now to point out some consequences of the theory advanced here.

Discussion: The importance of reducing the variance in evaluating this deposit springs from the fact that the standard deviation of distribution is large as compared to the ranges of quality into which output from the pit is to be divided. The standard deviation is the square root of the variance, and it is often used to express quantitatively the spread of a frequency distribution. Dimensions of standard deviation are the same as those of the mean, in this case, percent lime. In the simple case of the normal frequency distribution, 68.269 pct of the observations will be expected to lie within one standard deviation of the mean, 95.450 pct within two standard deviations, etc., cf. Cramer.[10] For other distributions, similar but less accurate limits can be set using the Bienaymé-Tchebychef inequality.[11]

In the present instance, the important dividing line between direct mining ore and beneficiating ore occurs on the low side of the average quality of the deposit. Therefore, as the variance and hence the

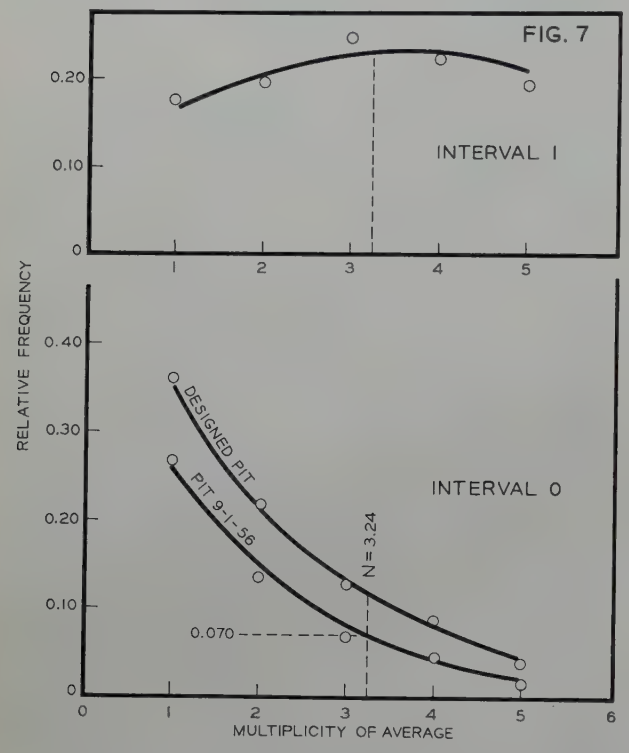

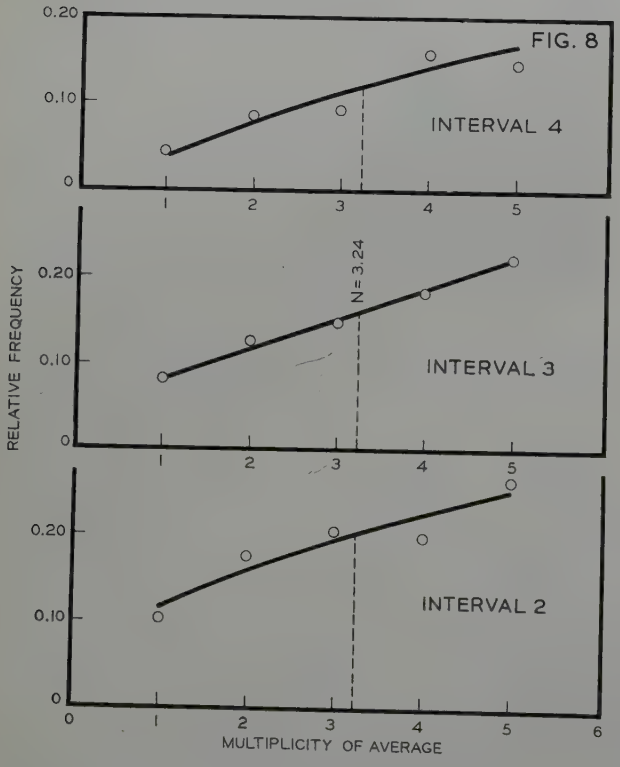

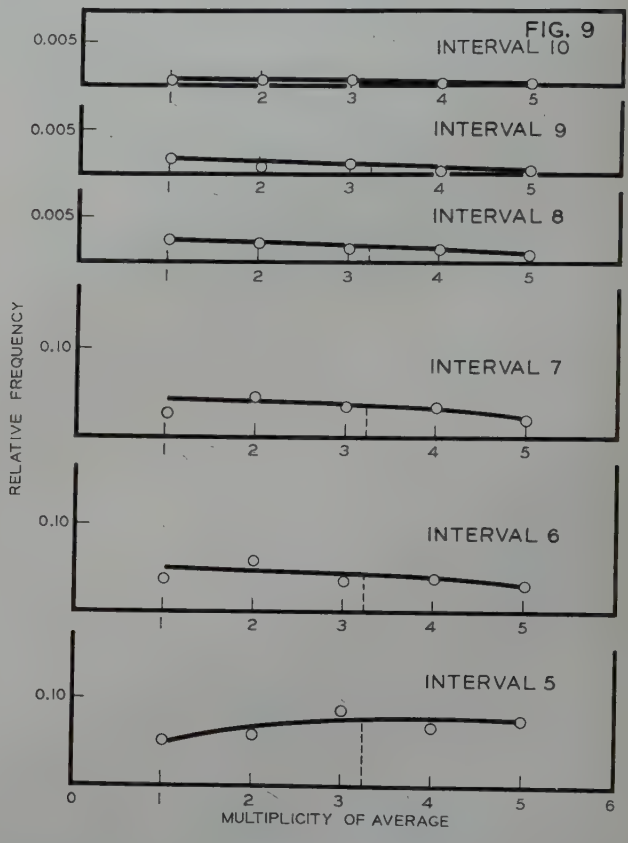

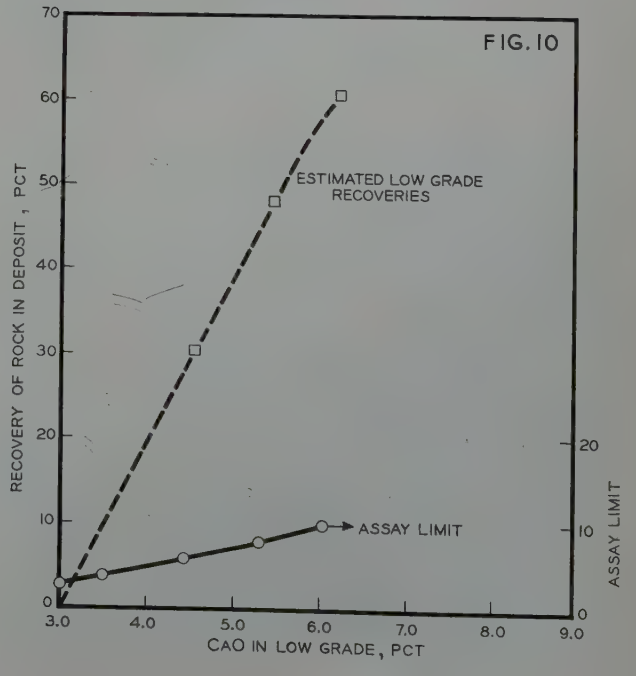

standard deviation are reduced, the clustering toward the average that must occur—unless the mining method is precise enough to distinguish between drill-core sized pieces—*moves ore upward* toward the average and out of the relatively narrow high-grade range. This, of course, increases the estimate of beneficiating ore available, although this is hardly a blessing.

The estimated amount of beneficiating-grade ore in this case is also augmented by the fact that ore *moves down* toward the average from the high-lime ranges. This occurs because the dividing line at about 10 pct lime between low-grade ore for direct use and waste is well on the high side of the average, so that the proportion of this grade is also increased over the expectation suggested by the unadjusted distribution of drill cores.

It is interesting to see how reduction of the variance and standard deviation of the distribution of assays for a metallic ore, say copper, might affect recovery in mining. Let it be assumed that the mean concentration of copper is 0.5 pct and the standard deviation of assays 0.1 pct. If the assay limit is 0.3 pct, the range of concentrations in samples accepted as ore runs from 0.3 pct upward. This range includes the average concentration, so reduction of variance resulting from the limited selective power of whatever mining method is used will be expected to concentrate the concentrations of copper observed during mining even more strongly in the range acceptable as ore. As standard deviation in this case is relatively small, the concentration effect will not be very important. For example, assuming a normal distribution of assays in the statistical sense, the number of samples having copper concentrations below 0.3 pct may be taken as equal to the proportion of the area of the normal distribution lying below the mean minus twice the standard deviation. This proportion is only 2.3 pct. If the reduced variance for mineable units is estimated to be one half the variance for samples, the standard deviation will be 0.071. Now the assay limit lies 2.82 standard deviations below the average and only 0.3 pct of the mineable units may be expected to be waste. The difference is not important.

However, if the standard deviation had been 0.3 pct, amounts of waste would have been estimated at 25.2 pct and 17.5 pct for samples and mineable units respectively, under the assumptions made in the preceding paragraph. This phenomenon accounts for the fact that such deposits, which have average concentrations above the assay limits, often produce more ore than is originally estimated.

Now let it be supposed that the cut-off assay is 0.6 pct, that the mean concentration is at 0.5 pct, that the standard deviation for samples is 0.3 pct, and that the assay distribution is again represented reasonably by a normal curve. Now only 37 pct of the deposit is ore when calculated by use of the unreduced variance. If the mining method selected, taken in conjunction with the characteristics of the deposit, brought about a reduction to half this variance, the standard deviation would be 0.21 pct and the expected amount of ore would fall to about 32 pct. If the reduced variance is one third the original variance, standard deviation would be 0.17 pct and the expected amount of ore would decrease to 28 pct. Although fairly subtle, these changes may cause large deviations between estimates and results if they are not taken into consideration.

Use of Analytic Frequency Functions: It often happens, in predictions of quality distribution, that there are not enough samples to form an acceptable frequency distribution. When this problem arises it is possible to use any one of the various analytic frequency functions having self-reproductive properties and adequately describing the distribution of quality in the deposit. The electronic computer may be used in this case also, but a synthetic frequency function is believed more reliable. Such functions, in a sense, embody the results of the geological influences that shaped the distribution of quality and for this reason may be expected to smooth out the random fluctuations, inevitable in a small group of samples, in a manner concordant with the factors that produced the deposit.

Of these functions, two are appropriate to the distribution of quality in the magnesite deposit at Gabbs, namely, the negative binomial distribution and the logarithmic normal distribution. The first of these will be illustrated here.

The frequency distributions from the Gabbs deposit are highly skewed positively and so are not adequately described by the normal distribution, which was used in the foregoing discussion only for the sake of simplicity. The equation of the negative binomial distribution is:

$$f(x) = \left(\frac{m}{1+Bm}\right)^x \frac{(1+B)\,(1+2B)\ldots[1+(x\text{-}1)B]f(0)}{x!} \qquad [7]$$

Details concerning this distribution may be found in Burrington and May,[12] Feller,[13] and Condon and Odishaw.[14] A recursion formula more useful for computing such a distribution over its whole range is given below along with the significance of the various symbols.

$$f(x) = f(n+1) = f(n)R\left[\frac{Bn+1}{n+1}\right] \qquad [8]$$

$$R = \left(\frac{m^2}{s^2}\right) \qquad [8a]$$

$$B = \frac{s^2-m}{m^2} \qquad [8b]$$

Table III. Negative Binomial Frequency Distributions

Grade Interval	Range, Percent CaO	Mined Ore Obs.	Mined Ore Calc.	Designed Pit Obs.	Designed Pit Calc.	Derived $n = 3.1$	X^2 Interval
0	0 to 2	267	247	360	317	109	0
1	2 to 4	218	186	178	185	198	1
2	4 to 6	129	140	103	127	213	2
3	6 to 8	71	105	80	91	178	3
4	8 to 10	31	79	46	67	126	4
5	10 to 12	75	60	54	50	80	4
6	12 to 14	39	45	37	39	47	5
7	14 to 16	41	34	27	29	26	5
8	16 to 18	42	25	21	22	14	6
9	18 to 20	9	19	17	17	7	6
10	20 to 22	23	14	6	13	3	7
11	22 to 24	18	11	21	10	—	7
12	24 to 26	13	8	17	8	—	8
13	26 to 28	10	6	16	6	—	8
14	28 to 30	7	5	11	5	—	8
15	30 to 32	7	4	6	4	—	8
	Chi-squared	—	12.38	—	8.04	—	
	$P(m = 6)$	—	0.11	—	0.24	—	
	Mean	—	3.05	—	2.75	2.75	
	Variance	—	12.32	—	12.96	3.99	
	B	—	1.00	—	1.35	0.16	
	$f(0)$	—	0.25	—	0.32	0.10	
	R	—	0.753	—	1.35	1.90	

$$f(O) = \left[\frac{s^2}{m}\right]^{\frac{-1}{B}} \qquad [8c]$$

Table III shows the calculated negative binomial distributions corresponding to the mined ore and the ore in the designed pit. The results of the chi-squared tests[15] show only moderately good fits. However, from a practical point of view, inspection of the table shows that the variations for the various grade intervals are, for the most part, not alarming in view of other uncertainties afflicting the case.

The negative binomial distribution for the mined ore was adjusted by reducing the variance and calculating several derived distributions so that a curve could be drawn relating n (multiplicity) with the amount of ore containing 2 pct lime. Fractional values were freely used for n, a recourse not readily available when distributions are derived on the computer. The estimated value for n turned out to be 3.1, in quite satisfactory agreement with the values of 3.1 and 3.2 found previously. The derived distribution for the ore in the designed pit is also shown in Table III for this value of n. The relative frequencies shown for the various grade intervals are in reasonable agreement with the computer results, which may be read from Figs. 7, 8, and 9, at the value 3.2 for n.

Table IV. Percent CaO in Core Analysis

2.62	11.48	15.68	1.98
0.66	1.12	0.77	3.45
15.80	11.91	0.77	2.36
1.81	3.20	3.51	0.60
2.59	1.99	11.58	10.48
0.89	1.03	1.52	

Now that the type of distribution to be used has been decided upon, and the value for n deduced, an illustration of an application to a single bench may be given. Table IV shows the analyses of 23 cores from the core drillholes passing through one of the benches in the pit. One of the problems encountered in planning production from this pit is that of predicting the rate at which ore of various grades will be produced in the future. To judge from the analyses in the table, well over half the ore on this bench should be of excellent quality, while there should be only a little ore lying in the intermediate range which is used for flotation feed.

These holes are roughly at random locations on the bench. They represent about 220,000 tons of ore. Taking moments in terms of the arbitrary grade intervals, $m = 1.84$, i.e., the average lime concentration is 4.68 pct. The variance is 6.306 in the arbitrary units, but this value must be adjusted for bias on account of the smallness of the sample (16) using the factor $(n\text{-}1/n)$ or 23/22 where n is the number of samples. The adjusted value is 6.593. When this is divided by 3.1, the multiplicity determined for the deposit gives the reduced variance 2.13. This value and Eqs. 7 and 8 are used to calculate Table V.

Table V. Expected Quality Distribution Single Bench

X	CaO, Pct	$f(x)$	X	CaO, Pct	$f(x)$
0	1.0	0.179	4	9.0	0.065
1	3.0	0.285	5	11.0	0.026
2	5.0	0.246	6	13.0	0.009
3	7.0	0.153	7	15.0	0.003

The amount of high-grade ore averaging 2 pct lime as estimated from this distribution is 35.8 pct. The amount estimated from the quality contour map prepared from the analysis of the blast drillholes was 42 pct. About 30 pct of the bench was actually recovered as ore of this grade. The amount of ore of a grade suitable for flotation feed at an average lime concentration of 4.5 pct is estimated from Table V to be 35.1 pct. The amount shown on the contour map was 38.2 pct. No record was kept of the amount of this quality actually mined from the bench in question, but it seems reasonable that the agreement between prediction and performance would have been acceptable. Certainly both the proportions calculated here are far more accurate than the expectation based on the unadjusted core drill analyses.

Conclusion: In presenting the results reported in these paragraphs, the writer has been constantly tempted to discuss each of the many side issues that have been raised either overtly or by implication. No doubt his attempt to steer a middle course will leave some readers with the impression that grievous omissions have been incurred and others with the impression that trivial facts have been belabored. All questions dealing with statistical theory have been left for investigation by those sufficiently interested to turn to the standard texts covering this subject. The author has not attempted to write a text on statistics and probability and does not claim the competence needed for such a task. The reference given will provide an excellent starting point for a fuller inquiry into the theories presented here.

The author does strongly believe that adjustments such as those proposed here and used with some success on the deposit in question have more theoretical justification than the blind practice of assigning uniform quality to large, sometimes vast blocks of ore and then expecting these blocks to distribute themselves quality-wise in accordance with the small number of samples that have been analyzed. When hand sorting is used this practice is justifiable, but with large-scale modern mining methods, some reduction in the spread of quality is inevitable and measures should be taken, using all the statistical tools available, to determine the amount of this reduction and the nature of the resulting distribution.

REFERENCES

[1] E. Callaghan: Brucite Deposit, Paradise Range, Nevada, A Preliminary Report. University of Nevada *Bull*, 27, 1933, p. 1.
[2] C. J. Vitaliano and E. Callaghan: Geologic Map of the Gabbs Magnesite and Brucite Deposits, Nye County, Nevada. *USGS Mineral Investigations Field Studies Map MF-35.*
[3] C. Martin and H. P. Willard: Quality Control in the Selective Mining of Magnesite at Gabbs, Nevada. Unpublished, 1956.
[4] L. H. Madow: Systematic Sampling and Its Relation to Other Sampling Designs. *Journal of the American Statistical Association*, 1946, vol. 41, pp. 207-214.
[5] H. J. de Wijs: Statistics of Ore Distribution. *Journal of the Royal Netherlands Geological and Mining Society*, Part I, November 1951, and Part II, January 1953.
[6] H. Cramer: *Mathematical Methods of Statistics*, p. 174 et seq. Princeton University Press, 1946.
[7] W. Feller: *An Introduction to Probability Theory and Its Applications*, p. 213 et seq. John Wiley & Sons Inc., New York, 1957.
[8] H. Cramer: *Mathematical Methods of Statistics*, p. 188 et seq.
[9] G. R. Stibitz and J. A. Larrivée: *Mathematics and Computers*, p. 191. McGraw-Hill Book Co. Inc., New York, 1957.
[10] H. Cramer: *Mathematical Methods of Statistics*, p. 558.
[11] H. Cramer: *Mathematical Methods of Statistics*, pp. 182-183.
[12] R. S. Burrington and D. C. May: *Handbook of Probability and Statistics*, p. 191. The Handbook Publishing Co., 1953.
[13] W. Feller: *An Introduction to Probability Theory and Its Applications*, p. 109 et seq. and p. 131.
[14] E. U. Condon and H. Odishaw: *Handbook of Physics*, pp. 1-158 et seq. McGraw-Hill Book Co. Inc., New York, 1958.
[15] R. S. Burrington and D. C. May: *Handbook of Probability and Statistics*, p. 178 et seq.
[16] H. Cramer: *Mathematical Methods of Statistics*, p. 351.

Discussion of this article sent (2 copies) to AIME before Nov. 30, 1959, will be published in MINING ENGINEERING.

TECHNICAL NOTE

FISHING TOOLS FOR RETRIEVING GAMMA-RAY LOGGING COMPONENTS

by CARL M. BUNKER and J. M. OHM

Two special tools for recovering gamma-ray probes and logging cable from drillholes have been designed by Ohm and Bunker and constructed by Ohm. Though intended specifically for U. S. Geological Survey equipment, they may be used with other equipment of the same general type.

Fishing Tool for Probes: A fishing tool of the overshot type (Fig. 1) was designed to retrieve logging probes (sondes) that become disconnected from the logging cable and are trapped in the drillhole. When the tool slides over the top of the gamma-ray probe, studs on the bottom engage the shoulder near the top of the probe (Fig. 2), which is then pulled to surface.

The barrel can be constructed from brass or steel tubing. Wall thickness is not a critical dimension, but the tool should be heavy enough to sink through mud or water in the drillhole.

The internal length of the tool must be enough to prevent interference with the upper end of the probe head as the tool slides over it. The design of the probe head used by the USGS required a minimum free space of 2½ in. inside the fishing tool, which was made 7½ in. long to increase the weight.

The lower end, which engages the shoulder of the upper end of the probe, contains three studs placed at 120° around the circumference of the tool and held in the engaging position by the tension of a spring wire. The studs can be made of any metal, such as steel, having high tensile strength. As the tool slides over the probe the studs are pushed outward from the center against the spring tension, allowing the tool to slide into position below the shoulder of the probe head. The spring tension forces the studs inward into the engaged position after they pass the shoulder. When the tool is raised the studs stop against the shoulder, preventing the tool from sliding up over the top of the probe. Once it engages the shoulder of the probe it cannot be freed until both probe and fishing equipment are recovered from the drillhole.

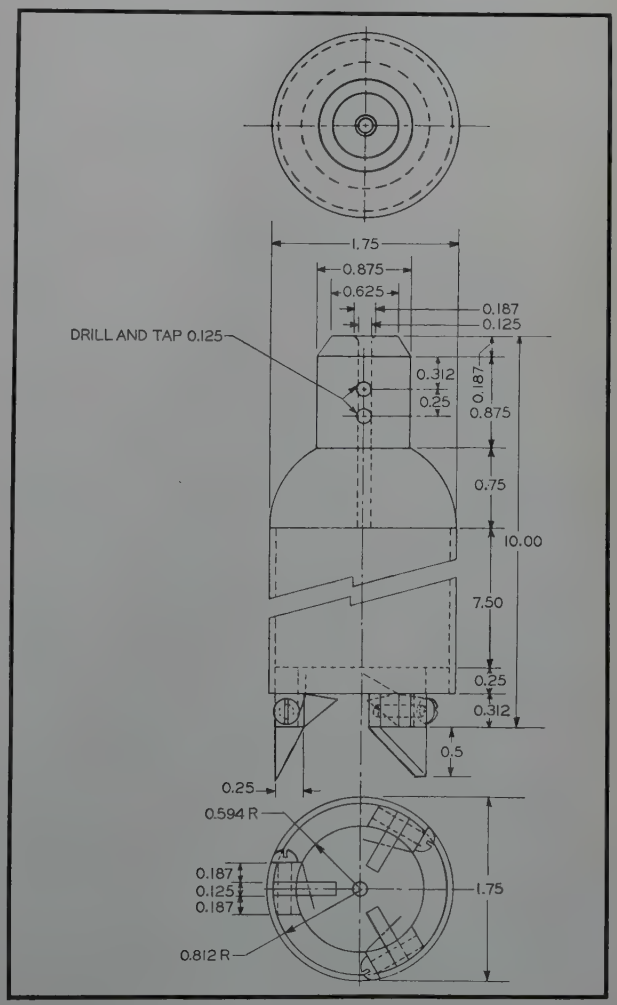

Fig. 1—Fishing tool for retrieving probes.

C. M. BUNKER and J. M. OHM are with the Geophysics Branch of the U. S. Geological Survey, Denver. TN 59 I 211. Manuscript, Feb. 16, 1959. AIME Trans., Vol. 214, 1959.

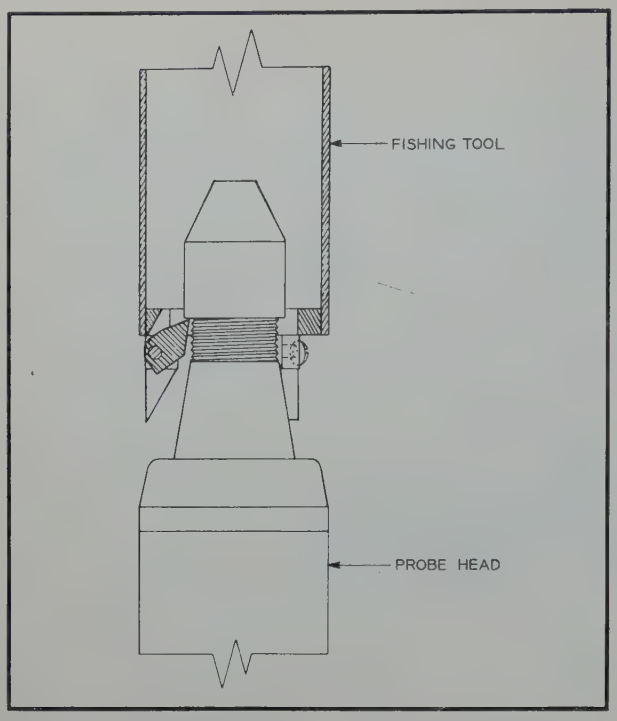

Fig. 2—Tool with probe in retrieving position.

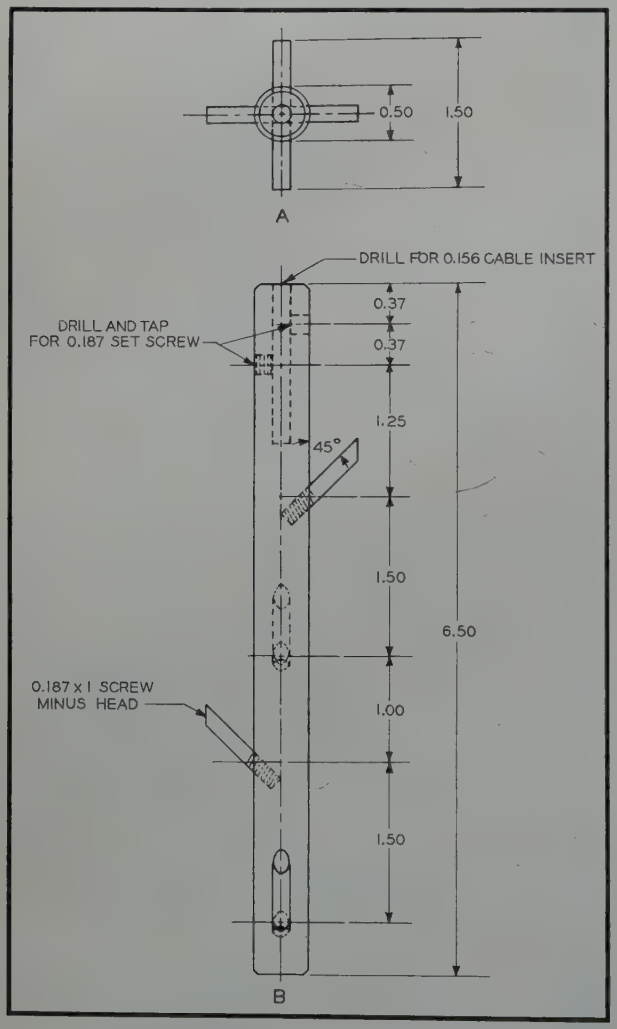

Fig. 3—Fishing tool for retrieving cable.

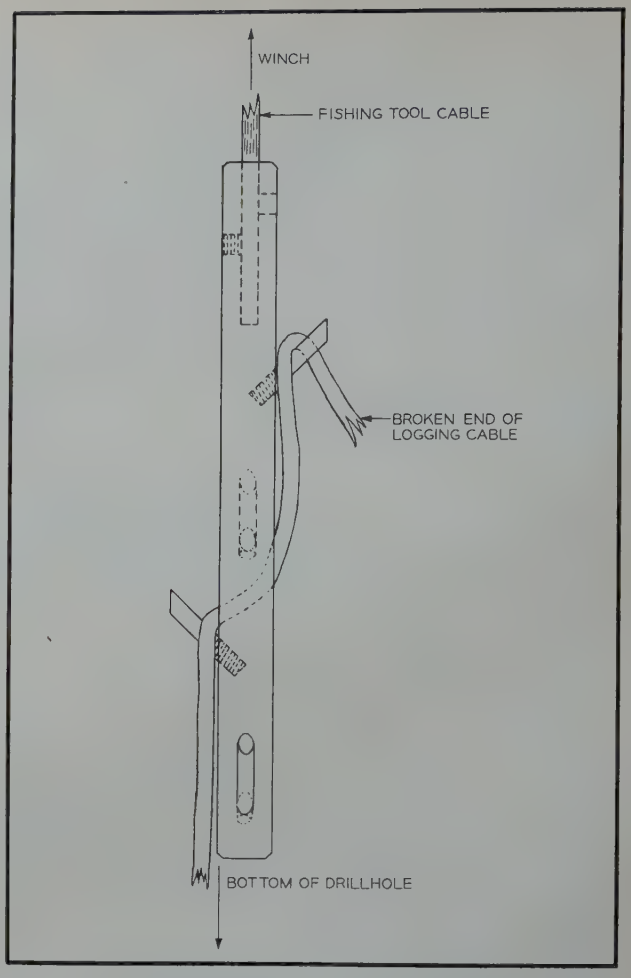

Fig. 4—Tool with cable in retrieving position.

The fishing tool is attached to a steel cable and lowered by hand into the drillhole. After the location of the probe has been determined, the tool is raised a few inches and then lowered rapidly to force it over the head of the probe. In a large drillhole it may be necessary to do this several times before the tool can be centered over the probe, but when the drillhole diameter is only slightly larger than the probe and fishing equipment, the tool is easily guided. Once the tool and probe are engaged, the upper end of the fishing cable can be attached to a winch or block and tackle and the equipment can be retrieved from the drillhole.

Fishing Tool for Cable: The tool designed for recovering broken logging cable from drillholes is simple but effective. A steel rod 7 to 8 in. long is drilled with four holes placed at 90° around the circumference (Fig. 3A), about 1½ in. apart vertically and pointing downward at a 45° angle from the center line of the rod (Fig. 3B). The holes are tapped and 5/32-in. screws 1 in. long are screwed into them. The heads of the screws are cut off at an angle parallel to the body of the tool. A hole is drilled in the center of the upper end of the tool to accept the winch cable. Two more are drilled into the side of the rods to intercept the hole drilled for the cable and are tapped for set screws.

The tool is lowered as far as possible into the drillhole containing the logging cable by a winch cable of high tensile strength. It is then raised and lowered repeatedly until the logging cable is entangled in the studs projecting from the tool (Fig.4).

PEBBLE MILLING PRACTICE AT THE SOUTH AFRICAN GOLD MINES OF UNION CORP. LTD.

by O. A. E. JACKSON

Pebble milling has been practiced in the reduction works of South Africa gold mines for well over 50 years. Originally flint pebbles were imported from Denmark to grind stamp-mill amalgamation-process tailing, which contained a good deal of extractable gold, but local operators soon found that large pieces of ore could be used for the same purpose.

The ore is a hard, tough conglomerate in which quartz pebbles are cemented together by a matrix of redeposited silica interspersed with pyrite crystals. The gold, rarely visible, occurs as fine particles mostly segregated at the interface of the pebble and matrix, although a small fraction occurs within the pyrite crystals. There is seldom any gold in the pebbles themselves.

Following the usual South African practice in pebble milling, Union Corp. grinds the ore wet in two or three milling stages incorporating classification. The sized broken ore used as grinding media is separated from the main ore stream in the crushing section that prepares the ore for milling.

Where the ore channel, or *reef*, is narrow there is a shortage of large pebbles. In this case primary grinding may be done in ball mills or, more recently, in rod mills, which cost less per ton to operate. The trend, however, is to prepare finer feed for the milling section. This makes it possible to use smaller primary pebbles and eliminates the need for steel.

REDUCTION WORKS OF UNION CORP. LTD.

Union Corp. Ltd. exercises financial and technical control over a group of seven gold mines in the Transvaal and Orange Free State. In the Transvaal, with one exception. the mines lie 20 to 40 miles east of Johannesburg, in flat or gently rolling countryside. Winkelhaak, the first of several new mines that will be developed by Union Corp., is located in similar terrain in an entirely new gold mining district about 80 miles east of Johannesburg.

Table I gives details of milling units for six of the Union Corp. mines, together with the tonnage milled in 1957. Winkelhaak Mines Ltd. is not included, as it did not begin milling until 1958. This reduction plant has no crushing section; ore is ground directly from the mine (autogenously) in 12x16-ft mills. Because these operations are still in development, they are not described in this article.

It will be noted that certain reduction works have mills of more than one size in the same milling stage. This came about when plant extensions incorporated larger units. In the case of Geduld Propty. Mines Ltd., which began milling operations 50 years ago, the primary stage is stamp milling.

The reduction works follow a uniform pattern and are usually joined to the main ore shaft. Ore from other shafts is brought by standard-gage railway and dumped into a common transfer bin. The trend is to increase surface storage capacity to enable the crushing and milling sections to operate at a steady rate, independent of fluctuating ore deliveries from mine.

Milling and cyanide extraction divisions of new mines are always designed to allow for extensions as mine production increases. The conveying, washing, and screening system of the crushing section is usually laid out in final form, with additional space for more crushing equipment. The crushing sections operate on one shift during early years of mine production; a second shift is introduced when the mining rate warrants it. Ample surge capacity is provided.

Crushing and milling is done only on weekdays, as the law does not allow these operations to take place on Sunday in any plants constructed since 1911. The cyanide extraction sections, however, operate continuously seven days a week, drawing on mill pulp gradually built up in the thickeners during the week.

Construction and equipment of milling plants follow standard practice. Dilution water is drawn from a large, high-level tank to obtain constant pressure, but gland service water for the pulp pumps is reticulated from high-pressure, two-stage pumps.

The mills are equipped with the most up-to-date machinery and are designed to save labor. They compare favorably with milling plants in countries where native labor does not exist, and automatic controls are being installed wherever feasible.

Hydrocyclone classifiers have replaced mechanical classifiers in modern milling plants, chiefly because of the saving in capital outlay, maintenance, and building space. The hydroclones are fed from steady head boxes rather than directly from pumps, and dilution water is introduced into these boxes. Tests have shown that in steadiness of operation and separating efficiency cyclones are comparable to mechanical classifiers, but protective stationary screens are needed to keep the spigots clear.

Rubber-lined pumps are used for pulp of about 3 mesh or finer and metal-lined pumps for coarser material.

None of the Union Corp. milling plants practices gravity concentration of coarse gold by amalgamation or the use of corduroy blankets. Studies have proved that no economic case can be made for these methods, which complicate the milling process and demand extra precautions against theft.

O. A. E. JACKSON is Consulting Metallurgist, Union Corp. Ltd., Springs, Transvaal, South Africa. TP 59B17. Manuscript, Nov. 10, 1958. San Francisco Meeting, February 1959. AIME Trans., Vol. 214, 1959.

This page of Mining Transactions AIME follows p. 1046. The intervening non-Transactions pages appeared in MINING ENGINEERING.

Feed Preparation and Pebble Production: Mill feed is prepared in the crushing section. Here the ore is washed to permit waste-sorting; pebbles of suitable sizes are separated for the various milling stages; and the remainder is crushed, in conjunction with closed-circuit screening, to the desired size as primary mill feed.

After going through a jaw crusher, the incoming ore is washed and sized as it passes over grizzlies and vibrating screens. The washings are classified, thickened, and pumped to the milling section to join the feed to the secondary circuit. Native sorters pick off waste quartzite and shale down to about 3-in. size, usually from two conveyor belts moving at 80 fpm. They average 10 tons per native-shift, sorting out roughly 10 pct from run-of-mine ore received.

Although primary pebbles are sorted by hand at present, in any new reduction works they will be separated by vibrating grizzlies or vibrating screens. Secondary and tertiary pebbles are separated by stationary grizzlies or by vibrating screens. Pebbles are transported to individual mill bins by 1-ton mine cars on an endless rope haulage system in the older plants and by conveyor belts, over weightometers, in the newer ones. The rest of the ore, usually about 80 pct of the crushing section feed, is crushed in two stages by both standard and shorthead Symons crushers in closed circuit with vibrating screens. The modern trend is to crush to about 95 pct —⅜ in., but some plants are not equipped to crush as fine as this. The crushed ore is carried by conveyor belts to mill bins of rather more than one day's milling capacity.

Slow-moving conveyor belts under the bins receive the crushed ore from chutes having adjustable gates and thence travel over weightometers and under the primary pebble bins, delivering their loads directly into the mill feed hoppers.

Feeding the relatively small proportion of pebbles into these hoppers from the storage bins has created problems in design. Among the devices currently in use are ratchet-driven conveyor belts, pan feeders, vibrating feeders, or roll feeders. In an 8x16-ft mill the pebble consumption, depending on prevailing conditions, is equivalent to a 1 to 3-in. load shrinkage per hr at the axis. The aim is to feed as continuously as possible. Guided by a meter on the control panel, the mill operator adds enough pebbles to maintain the power drawn by the mill motor at a maximum. The modern practice, however, is to employ vibrating feeders, which will be operated by the Williamson electronic automatic pebble feed controller recently developed and patented by Union Corp. Ltd.

Description of Mills: In recent years the size and speed of pebble mills has been increased. In reduction works constructed before 1930, 5½x22-ft and 6½x20-ft mills were installed. In the following decade four new reduction works were built containing 8x16-ft pebble mills. In 1948 two 21x16-ft pebble mills were installed as a self-contained unit to extend the reduction works at Grootvlei. These have proved very satisfactory, being cheaper in capital cost per ton of —200 mesh produced. Ten such mills have now been installed in reduction works of the Union Corp. group.

A number of mill drive installations have reverted to the spur gear and pinion system, with a reduction gear interposed between the driving motor and pinion shaft. Three large reduction works built in the late 1930's contain 8x12-ft mills driven by the center-drive principle: a torsion shaft fitted to a double-reduction gear box is coupled directly to a specially designed discharge trunnion. This system has operated satisfactorily but is more expensive to install than the conventional spur gear and pinion system.

All the mills are of the low-discharge type, with internal screens and lifter scoops fitted against the discharge ends. Trunnion bearings are of grease-lubricated white metal and trunnion liners of manganese steel. For 8-ft diam mills the bore of the inlet trunnions increases from 15 in. to 18 in. over 42 in. The outlet trunnion liner has a parallel bore of 12 in. For 12-ft mills the bore of both inlet and outlet trunnion liners is parallel and is 24 in. in each case.

With two exceptions all the mills are equipped with feed hoppers, fitted with heavy molded rubber gaskets. The whole assembly is spring-loaded to press against the rotating mill trunnion. Life of these gaskets varies from a few months to about a year. Recently it has been found advisable to have them molded with a metal core or else backed by a metal plate to which they adhere.

The mills of this group have been equipped during recent years with a wide variety of linings, and new types or modifications of older types have continually been designed and tested with a view to ultimate standardization. The liner situation is therefore in a state of flux. Data on typical linings

Table I. Union Corp. Ltd. Mills in Operation During 1957

Mine	Year Milling Commenced	Tons Milled per Month	Grade of Ore Dwt per Ton	Rod Mills, Primary		Ball Mills, Secondary		Pebble Mills						Total Mills
								Primary		Secondary		Tertiary		
				Dimensions, Ft	No.	Dimensions, Ft	No.	Dimensions, Ft	No.	Dimensions, Ft	No.	Dimensions, Ft	No.	
East Geduld Mines Ltd.	1931	135,000	6.37	—	—	—	—	8 x 16	5	6½ x 20	14	8 x 16	6	25
Geduld Propty. Mines Ltd.	1908	95,000	3.43	—	—	—	—	—	—	5½ x 22 6 x 20	9 9	— —	— —	18
Grootvlei Propty. Mines Ltd.	1938	196,000	4.43	—	—	—	—	8 x 16 12 x 16	6 1	8 x 16 12 x 16	14 1	8 x 16 —	6 —	28
Marievale Conc. Mines Ltd.	1939	71,000	5.45	6 x 12 8 x 12	1 1	8 x 8	2	— —	— —	8 x 16 —	4 —	— —	— —	8
St. Helena Gold Mines Ltd.	1951	116,000	6.02	8 x 12	3	—	—	12 x 16	1	8 x 16	3	8 x 16 12 x 16	6 1	14
Van Dyk Cons. Mines Ltd.	1938	77,000	3.66	—	—	—	—	8 x 16	4	8 x 16	8	—	—	12
Totals		667,000			5		2		17		62		19	105

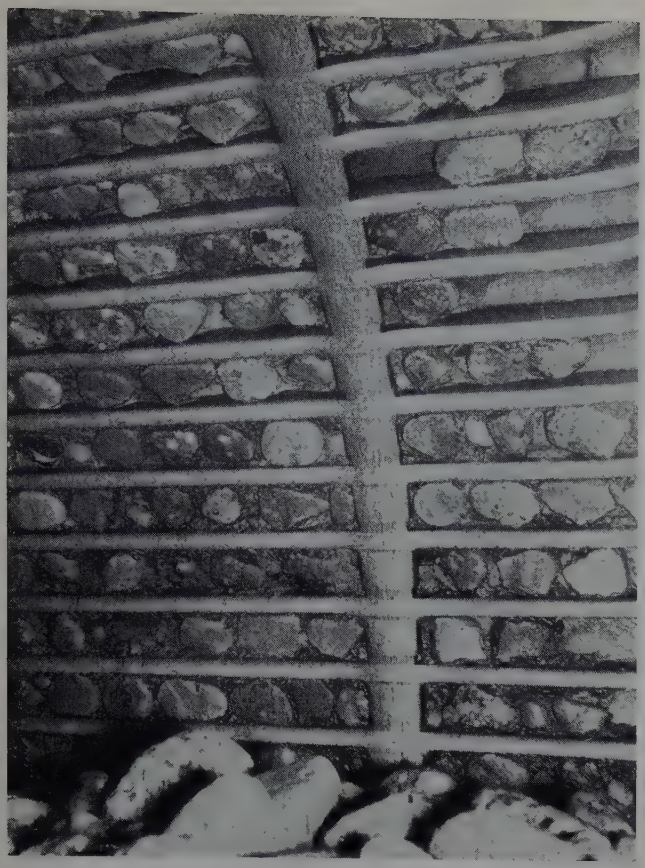

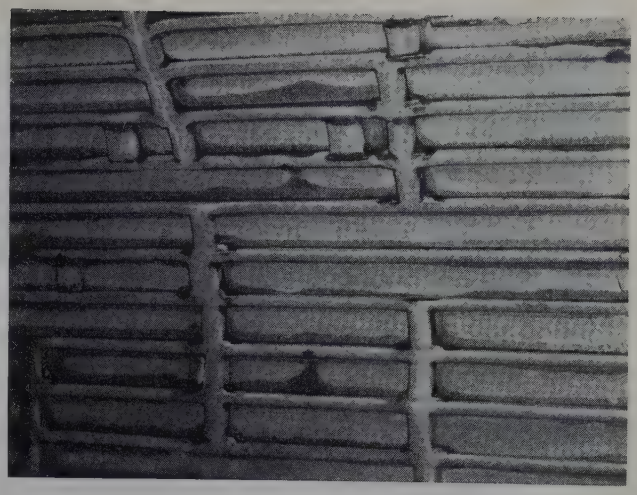

Fig. 1–(Above) Coarse pebbles packed between the Osborn bars form a semi-autogenous lining, reducing operating cost. Fig. 2–(Above, right) As bars wear down, toward the end of liner life, they no longer hold packing, and wear becomes more rapid. Fig. 3–(Right) These manganese-steel bars in a 12x16-ft primary mill are about 3½ in. in cross section, spaced about 15 in. apart and bolted down on grids worn to ¾ in. deep. Spaces between bars pack with pebbles and partly ground feed, so that only the bars are worn.

are given in Tables II-IV, arranged according to milling stage and type of lining. Three metals, in general, are used in construction of these linings, namely: white (cast) iron, with a Brinell hardness averaging 227; manganese (cast) steel, with a Brinell hardness averaging 285; and rolled steel bars, with a Brinell hardness of 183, containing 0.72 pct C, 0.86 pct Mn, 0.26 pct Cr, 0.36 pct Si, and 0.02 pct Ni. These steel bars form the Osborn bar liner referred to later.

Table II lists data concerning inlet end liners, which are cast in sections of appropriate size and bolted to the ends of the mills. To compensate for uneven rate of radial wear, their cross-sectional profiles vary in thickness according to operating experience.

Solid white-iron liners 3 to 4 in. thick have proved very satisfactory in the past, but they are heavy to handle and occasionally fracture toward the end of their lives. The more recent manganese-steel grid and plate developed at Marievale Consolidated Mines for its ball milling stage is lighter and more economical. The grids are open-work castings designed to allow the grinding medium to pack solidly; they are backed by plates about ¾ in. thick, which protect the shell when the grids eventually wear too thin to maintain the packing. Data are given for average life of both the steel grid and the plate. It will be seen that the plate backing outlasts many grids.

Table III lists data for shell liners. The peripheral speed refers to the mill shell liners less the thickness of half-worn liners. With the exception of the manganese-steel grid type, which is relatively new, two kinds of liners have been in use for many years: 1) Osborn bars are generally used in the primary and secondary milling stages of a three-stage unit and 2) white-iron blocks in the final stage. Both are held in place by thin plates driven by sledge hammer between the pieces making up the liner.

These boltless types have been adopted because the large pebbles used in the coarser milling stage will pack between the Osborn bars, as shown in Fig. 1, forming a semi-autogenous lining that reduces cost. As the bars wear down they can no longer hold their packing, as shown in Fig. 2, and wear becomes more rapid. The spacer bars can be used again in several relinings. In both cases the liners were well washed down before being photographed.

The white-iron block liners, cast in wave or sawtooth form, are used in the final milling stages because the smaller pebbles do not pack satisfactorily within the standard spacing of the Osborn bars.

Osborn bar liners consist of flat medium-carbon

Table II. Typical Mill Inlet End Line Data

Milling Stage	Liner Type	Mine	Mill		Average Liner Life, Days	Liner Wear	
			Dimensions, Ft	Speed, Rpm		Net Pounds per Horsepower-Day	Gross Pence per Ton Milled
Primary	Manganese steel, solid	Van Dyk	8 x 16	24.4	99	0.074	0.306
Primary	Manganese steel, solid	Grootvlei	12 x 16	20.2	51	0.126	0.925
Primary	Manganese steel, pocketed	St. Helena	12 x 16	20.5	61	0.068	0.466
Primary	White iron, solid	Grootvlei	8 x 16	24.8	90	0.101	0.157
Secondary three-stage	Manganese steel, grid and plate	Marievale*	8 x 8	19.6	250 to 1500	0.031	0.077
Secondary three-stage	White iron, solid	St. Helena	8 x 16	25.0	110	0.079	0.121
Secondary three-stage	White iron, solid	Grootvlei	8 x 16	19.6	114	0.081	0.240
Secondary two-stage	Manganese steel, solid	Grootvlei	12 x 16	20.2	73	0.072	0.701
Secondary two-stage	White iron, solid	Van Dyk	8 x 16	19.6	196	0.059	0.238
Secondary two-stage	White iron, solid	Van Dyk	8 x 16	22.8	167	0.066	0.279
Tertiary	Manganese steel, grid and plate	Marievale**	8 x 16	19.6	206 to 2744	0.018	0.121
Tertiary	White iron, solid	St. Helena	12 x 16	20.5	126	0.052	0.246
Tertiary	White iron, solid	St. Helena	8 x 16	25.0	162	0.058	0.165
Tertiary	White iron, solid	Grootvlei	8 x 16	19.6	260	0.041	0.052

* Ball mill.
** Composite load.

Table III. Typical Mill Shell Data

Milling Stage	Liner Type	Mine	Mill		Average Liner Life, Days	Liner Wear	
			Dimensions, Ft	Peripheral Speed, Fpm		Net Pounds per Horsepower-Day	Gross Pence per Ton Milled
Primary	Osborn bar	Grootvlei	8 x 16	597	117	0.246	0.755
Primary	Osborn bar	Van Dyk	8 x 16	588	113	0.382	1.025
Primary	Osborn bar	Grootvlei	12 x 16	740	58	0.423	1.326
Secondary three-stage	Manganese steel grids	Marievale*	8 x 8	472	334	0.062	0.177
Secondary three-stage	Osborn bar	Grootvlei	8 x 16	597	242	0.246	0.783
Secondary three-stage	White iron blocks	St. Helena	8 x 16	602	180	0.511	0.605
Secondary two-stage	White iron blocks	Van Dyk	8 x 16	472	460	0.196	0.598
Secondary two-stage	White iron blocks	Van Dyk	8 x 16	549	324	0.258	0.851
Tertiary	White iron blocks and manganese steel key bars	St. Helena	12 x 16	751	178	0.151	1.171
Tertiary	White iron blocks	Grootveli	8 x 16	472	575	0.185	0.341
Tertiary	White iron blocks	Marievale**	8 x 16	472	538	0.137	0.339
Tertiary	White iron blocks	Marievale**	8 x 16	590	314	0.240	0.604

* Ball mill.
** Composite load.

Table IV. Typical Mill Screen Data

Milling Stage	Liner Type	Mine	Mill		Average Screen Life, Days	Liner Wear	
			Dimensions, Ft	Speed, Rpm		Net Lb per Horsepower-Day	Gross Pence per Ton Milled
Primary	Manganese steel, solid	Grootvlei	12 x 16	20.2	90	0.063	0.537
Primary	Manganese steel grid and plate	Van Dyk	8 x 16	24.4	160 to 710	0.025	0.139
Primary	White iron, solid	Grootvlei	8 x 16	24.8	168	0.047	0.099
Primary	White iron, solid	St. Helena	12 x 16	20.5	78	0.050	0.508
Secondary three-stage	Manganese steel grid and plate	Marievale*	8 x 8	19.6	185 to 334	0.026	0.083
Secondary three-stage	White iron, solid	St. Helena	8 x 16	25.0	139	0.046	0.107
Secondary two-stage	Manganese steel grid and plate	Van Dyk	8 x 16	22.8	268 to 451	0.022	0.193
Secondary two-stage	Manganese steel, solid	Grootvlei	12 x 16	20.2	83	0.074	0.631
Secondary two-stage	White iron, pocketed	Van Dyk	8 x 16	19.6	262	0.023	0.201
Tertiary	Manganese steel grid and plate	Marievale**	8 x 16	24.5	354 to 1025	0.011	0.088
Tertiary	White iron, solid	St. Helena	8 x 16	25.0	180	0.041	0.179
Tertiary	White iron, solid	St. Helena	12 x 16	20.5	108	0.054	0.366

* Ball mill.
** Composite load.

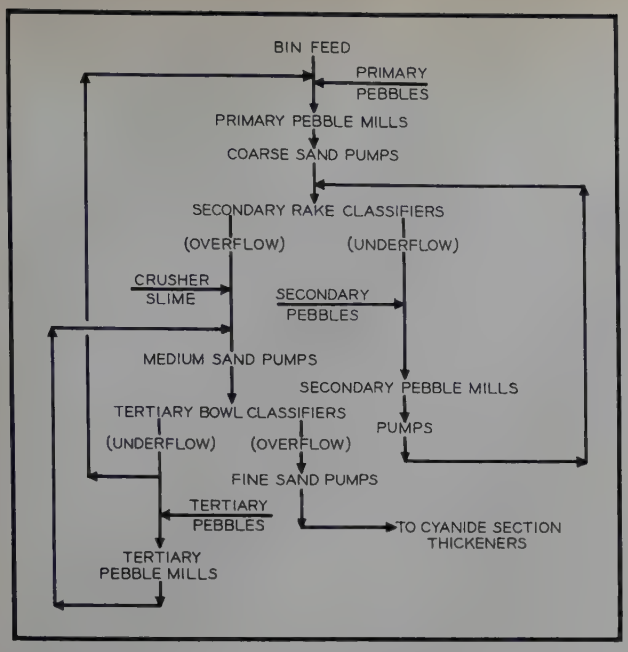

Fig. 4—In the East Geduld Mines plant the primary and tertiary mills alternate in one row. This accounts for division of sand flow from the tertiary bowl classifiers.

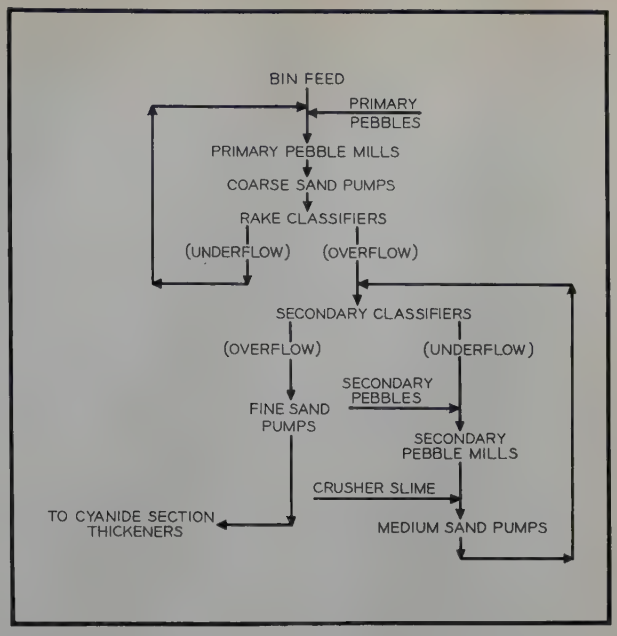

Fig. 5—Flowsheet of Van Dyk Consolidated Mines Ltd.

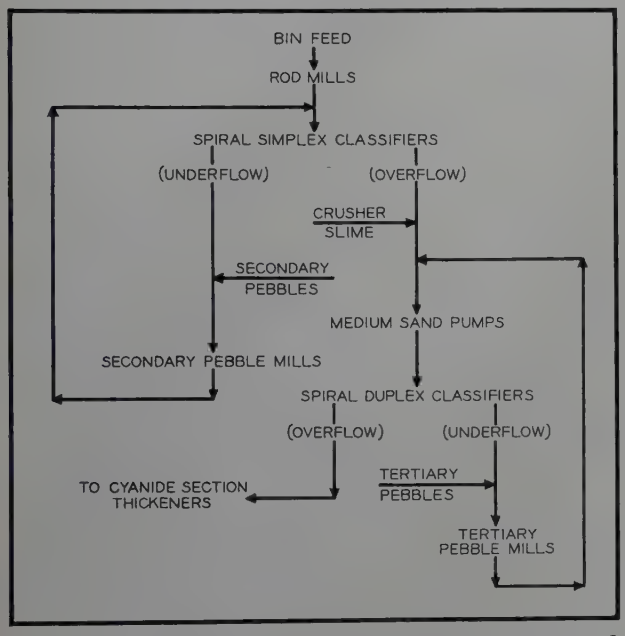

Fig. 6—Original flowsheet at St. Helena Gold Mines Ltd.

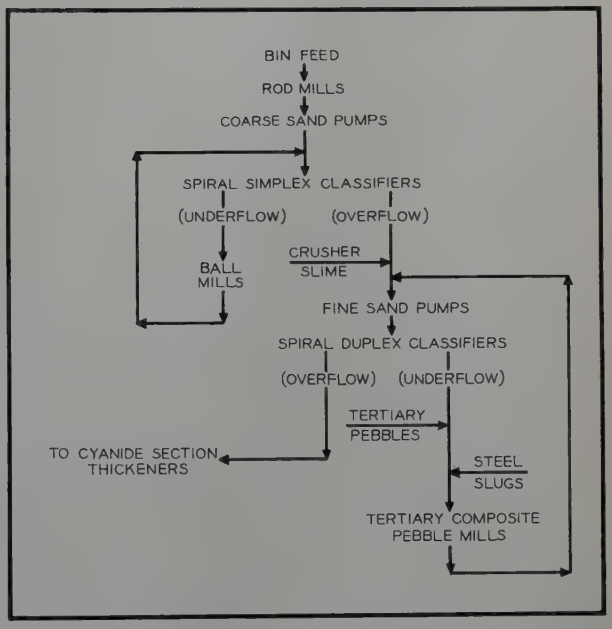

Fig. 7—Three-stage circuit of Marievale Consolidated Mines Ltd. incorporates rod, ball, and composite-load.

steel bars, 4½ in. deep by 1¼ in., tapering to ¾ in. These bars are placed on edge and separated at their 1¼-in. bases by flat steel spacers 3 in. wide and ¾ in. thick. They are further separated by cast-iron chocks, 3 x 2¼ x 2⅞ in., spaced about 2 ft apart, so that in a lined mill these appear as rings. An anti-creep bar is bolted to the shell along the full length of the mill to key the first and subsequent bars up against it and also to prevent any movement of the installed liners.

In the mills 16 ft long, Osborn bar liners are installed in two sectional rings. Steel jacks are set tightly against wooden blocks across the mill's diameter. The blocks press the liners hard against the shell, holding the bottom semi-circular lined section in place so that the mill can safely be turned through 180° while the assembly is completed. When properly installed these boltless liners are rarely displaced.

Because they are larger in diameter, liners in the 12x16-ft mills are of the bolted type. When Osborn bar liners are used they are installed in groups of 12 bars keyed up against wedge-shaped manganese-steel bars bolted to the shell. In the final-stage mills manganese-steel wedge bars, bolted to the shell, hold white cast-iron blocks in place.

The manganese-steel grid and plate-type liner, developed at Marievale for ball mills, bids fair to replace other shell liners used in this group of mines because it is relatively inexpensive per ton milled and is light and easy to install. The grids are cast in sections 45x15 in. and are 4 in. deep, forming openings 10 in. long by 3½ in. wide. They are backed by ½-in. thick sections of mild steel plate, and the whole is bolted to the shell. The grinding media pack within the openings, forming a partial autogenous liner as in the case of the Osborn liners, but the main advantage over the Osborn bar is the

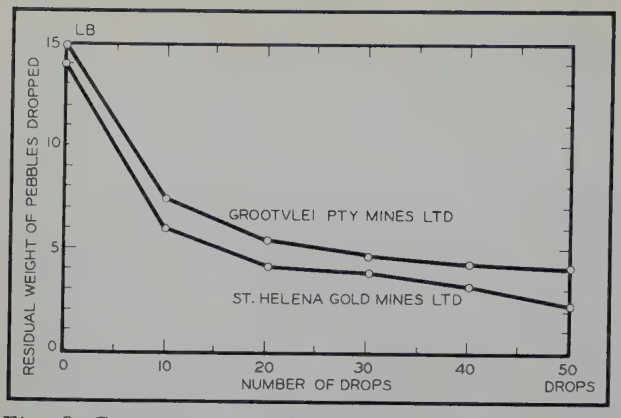

Fig. 8—Comparative results of pebble dropping test.

labor-saving installation.

A recent interesting development of this liner is the surprising fact that when manganese-steel bars, about 3½ in. square in cross section, are bolted down in a 12x16-ft primary mill parallel to the mill axis and spaced about 15 in. apart on grids worn down to only ¾ in. deep, the space between these bars packs solid with pebbles and partly ground feed, so that only the bars are worn. This system is illustrated in Fig. 3, where the packing can be clearly seen in the experimental end section next to the discharge screen. The packing was so dense that a chisel was required to dislodge it. The mill in this instance had not been washed down, so that most of the screen holes are full of fine sand but not blocked. Under work currently being conducted, this type of liner shows a good deal of promise, but like the Osborn bars, it does collect and retain a considerable amount of free gold within the pebble packing.

Mill doors are lined with one-piece blocks with a 1-in. center hole through which a graduated steel rod is inserted at least once a shift to measure the depth of pebble load relative to the axis of the mill. A wooden or rubber plug inserted into the hole prevents leakage of pulp. In this connection it might be mentioned that for optimum milling conditions the operators maintain the pebble loads in primary mills at about 5 in. below their axes, and in the final milling stages at approximately axis level. The 8x16-ft mills have one door each, but the 12x16-ft mills have two doors, placed at 180° from each other and staggered along the length of the mill to avoid undue weakening of the shell.

Table IV lists data for mill screens. White cast-iron solid screens were used almost exclusively in the past and are still used in great numbers, but new types made of manganese steel will probably replace white cast-iron in due course. All types of screens, however, are bolted in sections to the discharge end of their respective mills and are pierced with a multiplicity of circular holes varying from ½ to ⅞-in. diam on the new wearing face and tapering to larger diameters in the direction of pulp flow, at a conical angle of about 5°. All types of screens are bolted hard up against cast-steel lifter scoops cast in sections, varying in depth but averaging 4 in. These scoops discharge pulp from the mill through the outlet trunnions so that the fluid pulp within the mill can be maintained at a low level. This in turn allows greater horsepower to be absorbed by the mill load. Milling capacity is greater, therefore, than in mills of the overflow pulp type.

As in the case of the inlet-end liners, the cross-sectional profiles of screens vary in thickness to compensate for uneven radial wear, but white-iron screens have a tendency to fracture if worn too thin. For this reason, solid manganese screens were introduced in the primary milling stages, where there is greater impact from the larger pebbles.

Recent designs for manganese-steel grid and plate-type screens are similar to those developed for the inlet-end liners, but in this case the dimensions of the apertures of the grids are made larger so that they will not pack with grinding media. The

Table VI. Average Annual Classification Data for Milling Circuits

	East Geduld, 1957 (See Fig. 4)	Marievale, 1955 (See Fig. 7)	St. Helena, 1954 (See Fig. 6)	Van Dyk, 1957 (See Fig. 5)
Primary Classifiers				
Type	—	—	—	Duplex rake
Dimensions	—	—	—	8x18 ft
Number	—	—	—	4
Feed, tons per classifier-day	—	—	—	1551
Underflow, tons per classifier-day	—	—	—	805
Overflow, tons per classifier-day	—	—	—	746
Overflow, moisture, pct	—	—	—	42.7
Overflow, +200 mesh, pct	—	—	—	68.2
Classifier, 200-mesh efficiency, pct	—	—	—	37.6
Secondary Classifiers				
Type	Duplex rake	Simplex spiral High-weir	Simplex spiral High-weir	*
Dimensions	8x18 ft	72 in.	72 in.	—
Number	14	2	3	2777
Feed, tons per classifier-day	1173	5915	2523	1966**
Underflow, tons per classifier-day	760	4676	1182	811
Overflow, tons per classifier-day	413	1239	1341	87.8
Overflow, moisture, pct	82.6	73.5	52.6	15.3
Overflow, +200 mesh, pct	38.7	56.2	65.9	66.4
Classifier, 200-mesh efficiency, pct	64.1	61.4	38.0	
Tertiary Classifiers				
Type	Duplex rake Bowl	Duplex spiral Submerged	Duplex spiral Submerged	—
Dimensions	8x18 ft bowl	54 in.	54 in.	—
Number	6	4	6	—
Feed, tons per classifier-day	1390	1586	2258	—
Underflow, tons per classifier-day	472	915	1625	—
Overflow, tons per classifier-day	918	671	633	—
Overflow, moisture, pct	86.2	88.0	86.2	—
Overflow, +200 mesh, pct	17.0	15.0	28.0	—
Classifier, 200-mesh efficiency, pct	64.8	74.7	63.2	—

* 3 @ 16-ft quadruplex rakes with 18-ft bowl and 1 @ 54-in. duplex spiral.
** Each classifier feeds two secondary mills.

¾-in. plate behind the grid is of manganese steel and is pierced by a great number of tapered holes. As in the case of the inlet-end liners, the plate outlasts several protective grids.

Despite the higher cost of manganese steel, this type of screen can compete economically with white-iron screens. The sections are relatively light and are easier to install, they do not fracture towards the end of their life, and because the screen proper is thinner, there can be more holes per unit area. Because the holes are shallower, they are less likely to become choked with the smaller sizes of grinding media. Where high-circulating load milling is practiced, however, plain cast screens are more suitable, as the grids reduce the scouring action of the pulp across the holes that tend to become choked.

All sections of all mills are lined in place by a European tube mill reliner, an assistant, and a gang of about eight natives.

Constant vigilance is necessary to guard against theft of concentrate, which is readily disposable through illicit channels. A regulation of the Gold Law requires the presence of at least two Europeans when high-grade material is handled. In this respect it should be pointed out that fine metallic gold, usually not visible, lodges in the joints and also works its way behind tube mill liners as a very high-grade concentrate. The total quantity of gold a lined mill can adsorb varies with the type of liner. A 12x16-ft primary mill with a solid block liner does not absorb much gold, but when fitted with an Osborn bar liner it can absorb a considerable amount within and behind the metal, and a substantial quantity within the packed pebbles. Milling in cyanide solution is not practiced.

To reline the shell of an 8x16-ft mill, the whole load is emptied onto the concrete floor and shoveled back when the job is completed. The load averages 20 tons. In the case of the 12-ft mills, however, the load is not emptied, as there is enough head room for the mills to be relined by workers standing on the load. During relining, the mills are very slowly rotated by a motorized barring gear. Depending on rate of wear along the length of the mill, it is customary to reline only part of the shell liner at one time. An 8x16-ft mill is lined with Osborn bars in two sections, and one section can be relined and the mill reloaded within an 8-hr shift. Since the law prohibits milling operations on Sundays in any reduction works erected since 1911, it is common practice, under special permit, to reline mills on that day in order to minimize loss of running time.

Operational Data: Flowsheets of four milling plants are given to illustrate different types of Group

Table V. Average Annual Data for Four Milling Circuits

	East Geduld, 1957 (See Fig. 4)	Marievale, 1955 (See Fig. 7)	St. Helena, 1954 (See Fig. 6)	Van Dyk, 1957 (See Fig. 5)
Primary Mills				
Type	Pebble	Rod	Rod	Pebble
Number and dimensions	5 @ 8x16 ft	1 @ 6x12 ft 1 @ 8x12 ft	3 @ 8x12 ft	4 @ 8x16 ft
Average mill speed, rpm	24.0	20.8 to 19.4	18.6	24.4
Power consumed per mill, hp	289	187 to 366	293	299
Bin feed, + ⅜ in., pct	38	3	63	16
Bin feed, tons per mill-day	978	839 to 1773	1356	700
Sand, tons per mill-day	139	—	—	805
Pebbles, tons per mill-day	37	—	—	46
Pebbles, average weight, lb	11.1	—	—	14.9
3½-in. rods, lb per horsepower-day	—	4.80 to 5.60	7.45	—
Total feed per mill-day, tons	1154	839 to 1773	1356	1551
Discharge moisture, pct	18.1	19.7	—	21.6
Power per ton −200 mesh produced, kw-hr	30.4	25.7 to 24.1	24.2	27.0
Secondary Mills				
Type	Pebble	Ball	Pebble	Pebble
Number and dimensions	14 @ 6½x20 ft	2 @ 8x8 ft	3 @ 8x16 ft	8 @ 8x16 ft
Average mill speed, rpm	26.0	19.6	25.0	20.0
Power consumed per mill, hp	217	256	292	248
Sand feed per mill-day, tons	760	4676	1182	983
Pebbles per mill-day, tons	13	6	25	19
Pebbles, average weight, lb	3.3	—	0.9	—
Pebbles, screen analysis, pct:				
+2 in.	—	—	—	78.3
−2 in. +1½ in.	—	—	—	17.9
−1½ in. +1 in.	—	—	—	2.3
−1 in.	—	—	—	1.5
Steel per horsepower-day, lb	—	7.81	—	—
Total feed per mill-day, tons	773	4676	1207	1002
Discharge moisture, pct	21.8	26.1	—	31.3
Power per ton −200 mesh produced, kw-hr	24.2	15.6	23.5	20.9
Tertiary Mills				
Type	Pebble	Composite Load	Pebble	—
Number and dimensions	6 @ 8x16 ft	4 @ 8x16 ft	6 @ 8x16 ft	—
Average mill speed, rpm	19.5	23.3	25.0	—
Power consumed per mill, hp	233	367	274	—
Sand feed per mill-day, tons	360	915	1625	—
Pebbles per mill-day, tons	19	15	19	—
Pebbles, screen analysis, pct:				
+2 in.	11.3	45.1	50.5	—
−2 in. +1½ in.	18.9	38.5	39.4	—
−1½ in. +1 in.	36.6	15.1	8.9	—
−1 in.	33.2	1.3	1.2	—
Slugs per horsepower-day, lb	—	3.65	—	—
Total feed per mill-day, tons	379	930	1644	—
Discharge moisture, pct	32.3	28.8	—	—
Power per ton −200 mesh produced, kw-hr	26.6	23.8	21.0	—
Complete Milling Plant				
Total tons per plant-day	5530	2728	4119	3265
Overall circulating load ratio	2.4 to 1	4.8 to 1	3.4 to 1	3.4 to 1
Screen analysis of final pulp (+200 mesh), pct	17.0	15.0	28.0	15.3
Addition of steel per ton milled, lb	—	4.53	0.74	—
Cost per ton milled, pence	21.1	28.6	24.3	20.8
Power per ton milled (mills only), kw-hr	19.1	16.7	14.7	17.4
Power per ton −200 mesh produced (mills only), kw-hr	26.0	21.6	22.2	22.8
Total cost per ton −200 mesh produced (mills only), pence	28.7	37.0	36.7	27.2

Table VII. Primary Pebble Self-Comminution Tests

	Development Pebbles	
	Grootvlei	St. Helena
Initial pebble load, lb	20,000	20,000
Number of pebbles	1,412	1,502
Average weight of pebbles, lb	14.2	13.3
Duration of grind, min	15	15
Final load, lb	14,497	15,878
Final load, +1½ in., lb	13,252	11,378
Number of pebbles, +1½ in.	5,325	6,344
Average weight of pebbles +1½ in., lb	2.49	1.79
Final load of original, pct	72	79
Final load, +1½ in. of original, pct	66	57

Screen Mesh Sizes, In.	Percentage by Weight				Average Weight of Screened Fractions after Grind, Lb	
	After Grind		Of Original Charge			
	Grootvlei	St. Helena	Grootvlei	St. Helena	Grootvlei	St. Helena
+5	24.3	17.6	17.6	14.0	10.2	14.1
+4	63.6	31.8	46.1	25.3	6.7	6.1
+3	77.4	50.6	56.1	40.2	2.9	2.9
+2	87.9	65.5	63.7	52.0	0.9	1.1
+1½	91.5	71.8	66.3	56.9	0.3	0.4
−1½	8.5	28.2	33.7	43.1	—	—
	100.0	100.0	100.0	100.0	—	—

milling circuits. Details of their equipment and representative milling data for each of these circuits are given in Table V. Classification data are presented in Table VI.

It will be appreciated that direct comparisons between these four milling plants cannot easily be made, since operating conditions differ considerably as to addition of steel, number of milling stages, kilowatt-hours per ton milled, screen analyses of bin feed and final pulp, magnitude of circulating load and, to a lesser degree, relative hardness of ore.

Fig. 4 is the flowsheet of the East Geduld Mines mill, which is the oldest all-sliming plant of the Group and embodies a three-stage all-pebble-milling circuit. It will be noted that the circuit is rather unusual in that the sand from the tertiary bowl classifiers is split between the tertiary and primary pebble mills. This is done because the primary mills alternate with tertiary mills in one row.

Table V shows that overall power consumption per ton of −200 mesh produced is somewhat higher than that of the other plants given, owing to the small load in the primary and tertiary milling circuits. In the tertiary circuit, particularly in cold weather, this load has been found necessary to avoid or reduce sliming in the thickening plant, which consists mainly of two-deck thickeners. Milling costs are rather higher than for the Van Dyk two-stage pebble plant.

The flowsheet of this Van Dyk Consolidated Mines plant is presented in Fig. 5. Relevant operational data are given in Table V. This plant has the lowest costs of the four mills tabulated. It will be noted also that power consumption per ton of −200 mesh produced is less than for the East Geduld all-pebble milling plant and is comparable with power consumption in the other two mills, where steel grinding media are employed in certain stages.

Fig. 6 is the original flowsheet for the three-stage plant of St. Helena Gold Mines Ltd., where rod mills are used in the primary stage. St. Helena's reduction works were the first to be brought into operation in the Orange Free State's new gold field. To advance the date of production it was necessary to design the mill before enough mine development work had been carried out to reveal the milling properties of the ore, which was reported to be more brittle than the Transvaal Witwatersrand ore. This was disturbing information, since there would be a risk in incorporating a primary pebble milling stage if the primary pebbles broke up. A test was therefore devised to obtain a rough quantitative comparison between the St. Helena ore and ore from the Grootvlei Propty. Mines Ltd., a typical East Rand Group mine. Selected pieces of ore were dropped 50 times from a height of 9 ft onto a large solid manganese casting, chipping off part of the ore. Each residual piece was weighed after every ten drops. Comparative results of these tests are shown in Fig. 8.

Final residual weight of the Grootvlei pebbles was almost double that of the St. Helena pebbles. Owing to incipient planes of weakness, moreover, a greater number of St. Helena pebbles broke up during the first few drops. These were excluded from the test data.

Table VIII. Metallurgical Data per Pebble Milling Unit

	Van Dyk Cons. Mines Ltd. 1957				Grootvlei Propty. Mines Ltd. January-April 1958			
	Tons Per Calendar-Day		Moisture, Pct	+200 Mesh, Pct	Tons Per Calendar-Day		Moisture, Pct	+200 Mesh, Pct
	Dry Solids	Water			Dry Solids	Water		
Primary Pebble Mills								
Bin feed	629	19	3.0	94.2	1381	43	3.0	96.9
Primary classifier underflow	723	239	24.8	91.9	2958	1097	27.1	88.4
Primary pebbles	41	—	—	—	150	—	—	—
Added water	—	125	—	—	—	395	—	—
Discharge	1393	383	21.6	80.5	4489	1535	25.5	76.0
Primary Classifiers								
Primary mill discharge	1393	383	21.6	80.5	4489	1535	25.5	76.0
Added water	—	356	—	—	—	1783	—	—
Total feed:	1393	739	34.7	80.5	4489	3318	42.5	76.0
Underflow	723	239	24.8	91.9	2958	1097	27.1	88.4
Overflow	670	500	42.7	68.2	1531	2221	59.1	52.1
Secondary Pebble Mills								
Secondary classifier underflow	1799	752	29.5	86.8	3678	1629	30.7	80.5
Secondary pebbles	35	—	—	—	114	—	—	—
Added water	—	82	—	—	—	586	—	—
Discharge	1834	834	31.3	65.8	3792	2215	36.9	62.6
Secondary Classifiers								
Primary classifier overflow	670	500	42.7	68.2	1531	2221	59.1	52.1
Secondary mill discharge	1834	834	31.3	65.8	3792	2215	36.9	62.6
Crusher slime	34	63	65.0	29.3	—	—	—	—
Added water	—	4691	—	—	—	9871	—	—
Total feed:	2538	6088	70.5	65.6	5323	14307	72.9	59.6
Underflow	1799	752	29.5	86.8	3678	1629	30.7	80.5
Overflow	739	5336	87.8	15.3	1645	12678	88.5	12.9

Table IX. Supplementary to Table VIII

	Van Dyk 1957	Grootvlei January-April 1958
Number of primary mills per unit	1	1
Number of secondary mills per unit	2	1
Size of pebble mills, unlined shell	8x16 ft	12x16 ft
Speed of primary pebble mills	24.4 rpm	20.2 rpm
Speed of secondary pebble mills	19.6 rpm	20.2 rpm
Critical speed of primary mills with half-worn liners	88.3 pct	90.2 pct
Critical speed of secondary mills with half-worn liners	71.0 pct	90.2 rpm
Average power of primary mills per unit	299 hp	888 hp
Average power of secondary mills per unit	496 hp	828 hp
Average weight of pebbles, primary mills	14.9 lb	10.4 lb
Screen analysis of pebbles, secondary mills:		
+2 in.	78.3 pct	36.3 pct
−2 in. +1½ in.	17.9 pct	36.5 pct
−1½ in. +1 in.	2.3 pct	24.6 pct
−1 in.	1.5 pct	2.6 pct
Primary classifiers	1 @ 8 ft wide duplex rake	1 @ 36 in. x 15° cone cyclone
Secondary classifiers	1 @ 16 ft wide quadruplex rake with 18 ft bowl	4 @ 27 in. x 15° cone cyclones
Tons milled per housepower-day	1.026	0.959
Tons −200 mesh produced per ton milled	0.765	0.845
Kilowatt-hours per ton −200 mesh produced, primary	27.0	23.0
Kilowatt-hours per ton −200 mesh produced, secondary	20.9	21.1
Kilowatt-hours per ton −200 mesh produced, overall unit	22.8	22.1

To substantiate the test results, a shipment of primary-sized pebbles from the development ore dump at St. Helena was railed to Grootvlei for grinding tests against similar-sized pebbles from development ore from that mine. In each instance 10 tons were loaded into an empty selected mill (about half a normal mill load) and ground for 15 min at 24.5 rpm. Water was allowed to flow through the mill to wash out grit and slime through the ¾-in. holes in the mill screen. At the end of the tests the loads were dumped. The partly worn pebbles were screened through square mesh and each fraction was weighed and the number of pebbles counted, down to the +1½-in. size.

The results, given in Table VII, showed that the St. Helena pebbles wore away more quickly, for the +1½-in. pebbles in the original load, 57 pct remained, compared with 66 pct in the case of the Grootvlei pebbles. On the basis of this data, 8x12-ft rod mills were installed for the primary stage, as the 6x12-ft test mill installed in the Marievale reduction works had proved satisfactory and more economical for primary-stage milling than the ball mills operating at the same mine. It has since been established that it would have been quite safe and more economical to install primary pebble mills. A 12x16-ft primary pebble mill later installed in a plant extension has operated successfully, and a secondary primary mill of the same size is being installed in a new plant extension now under construction. A study of the savings in rod mill costs indicates that it should be profitable to convert the original rod mills to pebble mills.

Average milling data for 1954, presented in Table V, have been selected as representative of results from the original flowsheet before the first extension incorporating primary pebble milling came into operation. Screen analysis of the bin feed has since been reduced to 7 pct +⅜ in. The cost per ton milled given would be higher under 1957 prices.

Table V reveals that although the overall power consumption per ton of −200 mesh produced is 0.6 kw-hr lower than that of Van Dyk, the cost per ton of −200 mesh produced is 9.5 pence higher for a considerably coarser final pulp. This is due in part to the additional cost of rods. In 1957, however, with improved metallurgical practice, together with the benefit from the additional primary pebble milling unit and larger throughput, this cost differential has been reduced to 5.6 pence per ton of −200 mesh produced.

Fig. 7 is a flowsheet of the Marievale milling plant and Table V presents relevant operational data for 1955. Data from this mine are included here because steel is added to each of the three-stage milling circuits in the plant, which incorporates rod milling, ball milling, and composite-load pebble milling.

Because the width of the reef on this mine is narrow, it was believed that there would not be enough large pebbles for primary pebble milling, and the plant was designed to accommodate ball mills. In 1948 the writer paid a visit to the London milling plant of Tennessee Copper Co., where he was able to inspect and discuss operation of a 6x12-ft rod mill. Following this consultation, an experimental rod mill of the same size was installed at Marievale to test its economy as compared with that of ball mills in operation at that same plant. This was the first rod mill installed in a South African gold milling operation.

The installation was followed by several larger rod mills in this and other mining groups, since it was proved that in primary stages rod mills are more economical for South African gold ore than ball mills. Following the success of the prototype, an 8x12-ft rod mill was installed in parallel in 1953. The 3½-in. rods added cost 4.3 pence per lb; 3-in. cast steel balls cost 3.1 pence per lb.

The practice of milling with composite loads is not uncommon in South African gold ore reduction works. It was originally introduced to overcome a

Table X. Economics of 12x16-ft Mills Vs 8x16-ft Mills

	8x16-Ft Mills Van Dyk 1957		8x16-Ft Mills Grootvlei January-April 1958	
Power Costs				
Kilowatt-hours per ton −200 mesh produced	22.8		22.1	
Cost per kilowatt-hour (assumed average), pence	0.4		0.4	
Cost per ton −200 mesh produced, pence		9.12		8.84
Liner Costs				
Net wear per horsepower-day, lb	0.352		0.489	
Net wear per ton milled, lb	0.343		0.510	
Averaging cost per pound worn, pence	7.41		9.37	
Cost per ton milled, pence	2.54		4.78	
Cost per ton −200 mesh produced, pence		3.32		5.66
Total cost (power plus liners), pence		12.44		14.50
Capital Cost				
Number of mills per unit	3		2	
Mills, driving equipment and electrical controls (not erected)	£42,000		£53,000	
Amortization: Cost per ton −200 mesh produced, pence		4.28		2.43
Total cost per ton −200 mesh produced, pence		16.72		16.93

Table XI. Data on Pebble Consumption, 1947

Primary Pebbles:

Mine	Mill: Dimensions, Ft	Mill: Peripheral Speed, Fpm	Pebble: Average Weight Per Pebble, Lb	Pebble Consumption: Tons Per Day	Pebble Consumption: Tons Per Horsepower-Day
East Geduld	8x16	578	11.1	37	0.129
Grootvlei	8x16	597	12.3	41	0.138
Grootvlei	12x16	740	12.3	162	0.192
St. Helena	12x16	751	3.9	129	0.146
Van Dyk	8x16	588	14.9	46	0.154

Secondary Pebbles:

Mine	Mill: Dimensions, Ft	Mill: Peripheral Speed, Fpm	Pebble: Average Weight Per Pebble, Lb	Pebble Consumption: Tons Per Day	Pebble Consumption: Tons Per Horsepower-Day
East Geduld	6½x20	462	3.3	13	0.059
Grootvlei	8x16	597	2.3	43	0.141
St. Helena	8x16	602	1.1	40	0.136

Tertiary Pebbles:

Mine	Mill: Dimensions, Ft	Mill: Peripheral Speed, Fpm	Pebbles: Screen Analysis, Pct: +2 In.	−2 +1 In.	−1 In.	Consumption: Tons Per Day	Consumption: Tons Per Horsepower-Day
East Geduld	8x16	450	11.3	55.5	33.2	19	0.082
Grootvlei	8x16	472	33.7	60.9	5.4	23	0.092
Marievale	8x16*	472	45.4	54.5	0.1	15	0.041
St. Helena	8x16	602	50.5	48.3	1.2	20	0.072
St. Helena	12x16	751	50.5	48.3	1.2	118	0.138
Van Dyk	8x16**	549	78.3	20.2	1.5	19	0.077

* Composite load.
** Two-stage milling circuit.

shortage of suitably sized pebbles. In the case of Marievale, it was introduced to increase plant throughput, up to the ultimate safe working capacity of the motors and reduction gears driving the mills. The slugs used are about 1½ in. long and cost 1.1 pence per lb, being cut from discarded drill steel.

As to the economics of composite loading, a favorable case can be made for its increasing the tonnage output of a given plant, either as a temporary expedient or because expansion is not warranted by the expected life of the mine. But no economic case can be made for using steel balls to increase fineness of grind of Witwatersrand gold ores as a means of obtaining a higher gold recovery at the present price of gold.

The plant at Marievale is now being expanded to increase output and to eliminate composite-load milling.

It will be observed that the ball mills operate with a higher circulating load than the other group milling circuits. The net result of this appears to be chiefly a saving in liner wear and power, but the tons of −200 mesh produced per mill-day remain virtually constant, since the increased production per horsepower-day is offset by the horsepower drawn. This is the net effect of increasing the circulating load.

It will also be apparent from the data given in Table V that because of the use of 4.53 lb steel per ton milled, the power consumed per ton of −200 mesh produced is 1.2 kw-hr less than that of the Van Dyk all-pebble-milling two-stage circuit, but because of the addition of steel, the cost per ton of −200 mesh produced is 9.8 pence greater than that of Van Dyk. These data emphasize the economic advantage of the South African general practice of pebble milling over all-steel milling.

COMPARISON OF 12X16 AND 8X16 MILLS IN SIMILAR CIRCUITS

Average operational data in Tables VIII and IX allow comparison between two pebble milling units incorporated within the reduction works of the Van Dyk Consolidated Mines and the Grootvlei Propty. Mines Ltd. These have been selected as being of interest because, although both are two-stage units, each in closed circuit with its respective classification equipment, they differ in the size, speed, and number of mills per unit as well as in type of classification equipment, since the Van Dyk unit is a mechanical type and the Grootvlei a hydroclone unit. In this article, *calendar-days* include time lost through normal stoppages as opposed to *mill-days*, which represent 100 pct running time.

It will be noted that despite wide disparity of internal metallurgy, overall power consumption per ton of −200 mesh produced is of much the same order in each case, being 0.7 kw-hr per ton less for the Grootvlei unit despite a finer screen analysis of final pulp. The primary mill of this latter unit operated most of the time in conjunction with the Williamson pebble mill automatic controller, designed by the Group research metallurgist, J. E. Williamson.

The automatic controller senses the first differential of power consumed cyclically by a mill and controls the mean rate of pebble addition so that the power consumed by the mill is maintained very close to its maximum at all times. This maximum will vary with the quantity and quality of both the new feed and the circulating load, as well as with the moisture content of the mill. The device has been remarkably effective. Operational data have shown a mean increase of approximately 40 hp for a 12x16-ft pebble mill over that obtained by personal judgment of pebble addition.

It has already been mentioned that the trend of Group policy is to install large mills and to operate them at increased speeds. Table X compares the

Table XII. Screen Analysis of Composite Samples of one month's Operation, Van Dyk

	Mesh, Percentage Plus: ⅜ In.	4	8	14	28	48	100	200	Percent −200
Bin feed	11.4	52.2	68.2	73.5	80.8	86.6	90.8	93.1	6.9
Primary mill discharge	1.5	7.1	15.5	19.9	38.9	58.4	73.0	81.2	18.8
Secondary mill discharge	—	—	0.1	0.5	1.3	5.1	27.5	66.6	33.4
Primary classifier underflow	4.8	21.5	37.9	45.4	68.3	82.7	90.1	93.4	6.6
Secondary classifier underflow	—	4.1	6.1	8.4	13.2	24.4	54.4	91.9	8.1
Primary classifier overflow	—	—	—	2.8	16.9	41.3	61.8	73.6	26.4
Secondary classifier overflow	—	—	—	—	—	—	0.2	15.0	85.0

Fig. 9—Typical pebbles in East Geduld three-stage mill.

economics of 12x16-ft and 8x16-ft pebble mills per ton of — 200 mesh produced, based on data given in Tables VIII and IX and excluding all costs other than those of the mills. It will be noted that cost of power consumed under the given conditions is 0.28 pence per ton less in the case of the 12-ft mills, but this would be still less had the mill pulp screen analysis been equivalent to that of the 8-ft mills.

Liner replacement cost for the 12-ft mill is 2.34 pence per ton higher. This is chiefly due to the combination of larger-diameter mills and higher percentages of critical speed and partly to the higher cost of the manganese-steel liners used. It is probable that in due course this cost differential would be reduced by the use of less expensive metal. Amortization costs, calculated on the basis of 7.5 pct interest spread over 20 years, are 1.85 pence per ton less than for the 8-ft milling unit. The capital costs, quoted, include the mills with driving and control equipment only, exclusive of plant construction.

Total costs exceed those of the 8-ft unit by 0.21 pence per ton of — 200 mesh produced. This difference would be reversed by the additional amortization charges for a larger building necessitating an increased number of foundations; for equipment; and for more bins and also extra feed belts, particularly in view of the fact that the cost of the mills, *per se*, is only about one third of the complete milling plant. In addition, operational costs would be higher owing to a larger number of milling units to be controlled and maintained for an equivalent tonnage throughput. Finally, insofar as the milling of gold ore is concerned, there should be a net additional credit to the 12-ft unit of approximately 1.2 pence per ton for the extra gold that would be extracted from the finer pulp in the subsequent cyanide treatment process, since for the ores of this Group, within the normal range of screen analysis of mill pulp, the differential in extractable gold by cyanidation for every 1.0 pct of 200 mesh lies between 0.003 and 0.004 dwt gold per ton of ore milled.

With regard to increased speed alone, for mills of equivalent dimensions, a comparison showing the economic advantage has already been established.[1]

Pebble Consumption: Table XI lists average pebble consumption data for the Group mines for 1957. The peripheral speed refers to half-worn liners. Compared to steel ball consumption, pebble consumption is enormous, 200 to 300 lb per ton milled, depending on prevailing conditions. These data show that pebble consumption per horsepower-day progressively decreases from the primary to the tertiary milling stage, which also corresponds with a decrease in weight of pebble. In general, too, within milling stages, consumption per horsepower-day increases with both peripheral speed and diameter and appears to be more directly related to the latter. The large-diameter mills are thus heavy pebble consumers, but in view of the customary size distribution of run-of-mine ore this causes no embarrassment, particularly in the case of secondary and tertiary pebbles. In the case of primary pebble mills, it will be noted that for the St. Helena 12x16-ft mills an average pebble weight of 3.9 lb was fed, but in this case the bin feed was fine, being crushed to 6.9 pct + ⅜ in. Pebbles for any given milling stage should be as small as practicable, since this decreases both kilowatt-hours per ton of — 200 mesh produced and mill liner wear, but closely sized pebbles show no appreciable advantage in milling efficiency over those within a reasonable size range.

Fig. 9 shows typical pebbles used in the East Geduld three-stage milling plant. A 1-ft rule in the photograph gives a fair idea of their size.

RELATIONSHIP BETWEEN SCREEN ANALYSIS OF PULP, RATE OF MILLING, AND POWER TO PRODUCE —200 MESH MATERIAL

There is an empirical approximately linear relationship, shown in Fig. 10, between rate of milling and screen analysis of the final pulp. This relation-

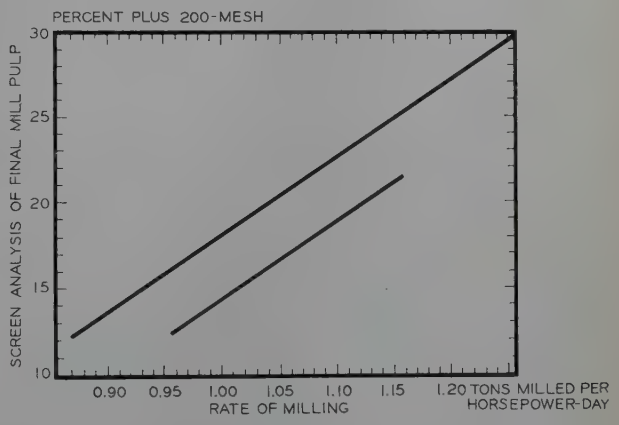

Fig. 10—Chart shows relationship between rate of milling per unit power and screen analysis of final pulp.

ship is useful in predicting performance of Group milling plants or in designing new plants and plant extensions. The slope of the curve appears to be nearly constant. For example, the equation of the upper curve in Fig. 10 is

$$y = 18 + 45\ (x\text{-}1) \qquad [1]$$

where x = the tons milled per horsepower-day and y = the percentge of + 200 mesh in the final mill pulp*

From such curves, interesting relationships can be deduced between the screen analyses of the final mill pulps and the power required per ton of material ground. An example of this is given in Fig. 11 for the Van Dyk milling circuit, milling at a rate of 1.0 tons per horsepower-day and producing a final

* In Group milling terminology it is customary to use either horsepower-days or kilowatt-hours, and also either percentage ±200-mesh, whichever is best to emphasize the point at issue.

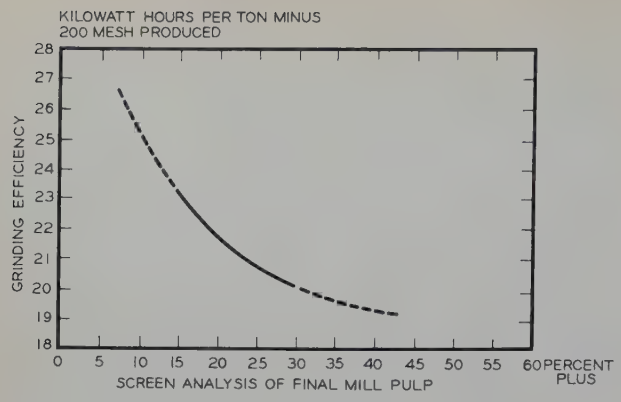

Fig. 11—Chart shows general theoretical shape of curve for relationship between screen analysis of final mill pulp and kilowatt-hours per ton of —200 mesh produced.

mill pulp at 15 pct + 200 mesh. It will be appreciated that a family of such curves must be constructed when, in practice, the screen analysis may vary according to the plant efficiency at a given milling rate. Monthly operating results for this mine over 18 consecutive months fitted these curves very closely. The writer is indebted to D. L. Carson, consulting metallurgist of the General Mining & Finance Corp., for developing an equation to fit this particular empirical curve:

$$y = (1.234 \times 10^{-13})\ x^7 + 18.9 \qquad [2]$$

where x = the percentage — 200 mesh and y = the kilowatt-hours per ton —200 mesh required to obtain such screen analysis. Using this equation, the curve has been extrapolated in broken lines in both directions to suggest a quantitative ratio for more extreme milling conditions.

Standardization of Screen Analysis Technique: In this group of mines, great care is taken to insure the highest practicable accuracy and concordance in screen analysis determinations, particularly for the 200 mesh determinations. Supervision of equipment and standardization of technique is the direct responsibility of the Group research metallurgist. Exhaustive tests were made of a large number of Tyled screens purchased about six years ago. Three of these which gave concordant results on a bulk sample of standard mill pulp from which the sulfides had been floated off were selected as master standards. One of the three screens was deposited in a safe as a final reference and has never been used since. The other two were used to standardize fresh bulk samples of sulfide-free mill pulps whenever these were required. The pulp samples are stored in air-tight containers, and the screens are renewed about every three years to be re-standardized against the standard bulk samples.

Upon request, the research laboratory supplies each mine of the Group with a numbered screen and a certificate giving its correction factor referred to the standard pulp sample. These screens are used by the mines for analyses of the monthly composite samples of cyanide residue pulp (considered to be the truest sample of the mill pulp) and also for their own standardization of all new 200-mesh screens, purchased on an average of one a month. Each mine submits a monthly composite of the cyanide residue to the Group research laboratory for check analysis. The screen analysis reported by the mine is required to agree within 0.5 pct.

All the Group mines retain, indefinitely, monthly composite samples of both original and cyanided mill pulp in air-tight glass preserving jars, in case any laboratory investigation is required into former milling or cyanidation practice.

Screen Analyses: Screen analyses of mill products through various mesh sizes are determined from time to time. Table XII shows analyses of composite samples of a typical month's operation at Van Dyk's two-stage pebble milling plant.

Infrasizer analyses of mill pulps are occasionally determined, as shown in Table XIII or a final mill pulp sample from the 12 x 16-ft two-stage milling unit of the Grootvlei Propty. Mines Ltd. Sulfur determinations of various fractions are included.

Table XIII. Typical Infrasizer Analysis of Final Pulp from the Grootvlei Two-Stage, 12-ft. X 16-ft. Milling Unit

Nominal Micron Size	Weight, Pct	Sulfur, Pct	
		Weight	Distribution
+56	14.4	1.0	14.4
−56 +40	17.1	1.2	20.5
−40 +28	12.9	1.2	15.4
−28 +20	9.8	1.2	11.8
−20 +14	8.1	1.1	8.9
−14 +10	4.2	1.3	5.5
−10	33.5	0.7	23.5

CONCLUSION

Steady progress in development of pebble milling in South Africa over half a century has brought the practice to its present state of efficiency. It has been established that for South African gold ores the use of pebbles as grinding media is considerably more economic than addition of steel balls or rods. Furthermore, the cost of producing suitable pebbles is unlikely to advance as fast as the price of steel grinding media. Although steel is sometimes employed in primary milling, recent experience has shown that, in nearly all cases, it could be eliminated by the preparation of finer mill feed.

The importance of accurate sampling and screen analysis cannot be too strongly stressed, and while pulp-density recording and controlling equipment is available, there is room for improvement. A further valuable development would be the continuous recording, coupled with automatic control, of equivalent screen analyses.

Owing to widespread staff shortages, progress since World War II has not been as rapid as could be wished and many details have not received the study they deserve. There is yet much to be learned about pebble milling. Reductions in both capital and operating costs are likely to be achieved principally by increased automatic control of large units and further simplification of the process.

The writer wishes to thank his colleagues, B. Fougner, assistant consulting metallurgist, and J. E. Williamson, research metallurgist, for assistance in preparing this article. He also extends thanks to technical staffs of the several Group reduction works whose operational data are partly recorded here, and to Union Corp. Ltd. for permission to publish this article.

Discussion of this article sent (2 copies) to AIME before Jan. 31, 1960, will be published in MINING ENGINEERING.

Reference

[1] O. A. E. Jackson: The Treatment of Ore from the Gold Mines of Union Corporation, Limited: a Summary of Metallurgical Practice. Accompanied by reply to discussion: Recent Development in Mineral Dressing. *The Institution of Mining and Metallurgy*, p. 623. London, 1953.

TIME ASPECTS OF GEOTHERMOMETRY

R. J. P. LYON

It is usually assumed[1, 2] that ore deposition is relatively slow, taking place over tens of thousands of years. Yet many syntheses and phase changes can be completed in the laboratory in a matter of hours, under essentially the same pressure and temperature conditions to be expected in nature.

Much has been written about geothermometry, and Ingerson's recent summary[2] can hardly be surpassed. Rather than review the whole field, this article will deal specifically with diffusion rates in solid solutions* of the sulfide minerals.

In the study and application of temperature-indicating phenomena to problems of ore genesis, the time factor has often been neglected. In the particular case of sulfide systems, the speed of unmixing and diffusion of the constituent phases in the solid solutions has seldom been considered when laboratory data are applied to the genesis of natural sulfide ores.

Chalcopyrite and Bornite Intergrowths: Chalcopyrite and bornite are copper iron sulfides often found in association. In many ores the individual grains appear to have mutual boundaries, but bladed intergrowths are quite common. Early workers in the field[5, 6] deduced that while these patterns could have been formed by replacement, they could be experimentally reproduced from the unmixing of solid solutions of the two previously homogenized at 475°C.

Much of the ore from Roan Antelope mine in the Rhodesian Copper Belt exhibits these bornite-chalcopyrite intergrowths, from which it has been deduced that the ores could have been subjected to a minimum temperature of 475°C. In several recent interpretations,[7] this temperature rise has been considered to result from a regional metamorphism of an original syngenetic copper-bearing sediment.

The same temperature rise to 475°C was suggested from similar intergrowths in the sulfide-bearing ore from the Happy Jack uranium mine[8] on the Colorado Plateau, although this temperature had a different origin.

In 1931 Schwartz[5] determined that 475°C represented the unmixing temperature of his bornite-chalcopyrite solid solutions but, more important, that the characteristic intergrowths of bornite and chalcopyrite could be preserved *only* if the solid solution were chilled quickly to room temperature. This significant corollary has been almost completely neglected by both Davis and Miller.[7, 8]

By suitably decreasing the cooling rate, Schwartz found that the original pattern of the intergrowth was reformed (Fig. 1). The cooling rate was critical. In cooling from 475°C to room temperature in

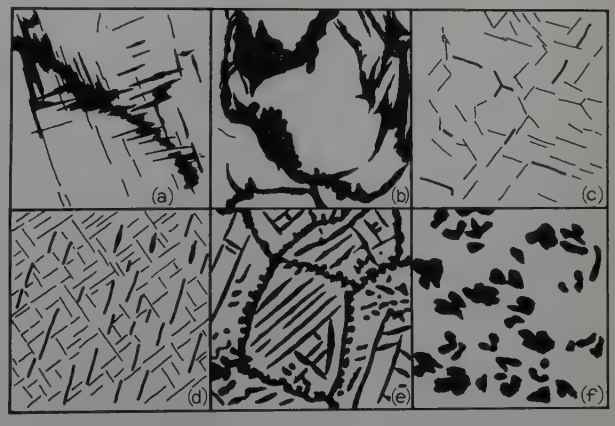

Fig. 1—Typical exsolution intergrowths of chalcopyrite in bornite. Micrographs reduced about one third. **a** *and* **b:** *Natural oriented intergrowths of chalcopyrite (black) in bornite (white) and segregation textures. Pine Vale ore. X90 (after Edwards, 1954).* **c:** *Natural intergrowth of tetrahedrite (black) in bornite (white). Pine Vale ore. X325 (after Edwards, 1954).* **d, e, f:** *Stages in unmixing of chalcopyrite (black) from same bornite solid solution (white). (After Schwartz, 1931.)* **d:** *Cooling from 475°C to room temperature in 5 min. X200.* **e:** *same solid solution, cooling time 1 hr. X100.* **f:** *same solid solution, cooling time 24 hr. X50.*

* The general subject of solid solution in structurally similar minerals is treated in many texts[1, 3, 4] and will not be further elucidated.

R. J. P. LYON, Member AIME, is a Mineralogist with Kennecott Copper Corp. Research Center, Salt Lake City. TP 4814 I. Manuscript, Jan. 19, 1959. AIME Trans., Vol. 214, 1959.

5 min, thin blades of chalcopyrite showed in the bornite-rich matrix (Fig. 1d). With 60 min cooling from 475°C to room conditions, the blades were broader and fewer in number and had some enlarged areas from the coalescing of the chalcopyrite blebs (Fig. 1e). In 24 hr cooling time an equigranular mass of bornite and chalcopyrite resulted (Fig. 1f).

Two things should be learned from these simple experiments: 1) diffusion rates in many sulfides are rapid and 2) equigranular mineral associations can be the end products of complete unmixing of a solid solution. The obvious corollary here is that intergrowths represent arrested diffusion, and it is difficult to see how this could come about under P-T conditions of regional metamorphism. In this most suitable environment for diffusion, what caused these processes to cease?

Chalcocite and Bornite Intergrowths: Frueh[9] has shown that there is a high degree of disorder in the bornite lattice above 175°C, and Latsky[10] described appreciable diffusion rates of chalcopyrite in bornite occurring even at 220°C. Bornite-chalcocite intergrowths are also well known in ore from the deep levels at Butte,[11] and the characteristic grating texture of chalcocite blades in bornite matrix appears in ore from the bornite-rich central pipe at Bingham, Utah. There are many other examples of bornite-chalcocite intergrowths[11] whose origin may be due to rapid diffusion rates during unmixing of the solid solutions, but this geometrical association is often complicated by replacement textures. For sulfide assemblages, however, evidence for exsolution is more positive, and rapid diffusion rates have been recorded in experimental work.

Diffusion of $Fe_{1-x}S$ in $CuFeS_2$: Borchert[12] has graphed the rate of solid state diffusion of $Fe_{1-x}S$ (from dissociating pyrite) through a chalcopyrite matrix as a function of temperature. The graph, reproduced as Fig. 2, gives a good idea of the rapid movement of the $Fe_{1-x}S$, increasing ten thousand fold from 1 μ per hr at 375°C to 1 cm per hour at 600°C.

Diffusion of $Fe_{1-x}S$ in ZnS: The most complete study of solution, diffusion, and unmixing in a synthetic sulfide system is that of the $Fe_{1-x}S$-ZnS system as studied by Kullerud.[13] This is a concise, detailed discussion of the behavior of synthetic (Fe, Zn)S mixed crystals and contains a graph of the time required for exsolution of $Fe_{1-x}S$ (as pyrrhotite) from the mixed crystals plotted as a function of temperature. This curve, as seen in Fig. 3, shows exsolution of the $Fe_{1-x}S$ to have been completed in laboratory tests in four days at about 875°C, or in two years at 500°C. Extrapolation down to 400°, 300°, and 200°C yields the corresponding unmixing times to be 5, 17 and 46 years.

Kullerud[13] notes that in most published descriptions of iron-rich sphalerites a maximum of 2 pct unmixed pyrrhotite laths in the sphalerite is recorded. In the Broken Hill, New South Wales, Australia ore, which is believed to have been subjected to at least 600°C temperatures induced by metamorphism,[14] or by hydrothermal[8] effects, the sphalerite contains above 20 weight pct dissolved $Fe_{1-x}S$. In the laboratory Kullerud found that this content of iron was in equilibrium with ZnS as a (Zn, Fe)S mixed-crystal at 620°C and that a synthetic crystal of this composition unmixed in 28 weeks.

We are faced with this situation. Here is one of the world's largest orebodies, thought to have been at elevated temperatures for long periods. There is a high content of iron sulfide, which has a known rapid rate of diffusion, yet only 10 pct of this $Fe_{1-x}S$ content has been able to unmix from a host. Kullerud believes that traces of impurities in natural materials could slow down these processes, but it is not necessary to resort to this explanation. The following account of annealing experiments will show that these conditions of arrested diffusion in the laboratory are also present in nature.

DIFFUSION IN MULTIPLE SULFIDE SOLID SOLUTIONS

Pine Vale, Queensland

A clear discussion of the sequence of deposition and unmixing of a multiple sulfide solid solution is given by Edwards[1,3,15] for the Pine Vale copper ore from Queensland. The three main ore minerals—bornite, chalcopyrite, and tetrahedrite—occur intergrown in definite proportions of 92:7:1. The tetrahedrite occurs in oriented intergrowths of blades (Fig. 1c), forming a discontinuous lattice work pattern in the bornite; the chalcopyrite forms a similar intergrowth pattern with the bornite but has mostly unmixed to show mutual boundaries (Figs. 1a, 1b). Silver content of the tetrahedrite is uniformly high and the straight line relationship between total copper content of the ore and silver assay (1 pct Cu is equivalent to ½ oz Ag) illustrates the overall constancy of the ratio between intergrown sulfides throughout the ore from different levels in the mine.

The Pine Vale copper ore can be restored to a single solid solution if the samples are heated* for about 100 hr at 480° to 500°C. If this homogeneous solid solution is cooled from 480°C to room temperature in several minutes, the original intergrowths of chalcopyrite in bornite can be reformed. Should the time of cooling be prolonged or the sample annealed at about 250° to 300°C, the chalcopyrite diffuses rapidly outward and segregates onto the bornite grain boundaries, yielding an even-grained pattern.

The tetrahedrite lamellae redissolve in the bornite areas if the samples are annealed for about 100 hr above 285°C. Again the cooling time is critical. If the new solid solution is cooled slowly from 285°C to room temperature, the tetrahedrite reforms and then rapidly diffuses to the grain boundaries of the bornite. The process is completed in a few minutes. The original pattern of the tetrahedrite lamellae in the bornite can be preserved only if the ore samples are quenched from above 480°C to below 250°C. Any prolonged exposure to temperatures above this level will enable the tetrahedrite to diffuse outward and destroy the lattice intergrowth with the bornite. The ore in the Pine Vale veins must have been introduced at over 500°C as a single homogeneous solid solution and crystallized in its present position (while being chilled to below 250°C) in a matter of minutes. The ore minerals were introduced about 200°C hotter than the country rocks and show the present geometry of intergrown sulfides as a result of arrested diffusion.

Aberfoyle, Tasmania

Another detailed discussion[16] of the intergrowth relationships between four sulfides has recently

* Small samples (1 to 5 cc) are placed in evacuated glass tubes (Vycor high silica glass). The furnaces are controlled to ±3°C.

been published. In the tin and wolfram-bearing quartz veins of the Aberfoyle tin mine, N. E. Tasmania, several sulfide minerals occur in patches, either intergrown with cassiterite and wolframite, forming clots of sulfides in the quartz cores of the wide veins, or filling the thinner veins. The sulfides are also disseminated in the underlying aplitic granite cupola. Vugs up to several cubic inches in volume are very common in the quartz; they are partially filled with well formed crystals of all the vein minerals.

The three important sulfides—sphalerite, chalcopyrite, and stannite—occur mutually associated; each sulfide is a host containing the other two as intergrowths. Pyrrhotite is nearly always present in tiny blades exsolved from and intergrown with the iron-rich sphalerite. The three sulfides of interest total 1.0 pct of the original vein and are present in the milled ore in a sphalerite-chalcopyrite-stannite ratio of 5:4.4:1. Individual specimens are usually sphalerite-rich or chalcopyrite-rich, the former occurring in a pronounced manner in the deeper levels.[16, 17]

Each of these minerals is really a partially unmixed solid solution whose outward diffusion has been arrested by chilling. It is very significant that well formed single crystals of the sulfides (especially sphalerite) found in the vugs still show oriented intergrowths of the other sulfides when sectioned and examined under the microscope. This is similar to the *chalcoborn* crystals found at Butte, Mont., which contained intergrowths of chalcocite in a bornite matrix while preserving the external crystal form of the bornite.[18]

Since the intergrowths of these three sulfides are unusual and complex and will have bearing on the later experimental results, each natural solid solution will be described in detail.

Sphalerite: The iron-rich sphalerite, containing 13 pct Fe, occurs in the quartz veins throughout the lode, and crystals occur in aplitic granite itself and in pegmatites within the aplitic granite in the deeper levels. It is much more common in the lower levels and there becomes the dominant sulfide mineral.

Under the microscope the sphalerite is crowded with chalcopyrite and stannite, with a persistent but low concentration of pyrrhotite blades. The pyrrhotite constitutes as much as 5 pct of some intergrowths in the sphalerite, the content being slightly higher in specimens from the lowest levels in the mine. The blades are common, showing up in 25 of the 57 polished sections of the ore examined.

The chalcopyrite-sphalerite intergrowths reveal all stages of arrested unmixing. The cores of many grains are drained of fine chalcopyrite, which has segregated in parallel rows of larger blebs. This host sphalerite is blue-gray and isotropic. The edges of these grains are clouded with chalcopyrite bodies ranging from 0.001 mm down to below the limit of microscope resolution. This clouded sphalerite is more brown in color and appears strongly anisotropic, often revealing the lamellar twinning of grains that is characteristic of low-temperature ZnS. X-rays of this intergrowth show the normal patterns of sphalerite, with a pattern of included chalcopyrite, confirming that this clouded sphalerite is not wurtzite. Bands of clouding tend to follow the boundaries of grains and run parallel to transecting gangue veins. In single crystals of sphalerite from the vugs, the clouding is in narrow bands running markedly parallel to the crystal faces. Width and

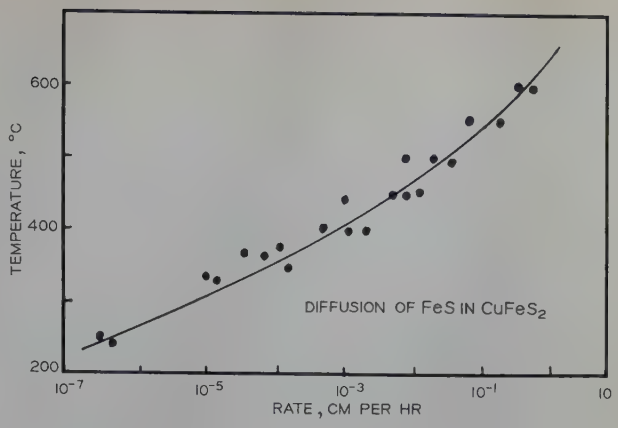

Fig. 2—Showing the diffusion velocities of FeS in chalcopyrite. Plotted in centimeters per hour in relation to the temperature. (After Borchert, 1934, Fig. 4)

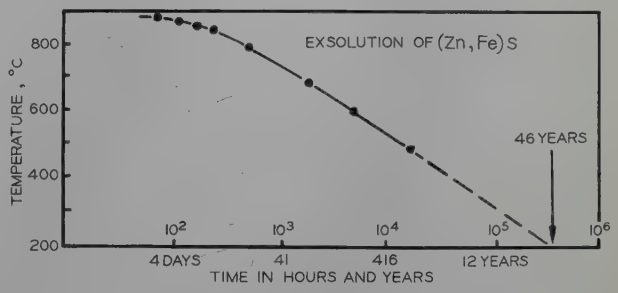

Fig. 3—Curve showing time required for complete exsolution of FeS from (Zn,F)S mixed-crystals as a function of temperature. (After Kullerud, 1953, Fig. 10.)

shape of the clouding vary from grain to grain in the ore depending upon the relative orientation of the plane of polished section to the crystal faces.

With a greater degree of segregation, the chalcopyrite has formed veinlets and in some grains has diffused out to the grain boundaries. The maximum recorded content of visible chalcopyrite in a large specimen (more than 2 sq in.) of sphalerite solid solution was 8.9 pct with an additional 11.4 pct of stannite in the same intergrown grain.

The stannite bodies appear in more clearly defined parallel rows, and have often served as nuclei for the chalcopyrite which unmixed later. Where the sphalerite is invaded by galena-matildite veinlets, the chalcopyrite segregations form a film around the margin of the galena. It is clear that the galena and matildite vein pre-dated the unmixing of the chalcopyrite from the sphalerite host solution.

Chalcopyrite: Chalcopyrite acts as a host mineral for the several other sulfides and often appears to have been the original solid solution mineral deposited in the upper parts in the veins (see later test data). Subsequent unmixing and controlled segregation of the several other intermixed solid solutions have yielded the distribution pattern of sulfides in the ore.

Sphalerite is the most common mineral intergrown with chalcopyrite. On all scales this sphalerite contains fine-grained disseminated chalcopyrite, indicating that the sphalerite itself unmixed from the chalcopyrite as a copper-bearing sphalerite solid solution rather than as a pure mineral (Fig. 6). In a large specimen of chalcopyrite 13 pct of exsolved sphalerite was measured in the form of

tiny asterisks, embayed patches, and small masses up to about 0.1 mm across.

The stannite content of the same chalcopyrite area was 16 pct but varied from specimen to specimen. As segregation of the stannite was more rapid than that of the sphalerite, stannite invariably lies on the boundaries of the chalcopyrite grains in thin curving films about 0.005 mm wide (Fig. 4). The unmixing of the stannite portion of the original solid solution with chalcopyrite, however, occurred later than that of the sphalerite, as it always surrounds the zinc sulfide. This stannite is impure and contains exsolved chalcopyrite in tiny rods and globules 0.001 to 0.01 mm long, which unmixed from a copper-bearing stannite solid solution.

Stannite: The stannite is invariably intergrown with chalcopyrite and sphalerite, any one of the three acting as host to the other two. Sphalerite occurs in the form of minute dots 0.001 mm to 0.002 mm across in the stannite, with occasional larger patches up to 0.1 x 0.01 mm which show a tendency to parallel orientation. For 0.05 mm outward from each large sphalerite patch the minute dots are absent, indicating that diffusion toward the larger areas has drained the stannite of zinc sulfide over that distance. This exact pattern of sphalerite patches, minute dots, and drained area persists without change throughout the vertical depth of the mine. In a measured specimen of stannite-rich ore the sphalerite content was 11 pct. This sphalerite contains in addition abundant small globules of

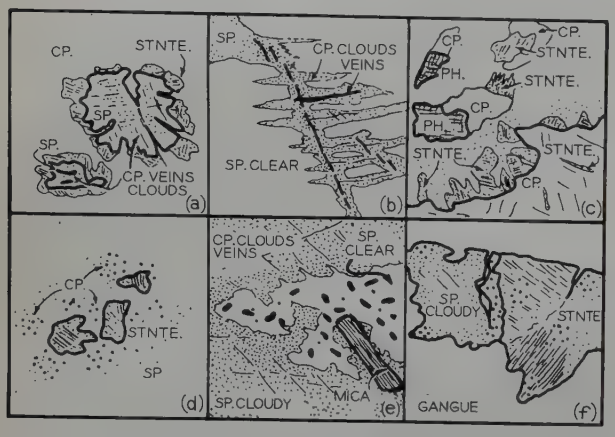

Fig. 4—Typical sulfide intergrowths in the Aberfoyle ore. Top row is from central veins (specimen used in annealing experiments). Bottom row from sphalerite clots and crystals in the aplite cupola, 300 ft below roof. X300. Micrographs reduced approximately one third. **a:** *Chalcopyrite (Cp) host; sphalerite (Sp) large exsolution patches clouded with chalcopyrite. Stannite (Stnte) molded on sphalerite and itself clouded with chalcopyrite. All stannite shows patchy inversion twinning.* **b:** *Partial unmixing of sphalerite yielding chalcopyrite clouds and veins. This sphalerite is anisotropic where clouded.* **c:** *Sphalerite host at top; chalcopyrite host in lower half. Early pyrrhotite (Ph) on which chalcopyrite and stannite are molded successively. Stannite is molded onto sphalerite-chalcopyrite boundaries, with stannite veins in the chalcopyrite.* **d:** *Sphalerite hosts, stannite exsolution patches, variable grain size of chalcopyrite blebs. In aplite cupola.* **e:** *Patch unmixing of clouded sphalerite yielding blue sphalerite and enlarged chalcopyrite blebs. Advanced stage of* (b). *In aplite cupola.* **f:** *Doublet grain of sphalerite and stannite in aplite gangue. Notice the patchy and variable clouding of the chalcopyrite in the sphalerite.*

Table I. Temperatures of Reformation of Solid Solutions, Depending on Criteria Used

	(A) Breakpoint of Temperature-Concentration Curves	(B) Initial Temperature of Dissolution of the Fine Threads	(C) Complete Resorption in 168 Hr
Chalcopyrite Host			
Sphalerite (solute)	400°C	550°C	700°C+
Stannite	375°C	475°C	625° to 700°C
Sphalerite Host			
Chalcopyrite	525°C	625° to 650°C	700°C+
Stannite	550°C	600° to 625°C	625° to 700°C
Stannite Host			
Chalcopyrite	400°C	475°C	Uncertain
Sphalerite	325°C	550°C	550°C

chalcopyrite which had unmixed after segregation of the sphalerite. This two-stage unmixing and segregation forms a constant pattern in the Aberfoyle ore.

Chalcopyrite is occasionally present in oriented intergrowths of rods 0.002 mm to 0.005 mm long, but most of it is in the form of veinlets crossing the stannite. Chalcopyrite of this type forms up to 4 pct of the stannite areas.

EXPERIMENTAL DATA AND RESULTS

The evidence from these detailed descriptions seems overwhelmingly in favor of origin of the intergrowths by exsolution after emplacement of the ore. The present geometry of the pattern was controlled by the arresting of diffusion. To determine the thermal history of this unmixing process, it was decided to make controlled annealing experiments of one week's duration (168 hr) at increasing temperatures until the solid solutions were reformed. This would reveal the pattern of a possible ore process.

A large specimen of typical chalcopyrite ore[16] was selected. The proportions of host mineral (solvent) and exsolved minerals (unmixed solute) were determined for each of the three solid solutions, with a Rossiwal integrating stage for the measurements. These values have been previously reported[16] and are graphed in Fig. 5.

The annealing experiments were performed by heating 2 to 5-cc fragments of this large specimen in evacuated pyrex glass tubes for 168 hr at temperatures ranging up to 700°C. After each run the tubes were quenched in cold water and the specimens repolished and remeasured for solvent and solute contents. Fig. 5 plots the changes in each of the three solid solutions with change in temperature of the annealing run.

Reformation of the Solid Solutions: Results of the annealing experiments are best summarized in Fig. 6. It should be borne in mind that the tests were conducted for only 168 hr, and Table I shows how the temperature of reformation of the various solid solutions changes with the criteria of re-solution used. These temperatures are a measure of at least two variables: 1) concentration and 2) diffusion rates of the solute in the solvent material. It is perhaps more correct to use the temperature at which the first signs of re-solution appear. A longer annealing time at this temperature will accomplish the same effects as those obtained by raising the temperature. The high temperature for re-solution of sphalerite in the chalcopyrite (700°C) is a function of its relatively slower diffusion rate, as the initial effects are apparent at 400°C.

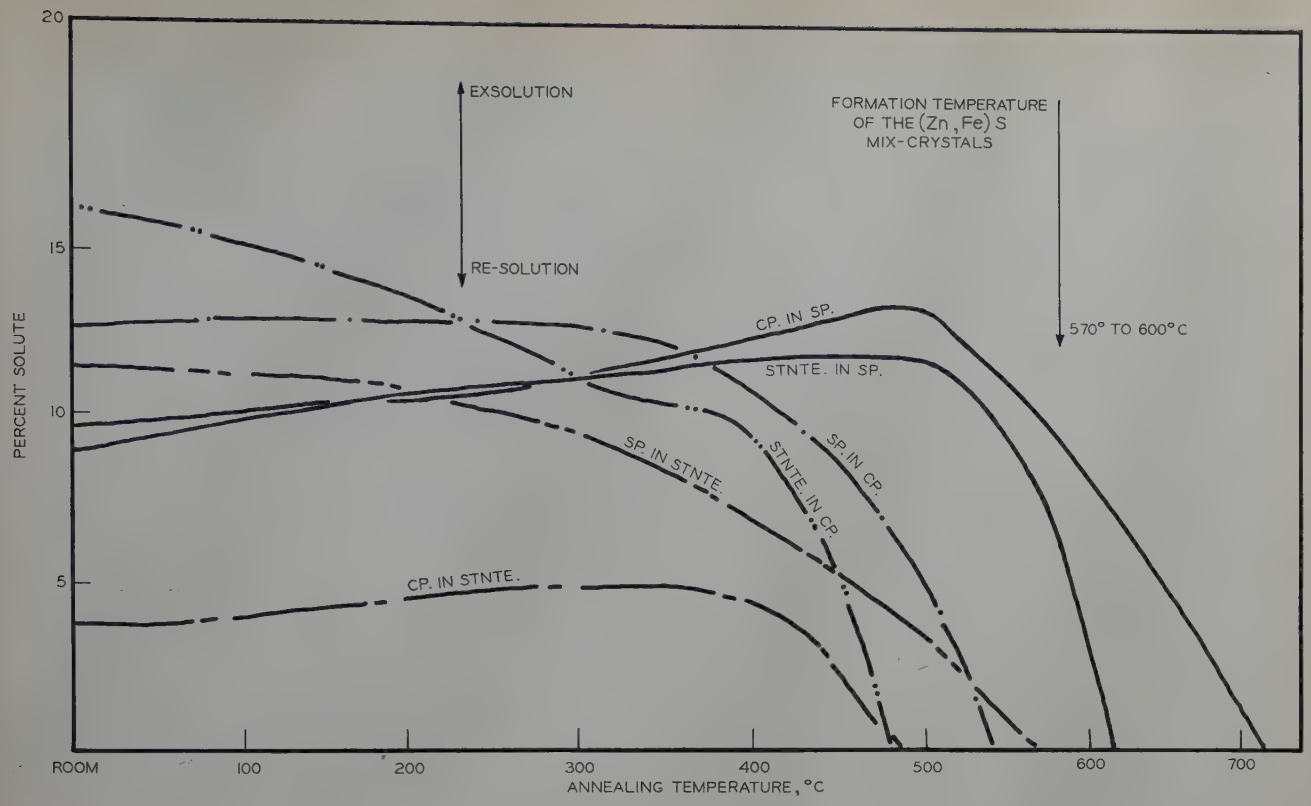

Fig. 5—Composition-temperature graph for 168-hr annealing experiments on Aberfoyle ore. Note similarity of re-solution temperatures for solid solutions and formation temperature of (Zn,Fe) mixed crystals. No pressure correction in either case. Chalcopyrite (Cp), Sphalerite (Sp), stannite (Stnte); "Stnte in Cp" is stannite content in chalcopyrite host.

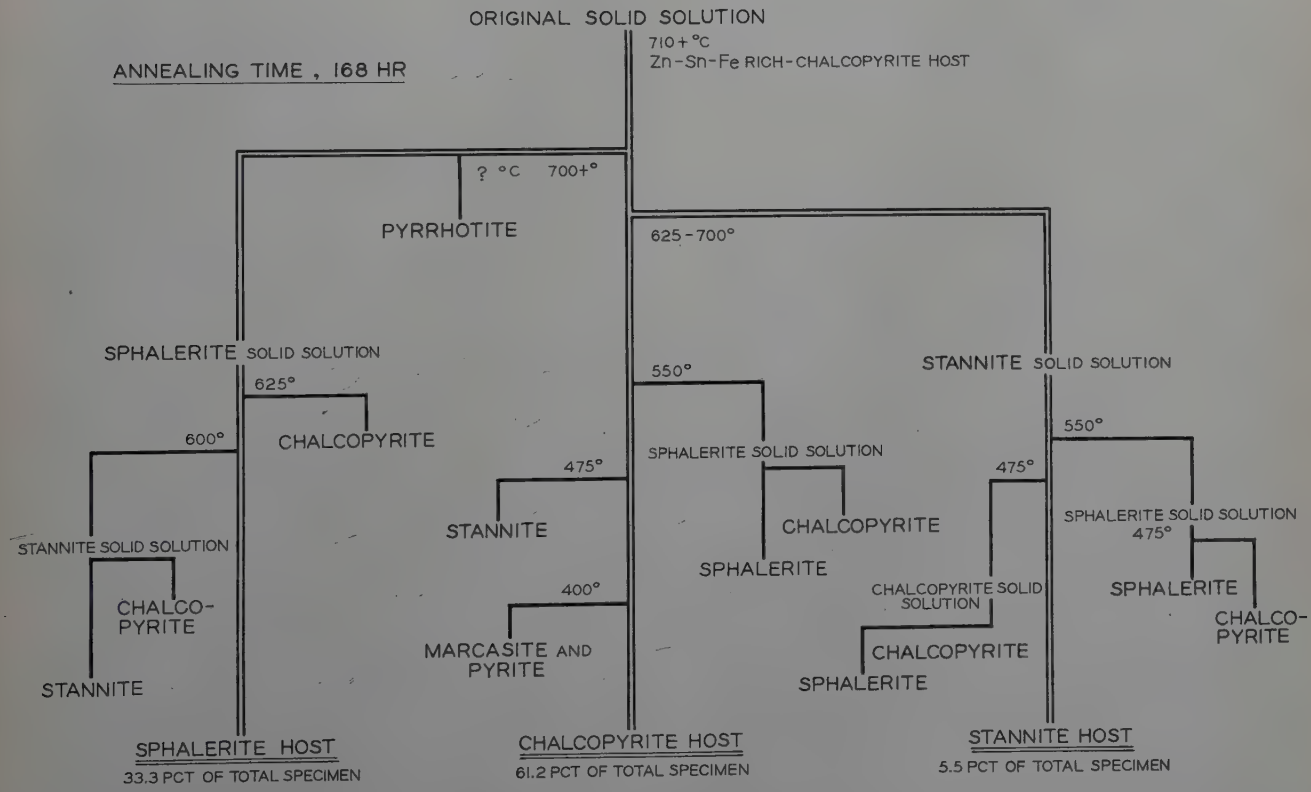

Fig. 6—Re-solution temperatures for a typical chalcopyrite-rich ore specimen. Temperatures indicate significant re-formation of solid solutions within the 168 hr of annealing, regardless of the grain size of the solute mineral.

Increased Diffusion: An interesting feature of the annealing experiments is the increased unmixing and diffusion of the chalcopyrite clouding in the sphalerite. When temperature was held at 475°C for 168 hr the clouding was intensified; more chalcopyrite was forming from the solid solution. Between 475° and 550°C this chalcopyrite segregated into enlarged patches, significantly raising the content of visible chalcopyrite (Fig. 5). Above 550°C the chalcopyrite redissolved in 168 hr until almost no trace of it remained at 700°C.

It appears obvious that the present geometry of the intergrown minerals is solely a result of arrested diffusion of several solid solutions. Given more time at temperatures higher than 325° to 400°C, increased diffusion and segregation would have removed all traces of the oriented intergrowths. Indeed the resulting even-grained granitoid texture would have indicated little of the complex thermal history. Regardless of the mechanism of ore transport, the rapid chilling of a solid solution series introduced into the veins at about 600°C appears to be the most likely way of achieving this state of suspended exsolution.

ADDITIONAL TEMPERATURE DATA

Iron Content of (Fe, Zn)S Mixed Crystal: The work of Kullerud[12] on the (Fe, Zn)S system has established a very useful geological thermometer. If the sphalerite was saturated with iron at the time of its formation, then that iron content is an indicator of the temperature of mixed crystal formation.

The Aberfoyle sphalerite on all mine levels has an iron content between 12.9 and 13.4 pct Fe. Of the 57 polished sections examined, pyrrhotite was found in a bladed intergrowth in 25, the iron sulfide covering 2 to 5 pct of the sphalerite surface. The other iron sulfides, pyrite and marcasite, occur frequently adjoining the sphalerite grains, and there is good reason to believe[16] that part of these minerals were originally pyrrhotite, either primary or exsolved from the sphalerite. This 2 to 5 pct iron sulfide is, therefore, a minimum content, and if it is assumed that the iron saturation requirements are thus satisfied, the temperature of mixed crystal formation may be calculated[13] as 570° to 600°C. This temperature apparently holds for all depths in the mine, as no significant change in the iron content can be determined. A pressure correction of 15°C for the 2000 ft of rock cover present during ore deposition can be calculated[13] which raises the deposition temperature to at least 585° to 615°C. This agrees well with the temperature of reformation of the sphalerite solid solutions (550°C) determined in the annealing experiments (see Fig. 5).

Kullerud[19] has commented upon the temperature calculated from the iron content in the Aberfoyle sphalerite, drawing attention to the very complex nature of the solid solution. Little can be done to refine these temperature data, however, until the study of this complex system is completed in synthetic form in much greater detail.

Metamorphism of the Country Rock: Thin sections over the country rock indicate that the shales and greywackes have undergone contact metamorphism sufficiently intense to develop fine-grained biotite in the matrix. It was assumed,[16] therefore, that this indicated that the country rock had not been heated over 200° to 300°C, as intense development of biotite appeared at about 400°C.[16]

SUMMARY

On the basis of experiments with ore from the Aberfoyle veins, the following hypotheses have been developed.

1) The ore was introduced at about 600°C.

Supporting Data: a) Annealing rate experiments; b) minimum figure from the iron content of sphalerite (see item 3 below).

2) Ore was introduced as a solid solution and crystallized in place before unmixing.

Supporting Data: Euhedral crystals of sphalerite from vugs show intergrowth patterns similar to those in the massive ore.

3) The solid solutions show the effects of diffusion, which has been arrested by chilling to below 325°C in a very short time. This diffusion was arrested at about 600°C (for sphalerite); all the sphalerites, therefore, contain the same amount of pyrrhotite. This proves that pyrrhotite was evenly distributed and all absorbed in ZnS, although not enough pyrrhotite was present to saturate the ZnS.

Supporting Data: a) Clouding of sphalerite varies markedly with annealing temperature (suspended exsolution); b) low grade of metamorphism of country rock, low biotite zone (200° to 300°C).

The data lead to the following conclusion:

The orebody (production total 550,000 long tons) was introduced at 600°C into a fracture zone between 100 and 1000 ft above an aplite cupola and chilled to below 325°C in a very few days.

Clearly defined data to refute this argument are hard to find. One of the points of conflict is quite significant and may hold a key to the problem:

The same pattern of complex intergrowths of the sulfides is present in the disseminated sphalerite dots in the aplite itself (300 ft beneath the cupola roof) in the pegmatite and quartz segregations, and intergrown with the wolframite as a selvage to the china-clay pipe—all in the aplitic granite cupola. It seems most unlikely that this part of the area could have been adequately cooled to freeze the diffusion of the sulfides, as all attempts to deduce the temperature gradient around an igneous intrusion[2] lead to exceedingly slow loss of heat.

It is not the purpose of this review to explain these conflicts in the data nor to propose a new theory of ore genesis. It is hoped that re-emphasizing the experimental studies will indicate the need for careful consideration of the time aspects of ore deposition as well as pressure, compositions, and temperatures of the ore fluids. Either the experimental data are incorrect by very large factors, or the classical hydrothermal theory—with its low concentrations of sulfides in aqueous solution and the implied grand expanse of time for deposition—should be critically examined. It has been assumed in these experiments, perhaps incorrectly, that the processes are reversible. It is quite possible that the position, frequency, and type of submicroscopic imperfections, defects, and dislocations in the natural crystal lattice[18] greatly influence the diffusion rates in the original deposition of the ore. Much more work must be done before these experimental data can be slavishly applied from one ore deposit

to another without very careful investigation of the ore minerals and their intergrowths.

The author would like to thank Kennecott Copper Corp. for assistance in the preparation and presentation of this article. He also extends thanks to A. B. Edwards of the Commonwealth Scientific and Industrial Research Organization, Melbourne, Australia, and C. Meyer and G. Curtis of the University of California at Berkeley for assistance in formulating the ideas presented. He is indebted to G. Kullerud, Carnegie Institute of Washington, who critically reviewed the manuscript.

REFERENCES

[1] A. B. Edwards: The Ore Minerals and Their Textures. Royal Society N. S. W., *Journal and Proceedings*, 1952, vol. 85, pp. 26-46.
[2] E. Ingerson: Methods and Problems of Geologic Thermometry. *Economic Geology*, 50th Anniversary Volume, 1130 pp. Lancaster, Pa. 1955.
[3] A. B. Edwards: *Textures of the Ore Minerals and Their Significance*, 242 pp. Australian Institute of Mining and Metallurgy, Melbourne, 1954.
[4] B. Mason: *Principles of Geochemistry*, 276 pp. John Wiley & Sons Inc., New York, 1952.
[5] G. Schwartz: Intergrowths of Bornite and Chalcopyrite. *Economic Geology*, 1931, vol. 26. pp. 186-201.
[6] R. van der Veen: *Mineragraphy and Ore Deposition*, 168 pp., The Hague, 1925.
[7] G. R. Davis: The Origin of the Roan Antelope Copper Deposit of Northern Rhodesia. *Economic Geology*, 1954, vol. 49, pp. 575-615.
[8] L. J. Miller: Uranium Ore Controls of the Happy Jack Deposit, White Canyon, San Juan County, Utah. *Economic Geology*, 1955, vol. 50, pp. 156-170.
[9] A. J. Frueh: Disorder in Sulfides. *GSA Bull.*, 1950, vol. 60, p. 1889 (Abstract).
[10] R. Latsky: The Magmatic Copper Ores of Namagualand. Geological Society of South Africa, *Trans.*, 1942, vol. 45, p. 137.
[11] G. Schwartz: Significance of Bornite-Chalcocite Intergrowths. *Economic Geology*. 1939, vol. 34, pp. 399-418.
[12] H. Borchert: Uber entmischungen im system Cu-Fe-S. *Chemie der Erde*, 1934, vol. 9, pp. 156-157.
[13] G. Kullerud: The FeS-ZnS System: A Geological Thermometer. *Norsk. geol. tidssk.*, 1953, vol. 32, pp. 61-147.
[14] P. Ramdohr: The Ore Deposit of Broken Hill in New South Wales, in the Light of New Geological Knowledge and Ore-Microscopic Investigations (English translation). *Heid. Beitrag. z. Min. u. Petr.*, Bd. 2. 1950.
[15] A. B. Edwards: Solid Solution of Tetrahedrite in Chalcopyrite and Bornite. Australian Institute of Mining and Metallurgy, *Proc.*, 1946, no. 143, pp. 141-155.
[16] A. B. Edwards and R. J. P. Lyon: Mineralization at Aberfoyle Tin Mine, Rossarden, Tasmania. Australian Institute of Mining and Metallurgy, *Proc.*, 1957, no. 181, pp. 93-145.
[17] R. J. P. Lyon: The Aberfoyle Vein System, Rossarden, Tasmania. Australian Institute of Mining and Metallurgy, *Proc.*, 1957, no. 181, pp. 75-93.
[18] C. Meyer: Personal communication.
[19] G. Kullerud: Personal communication.
[20] R. J. P. Lyon: Studies in the Geology of the Western Sierra Nevada, Pt. II. Mineralogical Study of the Ores of the Southern Foothill Copper Belt in California. Unpublished thesis, University of California, Berkeley, 1954.

Discussion of this article sent (2 copies) to AIME before Oct. 31, 1959, will be published in MINING ENGINEERING.

FACTORS AFFECTING THE CLEANING OF FINE COALS BY THE CONVERTOL PROCESS

by SHIOU-CHUAN SUN and W. L. McMORRIS III

The Convertol process was first described in Germany by Muschenborn[1] in 1952. In the U. S. Fraser[2] reported this new process in 1953, and Brisse and McMorris[3] presented the results of a Convertol pilot plant at the Alpheus preparation plant in Gary, W. Va., illustrating the mechanics of the process by a series of sketches.

The purpose of the present investigation was threefold: 1) to determine the relative effectiveness of various oils and hydrocarbons for recovering coal by the Convertol process, 2) to ascertain the behavior of coal pulps in this process under various operational conditions, and 3) to compare Convertol with flotation in the recovery of fine coals.

APPARATUS, PROCEDURE, AND COAL SAMPLES

In laboratory work with the Convertol process a Waring Blender equipped with a speed-regulating rheostat was used for wetting, conditioning, inversion, and retention of the coal pulp. A 5-in. International centrifuge was adapted to dewater the agglomerated clean coal product by installation of a 100-mesh screen inside the regular bronze basket of the centrifuge.

Except where otherwise stated, the Convertol testing was performed by the following steps:

1) A 450 to 500-cc coal slurry, containing 24 pct by weight of solids, was agitated in the blender for 10 min at 100 rpm to insure complete wetting and mixing.

2) Eight percent by weight of oil was added to the coal slurry in the blender and agitated for 1 min at 11,000 rpm to result in the phase inversion or agglomeration of oil-coated coal particles.

3) The agglomerated coal slurry was poured onto a 100-mesh sieve and wet-screened for about 2 min to remove most of the ash and some of the water.

4) The material remaining on the screen was transferred into the centrifuge for final dewatering.

5) A portion of the clean coal was immediately weighed out for moisture determination, while the

S. C. SUN, Member AIME, is Professor of Mineral Preparation, The Pennsylvania State University, University Park, Pa. W. L. McMORRIS III, Junior Member AIME, is Preparation Engineer, Wellington Coal Preparation Plant, Columbia-Geneva Steel, Drageron, Utah. TP 59F205. Manuscript, Feb. 5, 1959. New York Meeting, February 1958. AIME Trans., Vol. 214, 1959.

remaining clean coal was washed with acetone to remove the attached oil and then dried, weighed, and analyzed for ash and sulfur.

6) The refuses obtained from screening and centrifuging were combined and filtered, and the resultant filter-cake was dried, weighed, and analyzed for ash and sulfur. If the conditioning and retention stages were necessary, as in the case of Fig. 6, the blender was allowed to run at 1000 rpm for both stages. For brevity, the analytical results of ash and sulfur are only selectively presented, but are available in W. L. McMorris' thesis.[4]

The three coal samples used in this investigation came from the Robena, Alpheus, and Corbin preparation plants of U.S. Steel Corp. The Robena sample was obtained from the bowl-desilter overflow of Pittsburgh Seam coal in Greene County, Pa. The Alpheus sample, representing the Pocahontas No. 3 and 4 seams in McDowell County, W. Va., was taken from the feed to a Convertol pilot plant. The Corbin sample was taken from the bowl-desilter overflow of the *B, C,* and High Splint seams coal in Harlan County, Ky. All the coal samples were shipped to the University in sealed cans to prevent undue oxidation. Size distribution and chemical composition of these samples are given in Tables I and II, respectively.

EXPERIMENTAL RESULTS

Hydrocarbons and Oils: Tests were performed to determine the relative effectiveness of hydrocarbons and oils for cleaning Robena coal slimes by the Convertol process. The results, as given in Tables III-V and Figs. 1-3, show that the agglomerating power of the tested hydrocarbons and oils on the Robena coal can be roughly predicted from their

Table I. Screen and Chemical Analyses of Coal Samples

Tyler Screen,* Mesh	Robena			Corbin			Alpheus		
	Wt, Pct	Ash, Pct	S, Pct	Wt, Pct	Ash, Pct	S, Pct	Wt, Pct	Ash, Pct	S, Pct
48 to 65	Trace	—	—	Trace	—	—	Trace	—	—
65 to 100	12.03	6.36	0.80	12.78	1.40	0.48	9.05	5.59	0.41
100 to 150	19.60	5.82	1.76	6.93	2.30	0.56	8.03	5.63	0.42
150 to 200	18.27	5.68	1.91	7.41	3.90	0.92	6.84	5.99	0.69
200 to 270	6.04	6.42	1.34	5.42	6.63	0.52	8.03	6.62	0.60
270 to 400	3.02	9.18	1.36	4.51	8.13	0.81	7.02	7.37	0.69
−400	41.04	27.74	2.45	62.95	39.94	0.44	61.03	28.79	0.76
Head	100.00	14.00†	1.80†	100.00	28.00†	0.44†	100.00	18.00†	0.56†

* Wet screen analysis. † Average.

Table II. Ultimate Analyses of Oven Dried Coal Samples

Composition	Robena, Pct	Corbin, Pct	Alpheus, Pct
Carbon	70.35	57.00	72.59
Fixed carbon	52.61	42.85	64.09
Hydrogen	4.70	3.81	4.05
Sulfur	1.80	0.43	0.54
Nitrogen	1.02	0.81	0.76
Oxygen	5.28	6.23	2.95
Volatile matter	30.54	25.43	16.80
Ash	15.85	30.36	18.54
Moisture	1.00	1.36	0.57
B.T.U.	12435	9864	11036

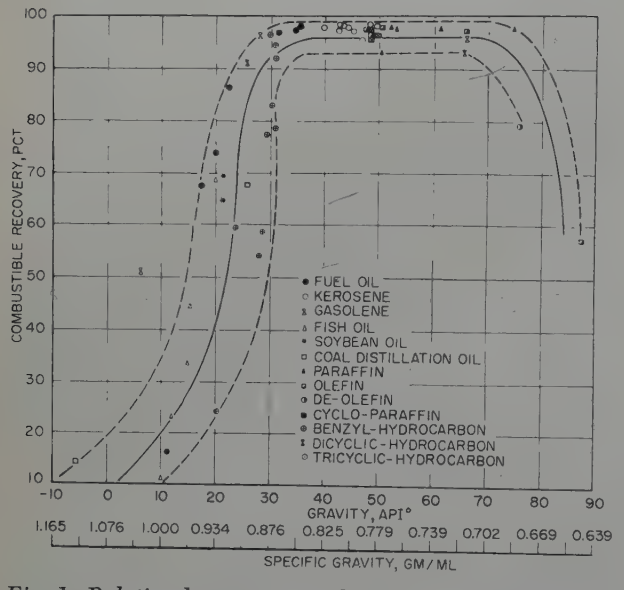

Fig. 1—Relation between specific gravity and agglomerating power of hydrocarbons and oils on Robena slime.

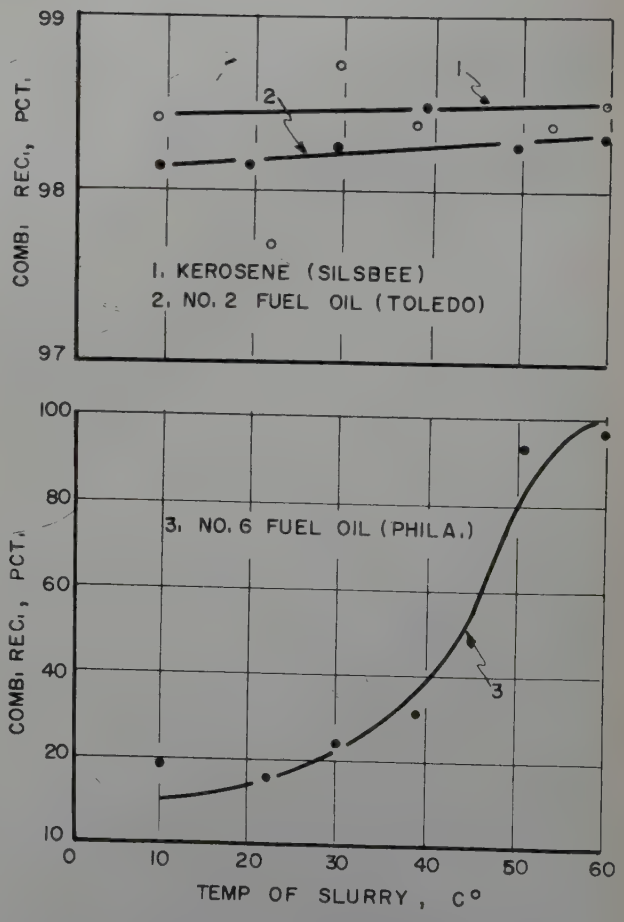

Fig. 2—Pulp temperature effects on agglomerating power of Gulf kerosene and No. 2 fuel oil on Robena slime.

Table III. Effects of Straight-Chain Hydrocarbons on Cleaning Robena Coal Slime by Convertol Process

Test Conditions: 10-min wetting, 13.5 pct pulp density, 8 pct by weight of oil, 1-min inversion at 11,000 rpm, and 1-min centrifuging at 1300 rpm.

Aliphatic Hydrocarbon								Clean Coal		
Name	Formula	Carbon Atom	Gravity API*	Sp Gr, G Per Ml	Viscosity 20°C Cp	Solu,† G Per Liter	Boiling Point, C°	Ash, Pct	S, Pct	Comb. Rec., Pct
(A) Paraffin Series										
n-Heptane	$CH_3(CH_2)_5CH_3$	7	75.3	0.684	0.409	$0.052^{15.5}$	98.25	5.30	1.69	97.23
n-Octane	$CH_3(CH_2)_6CH_3$	8	69.6	0.7036	0.539	0.015^{16}	125.8	5.38	1.71	97.50
n-Decane	$CH_3(CH_2)_8CH_3$	10	62.2	0.7301	0.907	Insoluble	174	3.62	1.70	97.68
n-Dodecane	$CH_3(CH_2)_{10}CH_3$	12	53.2	0.766	1.353^{25}	Insoluble	214.5	5.69	1.86	97.98
n-Tetradecane	$CH_3(CH_2)_{12}CH_3$	14	53.4	0.765	2.178	Insoluble	253.5	3.54	1.62	97.13
n-Hexadecane	$CH_3(CH_2)_{14}CH_3$	16	51.1	0.775	3.516	Insoluble	287.5	3.54	1.62	92.94
(B) Olefin Series										
l-Pentene	$CH_3(CH_2)_2CH{:}CH_2$	5	87.7	0.6454	0.239	Insoluble	30.1	4.44	1.38	56.95
di-iso-butylene	$(CH_3)_2C{:}CHC(CH_3)_3$	8	66.4	0.715	—	Insoluble	102.6	5.48	1.70	97.34
l-Octene	$CH_3(CH_2)_5CH{:}CH_2$	8	66.4	0.715	—	Insoluble	121.6	3.84	1.70	97.95
l-Decene	$CH_3(CH_2)_7CH{:}CH_2$	10	54.0	0.763	1.090	Insoluble	172	5.56	1.59	98.02
l-dodecene	$CH_3(CH_2)_9CH{:}CH_2$	12	51.6	0.7732	1.140^{30}	Insoluble	213	7.46	1.99	98.07
l-Tetradecene	$CH_3(CH_2)_{11}CH{:}CH_2$	14	51.1	0.775	—	Insoluble	246	5.64	1.83	98.56
l-hexadecene	$CH_3(CH_2)_{13}CH{:}CH_2$	16	49.3	0.7827	2.556^{30}	Insoluble	$158^{11.5}$	3.64	1.78	96.26
n-Octadecene	$CH_3(CH_2)_{15}CH{:}CH_2$	18	48.1	0.788	—	Insoluble	190^{15}	5.76	1.86	97.14
(C) Di-olefin Series										
Isoprene	$CH_2{:}C(CH_3)CH{:}CH_2$	5	76.4	0.6805	2.160	Insoluble	34.07	6.60	1.69	79.15

* API is the unit expressed in degree of gravity, as used by the American Petroleum Institute, and is calculated from the formula, Specific gravity = 141.5/(API + 131.5).
† Solution, solubility in water.

specific gravity. A study of Fig. 1 reveals that the specific gravity range of the highly effective hydrocarbons and oils is 0.7020 to 0.8498 or 70.0 to 35.0 API°; of the moderately effective ones, 0.6390 to 0.7019 or 90.0 to 70.1 API° at the right side of the curve and 0.8499 to 0.9658 or 34.9 to 15.0 API° at the left side; and of the non-effective ones, > 0.9658 and < 0.6390. On the basis of data in Tables III and IV it can be assumed that the large molecules of an extremely heavy hydrocarbon are too viscous to be dispersed in the coal pulp, while the small molecules of an extremely light hydrocarbon are not hydrophobic enough; thus neither can be effective in coal agglomeration. In contrast, the fluidity and hydrophobic property of a medium-weight hydrocarbon are both suitable for such a purpose. If the foregoing reasoning is accepted then some of the heavy hydrocarbons and oils might be sufficiently fluidized in a preheated coal slurry to become effective reagents. This proves to be true for the Gulf No. 6 fuel oil, as shown in curve 3 of Fig. 2. Curves 1 and 2 of the same graph show that the medium-weight oils, having enough fluidity at room temperature, are practically unaffected by preheating of slurry. Fig. 3a, however, shows that effectiveness of the No. 6 fuel oil is only slightly improved by preheating it to 110°C. It was observed that this oil was considerably more fluid at high temperatures but became viscous again when added to the slurry at room temperature.

The above classification does not lay claim to absolute accuracy, but it is sufficient as a crude rule for selecting oil. Table V shows that oils under different names and even under the same name may vary greatly in the agglomerating power on coal. While the specific gravities of oils are easily determined, or obtained from the manufacturers, their chemical compositions, boiling points, and viscosities are not. The irregularities of Fig. 1 are caused chiefly by differences among the types of hydrocarbons and oils and can be minimized by plotting each type separately.

Another series of tests determined the effects of concentration of oils on the cleaning of three different coal slimes by the Convertol process. Fig. 3A shows that with an increase in concentration of a heavy fuel oil the combustible recovery of coal increases, but after the maximum recovery is attained at the concentration of 4 pct oil, addition of more oil actually lowers recovery. This relationship is not changed by preheating the oil to 110°C. In contrast, Fig. 3B and Table VI show that the combustible recovery increases rapidly with an increase of the concentration of a medium-weight kerosene in the range of 2 to 6 pct, but a subsequent increase of kerosene results in only slight increases in combustible recovery. Fig. 3B shows also that while the concentration of kerosene is kept constant, combustible recovery of the three coal slimes tested is decreasing in the order of Robena, Alpheus, and Corbin. As can be seen from Tables I and II, these coals differ appreciably from each other not only in surface components[5] but also in size distribution and consequently have different affinities for any given agglomeration reagent.

Operational Variables: Tests were also made to determine the effects of pulp density, conditioning, inversion, retention time, and inverter speed on the cleaning of Robena coal slime by the Convertol process. Fig. 4 shows that with kerosene (Silsbee) of 0.8009 sp gr as the agglomerating reagent, the combustible recovery of coal increases rapidly with the increase of pulp density in the range of 5 to 15 pct solids, but a subsequent increase in pulp density results in only slight increases in combustible recovery. A similar relationship exists for the No. 2 fuel oil (Toledo) of 0.8477 sp gr except that the optimum pulp density is reached at 30 pct solids. The inefficiency of the low pulp density may be attributed to the relatively large distance between coal particles themselves and also between coal particles and oil droplets in the liquid phase; this lessens the frequency of collision and consequently slows the rate of agglomeration. The difference in

Table IV. Effects of Aromatic Hydrocarbons on Cleaning Robena Coal Slime by Convertol Process

Name	Aromatic Hydrocarbon Formula	C/H Ratio	Carbon Atom	Gravity API°	Sp Gr, G Per Ml	Viscosity at 20°C, Cp	Solu.,* G Per Liter	Boiling Point, C°	Clean Coal** Ash, Pct	S, Pct	Comb. Rec., Pct
(A) Cyclo-paraffin Series											
Methyl Cyclohexane	$C_6H_{11}CH_3$	0.5	7	48.4	0.7864	0.777^{15}	Insoluble	100.8	5.36	1.66	97.39
Trans., 1, 2, Dimethyl-cyclohexane	$C_6H_{10}(CH_3)_2$	0.5	8	50.8	0.776	0.863^{15}	Insoluble	123.7	3.66	1.69	96.31
Ethylcyclohexane	$C_6H_{11}CH_2CH_3$	0.5	8	49.0	0.784	0.838	Insoluble	131.8	4.32	1.61	96.65
(B) Benzyl Series											
Benzene	C_6H_6	1.0	6	29.4	0.8794	0.652	0.82^{22}	80.09	4.44	1.63	58.38
Toulene	$C_6H_5CH_3$	0.875	7	31.8	0.866	0.623^{15}	0.47^{16}	110.65	6.78	1.76	94.63
Ethylbenzene	$C_2H_5C_6H_5$	0.8	8	31.7	0.8669	0.691	0.14^{15}	136.15	1.65	1.65	82.78
o-Xylene	$C_6H_4(CH_3)_2$	0.8	8	30.3	0.8745	0.813	Insoluble	144.5	4.30	1.72	73.33
Styrene	$C_6H_5CH{:}CH_2$	1.0	8	24.4	0.9074	—	Very slightly soluble	146	4.80	1.46	59.39
Ethynylbenzene	$C_6H_5C{:}CH$	1.33	8	20.7	0.9295	—	Insoluble	143	2.80	1.31	24.48
Cumene	$C_6H_5CH(CH_3)_2$	0.750	9	32.0	0.864	0.73^{25}	Insoluble	152.4	4.14	1.69	91.87
Diethylbenzene	$C_6H_4(C_2H_5)_2$	0.714	10	31.9	0.8662	0.86^{25}	Insoluble	184	6.14	1.67	78.18
sec-Amylbenzene	$C_6H_7CH(CH_3)C_6H_5$	0.688	111	33.5	0.8576	—	Insoluble	192.5	5.56	1.68	96.95
Triethylbenzene	$C_6H_3(C_2H_5)_3$	0.667	12	28.9	0.8819	1.31^{27}	Insoluble	218	5.58	1.65	54.74
(C) Dicyclic Series											
decahydronaphtalene	$C_{10}H_{18}$	0.556	10	26.4	0.8963	3.381	Insoluble	194.6	3.80	1.63	91.30
Methylnaphthalene	$C_{10}H_7CH_3$	1.1	11	6.5	1.025	3.33	Insoluble	244.8	3.18	1.46	51.53
Dicyclohexyl	$CH_2(CH_2)_4CH{-}CH(CH_2)_4CH_2$	0.545	12	28.4	0.8848	4.027	Insoluble	238.5	5.40	1.62	96.71
(D) Tricyclic Series											
Fluorene	$C_6H_4CH_2C_6H_4$	1.3	13	23.0	0.916	—	Insoluble	298.0	—	—	None†

* Solu., solubility in water.
** Test conditions were same as that of Table III.
† No phase inversion.

Table V. Effects of Various Commercial Oils on the Cleaning of Robena Coal Slime by Convertol Process

Test No.	Oil Name and Source	Gravity API°	Sp Gr, G Per Ml	Clean Coal* Ash, Pct	S, Pct	Moisture, Pct	Comb. Rec., Pct
1	Fuel oil,[a] No. 2, (Toledo)	35.9	0.8477	5.86	1.70	13.5	98.13
2	Fuel oil,[a] Dieselect	35.6	0.8468	6.06	1.91	13.5	97.09
3	Fuel oil,[a] No. 2, (Port Arthur)	32.1	0.8649	6.44	1.90	12.0	96.65
4	Fuel oil,[a] Cracked No. 2	23.0	0.9195	5.84	1.86	11.0	88.62
5	Fuel oil,[a] No. 4, (N. Y.)	20.3	0.9321	5.61	1.62	12.2	74.07
6	Fuel oil,[a] No. 5, (Philadelphia)	18.0	0.9493	5.54	1.64	14.3	67.57
7	Fuel oil,[a] No. 6, (Philadelphia)	11.5	0.9895	5.38	1.77	10.5	16.00
8	Kerosene, (Mexico)	49.6	0.7814	5.32	1.81	16.5	98.22
9	Varsol,[b] (Canada)	50.3	0.7784	5.07	1.78	16.3	98.16
10	Kerosene,[b] (Canada)	44.6	0.8036	4.84	1.73	14.3	97.77
11	Kerosene,[a] (Silsbee)	45.2	0.8009	4.97	1.73	14.5	97.66
12	Kerosene,[a] (Venezuela)	40.4	0.8229	4.99	1.73	16.4	97.65
13	Kerosene,[a] (Houston)	43.3	0.8094	5.18	1.72	20.1	97.58
14	Kerosene,[c] (Norco)	43.9	0.8069	4.95	1.77	16.3	97.52
15	Kerosene,[a] (Port Arthur)	46.1	0.7967	5.92	2.06	12.5	97.11
16	Kerosene,[d] purified	47.8	0.7891	5.22	1.62	16.7	95.44
17	Gasoline,[e] imperial	67.1	0.7124	7.52	—	18.7	96.90
18	Gasoline,[e] regular	66.0	0.7164	7.76	—	19.2	93.50
19	Coal tar naphtha[f]	25.7	0.9000	7.45	1.91	16.0	67.87
20	Heavy creosote[f]	−6.3	1.13	4.88	1.55	15.7	14.48
21	Soybean oil,[g] white refined	21.6	0.9240	4.28	1.60	16.8	69.68
22	Soybean oil,[g] degummed raw	21.6	0.9240	4.86	1.68	13.5	64.77
23	Fish oil,[h] light, cold pressed	20.4	0.931	5.10	1.66	12.5	68.74
24	Fish oil,[h] crystol L	15.7	0.961	4.56	1.59	15.6	44.30
25	Fish oil,[h] crystol W	15.0	0.966	2.90	1.35	18.7	33.05
26	Fish oil,[h] Blown No. 3	12.2	0.985	5.26	1.44	18.7	22.36
27	Fish oil,[h] Blown No. 6	10.0	1.000	—	—	—	none†

Source: a, Gulf Research and Development Co., Pittsburgh, Pa.; b, Imperial Oil Co., Canada; c, Shell Oil Co., New York; d, local ESSO station; e, local Atlantic station; f, Koppers Co. Inc., Pittsburgh, Pa.; g, General Mills Inc., Kankakee, Ill.; and h, Archer-Daniels-Midland Co., Cleveland, Ohio.
* Test conditions were same as that of Table III, except that the pulp density was 24 pct.
† No phase inversion.

Table VI. Effects of Concentration of Gulf Kerosene (Silsbee) on Cleaning Robena, Alpheus, and Corbin Coal Slimes by Convertol Process

Test Conditions: 10-min wetting, 24.25 pct solids, 1-min inversion at 11,000 rpm and 1-min centrifuging at 1300 rpm

Kerosene, Wt, Pct	Robena Clean Coal Ash, Pct	S, Pct	Yield, Pct	Comb. Rec., Pct	Alpheus Clean Coal Ash, Pct	S, Pct	Yield, Pct	Comb. Rec., Pct	Corbin Clean Coal Ash, Pct	S, Pct	Yield, Pct	Comb. Rec., Pct
2	7.72	1.71	60.48	65.21	5.99	0.66	70.30	81.09	4.89	0.57	53.10	72.20
4	6.02	1.67	86.40	93.01	5.14	0.62	79.50	91.21	4.83	0.56	67.60	89.72
6	6.50	1.71	89.12	97.77	5.50	0.64	83.90	96.55	4.60	0.56	71.20	94.42
8	4.97	1.73	89.68	97.66	5.99	0.64	85.00	97.37	4.34	0.56	71.90	96.06
10	6.16	1.74	91.52	98.47	6.00	0.68	87.60	98.25	4.61	0.53	75.30	96.28

optimum pulp density between kerosene and fuel oil may be explained by the fact that kerosene is lighter and consequently less viscous and more dispersible than fuel oil, so that it can produce more oil droplets for collision with the widely dispersed coal particles in a relatively dilute pulp of 15 pct solids.

Fig. 5A shows that efficiency of the kerosene is only slightly improved by conditioning, prior to phase inversion, for 2 min or longer at 1000 rpm, whereas the effectiveness of the fuel oil is practically unchanged by conditioning. It can be deduced from Fig. 5B that the Robena coal is effectively coated and agglomerated by either of these two oils during the 1-min phase inversion at 11,000 rpm and consequently requires no conditioning. For the same reason, retention is not needed either, as indicated in Fig. 5C. Fig. 5B shows also that the optimum time for phase inversion, at a speed of 11,000 rpm, is 1 to 2 min. With less than 1 min, the coal particles are not sufficiently coated by oil for complete agglomeration. With more than 2 min, the large coal agglomerates are gradually disintegrated by the tearing force of eddying currents

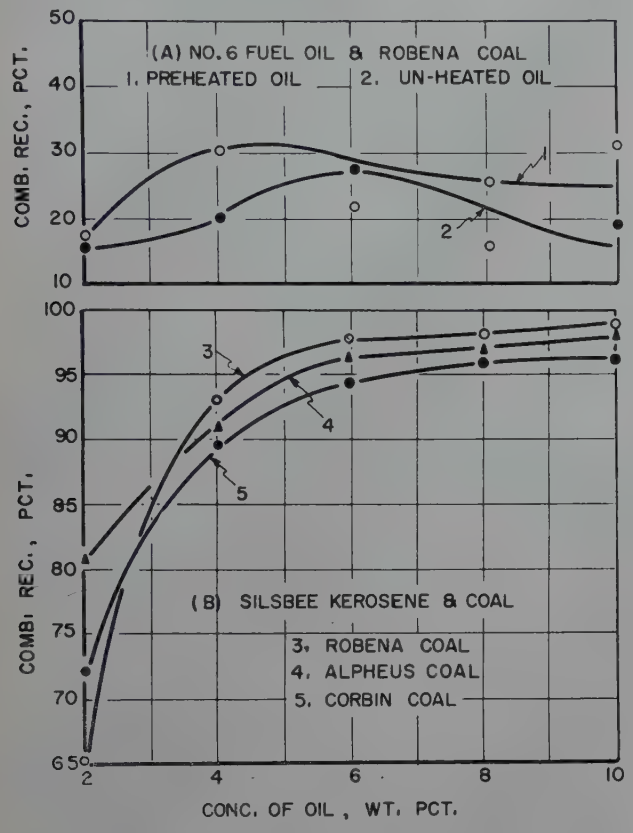
(A) NO. 6 FUEL OIL & ROBENA COAL
1. PREHEATED OIL
2. UN-HEATED OIL
COMB. REC., PCT.
(B) SILSBEE KEROSENE & COAL
3. ROBENA COAL
4. ALPHEUS COAL
5. CORBIN COAL
CONC. OF OIL, WT. PCT.

Fig. 3—Graph shows the effect of concentration of oils on the cleaning of coal slimes by the Convertol process.

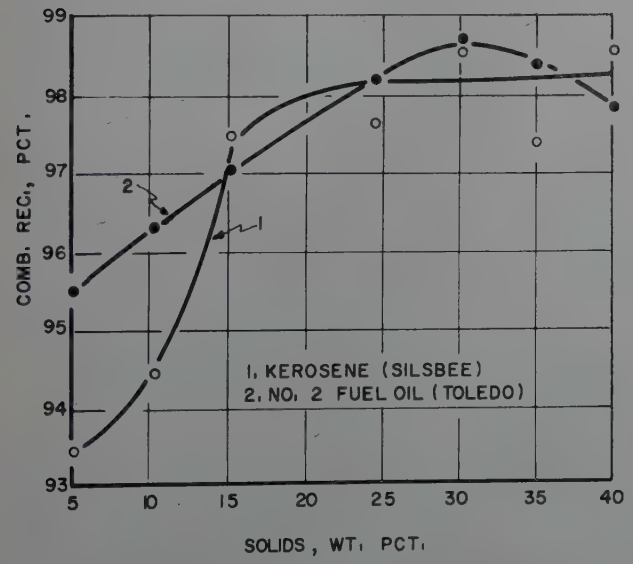

Fig. 4—Graph shows the effect of pulp density on the cleaning of Robena coal slime by the Convertol process.

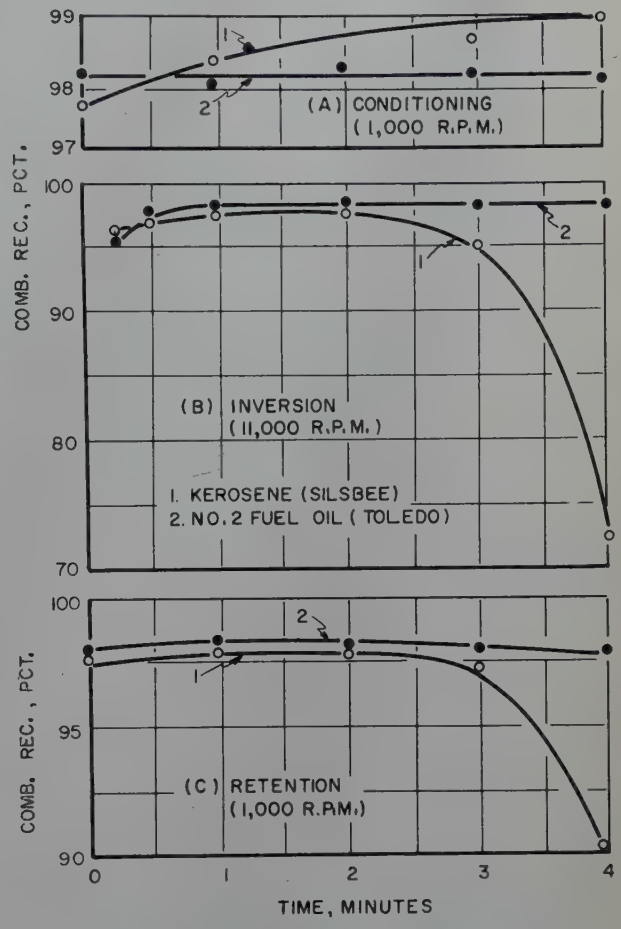

Fig. 5—Effects of conditioning, inversion, and retention time on cleaning Robena slime by Convertol process.

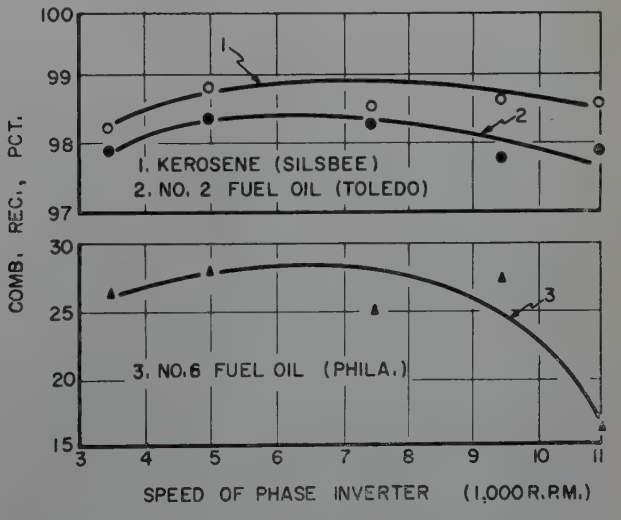

Fig. 6—Graph shows the effects of inverter speed on the cleaning of Robena coal slime by Convertol process.

Table VII. Rougher Flotation of Robena and Corbin Coal Slimes in Laboratory Fagergren Machine at pH 7.5

Test No.	Product				Reagent, Lb Per Ton			Flotation Time, Min
	Name	Wt, G	Ash, Pct	S, Pct	Comb. Rec., Pct	Silsbee Kerosene	Yarmour F Pine Oil	Carbinol*	
1	Robena	265.4	13.99	1.73	100.0				
	Conc.	130.4	8.48	1.72	99.9			0.14†	6
	Tail	15.0	98.80	1.91					
2	Robena	267.0	13.30	1.82	100.0				
	Conc.	240.5	8.70	1.80	94.9		0.14†		6
	Tail	26.5	55.17	2.00					
3	Robena	274.0	14.31	1.92	100.0				
	Conc.	261.0	10.84	1.91	99.2		0.53†		5
	Tail	13.0	86.68	2.12					
4	Robena	239.0	13.80	1.87	100.0				
	Conc.	220.0	9.24	1.85	96.9	0.33†	0.14		6
	Tail	19.0	66.25	2.10					
5	Robena	267.5	15.12	1.80	100.0				
	Conc.	246.5	9.56	1.78	98.2	5.35†	0.14		5
	Tail	21.0	80.90	2.04					
6	Corbin	202.7	10.51	0.82	100.0				
	Conc.	195.0	7.34	0.81	99.7			0.18†	4
	Tail	7.7	93.00	1.08					
7	Corbin	214.8	15.24	0.68	100.0				
	Conc.	199.6	11.38	0.66	97.1		0.18†		4
	Tail	15.2	65.76	0.92					
8	Corbin	155.4	27.91	0.70	100.0				
	Conc.	122.4	9.92	0.59	98.6		0.48†		4
	Tail	33.0	95.10	0.97					
9	Corbin	196.5	11.12	0.90	100.0				
	Conc.	186.0	7.34	0.89	98.7	0.84†	0.18		4
	Tail	10.0	78.61	0.91					
10	Corbin	201.0	10.10	0.83	100.0				
	Conc.	194.0	7.44	0.82	99.2	1.67†	0.18		4
	Tail	7.0	83.31	0.93					

* Methyl isobutyl carbinol. † Conditioning for 3 min.

and by the disruptive force of collision. The disintegration of coal agglomerates formed by kerosene is much more than that formed by fuel oil. This is probably due to the fact that coal particles are more easily dislodged from kerosene than from fuel oil, since kerosene is less viscous and more volatile. Fig. 5C shows that coal agglomerates also start to disintegrate after 2 min of retention.

Fig. 6 shows that the optimum speed of the phase inverter (Waring Blender) for a 1-min agglomeration of Robena coal slime with 8 pct by weight of kerosene, No. 2 fuel oil or No. 6 fuel oil, is 5000 to 7000 rpm. Efficiency is somewhat lower on either side of this range. The relatively weak agitation resulting from speeds lower than 5000 rpm is insufficient for effective mixing of coal and oil. Conversely, the violent turbulence resulting from speeds higher than 7000 rpm is capable of disintegrating the coal agglomerates.

Flotation: Table VII shows that both the Robena and Corbin coal slimes can be easily cleaned by flotation with methyl isobutyl carbinol, pine oil, or a combination of kerosene and pine oil as the reagent. Of the flotation reagents tested, methyl isobutyl carbinol is the most effective. Comparison of Tables VI and VII shows that the Convertol process is superior to rougher flotation in lowering the ash content of these two particular coal slimes. It is expected that flotation effectiveness will be improved by the inclusion of a cleaning circuit and/or by addition of a suitable depressant, although no such experiments were performed. Noteworthy also is the fact that flotation requires a much smaller amount of reagent than the Convertol process. However, it has been pointed out by other investigators[6] that the Convertol process can be economically justified for recovering metallurgical coal because the oil in the product is beneficial to coke plant operations. Selection of either method will depend upon the special conditions of each company and the ultimate use of the clean coal.

SUMMARY

1) A crude rule is established for selecting oils in the cleaning of coal slimes by the Convertol process.

2) The optimum pulp density ranges from 15 to 30 pct solids, depending on the oil used. The optimum time for phase inversion, at 11,000 rpm, is 1 to 2 min. Optimum inverter speed is 5000 to 7000 rpm.

3) Neither the conditioning or the retention stage is needed if the coal slurry is properly treated in the inversion stage.

4) The Convertol process and flotation are both effective for cleaning the Robena and Corbin coal slimes.

The writers are indebted to the coal division of U.S. Steel Corp. for furnishing the coal samples. They wish to thank P. D. Rao and D. J. Cook for assistance in the flotation experiments, and they also express appreciation to D. R. Mitchell and H. B. Charmbury for their encouragement and helpful criticism.

REFERENCES

[1] W. Muschenborn: Neve Versuche zur Feinstkornaufbereitung insbescondere zur Aufbereitung von Steinkohlenschlarmen. *Glückauf*, April 12, 1952, vol. 88, nos. 15-16, pp. 240-242.

[2] T. Fraser: Convertol Process of Coal-Slurry Treatment. *USBM Inf. Circ. 7660*, April 1953.

[3] A. H. Brisse and W. L. McMorris, Jr.: Convertol Process. *AIME Trans.*, 1958, vol. 211, pp. 258-261.

[4] W. L. McMorris, III: *Convertol Process for Recovery of Fine Coal*. Master's thesis, Pennsylvania State University, August 1957.

[5] S. C. Sun: Hypothesis for Different Floatabilities of Coals, Carbons, and Hydrocarbon Minerals. *AIME Trans.*, 1954, vol. 199, pp. 67-75.

[6] S. C. Sun: The Mechanism of Coarse Coal and Mineral Froth Flotation. *AIME Trans.*, 1950, vol. 187, pp. 616-622.

Discussion of this article sent (2 copies) to AIME before Dec. 31, 1959, will be published in MINING ENGINEERING.

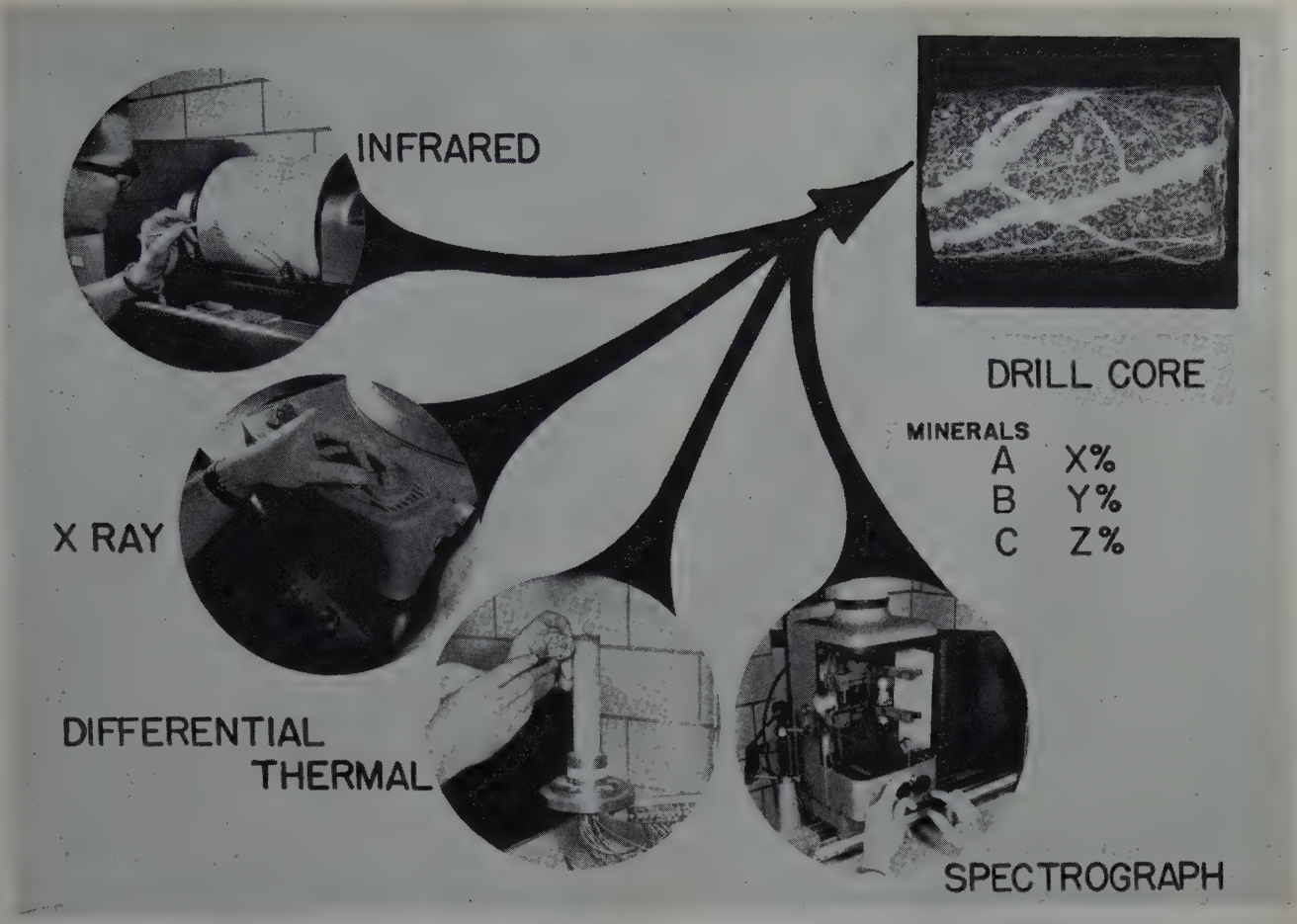

Fig. 1—Diagram of integrated instrumentation.

QUANTITATIVE MINERALOGY AS A GUIDE IN EXPLORATION

by R. J. P. LYON and W. M. TUDDENHAM

In many areas surrounding the orebodies in mining districts rocks have been bleached and altered by the ore-forming solutions and have been oxidized during later weathering processes. A number of the rock-forming silicates have been broken down to clay, sericitic micas and chlorites have been developed, and pyrite may be found hundreds of feet outside the economic limits of the orebody. These halos of altered ground are prime targets used by geologists in many districts to delineate promising sites for drilling.

Both in the field and in the laboratory it is often difficult to map these mineralogical changes in the halos in detail without numerous petrologic examinations. The secondary minerals are generally fine-grained, and since conversion of one mineral to another is often progressive, many alteration processes have not proceeded to completion (feldspars to clay to sericite mica). Qualitative detection of these minerals is difficult; quantitative determination is frequently impossible.

R. J. P. LYON, and W. M. TUDDENHAUM, Members AIME, are Senior Scientists, Kennecott Copper Research Center, Salt Lake City. TP 59177. Manuscript, April 17, 1959. San Francisco Meeting, February 1959. AIME Trans., Vol. 214, 1959.

This page of Mining Transactions AIME follows p. 1156. The intervening non-Transactions pages appeared in MINING ENGINEERING.

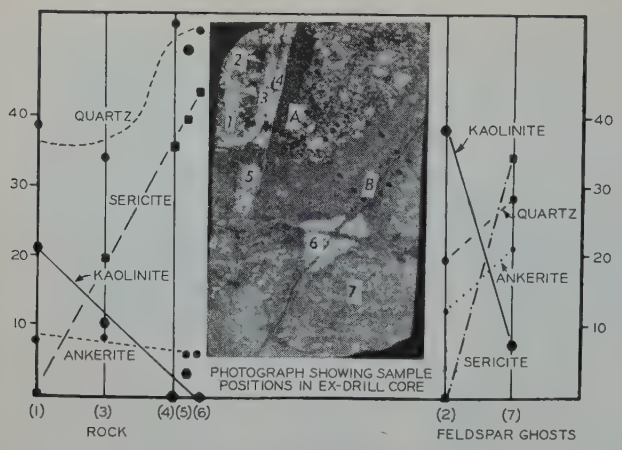

Fig. 2—The quantitative mineralogy of several alteration envelopes in drill core section (3, reduced approximately 12 pct.) The freshest rock (1) contains kaolinized feldspar phenocrysts (2). Alteration envelopes are chloritic fringe (3) and quartz-sericite zones (4, 5, 6), which contain feldspar ghosts (7).

Many studies made in the past have suffered from basic inadequacy in determining the fine-grained minerals. In consequence, the field mapping and ultimately the usefulness of the alteration study have been seriously handicapped. Quantitative mineralogy of samples collected on a grid basis in areas of pervasive alteration offers a guide little used to date in exploratory drilling.

INTEGRATED METHOD VS MICROSCOPE APPROACH

At Kennecott's Research Center techniques of mineral identification and quantification have been developed to aid the company's exploration department. Almost all samples received are now processed with the infrared spectrophotometer, X-ray diffraction, and differential thermal analysis units on a routine basis. These semi-automatic instruments are unaffected by the original grain size of the minerals and greatly assist rapid quantitative determinations. When coupled with thin-section and polished-section study of the rocks, this integrated approach gives better overall coverage, combining the area of mineralogy in which each particular instrument is most sensitive (Fig. 1).

Clays and hydrated minerals are thus best detected in thermal and infrared analysis, silicates by infrared analysis, micas and montmorillonite clays by X-ray diffraction, and sulfides and oxide minerals by examination of polished section. The textural relationship of adjacent minerals is seen most clearly in polished and in thin sections. Each instrument has a field of maximum sensitivity, and no one unit can possibly cover the range of minerals involved in mining and metallurgical research.

An excellent treatment of the problems encountered with optical determination of quartz in the presence of the talc and clays of fine-grained rocks was given 1949 by Foster,[1] who clearly showed that instrumental analysis is superior for the finer-grained materials. On the average, 30 pct of quartz was found by X-ray analysis, whereas only 5 pct was visible optically in the same samples. During the past three years the writers have found that infrared absorption analysis gives the most reliable single approach in quantitative mineralogy, being much less sensitive to the preferred orientation that makes X-ray diffraction analysis so hard to quantify.

To form the sample material for work with these instrumental methods, the Research Center now uses pulps exactly as prepared for chemical assays. Qualitative and quantitative mineralogy can be obtained ranging from samples of 1 mg, carefully drilled from a single phenocryst or groundmass area, to pulps prepared from lengths of drill core or from yearly mill head composites. This offers a great advantage over the usual thin-section mineralogical analysis.

The volume of rock contained in a thin section is only about 0.025 cc. To measure the average mineralogical composition of 100 ft of drill core it is necessary to assume that one thin section is a representative sample of that 100-ft section of core and then statistically examine the data to find out if the sampling has been adequate. It would be hard to determine the bulk mineralogy of mill feed by point-counting thin sections, but a method utilizing a powdered sample readily determines the mineralogy of this type of material. In routine mineralogical analysis of drill cores up to seven minerals have been quantitatively determined in a single analysis.

Table I lists the concentration limits for detection in routine infrared absorption analysis for typical minerals occurring in drill cores. Similar data are available for the X-ray[2] and differential thermal analysis[3] methods.

With the integrated approach, over 75 pct of the mineral content of the sample can be accounted for in a permanently recorded form. The personal factor of the operator is reduced to a minimum. A full petrographic study of an altered rock, including point-counting analysis to determine the modal composition, can take up to 8 hr; quantitative infrared, thermal, and X-ray analysis can each be completed in 1 hr.

DETAILED STUDY OF SMALL SAMPLES

Single Orthoclase Phenocryst

A single orthoclase phenocryst 3 mm square occurred in a quartz-sericite alteration zone around a sulfide veinlet. This was selected to determine the quantity of sericite formed in this phenocryst during the alteration. Infrared analysis of a 2.5-mg sample carefully drilled from the phenocryst showed 25 pct sericite, 4 pct kaolinite, 55 pct orthoclase, 10 pct albite, and 3 pct carbonate. The changing alteration of the small orthoclase phenocrysts that takes place within each of the adjacent alteration envelopes can

Table I. Estimated Infrared Limits of Detection and Sensitivity for Quantitative Analysis in Typical Rock Environments

Mineral	Rock Type	Lower Limit of Concentration for Detection, Pct	Percent of Sensitivity at 50 Pct Concentration
Carbonates	Any rock	0.5	±3
Quartz	Any rock	1	±3
Plagioclase (An_5 to An_{28})	Any rock	3	±5
Orthoclase	Granite	3	±5
Sericite	Alteration	15	±5
Biotite	Schist	50	±10
Augite	Diorite	10	±5
Kaolinite	Alteration	3	±3
Montmorillonite	Alteration	25	±10
Alunite	Alteration	3	±5
Jarosite	Alteration	3	±5
Chlorite	Alteration	15	±10

Fig. 3—A close-up of area B in Fig. 2 showing one side of a quartz-sericite envelope adjacent to a vein (vertical on right). Kaolinite zone (sample type 1) at left shows how quartz-sericite zone (samples 4-6) encroaches on the phenocrysts. Network of fine quartz ribbing is noticeable only in the quartz-sericite band. X12, reduced approximately one fourth.

be studied easily by this method. This type of work on single crystals is perhaps the field most suited for infrared analysis.[4]

Alteration Envelopes Adjacent to Veinlets

Altered wall rock adjacent to two veins in an andesitic tuff was selected for quantitative study of sericite and quartz alteration of the feldspar. Fig. 2 shows the sampling pits from which the powders were drilled and the location (B) of the close-up detailed photograph (Fig. 3). The data obtained from infrared analysis are expressed graphically in Fig. 2. The veins, which contain quartz, pyrite, and chalcopyrite, were deliberately excluded in the samples so that vein material would not mask the quartz in the adjacent wall rocks.

In the Fig. 3 micrograph the slight vertical illumination used in addition to oblique lighting shows up a ridge of harder material surrounding each feldspar ghost. This ridge appears in the quartz-sericite envelope but not in the chloritic fringe or clay zones; it does not seem to increase proportionately as the veins are approached. The ridge can be correlated with the increase of quartz content between samples 1 and 4, 5, and 6. This shows that the silica released when kaolinized feldspar is converted to sericite is reprecipitated outside each *feldspar* crystal as a hard wall. By defining accurately the content of free quartz and other silicates in the sample, infrared analysis gives valuable information on the movement of SiO_2 during the chemical reactions of alteration.

Petrography by Instruments—Rock Type Determination

Another quantitative application of this method has been the independent estimation of essential mineral content in a granite (G-1) whose mineralogical mode is known. The quartz content, microcline content, and plagioclase type and content of the powdered sample have been determined by instrumental analysis, details of which have been reported elsewhere.[5]

By rapidly determining the quartz: plagioclase: orthoclase ratios of rocks, it is possible to plot the data on composition diagrams and quickly deduce their petrologic types. This method has been applied on a routine basis to about 400 rocks in the general acid composition range.

APPLICATION TO EXPLORATION PROBLEMS

Areal Sampling of a Serpentine Belt

In prospecting an area of altered ultrabasic rocks, it was advantageous to know the ratio of chrysotile to antigorite in the natural mixtures of these minerals (usually called serpentine). It is difficult to distinguish them optically and hard to determine their relative abundance. To guide exploration a quick, accurate, and reproducible means of estimating the mineral content of the samples was desired.

As serpentine samples responded very well to both infrared and differential thermal analysis, it was possible to make quantitative determinations of the end members, chrysotile and antigorite. Instrumental data for the end members and a natural mixture of the two are shown in Fig. 4. Both instruments could be operated in a simple base camp laboratory, providing readily available information at nominal cost.[6]

Copper Prospect in Volcanic Rocks—Sampling and Analysis

The area of isolated outcrops of pervasively altered andesite lavas, tuffs, and agglomerates was 80 pct obscured by ice and glacial moraine. The study was to correlate the outcrops and drill cores and to give an idea of the size and type of zonal pattern of the alteration and its relationship to the metallized ground.

A suite of 28 samples collected over an area of 2 sq miles during field mapping and diamond drilling was examined in the laboratory. Sample locations were spotted on outcrop maps of the area, where the field parties had logged alteration types, but the quantitative data were obtained independently of these descriptions.

The samples were quartered, crushed as for assay pulps, and processed by differential thermal, infrared, and X-ray diffraction analysis. Specimens were mounted for polished-section study of the sulfide type and distribution, and thin sections were made for microscope study. The petrographic study was

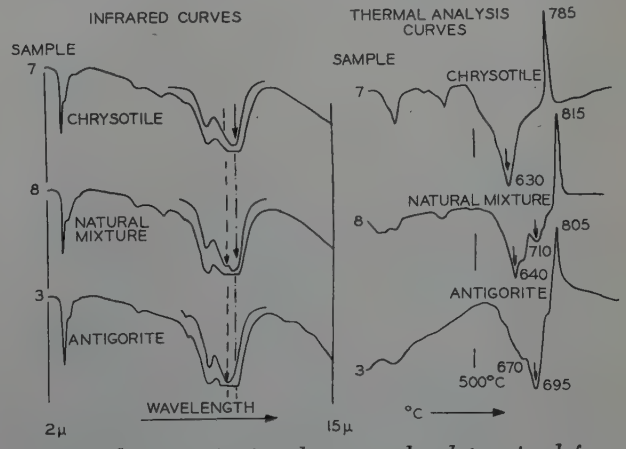

Fig. 4—The quantitative data may be determined from both the infrared curves and the thermal analysis curves for chrysotile-antigorite natural mixtures. Arrows indicate the criteria that are important for quantitative data.

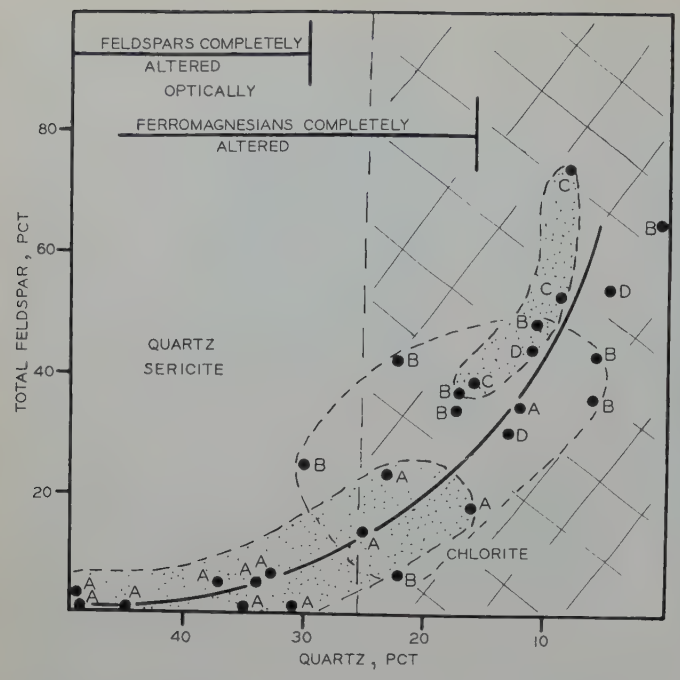

Fig. 5—The relationship between plot of quartz-total feldspar and degree (A and C, stippled) of alteration. Note broad division on the mica type (cross-hatched).

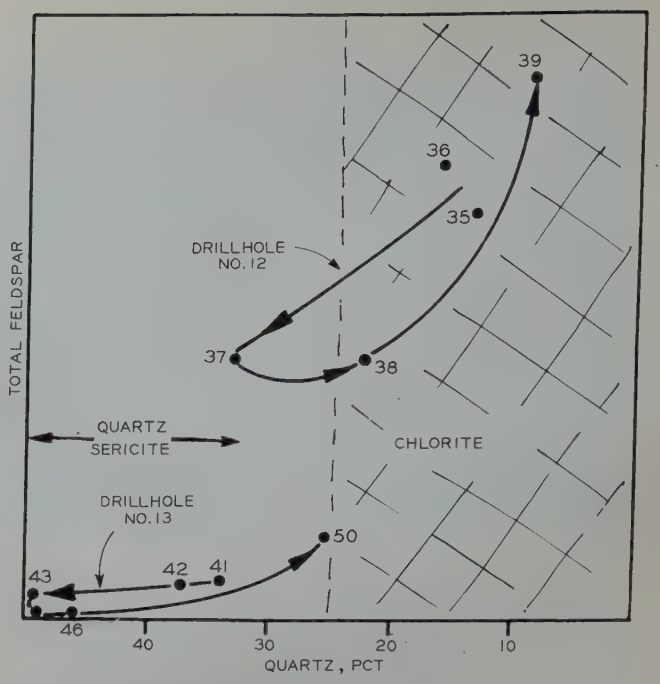

Fig. 6—The relationship between the same drillhole samples (12 and 13) shows the progressive changes in mineralogy and in the degree of alteration. (Curves are displaced vertically from Fig. 5).

performed by a different operator so optical and instrumental data could be obtained independently.

Data obtained from the various methods were as follows:

Microscope Analysis: Rock texture, chlorite content, and the minerals present in small amounts were determined. The degree of alteration of feldspars and ferromagnesians was assessed and classified as follows: *A*, both 100 pct altered; *B*, ferromagnesians 100 pct altered and feldspars 90 to 100 pct altered; *C*, ferromagnesians 100 pct altered and feldspars 80 to 90 pct altered; *D*, ferromagnesians 80 to 100 pct altered and feldspars less than 80 pct altered.

The type and ratio between opaque minerals and sulfides were obtained by study of polished sections.

Differential Thermal Analysis: This indicated the type of clay mineral and mica present. Quantitative data were difficult to obtain, as oxidation of sulfides invariably masked the thermal effects.

X-Ray Diffraction: X-ray diffraction indicated the type of mica mineral and gave a semi-quantitative determination of quartz content. Preferred orientation was found to be a very complex problem even when internal standards (brucite, fluorite, etc.) were used.

Infrared Absorption: This yielded the main qualitative and quantitative data on the quartz, feldspar, and sericite content. The type and content of the carbonates were determined by this instrument.

Discussion: Figs. 5 through 8 graph the serial variation of one or two minerals with another. Instrumental determinations of the quartz content are plotted as the abscissa with total feldspar content as the ordinate, indicating that feldspar content varies inversely with quartz content following a declining curve. At 20 pct quartz there is about 20 pct residual feldspar, whereas at 30 pct quartz only 7 pct feldspar remains. Given a quartz composition of a rock in the area, the content of several other minerals can be predicted. There is a definite relationship among minerals in the alteration halo which can be determined and contoured.

In detail, the figures show several interesting related sets of data. In Fig. 5 the microscopically determined degree of alteration (A-D) has been indicated near each sample point plotted from the quartz-total feldspar ratio. This shows the direct relationship between quartz-feldspar ratios and the visible degree of alteration. The cross-hatched field covers those samples in which chlorite occurs. In samples with lower quartz content chlorite is present, whereas those with higher quartz content have increasing amounts of sericite. A given point on an alteration curve, determined by the content of quartz and total feldspar, also indicates the type of mica present.

In Fig. 6 the sample from drillholes 12 and 13 have been separated and the decline curves displaced vertically. (Feldspar ordinates are on the same scale but displaced.) Drillhole 12, which was collared (samples No. 35, 36) in the chlorite zone, passed into the quartz sericite zone (No. 37) and returned into the chlorite zone in depth (Nos. 38, 39). Drillhole 13, collared in the sericite zone (No. 41), remained in that high alteration zone (Nos. 42 through 46) but bottomed in less altered ground (No. 50). Gypsum veinlets were found only in samples of the strongest altered ground (Nos. 42, 43, 45). Thus progressive degrees of alteration can be assessed within individual drillholes.

Fig. 7 shows the type of residual plagioclase for points plotted from their quartz and total feldspar contents. Results suggest that albitization steps during early and middle stages of alteration are reversed as the grade of alteration increases, and a residual amount of An_{18+} remains until a late stage in the process. Much more definitive data are required, but the determination of feldspar type when feldspar is below 10 pct in a highly altered and fine-grained rock unfortunately presents many difficulties.

Fig. 8 shows the carbonate type and content of the same samples plotted on the same quartz-total feldspar basis. Beneath the curves are histograms of the chalcopyrite (black) and pyrite (stippled) contents of the samples, determined by a polished-section study. It is noticeable that dolomite occurs with high quartz, high gypsum, and low feldspar and with sericite and pyrite. Calcite occurs with chalcopyrite in a chlorite-rich, low-quartz (less than 25 pct) high-feldspar sample. Ankerites occupy an intermediate position. Carbonate content increases somewhat as alteration proceeds, but its composition may be directly related to the type of sulfide and degree of alteration.

Correlation of Data: Fig. 5 shows good correlation between microscope data and instrumental data of the rock alteration. The microscope data, obtained independently, are thus compared with the infrared, X-ray, and differential thermal data. The data obtained principally by infrared analysis are obviously more precise and indicate the various alteration stages more accurately than the visual method.

Suggestions for Further Drilling: Drilling for hypogene copper in the rocks of this area should be confined to the chlorite-calcite alteration zones where quartz is low, feldspars are still visible, and original ferromagnesians are not yet converted to sericite.

SUMMARY

Several methods of mineralogical assistance in exploration have been shown. These provide mineral data with which to define or contour the drilling targets more exactly. The following instruments and techniques have been used in an integrated approach:

1) Infrared absorption.
2) X-ray diffraction.
3) Differential thermal analysis.
4) Petrographic, metallographic, and binocular microscopes.

These techniques were applied successively to the following problems:

1) Alteration of single feldspar phenocryst.
2) Alteration of rock in selvages around a sulfide veinlet.

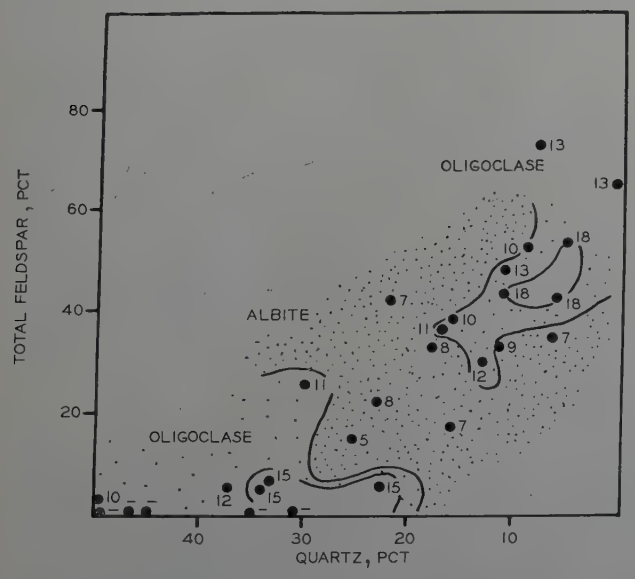

Fig. 7—Relation between Fig. 5 quartz-total feldspar plots and An content of their residual plagioclase.

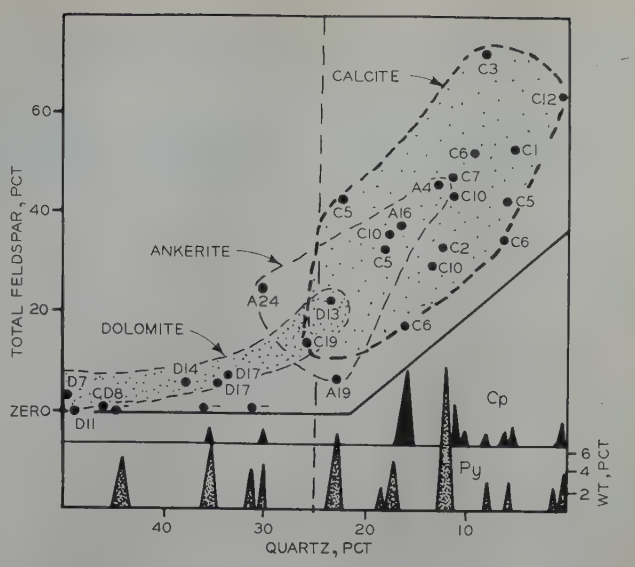

Fig. 8—The relationship between the same quartz-total feldspar plots and carbonate type (C, calcite; A, ankerite; D, dolomite) and content (A15). Histograms show the chalcopyrite content (black) and the pyrite content (stippled) for the same sample plots (see Fig. 5).

3) Quantitative mineralogy of large samples, rock type.
4) Area sampling for specific mineral content in a serpentine belt.
5) An exploration problem where outcrops are very limited and drillholes are few.

A single drillhole intersects only *one part in 700 million* of each square mile area, without consideration of depth as a further variable. Grid drilling is becoming increasingly expensive and the maximum data must be obtained from each hole. How near is the ore at each hole or, given two holes, where should the third be placed to intersect the ore? How close is a *near miss* drillhole? These are questions of great economic importance, particularly in determining the next drilling site, and anything that can be found to aid this decision will take some of the gamble out of the earlier stages in the search for metals.

The authors gratefully acknowledge the assistance of S. R. Zimmerley, Director of Research, Kennecott Copper Corp., who has vigorously supported the application of quantitative data to mineralogy. They also extend thanks to their colleagues, R. E. Wood, C. S. Thompson, G. Burgener, and M. C. Randle, without whose help much of the basic data would not have been determined.

REFERENCES

[1] W. D. Foster: Petrographic Determination of Quartz in the Presence of Clay-Like Minerals. *USBM R. I. 4573*, 1949, p. 13.
[2] L. V. Azaroff and M. J. Buerger: *The Powder Method*, p. 266. McGraw-Hill Book Co., New York, 1958.
[3] W. J. Smothers and Y. Chiang: *Differential Thermal Analysis*, p. 444. Chemical Publishing Co., New York, 1958.
[4] W. M. Tuddenham and R. J. P. Lyon: Relation of Infrared Spectra and Chemical Analysis for Some Chlorite and Related Minerals. *Analytical Chemistry*, 1959, vol. 31, pp. 377-380.
[5] R. J. P. Lyon, W. M. Tuddenham, and C. S. Thompson: Quantitative Mineralogy in 30 Minutes. *Economic Geology*, 1959, vol. 54, pp. 1047-1056.
[6] W. I. Watson: The Use of Differential Thermal Analysis in the Study of Ore Treatment Problems. Presented at AIME Pacific Southwest Mineral Industry Conference, March 1958.
[7] J. M. Hunt and D. S. Turner: Determination of Mineral Constituents of Rocks by Infrared Spectroscopy. *Analytical Chemistry*, 1953, vol. 25, pp. 1169-1174.
[8] C. S. Thompson and M. E. Wadsworth: Determination of the Composition of Plagioclase Feldspars by Means of Infrared Spectroscopy. *American Mineralogist*, 1957, vol. 42, pp. 334-380.

Discussion of this article sent (2 copies) to AIME before Jan. 31, 1960, will be published in MINING ENGINEERING.

RETENTION TIME IN CONTINUOUS VIBRATORY BALL MILLING

by D. W. FUERSTENAU

Recently R. J. Charles[1] showed that comminution of brittle or semi-brittle materials in batch operations is described more appropriately by a variable energy relationship than by the specific relationships proposed by Rittinger,[2] Kick,[3] and Bond.[4] That is, the value of n in the empirical differential operation which applies to crushing and grinding (Eq. 1) is variable. Independently, Holmes[5] developed an identical generalized equaton for size reduction. The experimental data of Charles and Holmes show that the value of n is determined by the material and the comminuting machine and is constant for a given combination of these two conditions.

The general objective of the present article is to extend the Charles-Holmes concepts to continuous ball milling. The specific objective is to analyze the operation of a vibratory ball mill dry-grinding chromite in a continuous open circuit and to develop an equation for the comminution of chromite in this mill.

Basic Principles: In a batch mill the length of time during which the material is ground is a direct measure of the energy expended on the material, except possibly for exceedingly fine grinding. However, in a continuous operation, the fraction of the total expended energy which is useful for grinding will vary according to feed rate and amount of material in the mill. If the amount of material within a continuously operating vibratory mill is low enough so that only part of the expended energy is used for grinding, the extent of size reduction at constant power input must depend upon the length of time the material is retained within the mill, namely, upon retention time. The following analysis pertains to a continuous mill operating under these conditions.

The empirical differential equation that applies to the comminution of brittle materials is:[6]

$$dE = -C\,dx/x^n \qquad [1]$$

where dE is an infinitesimal energy expenditure, C a constant, dx an infinitesimal size change, x the particle size, and n a constant. For continuous grinding in an open circuit at constant power input, P, Eq. 1 must be written as

$$(dt_r)_P = -C'\,dx/x^n \qquad [1a]$$

where dt_r is an infinitesimal time during which a particle of size x is in the mill, and C' is a constant.

A ground product never consists of particles of single size but always comprises a distribution of sizes. In comminution, the expenditure of energy causes a lateral shift in the size distribution.[1, 7, 8] The general objective of any engineering study of comminution is to correlate the magnitude of this size distribution shift with the energy expended, the ultimate aim being to cause the greatest shift with the least amount of expended energy. Although a number of criteria can be used to measure this shift, Schuhmann's size modulus has been found convenient.[1] Mathematically, the Schuhmann size distribution can be expressed as follows:[9]

$$y = 100\left(\frac{x}{k}\right)^{\alpha} \qquad [2]$$

or in differential form:

$$dy = \left[\frac{100\alpha}{k^{\alpha}}\,x^{\alpha-1}\,dx\right] \qquad [1a]$$

where y is percentage of material finer than size x, α is a constant that determines weight distribution among particles of various sizes, and k the size modulus that denotes the theoretically maximum-sized particle in any size distribution.

By considering the energy required to reduce an element of weight of material, dy, from size x_m to size x, the element of time during which the material must remain in the mill at constant power will be

$$\left(dt_{r'}\right)_P = \int_{x_m}^{x} \frac{-C\,dx'}{x'^n}\,(dy) \qquad [3]$$

Summing up all the elements of weight from zero to 100 for a product that conforms to the Schuhmann size distribution yields

$$(t_r)_P = \int_{x_0 \to 0}^{k} \int_{x_m}^{x} -\left(\frac{C\,dx'}{x'^n}\right)\left(\frac{100\alpha x^{\alpha-1}\,dx}{k^{\alpha}}\right) \qquad [4]$$

D. W. FUERSTENAU, Member AIME, is with the Department of Mineral Technology, University of California, Berkeley. TP 60B10. Manuscript, Jan. 5, 1959. New York Meeting, February 1960. AIME Trans., Vol. 214, 1959.

where x_o, the size of material when y is zero, approaches zero. Thus for reducing material of large initial size to a product conforming to the Schuhmann size distribution of size modulus, k, the retention time within a continuously operating mill is given by

$$(t_r)_P \approx \frac{C\alpha}{(n-1)\ (\alpha-n+1)}\ k^{1-n} \approx Ak^{1-n} \qquad [5]$$

Eq. 5 affords a method for obtaining n. If an ore is ground in the vibratory ball mill under conditions where the retention time varies, a log-log plot of the size modulus, k, vs the retention time at constant power, $(t_r)_P$, should yield a straight line of slope 1-n. For this method of determining n to be used, the material should have a reduction ratio great enough for the product to assume its natural value of α for the particular machine, and the approximation concerning the feed term must be valid. If the mill is operated at different power settings, the extent of size reduction must be stated as a function of retention time and power.

Where the feed and product size distributions have identical values of α, and where the feed term is not negligible, the general equation will have the following form:

$$(t_r)_P = A(k_p^{1-n} - k_f^{1-n}) \qquad [6]$$

where k_p and k_f are the size moduli of the product and feed, respectively. Thus a plot of retention time at constant power input vs the quantity, $(k_p^{1-n}-k_f^{1-n})$, should be a straight line of slope A. A plot of this type is used to evaluate A in Eq. 6.

Materials and Method: A 15x15-in. Allis-Chalmers vibratory ball mill was operated in continuous open circuit to dry grind chromite. This mill, which was charged with 332 lb of balls (3 pct 1 in. by ⅞ in., 60 pct ⅞ by ¾ in., 37 pct ¾ by ⅝ in.), required 5.60 ± 0.05 kw for operation at a frequency of 1260 rpm and a vibration radius of 9/32 in. With this ball load the mill was filled to 84 pct capacity. Regardless of feed rate, power to this mill was constant because weight of ore in the mill was negligible compared to the total weight of the mill.

To avoid dust loss the system from the feeder to the product hopper was sealed. The mill was fed dry from an Omega Gravimetric Model 50-8 feeder. Before each pass through the mill, the feeder was calibrated with the material to be fed to the ball mill. Accuracy of the feed rate during the runs was well within 1 pct. A flexible rubber chute connected the feeder with the ball mill. Since the mill was not air-swept, material passed through it by free flow and was discharged through a rubber hose into a covered hopper.

The ore being ground in the vibratory ball mill was Transvaal chromite ground previously in an Aerofall mill, nominally through 28 mesh. Since the product was the horizontal classifier discharge from the Aerofall mill, many of the fines had been removed and consequently the slope of the Schuhmann curve, α, for this material was high, i.e., 1.83 (see Fig. 1).

The procedure used in the experimentation was to pass about 1000 lb of ore through the mill at 1200 lb per hr. The product from the mill was passed through the mill again at 1200 lb per hr until five passes had been made. In each case, samples of the product were taken after 5, 10, 20, 30, and 40 min of operation. Size distributions of these samples were identical, which shows that steady state had been reached before 5 min had elapsed. While the mill was operating at steady state, the feed was shut off and the mill was stopped almost instantly with a wedge. The contents of the mill (balls plus ore) were carefully removed and separated, and the amount of ore retained in the mill was weighed so that average retention time could be determined. Repeat runs at a feed rate of 1200 lb per hr showed that the amount of ore retained in duplicate runs varied by no more than 4 pct. Four duplicate runs on ore that was 95 pct −325 mesh gave retention times agreeing within 1 pct. Before each subsequent run the mill was recharged with its contents. This procedure was repeated at a feed rate of 600 lb per hr, but at this lower feed rate only three consecutive passes were made.

Sizing was carried out by wet and dry-sieving and the −400 mesh material was sized with an Andreason pipette.

Experimental Results: Fig. 1 presents size distributions of the original feed and the products from each of the five consecutive passes through the mill at 1200 lb per hr. These data show that the product from the first pass through the mill has attained the equilibrium value of α, namely, 0.80, and that the size distributions are shifted laterally with each subsequent pass through the mill. In each case the size distributions are parallel straight lines over an important part, and the size modulus is the extrapolated straight-line portion to $y = 100$. Fig. 2 presents the size distributions for chromite ground in three consecutive passes through the mill at 600 lb per hr. In this case the curves again are parallel and α is again 0.80 in each case. Comparison of Figs. 1 and 2 shows that the product obtained by three passes through the mill at 1200 lb per hr is essentially identical to that obtained by two passes at 600 lb per hr.

Table I presents both the weight of material retained in the mill after each pass and the average retention time, t_r, for each pass. Study of Table I shows that the amount of ore in the mill decreases in general as the ore becomes finer. Only 12.5 lb of ore were in the mill at the highest feed rate, which means that retention time in the mill was only 0.63

Table I. Weight of Ore in Mill and Retention Time for Each Pass

	1200 Lb Per Hr Feed Rate				600 Lb Per Hr Feed Rate			
No. of Pass	k_p, Microns	Ore in Mill, Lb	Ret. Time, Min	Cumulative Ret. Time, Min	k_p, Microns	Ore in Mill, Lb	Ret. Time, Min	Cumulative Ret. Time, Min
1	200	12.6	0.63	0.63	120	10.1	1.01	1.01
2	100	10.3	0.51	1.14	67	5.1	0.51	1.52
3	67	6.7	0.34	1.48	44	5.1	0.51	2.03
4	46	8.9	0.44	1.92				
5	37	7.8	0.39	2.31				

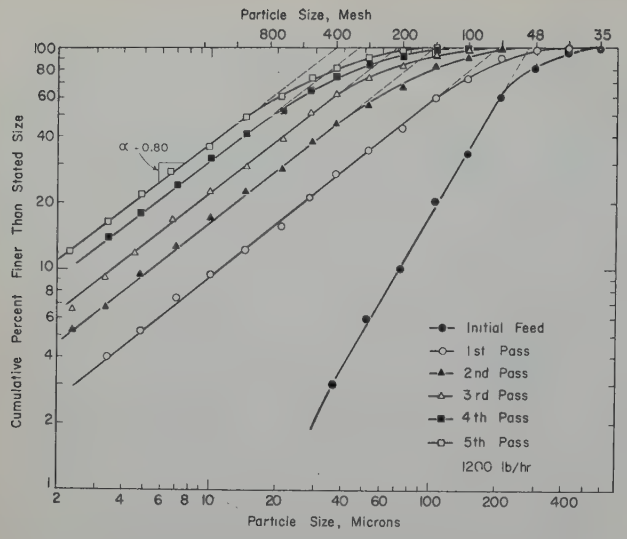

Fig. 1—The above graph shows the size distributions of chromite as a function of the number of passes through the vibratory ball mill at a feed rate of 1200 lb per hr.

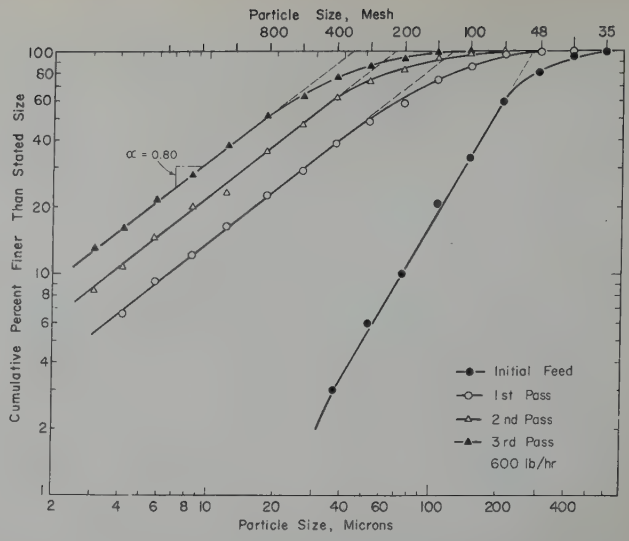

Fig. 2—The above graph shows the size distributions of chromite as a function of the number of passes through the vibratory ball mill at a feed rate of 600 lb per hr.

min during the first pass at 1200 lb per hr. The slightly larger amount of ore in the mill during the fourth pass is real because the same phenomenon was observed when the runs were repeated. Apparently ore of this size flows through the mill slightly slower than that of the third pass and fifth pass. At a feed rate of 600 lb per hr, there is somewhat less material within the mill than at the feed rate of 1200 lb per hr but the retention is somewhat greater. In Table I the cumulative retention time, $(T_r)_p$, is also presented, that is, after two passes the total retention time is the retention time for the first pass plus that for the second. As mentioned earlier, the product obtained by three passes at a feed rate of 1200 lb per hr is identical to that obtained by two passes at 600 lb per hr. As anticipated, the cumulative retention time required for production of this product was essentially the same for the two feed rates, namely, 1.48 min vs 1.52 min, which lies well within the experimental limit of error.

Since relatively coarse chromite was ground at constant power in the vibratory ball mill, n can be evaluated according to Eq. 5 by plotting on log-log paper the size modulus, k, vs the cumulative retention time, $(T_r)_p$. The data obtained at a feed rate of 1200 lb per hr and 600 lb per hr, which are plotted in Fig. 3, fall on a single straight line. The slope of this is −0.78. Since the slope of the curve is equal to the quantity, 1-n, the value of n for the comminution of chromite in the vibratory ball mill is 1.78.

An equation analogous to Eq. 6 can be written for the comminution of chromite in the vibratory ball mill for conditions where the feed term in Eq. 4 is not negligible and where size distribution of feed parallels that of the product. This can be done by considering the product from the first phase through the vibratory ball mill to be the feed for succeeding passes. For evaluation of Eq. 6, k_f will then be the material from the first pass and k_p the product from each of the succeeding four passes at 1200 lb per hr. The data for material ground at 600 lb per hr will be treated similarly. In Fig. 4 the cumulative retention time, $(T_r)_p$, is plotted vs $(k_p{}^{-0.78} - k_f{}^{-0.78})$ for the two different feed rates. This figure shows that the quantity, $(k_p{}^{1-n} - k_f{}^{1-n})$, depends on retention time and is independent of feed rate. The slope of the line drawn from the data obtained on grinding chromite (Fig. 4) is 38. Thus the continuous vibratory ball milling of chromite is described by the following equation if the feed and product have identical values of α:

$$(T_r)_p = 38(k_p{}^{-0.78} - k_f{}^{-0.78}) \text{ minutes} \qquad [7]$$

Discussion of Results: The experimental data reported in this paper show that for a vibratory ball mill operating continuously in open circuit, at constant power input, size moduli of the products are determined by total retention time within the mill, regardless of feed rate. Thus, for a continuously operating low-level discharge mill retention time determines how long any given particle is subjected to the mill action. In batch grinding the total grinding time is the retention time, and doubling the grinding time doubles the retention time. However, in continuous grinding the factors which determine retention time are complex in that retention time depends on flow characteristics of the material passing through the mill. For dry grinding in a vibratory mill, the scale-up of batch laboratory tests to continuous operation will be difficult without a knowledge of retention time, and this may entail experimental determination of retention time.

The data presented in Table I indicate that retention time must be included in a statement of grindability for this system. For example, consider the comminution of the −28 mesh chromite feed to a product with a size modulus of 67 μ in a 15-in. vibratory ball mill drawing 5.60 kw of power. To do this in open circuit at a feed rate of 1200 lb per hr three passes through the mill are necessary, whereas at 600 lb per hr only two passes are required. Thus, at a feed rate of 1200 lb per hr, the total energy requirements are 28 kw-hr per ton, whereas 37 kw-hr per ton are required to grind it at the rate of 600 lb per hr. If the total energy only were considered, it would be concluded that grindability depends upon feed rate. However, grindability of the ore does not vary with feed rate; only the retention time varies, and this in turn determines the fraction of the total energy which is useful for grinding. Therefore, for continuous grinding a statement of grindability must include an energy utilization fac-

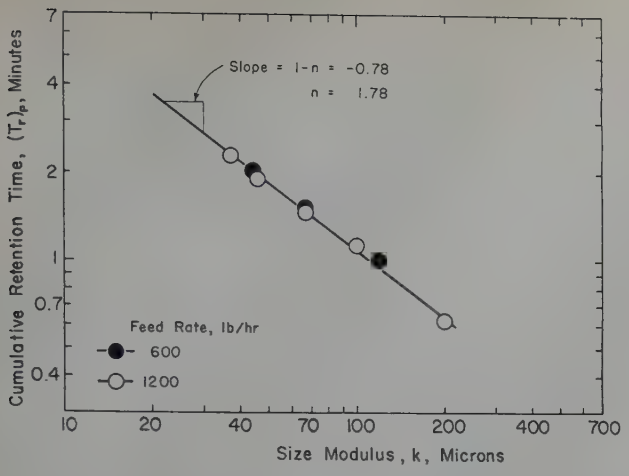

Fig. 3—Retention time–size modulus graph for chromite ground in continuous, open-circuit vibratory ball mill.

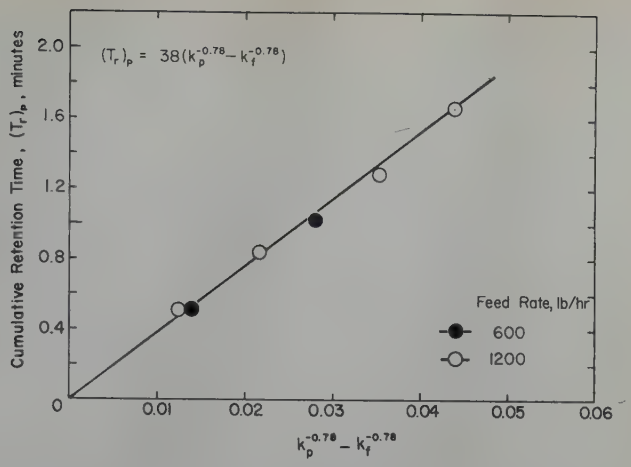

Fig. 4—Cumulative retention time as a function of $(k_p^{-0.78} - k_f^{-0.78})$, when product from first pass through the vibratory ball mill is considered to be the feed.

tor, f, which determines the fraction of the total energy that is being utilized for grinding. For continuous grinding the grindability, G, which is the energy expended per unit weight to reduce a material from size modulus k_f to k_p, is stated mathematically in terms of the power to the mill, P, the feed rate, F, and the energy utilization factor, f, as follows:

$$G = \frac{P}{F} \cdot f \qquad [8]$$

The factor f must depend on retention time. It will be the ratio of the retention time t_r to the hypothetically optimum retention time t_{rm} or it will be the ratio of the weight of ore W_r in the mill under steady state conditions to the optimum weight W_{rm}, which is the amount of material necessary to utilize the energy put into the mill.

$$f = \frac{t_r}{t_{rm}} = \frac{W_r}{W_{rm}} \qquad [9]$$

Thus the grindability of an ore in a continuously operating mill will be

$$G = \frac{P}{F}\left(\frac{W_r}{W_{rm}}\right) \qquad [8a]$$

The grindability of −28 mesh chromite to a size modulus of 67 μ can now be considered using Eq. 8a. At a feed rate of 1200 lb per hr the grindability is

$$G = \frac{5.6 \text{ kw}}{0.6 \text{ tph}}\left(\frac{29.6}{W_{rm}}\right) = \frac{276}{W_{rm}} \text{ kw-hr per ton}$$

At a feed rate of 600 lb per hr, the grindability is

$$G = \frac{5.6 \text{ kw}}{0.3 \text{ tph}}\left(\frac{15.2}{W_{rm}}\right) = \frac{284}{W_{rm}} \text{ kw-hr per ton}$$

The small difference (3 pct), which is within the experimental limit of error, indicates that the grindability, G, is constant. Since the hypothetical optimum weight of retained ore was not determined, grindability can be given only in terms of W_{rm}.

The energy utilization factor, f, apparently decreases with finer grinding in the vibratory ball mill. For example, Table I shows that almost twice as much power is required to grind chromite from a size modulus of 67 μ to about 45 μ at a feed rate of 600 lb per hr than is required at 1200 lb per hr. The reason for this is that the energy utilization factor at 600 lb per hr is $\frac{5.1}{8.9}$ or 57 pct of the energy utilization factor at a feed rate of 1200 lb per hr. To increase the energy utilization factor and thereby reduce the total power for any grinding operation, the flow of material through the ball mill must be constricted in order to increase the amount of ore retained within the mill. The increased retention time should cause the product to be ground finer in accordance with Eq. 6.

As seen in Figs. 1 and 2, the size distributions are shifted laterally with expenditure of increased energy. In each case the value of α is 0.80. Considerable discussion has centered around the constancy of α.[1, 6, 10] If the size distributions are not carried into fine enough sizes, α will appear to vary. Had the data been plotted only to 400 mesh, the curves would have had the appearance of those in

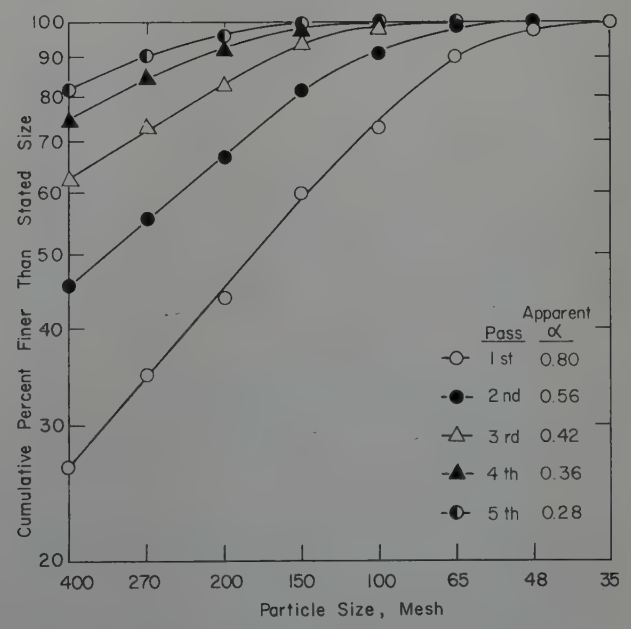

Fig. 5—Graph showing the apparent change in α when size distributions are plotted over a limited range only.

Fig. 5. As shown in Fig. 5, α would have had an apparent value of 0.80 after one pass through the mill but would have appeared to decrease to 0.28 after the fifth pass at 1200 lb per hr. The error would have been even greater if the data had been plotted only to —200 mesh.

Summary and Conclusions: The variable n hypothesis of Charles and Holmes can be extended to continuous grinding through the use of retention time as a measure of the fraction of the total energy which is useful for comminution. In the continuous vibratory ball milling of chromite, the equation for size reduction was found to have the following form:

$$(T_r)_p = A(k_p^{1-n} - k_f^{1-n})$$

where $(T_r)_p$ is the retention time at constant power input to the mill, A is a constant, k_p and k_f are the size moduli of the product and feed, respectively, and n is a constant for a given material and machine.

Experimentally, the size distribution of the products from continuous open-circuit grinding of chromite in a 15x15-in. vibratory ball mill were found to be shifted laterally with increased retention time. In each case the value of α, that is, the slope of the Schuhmann size distribution plot, was 0.80. The extent of the shift in size modulus depended on retention time, independent of a twofold change in feed rate. For the comminution of Transvaal chromite in the vibratory ball mill the value of n in the energy-size reduction equation was found to be 1.78, which lies about halfway between the values predicted by the Bond and Rittinger hypotheses.

In continuous ball milling the fraction of total energy which is useful for grinding depends upon weight of ore in the mill. Thus a statement of grindability for continuous grinding must include a factor that takes into account the efficiency of energy utilization, f, which is determined by the ratio of the weight of material retained in the mill at steady state, W_r, to the hypothetical optimum weight of retained material, W_{rm}. The grindability, G, of a material in a continuous mill is then:

$$G = \frac{P}{F} \cdot f = \frac{P}{F}\left(\frac{W_r}{W_{rm}}\right)$$

where P is the power input and F the feed rate. This statement permits comparison of grindabilities, which can be done only on a relative basis in the present work, since W_{rm} has not been determined.

This work was carried out in its entirety at the Metals Research Laboratories, Union Carbide Metals Co., Niagara Falls. The author wishes to acknowledge the assistance of J. J. Cunningham, J. M. Huse, and E. Laur for their part in making the experimental measurements.

REFERENCES

[1] R. J. Charles: *AIME Trans.*, 1957, vol. 208, p. 80.
[2] P. R. Rittinger: *Lehrbuch der Aufbereitungakunde.* Berlin, 1867.
[3] F. Kick: *Das Gesetz der proportionalen Widerstande und seine Andwendung.* Arthur Felix, Leipzig, 1885.
[4] F. C. Bond: The Third Theory of Comminution. *AIME Trans.*, 1952, vol. 193, p. 484.
[5] J. H. Holmes: *Institute of Chemical Engineers Trans.*, 1957, vol. 35, p. 125.
[6] W. H. Walker, W. K. Lewis, W. H. McAdams, and E. R. Gilliland: *Principles of Chemical Engineering,* McGraw-Hill Book Inc., New York, 1950.
[7] A. M. Gaudin: *AIME Trans.*, 1926, vol. 73, p. 253.
[8] A. M. Gaudin and R. T. Hukki: *AIME TP 1779*, 1944
[9] R. Schuhmann, Jr.: *AIME TP 1189*, 1940.
[10] F. C. Bond: Mining Engineering, 1958, vol. 10, p. 481.

Discussion of this article sent (2 copies) to AIME before Jan. 31, 1960, will be published in Mining Engineering.

DISCUSSION

F. C. Bond *(Consulting Engineer, Allis-Chalmers Mfg. Co.)*—This research study is ably presented and discussed. The data are consistent and well arranged. However, this very consistency raises some questions.

The exact parallel extending down to 3 μ of the plotted size distribution lines shown in Figs. 1 and 2 is rather remarkable when compared with the plotted lines of many other products. Even when no grain size excesses or deficiencies are evident, a plot pattern more similar to Fig. 5 would be expected, with perhaps a flattening of the steeper lines below 400 mesh.

Experience with the Andreason pipette has demonstrated the difficulty of preventing partial flocculation at sizes of 10 μ and smaller, where the efficiency of the ordinary dispersing reagents seems to decrease. Progressive flocculation at the finer sizes could accord with the straight lines plotted. A check of the size distributions below 10 μ by microscopic grain counts or by some other method would be helpful.

Of course, it is also quite possible that the dust seals used did not completely contain these fine particles in the grinding circuit. The loss of fine particles, either by flocculation or as dust, would increase as the particle size decreased and could result in a straight size distribution line on a log-log plot. In any case, the whole argument of the article rests upon the amount of fine particles produced, and these determinations are subject to many errors.

The data presented are calculated according to the Third Theory in Table II, which accompanies this discussion. The 80 pct passing size P and the slope Er were obtained from Third Theory exponential plots[10] and[11] from Figs. 1 and 2, and the crack length Cr was obtained as shown in Ref. 11. Since the feed had an unnatural deficiency of fines it was necessary to estimate the P and Er values for an equivalent feed containing its natural fines. A natural feed would have been preferable.

For each pass at 1200 lb per hr the work input W is 9.33 kw-hr per ton, and 148 joules are expended per cubic centimeter of chromite ore, assuming that it has a specific gravity of 4. The ball voids at rest should contain about 68 lb of chromite ore.

The joules per centimeter of crack length produced are fairly consistent down to the last period at both feed rates. However, they are very erratic in the last period, whose P and Er values are most dependent upon the Andreason pipette measurements.

The work index values at 1200 lb are about twice as high as those expected for ordinary dry grinding, and they are still higher at 600 lb per hr. The low level discharge of the mill and the small amount of material retained in it during grinding apparently permit many wasted metal to metal contacts and increase both the work index and the joules per centimeter. Only 7.5 pct of the ball voids are occupied by 5.1 lb of chromite ore retained in the last two test runs.

This introduces a new variable into the author's calculation of the exponent n which will change its value. For if the retention time is decreased with a constant power input to the mill, then the amount of work done per time unit is also decreased because the proportion of nonproductive metal to metal contacts is increased by the decreased volume of material within the mill. The exponent n and the size moduli of the products will be affected by this factor as well as by the retention time.

Table II

Lb Per Hr, Pass No.	Feed Equivalent	1200 (1)	1200 (2)	1200 (3)	1200 (4)	1200 (5)	600 (1)	600 (2)	600 (3)
Slope (Er)	0.340	0.360	0.425	0.500	0.572	0.568	0.387	0.475	0.375
−80 pct size (P)	390	170	98	64	43.3	35	126	68.4	41.6
Cm per cc (Cr)	26.0	37.5	49.6	61.2	73.7	78.5	43.2	58.7	64.0
$Cr\sqrt{P}$	513	490	492	489	408	465	485	485	413
Ball voids occupied, pct		18.4	15.0	9.8	13.0	11.4	14.7	7.5	7.5
Unit process work index		35.8	38.5	38.8	34.6	54.9	48.5	58.7	54.7
Joules per cm		12.9	12.3	12.7	12.2	27.9	17.2	19.1	55.9
Cumulative work index		35.8	37.1	37.6	36.5	39.4	48.5	53.0	53.6
Joules per cm		12.9	12.5	12.6	12.5	14.1	17.2	18.1	23.4

The Charles-Holmes relationship is empirical and is based upon no specific mechanism or pattern of rock breakage. It is always possible that two different mechanisms are operating simultaneously, and that the Charles-Holmes variable exponent n expresses the balance between them. However, this exponent has been applied only to a size modulus value, or to only one point on the plotted size distribution curve. It is assumed in the present article that the slopes of the plotted lines are parallel as shown, so that the size modulus would be a valid expression of the actual work done in reduction if there is no grind limit effect.

It is contended in this discussion that the log-log size distribution plots are normally curved and divergent in both the coarse and extremely fine size ranges, so that the exponent n is not a correct evaluation of the work input required for reduction.

More studies similar to this one, with increased attention to the measurement of fine particle sizes and specific work input to the material being ground, will advance our knowledge in this important field.

REFERENCE

[11] F. C. Bond: *Confirmation of the Third Theory.* Presented at AIME Annual Meeting, San Francisco, 1959.

D. E. Fuerstenau (*author's reply*)—F. C. Bond has questioned the possibility of flocculation during the determination of size distributions of the −400 mesh material with an Andreason pipette. Obtaining complete dispersion is of course the main concern in using any method which utilizes settling rates for size analysis. In the present case, dispersion must have been quite complete because 48 hr after the sizing tests had been completed, fine particles were still in suspension. After this elapsed period, essentially clear water existed only for a depth of about 1 cm. In addition, some sizing tests were made in the Infrasizer (which can size chromite down to about 5μ) and size distributions obtained by the two methods were identical. As for dust loss in the grinding operation itself, every effort was made to make the operation essentially dust-free, and this type of loss should have been quite negligible.

One of the real controversies which seems to exist in the field of comminution appears to concern the nature of size distributions. Bond contends that log-log size distribution plots are normally curved and are divergent at both ends. It might be pointed out that the best way to obtain a size distribution plot that bends at neither end is to use Bond's technique of grinding in simulated closed circuit with a sieve. The author is of the opinion that the concept that size distribution plots appear to flatten with finer grinding results from not carrying the size distribution to small particle size. For example, in the case of the products from the five passes through the mill at 1200 lb per hr, the pipette analyses of the first four products were identical and the fifth was parallel but displaced toward a finer size, indicating that the bend in the curve occurs considerably below 400 mesh for this latter product.

If one were to carry out a series of batch grinding tests for a given period of time at constant power input but with varying amounts of material inside the mill, three distinct types of grinding conditions should exist. When the mill contains only a very small amount of ore, the size modulus of the product (k_1) depends upon grinding time only. If the amount of ore in the mill is increased but is still below that where metal-to-metal contacts occur, the product obtained will also have a size modulus of k_1. However, if enough ore is put into the mill, that of the energy put into the mill is wasted on metal-to-metal impact; then the product should have size modulus determined by the relation:

$$\frac{(t)\ (P)}{W} = \frac{C}{W} = Ak_p^{1-n}$$

where t is the grinding time, P is the power input, W is the feed weight, A, C, and n are constants, and k_p is the size modulus of the product. If the amount of ore in the mill is increased until it impedes ball motion, this relationship no longer will hold and k_p will rapidly approach that of the feed, since grinding will be retarded. These phenomena should be more apparent in a vibratory ball mill in which a large amount of power is put into a small machine. The conditions under which the present grinding tests were run were certainly in the range where the mill was underloaded and the shift in the size distribution plot depends upon time within the mill only at constant power input.

A statement of grindability should include an energy utilization factor f for both batch and continuous grinding, and in the case of continuous grinding this statement has the following form:

$$G = \frac{P}{F} \cdot f$$

where P is the power and F is the feed rate. Under conditions where metal-to-metal impact occurs $f < 1$, and as the amount of ore in the mill is increased f increases to 1. Under intermediate loading conditions, $f = 1$. As the loading becomes excessive, f decreases to zero.

HIGH-INTENSITY MAGNETIC SEPARATION OF IRON ORES

by O. E. PALASVIRTA

Close examination of most so-called *new* processes in mineral dressing reveals that they were conceived and developed a long time ago. High-intensity magnetic separation is no exception. Although its application in iron ore beneficiation seems new, in Germany the process has been commercially successful for almost two decades. High-intensity separators have long been standard equipment in the glass sand industry; they have also been used in concentrating some of the more unusual para-magnetic minerals.

The basic features of an induced-rotor, high-intensity magnetic separator were described by Désiré Korda in Paris in 1905,[1] and many patents have since been issued for improvements on the original design. Fig. 1 shows the basic design of an induced-rotor separator. Several U. S. manufacturers have been supplying induced-rotor separators for many years, but these are all devices of relatively low capacity, not suitable for treating such low-cost commodities as iron ore. On the other hand, two German manufacturers are offering induced-rotor separators of high capacity, both proven in the field.

The present investigation was prompted by the apparent success of the German installations and by the discovery of iron ores on this continent which may be amenable to high-intensity separation. The objective was to gain better insight into the underlying principles of separation in a high-intensity field and to use this knowledge in selecting or designing an optimum separator.

THEORETICAL CONSIDERATIONS

The well known low-intensity magnetic separators are, without exception, of the multiple horseshoe magnet type with more or less similar field shapes. It is therefore permissible to speak of their comparative strengths in terms of field intensity alone. However, proper understanding of the high-intensity magnetic separation process requires somewhat deeper analysis of the relationship between the magnetic field and the attractive force.

Contrary to a widely held belief, a magnetic field of parallel lines of flux exerts no attractive force on a magnetically susceptible particle, but merely aligns its poles parallel to the lines of flux. On the other hand, a non-uniform field attracts a magnetically susceptible particle in the direction of the converging lines of flux. Thus the force of magnetic attraction varies as the product of the field intensity and the field gradient:

$$F_m \propto H\frac{dH}{ds} \qquad [1]$$

As the induced-rotor magnetic separator is primarily intended for separating feebly magnetic materials, it is important that maximum attraction be attained. For the designer, then, the relationship between the magnetic field and the attractive force has the following implications:

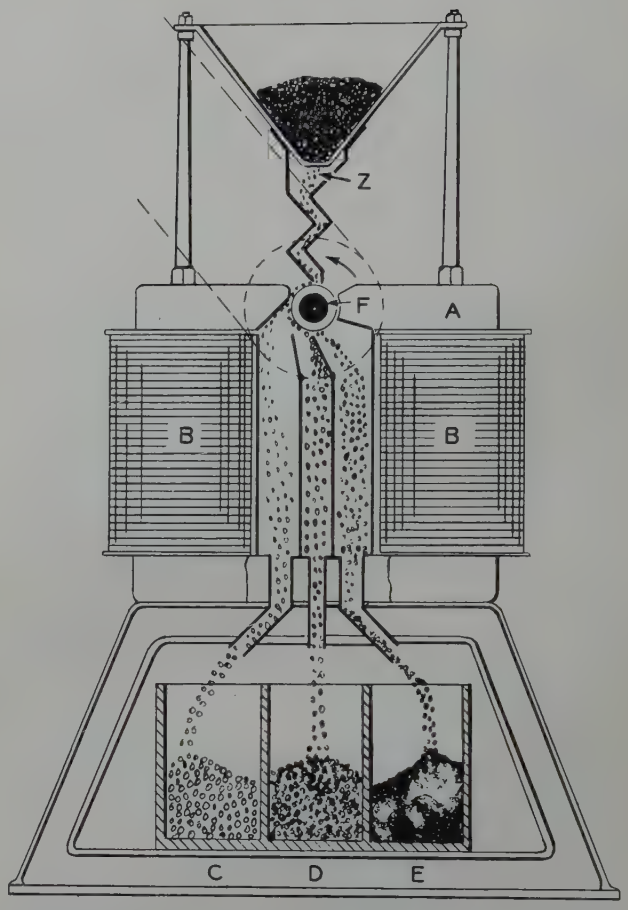

Fig. 1—Early type of high-intensity induced-rotor magnetic separator. A. Magnet poles. B. Coils. C. Tailing. D. Middling. E. Concentrate. F. Rotor. Z. Feed device.

1) Insofar as possible, the separation gap must be saturated with flux.

2) The rotor surface must be shaped to insure maximum convergence of lines of flux toward the rotor.

3) The primary pole face (opposite the rotor, on the other side of the separation gap) must be shaped so that the lines of flux do not diverge from it at any location in the effective separation zone.

The actual attractive force of the rotor, and its critical speed, can be calculated as shown by Runolinna,[2] provided that the true flux density, the field gradient, and the magnetic susceptibility of the mineral can be measured with sufficient accuracy. The irregular shape of the rotor surface makes flux measurements difficult, but it can be done if a suitable gaussmeter is available (see Fig. 2). Calculations by the author, and comparisons with the centrifugal force exerted by the rotor, indicate that the force pinning a hematite particle to the rotor is of the same order of magnitude as the force holding a

O. E. PALASVIRTA, Member AIME, is Development Engineer, Oliver Iron Mining Div., U. S. Steel Corp. TP59B73. San Francisco Meeting, February 1959. AIME Trans., Vol. 214, 1959.

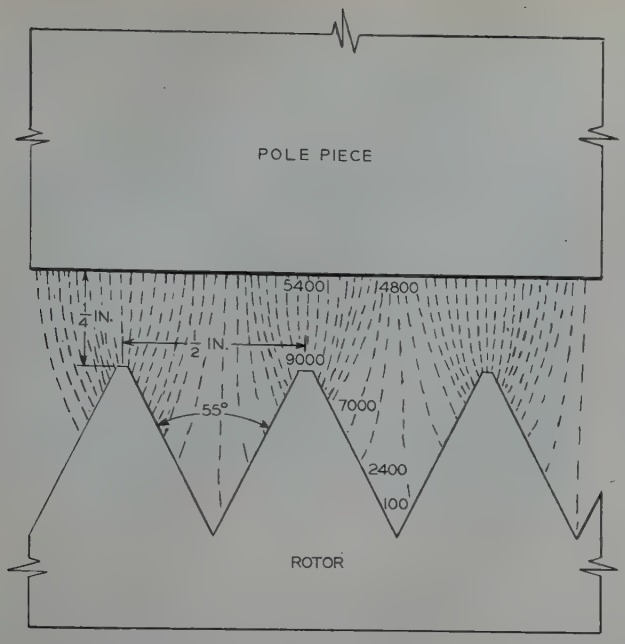

Fig. 2—Relative flux densities (gauss) and direction of flux in separation gap (triangular ridges on rotor). With ¼-in. ridges and ⅛-in. gap the mean flux density is a great deal higher but is difficult to measure locally.

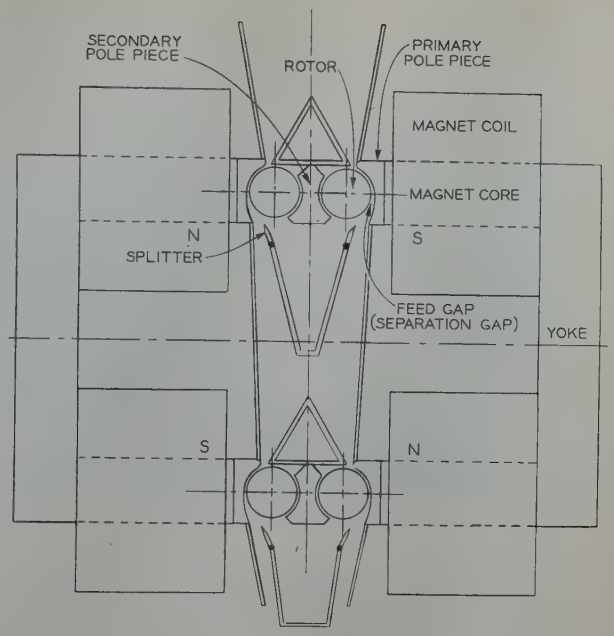

Fig. 3—The above sketch shows the magnetic circuit of a two-stage, double-rotor, high-intensity separator.

magnetite particle to a conventional low-intensity separator drum. It is important to note, however, that this pinning force (exerted when the particle is in contact with the rotor) is many times greater than the attractive force, say, in the middle of the separating gap.

BASIC DESIGN OF IDEAL SEPARATOR

The Magnetic Circuit: The critical nature of the magnetic circuit in an induced-rotor separator may be illustrated by a familiar textbook example dealing with magnetization of an iron ring. After the amount of magnetization corresponding to a given excitation is determined, a small gap is cut into the ring. Even if the width of the gap is negligible compared to the circumference of the ring, the magnetic reluctance of the system will be increased as much as ten times and the exciting current must be made tenfold in order to maintain the original degree of magnetization. Since any induced-rotor separator has at least two air gaps, on both sides of the rotor, and since the average intensity desired in the separation gap is about 20,000 gauss, the excitation coils must be massive as compared to the coils of a low-intensity separator. It is also known that magnetic flux tends to leak from sharp angles in the circuit. Thus the most effective location of the magnet coil is immediately behind the primary pole piece, as shown in Fig. 3.

Fig. 3 also illustrates two other important features of the proposed ideal separator. The distribution of dry feed, generally a difficult problem, is alleviated by arranging two rotors side by side so that they can treat a common feed flow. Since effective separation usually requires at least one cleaning pass of the tailing from the first pass, the separator is made into a two-stage machine by installation of another pair of coils and rotors in the lower half of the magnetic circuit. This also results in more economical use of iron, as the circuit would have to be closed with heavy members in any case.

Shape of Pole Pieces and Rotor Surface: The requirement that the attractive force must be directed toward the rotor affects the shaping of both pole pieces and the rotor surface. Fig. 4 presents profiles of eight pole pieces tested. A short description of each will help in understanding the final choice of shape.

Profile *A* in Fig. 4 was initially chosen with the idea that the sharply receding pole face would provide room for a high-speed trajectory of tailing particles which would prevent their rebounding to the concentrate flow. However, both separation efficiency and capacity were poor. Field intensity measurements then indicated that considerable flux was bypassing the narrowest separating zone by bridging, via the top of the rotor, between the sharp upper edges of the primary and secondary pole piece. A changeover to profile *B* decreased bridging, but performance remained poor.

Attempts at higher feed rates by free fall through the separation gap were not successful but showed that profile *D*, with a straight face, was superior to profile *C* with a convex pole face. The first good

Table I. Selected Data from High-Intensity Magnetic Separator Testing

Feed Sample	Mesh, 100 Pct Passing	Number of Passes	Feed Rate to First Rotor, L.T. Per Hr Per Ft	Concentrate Wt, Pct	Fe, Pct	SiO_2, Pct	Fe Rec., Pct
Coarse-grained specular hematite ore from Quebec	14	4	3.6	53.1	67.5	3.0	97.5
Coarse-grained specular hematite ore from Quebec	14	3	4.5	50.5	68.3	2.0	94.0
Coarse-grained specular hematite ore from Quebec	14	3	5.0	52.1	66.7	4.1	95.7
Coarse-grained specular hematite ore from Quebec	14	2	4.5	51.2	66.6	4.2	91.5
Spiral feed from Mesabi Range washing plant	20	4	1.9	33.0	58.4	9.2	79.3
Fine-grained specular hematite ore from Quebec	65	4	2.9	64.4	44.6		95.4

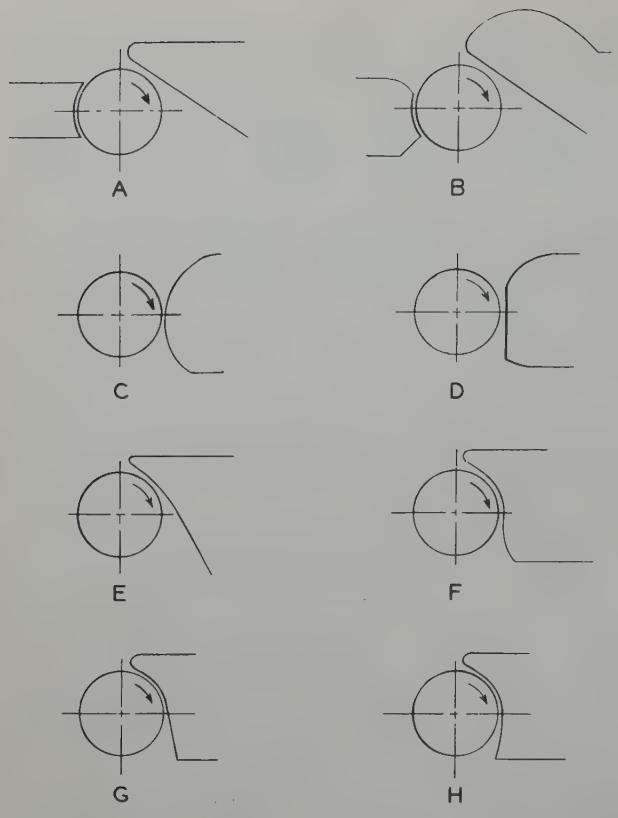

Fig. 4—Profiles of primary pole pieces.

results were obtained with the concave pole face depicted in sketch *E*, and very successful operation was finally attained with profile *H*.

It was concluded that the primary pole piece must provide the longest possible zone of high intensity as well as a consistently concave surface facing the rotor. The importance of consistently concave surface was further illustrated by the shapes of profiles *F* and *G*. The lower portion of pole piece *F* was made slightly convex by mistake, with the result that there was no clear distinction or empty zone between the tailing and concentrate flows. The situation was corrected by machining the convex surface straight as shown in sketch *G*.

Fig. 5 is a more detailed sketch of the preferred shapes and positioning of the pole pieces. The concave face of the primary pole piece has a cylindrical upper half and an involute lower half. The secondary pole piece hugs the rotor tightly but does not provide close edges that would serve to bunch up the flux from the upper and lower edges of the primary pole piece.

The shaping of the rotor surface offers at least as many possibilities as that of the pole pieces. Only two shapes will be discussed here.

Fig. 6A shows a rotor with square teeth in longitudinal cross-section. The valleys in this construction may or may not be filled with nonmagnetic material (flattened brass wire, for example, if the groove is a spiral). The square teeth converge the lines of flux toward the sharp edges, creating an attractive force directed toward the rotor surface, but tests with this kind of rotor gave mediocre results.

According to Derkatch,[3] triangular teeth or ridges, as shown in Fig. 6B, produce the maximum attractive force. Work at Oliver Iron Mining's research laboratory confirms this. Derkatch also claims, however, that the desired pitch or distance between the ridges is dependent on the particle size

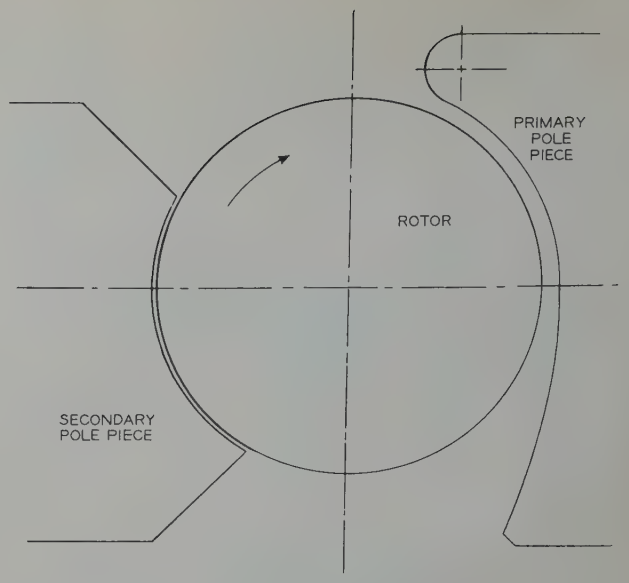

Fig. 5—Profiles of pole pieces.

treated. In this respect tests made in the present investigation have given conflicting results. It may be that the work mentioned by Derkatch was done with non-spiraling ridges on the rotor, whereas Oliver's laboratory rotors had a spiraling ridge. The inertia of the particles falling in the valleys between the ridges causes them to travel more slowly than the rotor surface, and while they are delayed they are caught by the sidewise-moving areas of strong attraction near the crests of the spiraling ridges.

Drives, Feeders, Feed Chutes, and Splitters: Capacity of the separator and grade of concentrate depend on how fast the rotor may be operated before the centrifugal force exceeds the magnetic attraction force. With a 4-in. rotor, speeds of 200 to 450 rpm have been found to be feasible. Optimum speed seems to vary according to feed rate or stage of separation; consequently, variable-speed drives should be specified for each stage.

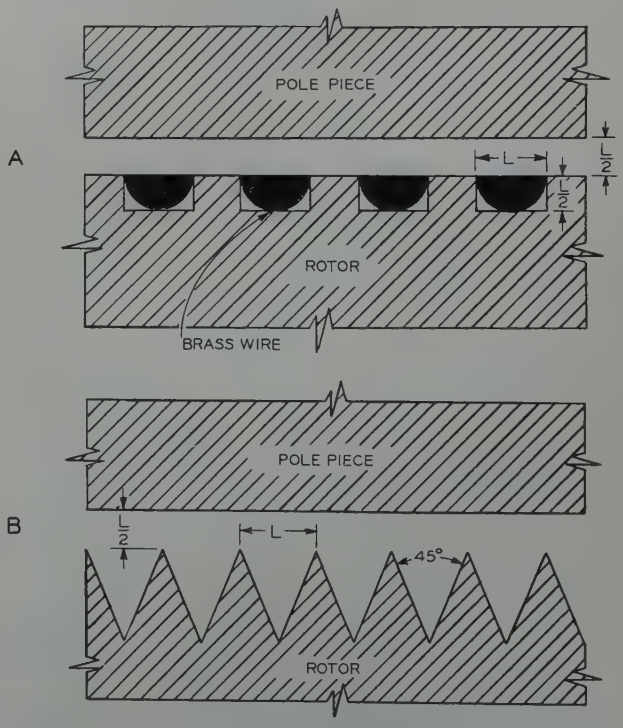

Fig. 6—Illustrated above are two types of rotor surface and their position with respect to the pole face.

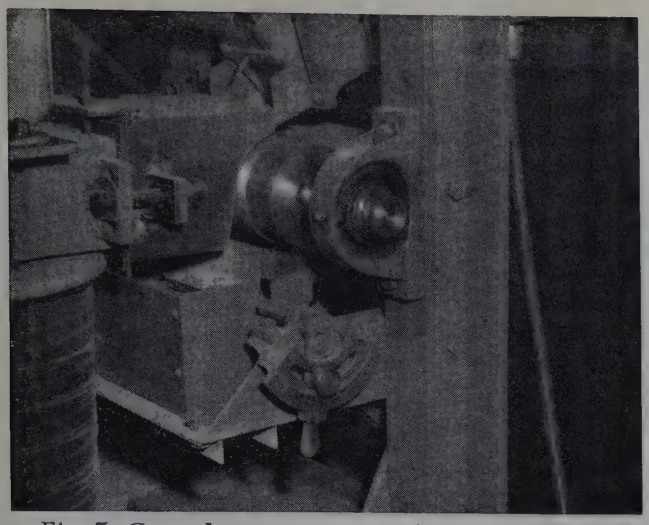

Fig. 7—General arrangement of the separator used.

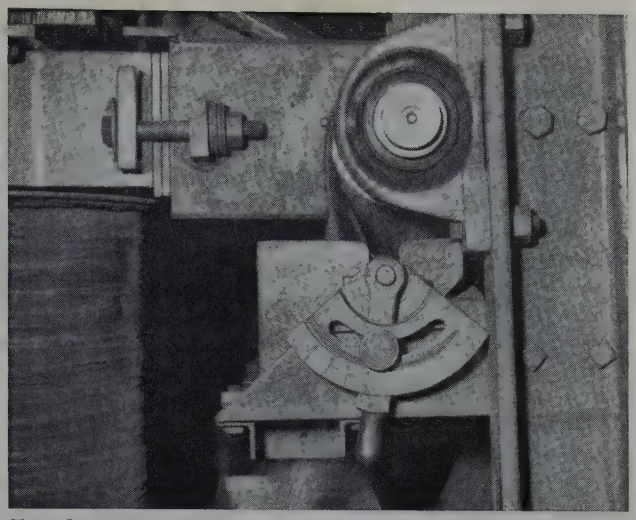

Fig. 8—Note separation of concentrate and tailing flows.

The design of feed chutes permits considerable freedom, but care should be taken that they provide an unhindered feed flow. There should be no problems in positioning the product splitters, but they should be placed where they can be easily observed and readjusted while the separator is in operation.

OPERATION OF SEPARATOR

Rebounding of tailing particles from the pole face into the concentrate is a serious problem affecting purity of product. This tendency will naturally increase as the rotor is speeded up to gain improved capacity. A fortunate circumstance was discovered, however—as feed rate was increased to the maximum the separator could receive, the stream of particles in the separation gap became so dense that contamination of concentrate by rebounding gangue ceased, although the particles still had considerable freedom of motion relative to one another. What might be called *choke feeding* thus turned out to be an important requirement for good separation efficiency as well as for capacity.

As the distance between the triangular ridges of the rotor is increased, without means of simultaneously increasing the excitation, the effective width of the separation gap, and consequently the reluctance, also increases. Correspondingly, the mean field intensity decreases. However, the remaining field is now divided between fewer ridges and, up to a point, the attractive force may actually increase. In testing at Oliver this was observed when the distance between the ridges was increased from ⅛ to ¼ in. The increased attractive force also seemed further to eliminate contamination of concentrate by rebounding gangue, regardless of rotor speed or whether the separator was choke-fed or not. Apparently choke feeding is essential only when the attractive force is relatively weak.

Table II. Combined High-Intensity Magnetic and High-Tension Separation Test on Fine-Grained Specularite from Quebec

	Wt, Pct	Fe, Pct	Fe Rec., Pct
High Tension Separator Concentrate	33.4	64.6	73.2
High-Tension Separator Tailing	23.5	24.8	
High-Intensity Magnetic Separator Tailing	43.1	4.8	

Selected Examples of Performance: The close-ups in Figs. 7 and 8 show the main features of the separator used in the testwork described. It should be noted that the excitation coil is smaller than used on most high-intensity separators and that there is no means of resaturating the core after the reluctance of the circuit has been increased past a certain value of widening the gap. The following selected test results should be considered, therefore, with the understanding that they are not the ultimate attainable by the high-intensity process.

Fig. 9 presents a comparison of two rotors, one with a ⅛-in. pitch and another with ¼-in. pitch. The coarser rotor did better in three passes than the finer rotor in five, although the mean field strength was considerably lower.

Table I offers additional selected test data. Results with a coarse-grained specularite ore from Quebec are excellent. Those obtained with sized Mesabi hematite (feed to the spiral section of a Mesabi Range washing plant) are considerably poorer, but concentration of Mesabi hematites did not fall into the scope of this investigation, and more exhaustive testing may produce better results. Those shown here about equal the average spiral performance. A difficult problem was presented by some fine-grained specularite ores from Quebec; a clean tailing of considerable weight could be produced, but concentrate grade remained poor. It was found that these ores contained low-grade middling particles of higher magnetic susceptibility than the liberated hematite itself. Superficially these middling particles resembled quartz, but microscopic examination revealed many small inclusions of iron oxide. The relatively high susceptibility of these middling particles is somewhat of a mystery because a chemical analysis showed only 0.6 pct Fe^{++}. A high-tension separator was *blind* to this middling and was able to make a high-grade product from the high-intensity concentrate. Table II shows results from a combination high-intensity—high-tension test.

Some Commercial High-Intensity Magnetic Separators: Schematic views of commercial types of high-intensity separators are given in Fig. 10. It should be noted that four of these separators, *A-D*, are now or have been employed successfully in concentrating iron ore in Germany. Sketches *E* and *F* feature separators of American design, so far exclusively employed in concentrating nonferrous minerals. In the following discussion the general layout of these separators is examined in the light

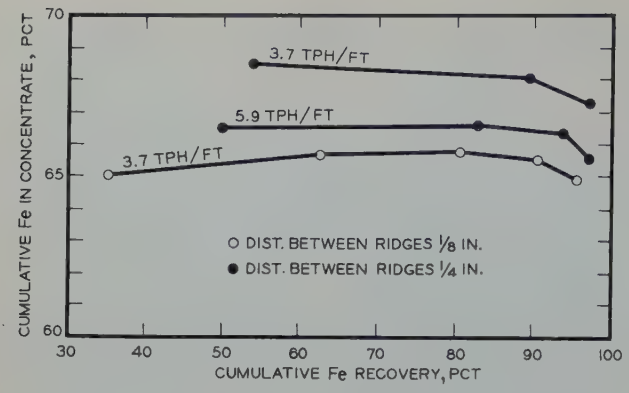

Fig. 9—Effect of rotor pitch on separator performance. Feed: coarse-grained specular hematite ore from Quebec.

of experience from laboratory testing or knowledge of magnetic circuits in general.

Separator *A* evidently was a forerunner of *B* and, as far as the writer knows, is no longer being built. Scant performance data are available, and the only comments would concern the need of apportioning feed between the two rotors and the lack of a second stage.

Both these limitations are overcome in the design of separator *B*, reported to be of high capacity and offering the advantage of two stages built into one circuit. Two features are viewed with some criticism, however:

1) The field between the two rotors is reduced by flux leakage from the secondary gaps between the rotors and the pole pieces.

2) The rotors weaken each other's field gradients. (They resemble a system consisting of a rotor and a primary pole piece with a convex face). Tests show that this has an adverse effect on recovery.

It is fair to assume that separator *C*, in turn, evolved from separator *B*. Item 1 in the preceding criticism still applies to this separator, but otherwise it must be considered an improvement. A common pole piece has been inserted to present a concave face to both rotors. Thus the field gradients have the right sign in all parts of the separation gaps.

In separator *D* the second stage has been eliminated and a parallel stage added. Reportedly, this was done at no expense of total capacity. On the other hand, this arrangement avoids the situation where the feed rate to the second stage is set by the output of the first stage. In the author's experience, however, this difficulty can be eliminated by proper design of the rotor surface as was described above.

The rotor-pole piece arrangement in sketch *E* generally follows the principles of preferred design except that the sharp upper edges of the pole pieces are too close to each other. Laboratory experiments show that in this arrangement the flux tends to bridge through the upper portions of the system, leaving the field weak in the rest of the separation gap. This would affect the separator's capacity adversely.

Sketch *F*, finally, presents the common, back-to-back layout favored by several American manufacturers of these separators. Generally a dummy pole, as shown, is included for pre-removal of highly magnetic minerals that might clog the high-intensity gaps. Compared to the ideal layout presented earlier, this design does not place the coil most effectively. The ideal separator also handles a single flow of feed, twice as large as the back-to-back separator.

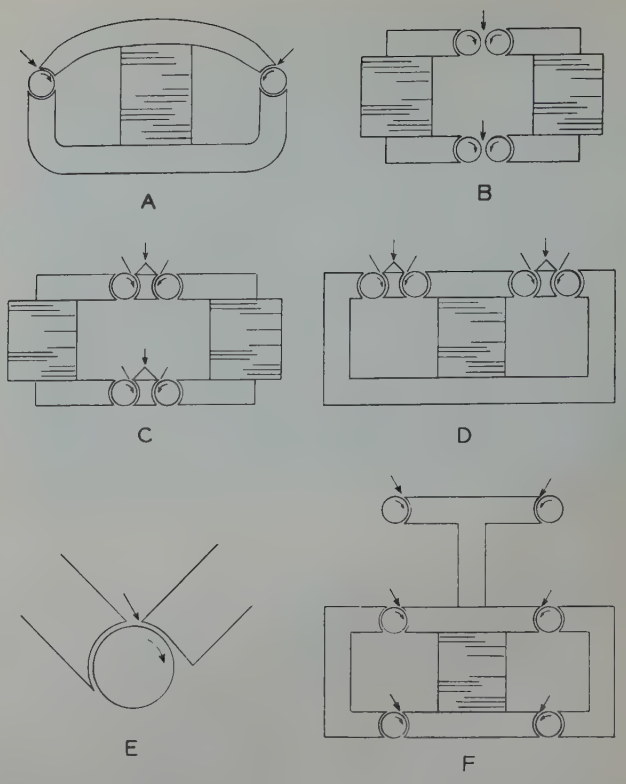

Fig. 10—Schematic view of several commercial types of high-intensity, induced-rotor magnetic separators.

CONCLUSION

There is no doubt that properly designed high-intensity separators will find wider application in concentrating iron ores. Being a dry process, high-intensity separation offers particular advantages whenever water supply is limited. But a thorough knowledge of the ore is needed before the process can be considered; some ores of seemingly simple mineralogy cannot be concentrated by this method.

The author expresses thanks to R. J. Morton, R. L. Bennett, and M. F. Williams, under whose supervision the present investigation was made. He also acknowledges, with appreciation, the valuable contribution by J. R. Andreachi of the Oliver research staff.

REFERENCES

[1] D. Korda: La Séparation Electromagnétique et Electrostatique Des Minerais. Paris, 1905, No. 6312, Engineering Societies Library, New York City.
[2] U. Runolinna: Dry Magnetic Separation of Finely Ground Magnetite. International Mineral Dressing Congress, Stockholm, Sweden, Sept. 13-21, 1957.
[3] Derkatch: Theory of Magnetic Separation of Weakly Magnetic Minerals. *Izvestia Akademii Nauk SSSR*, otdelenie tekhnitcheskikh Naouk, 1951, no. 6, pp. 852-862.
[4] "International" Separator, Fig. 46, *The Chemical World*, September 1913.
[5] H. H. Wait and F. T. Snyder: U. S. Pat. No. 832,822, Oct. 9, 1906.
[6] W. B. Moore: U. S. Pat. No. 922,800, May 25, 1909.
[7] C. Q. Payne: U. S. Pat. No. 901,368, Oct. 20, 1908.
[8] C. Q. Payne: U. S. Pat. No. 1 958,521, May 15, 1934.
[9] C. Q. Payne: U. S. Pat. No. 2,045,098, June 23, 1936.
[10] C. Q. Payne: U. S. Pat. No. 2,156,125, April 25, 1939.
[11] C. Q. Payne: U. S. Pat. No. 2,188,516, Jan. 30, 1940.
[12] C. Q. Payne: U. S. Pat. No. 2,188,517, Jan. 30, 1940.
[13] L. G. Rowand: U. S. Pat. No. 1,068,453, July 29, 1913.
[14] A. H. Pehrson, O. Fredricksborg, and E. O. E. Tydén: U. S. Pat. No. 1,967,723, July 24, 1934.
[15] A. L. J. Queneau: U. S. Pat. No. 2,290,892, July 28, 1942.
[16] A. Goltz and K. Neumann: U. S. Pat. No. 2,832,471, April 29, 1958.
[17] G. Sengfelder: German Patent No. 827,181, Jan. 7. 1952.
[18] H. Carpenter: U. S. Pat. No. 2,767,843, Oct. 23, 1956.
[19] R. N. Palmer: U. S. Pat. No. 2,826,303, March 11, 1958.
[20] J. de Robert: Colloque sur L'Enrichissement des Minerais de Fer. *IRSID*, Metz, Oct. 8, 1957.

Discussion of this article sent (2 copies) to AIME before Jan. 31, 1960, will be published in MINING ENGINEERING.

TRANSACTIONS

January-December 1959, Vol. 214

Society of Mining Engineers of AIME

A Decade of Development in Overvoltage Surveying ..... Mar 307
Activation and Deactivation Studies with Copper on Sphalerite ..... Apr 430
Advancing Through Caved Ground with Yieldable Arches ..... Jul 720
Airborne Gravity Meter Description and Preliminary Results ..... Aug 817
Aitkenhead, W. C., and Jaekel, J. A.: *Beneficiation of Autunitic Ores* ..... Jan 66
Application of Electron Diffraction and Electron Microscopy to Mineral Engineering ..... May 535
Archibald, R. S.: *Economic History of the Lake Superior Iron District* ..... May 513
Atchison, T. C., and Duvall, W. I.: *Rock Breakage with Confined Concentrated Charges* ..... Jun 605
Baldwin, R. W.: *A Decade of Development in Overvoltage Surveying* ..... Mar 307
Barnett, R. H., Wilson, E. E., and Vaughn, W. W.: *Drill Core Scanner Proved in Field* ..... Jun 617
Basic Studies of Percussion Drilling ..... Jan 68
Bauxitization in the Pocos De Caldas District, Brazil ..... Aug 805
Beneficiation of Autunitic Ores ..... Jan 66
Bunker, C. M., and Ohm, J. M.: *Fishing Tools for Retrieving Gamma-ray Logging Components* ..... Oct 1045
Canney, F. C.: *Geochemical Study of soil Contamination in the Coeur D'Alene District, Shoshone County, Idaho* ..... Feb 205
Cantwell, T., Hawkes, H. E., and Rasmussen, N. C.: *Nuclear Detector for Beryllium Minerals* ..... Sep 938
Carpenter, L. G., and Garrett, D. E.: *Tungsten in Searles Lake* Mar 301
Case History in Pillar Recovery ..... Jul 701
Chang, M. C., and Dasher, J.: *Mineral Dressing Fundamentals Applied to the Fine Coal Problem* ..... Mar 304
Charmbury, H. B., and Mitchel, D. R.: *Gravity Methods Clean Extreme Fine Sizes Of Bituminous Coal* ..... Feb 211
Crocker, B. S.: *Recent Developments in Pebble Milling* ..... May 527
Crosby, G. M.: *The Gem Stocks and Adjacent Orebodies, Coeur D'Alene District, Idaho* ..... Jul 697
Dasher, J., and Chang, M. C.: *Mineral Dressing Fundamentals Applied to the Fine Coal Problem* ..... Mar 304
Dietrich, W. F.: *Market Trends for Mineral Fillers in Western States* ..... Aug 813
Drill Core Scanner Proved in Field Jun 617
Duvall, W. I., and Atchison, T. C.: *Rock Breakage with Confined Concentrated Charges* ..... Jun 605
Economic History of the Lake Superior Iron District ..... May 513
Effect of Pulp Depth and Initial Pulp Density in Batch Thickening ..... Jun 613
Experiments in Concentrating Iron Ore from the Pea Ridge Deposit, Missouri ..... Mar 325
Face Ventilation for Continuous Miners ..... Sep 928
Factors Affecting the Cleaning of Fine Coals by the Convertol Process ..... Nov 1151
Ferrograde Concentrates from Arkansas Manganiferous Limestone ..... Aug 810
Fine, M. M.: *Ferrograde Concentrates from Arkansas Manganiferous Limestone* ..... Aug 810
Fine, M. M., and Frommer, D. W.: *Experiments in Concentrating Iron Ore from the Pea Ridge Deposit, Missouri* ..... Mar 325
Fishing Tools for Retrieving Gamma-ray Logging Components ..... Oct 1045
Flocculation To Improve Coal Slurry Filtration ..... Jul 715
Frischknecht, F. C.: *Scandinavian Electromagnetic Prospecting* Sep 932
Frommer, D. W., and Fine, M. M.: *Experiments in Concentrating Iron Ore from the Pea Ridge Deposit, Missouri* ..... Mar 325
Fuerstenau, D. W.: *Retention Time in Continuous Vibratory Ball Milling* ..... Dec 1238
Fuerstenau, D. W., Mao, G. W., and Gaudin, A. M.: *Activation and Deactivation Studies with Copper on Sphalerite* ..... Apr 430
Fuerstenau, M. C., Mitchell, S. R., and Gaudin, A. M.: *Effect of Pulp Depth and Initial Pulp Density in Batch Thickening* ..... Jun 613
Garrett, D. E., and Carpenter, L. G.: *Tungsten in Searles Lake* ..... Mar 301
Gaudin, A. M., Fuerstenau, D. W., and Mao, G. W.: *Activation and Deactivation Studies with Copper on Sphalerite* ..... Apr 430
Gaudin, A. M., Fuerstenau, M. C., and Mitchell, S. R.: *Effect of Pulp Depth and Initial Pulp Density in Batch Thickening* ..... Jun 613
Geer, M. R., Jacobsen, P. S., and Yancey, H. F.: *Flocculation To Improve Coal Slurry Filtration* ..... Jul 715
Geochemical Study of Pb-Ag-Zn Ore from the Darwin Mine, Inyo County, California ..... Sep 940
Geochemical Study of the Soil Contamination in the Coeur D'Alene District, Shoshone County, Idaho ..... Feb 205
Gillson, J. L.: *Sand Deposits of Titanium Minerals* ..... Apr 421
Gravity Methods Clean Extreme Fine Sizes of Bituminous Coal ..... Feb 211
Gyro-Compass Surveys Underground Workings and Boreholes ..... May 521
Hall, W. E.: *Geochemical Study of Pb-Ag-Zn Ore from the Darwin Mine, Inyo County, California* ..... Sep 940
Hartman, E. L.: *Basic Studies of Percussion Drilling* ..... Jan 68
Hawkes, H. E., Rasmussen, N. C., and Cantwell, T.: *Nuclear Detector for Beryllium Minerals* ..... Sep 938
High-intensity Magnetic Separation of Iron Ores ..... Dec 1244
Hines, P. R.: *Sphalerite Flotation With Guanidine Compounds and Derivates as Collectors* ..... Feb 219
Interaction of Minerals with Gases and Reagents in Flotation ..... Mar 319
Jackson, O. A. E.: *Pebble Milling Practice at the South African Gold Mines of Union Corp. Ltd.* ..... Nov 1133
Jacobsen, P. S., Geer M. R., and Yancey H. F.: *Flocculation To Improve Coal Slurry Filtration* ..... Jul 715
Jaekel, J. A., and Aitkenhead, W. C.: *Beneficiation of Autunitic Ores* ..... Jan 66
Kalasky, J. D.: *Face Ventilation for Continuous Miners* ..... Sep 928
Lawver, J. E., and Samsel, G. L.: *Application of Electron Diffraction and Electron Microscopy to Mineral Engineering* ..... May 535
Lundberg, H. T., and Ratcliffe, J. H.: *Airborne Gravity Meter Description and Preliminary Results* ..... Aug 817
Lyon, R. J. P., and Tuddenham, W. M.: *Quantitative Mineralogy As a Guide in Exploration* ..... Dec 1233
Lyon, R. J. P.: *Time Aspects of Geothermometry* ..... Nov 1145
Mao, G. W., Gaudin, A. M., and Fuerstenau, D. W.: *Activation and Deactivation Studies with Copper on Sphalerite* ..... Apr 430
Market Trends for Mineral Fillers in Western States ..... Aug 813
Meidav, T., Scharon, L., and Uhley, R.: *Sub-Surface Investigations of a Plant Site* ..... Feb 215
Meteorological Influence on Radon Concentration in Drillholes ..... Jul 706
Midnite Mine Geology and Development ..... May 531
Mineral Dressing Fundamentals Applied to the Fine Coal Problem Mar 304
Mitchel D. R., and Charmbury, H. B.: *Gravity Methods Clean Extreme Fine Sizes of Bituminous Coal* ..... Feb 211
Mitchell, S. R., Gaudin, A. M., and Fuerstenau, M. C.: *Effect of Pulp Depth and Initial Pulp Density in Batch Thickening* ..... Jun 613
McCarty, M. F., and Olson, R. S.: *Polyacrylamides for the Mining Industry* ..... Jan 61
McMorris, W. L., III, and Sun, S. C.: *Factors Affecting the Cleaning of Fine Coals by the Convertol Process* ..... Nov 1151
Nuclear Detector for Beryllium Minerals ..... Sep 938
Oglesby, S., Jr., and Thomas, A. L., Jr.: *Permissible-type Dust Counter for Coal Mines* ..... Mar 328
Ohm, J. M., and Bunker, C. M.: *Fishing Tools for Retrieving Gamma-ray Logging Components* ..... Oct 1045
Olson, E. H., Baroch, C. J., and Smutz, M.: *Processing California Bastnasite Ore* ..... Mar 315
Olson, R. S., and McCarty, M. F.: *Polyacrylamides for the Mining Industry* ..... Jan 61
Overstreet, W. C., Theobald, P. K., Jr., and Whitlow, J. W.: *Thorium and Uranium Resources in Monazite Placers of the Western Piedmont, North and South Carolina* ..... Jul 709
Overstreet, W. C., Whitlow, J. W., and Theobald, P. K.: *Thorium and Uranium Resources in Monazite Placers of the Western Piedmont, North and South Carolina*
Palasvirta, O. E.: *High-intensity Magnetic Separation of Iron Ores* ..... Dec 1244
Pebble Milling Practice at the South African Gold Mines of Union Corp. Ltd. ..... Nov 1133
Permissible-type Dust Counter for Coal Mines ..... Mar 328
Pfleider, E. P., and Rellensmann, O.: *Gyro-Compass Surveys Underground Workings and Boreholes* ..... May 521
Plaskin, I. N.: *Interaction of Minerals with Gases and Reagents in Flotation* ..... Mar 319
Polyacrylamides for the Mining Industry ..... Jan 61

Processing California Bastnasite Ore ..... Mar 315
Quantitative Mineralogy As a Guide in Exploration ..... Dec 1233
Quigley, J.: *Advancing Through Caved Ground with Yieldable Arches* ..... Jul 720
Rasmussen, N. C., Cantwell, T., and Hawkes, H. E.: *Nuclear Detector for Beryllium Minerals* ..... Sep 938
Ratcliffe, J. H., and Lundberg, H. T.: *Airborne Gravity Meter Decription and Preliminary Results* ..... Aug 817
Recent Developments in Pebble Milling ..... May 527
Reed, J. J.: *Case History in Pillar Recovery* ..... Jul 701
Relation of Land Subsidence to Ground-water Withdrawals in the Upper Gulf Coast Region, Texas ..... Oct 1030
Rellensmann, O., and Pfleider, E. P.: *Gyro-Compass Surveys Underground Workings and Boreholes* ..... May 521
Retention Time in Continuous Vibratory Ball Milling ..... Dec 1238
Rock Breakage with Confined Concentrated Charges ..... Jun 605
Samsel, G. L., and Lawver, J. E.: *Application of Electron Diffraction and Electron Microscopy to Mineral Engineering* ..... May 535
Sand Deposits of Titanium Minerals ..... Apr 421
Scandinavian Electromagnetic Prospecting ..... Sep 932
Scharon, L., Uhley, R., and Meidav, T.: *Sub-Surface Investigations of a Plant Site* ..... Feb 215
Sheldon, R. F.: *Midnite Mine Geology and Development* ..... May 531
Smutz, M., Olson, E. H., and Baroch, C. J.: *Processing California Bastnasite Ore* ..... Mar 315
Sphalerite Flotation With Guanidine Compounds And Derivates as Collectors ..... Feb 219
Subsurface Investigations of a Plant Site ..... Feb 215
Sun, S. C., and McMorris, W. L., III: *Factors Affecting the Cleaning of Fine Coals by the Convertol Process* ..... Nov 1151
Tanner, A. B.: *Meteorological Influence on Radon Concentration in Drillholes* ..... Jul 706
The Gem Stocks and Adjacent Orebodies, Coeur D'Alene District, Idaho ..... Jul 697
Theobald, P. K., Whitlow, J. W., and Overstreet, W. C.: *Thorium and Uranium Resources in Monazite Placers of the Western Piedmont, North and South Carolina* ..... Jul 709
Thomas, A. L., Jr., and Oglesby, S., Jr.: *Permissible-type Dust Counter for Coal Mines* ..... Mar 328
Thorium and Uranium Resources in Monazite Placers of the Western Piedmont, North and South Carolina ..... Jul 709
Time Aspects of Geothermometry Nov 1145
Tuddenham, W. M., and Lyon, R. J. P.: *Quantitative Mineralogy As a Guide in Exploration* ..... Dec 1233
Tungsten in Searles Lake ..... Mar 301
Uhley, R., Meidav, T., and Scharon, L.: *Sub-Surface Investigations of a Plant Site* ..... Feb 215
Vaughn, W. W., Barnett, R. H., and Wilson, E. E.: *Drill Core Scanner Proved in Field* ..... Jun 617
Webber, B. N.: *Bauxitization in the Pocos De Caldas District, Brazil* ..... Aug 805
Whitlow, J. W., Overstreet, W. C., and Theobald, P. K.: *Thorium and Uranium Resources in Monazite Placers of the Western Piedmont, North and South Carolina* ..... Jul 709
Wilson, E. E., Vaughn, W. W., and Barnett, R. H.: *Drill Core Scanner Proved in Field* ..... Jun 617
Winslow, A. G., and Wood, L. A.: *Relation of Land Subsidence to Ground-water Withdrawals in the Upper Gulf Coast Region, Texas* ..... Oct 1030
Wood, L. A., and Winslow, A. G.: *Relation of Land Subsidence to Ground-water Withdrawals in the Upper Gulf Coast Region, Texas* ..... Oct 1030
Yancey H. F., Geer, M. R. and Jacobsen, P. S.: *Flocculation To Improve Coal Slurry Filtration* ..... Jul 715